



National Library
of Canada

Acquisitions and
Bibliographic Services Branch

395 Wellington Street
Ottawa, Ontario
K1A 0N4

Bibliothèque nationale
du Canada

Direction des acquisitions et
des services bibliographiques

395, rue Wellington
Ottawa (Ontario)
K1A 0N4

Notice - Attention

Notice - Attention

NOTICE

The quality of this microform is heavily dependent upon the quality of the original thesis submitted for microfilming. Every effort has been made to ensure the highest quality of reproduction possible.

If pages are missing, contact the university which granted the degree.

Some pages may have indistinct print especially if the original pages were typed with a poor typewriter ribbon or if the university sent us an inferior photocopy.

Reproduction in full or in part of this microform is governed by the Canadian Copyright Act, R.S.C. 1970, c. C-30, and subsequent amendments.

AVIS

La qualité de cette microforme dépend grandement de la qualité de la thèse soumise au microfilmage. Nous avons tout fait pour assurer une qualité supérieure de reproduction.

S'il manque des pages, veuillez communiquer avec l'université qui a conféré le grade.

La qualité d'impression de certaines pages peut laisser à désirer, surtout si les pages originales ont été dactylographiées à l'aide d'un ruban usé ou si l'université nous a fait parvenir une photocopie de qualité inférieure.

La reproduction, même partielle, de cette microforme est soumise à la Loi canadienne sur le droit d'auteur, SRC 1970, c. C-30, et ses amendements subséquents.

UNIVERSITY OF ALBERTA

ASSESSING SEASONAL VARIATIONS IN COHESIVE SUBGRADE SOILS

by

Walaa Eldin Ibrahim Khogali



A THESIS SUBMITTED TO THE FACULTY OF GRADUATE STUDIES AND RESEARCH IN
PARTIAL FULFILLMENT OF THE REQUIREMENTS FOR THE DEGREE OF
DOCTOR OF PHILOSOPHY

DEPARTMENT OF CIVIL ENGINEERING

EDMONTON, ALBERTA

Spring, 1995



National Library
of Canada

Acquisitions and
Bibliographic Services Branch

395 Wellington Street
Ottawa, Ontario
K1A 0N4

Bibliothèque nationale
du Canada

Direction des acquisitions et
des services bibliographiques

395, rue Wellington
Ottawa (Ontario)
K1A 0N4

Your file: Votre référence

Our file: Notre référence

THE AUTHOR HAS GRANTED AN
IRREVOCABLE NON-EXCLUSIVE
LICENCE ALLOWING THE NATIONAL
LIBRARY OF CANADA TO
REPRODUCE, LOAN, DISTRIBUTE OR
SELL COPIES OF HIS/HER THESIS BY
ANY MEANS AND IN ANY FORM OR
FORMAT, MAKING THIS THESIS
AVAILABLE TO INTERESTED
PERSONS.

L'AUTEUR A ACCORDE UNE LICENCE
IRREVOCABLE ET NON EXCLUSIVE
PERMETTANT A LA BIBLIOTHEQUE
NATIONALE DU CANADA DE
REPRODUIRE, PRETER, DISTRIBUER
OU VENDRE DES COPIES DE SA
THESE DE QUELQUE MANIERE ET
SOUS QUELQUE FORME QUE CE SOIT
POUR METTRE DES EXEMPLAIRES DE
CETTE THESE A LA DISPOSITION DES
PERSONNE INTERESSEES.

THE AUTHOR RETAINS OWNERSHIP
OF THE COPYRIGHT IN HIS/HER
THESIS. NEITHER THE THESIS NOR
SUBSTANTIAL EXTRACTS FROM IT
MAY BE PRINTED OR OTHERWISE
REPRODUCED WITHOUT HIS/HER
PERMISSION.

L'AUTEUR CONSERVE LA PROPRIETE
DU DROIT D'AUTEUR QUI PROTEGE
SA THESE. NI LA THESE NI DES
EXTRAITS SUBSTANTIELS DE CELLE-
CI NE DOIVENT ETRE IMPRIMES OU
AUTREMENT REPRODUITS SANS SON
AUTORISATION.

ISBN 0-612-01709-5

Canada

UNIVERSITY OF ALBERTA

RELEASE FORM

NAME OF AUTHOR: **WALAA ELDIN IBRAHIM KHOGALI**
TITLE OF THESIS: **ASSESSING SEASONAL VARIATIONS IN COHESIVE SUBGRADE
SOILS**
DEGREE: **DOCTOR OF PHILOSOPHY**
YEAR THIS DEGREE GRANTED: **1995**

Permission is hereby granted to the University of Alberta Library to reproduce single copies of this thesis and to lend or sell such copies for private, scholarly or scientific research purposes only.

The author reserves all other publication and other rights in association with the copyright of the thesis, and except as hereinbefore provided neither the thesis nor any substantial portion thereof may be printed or otherwise reproduced in any material form whatever without the author's prior written permission.



211RH Michener Park
Edmonton, Alberta
Canada, T6H-4M5

UNIVERSITY OF ALBERTA

FACULTY OF GRADUATE STUDIES AND RESEARCH

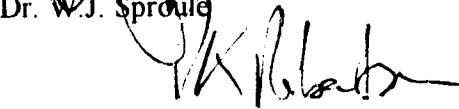
The undersigned certify that they have read, and recommend to the Faculty of Graduate Studies and Research for acceptance, a thesis entitled: **ASSESSING SEASONAL VARIATIONS IN COHESIVE SUBGRADE SOILS**, submitted by *Walaa Eldin Ibrahim Khogali* in partial fulfillment of the requirements for the degree of *Doctor of Philosophy*



Professor Emeritus, K.O. Anderson
(Supervisor)



Dr. W.J. Sproule



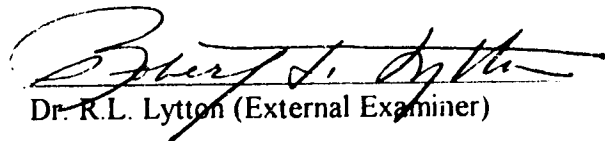
Dr. P.K. Robertson



Dr. J.T. Christison



Dr. K.W. Domier



Dr. R.L. Lytton (External Examiner)

Date: April 25, 1995

ABSTRACT

The long term performance of a pavement structure is strongly dependent on the subgrade soil conditions. This is particularly true in areas experiencing seasonal freezing and fluctuations in moisture and temperature existing within and around the pavement structure. To account for the adverse effects of such factors on the structural adequacy of pavements, it is necessary to have available realistic and reliable strength measures for the layer component materials. With the resilient modulus as a key parameter in such an evaluation, the current study is aimed at investigating the seasonal variation effects of moisture and temperature on pavement bearing capacity as assessed by non-destructive and other appropriate laboratory test procedures.

The present study consists of two phases: a field investigation phase and a laboratory testing program. Within the scope of the field testing program, a pavement section representative of the primary highway system within the Province of Alberta, was selected and instrumented with thermal conductivity suction sensors. FWD deflection tests were conducted at regular time intervals over a period of two years, and at various locations within the instrumented section. Output from these tests coupled with temperature and suction measurements were used in various forms to establish a procedure for measuring seasonal variations in the structural strength of the subgrade soil.

The laboratory investigation involved extensive repeated load testing on remolded samples of the subgrade material taken from the instrumented site. Representative resilient

modulus values, under different loading, temperature and moisture conditions, obtained from these test were used to develop predictive moduli relationships.

Both field and laboratory phases produced unique and practical approaches for quantifying the influence of seasonal variations on subgrade strength. Although traffic induced stresses were found to be significant in effecting subgrade strength, the soil matric suction was found to be more influential.

In addition to the benefits gained from this current research project, a new and relatively inexpensive resilient modulus test system has been developed and is now operational. This system can be utilized in the future for developing mechanistic-empirical procedures for the design and rehabilitation of flexible pavements.

ACKNOWLEDGEMENTS

My first and foremost sincere gratitude is due solely to ALLAH (swt) The Lord of the worlds. Al' praise is due to HIM, and it is to HIM I bow in submission.

I would also like to express my sincere appreciation to Professor Emeritus K.O. Anderson for his continued guidance, moral support and encouragement throughout my studies at the University of Alberta (U of A). Without his direction and invaluable suggestions the objectives of this research could not have been accomplished.

Special thanks are due to my mother, Fatima, my father, Ibrahim , my wife, Safaa and my children: Mohammed, Shemaa, Abdulrahman and Fatima for their continued support, understanding and sacrifices made throughout the years.

I would like also to extend my sincere thanks to the following individuals who contributed significantly during the course of the present study:

Dr. J.T. Christison of the Alberta Research Council; Dr. P.K. Robertson and Dr. W.J. Sproule of the U of A who served on my supervisory committee and gave invaluable suggestions throughout the present work.

Mr. Len Chase of the Alberta Research Council, Mr. Roy Gitzel and Mr. Dale Lathe of the Civil Engineering Electronics group at U of A, who participated in the development of the laboratory Resilient Modulus Testing System.

Mr. M. Kurlanda of Roadway Engineering Section of Alberta Transportation and Utilities for his generous support in providing all necessary information pertinent to the operation of the FWD deflection testing equipment and related matters.

Dr. D.G. Fredlund of the Civil Engineering Department of the University of Saskatchewan for providing much of the information needed for the chapter dealing with the review of current devices used for measuring soil suction.

Financial assistance from the following sources are acknowledged and appreciated. The primary source of funding for this study has been from Alberta Transportation and Utilities under various research contracts. Research assistantships from individual operating grants provided by the Natural Science and Engineering Research Council of Canada awarded to my supervisor helped during the latter stages of writing this Ph.D. dissertation. Other supplementary support came from the Alberta Research Council in the form of part of the hardware used in the development of the Resilient Modulus Testing System. The financial support provided by the Government of Sudan during the early stages of this study program is also recognized and greatly acknowledged.

Finally, I would like to extend my warmest thanks to all my friends in the Muslim Students' Association at the U of A and to all other unnamed individuals who helped in any way throughout the course of my studies at this University.

Table of Contents

Chapter		Page
1	INTRODUCTION	1
1.1	Research Problem Statement.....	1
1.2	Research Objectives.....	2
1.3	Study Approach.....	3
1.4	Scope and Limitations	4
1.5	Organization of the Thesis	5
	REFERENCES	8
2	FLEXIBLE PAVEMENT STRUCTURAL EVALUATION	9
2.1	Introduction.....	9
2.2	Methods of Pavement Design	9
2.2.1	Design Types	9
2.2.2	Mechanistic-Empirical Design Procedures	11
2.2.3	Pavement Model	12
2.2.4	Design Parameters	14
2.3	Pavement Performance	15
2.3.1	Functional and Structural Evaluation	16
2.3.2	Bearing Capacity.....	18
2.3.3	Non Destructive Deflection Testing.....	19
	2.3.3.1 Types of NDT Deflection Devices	20
	2.3.3.2 Recent Trends and Development Pertaining to NDT Deflection Equipment	24
	2.3.3.3 Comparison of the Different NDT Deflection Methods	25
	2.3.3.4 Factors Influencing Deflection Measurement.....	26

	2.3.3.5 Interpretation of Deflection Data	27
2.4	Materials Characterization	28
	2.4.1 Resilient Modulus	29
	2.4.2 Fine-grained Subgrade Soils	32
	2.4.3 Granular Materials	36
	2.4.4 Asphalt Bound Materials	40
	2.4.5 In Situ Moduli Determination	45
	2.4.5.1 Surface Waves Propagation Procedures	46
	2.4.5.2 Penetration Bowl Method	50
2.5	Effects of Environmental Factors on Pavements	57
	2.5.1 Temperature Effects	57
	2.5.2 Moisture Variation Effects	59
	2.5.3 Quantifying Seasonal Variations	60
2.6	Summary	64
	REFERENCES	66

3	MEASUREMENT OF SOIL MATRIC SUCTION	87
3.1	Introduction	87
3.2	Role of Soil Suction in Affecting Unsaturated soil Behaviour	87
3.3	Historical Development of Basic Concepts of Unsaturated Soil Mechanics	90
3.4	Theory and Components of Soil Suction	93
3.5	Thermal Properties of Frozen and Unfrozen Ground	96
	3.5.1 Theory of Soil Freezing	97
	3.5.2 Thermal Properties Relevant to Soil Suction Measurement	102
3.6	Measurement of Soil Suction	107
	3.6.1 Measurement of Total Suction	108
	3.6.1.1 Direct Measurement of Total Suction	108
	3.6.1.2 Indirect Measurement of Total Suction	112

3.6.2	Measurement of Osmotic Suction.....	115
3.6.3	Measurement of Matric Suction	116
3.6.3.1	Direct Measurement of Matric Suction	117
3.6.3.2	Indirect Measurement of Matric Suction	122
3.7	Summary	125
	REFERENCES	127
4	INSTRUMENTED PAVEMENT SECTION	151
4.1	Introduction.....	151
4.2	Selection Criteria	151
4.3	Structure and Geometry of Test Site	152
4.4	Traffic	153
4.5	Environmental Conditions.....	153
4.6	Instrumentation	154
4.6.1	Calibration of The AGWA - II Sensors.....	155
4.6.1.1	Description of Apparatus and Calibration Procedure.....	155
4.6.1.2	Calibration Data	157
4.6.2	Installation	157
4.7	Temperature and Soil Suction Data Collection	160
4.8	Summary	162
	REFERENCES	164
5	LABORATORY CHARACTERIZATION OF FINE-GRAINED SUBGRADE SOILS	177
5.1	General.....	177
5.2	Resilient Modulus Test Equipment.....	177
5.3	Soil Sample Classification and Grouping.....	180
5.4	Resilient Modulus Testing.....	181
5.4.1	Preparation of Soil Samples.....	181

5.4.2	Test Protocol	182
5.4.3	Conducting The Resilient Modulus Test	185
5.5	Scope and Limitations of The Laboratory Testing Program.....	187
5.6	Summary	188
	REFERENCES	189

6	PRESENTATION AND DISCUSSION OF LABORATORY TEST RESULTS	196
6.1	Introduction.....	196
6.2	Planning the Laboratory Testing Program	197
6.3	Establishing the Relationship(s) between Soil Matric Suction and Soil Water Content	198
6.4	Resilient Modulus Test Results and Analysis Methodologies	199
6.4.1	Graphical Analysis Method.....	200
6.4.1.1	Test Results of Soil Group #1	200
6.4.1.2	Test Results of Soil Group #2.....	203
6.4.1.3	Test Results of Soil Group #3.....	207
6.4.1.4	Test Results of Soil Group #5.....	209
6.4.1.5	Test Results of Soil Group #6.....	210
6.4.1.6	General Remarks on the Graphical Analysis Procedure ..	213
6.4.2	Postulated Predictive Resilient Modulus Models.....	216
6.4.2.1	Soil Group 1	217
6.4.2.2	Soil Group 2.....	218
6.4.2.3	Soil Group 3.....	219
6.4.2.4	Soil Group 5.....	222
6.4.2.5	Soil Group 6.....	222
6.5	Summary and Conclusions	223
	REFERENCES	229

7	PRESENTATION AND DISCUSSION OF FIELD TESTING PROGRAM RESULTS	269
7.1	Introduction.....	269
7.2	Objectives of The Field Testing Program	269
7.3	Temperature and Matric Suction Data	270
7.4	Presentation and Discussion of Temperature and Soil Suction Results...	270
	7.4.1 Temperature Variations.....	271
	7.4.2 Soil Matric Suction Variations	273
7.5	FWD Deflection Testing.....	275
	7.5.1 Test Protocol and Planned FWD Tests.....	277
	7.5.2 Analysis of Deflection Data.....	279
	7.5.3 Presentation and Discussion of Deflection Results	281
	7.5.3.1 Deflection Interpretation Analysis.....	281
	7.5.3.2 Modulus Back-calculation Analysis.....	290
	7.5.3.3 Correlating Temperature and Suction with Back-Calculated Moduli	294
7.6	Summary and Conclusions	297
	REFERENCES	303
 8	 SUMMARY, CONCLUSIONS AND RECOMMENDATIONS	 337
8.1	General.....	337
8.2	Major Research Findings	338
8.3	Linking Laboratory and Field Results.....	343
8.4	Recommendations and Areas of Future Research	345
 APPENDIX A	 CALIBRATION CHARACTERISTICS OF “AGWA-II” THERMAL CONDUCTIVITY SENSORS.....	 347
A-1	Calibration Curves of Installed AGWA-II Sensors	348
A-2	Limits of Accuracy of Installed AGWA-II Sensors.....	354

APPENDIX B	WATER RETENTION CURVES FOR TESTED SUBGRADE SOIL GROUPS.....	355
APPENDIX C	TEMPERATURE AND SOIL MATRIC SUCTION DATA FROM THE INSTRUMENTED SITE (HIGHWAY CONTROL SECTION 16:12) .	361
C-1	Data Presentation	362
C-2	Individual Sensor Responses.....	362
C-3	Limits of Sensors' Calibration.....	372
APPENDIX D	FALLING WEIGHT DEFLECTOMETER DEFLECTION DATA AND ANALYSIS TOOLS.....	388
D-1	Examples of FWD Field Program Outputs	389
D-2	Listing of Computer Program BOWL	393
APPENDIX E	RESILIENT MODULUS TRIAXIAL TEST SYSTEM (RMTS).....	399
E-1	Introduction.....	400
E-2	Repeated Loading Triaxial Test Equipment.....	400
E-3	Automated Data Recording System	406
E-4	Data Processing and Handling.....	409
E-5	Listing of Computer Programs Used for Repeated Loading Tests	411

List of Tables

Table	Page
4.1 Traffic Volume History for Hwy 16 (1983-1991)	165
4.2 Traffic Volume Breakdown and ESAL Statistics for Hwy 16 (1983-1991)	165
5.1(a) Properties of Tested Subgrade Soils	190
5.1(b) Bulk Fraction X-Ray Diffraction Data	190
5.2 Load Sequence for Testing Soil Type 2	191
5.3 Recommended Load Cell and LVDT Ranges for Different Test Specimen Configurations	191
6.1 Results of Regression Analysis Performed on Various Soil Groups	231
7.1 Dates of FWD Deflection Tests Performed on Highway 16	306
A.1 Limits of Accuracy of Installed <i>AGWA-II</i> Sensors	354
E.1 Typical Resilient Modulus Raw Data File	429
E.2 Typical Output File Produced by Program PDEF-IC (File D1-11.dat)	439
E.3 Typical Output File Produced by Program PDEF-IC (File DDIF1-11.dat)	443
E.4 Typical Output File Produced by Program MCALC-IC (File MR1-11.dat)	451
E.5 Typical Computed Temperature output file (File G1-11.tp)	457
E.6 Typical Output File Produced by Program MRCOMPL2 (File G1-1.dat)	463
E.7 Typical Output File Produced by Program TEMPCOMP (File G1-1.tpc)	465

List of Figures

Figure	Page
2.1 Straining of a Soil Sample Under a Repeated Load Test	81
2.2 Simplification of Actual Load Pulse as Sinusoidal and Triangular Wave Pulses ...	81
2.3 Resilient Modulus-Deviator Stress Relationship for Fine-Grained Soils (Thompson and Elliot, 1985)	82
2.4 Mr-Deviator Stress Relationship for Fine-Grained Soils (Fredlund et al., 1977) ..	82
2.5 Mr-Confining Pressure Relationship for Fine-Grained Soils	82
2.6 Shear Wave Velocity Dispersion Curve	83
2.7 Stress Zone Within A Typical Pavement Structure and Shape of Deflection Basin.....	84
2.8 A Flow Chart of the Back-calculation Process	85
2.9 Sources of Errors in the Back-calculation Process	86
3.1 The Capillary Model and the Concept of Soil Suction.....	136
3.2 Compressive Forces on the Walls of a Capillary Tube.....	137
3.3 A Typical Relative Humidity-Total Suction Relationship	138
3.4 Water Phase Diagram.....	139
3.5 Heat Capacity-Temperature Relationship for a Partially Frozen Bentonite	140
3.6 Screen-caged Single-junction Peltier Thermocouple Psychrometer	141
3.7 Principle of Operation of the Peltier Thermocouple Psychrometer	142
3.8 Typical Psychrometer Calibration Curves at Different Temperatures.....	143
3.9 Filter Paper Methods for Measuring Total and Matric Suction.....	144
3.10 Typical Filter Paper Calibration Curve.....	145
3.11 Osmotic Suction-Electrical Resistivity Relationship for Pore-water Containing Mixures of Dissolved Salts	146
3.12 Principle of Operation of a High Air Entry Disc.....	147
3.13 A Typical Conventional Tensiometer	148
3.14 A Cross Section of the AGWA-II Thermal Conductivity Sensor	149

3.15	Soil-Water Characteristic Curve for the Soil Used in the Calibration of the <i>AGWA-II</i> Thermal Conductivity Sensors	150
4.1	A Schematic Sketch of Site Location.....	166
4.2	Selected Pavement Section Profile.....	166
4.3	Selected Pavement Cross-section	167
4.4	A Cross Section of the <i>AGWA-II</i> Thermal Conductivity Sensor	168
4.5	Calibration Apparatus.....	169
4.6	Calibration Apparatus - Detail A	169
4.7	Time Response Curves for Sensors 1, 2, 3.....	170
4.8	Calibration Curve for Sensor 1	170
4.9	Instrumentation Layout	171
4.10	Sensor Depth Locations	172
5.1	Typical Load Trace Produced by Resilient Modulus Testing Equipment	192
5.2	Example Worksheet for Recording Resilient Modulus Test Results	193
6.1	Moisture-Density Report for Soils Sampled from CS 16:12	232
6.2	Moisture-Density Relation for Soil Group # 1	233
6.3	Moisture-Density Relation for Soil Group # 2	234
6.4	Moisture-Density Relation for Soil Group # 3	235
6.5	Moisture-Density Relation for Soil Group # 5	236
6.6	Moisture-Density Relation for Soil Group # 6	237
6.7	Resilient Modulus <i>versus</i> Deviator Stress for Soil Group 1	238
6.8	Resilient Modulus <i>versus</i> Soil Matric Suction for Soil Group 1.....	239
6.9	Resilient Modulus <i>versus</i> Confining Pressure for Soil Group 1	240
6.10	Resilient Modulus <i>versus</i> Deviator Stress for Soil Group 2.....	242
6.11	Resilient Modulus <i>versus</i> Soil Matric Suction for Soil Group 2.....	243
6.12	Resilient Modulus <i>versus</i> Confining Pressure for Soil Group 2	244
6.13	Resilient Modulus <i>versus</i> Deviator Stress for Soil Group 3	246
6.14	Resilient Modulus <i>versus</i> Soil Matric Suction for Soil Group 3.....	247
6.15	Resilient Modulus <i>versus</i> Confining Pressure for Soil Group 3	248
6.16	Resilient Modulus <i>versus</i> Deviator Stress for Soil Group 5.....	250

6.17	Resilient Modulus <i>versus</i> Soil Matric Suction for Soil Group 5.....	251
6.18	Resilient Modulus <i>versus</i> Confining Pressure for Soil Group 5	252
6.19	Resilient Modulus <i>versus</i> Deviator Stress for Soil Group 6.....	254
6.20	Resilient Modulus <i>versus</i> Soil Matric Suction for Soil Group 6.....	255
6.21	Resilient Modulus <i>versus</i> Confining Pressure for Soil Group 6	256
6.22	Selected Resilient Moduli for Soil Group # 1	258
6.23	Selected Resilient Moduli for Soil Group # 2.....	259
6.24	Selected Resilient Moduli for Soil Group # 3.....	260
6.25	Selected Resilient Moduli for Soil Group # 5.....	261
6.26	Selected Resilient Moduli for Soil Group # 6.....	262
6.27	Variation of Resilient Modulus with σ_d and ψ for Soil Group 1	263
6.28	Variation of Resilient Modulus with σ_d and ψ for Soil Group 2	264
6.29	Variation of Resilient Modulus with σ_d and ψ for Soil Group 6	265
6.30	Variation of Resilient Modulus with σ_d and σ_3 for Soil Group 1.....	266
6.31	Variation of Resilient Modulus with σ_d and σ_3 for Soil Group 2.....	267
6.32	Variation of Resilient Modulus with σ_d and σ_3 for Soil Group 6.....	268
7.1	Seasonal Variations in Temperature and Soil Matric Suction for Sensors 1, 2, 3 (Shoulder Area)	307
7.2	Seasonal Variations in Temperature and Soil Matric Suction for Sensors 8, 9, 11 (OWP Area).....	308
7.3	Seasonal Variations in Temperature and Soil Matric Suction for Sensors 4, 6, 12 (IWP Area)	309
7.4	Seasonal Variations in Temperature and Soil Matric Suction for Sensors 1, 4, 8 (Depth Horizon 0.14 to 0.21m from top of Subgrade)	310
7.5	Seasonal Variations in Temperature and Soil Matric Suction for Sensors 3, 9, 12 (Depth Horizon 0.32 to 0.36m from top of Subgrade)	311
7.6	Seasonal Variations in Temperature and Soil Matric Suction for Sensors 5, 6 (Depth Horizon 1.00 to 1.14m from top of Subgrade)	312
7.7	Plan View of FWD Test Locations	313

7.8	Variation of Deflection Basin Area Ratio with Season for Both Cut and Fill Sections (under FWD load of 40 kN)	314
7.9	Variation of Deflection Basin Area Ratio with Season for Both Cut and Fill Sections (under FWD load of 53 kN)	315
7.10	Variation of Subgrade Stiffness Index, SSID4, with Season for Both Cut and Fill Sections (under FWD load of 40 kN)	316
7.11	Variation of Subgrade Stiffness Index, SSID7, with Season for Both Cut and Fill Sections (under FWD load of 40 kN)	317
7.12	Variation of Subgrade Stiffness Index, SSID4, with Season for Both Cut and Fill Sections (under FWD load of 53 kN)	318
7.13	Variation of Subgrade Stiffness Index, SSID7, with Season for Both Cut and Fill Sections (under FWD load of 53 kN)	319
7.14	Temperature Adjustment Factor Curves for Central Deflection.....	320
7.15	Variation of Actual Central Deflection with Season for Both Cut and Fill Sections (under FWD load of 40 kN)	321
7.16	Variation of Corrected Central Deflection with Season for Both Cut and Fill Sections (under FWD load of 40 kN)	322
7.17	Variation of Corrected Central Deflection Ratio with Season for Both Cut and Fill Sections (under FWD load of 40 kN)	323
7.18	Variation of Corrected Impulse Stiffness Modulus Ratio, ISMratio, with Season for Both Cut and Fill Sections (under FWD load of 40 kN)	324
7.19	Variation of ACP Back-calculated Modulus with Season for the Sections in OWP Area (FWD measurements performed @ 10:00 A.M.)	325
7.20	Variation of ACP Back-calculated Modulus with Season for the Sections in IC Area (FWD measurements performed @ 10:00 A.M.)	326
7.21	Variation of GB Back-calculated Modulus with Season for the Sections in OWP Area (FWD measurements performed @ 10:00 A.M.)	327
7.22	Variation of GB Back-calculated Modulus with Season for the Sections in IC Area (FWD measurements performed @ 10:00 A.M.)	328

7.23	Variation of SG Back-calculated Modulus with Season for the Sections in OWP Area (FWD measurements performed @ 10:00 A.M.)	329
7.24	Variation of SG Back-calculated Modulus with Season for the Sections in IC Area (FWD measurements performed @ 10:00 A.M.)	330
7.25	Variation of ACP Back-calculated Modulus with Season for the Sections in OWP Area (FWD measurements performed @ 12:00 P.M.).....	331
7.26	Variation of ACP Back-calculated Modulus with Season for the Sections in IC Area (FWD measurements performed @ 12:00 P.M.).....	332
7.27	Variation of GB Back-calculated Modulus with Season for the Sections in OWP Area (FWD measurements performed @ 12:00 P.M.).....	333
7.28	Variation of GB Back-calculated Modulus with Season for the Sections in IC Area (FWD measurements performed @ 12:00 P.M.).....	334
7.29	Variation of SG Back-calculated Modulus with Season for the Sections in OWP Area (FWD measurements performed @ 12:00 P.M.).....	335
7.30	Variation of SG Back-calculated Modulus with Season for the Sections in IC Area (FWD measurements performed @ 12:00 P.M.).....	336
A.1	Calibration Curve for Sensor 1	348
A.2	Calibration Curve for Sensor 2	348
A.3	Calibration Curve for Sensor 3	349
A.4	Calibration Curve for Sensor 4	349
A.5	Calibration Curve for Sensor 5	350
A.6	Calibration Curve for Sensor 6	350
A.7	Calibration Curve for Sensor 7	351
A.8	Calibration Curve for Sensor 8	351
A.9	Calibration Curve for Sensor 9	352
A.10	Calibration Curve for Sensor 10	352
A.11	Calibration Curve for Sensor 11	353
A.12	Calibration Curve for Sensor 12	353
B.1	Moisture Retention Curve for Soil Group 1	356
B.2	Moisture Retention Curve for Soil Group 2	357

B.3	Moisture Retention Curve for Soil Group 3	358
B.4	Moisture Retention Curve for Soil Group 5	359
B.5	Moisture Retention Curve for Soil Group 6	360
C.1	Seasonal Variation in Temperature for Sensor 1	373
C.2	Seasonal Variation in Soil Matric Suction for Sensor 4	374
C.3	Seasonal Variation in Temperature and Soil Matric Suction for Sensor 1 (@ depth of 0.21m)	375
C.4	Seasonal Variation in Temperature and Soil Matric Suction for Sensor 2 (@ depth of 0.59m)	376
C.5	Seasonal Variation in Temperature and Soil Matric Suction for Sensor 3 (@ depth of 0.32m)	377
C.6	Seasonal Variation in Temperature and Soil Matric Suction for Sensor 4 (@ depth of 0.14m)	378
C.7	Seasonal Variation in Temperature and Soil Matric Suction for Sensor 5 (@ depth of 1.14m)	379
C.8	Seasonal Variation in Temperature and Soil Matric Suction for Sensor 6 (@ depth of 1.00m)	380
C.9	Seasonal Variation in Temperature and Soil Matric Suction for Sensor 7 (@ depth of 0.59m)	381
C.10	Seasonal Variation in Temperature and Soil Matric Suction for Sensor 8 (@ depth of 0.16m)	382
C.11	Seasonal Variation in Temperature and Soil Matric Suction for Sensor 9 (@ depth of 0.32m)	383
C.12	Seasonal Variation in Temperature and Soil Matric Suction for Sensor 10 (@ depth of 1.01m)	384
C.13	Seasonal Variation in Temperature and Soil Matric Suction for Sensor 11 (@ depth of 0.84m)	385
C.14	Seasonal Variation in Temperature and Soil Matric Suction for Sensor 12 (@ depth of 0.35m)	386
C.15	Extended Calibration Curve for Sensor 1	387

D.1	Example Output of FWD Field Program - Edition 20	389
D.1	Example Output of FWD Field Program - Edition 25	391
E.1	Repeated Loading Triaxial Test System.....	466
E.2	Cross Sectional and Plan View of the Axial Load Cell Compression Transducer.....	467
E.3	Calibration Curve for Load Cell "B"	468
E.4(a)	Schematic Diagram of a Typical LVDT - Model DC-DC series 240	469
E.4(b)	Calibration Curve for LVDT # 2	470
E.5	Repeated Load Triaxial Chamber	471
E.6	Schematic Diagram of the Data Acquisition System.....	472

List of Plates

Plate	Page
4.1	Preparation of a Pilot Hole for Instrumentation 173
4.2	Obtaining an Undisturbed Shelby Sample 173
4.3	Preparation of a Punched Hole at the Bottom of the Shelby Cavity to Host the <i>AGWA-II</i> Sensor 174
4.4	Finished Pilot Hole..... 174
4.5	A Picture Showing the <i>AGWA-II</i> Sensor with the Special Rod Used to Situate the Sensor Inside the Prepared Hole 175
4.6	Preparation of Transverse and Longitudinal Trenches for Laying Sensors' Cables..... 175
4.7	A Picture Showing the Connection of the Sensors' Cables to the Data Acquisition Box 176
4.8	Finished Instrumented Site 176
E.1	Resilient Modulus Testing System (RMTS)..... 473
E.2	Loading Frame - Triaxial Chambers Assembly 473
E.3	Data Acquisition Arrangement Used for Operating the RMTS..... 474
E.4	Loading Panel Used for Setting Applied Deviator Stress and Confining Pressure 474

CHAPTER ONE

INTRODUCTION

1.1 Research Problem Statement

The impact of the environment on pavement response and performance has been an important issue of concern to many highway engineers and researchers. Among the many environmental factors, moisture and temperature conditions within and around pavement structures represent the most significant parameters that influence pavement response to traffic loads.

The effects of both temperature and moisture variations on pavements can be viewed through their influences on the properties of the constituent materials. Such seasonal variations tend to change the strength of the pavement materials so that their resistance to traffic induced stresses are altered.

It then follows that quantitative evaluation of the influences of both temperature and moisture variations on pavement response is essential to properly design and rehabilitate new and existing pavements. This necessitates establishing a procedure for measuring seasonal variations.

In the present research a methodology was developed for quantifying seasonal variations in subgrade strength as assessed by non-destructive and other appropriate laboratory test procedures.

1.2 Research Objectives

The main theme of the current research concentrates on developing suitable resilient modulus relationships for a typical subgrade soil material that is frequently encountered within the Province of Alberta. These models incorporate the effects of both temperature and moisture influences on pavement structures situated in cold regions.

The primary objective of the investigation was to establish seasonal variation-moduli relationships for the purpose of future implementation of mechanistic-empirical pavement design procedures.

Specific objectives of the study are to:

1. Establish temperature and soil matric suction distribution trends within a typical subgrade soil material in Alberta.
2. Assess the effects of seasonal variations in temperature and soil matric suction on flexible pavement structural capacity to withstand traffic loadings particularly during the thaw-weakening period in the spring time. This will be accomplished through the use of non-destructive deflection testing and modulus back-calculation techniques.
3. Describe currently available laboratory procedures for determining pavement layer moduli.
4. Develop an improved, relatively inexpensive laboratory resilient modulus testing system. This also includes establishing a procedure, or a set of procedures, for efficient analysis of obtained test results. The purpose behind the development of

such a system is to provide a means for future implementation of mechanistic-empirical pavement design procedures in the Province of Alberta.

5. Develop a testing protocol to be used for repeated load tests on cohesive subgrade soils.
6. Develop laboratory predictive resilient moduli models for typical Alberta subgrade soils in terms of pertinent soil properties and conditions. This will be achieved through the utilization of the developed dynamic repeated load testing system.
7. Correlate laboratory-determined resilient moduli relationships with field-obtained moduli.
8. Provide guidelines for future implementation of mechanistic-empirical pavement design methodologies.

1.3 Study Approach

To achieve the research objectives, a two-phase investigation was conceived. The first phase was a field testing program and the second phase was a laboratory testing program.

The proposed field testing program consisted of instrumenting a pavement section that is representative of the primary highway system within Alberta, with thermal conductivity suction sensors. Falling Weight Deflectometer (FWD) deflection tests (Bush, 1980; Hoffman and Thompson, 1982; Coetzee and Hicks, 1989; and AASHTO, 1993) were conducted at various locations within the instrumented section. This was done at different time intervals throughout the seasons with particular emphasis on the spring time. Output from these tests were used to back-calculate the resilient moduli of the various component layers of the pavement structure. The back-calculated moduli in conjunction

with temperature and soil suction measurements were linked together to describe the changes in subgrade resilient characteristics under varying environmental conditions.

Within the scope of the laboratory testing phase, extensive repeated load testing on remolded samples of the subgrade material taken from the instrumented site were conducted to obtain representative resilient moduli values under different loading, temperature and moisture conditions. Predictive moduli relationships linking the resilient modulus of the subgrade material to the stress state variables were postulated.

The final stage in the research plan linked in situ obtained moduli with laboratory determined moduli. This provides guidelines for implementing mechanistic-empirical methodologies for designing and rehabilitating flexible pavements in Alberta. Moreover, better understanding of thaw-weakening behaviour of subgrade soils within the Province is expected to provide more sound and rational design mechanisms to cater for the adverse effects of such phenomenon.

1.4 Scope and Limitations

The scope of this study is limited to conventional asphalt concrete pavements. Furthermore, only one type of subgrade soil has been investigated in this study. The soil chosen represents a typical subgrade material that is frequently encountered in Alberta. It is a medium to low plasticity silty clay material that classifies as a CL-CI type soil according to the Unified Soil Classification System. This soil also classifies as a soil Type 2 according to the AASHTO T 294-92 Resilient Modulus Test Procedure (AASHTO, 1992).

Inability to continuously monitor soil matric suction under repeated loading test conditions necessitated the estimation of this parameter from water content-matric suction relations known as moisture retention curves. Because of the anticipated significant effect of matric suction on the resilient modulus, great care was exercised in estimating this parameter from the moisture retention curves. Continuous measurement of the other parameters during the repeated loading test did not present any problem.

The results obtained from repeated load tests are accurate within the error range of the devices used. This includes loading cells, pressure transducer, LVDT's, and temperature-measuring thermocouples.

Back-calculation of layer moduli was performed using only the MODULUS computer program (Uzan et al., 1988 and MODULUS, 1990). This implies that the results and research findings obtained from this study are interpretable only within the limits of accuracy associated with this program.

1.5 Organization of the Thesis

This thesis is divided into eight chapters and five appendices. Chapter one contains the problem background, the research objectives, the study plan and the scope and limitations of the research work.

Chapter two is a state-of-the-art review of current techniques used in the structural evaluation of flexible pavements. This encompasses methods of pavement design, pavement performance criteria, non-destructive deflection testing, materials characterization and seasonal effects of environmental factors on pavements. Particular emphasis is placed on methods used in obtaining pavement materials' resilient moduli both

in situ and under controlled laboratory conditions. The phenomenon of seasonal variations in pavement strength pertaining to pavement structures that are situated in areas experiencing cyclic freezing and thawing was also discussed in detail.

Chapter three is an in-depth summary of methods and devices used for measuring soil suction. The theoretical concepts underlying the mechanical behaviour of frozen and non frozen unsaturated soils and their relation to soil suction are briefly reviewed. This is then followed by a description of the various devices used for measuring the different components of soil suction.

Chapter four describes the general outline of the field testing program. This involves the description of the pavement test site selected for instrumentation together with the selection criteria used. Instrumentation details and the procedure used for collecting and monitoring temperature and matric suction data are also included in this chapter.

Chapter five overviews the general framework of the laboratory testing phase of the research study. This chapter consists of three main sections. The first section is devoted to the description of the resilient modulus test system developed for the laboratory investigation. The second section deals with the identification, grouping and preparation of the soil samples tested. The third section documents the test protocol used and also the testing plan carried out.

Chapters six and seven present and discuss the research findings from the laboratory and the field testing phases, respectively.

Chapter eight contains a summary of the whole research study together with the final conclusions and recommendations for future research. Practical implications of the research findings are also included in this chapter.

Appendix A includes the calibration curves of the twelve AGWA-II thermal conductivity sensors used in this study together with a table displaying the limits of accuracy associated with these sensors.

Appendix B contains the water retention characteristic curves for the different soil groups tested.

Appendix C contains the collected temperature and soil matric suction data presented in a graphical form.

Appendix D contains typical printouts of FWD deflection data collected using two different versions of the Dynatest FWD Field Program. Listing of the BOWL computer program developed and used for the analysis of the deflection data is also included in this appendix.

Appendix E provides detailed information on the laboratory resilient modulus testing system that was developed and used in the current study.

References

1. AASHTO (1992), "*Resilient Modulus of Unbound Granular Base/Subbase Materials and Subgrade Soils - SHRP Protocol P46: AASHTO Standard Test Designation T-294-92*," American Association of State Highway and Transportation Officials.
2. AASHTO (1993), "*AASHTO Guide for Design of Pavement Structures 1993*," American Association of State Highway and Transportation Officials.
3. Bush A.J., III (1980a), "*Nondestructive Testing for Light Aircraft Pavements. Phase 1: Evaluation of Nondestructive Testing Devices*," USDOT, Federal Aviation Administration, Report No.FAA-RD-80-9, Washington D.C.
4. Coetzee N.F. and R.G. Hicks (1989), "*NDT in Cold Regions: A Review of the State-of-the-Art of Deflection Testing*," Proceedings, First Symposium on State-of-the-Art of Pavement Response Monitoring Systems for Roads and Airfields, West Lebanon, N.H., pp. 198-209.
5. Hoffman M.S. and M.R. Thompson (1982), "*Comparative Studies of Selected Nondestructive Testing Devices*," Transportation Research Board, TRR 852, Washington D.C.
6. MODULUS (1990): Preliminary User's Manual - Version 4, Texas Transportation Institute, Texas A&M University, College Station, TX.
7. Uzan J., R.L. Lytton and F.P. Germann (1988), "*General Procedure for Backcalculating Layer Moduli*," First International Symposium on Nondestructive Testing of Pavements and Backcalculation of Moduli, ASTM, Baltimore, MD.

CHAPTER TWO

FLEXIBLE PAVEMENT STRUCTURAL EVALUATION

2.1 Introduction

In this chapter, an extensive review of current knowledge of flexible pavement design is given, including flexible pavement design procedures, pavement performance and its linkage to pavement response, materials characterization and the phenomenon of seasonal variations in pavement strength. The emphasis in this chapter is on available techniques for the structural evaluation of flexible pavements.

2.2 Methods of Pavement Design

Although flexible pavements have been in use since the late 1800's, subjectivity still plays an important role within the pavement design process. Prior to the early 1920's, thickness design of pavements was based solely on experience. As experience was gained throughout the years, various methods were developed by various agencies and highway departments for determining the required pavement thickness. In the following sections, an overview of some of these methods will be presented.

2.2.1 Design Types

As it stands today, procedures for flexible pavement design can be categorized into five groups (Huang, 1993):

1. Empirical methods with or without a soil strength test: These methods were among the first to be developed for the purpose of determining the thicknesses of flexible pavements. An example is the Group Index method developed by the Highway Research Board (HRB, 1945). This procedure uses a modified version of the Public Roads Soil Classification System, developed by Hogentogler and Terzaghi in 1929, to estimate the

subbase and pavement thickness without a strength test. Another example of a method that uses a soil strength test is the CBR method developed, for airfield pavements, by the California Highway Department in 1929 (Porter, 1950) and modified by the Corps of Engineers to include flexible pavements (Middlebrooks and Bertram, 1950). This method received much attention and became very popular after the Second World War.

2. Limiting shear failure methods: The limiting shear failure methods utilize the shear strength parameters (cohesion and angle of internal friction) of pavement component materials to prevent shear failures (Barber, 1945 and McLeod, 1953). Such procedures were virtually discontinued because of the fact that pavements should be designed for riding comfort rather than for merely preventing shear failures.

3. Limiting deflection methods: The deflection method uses the principle of the vertical deflection at the top of the subgrade layer as a limiting criterion for thickness design. Pavement thicknesses are determined in such a way that the vertical deflection will not exceed a specified maximum value. Examples of these methods are the Kansas State Highway Commission procedure (1947) and the U.S. Navy procedure (1953).

4. Regression methods based on pavement performance or road tests: These methods link the performance of in-service pavements and/or full scale road tests with the factors that influence such performance. Examples are the two AASHTO (1972 and 1986) procedures that were based on results from the AASHO Road Test. Other examples that utilize in-service pavements rather than road tests are the Canadian studies in the late 1950's and early 1960's (CGRA, 1962), COPEs (Darter et al., 1985) and EXPEAR (Hall et al., 1989) procedures.

5. Mechanistic-Empirical methods: Since the emphasis in this thesis is on the utilization of mechanistic-empirical (M-E) methodologies for the purposes of pavement design and evaluation, the details pertaining to these procedures will be reviewed more thoroughly in the next section.

2.2.2 Mechanistic-Empirical Design Procedures

Pavement structures are considered extremely complicated physical systems that involve the interaction of a large number of complex and interrelated factors. As a result, a systematic and logical approach must be followed in developing rational and generally applicable method(s) for pavement thickness design.

Historically, many thickness design procedures have been developed by various highway departments and transportation research institutes. Unfortunately, most, if not all, lack the rationale for making them universal in terms of application. Realizing the problem, several researchers, during the past four decades, have put a great deal of effort into developing a mechanistic basis for designing and evaluating pavement structures. As a result, many theoretically-based design procedures evolved. However, all these procedures include an empirical element as well, and are therefore usually referred to as mechanistic-empirical or analytical-empirical procedures (AASHTO, 1993 and Ullidtz, 1987).

A mechanistic-empirical (M-E) method is a design approach whereby the performance of a pavement system is postulated to be closely related to the mechanistic responses of stress, strain and displacement induced in the pavement under traffic loading and/or environmental influences. Within this context, the thickness design process involves selecting a pavement structure in which an appropriate combination of materials and layer thicknesses is chosen to counter the adverse effects of the various forms of distress induced in the pavement from traffic and environmentally-related factors. Thus, several

design inputs are needed for mechanistic design. These include traffic, materials and environmental factors.

Examples of M-E design methods are the Asphalt Institute (AI, 1982) and the Shell (Shell, 1978) procedures. In both methodologies, the horizontal tensile strain at the bottom of asphalt bound layer(s) and the vertical compressive strain at the top of the subgrade constitute the design parameters used to control both fatigue cracking and permanent deformation within these layers, respectively. These failure criteria were first suggested by Saal and Pell (1960) and Kerkhoven and Dormon (1953).

The merits of adopting a mechanistic-empirical design approach over other procedures described in section 2.2.1 can be viewed as follows:

- (I) An M-E procedure permits the effective and expeditious use of existing materials and the incorporation of new materials into the design process (this is in contrast to the purely empirical and regression methods in which embedded empiricism prevents such versatility in application).
- (II) Relating pavement prime responses under load to the distress design criteria in a rational and applicable manner improves the reliability of the overall pavement design process.
- (III) M-E methods provide for the ability to extrapolate the design equations for other sets of loading and/or environmental conditions.

2.2.3 Pavement Model

Utilizing the M-E design concepts, pavement systems have been modeled as multi-layered systems that can be analyzed using the principles of continuum mechanics. During the forties and fifties, Burmister (1943 and 1958) developed and verified a multi-layered elastic theory for a two-layer pavement system. Other researchers followed (Warren and

Dieckmann, 1963; De Jong et al., 1973; Hwang and Witczak, 1979; and Kopperman et al., 1986) and extended Burmister's solution to more generalized pavement conditions in terms of the number of layers within the pavement structure, axle load configurations and conditions of friction at pavement layer interface surfaces.

A major disadvantage of the elastic layered-theory seems to be the incorrect assumption that each layer within the pavement is considered homogeneous with the elastic properties being the same throughout the layer. This assumption ignores the fact that most pavement materials, especially granular bases and fine-grained subgrades, have nonlinear load-deformation characteristics. This in turn necessitates complete mapping of the stress-strain characteristics within each pavement layer for proper assignment of an elastic modulus that will be representative of the whole layer. Taking this into account, some investigators have employed finite element techniques to the solution of layered systems (Duncan et al., 1968; Raad and Figueroa, 1980; and Harichandran et al., 1989).

Due to the temperature-dependency of asphalt-stabilized materials, some researchers have used the viscoelastic analysis approach to model the behaviour of these materials (Monismith and Secor, 1962 and Barksdale and Leonards, 1967).

As a result of the aforementioned studies, several multi-layered elastic solutions for modeling flexible pavement structures are available today in the form of either graphical solutions or computer programs, including the well known CHEV program developed by Chevron Research Company (Warren and Dieckmann, 1963), the DAMA program of the Asphalt Institute (Hwang and Witczak, 1979), the BISAR program of Shell International Inc. (De Jong et al., 1973) and the ELSYM5 program developed at the University of California (Kopperman et al., 1986). Other programs that are based on linear viscoelastic theory are also available. Examples of these are the ILLI-PAVE program (Raad and

Figueras, 1980), the MICH-PAVE (Harichandran et al., 1989) and the Federal Highway Administration VESYS-II program (FHWA, 1978).

The selection of a specific mathematical model to represent the pavement structure should depend on whether there are any benefits gained in using a more sophisticated approach. Over the years, however, the elastic layered approach has proven to have worked adequately, from a practical stand point, in estimating actual pavement response to load and in predicting field performance.

2.2.4 Design Parameters

The pertinent design variables that are needed as inputs in an M-E design procedure can be listed under four categories: traffic, environment, materials characterization and failure criteria.

Traffic and environmental factors are those that impose a load on the pavement structure, whereas materials variables are those that characterize pavement response to load. On the other hand, failure criteria constitute the design equations that govern the relationship between pavement response and pavement performance. Another important concept is that of variability. All aspects of pavement design involve inherent variations that can not be measured adequately or predicted in the deterministic sense. Therefore, neither the exact determination of traffic to be carried by the pavement structure at any point in time during its service life nor the precise prediction of the prevailing environmental conditions at any particular site are possible. As a result, any pavement design procedure must have a reliability component that includes such variations in the design inputs and the model or model coefficients selected for the design purposes.

Traffic variables include all those related to the vehicle loads applied to the pavement. Such variables include total vehicle load, wheel load, tire pressure, axle load configuration, lateral distribution of wheel loads, number of wheel load applications, lane and directional wheel load distribution, sequence of load application of various types and variability of traffic. Historically, two trends have been followed in estimating traffic loading for pavement design purposes:

- (I) The direct analysis of the actual mixed traffic loads encountered.
- (II) The introduction of the equivalent single axle load concept (ESAL), which involves converting all mixed traffic into equivalent load applications of a standard single axle load (usually taken as 80 kN single axle load).

An extensive review of the merits and drawbacks of both techniques can be found elsewhere (Monismith et al., 1986 and Khogali, 1988).

The details pertaining to the other variables including materials and environmental influences will be presented in sections 2.4 and 2.5 of this chapter.

2.3 Pavement Performance

The condition of a highway network is of extreme importance to the economy of any country. In connection with the recent Strategic Highway Research Program (SHRP) in the U.S, it has been estimated that replacing and rehabilitating existing pavements will cost about 400 billion dollars over the next 15 years (Ullidtz, 1987). This example and many others serve to illustrate the point that highway authorities and other decision makers must carefully evaluate the best and most cost effective ways of maintaining such facilities. The importance of such planning has been made evident, in recent years, by many research initiatives within the field. The largest of these is the aforementioned Strategic Highway Research Program. A major portion of this program, named the Long

Term Pavement Performance (LTPP) study (SHRP, 1986; Hudson and Elkins, 1989; and Teng, 1993), is aimed at developing better models for predicting pavement performance.

In countries such as France, Australia, Switzerland, the United Kingdom and South Africa, efforts have taken the form of building full-scale testing facilities and initiating accelerated pavement test research.

The two above-mentioned types of research efforts will serve to complement each other and provide for a better understanding of pavement behaviour in the future.

2.3.1 Functional and Structural Evaluation

The importance of evaluating pavement performance stems from the fact that pavements must withstand structural failure due to traffic loading, and the design process should include a means of measuring pavement condition deterioration over time. This is because pavements, unlike other structures, tend to deteriorate gradually with time as a result of material quality, traffic loading and environmental conditions. Also, observed pavement performance under actual field conditions is the final criterion to judge the adequacy of any design procedure. Thus, measuring performance and relating this to pavement response serve to validate the design approach.

During the process of pavement evaluation, one should be able to distinguish between pavement response and pavement performance. Pavement response refers to the mechanistic responses of stress, strain and deflection induced in the pavement structure by traffic loading and/or climatic factors. On the other hand, performance is the term used to describe the condition of the pavement structure at any time as measured or observed through manifested pavement distress such as surface cracking and/or permanent deformation.

Current concepts of pavement performance should include functional, structural and safety evaluations (AASHTO, 1986 and 1993). For the purposes of this research study, only functional and structural evaluations will be reviewed with specific attention being given to the latter. Details on safety considerations can be found elsewhere (Yoder and Witczak, 1975; Leu and Henry, 1978; FHWA, 1980; and Huang, 1993).

Functional performance relates to how well a pavement serves the user. In this context, riding comfort, or ride quality, constitutes the major parameter of interest. To quantify this factor, various highway departments have adopted two approaches. Both approaches use the "serviceability-performance" concept developed by the AASHO Road Test staff in 1957. In the first approach, serviceability is measured in terms of the Present Serviceability Index (PSI). This index is expressed in terms of pavement roughness and distress conditions such as rutting, cracking and patching. In the second approach, the serviceability is measured in terms of the International Roughness Index (IRI), which is based on roughness only (Sayers et al., 1986a and 1986b).

Structural performance deals with the pavements' physical conditions, i.e. occurrence of cracking, raveling and other conditions that adversely affect the road-carrying capability of the pavement structure. Such ability is usually referred to as the "bearing capacity" of the pavement structure. Bearing capacity is the main issue of concern in the current research investigation, and, therefore, the remaining parts of this chapter will be devoted solely to the discussion of all the aspects pertaining to this parameter.

One further point of concern is that functional and structural performance should not be combined into one index since these are two incommensurable quantities. Rather,

each evaluation should be conducted independently, and the adequacy of the pavement design procedure should then be checked against each of these evaluations separately.

2.3.2 Bearing Capacity

The evaluation of the pavement bearing capacity has long been the focus of attention of many highway engineers and researchers. Plate-bearing tests and CBR tests were among the first to be used for determining the in situ structural strength of individual component layers of pavements. Traditionally, the plate-bearing test was used to obtain the supporting capacity of subgrades, bases, and in some cases, completed pavements by utilizing relatively large diameter plates. The evaluation took the form of obtaining a modulus of elasticity in the case of flexible pavements and a modulus of subgrade reaction in the case of rigid pavements. On the other hand, the CBR test has also been in use for determining the subgrade CBR value both in the laboratory and in situ. A major disadvantage of the plate-bearing and the CBR tests is that both are destructive tests which involve both expensive and time consuming efforts.

The development of the Benkelman Beam device in the early 1950's marked the first use of nondestructive evaluations of in service pavements. This device, developed by A.C. Benkelman, was used during the WASHO Road Test (1955) to measure pavement surface deflection and relate that to the pavement load-carrying capacity. The device proved to be adequate and had great potential for such purposes.

Extensive use of the Benkelman Beam for assessing the structural strength of pavement was also conducted by the Canadian Good Road Association in the late 1950's and early 1960's (CGRA, 1962). In these studies, the CGRA revised and standardized the WASHO test procedure to achieve more reproducible results. The modified test

procedure, known as the CGRA Rebound Method, is described in detail elsewhere (CGRA, 1959).

During the 1950's and 1960's a number of other non-destructive methods were developed to determine the geometric and elastic parameters of pavement structures. These methods were based on the theory of surface wave propagation in an elastic medium. Details on these procedures will be given in section 2.4.5.1.

In addition to in situ evaluation of pavement bearing capacity, various laboratory tests of different kinds have also been in use. Some of these involve determining basic material properties such as the gradation of base courses, moisture-density relationships for subgrade soils and mix characteristics of asphalt concrete materials. Other tests are of special types in which one or more of the fundamental elastic properties of pavement materials are determined. Examples include the indirect tensile test for asphalt-stabilized materials and the triaxial resilient modulus test for granular base courses and subgrade soils.

2.3.3 Non Destructive Deflection Testing

The use of non destructive (NDT) deflection testing has been an integral part of pavement structural evaluation for many decades. Since its inception in the early 1950's (WASHO, 1955), it has become apparent that surface deflection constitutes an excellent tool for determining pavement load-carrying capacity for the purposes of checking pavement structural integrity and providing remedial measures where needed. Several agencies started developing failure criteria based on maximum deflection as represented by the number of allowable load repetitions. As experience grew with the Benkelman Beam testing procedure, only the "rebound", "recoverable", or "elastic" portion of the deflection was used as an indicator of pavement strength. The CGRA rebound procedure (CGRA,

1965) and the Asphalt Institute overlay design method (AI, 1969) are two examples of procedures that utilized this parameter.

Recent technical advances indicate that the use of the deflection rebound value as a sole indicator of strength is inadequate and needs to be supplemented by other strength measures. This fact, as has been referred to in the 1986 AASHTO Guide, stems from two fundamental principles of deflection testing:

- (1) multiple structural distress types (such as deformation and fracture) must be separately accounted for in the interpretation of deflection test results; and
- (2) pavement material type and layer thickness are also important factors to be considered in the structural evaluation of pavements.

As a result, many transportation agencies have refined their deflection design criteria to include a measure of pavement flexural strength. An example is the design procedure developed at the Laboratoire Central des Ponts et Chaussees (LCPC) (Guillemin and Gramsamer, 1971). The LCPC method makes extensive use of empirical relations based on the product of deflection and pavement radius of curvature to evaluate structural conditions of in-service roads.

In summary, accurate assessment of pavement structural performance cannot be achieved through the use of maximum rebound deflection alone; an indicator of the pavement radius of curvature under load must also be included in the design criteria. Implementation of these concepts in the design and rehabilitation of flexible pavements will be further elaborated on in the following sections.

2.3.3.1 Types of NDT Deflection Devices

Many devices for performing NDT testing on pavements are available today. The most widely used ones are those that measure pavement surface deflection (Bush, 1980; Smith and Lytton, 1984; Epps and Monismith, 1986; Hudson et al., 1987; and Coetzee

and Hicks, 1989). Other NDT approaches include spectral analysis of surface waves (SASW) (Heisey et al., 1982 and Nazarian and Stokoe, 1983) and laser and/or ground-penetrating radar measurement of deflection under moving loads (Elton and Harr, 1988 and Briggs et al., 1992). These latter devices are still in the developmental stage and need further study before they can be used on a routine basis for pavement evaluation.

The currently used NDT deflection measuring equipment can be classified into three groups according to the type of load application to the pavement surface (Coetzee and Hicks, 1989):

- (1) Static or slowly moving load systems
- (2) Steady-state vibratory load systems
- (3) Transient dynamic impulse load systems

Following is a brief description of these NDT devices.

(1) Static or slowly moving load systems: Equipment in this category includes the static plate-loading test, the Benkelman Beam, automated deflection beams such as the California Traveling Deflectometer, the La Croix Deflectograph, the Transport and Road Research laboratory Pavement Deflection Data Logging (PDDL) machine and the CEBTP Curviameter. Specific details on these devices can be found elsewhere (Bush, 1980; Smith and Lytton, 1984; Epps and Monismith, 1986; and Hudson et al., 1987). Use of this type of equipment requires an application of a realistic load magnitude, usually an 80 kN single axle load at the pavement surface. Deflections are then measured by means of a long beam placed between the dual wheels of the truck applying the load. This procedure can be performed manually or can be automated as in the case of the California Traveling Deflectometer measuring system (California Division of Highways, 1972). Major disadvantages associated with static or slowly moving load deflection testing are the following:

- (i) Load duration is typically not representative of actual traffic load duration. This in turn produces unrealistic deflection measurements as compared to those expected under dynamic traffic loads because most flexible pavement materials tend to exhibit nonlinear load-deformation behaviour.
- (ii) A fixed reference point is needed for this type of measurement. This is usually provided by the beam supports. Erroneous measurements result if the support points fall within the deflection basin created by the wheel load (CGRA, 1962; Epps and Monismith, 1986; and Hudson et al., 1987).
- (iii) Measurements of a deflection basin rather than a single central deflection are difficult and time consuming.

(2) Steady-state vibratory load systems: Equipment falling under this category includes the commercially produced Dynaflect and Road Rater, the custom built Waterways Experiment Station (WES) 16 kip Heavy Vibrator and the FHWA Cox Vibrator. These devices impose a sinusoidal steady-state vibration on the pavement surface. This sinusoidal force is superimposed on a static preload placed on the pavement surface (Coetzee and Hicks, 1989). The peak to peak dynamic force must be less than twice the static force magnitude in order to prevent the loading plate from lifting off the pavement surface during the loading period. The equipment available has variable frequencies and dynamic force ranges. Typical values are 40 kN maximum force and a frequency range of 5 to 80 Hertz (Hudson et al., 1987). Advantages of this type of equipment (Coetzee and Hicks, 1989) are that:

- (i) Deflection basins can be measured.
- (ii) No fixed reference is needed since velocity transducers are used.
- (iii) Data collection is relatively quick.
- (iv) The units are relatively inexpensive.

On the other hand, disadvantages include the following:

- (i) Load characteristics are unrealistic compared to those induced by actual traffic. A moving vehicle typically applies discrete dynamic load pulses separated by rest periods. This is different from vibratory steady-state loading. Consequently, deflections measured under the latter mode of loading are not representative of actual deflections under traffic.
- (ii) The static preload is of a similar order of magnitude as the dynamic sinusoidal force. This fact will have a significant effect on the stress state induced within the pavement structure, which will in turn produce erroneous estimates of elastic properties of pavement materials.

(3) Transient impulse load systems: Measuring systems in this category include the well-known Falling Weight Deflectometers (FWD's). The principle of operation of the FWD equipment consists of applying a dynamic impulse force to the pavement surface and measuring the resulting deflections at various radial distances from the centre of the load application. The provision of the transient impulse load is achieved by dropping a mass of known magnitude from some specified height onto the pavement, with the load being transferred through a buffer system to the loading plate. The output is a haversine load pulse. The width of the loading pulse is controlled by the buffer characteristics to simulate actual moving wheel loads. Typically these loads are in the order of 25 to 35 milliseconds. Variable load intensities can be obtained by varying both the weight of the masses being used and the dropping distances. Four commercial types of FWD's are available on the market today: the Dynatest, KUAB, Phoenix and the JILS systems.

A major advantage of the FWD testing device is that all data collection and equipment functions are automated through the use of microcomputers. Other advantages include:

- (i) Deflection basins can be measured using up to 9 sensors.

- (ii) No fixed reference is necessary since typically velocity transducers are used.
- (iii) Excellent simulations of traffic loads are possible in terms of magnitude, duration and repetition.
- (iv) No preload is required (as with steady-state vibratory devices).
- (v) A wide range of loading is available.

The disadvantages in the use of FWD systems are as follows:

- (i) Measuring systems have high initial cost.
- (ii) Measuring systems are complex systems that involve significant maintenance and operational costs.
- (iii) Needs rigorous calibration to validate manufacturers' measurement accuracy criteria (procedures to accomplish this have recently been developed by SHRP and are currently available).

2.3.3.2 Recent Trends and Development Pertaining to NDT Deflection Equipment

The major trend in deflection measurement in recent years appears to be the increasing use of the FWD equipment. In the United States, for example, as of 1989, there were about 25 states and one territory using the machine (Coetzee and Hicks, 1989). Also, within the framework of the LTPP study of the Strategic Highway Research Program, FWD's represent the equipment of choice for collecting surface deflection of in service pavements.

The increased popularity of the FWD equipment is also noticeable in Canada and in other countries worldwide. In Alberta, for instance, Alberta Transportation and Utilities (a department of highways) purchased one Dynatest 8000 FWD machine in 1989 to replace the Benkelman Beam testing device. In 1992 the number of operational FWD's increased to four. The reasons behind this trend seem to be related to the productivity of the equipment and its ability to measure deflection basins comparable to those produced

by actual traffic loads. These features are important considerations in terms of applying mechanistic-empirical design principles for pavement analysis and rehabilitation.

Despite the aforementioned trend, there are some concerns regarding the use of FWD systems for routine deflection measurement. Most important among these are the accuracy of the deflection measurements and the repeatability of test results. To some extent, however, these issues have recently been addressed by the independent calibration verification techniques developed by SHRP (SHRP Product Designations 5003-5008, 1992 and Irwin, 1994).

2.3.3.3 Comparison of the Different NDT Deflection Methods

Although versatility and efficiency of any NDT device for obtaining deflection basin measurements are important considerations, conformity of such measurements with pavement response under realistic traffic loads is the final criterion to judge the selection of the equipment to be used. With due regard to this issue, various studies using different approaches and criteria (Bush, 1980; Heisey et al., 1982; Nazarian and Stokoe, 1983; Smith and Lytton, 1984; and Hudson et al., 1987) were conducted to evaluate and compare the various types of the currently available NDT deflection devices. Hoffman and Thompson (1982) compared results obtained from the Benkelman Beam, Road Rater, and Dynatest FWD and actual deflections under a moving wheel load and concluded that the FWD is the best NDT device to simulate pavement response under moving loads. This conclusion was further supported by findings from other investigations (Bush, 1980; Smith and Lytton, 1984; Hudson et al., 1987; and Ullidtz, 1987). Smith and Lytton (1984) and Hudson et al. (1987) also reported that extrapolated deflections from measurements by a light load vibratory device were very different from the actual deflections measured at higher load levels by the FWD. These observations, coupled with the fact that the FWD load pulse is the one that most closely simulates actual load pulses under moving traffic

load, tend to support the argument that impulse dynamic loading devices are the ones that are best suited for use in pavement structural evaluation.

2.3.3.4 Factors Influencing Deflection Measurement

The amount a pavement will deflect under load is dependent upon many factors, including loading, environment and pavement conditions. For deflection measurements to be adequately interpreted in the context of pavement performance, the effects of these factors must be properly quantified. This usually involves test standardization and deflection measurement adjustment to reference conditions.

Loading factors are concerned with magnitude, duration and frequency of load application. An NDT device that is capable of applying a load to the pavement similar to actual traffic load should be used (AASHTO, 1986) because most pavement materials either have a time-dependent deformation component or exhibit stress-sensitive (or nonlinear) elastic behaviour. Furthermore, an NDT device that is capable of measuring deflection basins rather than single maximum deflection at one point should be used to provide for the direct utilization of measured deflections in mechanistic-empirical design procedures. As has been alluded to in previous sections, the FWD machine is the equipment of choice to achieve the above-mentioned objectives.

Temperature and moisture distributions within and around pavement structures represent the two most influential climatic factors that affect pavement deflections. Since the emphasis in the current research study is on evaluating the adverse effects of these factors on pavement load-carrying capacity, a thorough discussion of these factors will be given later in this chapter in the section dealing with the phenomenon of seasonal variations.

Pavement condition is the third factor that significantly affects measured deflections. Deflections obtained in areas with cracking and rutting are normally higher than those taken in areas free of distress. Also, deflections taken over or near a culvert may be high, and pavements in cut or fill sections may show significantly different deflection measurements. As a result, proper selection of sections for deflection testing is extremely important to provide a representative picture of the structural capacity of the roadway under consideration.

2.3.3.5 Interpretation of Deflection Data

Sound interpretation of deflection is directly dependent on the accuracy of the deflection measurements obtained, the test procedure used and the representation of the roadway section under consideration. As has been discussed before, this interpretation usually takes the form of measuring deflection basins under different levels of load application. The resulting data from these measurements are then analyzed using one of the following two approaches (AASHTO, 1986):

- (i) Direct deflection analysis
- (ii) Back calculation of layer moduli

The first approach was criticized by many researchers based on justified scientific evidence. Ullidtz, for example, discusses the problem of the incompatibility of the deflection criterion as compared to the strain criterion to be used as a basis for pavement structural evaluation (Ullidtz, 1987). He also points out that it is the critical stresses and strains, and not the deflections, that are of prime concern in any analytically-based design procedure. Deflection measurements cannot be applied directly as input in any of the currently available mechanistic-empirical design methods. These and other similar observations made by many pavement engineers lead to the conclusion that the second approach, i.e. back-calculation of layer moduli, is more appropriate for use in pavement structural evaluation.

In addition to accurate deflection measurements, proper planning, organization and implementation of NDT deflection testing programs constitute other essential considerations toward proper interpretation and utilization of deflection test results. These issues have been discussed in detail by Pumphrey et al. (1989). The Pumphrey et al. study involved developing an overlay thickness design procedure for the Indiana Department of Highways (IDOH) that is based on NDT deflection tests. Many of the basic concepts pertaining to the planning and conducting of such tests were investigated and reported.

Adjustment of deflection data to reflect the influence of loading, environmental and roadway condition variables is also of paramount importance for adequate interpretation of this data.

It is important to mention that although NDT deflection basin methodologies represent the current state-of-the-art of pavement structural analysis and rehabilitation, these methods may be modified as technology and use advances. This is very important since, apart from NDT equipment limitations, available analytical techniques in use today also have their own limitations and drawbacks. This point will be discussed further in the section dealing with back-calculation of pavement materials moduli.

2.4 Materials Characterization

An important element of the development of a mechanistic-empirical design procedure for flexible pavements is the adequate characterization of the constituent materials in the context of the part they play in the pavement structure. This fact and its consequences have been emphasized in both the 1986 and the 1993 versions of the AASHTO Guide for the Design of Pavement Structures and also in the recent SHRP Long-Term Pavement Performance study (SHRP, 1991).

Even though a great deal of research effort has gone into describing the response of pavement materials to load, there are still many difficulties associated with such characterizations. These difficulties stem from the variety of materials involved, the types of pavement structures, the influence of environmental conditions and the modeling of the material behaviour under load. A list of pertinent variables affecting material response to load is given by Deacon (1971).

Many tests and types of test equipment have been devised for measuring the characteristics of pavement materials. They can be divided into three groups (Deacon, 1971 and Yoder and Witczak, 1975):

- (i) conventional or routine tests
- (ii) specialized tests for characterizing the deformability of materials
- (iii) test procedures used to determine fundamental material distress conditions (such as fatigue cracking of asphalt-stabilized materials and permanent deformation).

In the context of dynamic behaviour, materials characterization usually takes the form of determining the resilient (or stiffness) modulus of the various layers comprising the pavement system. The acceptability of these mechanical responses may then be assessed in terms of the anticipated life of the pavement structure as controlled by the various failure criteria such as fatigue and/or permanent deformation.

2.4.1 Resilient Modulus

The resilient modulus, M_r , is a measure of the elastic property of soil, recognizing certain nonlinear characteristics. In repeated triaxial load tests, M_r is defined as the ratio of the peak repetitive deviator stress to the recoverable measured axial strain i.e.:

$$M_r = \frac{\sigma_d}{\epsilon_r} \quad (2.1)$$

Figure 2.1 shows the straining of a soil specimen under repeated load test.

Due to the nonlinear behaviour of pavement materials, the type and duration of loading used in the repeated load test must simulate that occurring in the field. When a wheel load is at a large distance from a given point in the pavement, the stress at that point is zero. As the wheel load starts moving toward the point, the stress starts increasing until it reaches a maximum when the load is exactly above the point. Such loading had traditionally being simulated in the laboratory by either a haversine or triangular load pulse as shown in Figure 2.2.

Barksdale (1971), Brown (1973) and Mclean (1974) investigated the vertical stress pulse for sinusoidal, triangular and square wave forms and derived the loading times for a bituminous layer as a function of vehicle speed and layer thickness. Based on these and other studies (AI, 1973; AASHTO, 1982; and SHRP, 1989), researchers recommended using a haversine load pulse with a duration of 0.1 second and a rest period of 0.9 second in repetitive triaxial load testing for determining the resilient characteristics of unbound soil materials (both granular and fine-grained soils). Although repeated triaxial load tests can also be used for other pavement materials, it is the indirect tensile test that is recommended for use with asphalt-stabilized materials.

Advantages of using the resilient modulus as a key parameter for pavement materials characterization as stated in the 1986 AASHTO Guide are:

- (1) M_r is a basic material property that can be used directly in mechanistic-empirical pavement design procedures.
- (2) Methods for obtaining M_r are well established and standardized.

- (3) M_r is recognized internationally as a method for pavement materials characterization.
- (4) Techniques for estimating M_r from nondestructive testing are also available.

Currently, there are three approaches available for obtaining representative moduli values for the different materials within the pavement system:

1. Laboratory Testing: As has been mentioned before, laboratory testing is usually done through some type of a dynamic testing procedure. The most widely accepted testing procedure for granular and fine-grained soils is the repeated load triaxial test (AASHTO, 1982; Cole et al., 1986; SHRP, 1989; Claros et al., 1990; and AASHTO, 1992). Tests are usually performed either on samples of the representative material prepared in the laboratory under controlled conditions or on undisturbed samples that are obtained from the field.

2. In-Situ Modulus Determination: This is normally accomplished by using any NDT deflection procedure and a suitable mathematical model for the pavement structure to back-calculate the resilient moduli of the constituent materials from surface deflection measurements. Short wave propagation techniques and Falling Weight Deflectometers (FWD) are among the most widely used methodologies for obtaining such moduli. More details on these methods are provided in section 2.4.5.

3. Empirical Correlations: Certain empirical correlations have been developed that relate the resilient modulus of untreated granular and cohesive materials to more easily measured parameters like the CBR and the R-value of such materials (AI, 1982). Although these correlations provide for preliminary estimate of the modulus value, caution should be exercised when using such relationships in actual design or rehabilitation analysis of

flexible pavements due to the fact that large scatter in the original data used to derive such relations does exist.

2.4.2 Fine-grained Subgrade Soils

Since the Seed and McNeill (1957) study of the resilient characteristics of unbound materials in the late 1950's, very many experiments and studies have been conducted by other investigators on the subject. Dehlen and Monismith (1970) studied the behaviour of clay under load and stated that:

" a clay subjected to stress shows immediate and time-dependent recoverable and permanent strains, the immediate strain being predominant under short-duration loads, and the permanent strain per cycle decreasing to an insignificant amount after many cycles of stress. Stress history may have a significant effect on the response. The response is markedly nonlinear."

Other studies (Seed et al., 1962 and 1967; and McLeod, 1971) also confirmed the following observations:

1. Resilient modulus determined under relatively small number of stress applications seem to give a misleading picture of actual resilience characteristics of cohesive soils due to the stress conditioning effect. This effect can be eliminated by obtaining moduli values after a large number of load applications.
2. Changing the stress level was found to significantly affect the modulus value. This is a further indication that fine-grained soil materials are highly nonlinear.
3. Compaction methods that produce dispersed soil structures tend to produce lower moduli values.
4. Changes in water content and density after compaction tend to alter significantly the moduli values obtained. Increased water content produces adverse effects on

the modulus whereas increased density tend to produce beneficial influences on the other hand.

5. Cohesive soils possess cross isotropic properties with the horizontal moduli exceeding the vertical moduli.
6. Poisson's ratio for cohesive materials remain more or less constant during repeated load tests. Typical values are in the range 0.35 to 0.50.

Different constitutive relations have been developed to describe the resilient modulus of cohesive materials. The most famous is the resilient modulus-deviator stress equation defined as follows:

$$M_r = A[\sigma_d]^B \quad (2.2)$$

where,

M_r = resilient modulus of cohesive soil,

σ_d = deviator stress ($= \sigma_1 - \sigma_3$ in the case of the triaxial test),

A & B = experimentally determined constants.

Seed et al. (1967) showed that the magnitude of the deviator stress has a significant effect on the resilient modulus for plastic soils. They suggested a bilinear relation such as the one shown in Figure 2.3 in which:

$$M_r = K_1 + K_3 (K_2 - \sigma_d) \quad \text{when } \sigma_d < K_1 \quad (2.3a)$$

$$\& \quad M_r = K_1 - K_4 (\sigma_d - K_2) \quad \text{when } \sigma_d > K_1 \quad (2.3b)$$

where K_1 , K_2 , K_3 and K_4 are material constants.

Thompson and Elliot (1985) indicated that the value of M_r at the breakpoint in the bilinear curve, as indicated by K1 in Figure 2.3, is a good indication of resilient behaviour, while other constants K2, K3 and K4 display less variability and affect the modulus parameter to a smaller degree than K1. Thompson and Elliot classified fine-grained soils into four groups: very soft, soft, medium and stiff with different values of K1, K2, K3 and K4 assigned to each group. They further defined a maximum resilient modulus as the one governed by a deviator stress of 13.8 kPa (or 2 psi), and a minimum resilient modulus that is limited by the material unconfined compression strength, shown in Figure 2.3.

Fredlund et al. (1975) indicated that the resilient modulus of fine-grained soils can be described in terms of three independent stress state variables, namely, the deviator stress ($\sigma_1 - \sigma_3$), the confining pressure ($\sigma_3 - u_a$) and soil matric suction ($u_a - u_w$) i.e.:

$$M_r = f \{ (\sigma_1 - \sigma_3), (\sigma_3 - u_a), (u_a - u_w) \} \quad (2.4)$$

where,

- M_r = resilient modulus,
- σ_1 = major principal stress,
- σ_3 = minor principal stress,
- u_a = air pressure, and
- u_w = pore water pressure.

Using these concepts, Fredlund et al. (1977) were successful in adequately describing the resilient properties of some glacial till and clay soils in Saskatchewan. The general form of the postulated equation is as follows:

$$\text{Log } M_r = c_{1d} - m_{1d} (\sigma_1 - \sigma_3) \quad (2.5)$$

where, c_{1d} and m_{1d} are the intercept and slope of the linearized M_r - σ_d relationship shown in figure 2.4, respectively. These two parameters are dependent on matric suction. In this

way, the resilient modulus is related to both the deviator stress and matric suction. It was also suggested that the influence of the confining pressure could either be ignored, since it is often insignificant for cohesive soils, or corrected for by using an equation of the form,

$$\Delta M_r = m_c \cdot \Delta (\sigma_3 - u_a) \quad (2.6)$$

where, ΔM_r = change in resilient modulus due to change in confining pressure,
 m_c = slope of the plot of $(\sigma_3 - u_a)$ versus M_r , see Figure 2.5, and
 $\Delta (\sigma_3 - u_a)$ = change in confining pressure from that used to define the plot for resilient modulus versus deviator stress.

Although the use of equation 2.5 and 2.6 seems appealing, one difficulty does exist which is associated with laboratory soil suction measurement. Presently, there is no existing device that is capable of measuring soil matric suction under dynamic loading conditions. This is due to the slow response of available measuring devices. This problem can, however, be partially solved by measuring soil suction either before or after the resilient modulus test is performed, and assume that it is the same during testing. Alternatively, the M_r -suction relationship can be obtained by cross-plotting from M_r -water content and suction-water content relationships.

In an attempt to avoid the cost and technical complexities usually involved in dynamic-type testing, some agencies developed equations that relate the resilient modulus to more easily measured soil indices such as the CBR and the R-value. The Shell method of pavement design (Shell, 1978), for example, uses the following relation to estimate the resilient modulus from CBR measurements:

$$M_r = 10.3 \text{ CBR} \quad (\text{MPa}) \quad (2.7)$$

It is important, however, to note that the coefficient in equation 2.7 can vary from 5.15 to 20.6 CBR. Another example relating the resilient modulus to the R-value is the equation used by the Asphalt Institute (AI, 1982). This relationship is of the form:

$$M_r = 7.96 + 3.83R \quad (\text{MPa}) \quad (2.8)$$

The aforementioned empirical relations do not substitute the need for actual resilient modulus testing. However, they can be used temporarily until such ability become available. Moreover, extreme caution should be exercised in applying any of these relationships to actual pavement design since the scatter in the data from which these equations were originally developed is great.

2.4.3 Granular Materials

Cohesionless soils include both sand and granular materials. The behaviour of these materials under load is both instantaneous and time dependent (Dehlen and Monismith, 1970). Large permanent strains may occur during the first few cycles of stress, but the behaviour becomes almost elastic after several cycles. Stress history has a profound effect, initially, on these materials but is generally less marked than in the case of cohesive materials.

Many investigators (Ko and Scott, 1967a, 1967b, and 1967c; Seed et al., 1967; Dehlen and Monismith, 1970; and Pell and Brown, 1972) have shown that the behaviour of untreated granular materials, usually used as bases and subbases in pavement structures, is highly nonlinear and stress dependent. Of particular influence is the degree of confinement. To study such an effect, several tests were used to characterize these

materials. In these test several techniques for applying the confining pressure were used. Basically, this can be divided into three categories (Seed et al., 1967):

1. Triaxial repeated load tests with either constant or varying cell pressures.
2. Repeated load tests performed in the Hveem Resiliometer.
3. Tests wherein specimens are compacted and tested in hollow rigid cylinders in the absence of any confining pressure.

Several expressions have been proposed by many researchers to describe the nonlinear behaviour of granular materials. This can be listed as follows:

1. Resilient modulus as a function of the first stress invariant, J_1 , (Seed et al., 1967):

$$M_r = k[J_1]^n \quad (2.9)$$

where M_r = resilient modulus of granular material,

$$J_1 = \sigma_1 + \sigma_2 + \sigma_3 \quad (= \sigma_1 + 2\sigma_3 \text{ in the case of the triaxial test}), \text{ and}$$

k & n = material constants.

2. Resilient modulus as a function of the confining pressure (McLeod, 1971):

$$M_r = k_1[\sigma_3]^{n_1} \quad (2.10)$$

where σ_3 = confining pressure, and

k_1, n_1 = experimentally determined constants.

3. Resilient modulus as a function of the mean normal stress, p , and deviator stress, σ_d (Brown, 1974):

$$M_r = f(p, \sigma_d) \quad (2.11)$$

where $p = \frac{1}{3}[\sigma_1 + 2\sigma_3]$, and

$$\sigma_d = \text{deviator stress} = \sigma_1 - \sigma_3.$$

An alternative, although relatively crude, procedure for estimating the resilient modulus of granular materials is through the use of the stiffnesses and thicknesses of other supporting pavement layers. Two such relationships were proposed and used by Shell and the Asphalt Institute design procedures (Shell, 1978 and AI, 1982). The equations, respectively, are:

$$M_r = K E_{sg} \quad (2.12)$$

where M_r = granular base layer modulus,
 E_{sg} = subgrade layer modulus, and
 $K = 0.2 (h_2)^{0.45}$ where h_2 is the granular layer thickness in mm,
 and K is applicable in the range $2 < K < 4$

and,
$$E_{ua} = M_r = g_0 (h_1)^{g_1} (h_3)^{g_2} (E_1)^{g_3} (E_{sg})^{g_4} (K')^{g_5} \quad (2.13)$$

where g_0, \dots, g_5 = regression constants,
 E_{sg} = subgrade modulus, psi,
 E_1 = modulus of asphalt layer, psi,
 h_1 = asphalt layer total thickness, in.,
 h_3 = granular layer thickness, in., and

K' = a factor with range between 8000 and 12000.

Examples of more recent studies that aimed at improved characterization of cohesionless materials are the two studies conducted by Pappin and Brown (1981) and the U.S. Army Corps of Engineers Cold Region Research and Engineering Laboratory, CRREL, (Cole et al., 1986). In the first investigation, Pappin and Brown studied the effect on the resilient modulus of cyclic confining pressure and used that capability to investigate the effect of the stress path on crushed rock specimens. On the other hand, the CRREL study concentrated on evaluating the effect of soil suction and temperature fluctuations on the resilient modulus of granular materials.

In the CRREL study, the behaviour of cohesionless soils under load was modeled using a resilient modulus equation of the form:

$$M_r = K_1 [f(\sigma)]^{K_2} \quad (2.14)$$

where K_1 and K_2 are constant for a given soil state and $f(\sigma)$ is a stress parameter normalized to a reference stress σ_0 of 1.0 kPa.. Furthermore, elaboration on the basic model, of equation 2.14, to include the effects of soil matric suction, dry density and temperature fluctuations were made. This is accomplished by considering K_1 as a function of soil suction and, in some cases, dry density. Also more liberty was exercised in the form of the stress function $f(\sigma)$ by developing models based not only on the bulk stress (i.e. first stress invariant) but also on a ratio of the second stress invariant to the octahedral shear stress. The final general form for equation 2.14 thus become:

$$M_r = K_1 [f_i(\sigma)]^{K_2} \quad (2.15)$$

where $K_1 = C_0 [f(\psi)]^{C_1}$ or $= C_0 [f(\psi)]^{C_1} (\gamma_d/\gamma_0)^{C_2}$
 and $f(\psi) = [(101.38 - \psi)/\psi_0]$ and ψ is the soil suction, ψ_0 is a
 reference suction of 1.0 kPa, γ_d is the soil dry density and γ_0 is
 a reference dry density of 1.0 Mg/m³.
 and $f_1(\sigma) = f_1(\sigma) = (J_1/\sigma_0)$ or $f_1(\sigma) = f_2(\sigma) = [(J_2/\tau_{oct.})/\sigma_0]$
 and $J_1 = (\sigma_1 + \sigma_2 + \sigma_3)$, $J_2 = (\sigma_1\sigma_2 + \sigma_2\sigma_3 + \sigma_3\sigma_1)$
 $\tau_{oct.} = [(\sigma_1 - \sigma_2)^2 + (\sigma_2 - \sigma_3)^2 + (\sigma_3 - \sigma_1)^2]^{1/3}$
 and σ_0 is a reference stress $\sigma_0 = 0$

$C_0, C_1, C_2, K_2 =$ constants determined experimentally

Using the general form of equation 2.15 and repeated load tests, the CRREL study involved developing approximately 33 different moduli relationships for six types of granular soils obtained from test sites in Winchendon, Massachusetts.

As far as the Poisson's ratio, μ , of granular material is concerned, investigations have shown that this ratio is highly dependent on the principal stress ratio, σ_1/σ_3 , (Hicks, 1970 and Cole et al., 1986). An equation for estimating μ was suggested by Hicks (1970) which is of the following form:

$$\mu = A_0 + A_1 (\sigma_1/\sigma_3) + A_2 (\sigma_1/\sigma_3)^2 + A_3 (\sigma_1/\sigma_3)^3 \quad (2.16)$$

From other studies, it was also found that μ for granular materials usually fall within a range of 0.23 to 0.42. Typical value used in pavement analysis is 0.35 (AI, 1982).

2.4.4 Asphalt Bound Materials

The response of asphalt stabilized materials under load is extremely complex. This is believed to be due to the following:

1. Asphalt concrete materials under load exhibit immediate and time-dependent responses, both of which may be partly recoverable and partly permanent. The time-dependent response may be either viscous or non viscous (Dehlen and Monismith, 1970).
2. Range of linearity of these materials is extremely small. Monismith et al. (1966) found that these materials behave reasonably linear as long as the strains are less than 0.1 percent. Sayegh (1967) reported that the domain of linearity for a particular mix is limited to deformations of less than 4×10^{-5} . Korkosky and others (1963) observed nonlinear viscoelastic behaviour for most part of the response of asphalt mixes.
3. Asphalt mixture in situ appears to be anisotropic due to layering and particle orientation inherent in the construction process. Monismith and Dehlen (1970) found that the behaviour of asphalt mixes seems to be cross-isotropic with the horizontal stiffness exceeding the vertical stiffness. They also concluded that there is a significant degree of stress-induced cross-isotropy. Further, studies by Coffman et al., Deacon (1965) and Gradowczyk (1969) also revealed that asphalt concrete mixes have compression moduli that are different from tension moduli. However, Coffman et al. concluded that, for practical purposes, asphalt bound materials can be considered isotropic in compression at the phenomenological level.
4. Observed moduli of asphalt mixes appear to be sensitive to the testing procedure used. According to Kallas and Riley (1967) there are significant differences between moduli determined by repeated load flexure and dynamic complex modulus test procedures. Such differences may be attributed, in part, to the fact that the deformational responses are different due to different loading modes (repeated flexural loading versus steady state sinusoidal loading in the case of the dynamic complex test procedure).

In summary, the behaviour of asphalt bound materials is highly nonlinear. This nonlinearity would appear to depend upon the properties of the mix and the environmental and loading conditions to which such materials would be subjected to in service (Pell and Taylor, 1969).

Observations such as the ones listed above led investigators to search for procedures that enable the prediction of the dynamic modulus of asphalt paving mixtures based on routine test parameters. Van der Poel (1954a and 1954b) was perhaps the first to provide a simple basis for the determination of such characteristics. Based on extensive static and dynamic testing, Van der Poel developed a nomographic procedure for predicting the stiffness of pure bitumen, S_{bit} , such that:

$$S_{bit} = f(\text{frequency of loading, temperature, penetration of bitumen, ring- and-ball softening point of bitumen})$$

where f is some function (Ullidtz, 1987). A second nomograph was also developed by Van der Poel to enable the estimation of the mix stiffness, S_{mix} , from a knowledge of S_{bit} and the volume concentration of mineral aggregates, C_v .

Heukelom and Klomp (1964) slightly modified the Van der Poel's nomograph for S_{bit} and suggested that S_{mix} could be obtained as follows:

$$\frac{S_{mix}}{S_{bit}} = \left(\frac{1 + 2.5C_v}{n - nC_v} \right)^n \quad (2.17)$$

where,

$$S_{mix} = \text{mix stiffness in kg/cm}^3$$

S_{bit} = bitumen stiffness in kg/cm³

C_v = volume concentration of aggregates in mix and is equal

$[V_A/(V_A + V_B)]$ where V_A is the volume of aggregates

and V_B is the volume of bitumen in the mix,

$$n = 0.83 \log_{10} (4 \times 10^5 / S_{bit})$$

Heukelom and Klomp method was applicable to mixtures having air voids content of less than or equal to 3 percent. Van Draat and Sommer (1965) suggested that the applicability of equation 2.16 can be extended to mixtures having air voids content of more than 3 percent by applying a correction to the volume of aggregate concentration, C_v , as follow:

$$C_{v'} = \frac{C_v}{1 + \Delta H} \quad (2.18)$$

where,

ΔH = the difference between the actual air voids content and 3 percent, expressed as a decimal fraction.

Bazin and Saunier (1967) also presented a nomograph similar to Van der Poel's that is applicable for linear deformations in bending and that uses binder properties determined before mixing. Independent parameters considered in the construction of this nomograph included time of loading, temperature, binder type and mixture void content.

More recently, the research and development branch of the Shell company produced computer simulations of a number of Bitumen and Asphalt Nomographs that were used previously in the Shell design procedure for designing flexible pavements. This computerized version, known as the BANDS Program (BANDS-PC, 1990), was intended

to be used for obtaining bitumen and asphalt mix stiffnesses based on bitumen properties and aggregate content in the asphalt mix.

Other studies have suggested using more direct methods for determining the influence of temperature and rate of loading on resilient characteristics of asphalt concrete mixes through tension, compression and flexural testing. Secor and Monismith (1965) and Secor et al. (1965) performed creep and relaxation tests on asphalt concrete mixes and suggested that these materials can be modeled as linear viscoelastic materials whose stiffness can be determined from creep compliance and/or relaxation modulus as a function of both temperature and time of loading.

Papazian (1962) and Pagen (1965) used a complex modulus to describe the time of loading and temperature dependency of asphalt concrete.

Pell and Cooper (1975) used results from fatigue testing to obtain asphalt concrete moduli.

The Asphalt Institute (1982) developed a regression equation relating the asphalt dynamic stiffness to rate of loading, temperature and mixture properties. The mix characteristics incorporated in this equation are percent air voids, percent aggregate finer than 75 μm (number 200 sieve), absolute viscosity of asphalt liquid at 21° C (70° F) and percent asphalt content by weight of mix. The validity of this stiffness equation was checked for 41 different mix types at three levels of temperature (4.4, 21.2 and 37.8° C) and at three rates of loading (1, 4, 16 Hz).

From the aforementioned discussion and today's state-of-knowledge pertaining to asphalt concrete materials characterization, it seems that there are two general approaches that can be used for estimating asphalt concrete stiffness (or dynamic moduli):

1. Direct measurement of the modulus using any of the available strength tests (e.g. bending, compression, tension, indirect tensile test etc.).
2. Use of empirical relationships that correlate asphalt moduli with other routinely measured mix parameters (this include any or all of the mix properties as well as other environmental and loading variables such as temperature and rate of loading).

Moreover, studies that aimed at investigating asphalt concrete modulus sensitivity to level of applied stress revealed that this parameter has an insignificant effect on the modulus compared to the other variables noted above and as such it can safely be ignored.

Limited information is available pertaining to Poisson's ratio of asphalt bound materials. Nevertheless, it was found (Dehlen and Monismith, 1970) that this parameter remains constant or increases very slightly with increasing applied compressive stress and is independent of transverse stress. Also the ratio was found to be insensitive to mixture type (Heukelom and Klomp, 1964). From various studies the range for Poisson's ratio for asphalt concrete materials was set to be between 0.1 and 0.5 with 0.35 as the value typically used in many design procedures (Shell, 1978; AI, 1982; and AASHTO, 1986).

2.4.5 In Situ Moduli Determination

In situ modulus determination is another attractive alternative for characterizing pavement materials. The advantage of this approach is its ability to estimate pavement material moduli under actual field conditions that may be difficult to reproduce in laboratory testing.

Over the years, a number of different techniques were developed for in situ moduli determinations. The two most famous are the deflection bowl (or basin) method and the wave propagation procedure. Detailed description of each of these two techniques are given below.

2.4.5.1 Surface Waves Propagation Procedures

For more than four decades, elastic waves have extensively been used to evaluate, both destructively and non destructively, the elastic properties of the media in which these waves propagate.

An elastic wave is defined as one that has a small amplitude and that does not permanently deform the medium in which it travels. Elastic waves are commonly classified on basis of either the conditions under which they exist or their frequency content (Addo, 1992). Based on their frequency content, elastic waves can be (Winkler, 1986):

- (i) Seismic (10 - 100 Hz),
- (ii) Sonic (100 - 1000 Hz), or
- (iii) Ultrasonic (100,000 - 1,000,000 Hz).

On the other hand, based on the condition under which they exist, elastic waves can be classified as follows (Addo, 1992):

- (I) **Body waves:** These consist of compressional (primary or P-) and shear (secondary or S-) waves. Under anisotropic conditions, body waves are difficult to discern into separate compressional and shear waves. However, for relatively small anisotropy and inhomogeneity conditions such as those found in most soils and other pavement materials, the assumption for the existence of distinct P- and S-waves is justified (Sheriff and Geldart, 1982). Both P- and S- waves have high rate of damping from the source of disturbance (proportional to $1/r^2$ where r is the distance from the generating source of disturbance (Timoshenko and Goodier,

1943). Also S-waves are difficult to detect and measure in the presence of P-waves.

- (II) **Surface waves:** These waves, usually referred to as R- or Rayleigh waves, were discovered by Rayleigh in 1885 (Rayleigh, 1885). Based on Rayleigh's work and other researchers (Timoshenko and Goodier, 1943), R-waves were found to possess the following characteristics:
- (a) have larger amplitude than either P- or S-waves,
 - (b) attenuate less rapidly with distance from the energy source than both P- and S-waves, and
 - (c) are easy to generate, detect and measure at several wavelengths from the source.

Miller and Pursey (1955) discovered that under conditions where both body and surface waves coexist, 67 % of the input energy propagated as Rayleigh waves, 26 % as shear waves and 7 % as compressional waves. Based on this and other characteristics of R-waves, it is thus more convenient to measure surface (or R-waves) wave velocities and then infer the desired P- and/or S-wave velocities on the basis of elastodynamic relationships between body and surface waves.

Methods for determining body wave velocities involve either intrusive (i.e. destructive) or non-intrusive test procedures. Addo (1992), in a recent study, gave an excellent overview of these techniques. He further pointed out that for both geotechnical and pavement engineering purposes, the steady state vibration and Spectral Analysis of Surface Waves (SASW) procedures qualify as some of the best available methods for such applications. The SASW procedure is an improvement of the steady state vibration technique. Beside sharing all the advantages of the latter, SASW procedure provide for a much quicker and more accurate estimation of field dispersion curves.

The use of the SASW, or any of the other wave propagation techniques, for evaluating materials properties involves the following steps:

- (1) Generate and measure R-wave velocities at different but known wavelengths using the relationship:

$$v_R = f.L \quad (2.19)$$

where, v_R = Rayleigh wave velocity at frequency f ,

f = applied excitation frequency,

L = measured wavelength.

- (2) Compute shear wave velocities from R-wave velocities using elastodynamic relationships. An example equation used in the steady state vibration method (Addo, 1992) is:

$$v_s = k_v \cdot v_R \quad (2.20)$$

where, v_s, v_R = shear and Rayleigh wave velocities,

k_v = ratio of Rayleigh wave to body wave velocities and k_v can be

determined from the relationship:

$$k_v^6 - 8k_v^4 + 8(3-2\zeta^2)k_v^2 - 16(1-\zeta^2) = 0 \quad (2.21)$$

where $\zeta^2 = v_s^2/v_p^2 = (0.5 - \mu)/(1-\mu)$

v_p = P-wave velocity

μ = Poisson's ratio.

Thus knowing the Poisson's ratio, equation 2.21 can be solved for the valid root of k_v . Alternatively, approximate solutions can be obtained for k_v within the normal

range of Poisson's ratio ($0 < \mu < 0.5$). Filipczynski et al. (1966) gave a simpler but approximate solution of equation 2.20 as :

$$1/k_v = (0.87 + 1.12\mu)/(1 + \mu) \quad (2.22)$$

- (3) The data obtained from the computation in step 2 is then used to construct a dispersion curve, i.e. variation of shear wave velocity with wavelength, like the one shown in Figure 2.6.
- (4) The desired elastic constants pertaining to each layer are then estimated using the dispersion curve obtained in step 3 and the following relationships (Timoshenko and Goodier, 1943):

$$E = 2\rho v_s^2(1+\mu) \quad (2.23a)$$

$$G = \rho v_s^2 \quad (2.23b)$$

$$K = \rho(v_p^2 - 0.5 v_s^2) \quad (2.23c)$$

$$\mu = [(v_s/v_p)^2 - 0.5]/[(v_s/v_p)^2 - 1] \quad (2.23d)$$

where E = Young's, or elastic, modulus

G = shear modulus

K = Bulk, or volume, modulus, and

ρ = material bulk density.

- (5) Average layer thickness is determined using the following relationship (Das, 1983 and Addo, 1992):

$$Z = k_z L \quad (2.24)$$

where Z = thickness of layer in question

L = R-wave wavelength

k_z = a constant relating depth and wavelength (typical values used are in the range of 0.3 to 0.5).

Several researchers used the aforementioned techniques in pavement evaluation studies (Heukelom and Klomp, 1962; Dormon and Ewing, 1962; Jones et al., 1967; Christison and Shields, 1974; and Nazarian, 1984). However, the main difficulty or disadvantage in using wave propagation methods for estimating pavement materials properties is that most of these materials are highly nonlinear elastic. The stresses induced during either the steady-state vibration or SASW tests are very small, and are thus in no way comparable to those induced by heavy traffic loads. This results in over estimation of the materials' moduli and hence provide for a non conservative basis for the analysis and design of pavement structures. This observation was noted by Christison and Shields (1974) and others (Ullidtz, 1987 and Lytton, 1989).

2.4.5.2 Deflection Bowl Method

The deflection bowl method involves measuring the surface deflection basin for the particular pavement under consideration and then infers the in situ material moduli using the measured basin and a suitable analytical model. Deflection basin procedures are often termed near field impulse methods whereas wave propagation techniques are referred to as far field impulse methods (Lytton, 1989). The terms "near field" and "far field" refer to the behaviour of the surface of the pavement where the measurements are made. The "near field" is within the deflection basin around the applied load whereas "far field" is outside the deflection basin area. A clear distinction should be drawn between the two methods since the behaviour of the material beneath the load is different from that in the far field. This consideration is of paramount significance in the case of many pavement materials whose behaviour are proved to be, beyond any doubt, stress dependent i.e. have nonlinear rather than linear load-deformation characteristics. This leads to the conclusion that "near

field" responses are more suitable to use in the analysis, design and rehabilitation of pavement structures than "far field" measurements.

The significance of using NDT deflection data for estimating pavement layer properties has been stressed in the 1993 AASHTO Guide for pavement design. As a matter of fact, specific guidelines have been proposed for estimating and using back-calculated moduli for both rehabilitating in service pavements and designing new ones. In Canada and worldwide, the same trend is also evident.

The pursuit for obtaining pavement material elastic properties from nondestructive deflection testing dates back to the early 1960's when Shields and Hutchinson (1961) conducted a study for evaluating cement treated bases in Alberta. In this study, surface deflection bowls using the Benkelman Beam device were obtained for both soil cement and conventional pavements. These deflection bowls were then analyzed using elastic layer theory. Based on deflection coefficients for a two-layer system (Mehta and Veletsos, 1959), the modular ratio, and subsequently pavement and subgrade moduli, was obtained from the measured deflection bowls.

In 1973, Scrivner et al. (1973) developed the first closed-form solution for back calculating material moduli for two-layered systems. The equation took the form:

$$\left[\frac{4\pi\omega r}{3p} \right] E_1 = 1 + \int_0^{(10r/h)} (v-1) J_0(x) dx \quad (2.25)$$

where,

ω = surface deflection at a radial distance r , from the applied load p ,

E_1 = the elastic modulus of the surface layer,

h = thickness of the surface layer,

$J_0(x)$ = Bessel function of first kind and 0th order,

$x = mr/h$, and m is a continuous variable of integration,

$v = (1 + 4Ne^{-2m} - Ne^{-4m})/[1 - 2N(1 + 2m)e^{-2m} + N^2e^{-4m}]$, and

$N = (E_1 - E_2)/(E_1 + E_2)$.

Scrivner found that the ratio $\omega_1 r_1 / \omega_2 r_2$ was useful in analyzing Dynaflect deflection basins and consequently a graphical solution for equation 2.24 was developed.

Swift (1973) developed another graphical procedure for obtaining moduli of a two-layer pavement system. He also suggested an empirical equation with great ability for fitting measured and calculated deflection basins for two-layer pavement systems (Swift, 1972).

Other solutions for multi-layered systems were also developed by several researchers. During the process, three different approaches were utilized for modeling the pavement structure, namely, the elastic layer theory (Yiu Hou, 1977), the equivalent thickness procedure (Ullidtz, 1987 and Lytton and Michalak, 1979) and the finite element techniques (Chua, 1989). Among these, the multi-layered elastic approach gained wide popularity and as a consequence several microcomputer program solutions were developed that back-calculate layer moduli for pavements with three or more layers. Figure 2.7 illustrates the mechanism of modulus back-calculation from surface deflection measurements for a three layer system. Here, five deflection sensors are situated at radial distances $r_1, r_2, r_3, \dots, r_5$ from the point of load application. The applied load is arbitrarily assumed to distribute itself through the various layers according to the broken lines shown in the upper part of Figure 2.7. Since sensors 4 and 5 are outside the stress zone of the asphalt concrete (ACP) and granular base (GB) layers, then it is justified to assume that the deflections at sensors 4 and 5 are only influenced by the subgrade modulus and are

independent of the asphalt concrete and granular base moduli. Therefore, in applying layer system analysis, any reasonable moduli can be assumed for the ACP and GB materials, and the subgrade modulus can be varied until a satisfactory match between computed and measured deflections at sensors 4 and 5 is achieved. After obtaining the subgrade modulus in this fashion, the base modulus can be varied until a satisfactory match between the computed and measured deflections at sensor 3 is achieved. The procedure is repeated again to obtain the asphalt concrete layer modulus from the deflections of sensors 1 and 2.

The procedure outlined above for obtaining the in situ moduli is over simplified. Other considerations like the suitability of the analytical model selected, inherent material dependency on stress level and other factors should be investigated and catered for. Nevertheless, several computer codes i.e. programs, have been developed for obtaining moduli based on the aforementioned procedure. The features which all of these programs have in common have been discussed by Lytton (1989) and are illustrated in Figure 2.8. The flow chart shown in Figure 2.8 can briefly be explained as follows (Lytton, 1989):

Measured Deflections: These are the deflections measured by any NDT device and their respective distances from the applied load.

Layer Thickness and Load: These describe the pavement that is tested, the load level and the area over which it is applied.

Seed Moduli: These are the assumed initial values of the layer moduli. In some methods, these values are either generated from the measured deflections, through regression equations, or they are presumed values. Assumed values of Poisson's ratios are used in all methods.

Deflection Calculation: A number of elastic computer programs are used here. Examples of such programs are BISAR, CHEVRON, ELSYM5. The programs utilize the layer thicknesses, load, the latest set of layer moduli, and radii to the deflection sensors and

calculates the surface deflections at each. In methods where adjustments are made for nonlinearity, stresses and strains at selected locations are also calculated.

Error Check: Several types of error checks are used to evaluate the adequacy of the calculated moduli. Some of these are the sum of the squared differences between the measured and calculated deflections, the sum of absolute differences and the sum of the squared relative errors, in which the difference is divided by the measured deflection before the ratio is squared and summed. If the error check indicates convergence within acceptable levels of tolerance, the results are printed out. Otherwise, a new iteration is started.

Results: These usually include an array of outputs such as the measured and calculated deflections, the differences and percent differences, the final set of layer moduli and the error sums.

Constitutive Relations: These are the relationships used to describe the load-deformation characteristics of the different layer materials. Types of relations used by different methods vary considerably from linear elastic theory with no correction for nonlinearity to various forms of assumed relations between the stress and strain beneath the load to the modulus of the layer.

Stress and Strain Level Corrections: These make use of the constitutive equations for each layer and any calculated stresses or strains to estimate new layer moduli to try in the next iteration.

Search for New Moduli: This is one of the major distinguishing features of all the microcomputer methods. The error criterion (mentioned above) when plotted against the layer moduli in multi-dimensional space will form an "error surface" which may have a local minimum and several global minima, depending upon the radii where deflections are measured, the number of layers, the error criterion and the degree of nonlinearity introduced by the constitutive relations and corrections. The search methods then attempt, by using efficient multi-dimensional search techniques, to find a global minimum which

represent the least error, the best fit of the measured basin and the best set of layer moduli. During the process of converging to such a minimum, one or more viable solutions can be obtained.

Control of the Range of Moduli: In order to guide the iterative search toward an acceptable set of layer moduli, numerous controls are programmed to direct the search away from unwanted or unreasonable values of the moduli. In most cases this takes the form of asserting upper and lower limits on the moduli of the different layers. This, of course, requires some prior knowledge and experience with the type of the pavement structure being analyzed. Stabilized layers or thin soft layers are difficult to assess and therefore may cause difficulty in convergence or in the final results.

Examples of computer codes utilizing the steps described above and shown in Figure 2.8 are the MODCOMP programs originally developed by Irwin (1983), the "_DEF" series of programs developed by Bush (1980) at the U.S. Army Corps of Engineers Waterways Experiment Station and the MODULUS Program developed by Uzan et al. (1988) at Texas A & M University. Two versions of the MODCOMP program (Irwin, 1983 and Irwin and Szebenyi, 1991) and four different "_DEF" programs (CHEVDEF, BISDEF, ELSDEF and WESDEF) are available today (Bush, 1980; Jordahl, 1985; and Van Gauwelaert et al., 1989). Also three versions of the NCHRP MODULUS program exist (version 2, 1988; version 4, 1990; and version 5, 1994). Differences among these computer programs involve mainly the selection of the analytical model and/or the convergence criterion used to perform the following tasks:

- (i) Deflection calculations
- (ii) Error checks
- (iii) Constitutive relations used for the various material types
- (iv) New moduli search techniques

Several limitations and problem areas have been identified by the researchers and engineers using the modulus back-calculation methodologies. The sources of errors in the back-calculated moduli, shown in Figure 2.9, can be classified into:

- (i) Systematic errors
- (ii) Random errors

Systematic errors are introduced by the deflection calculation model and its presumed constitutive relationships. These errors can not be reduced or eliminated by repeated measurements or calculations. On the other hand, random errors can be reduced or even completely eliminated. The sources of random errors are in the measurements that are made, i.e. in force, deflections and pavement layer thickness determinations. Irwin et al. (1989) showed how random errors produced by inaccurate deflection and layer thickness measurements can significantly affect material moduli especially those pertaining to upper layers such as ACP and GB layers. However such variability in the back-calculated moduli had only a minimal effect on the estimated overlay thickness requirements. Stolle and Hein (1989) investigated the uniqueness of the solution of the back-calculated moduli of a pavement structure subjected to axisymmetric loading. They concluded that back-calculation is an ill-conditioned problem since a small change in measured deflections can result in large changes in moduli predictions. Consequently, if an iterative solver was to be used to obtain a solution, convergence would be slow and, unless the tolerance for convergence is very stringent, the procedure may not converge to a proper solution.

The above mentioned studies and many others (Irwin, 1992; Thompson, 1992; Smith, 1992; Rada et al., 1992; Rauhut and Jordahl, 1992; Siddharthan et al., 1992; and Zaniewski and Hossain, 1992) appear to support the conclusion that reducing and/or eliminating random errors, improving analytical tools and material constitutive relationships is the only way of achieving the strategic objective of making NDT testing the primary method for measuring pavement material properties.

2.5 Effects of Environmental Factors on Pavements

The impact of the environment on pavement response and performance has been an important issue of concern to many highway engineers and researchers. Among the many environmental factors, moisture and temperature conditions within and around pavement structures represent the most significant parameters that influence pavement response to loads.

The effects of both temperature and moisture variations on pavements can be viewed through their influences on the properties of the constituent materials. Such seasonal variations tend to change the strength of the pavement materials so that their resistance to traffic induced stresses are altered (AI, 1982 and AASHTO, 1986). Furthermore, there is much evidence from previous research that pavements are deteriorated by climatic factors even in the absence of traffic variables. This stems from the fact that temperature and moisture variations, among other environmental factors, can produce internal stresses in the pavement materials which may become excessive and ultimately lead to structural failure.

It follows that quantitative evaluation of the effects of both temperature and moisture variations on pavement response is essential to properly rehabilitate existing pavements and design new ones. This fact necessitates establishing a way for measuring seasonal variations.

2.5.1 Temperature effects

Of all environmental factors, temperature is the easiest to estimate and use in a mechanistic-empirical design procedure.

Temperature conditions affect pavement structures in one or more of three ways:

(1) **Internal stresses:** Daily and seasonal fluctuations in temperature induce internal stresses within the pavement structure due to thermal expansion and contraction. Diurnal variations usually produce bending stresses whereas seasonal fluctuations manifest itself in terms of either tensile or compressive stresses. The effects of these stresses in producing temperature associated cracks were studied by many investigators. Worth mentioning among these, is the work reported by Secor et al. (1965b) and Haas and Topper (1969) on the phenomenon of low temperature cracking.

(2) **Changing material properties:** It is well known that all asphalt-stabilized materials are viscous materials and as such their properties are highly dependent on temperature. Therefore, changes in temperature will in turn alter the ability of these materials to withstand traffic loads. Low temperatures, for example, have beneficial effects in terms of increasing the stiffness of the asphalt concrete layer whereas high temperatures tend to soften these materials and thus increase its susceptibility to traffic-induced damage.

(3) **Combined temperature and moisture effects:** In seasonal frost areas the interaction between subzero surface temperature conditions and moisture present within the pavement structure leads to significant reduction in the pavement system ability to withstand traffic loading during the spring time due to reduced subgrade strength under thawing conditions.

Due to the above discussed temperature influences on pavement thickness design requirements, various approaches were tried for predicting appropriate temperature inputs to be included in the design and rehabilitation of pavement structures. Hudson (1973) summarized the approaches adopted by the different investigators as follows:

1. Applying regional or environmental factors to adjust the design (or overlay) thickness. An example of this is the 1961 AASHO Interim Guide procedure (1961).

2. Developing design procedures that will relate to a general climatic area where an annual cycle of temperature, freezing and so on will be about the same from year to year. This is similar to the procedure developed by Haas and Topper (1969) for investigating low temperature cracking.
3. Developing temperature prediction models whereby temperature profile and history of a particular pavement can be predicted from available weather data (Secor et al., 1965b; Christison, 1972; Shahin and McCullough, 1973; and Robinson, 1986).

Recently, Pufahl et al. (1990) developed an integrated computer model to estimate both moisture and temperature effects beneath pavement structures. Extensive meteorological data, as well as other data, represent the inputs needed by the program to produce the temperature- and moisture-time profiles.

2.5.2 Moisture variation effects

The presence of moisture and its seasonal variations within the pavement structures can produce one or more of the following effects:

1. Combination of moisture and sunlight can lead to the oxidation of the asphalt concrete layer and thus change the layer resistance to traffic loads.
2. Development of excessive pore-water pressure in pavement embankments can lead to base and slope stability failures.
3. Undesirable volume changes may occur in certain soils that are more susceptible to changes in moisture. Examples of these soils are expansive clays and frost susceptible soils.
4. Prevailing subzero surface temperature conditions in conjunction with moisture present in the subgrade layer leads to freezing and subsequent thawing of these

materials. Such conditions tend to reduce the subgrade soil bearing capacity during the spring time, and thus enhance the damage induced by traffic during this period.

5. Seasonal fluctuations in moisture also induce internal stresses within the pavement structure which may become excessive and eventually produce structural failure.

Since moisture cycling is seasonal and not a daily change, moisture variations do not impose the large number of repeated stresses that temperature variations do. Therefore, the major concern with moisture influences on pavements is only to cater for its effect in changing material properties. This is particularly emphasized in areas experiencing seasonal freezing and thawing of the subgrade soil material.

2.5.3 Quantifying seasonal variations

Efforts for measuring the loss in pavement load carrying capacity due to reduced subgrade supporting capacity during the frost-melt period in the spring time dates back to the early 1940's when Motl (1948) developed his familiar curve that relates loss in bearing capacity as measured by plate-loading tests, with seasons. Further investigations by the U.S. Army Corps of Engineers (Sayman, 1955) substantiated the Motl work. Although these studies brought into attention the importance of seasonal adverse effects on pavement strength, however, it was only a very broad generalization of what actually happens in a specific pavement section. This fact called for more definitive methods for measuring pavement structural response to load and quantification of the effects of seasonal variations on such measure(s).

With the emergence of the Benkelman Beam surface deflection as an acceptable index of the pavement ability to carry load (WASHO, 1955), it became evident that the seasonal effects of temperature and moisture on pavements must be incorporated in this measure. This conclusion was arrived at after extensive deflection testing at the WASHO

Road Test. The following observations are among the important findings from the Road Test (WASHO, 1955):

- (i) The effect of the condition of the separate components of the pavement on the ability of the structure to support load should further be studied. Of prime importance is the moisture content at the surface of the subgrade soil.
- (ii) A strong relationship between the Benkelman Beam deflection and asphalt concrete surface temperature is evident. However, further research is needed to substantiate and quantify this effect.

Similar findings had also been reported by the Canadian Good Roads Association (CGRA) during their evaluation of Canadian roads in the late 1950's and the early 1960's (CGRA, 1959 and 1962). From stage two of the CGRA study, attempts had been made to relate characteristics of the seasonal deflection curve such as peak spring deflection and mean fall deflection to various pavement and environmental parameters such as soil type, pavement thickness, traffic, spring axle load restrictions, freezing index and average annual precipitation. Regression analyses of these parameters versus peak spring and/or mean fall deflection proved inadequate for fully characterizing seasonal behaviour.

Further attempts that used the surface deflection as a means of assessing pavement strength followed. In Alberta, Shields and Dacyszyn (1965) used this procedure to detect seasonal variation influences in the strength of flexible pavements within the Province. In their study, the ratio of the spring rebound deflection, defined as the maximum value, to the fall rebound, defined as the average value during the 60 day period prior to the inception of freezing, was used as an indicator of the effect of the season on the pavement load-carrying capacity. Findings indicated that there was a substantial loss in the strength of pavements during the spring period. Practical implementation of the research findings took the form of imposing spring load restrictions on major highways within the Province for more than twenty years. More recently, Christison and Leung (1988) employed the

same technique used by Shields and Dacyszyn to a larger database and obtained similar results to those reported earlier.

With the advent of new nondestructive deflection measuring devices, such as the Dynaflect and the FWD, that more closely simulate in situ traffic loading conditions, extensive use and adjustment of measured surface deflections to cater for seasonal variations continued. Parker (1991) and Germann and Lytton (1989) used different temperature correction procedures to adjust measured FWD deflection data to a standard temperature of 21⁰ C (70⁰ F). In both studies, the correction factors were applied to layer moduli back-calculated from deflection data rather than the measured deflections, per se. In Alberta, Kurlanda (1993) used temperature-adjusted FWD central deflections to evaluate flexible pavement bearing capacity. The aim behind that was to identify those pavements in need for structural rehabilitation at the network level.

Newcomb et al. (1989) also investigated the phenomenon of seasonal variations in the states of Nevada and Washington. Ratios of the subgrade moduli during the spring time, or wet season, to those under no thaw, or dry, conditions were computed from FWD deflection measurements and related to environmental and soil parameters such as the freezing index, thawing index, permeability and percent soil passing the 0.076 mm sieve (#200 sieve). The major finding from this study was that there is no appreciable change in subgrade moduli from season to season.

Janoo and Berg (1990 and 1992) investigated thaw-weakening behaviour of flexible pavements in seasonal frost areas. In these studies, four test sections were built in the Frost Effects Research Facility (FERF) at the U.S. Army Cold Region Research and Engineering Laboratory (CRREL). These sections were instrumented with thermocouples and electrical resistivity gauges for recording the temperature distribution within the

asphalt concrete, base, subbase and subgrade layers. The combined use of thermocouples and resistivity gauges was meant to provide a better estimate of freezing and thaw depths. The test sections were subjected to several freezing and thawing cycles. FWD deflection measurements were conducted prior to and during the thaw cycles. The data collected from these tests were then analyzed to identify and interpret seasonal behaviour. Two types of analyses were performed. In the first analysis, explicit utilization of the deflection data was made. This took the form of determining seasonal variation effects through the interpretation of some deflection parameters like the centre deflection, the fourth sensor deflection and the deflection basin area. In the second analysis, the information gathered from the first stage was used to back-calculate the layer moduli during one full freeze-thaw cycle. These moduli were then used to estimate changes in pavement load carrying capacity with the seasons.

To summarize, detection of seasonal variation trends and their influences on pavement bearing capacity can be achieved through the following steps:

- (i) Adjust the measured surface deflections (or back-calculated moduli) to a standard temperature, usually taken as 21°C .
- (ii) Use different corrected deflections and/or modulus ratios to quantify the effects of moisture changes.

With the ever-growing trend of using mechanistic-empirical methods for pavement design and evaluation, the resilient modulus represents the most adequate and popular measure to be used for quantifying seasonal variations. Apart from the fact that the resilient modulus represents a basic material property, it is an essential primary input that is required by all available mechanistic-empirical procedures. Furthermore, today's technology and state-of-the-art knowledge of pavement design and analysis, lend itself quite easily to the determination of the resilient moduli of all pavement materials within a reasonable degree of accuracy both in situ and under controlled laboratory conditions.

2.6 Summary

This chapter is intended to present the current state-of-the-knowledge pertaining to flexible pavement structural evaluation procedures.

In the first part of the chapter, a review of available pavement design methodologies is given. The need for rationalizing the process of pavement thickness design and rehabilitation through the use of mechanistic-empirical procedures is emphasized. Pavement performance and its linkage to pavement response, materials characterization and the phenomenon of seasonal variations in pavement strength are among the crucial issues that need to be further studied.

In the second part of the chapter, the question of measuring the pavement bearing capacity through nondestructive testing techniques was discussed. Nondestructive deflection testing and surface wave propagation procedures are the two most popular approaches currently available for evaluating pavement load-carrying capability. Both techniques involve back calculating fundamental material properties from some measured pavement response(s). These properties are then used in designing new pavements and/or rehabilitating in-service ones. The merits and disadvantages of both evaluation techniques are presented and discussed.

Laboratory testing is another way of characterizing pavement materials. Although such characterization is of a destructive nature, however, its potential use for designing new pavements should not be ignored. Furthermore, laboratory materials testing supplements and substantiates the information collected by nondestructive testing procedures.

Environmental considerations and their influence on pavement bearing capacity are discussed in the last part of this chapter. In particular, temperature and moisture fluctuations and their adverse effects on pavement conditions are addressed here. As a matter of fact, the need for better quantification of the effects of such factors on pavement structural performance is the reason behind the pursuit of the current research project.

References

1. AASHTO (1972), "*AASHTO Interim Guide for Design of Pavement Structures*," American Association of State Highway and Transportation Officials.
2. AASHTO (1982), "*Standard Method of Test for Resilient Modulus of Subgrade Soils - AASHTO Designation: T 274-82*," AASHTO Methods of Sampling and Testing, pp. 1157-1177. (N.B.: This test procedure is discontinued as of 1992)
3. AASHTO (1986), "*Guide for Design of Pavement Structures*," American Association of State Highway and Transportation Officials.
4. AASHTO (1992), "*Resilient Modulus of Unbound Granular Base/Subbase Materials and Subgrade Soils - SHRP Protocol P46: AASHTO Standard Test Designation T-294-92*," American Association of State Highway and Transportation Officials.
5. AASHTO (1993), "*AASHTO Guide for Design of Pavement Structures 1993*," American Association of State Highway and Transportation Officials.
6. Addo K.O. (1992), "*Development of a Computerized SASW Technique*," Ph.D. Dissertation, Department of Civil Engineering, University of Alberta, Alberta, Fall 1992, 271 p.
7. AI (1969), "*Asphalt Overlays and Pavement Rehabilitation*," 1st Edition, Manual Series No. 17 (MS-17), Asphalt Institute, 134 p.
8. AI (1973), "*Full-Depth Asphalt Pavements for Air Carrier Airports*," Manual Series No. 11 (MS-11), Asphalt Institute, 164 p.
9. AI (1982), "*Research and Development of the Asphalt Institute's Thickness Design Manual (MS-1). 9th Edition*," Research Report 82-2, Asphalt Institute.
10. BANDS-PC User Manual (1990), "*Computerized Bitumen and Asphalt Nomographs*," Shell Company.
11. Barber E.S. (1945), "*Application of Triaxial Compression Test Results to the Calculation of Flexible Pavement Thickness*," Proceedings. Highway Research Board, pp.26-39.
12. Barksdale R.D. and G.A. Leonards (1967), "*Predicting Performance of Bituminous Surface Pavements*," Proceedings, Vol. 1, Second International Conference on the Structural Design of Asphalt Pavements, University of Michigan, Ann Arbor, Michigan, pp. 321-340.

13. Barksdale R.G. (1971), "*Compressive Stress Pulse Times in Flexible Pavements for Use in Dynamic Testing*," Highway Research Record 345, Highway Research Board, pp. 32-44.
14. Bazin P. and J.B. Sauneir (1967), "*Deformability, Fatigue and Healing Properties of Asphalt Mixes*," Proceedings, Vol. 1, Second International Conference on the Structural Design of Asphalt Pavements, University of Michigan, Ann Arbor, Michigan, pp. 553-569.
15. Briggs R.C., T. Scullion and K.R. Maser (1992), "*Asphalt Thickness Variation on Texas Strategic Highway Research Program Sections and Effect on Backcalculated Moduli*," Transportation Research Board, TRR 1377, Washington D.C., pp. 115-127.
16. Brown S.F. (1973), "*Determination of Young's Modulus for Bituminous Materials in Pavement Design*," Highway Research Record 431, Highway Research Board, pp. 38-49.
17. Brown S.F. (1974), "*Repeated Load Testing of a Granular Material*," Journal of the geotechnical Engineering Division, Vol. 100, No. G77, pp. 825-841.
18. Brown S.F. and J.W. Pappin (1981), "*Analysis of Pavements with Granular Bases*," Transportation Research Record 810, Transportation Research Board, pp. 17-22.
19. Burmister D.M. (1943), "*The Theory of Stresses and Displacements in Layered Systems and Application to the Design of Airport Runways*," Proceedings, Highway Research Board, Vol. 23, pp. 126-144.
20. Burmister D.M. (1958), "*Evaluation of Pavement Systems of the WASHO Road Test by Layered Systems Methods*," Bulletin 177, Highway Research Board, pp. 26-54.
21. Bush A.J., III (1980a), "*Nondestructive Testing for Light Aircraft Pavements. Phase I: Evaluation of Nondestructive Testing Devices*," USDOT, Federal Aviation Administration, Report No. FAA-RD-80-9, Washington D.C..
22. Bush A.J., III (1980b), "*Nondestructive Testing for Light Aircraft Pavements, Phase II: Development of the Nondestructive Evaluation Methodology*," Report No. FAA-RD-80-9-II, Federal Aviation Administration, Washington, D.C..
23. Canadian Good Roads Association (1959), Manual on Pavement Investigations, CGRA Technical Publication No. 11.
24. Canadian Good Roads Association (1962), "*Pavement Evaluation Studies in Canada*," Proceedings, Vol. 1, First International Conference on the Structural Design of Asphalt Pavements, University of Michigan, Ann Arbor, Michigan, pp. 137-218.

25. Canadian Good Roads Association (1965), *"A Guide to the Structural Design of Flexible and Rigid Pavements in Canada,"* CGRA 1965 Guide, 65 p.
26. California Division of Highways, Materials and Research Department (1972), *"Methods of Test to Determine Overlay and Maintenance Requirements by Pavement Deflection Measurements,"* Test Method No. Calif. 356-C.
27. Christison J.T. (1972), *"The Response of Asphaltic Concrete Pavements to Low Temperatures,"* Ph.D. Dissertation, University of Alberta, Edmonton, 323 p.
28. Christison J.T. and B.P. Shields (1974), *"Pavement Elastic Moduli by the Surface Wave Method Correlated with In-Situ Measurements of Elastic Response Under Moving Vehicle Loads,"* A Paper Presented to the Annual Meeting of the Canadian Technical Asphalt Association, Regina, Saskatchewan, Contribution No. 703, Alberta Research Council HTE/74/4, 33 p.
29. Christison J.T. and P.S. Leung (1988), *"Temperature Adjustment Factors for Benkelman Beam Rebound Deflections and Seasonal Variations in Pavement Strength,"* Alberta Research Council, Technical Report No. HTE 88/07, 12 p.
30. Chua K.M. (1989), *"Evaluation of Moduli Backcalculation Programs for Low Volume Roads,"* Nondestructive Testing of Pavements and Backcalculation of Moduli, ASTM STP 1026, A.J. Bush III and G.Y. Baladi, Eds., American Society of Testing and Materials, Philadelphia, pp. 398-414.
31. Claros G., W.R. Hudson and K.H. Stokoe (1990), *"Modifications to the Resilient Modulus Testing Procedure and the Use of Synthetic Samples for Equipment Calibration,"* Presented at the 69th Annual Meeting of the Transportation Research Board, 1990 TRB Convention, Washington, D.C., p. 27.
32. Coetzee N.F. and R.G. Hicks (1989), *"NDT in Cold Regions: A Review of the State-of-the-Art of Deflection Testing,"* Proceedings, First Symposium on State-of-the-Art of Pavement Response Monitoring Systems for Roads and Airfields, West Lebanon, New Hampshire, pp. 198-209.
33. Coffman B.S., G. Ilves and W.F. Edwards, *"Isotropy and an Asphaltic Concrete,"* Unpublished.
34. Cole D., D. Bentley, G. Durell and T. Johnson (1986), *"Resilient Modulus of Freeze-Thaw Affected Granular Soils for Pavement Design and Evaluation: Part 1. Laboratory Tests on Soils from Winchendon, Massachusetts, Test Sections,"* CRREL Report 86-4, 71 p.

35. Committee on Design (1961), *"AASHO Interim Guide for the Design of Flexible Pavement Structures,"* AASHO.
36. Darter M.I., J.M. Becker, M.B. Snyder and R.E. Smith (1985), *"Portland Cement Concrete Pavement Evaluation System (COPEs),"* NCHRP Report 277, Transportation Research Board.
37. Das B.M. (1983), *"Fundamental of Soil Mechanics,"* Elsevier, Oxford, Eng'land.
38. Deacon J.A. (1965), *"Fatigue of Asphalt Concrete,"* Institute of Transportation and Traffic Engineering, Graduate Report, University of California, Berkeley, CA.
39. Deacon J.A. (1971), *"Materials Characterization - Experimental Behaviour,"* Highway Research Board, Special Report No. 126, Washington, D.C., pp. 150-179.
40. Dehlen G.L. and C.L. Monismith (1970), *"The Effect of Nonlinear Material Response on the Behaviour of Pavements Under Traffic,"* Highway Research Record 310, Highway Research Board, pp. 1-16.
41. De Jong D.L., M.G.F. Peatz and A.R. Korswagen (1973), *"Computer Program BISAR Layered Systems Under Normal and Tangential Loads,"* Konin Klijke Shell Laboratorium, Amsterdam, External Report AMSR.0006.73.
42. Dorman J. and M. Ewing (1962), *"Numerical Inversion of Seismic Surface Wave Dispersion Data and Crust-Mantle Structure in the New York - Pennsylvania Area,"* Journal of Geophysical Research, Vol. 67, No. 13, pp. 5227-5241.
43. Duncan J.M., C.L. Monismith and E.L. Wilson (1968), *"Finite Element Analysis of Pavements,"* Highway Research Record 228, Highway Research Board, pp. 18-33.
44. Elton D.J. and M.E. Harr (1988), *"New Nondestructive Pavement Evaluation Method,"* Journal of Transportation Engineering, ASCE, Vol. 114 No. 1, New York.
45. Epps J.A. and C.L. Monismith (1986), *"Equipment for Obtaining Pavement Condition and Traffic Loading Data,"* NCHRP Synthesis of Highway Practice No. 126, Transportation Research Board, Washington D.C..
46. FHWA (1978), *"Predictive Design Procedures, VESYS User's Manual,"* Report No. FHWA-RD-77-154, Federal Highway Administration.
47. FHWA (1980), *"Skid Accident Reduction Program,"* Technical Advisory T-5040.17, Federal Highway Administration.

48. Filipczynski L., Z. Pawlowsky and J. Wehr (1966), *"Ultrasonic Methods of Testing Materials,"* Butterworths, London, England.
49. Fredlund D.G., A.T. Bergan and E.K. Sauer (1975), *"Deformation Characterization of Subgrade Soils for Highways and Runways in Northern Environments,"* Canadian Geotechnical Journal, Vol. 12, No. 2, pp. 213-223.
50. Fredlund D.G., A.T. Bergan and P.K. Wong (1977), *"Relation Between Resilient Modulus and Stress Conditions for Cohesive Subgrade Soils,"* Transportation Research Record 642, Transportation Research Board, pp. 73-81.
51. Germann F.P. and R.L. Lytton (1989), *"Temperature, Frequency and Load Level Correction Factors for Backcalculated Moduli Values,"* Nondestructive Testing of Pavements and Backcalculation of Moduli, ASTM STP 1026, A.J. Bush III and G.Y. Baladi, Eds., American Society of Testing and Materials, Philadelphia, pp. 431-451.
52. Gradowczyk M.H. and F. Moavenzadeh (1969), *"Characterization of Linear Viscoelastic Materials,"* Transportation Society of Rheology, Vol. 13, No. 2, pp. 173-191.
53. Guillemain R. and J.C. Gramsammer (1971), *"Auscultation Dynamique des Chaussees a l'aide du Vibreur Leger,"* Note d'information Technique, Laboratoire Centrale des Ponts et Chaussees.
54. Haas R.C.G. and T.H. Topper (1969), *"Thermal Fracture Phenomena in Bituminous Surfaces,"* HRB Special Report No. 101, pp. 136-153.
55. Hall K.T., J.M. Connor, M.I. Darter and S.H. Carpenter (1989), *"Rehabilitation of Concrete Pavements, Vol. 3, Concrete Pavement Evaluation and Rehabilitation System,"* Report No. FHWA-RD-88-073, Federal Highway Administration.
56. Harichandran R.S., G.Y. Baladi and M. Yeh (1989), *"Development of a Computer Program for Design of Pavement Systems Consisting of Bound and Unbound Materials,"* Department of Civil and Environmental Engineering, Michigan State University.
57. Heisey J.S., K.H. Stokoe, W.R. Hudson and A.H. Meyer (1982), *"Determination of In Situ Shear Wave Velocities from Spectral Analysis of Surface Waves,"* Centre for Transportation Research, Research Report 256-2, The University of Texas at Austin, Austin, TX.
58. Heukelom W. and A.J.G. Klomp (1962), *"Dynamic Testing as a Means of Controlling Pavements During and After Construction,"* Proceedings, Vol. 1, First

International Conference on the Structural Design of Asphalt Pavements, University of Michigan, Ann Arbor, Michigan, pp. 667-679.

59. Heukelom W. and A.J.H. Klomp (1964), "*Road Design and Dynamic Loading*," Proceedings, Vol. 33, AAPT, pp. 92-125.
60. Hicks R.G. (1970), "*Factors Influencing the Resilient Properties of Granular Materials*," Institute of Transport and Traffic Engineering, University of California, Berkeley, Ph.D. Dissertation.
61. Hoffman M.S. and M.R. Thompson (1982), "*Comparative Studies of Selected Nondestructive Testing Devices*," Transportation Research Board, TRR 852, Washington D.C..
62. HRB (1945), "*Report of Committee on Classification of Materials for Subgrades and Granular Type Roads*," Proceedings, Highway Research Board, Vol.25, pp. 376-384.
63. Hudson W.R. (1973), "*Other Input Variables: Traffic and Environmental*," TRB Special Report No. 140, pp. 65-77.
64. Hudson W.R., G.E. Elkins, W. Eden and K.T. Reilley (1987), "*Evaluation of Pavement Deflection Measuring Equipment*," USDOT, Federal Highway Administration, Report No. FHWA-TS-87-208, Washington D.C..
65. Hudson W.R. and G.E. Elkins (1989), "*SHRP - Long-Term Asphaltic Pavement Performance Studies*," Proceedings of the fifth Conference on Asphalt Pavements for Southern Africa, Swaziland, South Africa, pp. III-38 to III-42.
66. Huang H.Y. (1993), "*Pavement Analysis and Design*," Prentice Hall, Englewood, New Jersey, 785 p.
67. Hwang D. and M.W. Witczak (1979), "*Program DAMA (Chevron), User's Manual*," Department of Civil Engineering, University of Maryland.
68. Irwin L.H. (1983), "*User's Guide to MODCOMP 2*," Report No. 83-8, Cornell University Local Roads Program, Cornell University, Ithaca, NY.
69. Irwin L.H., W.S. Yang and R.N. Stubstad (1989), "*Deflection Reading Accuracy and Layer Thickness Accuracy in Backcalculation of Pavement Layer Moduli*," Nondestructive Testing of Pavements and Backcalculation of Moduli, ASTM STP 1026, A.J. Bush III and G.Y. Baladi, Eds., American Society of Testing and Materials, Philadelphia, pp. 229-244.

70. Irwin L. and T. Szebenyi (1991), "*User's Guide to MODCOMP 3, Version 3.2*," CLRP Reptot 91-4. Cornell University local Roads Programs, Ithasca, NY.
71. Irwin L.H. (1992), "*Report of the Discussion Group on Practical Limitations and What Can Be Done To Overcome Them*," Transportation Research Record 1377, Highway Research Board, Washington, D.C., pp.1-2.
72. Irwin L.H., G. Cumberledge and B. Henderson (1994), "*Implementation of a Calibration Procedure for Falling Weight Deflectometers*," A Paper presented at the Third International Conference on Managing Pavements, May 22-26, San Antonio, Texas, USA.
73. Janoo V.C. and R.L. Berg (1990), "*Thaw Weakening of Pavement Structures in Seasonal Frost Areas*," Transportation Research Record 1286, Highway Research Board, Washigton, D.C., pp. 217-233.
74. Janoo V.C. and R.L. Berg (1992), "*Layer Moduli Determination During Freeze-Thaw Periods*," Transportation Research Record 1377, Highway Research Board, Washigton, D.C., pp. 26-35.
75. Jones R., E.N. Thrower and E.N. Gatfield (1967), "*The Surface Wave Method*," Proceedings, Vol. 1, Second International Conference on the Structural Design of Asphalt Pavements, University of Michigan, Ann Arbor, Michigan, pp. 505-520.
76. Jordahl P. (1985), "*ELSDEF User's Guide*," Brent Rauhut Engineers, Austin TX.
77. Kallas B.F. and J.C. Riley (1967), "*Mechanical Properties of Asphaltic Pavement Materials*," Proceedings, Vol. 1, Second International Conference on the Structural Design of Asphalt Pavements, University of Michigan, Ann Arbor, Michigan, pp. 931-952.
78. Kansas State Highway Commision (1947), "*Design of Flexible Pavement Using the Triaxial Compression Test*," Bulltein 8, Highway Research Board.
79. Kerkhoven R.E. and G.M. Dormon (1953), "*Some Considerations on the California Bearing Ratio Method for the Design of Flexible Pavement*," Shell Bitumen Monograph No. 1.
80. Khogali W.E.I. (1988), "*A Parametric Evaluation of a Mechanistic-Empirical Design Procedure for Asphalt Concrete Pavements*," M.Sc. Thesis, Department of Civil Engineering, University of Alberta, 257 p.
81. Ko H.Y. and R.F. Scott (1967a), "*Deformation of Sands in Hydrostatic Compression*," Journal of Soil Mechanics and Foundation Division, ASCE, Vol. 93, No. SM3, May, pp. 137-156.

82. Ko H.Y. and R.F. Scott (1967b), "*Deformation of Sands in Shear*," Journal of Soil Mechanics and Foundation Division, ASCE, Vol. 93, No. SM5, September, pp. 283-310.
83. Ko H.Y. and R.F. Scott (1967c), "*A New Soil Testing Apparatus*," Geotechnique, Vol. 14, No. 1, March, pp. 40-57.
84. Kopperman S., G. Tiller and M. Tseng (1986), "*ELSYM5, Interactive Microcomputer Version, User's Manual*," Report No. FHWA-TS-87-206, Federal Highway Administration.
85. Korkosky E.M., E. Tons and R.D. Andrews (1963), "*Rheological Properties of Asphalt-Aggregate Compositions*," Proceedings, Vol. 63, ASTM, pp. 1263-1286.
86. Kurlanda M. (1993), "*Network Level Evaluation of Pavement Bearing Capacity with Use of Falling Weight Deflectometer*," Proceedings of the fifth Conference on Paving in Cold Areas, Vol. II, Kananaskis, Alberta, Canada, pp. 37-55.
87. Leu M.C. and J.J. Henry (1978), "*Prediction of Skid Resistance as a Function of Speed from Pavement Texture*," Transportation Research Record 666, Transportation Research Board, pp. 38-43.
88. Lytton R.L. and C.H. Michalak (1979), "*Flexible Pavement Deflection Equation Using Elastic Moduli and Field Measurements*," Research Report 207-7F, Texas Transportation Institute, Texas A&M University, College Station TX.
89. Lytton R.L. (1989), "*Backcalculation of Pavement Layer Properties*," Nondestructive Testing of Pavements and Backcalculation of Moduli, ASTM STP 1026, A.J. Bush III and G.Y. Baladi, Eds., American Society of Testing and Materials, Philadelphia, pp. 7-38.
90. McLean D.B. (1974), "*Permanent Deformation Characteristics of Asphalt Concrete*," Ph.D. Dissertation, University of California, Berkeley.
91. McLeod N.W. (1953), "*Some Basic Problems in Flexible Pavement Design*," Proceedings, Highway Research Board, pp. 91-118.
92. McLeod D.R. (1971), "*Some Fatigue Considerations in the Design of Thin Pavements*," M. Sc. Thesis, University of Saskatchewan, Saskatoon, Saskatchewan.
93. Mehta M.R. and A.S. Veletsos (1959), "*Stresses and Displacements in Layered Systems*," Structural Research Series No. 178, University of Illinois.

94. Middlebrooks and Bertram (1950), "*Development of CBR Flexible Pavement Design Methods for Airfields*," Symposium Transactions, Vol. 115, American Society of Civil Engineers.
95. Miller G.f. and H. Pursey (1955), "*On the Partition of Energy between Elastic Waves in a Semi-infinite Solid*," Proceedings of the Royal Society of London, Series A, Mathematical and Physical Sciences, Vol. 233, pp. 55-59.
96. MODULUS (1988): Preliminary User's Manual - Version 2, Texas Transportation Institute, Texas A&M University, College Station.
97. MODULUS (1990): Preliminary User's Manual - Version 4, Texas Transportation Institute, Texas A&M University, College Station.
98. MODULUS (1994): Preliminary User's Manual - Version 5, Texas Transportation Institute, Texas A&M University, College Station.
99. Monismith C.L. and K.E. Secor (1962), "*Viscoelastic Behaviour of Asphalt Concrete Pavements*," Proceedings, Vol. 1, First International Conference on the Structural Design of Asphalt Pavements, University of Michigan, Ann Arbor, Michigan, pp. 476-498.
100. Monismith C.L., R.L. Alexander and K.E. Secor (1966), "*Rheologic Behaviour of Asphalt Concrete*," Proceedings, Vol. 35, AAPT, pp. 400-450.
101. Monismith C.L. and J.A. Epps (1986), "*Update of Asphalt Concrete Rehabilitation*," Solutions for Pavement Rehabilitation of a Conference held in Atlanta, Georgia, May 19-21, pp. 51-96.
102. National Research Council Committee on Load-Carrying Capacity of Roads and Bridges (1960), "*Report of the Committee on Load-Carrying Capacity of Roads and Bridges*," Proceedings, HRB, Vol. 28.
103. Nazarian S. and K.H. Stokoe (1983), "*Evaluation of Moduli and Thicknesses of Pavement Systems by Spectral-Analysis-of Surface-Waves Method*," Centre for Transportation Research, Research Report 256-4, The University of Texas at Austin, Austin, TX.
104. Nazarian S. (1984), "*In-Situ Determination of Elastic Moduli of Soil Deposits and Pavement Systems by Spectral Analysis of Surface Waves Method*," PH.D. Dissertation, Department of Civil Engineering, University of Texas at Austin, Austin, TX, 453 p.
105. Newcomb D.E., S.W. Lee, J.P. Mahoney and N.C. Jackson (1989), "*The Use of Falling Weight Deflectometer Data in Monitoring Flexible Pavement Systems*,"

- Nondestructive Testing of Pavements and Backcalculation of Moduli, ASTM STP 1026, A.J. Bush III and G.Y. Baladi, Eds., American Society of Testing and Materials, Philadelphia, pp. 470-485.
106. Pagen C.A. (1965), "*Rheological Response of Bituminous Concrete*," Highway Research Record 67, Highway Research Board, pp. 1-26.
 107. Papazian H.S. (1962), "*The Response of Linear Viscoelastic Materials in the Frequency Domain with Emphasis on Asphalt Concrete*," Proceedings, Vol. 1, First International Conference on the Structural Design of Asphalt Pavements, University of Michigan, Ann Arbor, Michigan, pp. 454-463.
 108. Parker F., Jr. (1991), "*Estimation of Paving Materials Design Moduli from FWD Measurements*," Transportation Research Board 70th Annual Meeting, Paper No. 910052, Washington, D.C., 34 p.
 109. Pell P.S. and I.F. Taylor (1969), "*Asphaltic Road Materials in Fatigue*," Proceedings, Vol. 38, AAPT, pp. 371-422.
 110. Pell P.S. and S.F. Brown (1972), "*The Characteristics of Materials for the Design of Flexible Pavement Structures*," Proceedings, Vol. 1, Third International Conference on the Structural Design of Asphalt Pavements, London, England, pp. 326-342.
 111. Pell P.S. and K.E. Cooper (1975), "*The Effect of Testing and Mix Variables on the Fatigue Performance of Bituminous Materials*," Proceedings, Vol. 44, AAPT, pp. 1-37.
 112. Porter O.J. (1950), "*Development of the Original Method for Highway Design: Symposium on Development of CBR Flexible Pavement Design Method for Airfields*," Transactions, ASCE, pp. 461-467.
 113. Pufahi D.E., R.L. Lytton and H.S. Liang (1990), "*Integrated Computer Model to Estimate Moisture and Temperature Effects Beneath Pavements*," Transportation Research Record 1286, Highway Research Board, Washington, D.C., pp. 259-269.
 114. Pumphrey N.D., J.K. Lindly and T.D. White (1989), "*Planning and Implementing a Nondestructive Pavement Testing Program*," Nondestructive Testing of Pavements and Backcalculation of Moduli, ASTM STP 1026, A.J. Bush III and G.Y. Baladi, Eds., American Society of Testing and Materials, Philadelphia, pp. 599-611.
 115. Raad L. and J.L. Figueroa (1980), "*Load Response of Transportation Support Systems*," Transportation Engineering Journal, ASCE, Vol. 106, No. TE1, pp. 111-128.

116. Robinson R.G. (1986), "*A Model for Calculating Pavement Temperatures from Meteorological Data*," Transport and Road Research Laboratory, Digest of Research Report rr44.
117. Rada G.R., S.D. Rabinow, M.W. Witczak and C.A. Richter (1992), "*Strategic Highway Research Program Falling Weight Deflectometer Quality Assurance Software*," Transportation Research Record 1377, Highway Research Board, Washington, D.C., pp. 36-44.
118. Rauhut J.B. and P.R. Jordahl (1992), "*Variability in Measured Deflections and Backcalculated Moduli for the Strategic Highway Research Program Southern Region*," Transportation Research Record 1377, Highway Research Board, Washington, D.C., pp. 45-56.
119. Rayleigh J.W.S. (1885), "*On Waves Propagated Along the Plane Surface of an Elastic Solid*," Proceedings of the London Mathematical Society, England, Vol. 17 (Series 1), pp. 4-11.
120. Richter C. (1991), "*FWD Calibration Centres: Why Do We Need Them?*," A Video Tape Recorded by SHRP Staff, Running Time 7:20 Minutes.
121. Saal R.N. and P.S. Peil (1960), *Kolloid-Zeitschrift* MI, pp. 61-71.
122. Sayegh G. (1967), "*Viscoelastic Properties of Bituminous Mixtures*," Proceedings, Vol. 1, Second International Conference on the Structural Design of Asphalt Pavements, University of Michigan, Ann Arbor, Michigan, pp. 743-755.
123. Sayers M.W., T.D. Gillispie and W.D. Paterson (1986a), "*Guidelines for the Conduct and Calibration of Road Roughness Measurements*," Technical Paper 46, The World Bank, Washington D.C..
124. Sayers M.W., T.D. Gillispie and C.A. Queiroz (1986b), "*The International Road Roughness Experiment: Establishing Correlation and a Calibration Standard for Measurements*," Technical Paper 46, The World Bank, Washington D.C..
125. Sayman W.C. (1955), "*Plate-Bearing Study of Loss of Pavement Supporting Capacity due to Frost*," Bulletin 111, Highway Research Board, pp. 99-106.
126. Scrivner F.H., C.H. Michalak and W.M. Moore (1973), "*Calculation of the Elastic Moduli of a Two-Layer Pavement System from Measured Deflections*," Highway Research Record 431, Highway Research Board, Washington, D.C., pp. 12-24.

127. Secor K.E. and C.L. Monismith (1965), "*Viscoelastic Response of Asphalt Paving Slabs Under Creep Loading*," Highway Research Record 67, Highway Research Board, pp. 84-97.
128. Secor G.A., K.E. Secor and C.L. Monismith (1965), "*Temperature Induced Stresses and Deformations in Asphalt Concrete*," Proceedings, Vol. 34, AAPT, pp. 248-285.
129. Seed H.B. and R.L. McNeill (1957), "*Soil Deformation Under Repeated Stress Applications*," Proceedings, Conference on Soils for Engineering Purposes, Universidad de Mexico.
130. Seed H.B., C.K. Chan and C.E. Lee (1962), "*Resilience Characteristics of Subgrade Soils and Their Relation to Fatigue Failures in Asphalt Pavements*," Proceedings, Vol. 1, First International Conference on the Structural Design of Asphalt Pavements, University of Michigan, Ann Arbor, Michigan, pp. 611-636.
131. Seed H.B., F.G. Mitry, C.L. Monismith and C.K. Chan (1967a), "*Prediction of Flexible Pavement Deflections from Laboratory Related Load Tests*," NCHRP Report No. 35, Highway Research Board, pp. 6-28.
132. Seed H.B., F.G. Mitry, C.L. Monismith and C.K. Chan (1967b), "*Factors Influencing the Resilient Deformations of Untreated Aggregate Base in Two-Layer Pavements Subjected to Repeated Loadings*," Highway Research Record 140, Highway Research Board, 1967, pp. 19-57.
133. Shahin M.Y. and B.F. McCullough (1973), "*Prediction of Low Temperature and Thermal Fatigue Cracking*," Texas Highway Department, Texas Transportation Institute, Texas A&M University, and Centre for Highway Research of Texas at Austin, Research Report 123-14.
134. Shell (1978), "*Shell Pavement Design Manual - Asphalt Pavements and Overlays for Road Traffic*," Shell International Petroleum, London.
135. Sheriff R.E. and L.P. Geldart (1982), "*Exploration Seismology Vol. 1: History, Theory and Data Acquisition*," University Press, Cambridge, 253 p.
136. Shields B.P. and B.G. Hutchinson (1961), "*Cement Bases In Alberta*," Proceedings, Canadian Good Roads Association, pp. 424-437.
137. Shields B.P. and J.M. Dacyszyn (1965), "*Seasonal Variations in Flexible Pavement Strength*," Proceedings, Canadian Good Roads Association, pp. 394-409..
138. Strategic Highway Research Program (1986), "*Strategic Highway Research Program - Research Plans*," Final Report, AASHTO, FHWA and TRB, May.

139. Strategic Highway Research Program (1989), SHRP PROTOCOL: P46 for SHRP Test Designation: UG07, SS07, "*Resilient Modulus of Unbound Granular Base/Subbase Materials and Subgrade Soils*," November.
140. Strategic Highway Research Program (1991), Long-Term Pavement Performance Information Management System Researchers Guide, SHRP Publication, January.
141. Strategic Highway Research Program (1992), "*SHRP Product Catalog*," SHRP Publication, National Research Council, pp. 45-49.
142. Siddharthan R., P.E. Sebaaly and M. Javaregowda (1992), "*Influence of Statistical Variation in Falling Weight Deflectometers on Pavement Analysis*," Transportation Research Record 1377, Highway Research Board, Washington, D.C., pp. 57-66.
143. Smith R.E. and R.L. Lytton (1984), "*Synthesis Study of Nondestructive Testing Devices for Use in Overlay Thickness Design of Flexible Pavements*," USDOT, Federal Highway Administration, Report No. FHWA-RD-83-097, Washington D.C..
144. Smith R.E. (1992), "*Report of the Discussion Group on Current and Future Applications of Nondestructive Deflection Measurements*," Transportation Research Record 1377, Highway Research Board, Washington, D.C., pp. 5-6.
145. Stolle D. and D. Hein (1989), "*Parameter Estimates of Pavement Structure Layers and Uniqueness of the Solution*," Nondestructive Testing of Pavements and Backcalculation of Moduli, ASTM STP 1026, A.J. Bush III and G.Y. Baladi, Eds., American Society of Testing and Materials, Philadelphia, pp. 313-322.
146. Swift G. (1972), "*An Empirical Equation for Calculating on the Surface of a Two-Layer Elastic System*," Texas Transportation Institute Research Report 136-4, Texas A&M University, College Station, TX.
147. Swift G. (1973), "*Graphical Technique for Determining the Elastic Moduli of a Two-Layer Structure from Measured Surface Deflections*," Highway Research Record 432, Highway Research Board, Washington, D.C..
148. Teng P. (1993), "*Long-Term Pavement Performance Program for Years 1992-1997: A Strategic Plan*," Proceedings, Pacific Rim TransTech Conference, Vol. II, pp. 256-262.
149. Timoshenko S.P. and J.N. Goodier (1943), "*Theory of Elasticity*," McGraw-Hill Book Company, London, England, 567 p.

150. Thompson M.R. and R.P. Elliot (1985), *"ILLI-PAVE-Based Response Algorithms for Design of Conventional Flexible Pavements,"* Transportation Research Record 1043, Transportation Research Board, pp. 50-57.
151. Thompson M.R. (1992), *"Report of the Discussion Group on Backcalculation Limitations and Future Improvements,"* Transportation Research Record 1377, Highway Research Board, Washington, D.C., pp. 3-4.
152. U.S. Navy (1953), *Airfield Pavement*, Bureau of Yards and Docks, Technical Publication, NAVDOCKS TP-PW-4.
153. Ullidtz P. (1987), *"Pavement Analysis,"* Elsevier Science Publishing Co. Inc., New York, 314 p.
154. Uzan J., R.L. Lytton and F.P. Germann (1988), *"General Procedure for Backcalculating Layer Moduli,"* First International Symposium on Nondestructive Testing of Pavements and Backcalculation of Moduli, ASTM, Baltimore, MD.
155. Van der Poel C. (1954a), *"A general System Describing the Viscoelastic Properties of Bitumens and Its Relation to Routine Test Data,"* Journal of Applied Chemistry, pp. 221-236.
156. Van der Poel C. (1954b), *"Road Asphalt. In Building Materials, Their Elasticity and Inelasticity,"* (Reiner, M., ed.), Interscience Publishers, New York, pp. 361-443.
157. Van Draat W.E.F. and P. Sommer (1965), *"Ein Gerat zur Bestimmung der Dynamischen Elastizitätsmoduln von Asphalt,"* Strasse und Autobahn, Vol. 35, pp. 206-211.
158. Van Gauwelaert F.J., D.R. Alexander, T.D. White and W.R. Barker (1989), *"Multilayer Elastic Program for Backcalculating Layer Moduli in Pavement Evaluation,"* Nondestructive Testing of Pavements and Backcalculation of Moduli, ASTM STP 1026, A.J. Bush III and G.Y. Baladi, Eds., American Society of Testing and Materials, Philadelphia, pp. 171-188.
159. Warren H. and W.L. Dieckmann (1963), *"Numerical Computation of Stresses and Strains in a Multipl-layer Asphalt Pavement System,"* Internal Report, Chevron Research Corporation, Richmond, California.
160. WASHO (1955), *"The WASHO Road Test- Part 2: Test Data, Analysis, Findings,"* Highway Research Board Special Report 22.
161. Winkler K.W. (1986), *"Estimates of Velocity Dispersion between Seismic and Ultrasonic Frequencies,"* Geophysics, Vol. 51, No. 9, pp. 183-189.

162. Yih Hou T. (1977), "*Evaluation of Layered Material Properties from Measured Surface Deflections*," Ph.D. Dissertation, University of Utah, UT.
163. Yoder E. J. and M.W. Witczak (1975), "*Principles of Pavement Design*," Wiley, New York, N.Y.
164. Zaniewski J.P. and M. Hossain (1992), "*Effect of Thickness and Temperature Corrections on Prediction of Pavement Structural Capacity Using Falling Weight Deflectometer Data*," Transportation Research Record 1377, Highway Research Board, Washington, D.C., pp. 193-199.

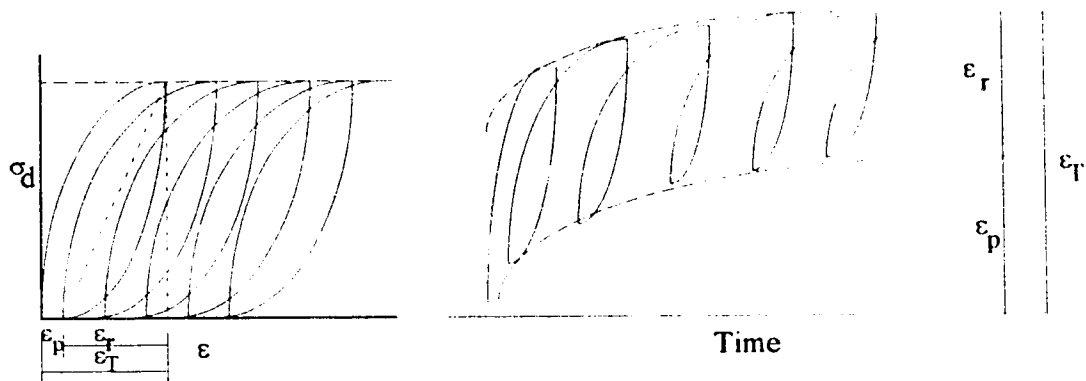


Figure 2.1: Straining of a Soil Sample Under a Repeated Load Test

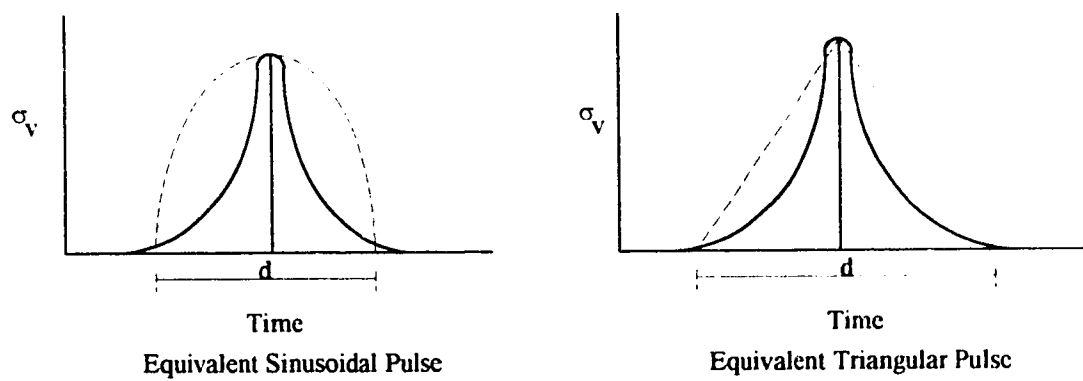


Figure 2.2: Simplification of Actual Load Pulse as Sinusoidal and Triangular Wave Pulses (After Barksdale, 1971)

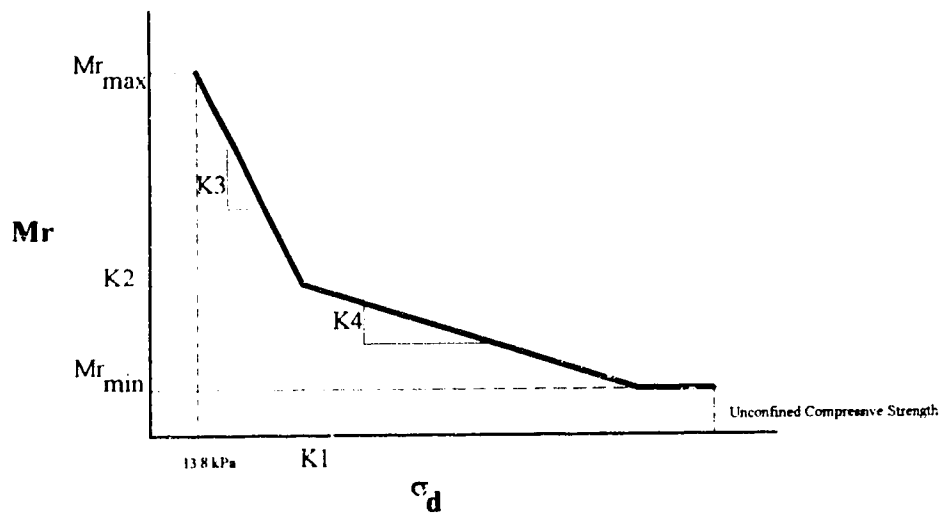


Figure 2.3: Resilient Modulus - Deviator Stress Relationship for Fine-Grained Soils
(After Thompson and Elliot, 1985)

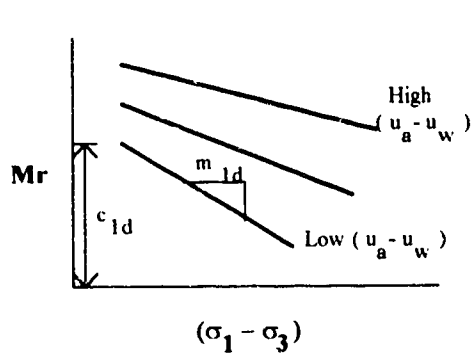


Figure 2.4: Mr - Deviator Stress for Fine-Grained Soils
(After Fredlund et al., 1977)

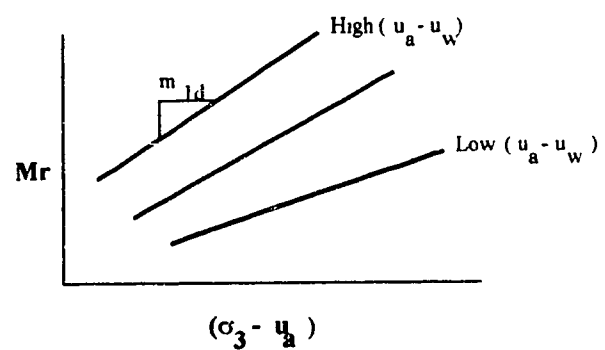


Figure 2.5: Mr - Confining Pressure for Fine-Grained Soils
(After Fredlund et al., 1977)

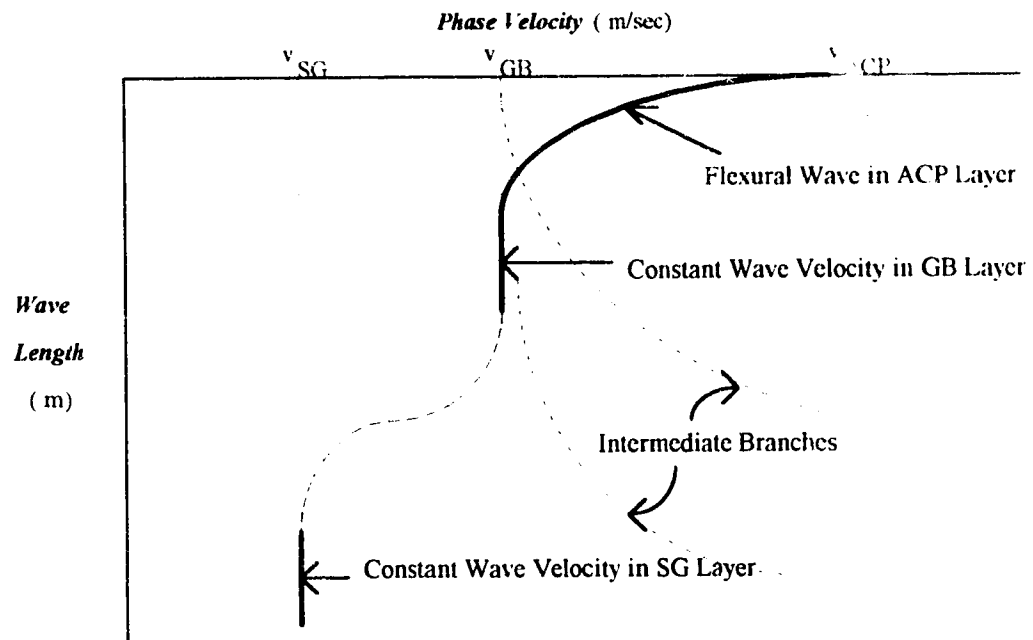


Figure 2.6: Shear Wave Velocity Dispersion Curve
(After Shields and Christison, 1974)

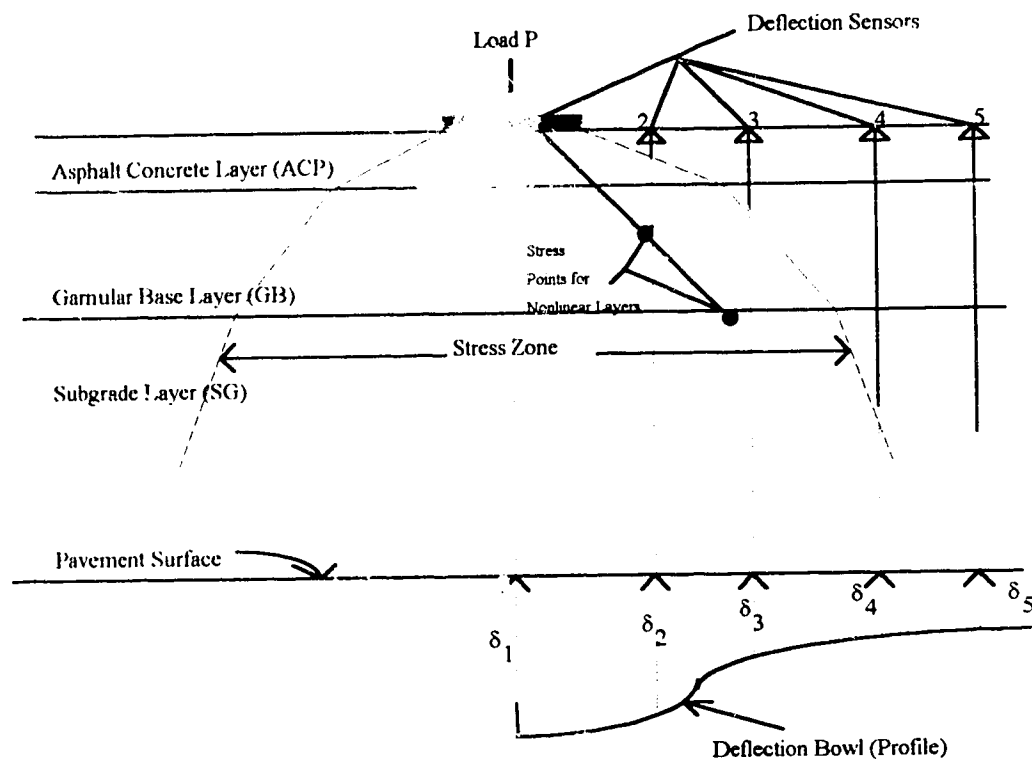


Figure 2.7: Stress Zone Within A Typical Pavement Structure and Shape of the Deflection Basin

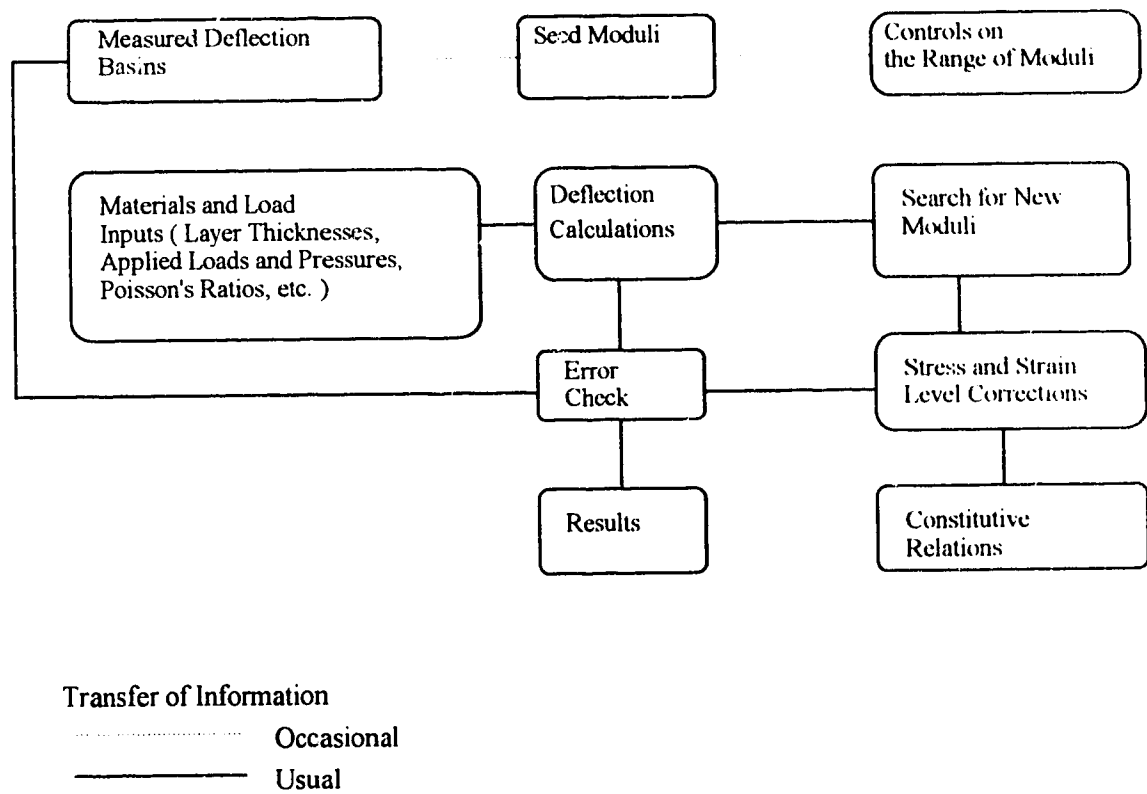


Figure 2.8: A Flow Chart of the Back-calculation Process
(After Lytton, 1989)

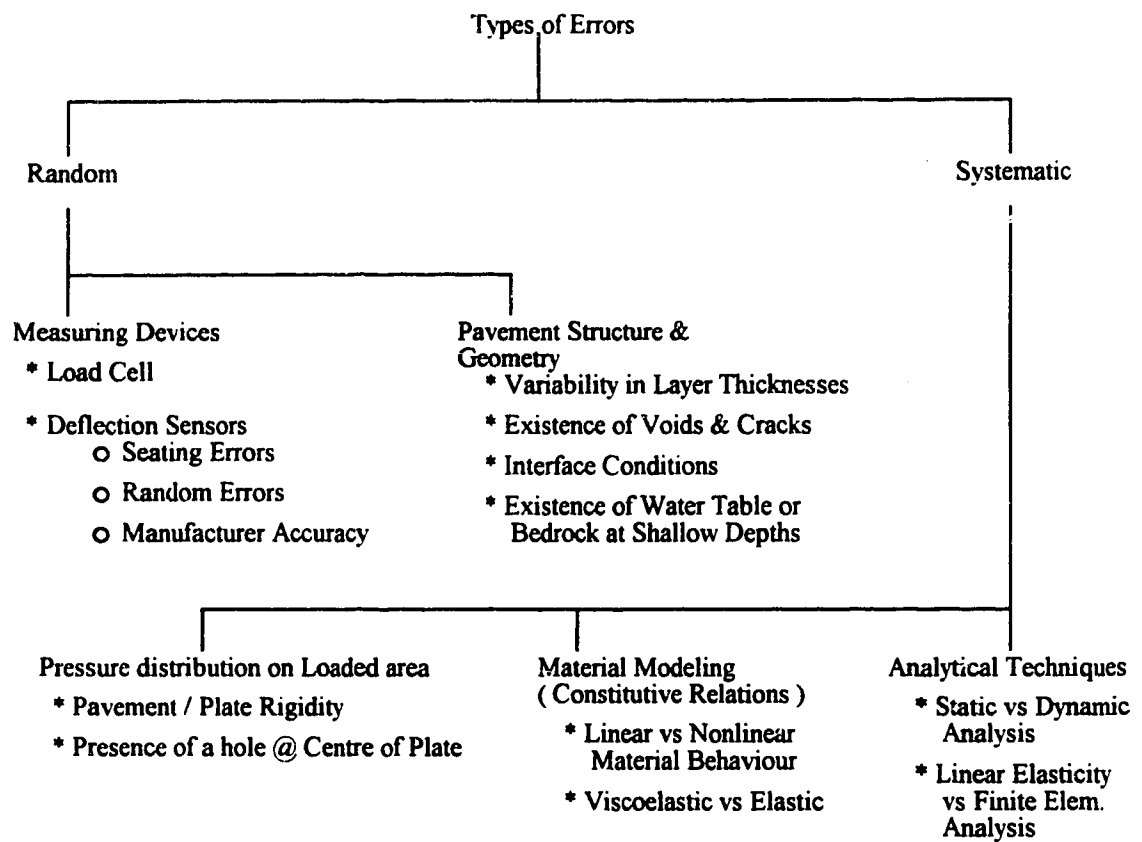


Figure 2.9: Sources of Errors in the Back-calculation Process

CHAPTER THREE

MEASUREMENT OF SOIL MATRIC SUCTION

3.1 Introduction

The construction of highway embankments and preparation of subgrade soils usually involves dealing with compacted soils that are unsaturated. Furthermore, microclimatic conditions in the vicinity of a pavement tend to produce a surface flux boundary condition which produces flow through the upper portion of the soil profile. If the net upward flux, due to evaporation, is greater than the net downward flux, due to rainfall and other forms of precipitation, the pore-water pressure within the soil will be negative, otherwise a saturated soil condition with positive pore-water pressure will prevail. The existence of such negative pore-water pressure in the soil has been advocated by many (Fredlund and Morgenstern, 1977; Fredlund, Bergan and Sauer, 1975; Edil and Motan, 1984; and Fredlund and Rahardjo, 1993) researchers to have beneficial effects on the soil structural strength. Based on this, a quantitative evaluation of the influence of negative pore-water pressures (i.e. soil suction) on soil bearing capacity is considered an essential part towards proper understanding of the mechanical behavior of unsaturated soils and its relation to pavement design and rehabilitation.

In this chapter, the underlying principles of unsaturated soil mechanics together with the various techniques used for measuring soil suction are presented and discussed. A separate section on the behaviour of frozen soils is also included in this review.

3.2 Role of Soil Suction in Affecting Unsaturated Soil Behaviour

An unsaturated soil is a mixture of four distinct phases: i) solid particles, ii) water, iii) air and iv) air-water interface. Fredlund and Morgenstern (1977) justified the use of

the air-water interface as a separate phase based on the fact that it has different properties from the contiguous materials and has definite bounding surfaces. These two attributes qualify any portion of the material within a mixture to be identified as an independent phase (Sisler et al., 1953; Davies and Rideal, 1963;). A unique property of the air-water interface, or contractile skin as it is often called, is its ability to exert a tensile pull on the soil solid particles. This allows the contractile skin to behave as "an elastic membrane interwoven throughout the soil structure" (Fredlund and Rahardjo, 1993). The contractile skin has a thickness in the order of only a few molecular layers. This fact makes the physical subdivision of the contractile skin unnecessary when establishing volume-mass relationships for unsaturated soils. However, when considering the stress state equilibrium analysis of the multiphase continuum, it is necessary to realize that the contractile skin behaves as an independent phase.

To illustrate how the contractile skin influences the mechanical behaviour of unsaturated soils, let us consider the case of a thin glass tube that is inserted into water under atmospheric conditions (Figure 3.1). According to the capillary law, water starts rising up in the tube as a result of its tendency to wet the surface of the glass. As this happens, water molecules at the water-air interface start experiencing an unbalanced force towards the interior of the water due to the pressure exerted by the column of water of height h_c . In order for the contractile skin to be in equilibrium, a tensile pull is generated along the circumference of the contractile skin. This force is called surface tension, T_s , and is usually measured as force per unit length of the contractile skin. The surface tension acts at an angle, α , from the vertical. This angle is known as the contact angle and its magnitude depends on the adhesion between the molecules of contractile skin and the material comprising the tube.

Let us now consider the equilibrium of forces in the vertical direction in the capillary water in the tube in Figure 3.1. The vertical component of surface tension (i.e. $2\pi r T_s \cos(\alpha)$) is responsible for holding the water column of height h_c (i.e. $\pi r^2 h_c \rho_w g$)

Then,

$$2\pi r T_s \cos(\alpha) = \pi r^2 h_c \rho_w g \quad (3.1)$$

where,

ρ_w = density of water

T_s = surface tension

g = gravitational acceleration

r = radius of the capillary tube

α = contact angle

but, from the condition of hydrostatic equilibrium at point C, we have

$$u_w = -h_c \rho_w g \quad (3.2)$$

where,

u_w = water pressure at C

also at Point C, the pore-air pressure is atmospheric, i.e.

$$u_a = 0 \quad (3.3)$$

combining equations (3.2) and (3.3), we have

$$(u_a - u_w) = h_c \rho_w g \quad (3.4)$$

substituting equation (3.4) in equation (3.1), we get:

$$(u_a - u_w) = \frac{2T_s}{R_s} \quad (3.5)$$

where,

$(u_a - u_w)$ = soil matric suction

& R_s = radius of curvature of the meniscus

= $r/\cos(\alpha)$

Equation 3.5 is called the “matric suction — surface tension” relationship. Note that in the case of soils, R_s can be substituted for by the pore radius, r , assuming a zero contact angle. As a result, the smaller the pore radius of a soil, the higher will be the matric

suction (in other words, soils composed of fine particles such as clay and silty soils experience high suction).

Referring to Figure 3.2, the surface tension associated with the contractile skin results in a compressive reaction force on the wall of the capillary tube. The vertical component of this reaction produces compressive stresses on the wall of the tube. In other words, the weight of the water column is transferred to the tube through the contractile skin. In the case of unsaturated soils, the compressive stresses resulting from surface tension in the contractile skin produce an increase in the compression of the soil structure. As a result, the presence of matric suction in an unsaturated soil increases its shear strength (Fredlund and Rahradjo, 1993).

3.3 Historical Development of Basic Concepts of Unsaturated Soil Mechanics

The principle of effective stress introduced by Terzaghi in 1936 laid the foundation for understanding the behavior of classical saturated soil mechanics. The principle states that :

The stresses in any point of a section through a mass of soil can be computed from the total principal stresses $\sigma_1, \sigma_2, \sigma_3$, which act at this point. If the voids of the soil are filled with water under a stress, u_w , the total principal stresses consist of two parts. One part, u_w , acts in the water and in the soil in every direction with equal intensity. It is called the neutral (or the pore-water) pressure). The balance $\sigma_1' = \sigma_1 - u_w$, $\sigma_2' = \sigma_2 - u_w$, and $\sigma_3' = \sigma_3 - u_w$ represents an excess over the neutral stress, u_w , and it has its seat exclusively in the solid phase of the soil. All the measurable effects of a change in stress, such as compression, distortion and a change in shearing resistance are exclusively due to changes in the effective stress.

(Terzaghi, 1936)

The validity of the effective stress as a stress state variable that can be used in describing the mechanical behavior of saturated soils has been well accepted and experimentally verified (Rendulic, 1936; Bishop and Eldin, 1950; and Skempton, 1961). Moreover, evidence has shown that only a single-valued effective stress relation is required to completely describe the mechanical behavior of saturated soils.

Following the successful evaluation and implementation of the principle of effective stress for saturated soils, many attempts had been made to develop a similar concept of effective stress for unsaturated soils. Fredlund and Rahardjo (1993) gave an extensive review of these efforts. In summary, they stated the following:

- i) Numerous equations had been proposed by several researchers (Croney et al., 1958; Bishop, 1959; Bishop and Donald, 1961; Jennings, 1961; Coleman, 1962; and Richards, 1966).
- ii) All proposed relations incorporated a soil property to form a single-valued effective stress expression. However, these equations proved unsuccessful in explaining fully the soil behaviour and further suggested a dependency of behaviour on stress path followed.
- iii) The incorporation of a soil property into the description of the stress state for unsaturated soils lead to difficulties. First, experiments have demonstrated that the effective stress equation is not single-valued (Jennings and Burland, 1962). Second, and more importantly, the incorporation of a material property in the description of the stress state within that material is in violation of the basic concepts of continuum mechanics (Fung, 1969). This is because such relations are in essence constitutive relations and not stress state equations.
- iv) Re-examination of the proposed effective stress equations had led many researchers to suggest the use of independent stress state variables, e.g., $(\sigma - u_w)$

and $(u_a - u_w)$, to describe the mechanical behavior of unsaturated soils (Bishop and Blight, 1963; Burland, 1965; Aitchison, 1967; Brackley, 1971).

In the late 1970's, Fredlund and Morgenstern (1977) presented a theoretical stress analysis of an unsaturated soil on the basis of multiphase continuum mechanics. The analysis revealed that any two of three possible normal stress variables can be used to fully describe the stress state of an unsaturated soil. These stress state variables are:

- i) $(\sigma - u_a)$ and $(u_a - u_w)$;
- ii) $(\sigma - u_w)$ and $(u_a - u_w)$;
- iii) $(\sigma - u_a)$ and $(\sigma - u_w)$.

where,

- σ = total vertical stress,
- u_a = pore-air pressure,
- u_w = pore-water pressure.

It is worth noting that the stress state variables are expressed in terms of readily measurable physical quantities (i.e. normal stress, pore-air stress, and pore-water pressures). This makes the utilization of the proposed stress state variables in solving engineering problems an easy job once the in situ measurements of the physical quantities become available.

Although any two of the three possible combinations of the stress state variables can be used, however, the $(\sigma - u_a)$ and $(u_a - u_w)$ combination appears to be the best choice for two reasons (Fredlund and Rahardjo, 1993):

- i) The effects of a change in total stress, σ , can be separated from the effects caused by a change in pore-water pressure, u_w ;

- ii) Pore-air pressure is atmospheric (i.e. $u_a = 0$ gauge pressure) for most practical engineering problems and as such serves as an excellent reference for both the total stress and pore-water pressure.

The aforementioned stress state variables for unsaturated soils have been experimentally tested and verified (Fredlund, 1973).

3.4 Theory and Components of Soil Suction

The significance of soil suction in explaining the mechanical behavior of unsaturated soils relative to engineering problems was first recognized by a group of researchers at the Road Research Laboratory in London in the early 1950's (Croney and Coleman, 1948; and Croney, Coleman and Lewis, 1950). This is followed, in 1965, by the adoption of the review panel for the soil mechanics symposium, "Moisture Equilibrium and Moisture Changes in Soils", of the quantitative definitions of soil suction and its components (Aitchison, 1965).

From a thermodynamic standpoint, soil suction is defined as the free energy state of soil water (Edlefsen and Anderson, 1943). The free energy of the soil water can be measured in terms of the partial vapor pressure of the soil water (Richards, 1966). The equation that governs the relationship between soil suction and the partial pressure of the pore-water vapor is known as the Kelvin's equation and is expressed as follows (Fredlund and Rahardjo, 1993):

$$\psi_T = \frac{RT}{V_{wo} W_v} \ln \left(\frac{\bar{u}_v}{u_{vo}} \right) \quad (3.6)$$

where,

ψ_T = soil or total suction (kPa),

R = universal gas constant (=8.3143231 mol K),

- T = absolute temperature in °Kelvin ($T = (t + 273) ^\circ\text{K}$),
 t = temperature in °C,
 v_{wo} = specific volume of water or the inverse of the water density
 (i.e. $1/\rho$) (m^3/kg),
 ρ_w = water density (kg/m^3),
 w_v = molecular mass of water vapor (=18.016 kg/Kmol),
 \bar{u}_v = partial pressure of pore-water vapor (kPa),
 \bar{u}_{v0} = saturation pressure of pure water vapor over a flat surface of pure
 water at the same temperature as that of the pore-water vapor (kPa).

The term $\left(\frac{\bar{u}_v}{\bar{u}_{v0}}\right)$ is called the relative humidity, RH%. By combining all constant terms in equation 3.6 into one constant, say C, this equation can be re-written as follows:

$$\psi_T = C \ln \left(\frac{\bar{u}_v}{\bar{u}_{v0}} \right) \quad (3.7)$$

The relation between suction, ψ_T , and relative humidity, $\left(\frac{\bar{u}_v}{\bar{u}_{v0}}\right)$, is depicted in Figure 3.3. From Figure 3.3 and equation 3.7 above, it is clear that at RH% of 100% $\psi_T = 0$. At RH% less than 100%, suction will be present in the soil. Also, extremely high suction values are experienced for RH% > 90% and < 100%. For example, at a reference temperature of 20 °C, the constants in equation 3.6 give a suction range of 1350 kPa - 13500 kPa for RH% of 90.5% to 99%, respectively. This is the range of soil suction usually encountered in compacted cohesive subgrade soil that is used as a foundation layer in roadway construction.

The soil suction expressed by equation (3.6) above is called the total suction. Total suction has two components usually referred to as matric and osmotic suctions. The definitions of total, matric and osmotic suctions as quoted by the International Society of Soil Science are as follows (Aitchison, 1965):

Total suction or free energy of the soil water — In suction terms, it is the equivalent suction derived from the measurement of the partial pressure of the pore-water vapor in equilibrium with free pure water.

Matric or capillary component of free energy of the soil water — In suction terms, is the equivalent suction derived from the measurement of the partial pressure of the water vapor in equilibrium with the soil water, relative to the partial pressure of the water vapor in equilibrium with a solution identical in composition with the soil water.

Osmotic (or solute) component of free energy of the soil water — In suction terms, it is the equivalent suction derived from the measurement of the partial pressure of the water vapor in equilibrium with a solution identical in composition with the soil water, relative to the partial pressure of water vapor in equilibrium with free pure water.

From the above definitions, it is clear that total suction is the free energy of soil water while matric and osmotic suctions are the components of the free energy i.e.

$$\psi_T = \psi_m + \psi_\pi \quad (3.8)$$

where,

$$\psi_m = \text{matric suction (i.e. } \psi_m = u_a - u_w), \text{ and}$$

$$\psi_\pi = \text{osmotic suction (sometimes referred to as } \pi)$$

Therefore, equation (3.8) can be written as:

$$\psi_T = (u_a - u_w) + \pi \quad (3.9)$$

The assertion that total suction equals the sum of matric and osmotic suctions has been experimentally verified (Fredlund and Krahn, 1972; and Edil and Motan, 1984). Also, researchers found that a unique relationship exists between matric suction and soil water content irrespective of the soil dry density (Croney and Coleman, 1960; and Fredlund and Krahn, 1972). Box and Taylor (1961) used null-point tensiometer and showed that at constant water contents, higher densities resulted in a decrease of matric suction. However, the variations appear to be small that from an engineering point of view they could be neglected. The work of Olson and Langfelder (1965) further substantiated the findings of Croney and Coleman (1960) and Fredlund and Krahn (1972).

3.5 Thermal Properties of Frozen and Unfrozen Ground

It is a fact that the engineering properties of unsaturated soils are affected by the amount of moisture present in these materials. Also, the phase composition of water in frozen soils, i.e. ratio of unfrozen water to ice, plays an important role in defining the engineering properties of such soils.

In unfrozen soils, the main forces acting on the soil water are those due to capillarity and adsorption (Hoekstra, 1969). Capillary forces are surface tension forces created at the water-air interfaces due to difference in pressure between the two phases. On the other hand, adsorption forces are those emanating from negatively charged soil particles. The latter forces tend to attract and keep in close contact to the soil particles a thin film of water. This type of adsorbed water is strongly bound to the surfaces of the soil particles and have distinctively different characteristics than those of the remaining soil water. In the unfrozen state, the effect of temperature on both surface tension forces and adsorption forces is either small or difficult to quantify. Consequently, the effect of temperature on the value of engineering properties of unfrozen soils is usually neglected in practice.

The behavior of frozen soils, on the other hand, is highly temperature-dependent because temperature tends to change the interaction of water with soil, and also the ratio of the remaining unfrozen water to ice.

In this section, some considerations pertaining to ground freezing and definitions of some essential thermal properties of soils and other materials (usually used for constructing soil suction measuring devices) will be given.

3.5.1 Theory of Soil Freezing

In fine-grained soils, freezing of the soil water does not occur at a single freezing temperature but rather over a wide range of negative temperatures below 0°C (Lovell, 1957; Williams, 1964a; Hoekstra, 1969). As the soil freezes, the soil water occupying the larger soil pores starts turning into ice. This is then followed by the gradual freezing of the adsorbed water adjacent to soil particles as the temperature drops further below 0°C . This results in a decrease in the thickness of the unfrozen film. Hoekstra (1969) reported that the unfrozen adsorbed water can coexist in equilibrium with the ice formed over a wide temperature range below freezing. In other words, the ice phase at each freezing temperature is in equilibrium with the unfrozen water layer whose properties are constantly changing as the temperature is lowered.

Nersesova and Tsytoich (1966) found that three types of water exist in frozen ground: ice, strongly-bound water, and water, depending on temperature, that may be either frozen or unfrozen.

As freezing progresses and ice starts forming, it becomes more difficult to freeze the remaining water due to increased adsorptive forces on the thinning unfrozen water film. This is further augmented by the increase in salt concentration of the remaining unfrozen water (this is because when ice is formed, it does not contain within its

crystalline structure any salt constituents which means that the concentration of salts in the remaining unfrozen water will increase). The result of the observed phenomenon will be a depression in the freezing point of the remaining unfrozen water (Schofield, 1935).

Several factors were reported in the literature (Hoekstra, 1969) that influence the amount of unfrozen water content. Most important among these are:

- (a) temperature,
- (b) surface area of clay minerals,
- (c) salt content,
- (d) mineralogical composition of soil,
- (e) soil structure, and
- (f) external pressure.

Edlefsen and Anderson (1943) suggested that very little, if any, of the soil water, in frozen soil, is under reduced pressure, or suction. Rather, most of the soil water is under the influence of adsorption forces acting normally to the particles surfaces and resulting in raised pressure, i.e. positive pore pressure, in the adjacent water. Ice present in the frozen soil under these conditions will also be subjected to these pressures with the result being that of a depressed freezing point. They also believed that such adsorptive forces could be responsible for the suction in the soil.

Schofield (1935), on the other hand, believed that much of the soil water in a frozen soil is actually under a reduced pressure, or tension, but that the ice first formed would be under atmospheric pressure (i.e. zero gauge pressure). If such is the case then the result will again be that the freezing point of the remaining unfrozen water will be depressed because of the pressure difference between the ice and the liquid water content.

Williams (1964b) proved experimentally that Schefield's proposed explanation of what happens during soil freezing is the correct explanation. He further added that even when large quantities of ice are present for temperatures down to at least -1°C , the pressure on ice is still different from that on the remaining unfrozen water. Therefore, the development of this cryogenic suction is the real reason behind the observed phenomenon of freezing point depressions.

The presence of unfrozen water in frozen soils down to negative temperatures as low as -40°C (Farouki, 1985), is an important issue of concern in terms of the associated engineering properties of these soils. This importance motivated several researchers to find relationship(s) between the amount of the unfrozen water content and other soil strength indices. Williams (1964b) used calorimetric experiments and the soil water retention curve, soil suction-moisture content relationship, to relate the negative temperature at which a given unfrozen moisture content occurs and the suction corresponding to a similar moisture content at room temperature. He also found that the equilibrium freezing temperature associated with a particular amount of unfrozen water content is not significantly affected by the amount of ice already present.

Anderson and Tice (1972) showed that the amount of unfrozen water content is a function of the equilibrium freezing temperature. Anderson and Morgenstern (1973) postulated a power model for the relation between the freezing temperature and the amount of unfrozen water content. This relation is of the following form:

$$W_u = m\theta^n \quad (3.10)$$

where,

W_u = unfrozen water content

θ = equilibrium freezing temperature

m, n = characteristic soil parameters that can be determined experimentally.

Another relation, using regression analysis on phase composition data for a group of soils having widely varying properties and characteristics, was also reported by Anderson et al. (1973). This relation is of the form:

$$\ln W_u = a + b \ln S + c S^d \ln \theta \quad (3.11)$$

where,

W_u & θ = are as defined before

S = specific surface area of the soil

a, b, c, d = experimental constants of regression.

Black (1991) also derived an expression, for saturated frozen soils, relating the amount of the unfrozen water to the difference in pressure between the ice and the liquid phases as follows:

$$W_u = a(\phi_{iw})^b \quad (3.12)$$

where,

ϕ_{iw} = $u_i - u_w$

u_i = ice pressure

u_w = water pressure

a & b = regression constants that can be determined from experimental data

Another issue of concern pertaining to frozen soil strength characteristics is the development of the cryogenic suction, mentioned previously, as a result of freezing point depression phenomenon. Using traditional thermodynamic concepts and the phase diagram of water, a theoretical expression for determining this cryogenic suction can be derived.

A water phase diagram, shown in Figure 3.4, is a diagram that shows the three phases of water under different conditions of temperature and pressure. Three curves in this diagram are of special importance, namely: the fusion curve, the sublimation curve and the evaporation curve. The fusion curve is the one that is associated with the freezing and thawing processes. At a specified temperature, water and ice can co-exist under a given pressure as determined by the fusion curve. Using the concepts of thermodynamics, the slope of the fusion curve is given by the Clausius-Clapeyron equation (Miller, 1972; Law et al., 1968a & b):

$$\frac{\partial P}{\partial \theta} = - \frac{L}{\theta V_w} \quad (3.13)$$

where,

∂P = change in pressure

$\partial \theta$ = change in temperature

L = latent heat of fusion (= 333 kJ/kg) liberated when water turns to ice or heat absorbed when ice turns to water.

θ = temperature in degrees Kelvin

V_w = $1/\rho_w$ (where ρ_w is the mass density of water)

For a freezing soil, suction will develop as a consequence of the difference in pressure between the ice and the unfrozen water phases i.e. $\partial P = \partial (u_i - u_w)$, where u_i and u_w are as defined before. The development of this suction will be accompanied by a depression in the freezing point of the remaining unfrozen water i.e. $\partial \theta = (\theta - \theta_0) = \partial \theta_0$, where $\partial \theta_0$ is the freezing point depression. Thus equation (3.13) can be written as:

$$\frac{\partial (u_i - u_w)}{\partial \theta_0} = - \frac{L}{\theta_0 V_w} \quad (3.14)$$

where,

θ_0 = normal freezing temperature in Kelvin (i.e. 273.15 °K or 0°C).

According to Scheffield (1935), u_i is atmospheric or near atmospheric pressure (i.e. $u_i = 0$ gauge pressure). Substituting this in equation (3.14) then:

$$\partial(-u_w) = -\frac{L}{\theta_0 V_w} \cdot \partial\theta_0 \quad (3.15)$$

The term $\partial(-u_w)$ refers to the increase in soil suction as the freezing temperature θ_0 is lowered by $\partial\theta_0$ from 0°C . It can thus be concluded that soil freezing is a dehydration process that is analogous to the drying process that occurs in soils above 0°C . The unfrozen water content in frozen soils is comparable to the “adsorbed water” contained in air-dry soils at temperature above freezing (Tyutyunov, 1963). The ice crystals formed in frozen soils are analogous to the air pockets in air-dry unfrozen soil. And the cycles of freezing/thawing are like cycles of drying/wetting (Koopmans and Miller, 1966).

From the above discussion it is very evident that the engineering properties of frozen soils are strongly dependent on temperature. And since these properties are also linked to the amount of unfrozen water, then one could expect that the strength properties of frozen soils to change drastically over a relatively small temperature interval (zero to -10°C) (Hoekstra, 1969).

3.5.2 Thermal Properties Relevant to Soil Suction Measurement

Many soil scientists and agricultural engineers advocated the use of thermal characteristics of soils as indices of soil moisture and/or soil suction. In this section, definitions of some of the basic thermal properties pertaining to the theory of heat dissipation in a porous medium will be given.

One criticism pertaining to any method of measuring soil moisture based on applied heat is the fact that moisture will move away from the heat source. Shaw and Baver (1939), and Bloodworth and Page (1957), stated that the amount of movement depends upon both the temperature of the heat source and the length of time the heat is applied. These researchers further demonstrated that if both the amount of heat applied and the time interval during which that happens were chosen to be as small as possible,

then the corresponding moisture movement from the point where the heat is applied would be negligible.

In frozen and unfrozen soils, heat is transferred mainly by conduction i.e. the transfer of thermal energy on a molecular level. To this end, quantitative description of heat transfer by conduction can be performed using two independent thermal properties of the medium i.e.:

- (i) thermal conductivity, k , and
- (ii) heat capacity per unit weight, c .

The ratio (k/c) often appears in heat flow equations and is called thermal diffusivity. following are definitions of these parameters and some considerations associated with their use for soil suction (and/or moisture content) measurement.

Heat Capacity and Apparent Specific Heat of Soils

The heat capacity is defined as the amount of heat that is needed to raise the temperature of a unit mass of the material by 1°C . It is measured in $\text{kJ/kg } ^{\circ}\text{C}$.

The specific heat capacity is the ratio of the heat capacity of the material relative to that of water. For many substances, specific heat capacities are tabulated. These can also be expressed in terms of temperature as simple polynomial relationships (Anderson and Morgenstern, 1973).

For mixtures, the specific heat capacity of the mixture is the sum of the products of the specific heat capacities of the individual constituents and their respective weight fractions. For example, for unfrozen soils with x_s , x_w , and x_a as the respective weight proportions of soil particles, pore-water and pore-air, the specific heat capacity of the soil is:

$$c_a = c_s x_s + c_w x_w + c_a x_a \quad (3.16)$$

where,

c_s, c_w, c_a = are the specific heat capacities of soil solids, pore-water and pore-air, respectively.

For mixtures containing constituents that undergo phase changes, additional terms containing the appropriate latent heats of phase change multiplied by the respective mass fractions of these constituents suffice to describe the situation. For these materials, the term “apparent” specific heat capacity is usually used to emphasize that heat is not transferred in soils through conduction only. However, for practical purposes, other modes of heat transfer can be neglected (Frivik, 1980).

In a freezing soil, the amount of heat required to change the temperature of one gram of frozen soil over a temperature interval ΔT is given by (Anderson, 1966):

$$Q = (c_s x_s + c_i x_i + c_u x_u) \Delta T + \int_T^{T+\Delta T} L \left(\frac{\partial x_u}{\partial T} \right) \cdot \partial T \quad (3.17)$$

where,

c_s, c_i, c_u = are the specific heat capacities of soil solids, ice and unfrozen water, respectively.

x_s, x_i, x_u = are the respective mass proportions of solids, ice and unfrozen water.

L = latent heat of phase change of unfrozen water in Cal./gm

The last term in equation (3.17) is a term that takes into account the contribution of the latent heat involved when the phase composition changes with temperature. Now if the total amount of moisture in the soil prior to freezing is given by:

$$x_w = x_i + x_u \quad (3.18)$$

then substituting equation (3.18) in equation (3.17) and dividing by ΔT yields:

$$\frac{Q}{\Delta T} = c_s x_s + c_i (x_w - x_u) + c_u x_u + \frac{1}{\Delta T} \int_T^{T+\Delta T} L \left(\frac{\partial x_u}{\partial T} \right) \cdot \partial T$$

or,

$$c_a = c_s x_s + c_i (x_w - x_u) + c_u x_u + \frac{1}{\Delta T} \int_T^{T+\Delta T} L \left(\frac{\partial x_u}{\partial T} \right) \cdot \partial T \quad (3.19)$$

Equation (3.19) is an expression of the apparent specific heat capacity of frozen soils that undergo phase transformation. As it can be seen from this equation, apparent specific heats of frozen soils are significantly influenced by the latent heat of phase change. This conclusion was verified experimentally by Williams (1962 and 1964a). He also found that different values of the apparent specific heat are obtained depending on whether the soil is freezing or thawing.

Thermal Conductivity

Thermal conductivity, k , is defined as the amount of heat transferred in a unit time through a unit length of the material with a unit cross-sectional area under a unit temperature gradient (Fredlund and Rahardjo, 1991). It is a property that is used in classical heat transfer problems to describe heat flow in frozen ground (Anderson and Morgenstern, 1973). The units of measurement of k are Watts/metre °Kelvin (W/mK). typical values for k for soil solids, water, air (at 20°C and 1 atmosphere) and ice are: 2.9, 0.6, 0.026 and 2.24 W/mK, respectively (Fredlund and Rahardjo, 1991; Frivik, 1980). From these values it is clear that the conductivity of ice is about four times that of unfrozen water. Since the apparent thermal conductivity of the soil equals the sum of the products of the conductivities and volume fractions of the soil constituents i.e. solids, ice and water, then it is expected that as the soil freezes, the overall k of the soil increases.

Frivik (1980) stated that for a coarse material the conductivity changes almost instantaneously near 0°C, but for fine-grained materials with much unfrozen water content

below 0°C, the change in conductivity usually takes place over an interval. Johansen and Frivik (1980) proposed that the conductivity within the interval can be estimated from:

$$k = k_f + (k_u - k_f)\eta \quad (3.20)$$

where,

- k = conductivity in the interval
- k_f = frozen-state conductivity
- k_u = unfrozen-state conductivity
- η = ratio of the unfrozen water to total water content.

Kersten (1949) also found that the initial degree of saturation of the soil affects the ratio of the thermal conductivity below freezing to that above freezing. For high degrees of saturation, the thermal conductivity of the unfrozen soil, k_u , is expected to be lower than that when the soil is frozen, k_f , due to the fact that k_{ice} is four times that of unfrozen water. However, for low degrees of saturation, Kersten found that k_f is actually lower than k_u . This may be explained in view of the fact that at low moisture contents some of the effective bridge water between the soil particles is removed to form ice in the pores. the consequence of this is that the efficiency of heat conduction at the particle contact point decreases making k_f less than k_u (Farouki, 1985).

Thermal Diffusivity

The thermal diffusivity, α , is defined as the ratio of the thermal conductivity of the material to its volumetric specific heat capacity i.e.:

$$\alpha = \frac{k}{\rho c} \quad (3.21)$$

where,

- k, c = are as defined before
- ρ = mass density of the material (kg/m³)

Thermal diffusivity of the material is the property that controls the rate at which a temperature change spreads through a mass. The thermal diffusivity of ice is eight times

that of water (because $k_{ice} = 4 k_w$ & $c_{ice} = 0.5 c_w$). Therefore, heat conduction and dissipation in frozen soils occurs at a faster rate than that in unfrozen soils.

Hoekstra (1969) reported that both the thermal conductivity and specific heat capacity are temperature-dependent. This makes the diffusivity dependent on temperature as well.

Latent Heat

The latent heat is the heat or energy needed in a phase change. For water, it is called the latent heat of fusion when heat is liberated upon the formation of ice or when heat is absorbed upon the conversion of ice into water. The latent heat of fusion of water is 333 kJ/kg.

The latent heat of fusion plays an important role during the freezing and thawing of cohesive soils. Johansen (1977) reported that as water in fine-grained soils starts freezing gradually, its latent heat is released in stages. The result of this heat release will be a sudden change in the specific heat capacity immediately below the temperature at which freezing begins (see Figure 3.5 - Low et al., 1968a). This change in the specific heat capacity will be accompanied by a corresponding change in diffusivity (Hoekstra, 1969).

3.6 Measurement of Soil Suction

The successful application of the basic principles of unsaturated soil mechanics to highway engineering necessitates the accurate determination of the magnitudes of the stress state variables discussed in section 3.3 above. This involves measuring both the net normal stress, $(\sigma - u_a)$ resulting from traffic loading, and soil matric suction, $(u_a - u_w)$.

In the following sections of this chapter, a revision of available techniques for measuring soil suction both in the laboratory and in the field will be given. Although matric suction is the main parameter of concern in the current study, the review will include, for the purpose of completeness, techniques used for all types of suction measurements. For each category of suction measurements, the review will include i) the devices used, ii) the underlying working principle of each device and iii) the experience of the various researchers with these devices.

3.6.1 Measurement of Total Suction

Microclimatic changes in the vicinity of pavement structures produce changes in the water content of the foundation soil (i.e. the subgrade layer). As stated previously, initial water content of compacted soils appears to have direct relationships with the soil matric suction. On the other hand, the osmotic suction appears to be insensitive to changes in the soil water content (Fredlund and Krahn, 1972). As a result, a change in total suction can be representative of a change in the matric suction. Therefore, measurements of total suction are important particularly in the high suction range where matric suction measurements are difficult to obtain.

In this section, different techniques for performing total suction measurements will be reviewed. This includes both direct and indirect procedures.

3.6.1.1 Direct Measurement of Total Suction

Direct measurements of total suction involve the use of thermocouple psychrometers. When properly used, the psychrometer provides good estimates of the total suction present in the soil.

Thermocouple psychrometers are used to measure total soil suction up to a maximum suction of 8,000 kPa. Two basic types of thermocouple psychrometers exist.

These are the Peltier psychrometer and the wet-loop type psychrometer. Both types of psychrometers operate on the basis of temperature measurements between a non evaporating surface and an evaporating surface. The difference in temperature between these surfaces is then related to the relative humidity of the surrounding which in turn is related to total suction by means of equation (3.6) above.

The difference between the Peltier type and the wet-loop type psychrometers is in the manner by which the evaporating junction is wetted to induce evaporation. Further details on this subject can be found elsewhere (Fredlund and Rahardjo, 1993).

The Peltier psychrometer is the one that is most frequently used in engineering applications. Figure 3.6 shows a typical single-junction Peltier psychrometer. The principle of operation of Peltier psychrometers is based on the Seebeck and Peltier effects. Seebeck effect states that an electromotive force will be generated in a closed circuit of two dissimilar metals when the two junctions of the circuit have different temperatures (i.e. T and $(T + \Delta T)$). A microvoltmeter installed in the circuit will measure the Seebeck electromotive force as a function of the temperature difference between the two junctions.

The Peltier effect states that a current passed through a circuit of two dissimilar metals will cause one junction to become warmer while the other become cooler. Passing the current in the opposite direction will produce a reverse thermal condition at the two junctions. This phenomenon makes it possible to use the thermocouple for measuring relative humidity.

The application of the Seebeck and Peltier effects to measure soil total suction can be illustrated by Figure 3.5 with the following explanation (Fredlund and Rahardjo, 1993):

- i) The psychrometer suspended in a closed chamber containing the soil specimen is allowed to achieve isothermal equilibrium with the surrounding atmosphere. This is indicated by a zero voltage reading being registered in the microvoltmeter.
- ii) A small electrical current (i.e. 5mA) is passed through the psychrometer from the constantan wire (+ve) to the chromel wire(-ve) for a period of 15 seconds. The passage of the electric current in this direction causes the measuring junction to cool due to the Peltier effect. As the temperature at the measuring junction drops below the dew point corresponding to the surrounding atmosphere, water vapor starts condensing on the measuring junction. during the condensation process the temperature at the measuring junction remains at the corresponding dew point temperature.
- iii) At the end of the 15 second period of cooling, the Peltier current is terminated.
- iv) As soon as the cooling process is stopped, the condensed water on the measuring junction starts to evaporate back to the surrounding atmosphere. The temperature at the measuring junction starts to drop below the dew point temperature as evaporation begins. As a result, the microvoltmeter records the electromotive force on a strip chart recorder. According to the Seebeck effect, the generated electromotive force is a function of the temperature difference between the measuring junction and the reference junction. The microvolt reading increases rapidly to a maximum value which is a function of the relative humidity in the surrounding atmosphere. The drier the

atmosphere, the higher will be the microvolt output during the evaporation process.

- v) Having reached the maximum output corresponding to the maximum evaporative cooling, the microvolt output decreases rapidly to approach a zero reading. The decreasing outputs indicate that the temperature at the measuring junction is increasing back towards the ambient or the reference junction temperature.
- vi) The microvoltmeter reads a zero reading when the temperature at the measuring junction becomes equal to that of the reference junction.

Since thermocouple psychrometers produce measurements in terms of microvolt outputs, calibration curves relating these outputs to corresponding total suction are needed. The calibration procedure is normally conducted by suspending the psychrometer over a salt solution with a known osmotic suction and measuring the corresponding microvolt maximum reading. Repeating this procedure with different concentrations of the salt solute produces the needed calibration curve. It should be mentioned, however, that temperature constitutes an important consideration during psychrometer calibration. As a consequence of this, the calibration process results in a set of calibration curves corresponding to various temperatures, shown in Figure 3.8. The obtained calibration curves can then be used to estimate the total suction in soil specimens.

Psychrometers have been used successfully by several researchers (Fredlund and Krahn, 1972; Edil and Motan, 1984; Van der Raadt and Clifton, 1985) to measure total suction. The following constitutes the advantages of using thermocouple psychrometers:

- i) Capable of measuring high suctions in soils (range of 100 kPa to 8,000 kPa).

- ii) Highly accurate.
- iii) Relatively easy to calibrate and use.
- iv) Insensitive to changes in bulk density.

There are also disadvantages to using psychrometers, such as the following:

- i) Easily corroded by acidic soils (this makes the interpretation of the psychrometer response difficult and unreliable).
- ii) Relatively long response time (hours), particularly at low suction range.
- iii) A controlled temperature environment ($\pm 0.001^\circ\text{C}$) is needed for the measurements (this renders the utilization of psychrometers for in situ measurements useless due to significant temperature fluctuations generally occurring in the field).

3.6.1.2 Indirect Measurement of Total Suction

The technique known as the filter paper method can be used indirectly to measure the soil suction. The technique has been extensively used by several soil scientists and agronomists (Gardner, 1937; Fawcett et al., 1967; McQueen and Miller, 1968; and Al-Khafaf and Hanks, 1974), and to some degree by other researchers in the geotechnical engineering discipline (Ho, 1979; Ching and Fredlund, 1984; Gillen, 1985; and Van der Raadt and Clifton, 1985).

The filter paper method can be used to measure either the soil total suction (non-contact method) or the soil matric suction (contact method). The non-contact method involves suspending a dry filter paper above a soil specimen, vapor flow of water will then occur from the soil to the paper until equilibrium in the water content between the filter paper and the surrounding is achieved. After equilibrium is established, the water content in the filter paper is measured and total suction is inferred from this measurement. On the other hand, the contact method involves placing the filter paper in direct contact with the soil and measure water content of the filter paper after equilibrium is achieved. Soil

suction inferred from such measurement gives the matric suction of the soil specimen. Figure 3.9 illustrates both the contact and non-contact filter paper methods for measuring soil suction.

The measurement and calibration technique of the filter paper method is done in accordance with a tentative ASTM Standard procedure (ASTM Committee D18 on Soil and Rock). The steps of measurements of this procedure can be summarized as follows (Fredlund and Rahardjo, 1993):

- i) The filter papers are oven dried and then cooled and stored in a desiccant container.
- ii) A soil specimen is placed in a large container with most of the container space being filled with the soil to reduce time needed for equilibrium.
- iii) Two dry filter papers are placed on top of a perforated brass disc that is seated on the top of the soil specimen (non-contact method); alternatively, three stacked filter papers are placed in contact with the soil. Two of these papers are used to avoid contamination of the middle filter paper with the soil which will later be used in obtaining suction measurements (contact method).
- iv) The large container, containing the soil material and the filter papers, is sealed with plastic electrical tape. The whole assembly is then stored inside an insulated box.
- v) Suction is allowed to equilibrate for a minimum of seven days.
- vi) At the end of the equilibration time, the filter papers are taken out from the large container using a pair of tweezers and the water content of the papers are determined in a manner similar to the determination of the gravimetric water content of soil specimens.
- vii) Suction is then determined from the water content measurements using the filter paper calibration curve (A water content versus suction relationship).

It is worth mentioning that the calibration curve for the filter paper method is obtained using the same measurement steps described above and a salt solution of known osmotic suction values at different concentrations (a procedure similar to psychrometer calibration). Figure 3.10 shows a typical filter paper calibration curve (McQueen and Miller, 1968). In contrast to psychrometer calibration curves, the filter paper calibration curves always exhibit bilinearity as depicted in Figure 3.10.

Researchers' experience with the filter paper method proved satisfactory. However, the technique is highly user dependent and extreme caution should be exercised when measuring the water content of the filter paper. The latter consideration stems from the fact that filter papers have very small masses (each dry filter paper has a mass of about 0.52 grams) and with a water content of, for example, 30%, the mass of water is about 0.16 grams. As it can be seen, measurement of quantities of this nature should be done very precisely or otherwise unreliable estimates of soil suction will result.

The following are some advantages of the filter paper technique:

- i) The procedure is simple.
- ii) It is inexpensive since only filter papers are used as sensors for measurement.
- iii) Can measure either total or matric suction.
- iv) Can be used with a wide range of suction measurements (from a few kPa to several hundred thousands kPa).
- v) Can be used for both laboratory and field measurements.

The disadvantages of the method include:

- i) Non-contact method is the only procedure that can be assured for measuring total suction. However, under in situ conditions it is difficult to assure non-contact.
- ii) The procedure is extremely sensitive and user dependent.

3.6.2 Measurement of Osmotic Suction

As mentioned previously, osmotic suction results from the presence of salts and other impurities in soil pore-water. It also appears that osmotic suction is relatively constant at various water contents (Fredlund and Krahn, 1972; and Edil and Motan, 1984). Therefore, this type of soil suction is of little significance in highway engineering applications. Nonetheless, measurement techniques used for osmotic suction determinations will briefly be reviewed in this section for the purpose of completeness. Further, it is also possible to use osmotic suction measurements once they become available to infer matric suction values by subtracting the former measurements from total suction measurements.

Several procedures are available to obtain osmotic suction measurements. One procedure, known as the saturation extract procedure, consists of adding distilled water to a soil until the soil is in a near fluid condition. Some effluent is then drained off and its electrical conductivity is measured. Osmotic suction is then inferred from the conductivity measurement through the use of a calibration curve. This procedure is simple but it does not yield accurate measurement of the osmotic suction (Fredlund and Krahn, 1972).

A second procedure for determining osmotic suction measurements involves the use of the psychrometer. A psychrometer is placed over the fluid extract to measure its osmotic suction. This procedure also gives poor results (Fredlund and Krahn, 1972).

The use of the pore-fluid squeezing technique constitutes the third method that can be utilized to measure osmotic suction. This procedure proved superior to both the above-mentioned methods in producing reasonable measurements of osmotic suction. The steps involved in using this technique can be summarized as follows:

- i) The pore-water in the soil is extracted using a pore-fluid squeezer device which consists of a heavy-walled cylinder and piston squeezer. This device was first used by Manheim (1966).
- ii) The electrical conductivity of the extracted pore-water is then measured;
- iii) The osmotic suction is then inferred from the measured electrical conductivity using a calibration curve like the one displayed in Figure 3.11.

The squeezing technique appears to produce good results; however, the results seem to be affected to some degree by the magnitude of the extraction pressure applied (Fredlund and Krahn, 1972).

3.6.3 Measurement of Matric Suction

Measurement of the unsaturated soil negative pore-water pressure, or matric suction is central to the application of unsaturated soil mechanics to highway engineering. This is particularly true in areas experiencing large fluctuations in matric suction as a result of significant environmental changes (excessive wetting and drying and/or seasonal freezing and thawing).

In this section a comprehensive review of currently available techniques for measuring matric suction will be presented.

Matric suction can be measured either directly or indirectly. Direct measurements involve the use of high air entry discs for measuring the negative pore-water pressure. Examples of direct measurements are the tensiometer and the use of the axis-translation technique. On the other hand, the indirect method involves the use of several porous sensors for performing the measurements. Among the devices used for this type of measurements, are electrical resistivity and thermal conductivity sensors.

Measurement techniques that are going to be reviewed in this section include:

- i) Tensiometers.
- ii) Axis-translation technique.
- iii) Thermal conductivity sensors.

Electrical resistivity gauges and other types of indirect measurement devices can be referred to elsewhere (Berg, 1989; Nieber and Baker, 1989; and Nieber et al., 1991).

3.6.3.1 Direct Measurement of Matric Suction

Direct measurements of matric suction involve measuring the negative pore-water pressure within the soil mass using high air entry discs. A high air entry disc is a porous disc that has many small pores of relatively uniform size. The disc acts as a membrane between air and water, see Figure 3.12. High air entry discs are commonly made from ceramic material that consists of compressed and sintered kaolin.

The principle of operation of the high air entry disc was explained by Fredlund and Rahardjo (1993). This can be illustrated by reference to Figure 3.12 with the following explanation:

- i) As the high air entry disc becomes saturated with water, air cannot pass through the disc due to the ability of the contractile skin (i.e. air-water interface) to resist the flow of air.
- ii) The ability of the disc to resist the inflow of air through the contractile skin results from the surface tension, T_s , developed by the contractile skin. This contractile skin acts as a thin membrane joining the small pores of radius, R_s , on the surface of the ceramic disc.
- iii) The difference between the air pressure above the contractile skin and the water pressure below the contractile skin is defined as matric suction.
- iv) The maximum matric suction that can be maintained across the surface of the disc is called its air entry value, $(u_a - u_w)_d$, and is given by Kelvin's equation:

$$(u_a - u_w)_d = \frac{2T_s}{R_s} \quad (3.22)$$

where,

$(u_a - u_w)_d$ = air entry value of the ceramic disc

T_s = surface tension of contractile skin

R_s = radius of curvature of the contractile skin or the
radius of the maximum pore-size.

The air entry value of the ceramic disc is largely controlled by the radius of curvature, R_s . Therefore, by manipulating the size of the pores within the ceramic disc, different air entry values can be obtained. This is usually controlled by the preparation and sintering process used to fabricate the ceramic discs.

In using high air entry discs (either in tensiometers or in the axis-translation technique) for negative pore-water measurements, one should make sure that the ceramic disc is fully saturated with water. In addition to the fact that the water in the ceramic disc provides the necessary surface tension to be developed for measurement purposes, it is also essential since this water acts as a link between the pore-water in the soil and the water in the measuring system. In other words, the water in the saturated ceramic disc provides continuity between the pore-water in the soil and the water in the measuring system.

It should also be mentioned that during suction measurement, the air entry value of the ceramic disc should never be exceeded, otherwise air will diffuse through the disc and enter the measuring system. The presence of air in the measuring system causes erroneous suction measurements.

There are two commonly used techniques for performing the direct measurement of negative pore-water pressure. These are the tensiometer method and the axis-translation technique. Both methods involve the use of high air entry discs.

(a) The Tensiometer

The tensiometer utilizes a high air entry ceramic cup as the interface between the measuring system and the negative pore-water pressure in the soil. It can be used for both laboratory and field suction determinations.

The tensiometer consists of a porous ceramic cup attached to a pressure measuring device through a small pore tube. The tube is usually made of plastic because of its low heat conductivity and non-corrosive nature. A conventional tensiometer is shown in Figure 3.13. The pore tube and ceramic cup are filled with air-free water and inserted into a pre-cored hole until good contact is established between the tensiometer and the surrounding soil. After equilibrium is achieved between the water in the ceramic cup and the surrounding soil, the water in the tensiometer will have the same negative pore-water pressure as that existing in the soil. This negative pressure numerically equals the matric suction in the soil under atmospheric conditions (i.e. $u_a = 0$).

It should be mentioned that tensiometers cannot measure osmotic suction since the soluble salts in the soil can freely move through the ceramic cup.

The negative water pressure in the tensiometer tube can be measured by any one of the following:

- i) a water-mercury manometer
- ii) a vacuum gauge
- iii) an electrical pressure transducer

The system that provides for the greater gauge sensitivity is recommended for the following reasons (Fredlund and Rahardjo, 1993):

- i) will decrease the response time of the tensiometer;
- ii) will result in less water movement between the tensiometer and the surrounding soil which will in turn provide for more accurate measurements.

Also, ceramic cups with higher permeability are recommended for use since they result in a quicker response time for the tensiometer.

Tensiometers must be serviced before and after installation to ensure that:

- i) the ceramic cup is not plugged;
- ii) the system is free from air bubbles; and
- iii) the tensiometer response time is adequate.

The details of servicing tensiometers was described by Fredlund and Rahardjo (1993). Failure to adequately service the tensiometer before and after installation results in erroneous suction measurements and the possibility of breakage of the ceramic cup.

Several types of commercial tensiometers are available. To name a few, there are the jet fill tensiometers, the small tip tensiometers, the quick draw tensiometers and the Bourden - vacuum gauge tensiometers (Fredlund and Rahardjo, 1993).

A major disadvantage of the tensiometer is its inability to measure negative pore-water in excess of 90 kPa. This is due to the phenomenon of water cavitation at pressures equal to or greater than one atmosphere (i.e. zero absolute pressure or -100 kPa). As cavitation occurs, the measuring system becomes filled with air and water from the measuring system is forced into the soil. To overcome this difficulty, one can use either the osmotic tensiometer or the axis-translation technique. Details pertaining to the theory and use of the osmotic tensiometer can be found elsewhere (Peck and Rabbidge,

1969; and Bocking and Fredlund, 1979). The basic principles of the axis-translation technique will be presented in the next section.

In summary, the tensiometer is a good device for obtaining direct measurements of negative pore-water pressure provided that the following points are observed:

- i) measurements are restricted to soils having suction values in the range of 0 to 90kPa; and
- ii) adequate servicing of the device is performed before and after installation.

The advantages of the tensiometer are (Berg, 1989):

- i) Moderate response time (minutes).
- ii) High accuracy and precision.
- iii) Useful under conditions near saturation.
- iv) Adaptable to low temperatures.

(b) Axis-translation technique

Direct measurements of negative pore-water pressure can also be performed using the axis-translation technique. This technique can be used to perform the measurements on either disturbed or compacted specimens in the laboratory.

The axis-translation technique was first proposed by Hilf in 1948. This technique basically translates the origin of reference for the negative pore-water pressure from standard atmospheric conditions to an elevated air pressure at which equilibrium between the water in the measuring system and that in the unsaturated soil specimen is achieved. The technique was developed to resolve the problem of cavitation of the water in the measuring system as the negative pore-water pressure in the soil approaches -1 atmosphere (i.e. zero absolute pressure).

Many researchers used the axis-translation technique and reported good results (Olson and Langfelder, 1965; and Fredlund and Rahardjo, 1993).

The axis-translation technique can only be used in the laboratory. Furthermore, the technique is best suited for soils with a continuous air phase (Bocking and Fredlund, 1980). The presence of occluded air bubbles in the soil specimen can result in over-estimation of the matric suction. In addition, air diffusing through the high air entry disc can cause an under-estimation of the measured matric suction. This is because accumulated air bubbles beneath the high air entry disc makes the pressure approach atmospheric conditions and hence a reduction in measured suction results.

3.6.3.2 Indirect Measurement of Matric Suction

The indirect measurement of matric suction can be performed using any of several types of porous sensors. The electrical and thermal properties of the sensor are a function of the water content within the porous block of the sensor which is in turn a function of the matric suction.

Electrical properties of the porous block have been found to be sensitive to the presence of dissolved salts in the pore-water. On the other hand, thermal properties are free from such effects and are shown to be very little affected by variations in ambient temperature (Fredlund and Rahardjo, 1993). Therefore, the use of the thermal properties in performing the indirect measurements of matric suction is preferred over the use of the electrical properties. Only indirect matric suction measurements based on the thermal properties of the sensing device are described in the following sections of this chapter.

Principle of Operation of the Thermal Conductivity Sensor

The devices used for indirect measurements of matric suction through the utilization of their thermal properties are referred to as thermal conductivity sensors

(TCS's). A thermal conductivity sensor consists of a porous ceramic block that contains a heater coil and a temperature sensing circuit. A schematic diagram of a typical thermal conductivity sensor is shown in Figure 3.14. The thermal conductivity of the porous block of the sensor is a function of the amount of the water contained in the block. This water content is in turn a function of the matric suction applied to the block by the surrounding soil. Therefore, the thermal conductivity of the porous block can be calibrated with respect to the applied matric suction. The calibrated sensor can then be used to infer matric suction measurements using the calibration curve and the measured sensor response at equilibrium with the soil in question.

Fredlund and Rahardjo (1993) gave an excellent summary of the historical development of the thermal conductivity sensor. This development spanned the period from the late 1930's (Show and Baver, 1939) to the early 1980's (Johnston, 1942; Richards, 1955; Bloodworth and Page, 1957; Phene et al., 1971a & 1971b; and Lee and Fredlund, 1984). As a result of these efforts, several TCS's became commercially available. Two examples are the MCS 6000 sensor, manufactured by Moisture Control System Incorporated of Findlay, Ohio, and the AGWA-II sensor, developed by Agwatronics Incorporated of Merced, California.

The principle of operation of the thermal conductivity sensor utilizes the theoretical concepts of heat dissipation within a porous body. The steps of measurements can be summarized as follows (Fredlund and Rahardjo, 1993):

- i) First, a controlled amount of heat is generated by the heating element at the center of the ceramic block for a specified period of time (usually one minute).
- ii) A portion of the heat pulse generated will be dissipated throughout the block. The amount of heat dissipated is controlled by the amount of water present within the porous block. The change in the thermal conductivity of the sensor is directly

- related to the change in the water content of the block (i.e. more heat will be dissipated as the water content in the block increases).
- iii) The undissipated heat will result in a temperature increase (i.e. rise) at the center of the block. This temperature rise, measured by the sensing element after a specified period of time, is inversely proportional to the water content of the block. The measured temperature rise can be expressed in terms of either a voltage output or a difference in temperature output.
 - iv) The matric suction value is then inferred from the sensor's calibration curve using the corresponding sensor output.

Calibration of Sensors

The calibration of the thermal conductivity sensors is performed by applying a range of matric suction values to the sensors which are mounted in a calibration soil. The specifics of the calibration procedure are described in chapter 4. A modified pressure plate apparatus is used for calibration purposes (Wong et al., 1989; and Fredlund and Wong, 1989). The purpose of using a calibration soil is to provide continuity between the water phase in the porous block and the water in the high air entry pressure plate. Figure 3.15 shows the soil-water characteristic curve of the soil used in the calibration process as described by Fredlund and Wong (1989).

The calibration curves for the AGWA-II thermal conductivity sensors are typically non-linear. The non-linear response of the sensors is attributed to the pore size distribution of the ceramic porous block (Fredlund and Wong, 1989). Similar non-linear behavior was also observed in the calibration curves of the MCS 6000 sensors (Lee, 1983).

The AGWA-II sensors have been found to provide consistent, reproducible and stable output readings with time (Fredlund and Wong, 1989). The sensors have also been

found to be responsive to both the wetting and drying process. However, submergence in water for long periods of time may render the sensor inoperative. This effect which is irreversible is attributed to the intrusion of water inside the sealed electronics compartment within the porous block (Wong et al., 1989).

Performance of Thermal Conductivity Sensors

Several studies for measuring matric suction using thermal conductivity sensors have been completed (Picornell et al., 1983; Lee and Fredlund, 1984; Van der Raadt and Clifton, 1985; Curtis and Johnston, 1987; Van der Raadt, 1988; Sattler and Fredlund, 1989; Khogali et al., 1991; and Loi et al., 1992). The results from all these studies are encouraging and clearly demonstrate the great potential of the thermal conductivity sensors for measuring soil matric potential on a routine basis. However, extreme care should be exercised in handling the sensors during installation and further research is definitely needed to improve the quality of the ceramic material used for the construction of the porous block. In addition, a better seal around the electronics within the sensor can greatly reduce the risk of sensor failure particularly under saturation and/or flooding conditions.

3.7 Summary

The special significance water has for pavement systems stems from the fact that such structures are strongly associated with soils close to the ground surface. These soils are commonly unsaturated, experience large fluctuations in moisture content and are strongly influenced by environmental conditions.

In this chapter, the importance of using soil suction as a stress parameter for describing unsaturated soil behaviour is illustrated. The chapter constitutes a state-of-the-art review of the theory of soil suction. Basic fundamentals underlying the theory and the various techniques used for obtaining the measurements are given. For each device used

in suction measurements, the underlying working principle, range of application, limitations and advantages of usage have all been presented and discussed.

From the literature review, it is clearly evident that adequate theoretical background and appropriate technology are currently available for obtaining the different suction components for a wide spectrum of soil types. Of particular interest to highway applications is the measurement of the soil matric suction. The influence this has on the resilient characteristics of subgrade materials is the main reason for pursuing current research study.

The device of choice for matric suction measurements in the current investigation is the AGWA-II thermal conductivity sensor. The decision to use this device was made based on three reasons. First, the device has numerous merits and lends itself quite easily to suction measurement over a prolonged time period under different in situ climatic conditions. Second, monitoring and collection of the suction data can be performed using relatively simple portable devices (such as a portable personal computer). Third, other researchers' experience with the thermal conductivity sensor is quite encouraging and promising. In addition to the aforementioned reasons, the AGWA-II sensors are easy to obtain from the manufacturer and are relatively inexpensive.

The basic concepts of soil freezing and pertinent thermal properties of fine-grained soils were also reviewed. The utilization of this and other information pertaining to the behaviour of unfrozen unsaturated soils constitute the knowledge base that will be used later to interpret the temperature and soil matric suction measurements collected during the current investigation.

References

1. Aitchison, G.D. (1960), "*Relationship of Moisture Stress and Effective Stress Functions in Unsaturated Soils*," Pore Pressure and suction in Soils. Conference Organized by the British National Society of the International Society of Soil Mechanics and Foundation Engineering at the Institution of Civil Engineers, March 30-31, 1960. Butterworths, London, England, 1961, pp.47-52.
2. Aitchison, G.D. (1965), "*Moisture Equilibria and Moisture changes in Soils Beneath Covered Areas*," Statement of the Review Panel, Engineering Concepts of Moisture Equilibria and Moisture Changes in Soils, Butterworths, London, England, pp.7-22.
3. Aitchison, G.D. (1967), "*Separate Roles of Site Investigation, Quantification of Soil Properties and Selection of Operational Environment in the Determination of Foundation Design on Expansive Soils*," Proceedings of the Third Asian Regional Conference on Soil Mechanics and Foundation Engineering, Haifa, Israel.
4. AL-Khafaf, S. and R.J. Hanks (1974), "*Evaluation of the Filter Paper Method for Estimating Soil Water Potential*," Soil Science, Volume 117, No.4, pp. 194-199.
5. Anderson, D. M. (1966) "*Phase Composition of Frozen Montmorillonite-Water Mixtures from Heat Capacity Measurements*," Soil Science Society of America Proceedings, Vol. 30, pp.670-675.
6. Anderson, D. M. and A. R. Tice (1972), "*Predicting Unfrozen Water Contents in Frozen Soils from Surface Area Measurements*," Highway Research Record 393, pp. 12-18.
7. Anderson, D. M. and N. R. Morgenstern (1973), "*Physics, Chemistry and Mechanics of Frozen Ground: A Review*," Proceedings of Second International Conference on Permafrost, Yakutsk, U.S.S.R., North American Contribution, U.S. National Academy of Sciences, pp. 257-288.
8. Anderson, D. M., A. R. Tice and H. L. McKim (1973), "*The Unfrozen Water and the Apparent Specific Heat Capacity of Frozen Soils*," Proceedings of the Second International Conference on Permafrost, National Academy of Sciences, Washington, D.C., pp. 289-295.

9. Barden, L., A.O. Madedor and G.R. Sides (1969), "*Volume Change Characteristics of Unsaturated Clay*," Journal of the Soil Mechanics and Foundation Division, ASCE, Vol. 95, No. SM1, Proceedings Paper 6338, pp. 33-52.
10. Berg, R.L. (1989), "*Monitoring Pavement Performance in Seasonal Frost Areas*," Proceedings of the State of the Art Symposium of Pavement Response Monitoring Systems for Roads and Airfields, U.S. Army Corps of Engineers Cold Regions Research and Engineering Laboratory, Special Report 89-23, pp. 10-19.
11. Bishop, A.W. and G. Eldin (1950), "*Undrained Triaxial Tests on Saturated Sands and Their Significance in the General Theory of Shear Strength*," Geotechnique, Vol. 2, pp. 13.
12. Bishop, A.W. (1959), "*The Principle of Effective Stress*," Tecknisk Ukeblad, No. 39.
13. Bishop, A.W. and I.B. Donald (1961), "*The Experimental Study of Partly Saturated Soil in the Triaxial Apparatus*," Proceedings of the Fifth International Conference on Soil Mechanics and Foundation Engineering, pp. 13-21.
14. Bishop, A.W. and G.E. Blight (1963), "*Some Aspects of Effective Stress in Saturated and Unsaturated Soils*," Geotechnique, London, England, Vol. 13, pp. 177-197.
15. Bock, J. B. (1991), "*Interpreting Unconfined Unfrozen Water Content*," Sixth International Symposium on Ground Freezing, Beijing, People's Republic of China, Vol. 1, pp. 3-6.
16. Bloodworth, M.E. and J.B. Page (1957), "*Use of Thermistors for the Measurement of Soil Moisture and Temperature*," Soil Science Society of America Proceedings, Vol. 21, pp. 11-15.
17. Bocking, K.A. and D.G. Fredlund (1979), "*Use of the Osmotic Tensiometer to Measure Negative Pore Water Pressure*," Geotechnical Testing Journal, GTJODJ, Vol. 2, No. 1, pp. 3-10.
18. Bocking, K.A. and D.G. Fredlund (1980), "*Limitations of the Axis-Translation Technique*," Proceedings of the Fourth International Conference on Expansive Soils, Vol. I, pp. 117-135.
19. Box, L., J.E. and S.A. Taylor (1961), "*Influence of Soil Bulk Density on Matric Suction*," Soil Science of America Proceedings.
20. Brackley, I.J.A. (1971), "*Partial Collapse in Unsaturated Expansive Clay*," Proceedings, Fifth Regional Conference on Soil Mechanics and Foundation Engineering, South Africa, pp. 23-30.

21. Brown, R.W. and D.L. Bartos (1982), "*A Calibration Model for Screen-Caged Peltier Thermocouple Psychrometers*," U.S. Department of Agriculture, Research Paper INT-293.
22. Brown, R.W. and J.M. Collins (1980), "*A Screen-Caged Thermocouple Psychrometer and Calibration Chamber for Measurements of Plant and Soil Water Potential*," *Agronomy Journal*, Vol. 72, pp. 852-854.
23. Burland, J.B. (1964), "*Effective Stresses in Partly Saturated Soils*," discussion of "*Some Aspects of Effective Stress in Saturated and Partly Saturated Soils*," by G.E. Blight and A.W. Bishop, *Geotechnique*, London, England, pp. 65-68.
24. Burland, J.B. (1965), "*Some Aspects of the Mechanical Behaviour of Partly Saturated Soils*," *Moisture Equilibrium and Moisture Changes in Soils Beneath Covered Areas*, Butterworth, Sydney, Australia, pp. 270-278.
25. Ching, R.K.H. and D.G. Fredlund (1984), "*A Small Saskatchewan Town Copes with Swelling Clay Problems*," *Proceedings of the Fifth International Conference on Expansive Clays*, Adelaide, South Australia, pp. 306-310.
26. Coleman, J.D. (1962), "*Stress/Strain Relations for Partly Saturated Soils*," *Correspondence in Geotechnique*, London, England, Vol. 12, No. 4, pp. 348-350.
27. Croney, D. and J.D. Coleman (1948), "*Soil Thermodynamics Applied to the Movement of Moisture in Road Foundations*," *Proceedings of the Seventh International Conference on Applied Mechanics*.
28. Croney, D., J.D. Coleman and W.A. Lewis (1950), "*Calculation of the Moisture Distribution Beneath Structures*," *Cov. Eng. (L.)*, 45 (524).
29. Croney, D., J.D. Coleman and W.P.M. Black (1958), "*The Movement and Distribution of Water in Soil in Relation to Highway Design and Performance*," *Highway Research Board Special Report No. 40*, Washington, D.C.
30. Croney, D. and J.D. Coleman (1960), "*Pore Pressures and Suction in Soils*," *Pore Pressures and Suction in Soils Conference*, Butterworths, London, England.
31. Curtis, A.A. and C.D. Johnston (1987), "*Monitoring Unsaturated Soil Water Conditions in Groundwater Recharge Studies*," *Proceedings of International Conference on Measurement of Soil and Plant Water Status at Utah State University*, U.S.A., Vol. 1, pp. 267-274.
32. Davies, J.T. and E.K. Rideal (1963), "*Interfacial Phenomena*," Second Edition, Academic Press, New York, N.Y., U.S.A.

33. Edlefsen, N.E. and A.B.C. Anderson (1943), "*Thermodynamics of Soil Moisture*," Hilgardia, Vol. 15, No. 2, Berkeley, California, pp. 31-298.
34. Edil, T.B. and S.E. Motan (1984), "*Laboratory Evaluation of Soil Suction Components*," Geotechnical Testing Journal, GTJODJ, Vol. 7, No. 4, pp. 173-181.
35. Farouki, O.T. (1985), "*Ground Thermal Properties*," Thermal Design Considerations in Frozen Ground Engineering, Technical Council on Cold Regions Engineering Monograph, ASCE Publication, pp. 186-203.
36. Fawcett, R.G. and N. Collis-George (1967), "*A Filter Paper Method for Determining the Moisture Characteristics of Soil*," Australian Journal of Experimental Agriculture and Animal Husbandry, Vol. 7, April.
37. Fredlund, D.G. and J. Krahn (1972), "*On Total, Matric and Osmotic Suction*," Soil Science, Vol. 114, No. 5, November, pp. 339-348.
38. Fredlund, D.G. (1973), "*Volume Change Behaviour of Unsaturated Soils*," Ph.D. Thesis presented to the University of Alberta, Edmonton, Alberta, Canada.
39. Fredlund, D.G., A.T. Bergan and E.K. Sauer (1975), "*Deformation Characterization of Subgrade Soils for Highways and Runways in Northern Environments*," Canadian Geotechnical Journal, Vol. 12, No. 2, pp. 213-223.
40. Fredlund, D.G. and N.R. Morgenstern (1977), "*Stress State Variables for Unsaturated Soils*," Journal of the Geotechnical Engineering Division, ASCE, Vol. 103, No. GT5, pp. 447-466.
41. Fredlund, D.G. and D.K.H. Wong (1989), "*Calibration of Thermal Conductivity Sensors for Measuring Soil Suction*," ASTM Geotechnical Journal, GTJODJ, Vol. 12, Number 3, pp. 188-194.
42. Fredlund, D. G., J. K. Gan and H. Rahardjo (1991), "*Measuring Negative Pore Water Pressures in a Freezing Environment*," Transportation Research Record 1307, Washington, D.C., pp. 291-299.
43. Fredlund, D.G. and H. Rahardjo (1993), "*Soil Mechanics for Unsaturated Soils*," John Wiley & Sons Inc., 517 p.
44. Frivik, P. E. (1980), "*State-of-the-art. Ground Freezing: Thermal Properties, Modelling of Processes and Thermal Design*," Second International Symposium on Ground Freezing, Trondheim, Norway, pp. 115-134.

45. Fung, Y.C. (1969), *"A First Course in Continuum Mechanics,"* Prentice-Hall, Inc., Englewood Cliffs, N.J.
46. Gallen, P.M. (1985), *"The Measurement of Soil Suction Using the Filter Paper Method,"* M.Sc. Thesis, University of Saskatchewan, Saskatoon, Canada.
47. Gardner, R. (1937), *"A Method for Measuring the Capillary Tension of Soil Moisture Over a Wide Moisture Range,"* Soil Science, Vol. 43, No. 4, April.
48. Hilf, J.W. (1948), *"Estimating Construction Pore Pressures in Rolled Earth Dams,"* Second International Conference on Soil Mechanics and Foundation Engineering, Rotterdam, Vol. III, pp. 234-240.
49. Hoekstra, P.(1969), *"The Physics and Chemistry of Frozen Soils,"* Effects of Temperature and Heat on Engineering Behaviour of Soils, Highway Research Board Special Report 103, pp. 78-90.
50. Ho, D.Y.F. and D.G. Fredlund (1982), *"Increase in Strength Due to Suction for Two Hong Kong Soils,"* Conference on Engineering and Construction in Tropical and Residual Soils, Honolulu, Hawaii, U.S.A.
51. Jennings, J.E.D. (1961), *"A Revised Effective Stress Law for Use in the Prediction of The Behaviour of Unsaturated Soils,"* Pore Pressure and Suction in Soils Conference, Butterworths, London, England, pp. 26-30.
52. Jennings, J.E. and J.B. Burland (1962), *"Limitations to the Use of Effective Stresses in Partly Saturated Soils,"* Geotechnique, London, England, Vol. 12, No. 2, pp. 125-144.
53. Johansen, O. (1977), *"Thermal Conductivity of Soils,"* Draft Translation 637, U.S. Army Cold Regions Research and Engineering Laboratory, Hanover, N. H.
54. Johansen, O. and P. E. Frivik (1980), *"Thermal Properties of Soils and Rock Materials,"* Second International Symposium on Ground Freezing, Trondheim, Norway, Unpublished Paper.
55. Johnston, L.N. (1942), *"Water Permeable Jacketed Thermal Radiators as Indicators of Field Capacity and Permanent Wilting Percentage in Soils,"* Soil Science, Vol. 54, pp. 123-126.
56. Kersten, M. S. (1949), *"Laboratory Research for the Determination of the Thermal Properties of Soils,"* Technical Report 23, Arctic Construction and Frost Effects Laboratory, U. S. Army Engineer Division, New England, Waltham, Mass.
57. Khogali, W.E., K.O. Anderson, J.K. Gan and D.G. Fredlund (1991), *"Installation and Monitoring of Thermal Conductivity Suction Sensors in a Fine-Grained Subgrade Soil Subjected to Seasonal Frost,"* Proceedings of Conference on

Road and Airport Pavement Response Monitoring Systems, West Lebanon, New Hampshire, pp. 153-167.

58. Koopsman, R. W. R. and R. D. Miller (1966), "*Soil Freezing and Soil Water Characteristic Curves*," Proceedings of the Soil Science Society of America, Vol. 30, pp. 680-685.
59. Lee, R.K. and D.G. Fredlund (1984), "*Measurement of Soil Suction Using the MCS 6000 Gauge*," Proceedings, Fifth International Conference on Expansive Soils, The Institution of Engineers, Australia, pp. 50-54.
60. Lee, R.K.C. (1983), "*Measurement of Soil Suction Using the MCS Sensor*," M.Sc. Thesis, University of Saskatchewan, Saskatoon, Canada.
61. Loi, J., D.G. Fredlund, J.K.M. Gan and R.A. Widger (1992), "*Monitoring Soil Suction in an Indoor Test Track Facility*," Transportation Research Record 1362, Washington, D.C., pp. 101-110.
62. Lovell, C. W. (1957), "*Temperature Effects on Phase Composition and Strength of Partially Frozen-Soils*," Highway Research Board Bulletin 168, pp. 74-95.
63. Low, P. F., D. M. Anderson and P. Hoekstra (1968a), "*Some Thermodynamics Relationships for Soils at or Below the Freezing Point: 1. Freezing Point Depression and Heat Capacity*," Water Resources Res., Vol 4, pp. 379-394.
64. Low, P. F., D. M. Anderson and P. Hoekstra (1968b), "*Some Thermodynamics Relationships for Soils at or Below the Freezing Point: 2. Effects of Temperature and Pressure on Unfrozen Soil Water*," Water Resources Res., Vol 4, No. 3, pp. 541-544.
65. Manheim, F.T. (1966), "*A Hydraulic Squeezer for Obtaining Interstitial Water from Consolidated and Unconsolidated Sediment*," U.S. Geological Survey Prof. Paper 550-C, pp. 256-261.
66. Matyas, E.L. and H.S. Radhakrishna (1968), "*Volume Change Characteristics of Partially Saturated Soils*," Geotechnique, London, England, Vol. XVIII, No. 4, pp. 432-448.
67. McQueen, I.S. and R.F. Miller (1968), "*Calibration and Evaluation of a Wide Range Method for Measuring Moisture Stress*," Soil Science, Vol. 106, No. 3, pp. 225-231.
68. Miller, R. D. (1972), "*Freezing and Heaving of Saturated and Unsaturated Soils*," Highway Research Record 393, Washington, D.C., pp. 1-11.

69. Nersesova, A. A. and N. A. Tsytovich (1966), "*Unfrozen Water in Frozen Soils*," Proceedings of the International Conference on Permafrost, National Academy of Sciences, Washington, D.C., pp. 230-234.
70. Nieber, J.L. and J.M. Baker (1989), "*In-Situ Measurement of Soil Water Content in the Presence of Freezing/Thawing Conditions*," First Symposium on the State of the Art of Pavement Response Monitoring Systems for Roads and Airfields, New Hampshire, CRREL Special Report 89-23, pp. 45-62.
71. Nieber, J.L. J.M. Baker and E. Spaans (1991), "*Evaluation of Soil Water Sensors in Frozen Soils*," Proceedings of Conference on Road and Airport Pavement Response Monitoring Systems, West Lebanon, New Hampshire, pp. 168-181.
72. Olson, R.E. and L.J. Langfelder (1965), "*Pore Pressures in Unsaturated Soils*," Journal of Soil Mechanics and Foundations Division, ASCE, Vol. 91, SM4.
73. Peck, A.J. and R.M. Rabbidge (1969a), "*Direct Measurement of Moisture Potential: A New Technique*," in Proceedings of the UNESCO-Netherlands Government Symposium on Water in the Unsaturated Zone, UNESCO, Paris, pp. 165-170.
74. Peck, A.J. and R.M. Rabbidge (1969b), "*Design and Performance of an Osmotic Tensiometer for Measuring Capillary Potential*," Proceedings of the Soil Science Society of America, Vol. 33, No. 2 March-April, pp. 196-202.
75. Phene, C.J., G.J. Hoffman and S.L. Rawlins (1971a), "*Measuring Soil Matric Potential In-Situ by Sensing Heat Dissipation Within A Porous Body: I. The Theory and Sensor Construction*," Soil Science Society of America, Vol. 35, pp. 27-33.
76. Phene, C.J., G.J. Hoffman and S.L. Rawlins (1971b), "*Measuring Soil Matric Potential In-Situ by Sensing Heat Dissipation Within A Porous Body: II. Experimental Results*," Soil Science Society of America, Vol. 35, pp. 225-229.
77. Picornell, M., R.L. Lytton and M. Steinberg (1983), "*Matrix Suction Instrumentation of a Vertical Moisture Barrier*," Transportation Research Record 945, TRB, National Research Council, Washington, D.C., pp. 16-21.
78. Rahardjo, H., H. Loi and D.G. Fredlund (1989), "*Typical Matric Suction Measurements in the Laboratory and the Field Using Thermal Conductivity Sensors*," Indian Geotechnical Conference - '89, Visakhapatnam, India.
79. Rendulic, L. (1936), "*Discussion on Relation Between Void Ratio and Effective Principal Stresses for a Remoulded Silty Clay*," Proceedings, First International Conference on Soil Mechanics and Foundation Engineering, Cambridge, Vol. 3, pp. 48-51.

80. Richards, L.A. (1966), *"A Soil Salinity Sensor of Improved Design,"* Soil Science Society of America Proceedings, Vol. 30, pp. 333-337.
81. Richards, B.G. (1966), *"The Significance of Moisture Flow and Equilibria in Unsaturated Soils in Relation to the Design of Engineering Structures Built on Shallow Foundations in Australia,"* Symposium on Permeability and Capillarity, American Society for Testing Materials (ASTM), Atlantic City, N.J.
82. Sattler, P.J. and D.G. Fredlund (1989), *"Use of Thermal Conductivity Sensors to Measure Matric Suction in the Laboratory,"* Canadian Geotechnical Journal, Vol. 26, No. 3, pp. 491-498.
83. Schofield, R.K. (1935), *"The pF of Water in Soils,"* Trans. Third International Congress of Soil Science, Vol. 2, pp. 38-48.
84. Shaw, B. and L.D. Baver (1939), *"An Electrothermal Method for Following Moisture Changes of the Soil In-Situ,"* Soil Science Society of America Proceedings, Vol. 4, pp. 78-83.
85. Sisler, H.H., C.A. Vanderwerf and A.W. Davidson (1953), *"General Chemistry – A Systematic Approach,"* The MacMillan Company, New York, N.Y.
86. Skempton, A.W. (1961), *"Effective Stress in Soils, Concrete and Rocks,"* Pore Pressure and Suction in Soils, Butterworths, London, pp. 4.
87. Soilmoisture Equipment Corporation (1985), *"Commercial Publications,"* P.O. Box 30025, Santa Barbara, CA.
88. Terzaghi, K. (1936), *"The Shearing Resistance of Saturated Soils,"* Proceedings of the First International Conference on Soil Mechanics, Vol. 1.
89. Tyutvunov, I. A. (1963), *"Phase Transformations of Water in Soils and the Nature of Migration and Heaving,"* Proceedings of the First International Conference on Permafrost, Building Research Advisory Board, National Academy of Sciences, National Research Council, Washington, D.C., pp. 234-239.
90. U.S.D.A. Agricultural Handbook No. 60 (1950), *"Diagnosis and Improvement of Saline and Alkali Soils."*
91. Van der Raadt, P. and A.W. Clifton (1985), *"Soil Suction Measurement: Final Report,"* A Report prepared for CP Rail – Canadian National Railways, Transportation Development Centre.

92. Van der Raadt, P. (1988), *"Field Measurement of Soil Suction Using Thermal Conductivity Matrix Potential Sensors,"* M.Sc. Thesis, University of Saskatchewan, Saskatoon, Canada, 245 pp.
93. Van Haveren, B.P. and R.W. Brown (1972), *"The Properties and Behaviour of Water in the Soil-Plant-Atmosphere Continuum,"* in *Psychrometry in Water Relations Research*, R.W. Brown and B.P. Haveren, Eds., Utah Agricultural Experimental Station, Utah State University, Logan, pp. 1-27.
94. Williams, P. J. (1962), *"Specific Heats and Unfrozen Water Content of Frozen Soils,"* Proceedings of the First Canadian Conference on Permafrost, National Research Council of Canada, Technical Memorandum No. 76, pp. 109-126.
95. Williams, P. J. (1964a), *"Specific Heat and Apparent Specific Heat of Frozen Soils,"* Geotechnique, Vol. 14, No. 2, pp. 133-142.
96. Williams, P. J. (1964b), *"Unfrozen Water Content of Frozen Soils and Soil Moisture Suction,"* Geotechnique, Vol. 14, No. 3, pp. 231-246.
97. Wong, D.K.H. and A. Ho (1987), *"An Evaluation of a Thermal Conductivity Sensor for the Measurement of Soil Matrix Suction,"* A Report Submitted to the Saskatchewan Highways and Transportation Department, Regina, Saskatchewan, Canada.
98. Wong, D.K.H., D.G. Fredlund, E. Imre and G. Putz (1989), *"Evaluation of AGWA-II Thermal Conductivity Sensors for Soil Suction Measurements,"* Transportation Research Record 1219, pp. 131-143.

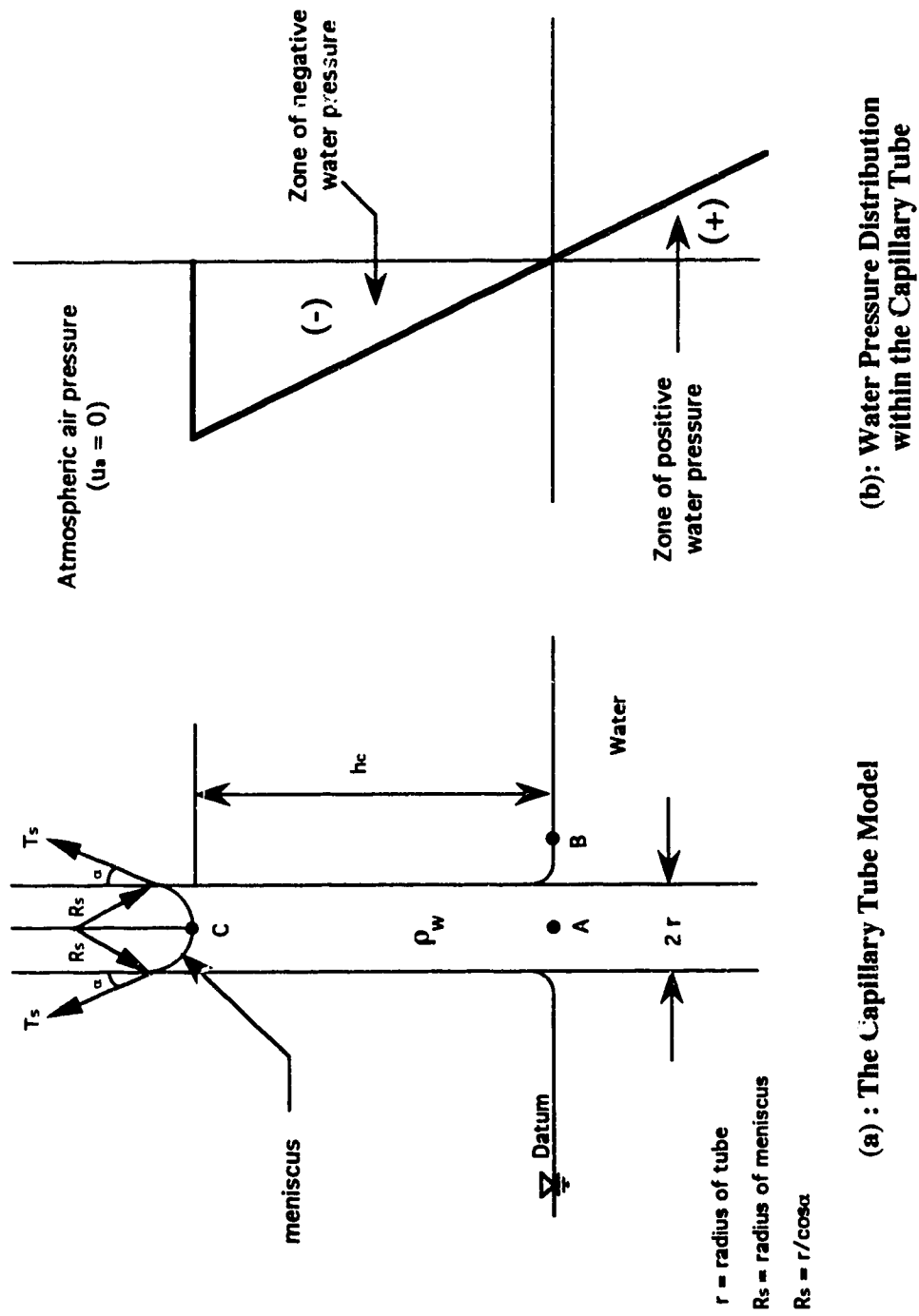


Figure 3.1: The Capillary Model and the Concept of Soil Suction
 (After Fredlund and Rahaijoo, 1993)

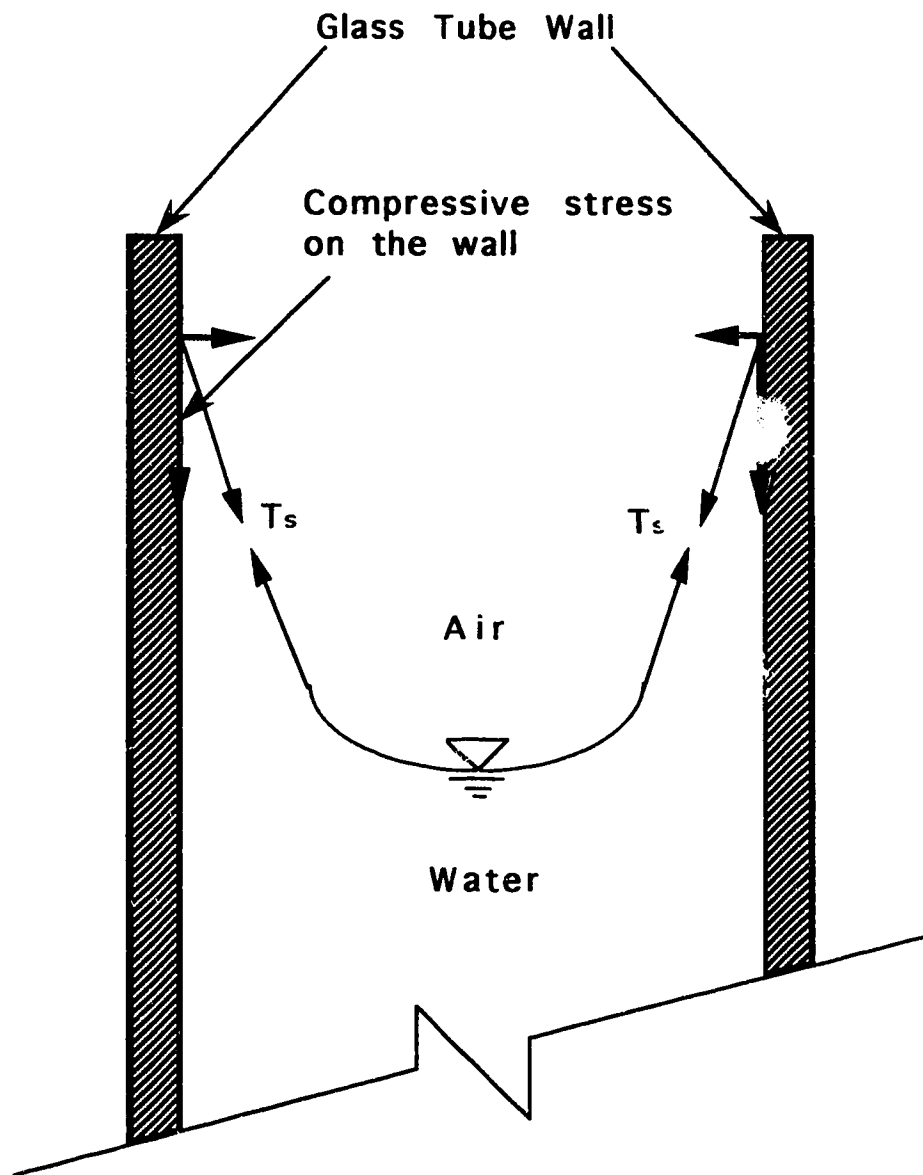


Figure 3.2: Compressive Forces on the Walls of a Capillary Tube
(After Fredlund and Rahardjo, 1993)

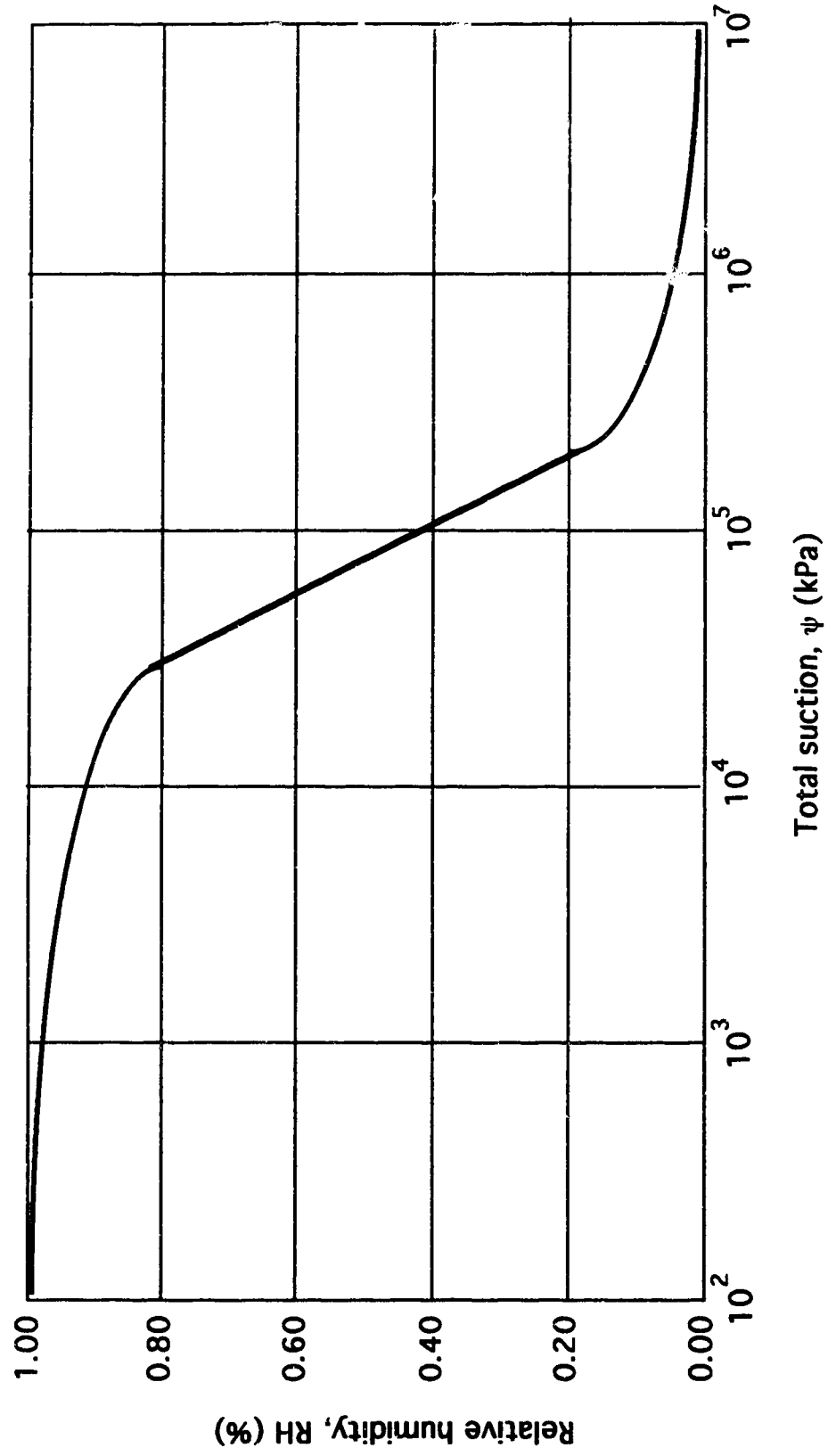


Figure 3.3: A Typical Relative Humidity - Total Suction Relationship

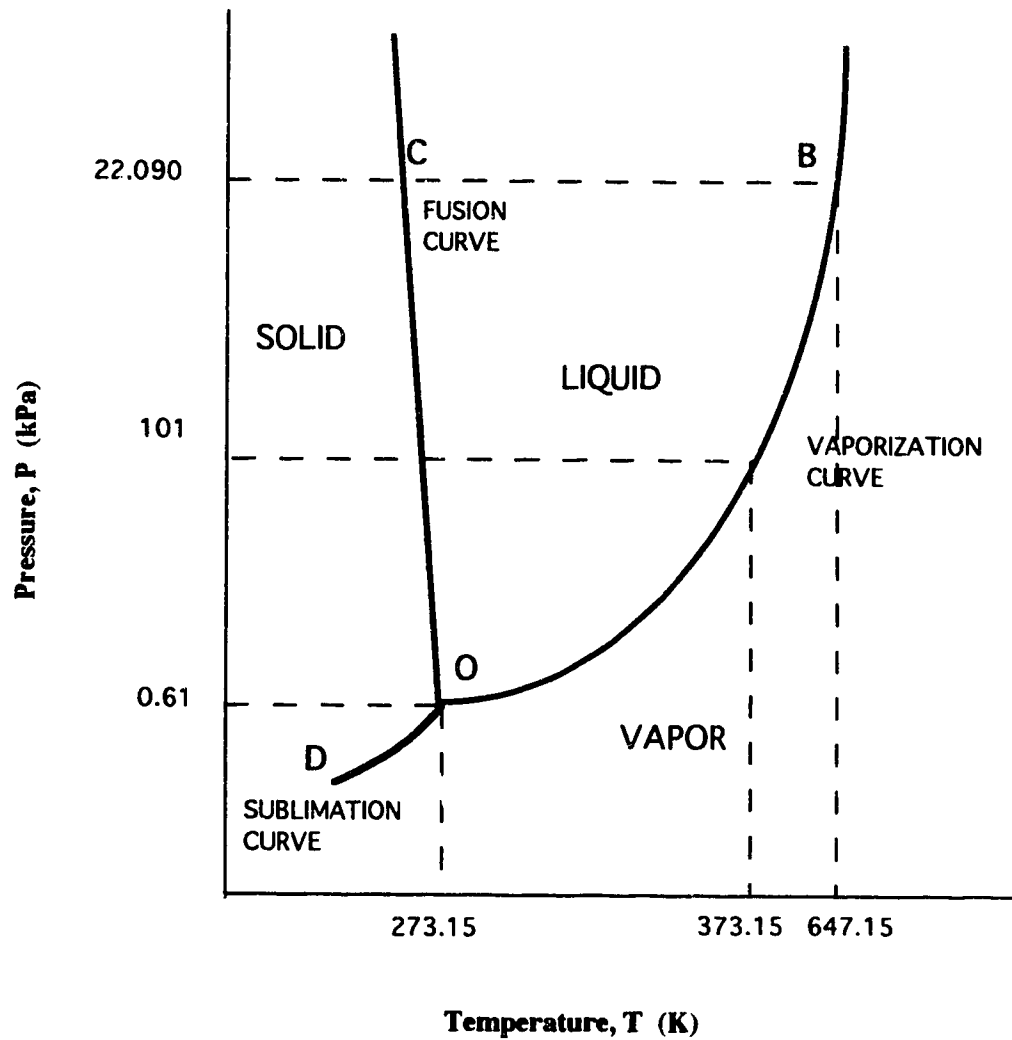


Figure 3.4: Water Phase Diagram (After Van Haveren and Brown, 1972)
(Not to Scale)

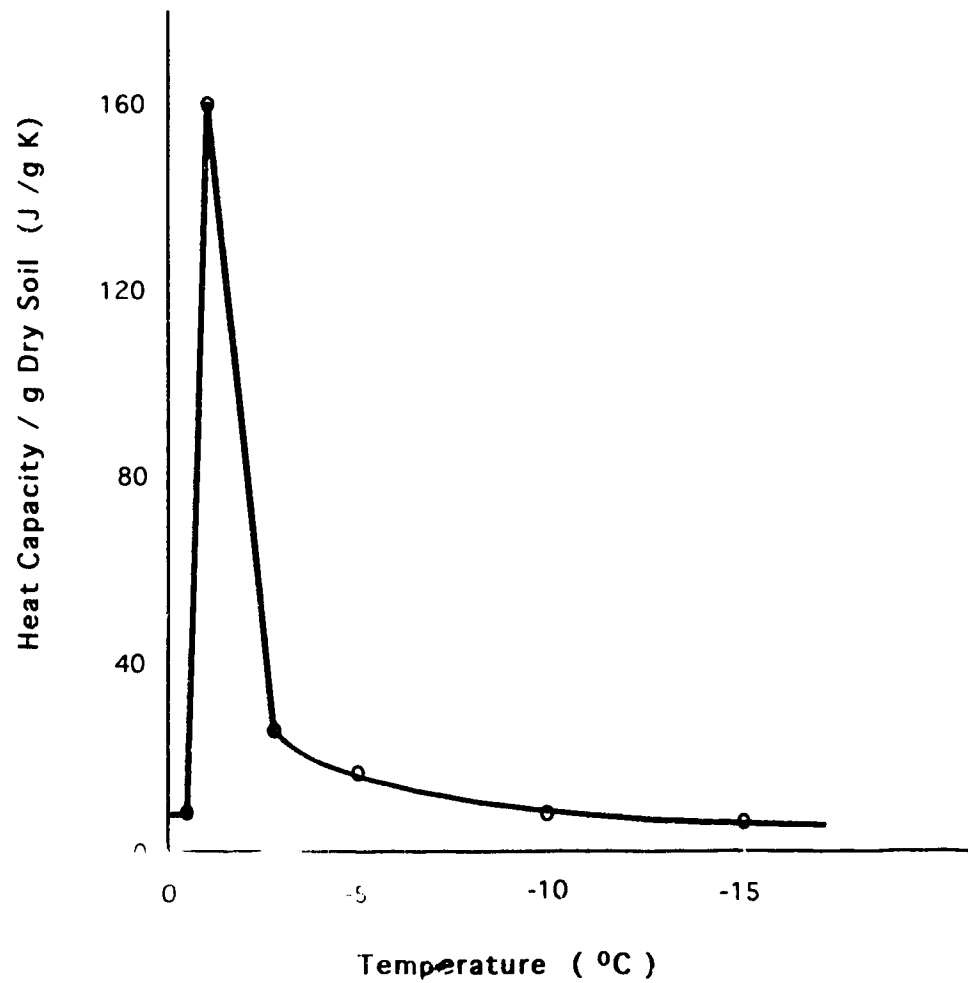


Figure 3.5: Heat Capacity - Temperature Relationship for a Partially Frozen Bentonite

(Modified after Low et al., 1968 a)

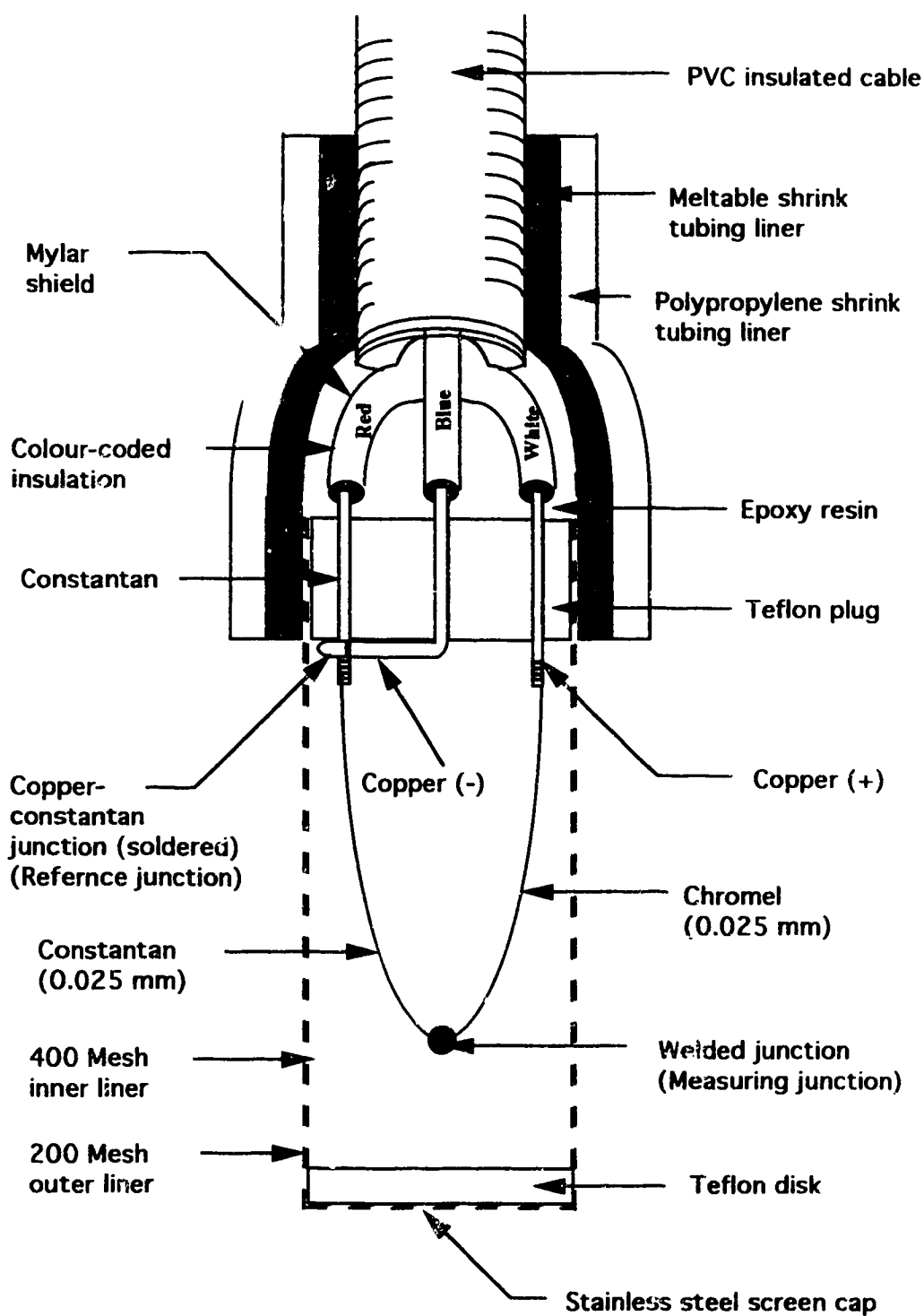


Figure 3.6: Screen-caged Single-junction Peltier Thermocouple Psychrometer
(After Brown and Collins, 1980)

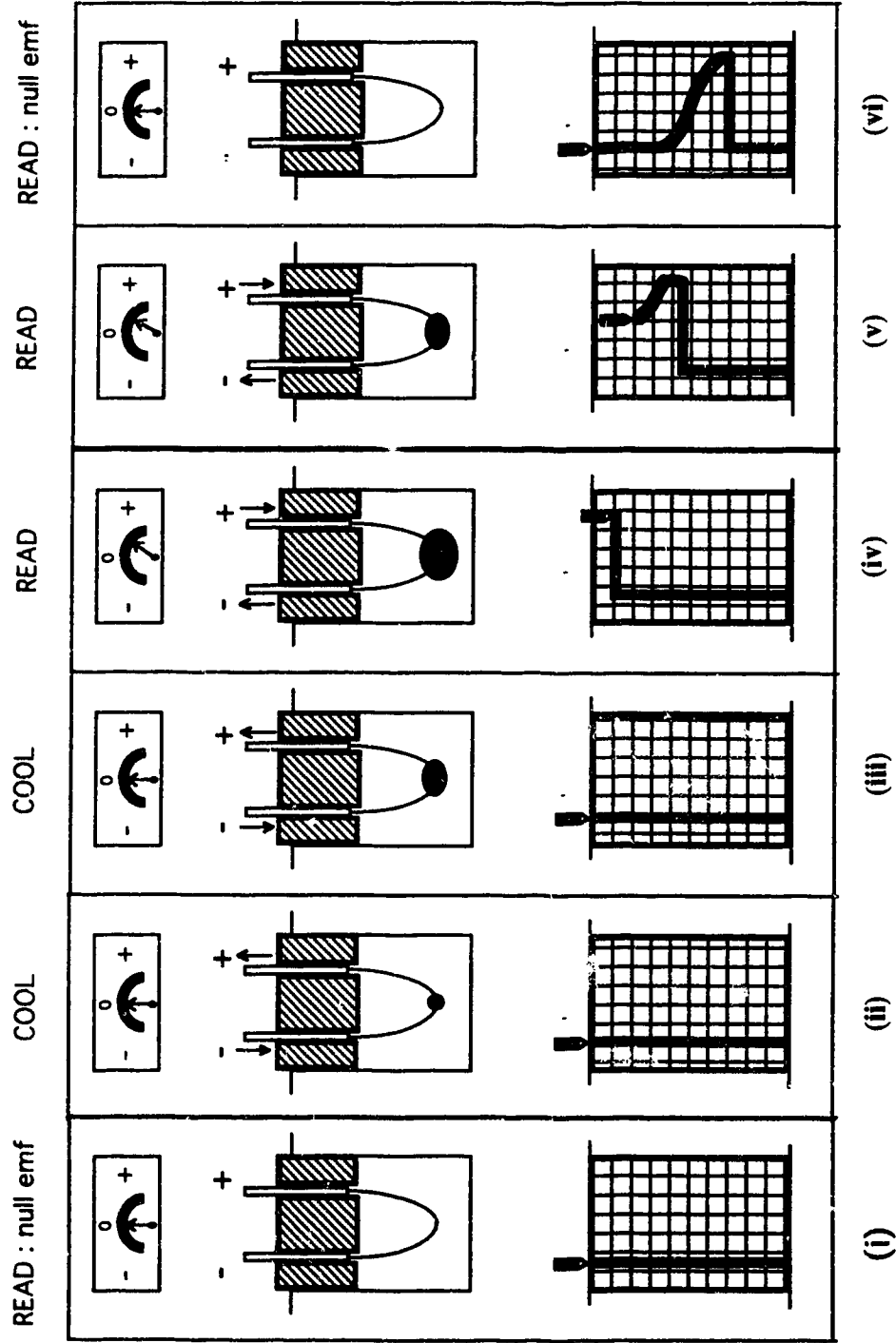


Figure 3.7: Principle of Operation of the Peltier Thermocouple Psychrometer

(After Van Haveren and Brown, 1972)

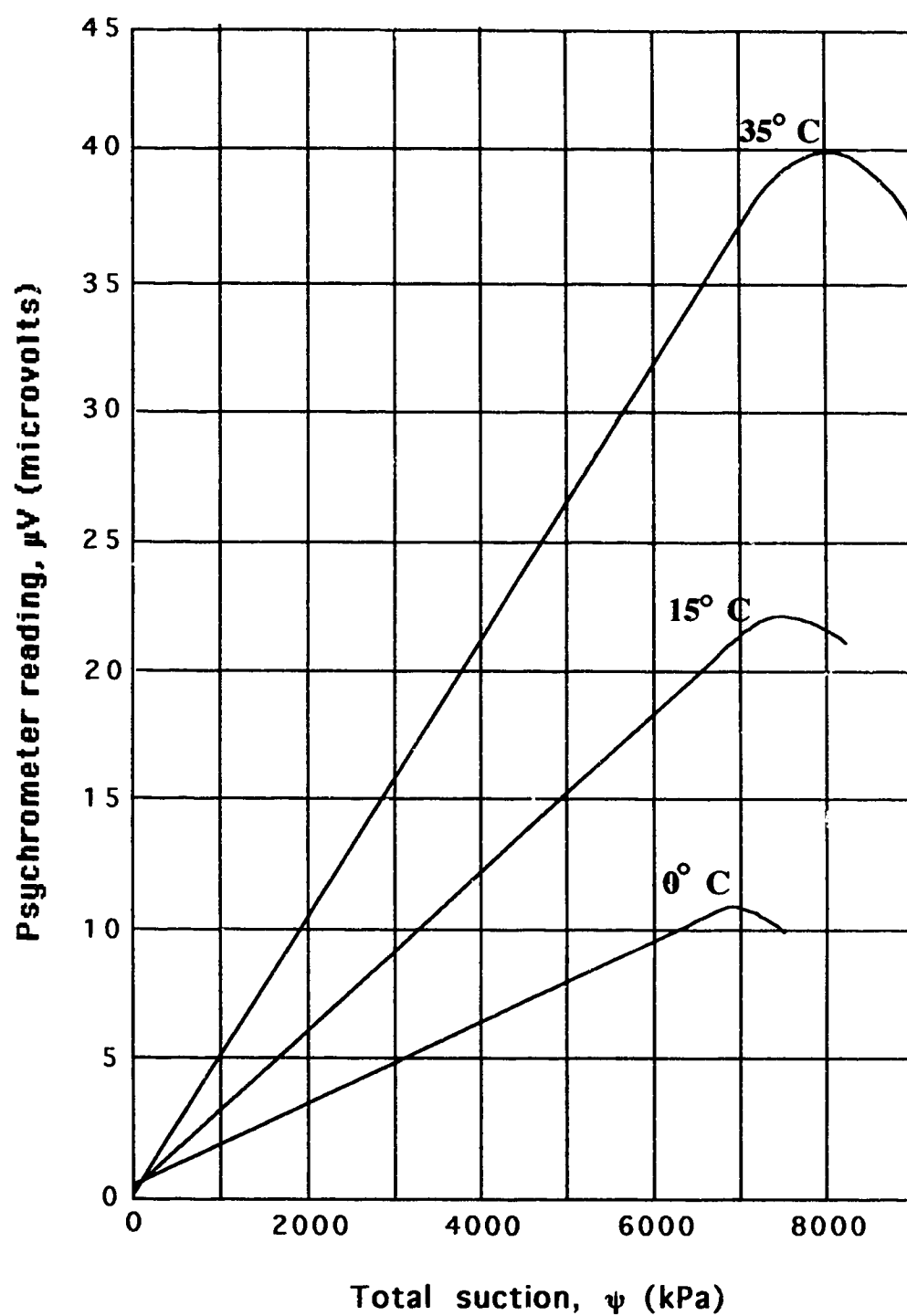


Figure 3.8: Typical Psychrometer Calibration Curves at Different Temperatures
(Modified after Brown and Bartos, 1982)

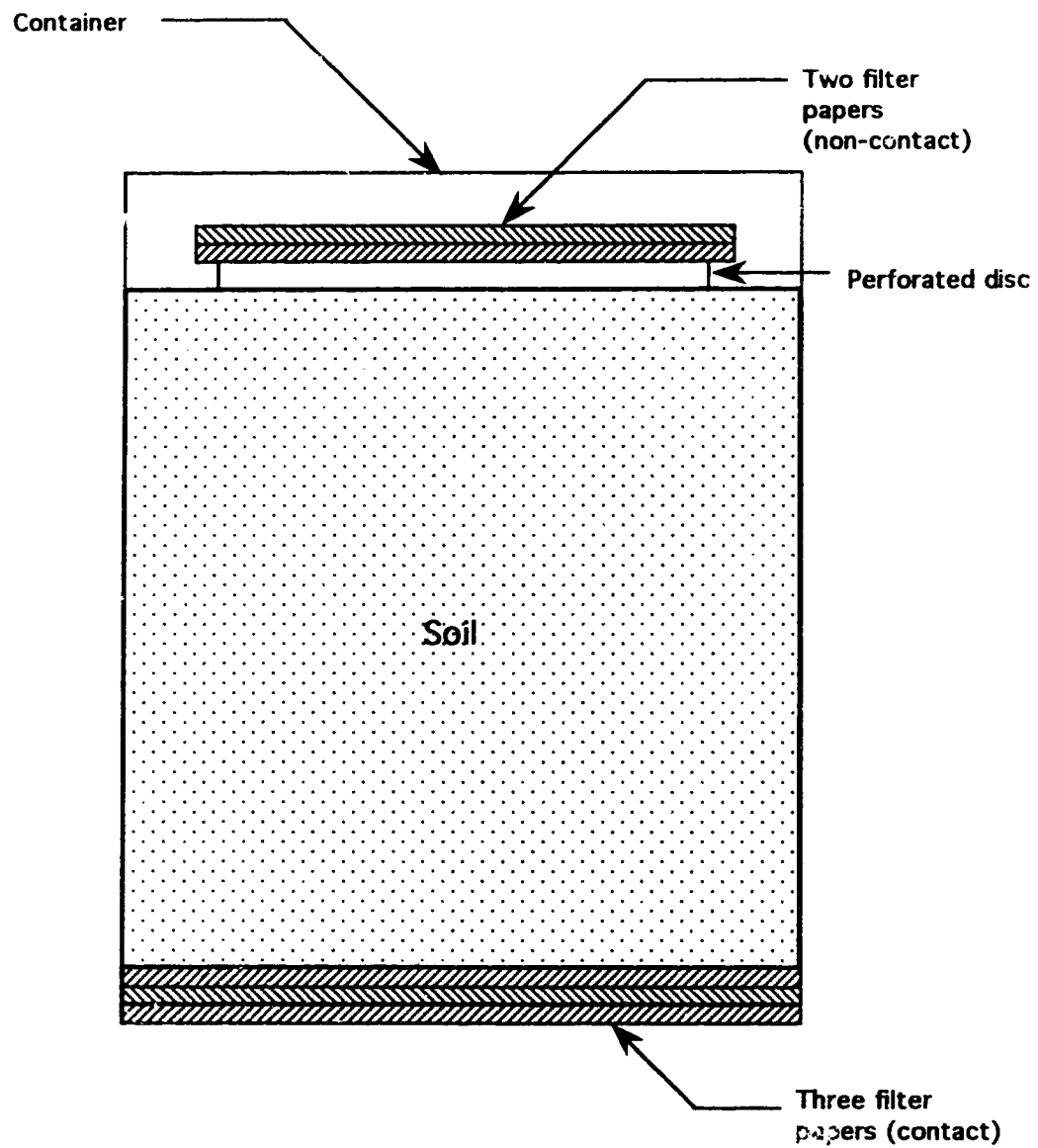


Figure 3.9: Filter Paper Methods for Measuring Total and Matric Suction
(After Al-khafaf and Hanks, 1974)

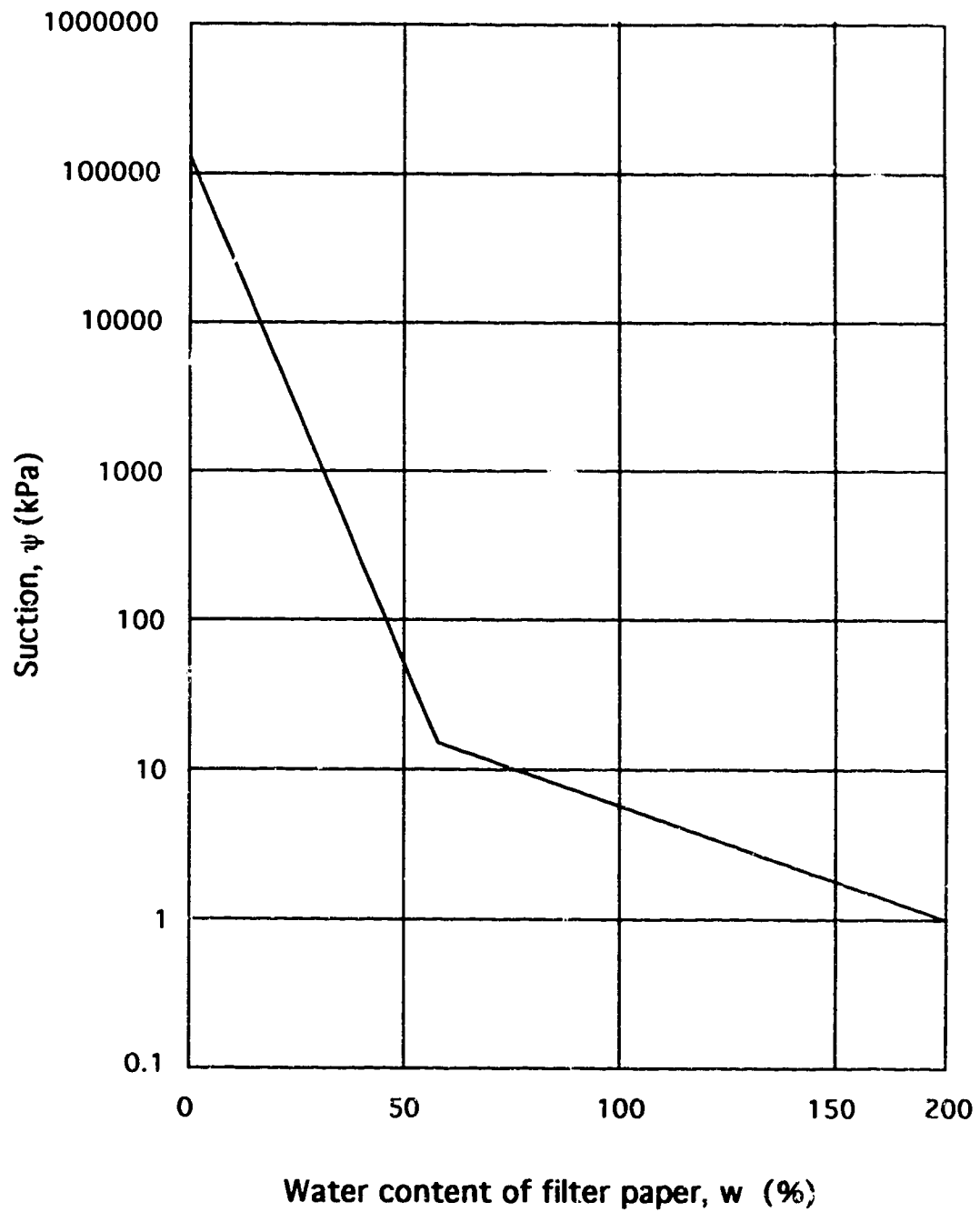


Figure 3.10: Typical Filter Paper Calibration Curve
(Modified After McQueen and Miller, 1968)

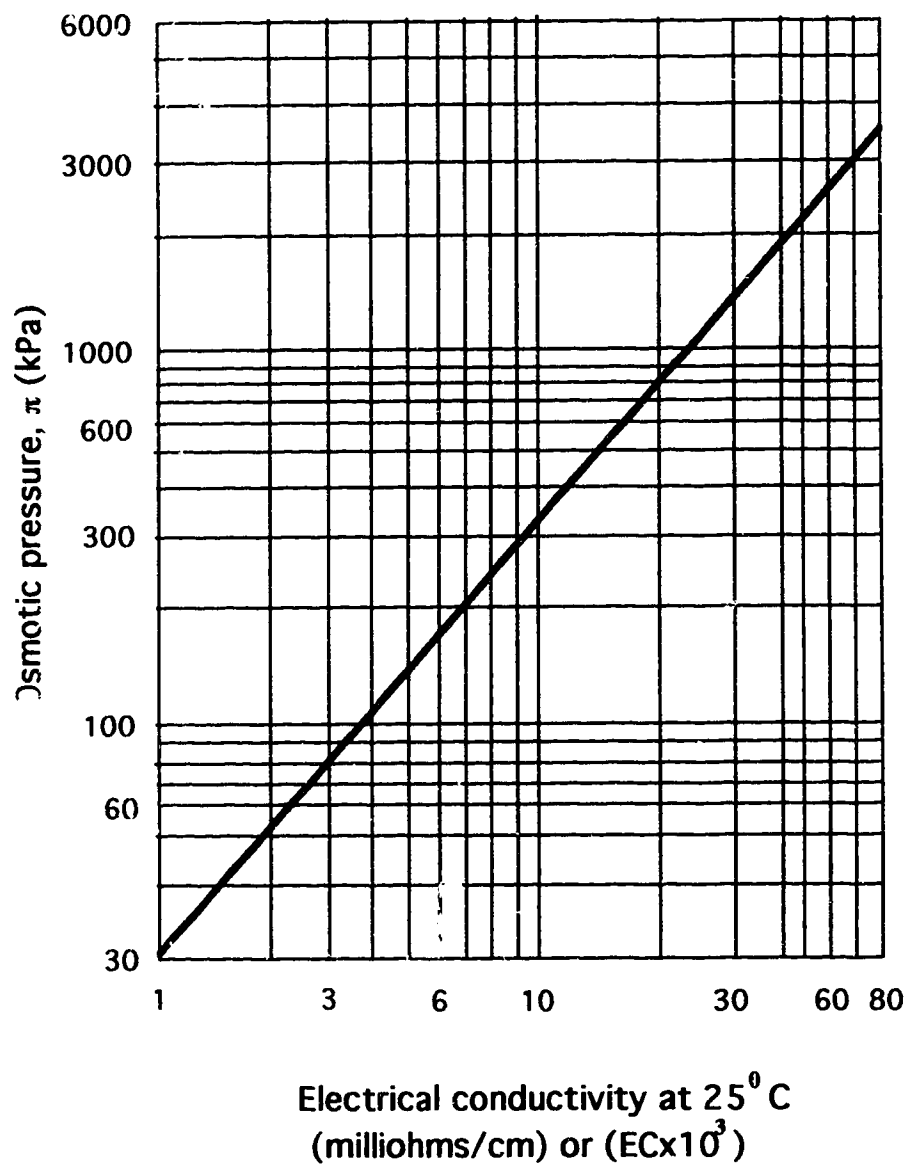


Figure 3.11: Osmotic Suction - Electrical Conductivity Relationship for Pore-water Containing Mixtures of Dissolved Salts
(from USDA Agricultural Handbook No. 60, 1950)

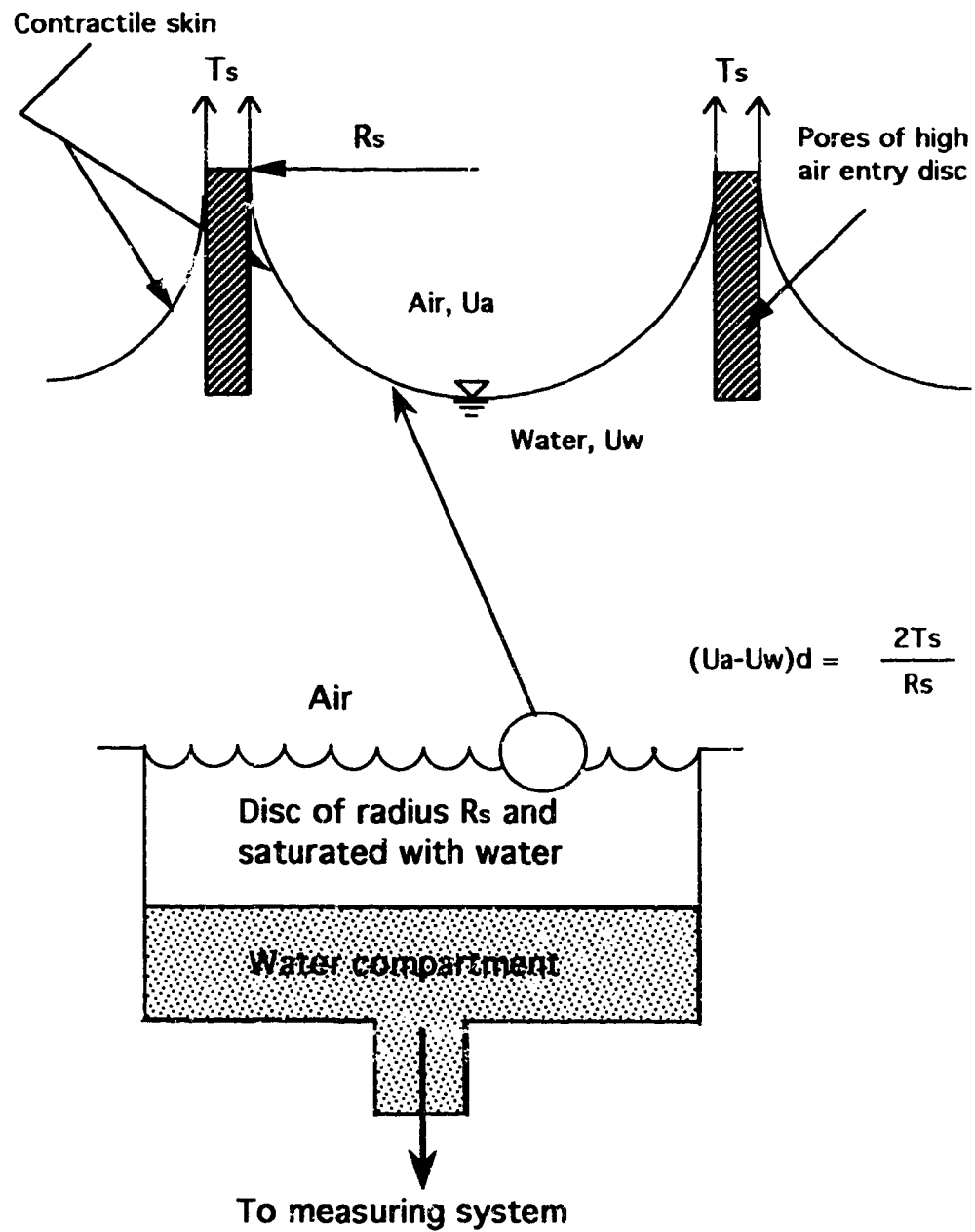


Figure 3.12: Principle of Operation of a High Air Entry Disc
 (After Fredlund and Rahardjo, 1993)

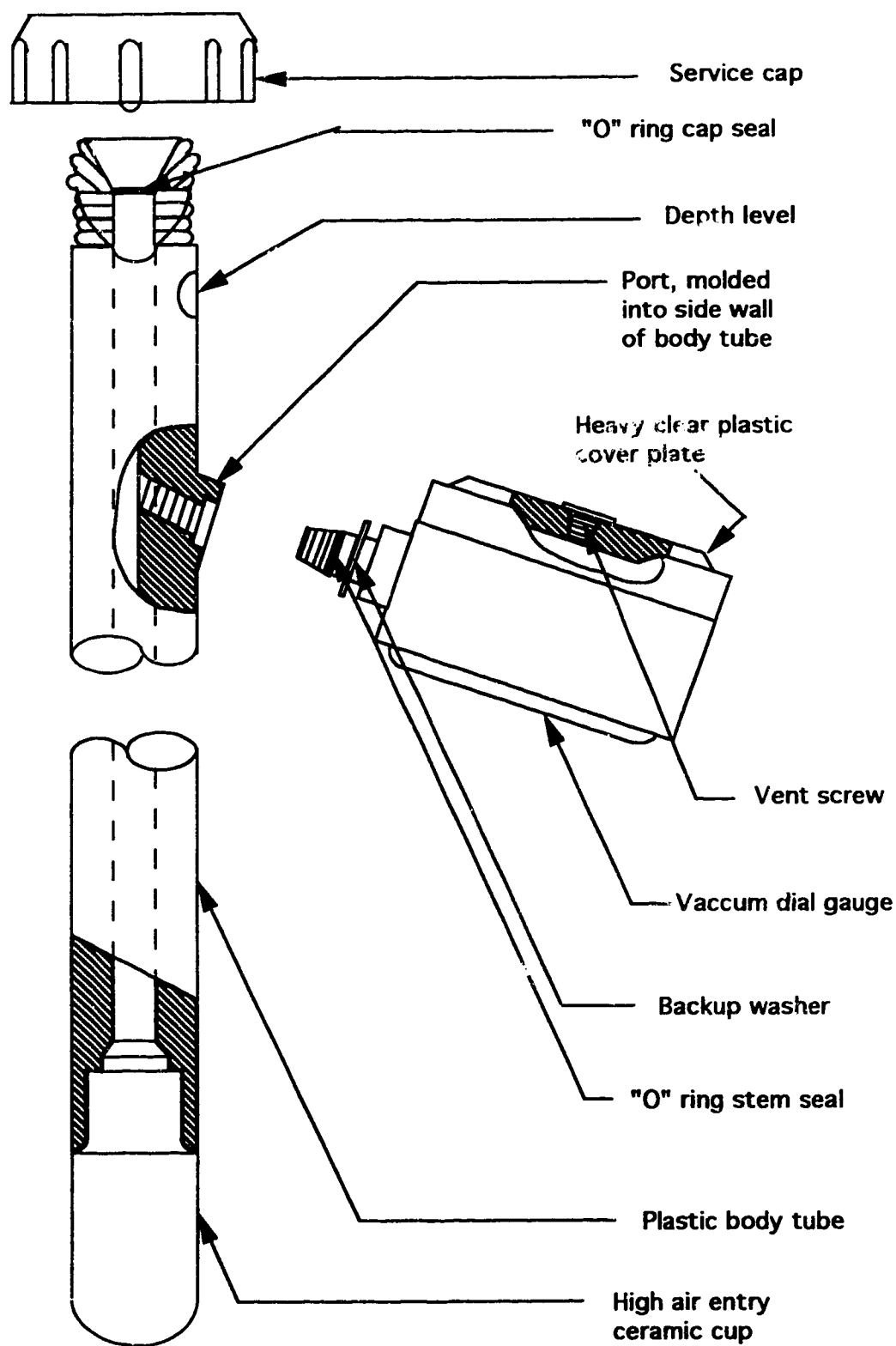


Figure 3.13: A Typical Conventional Tensiometer
(Soilmoisture Equip. Corporation, 1985)

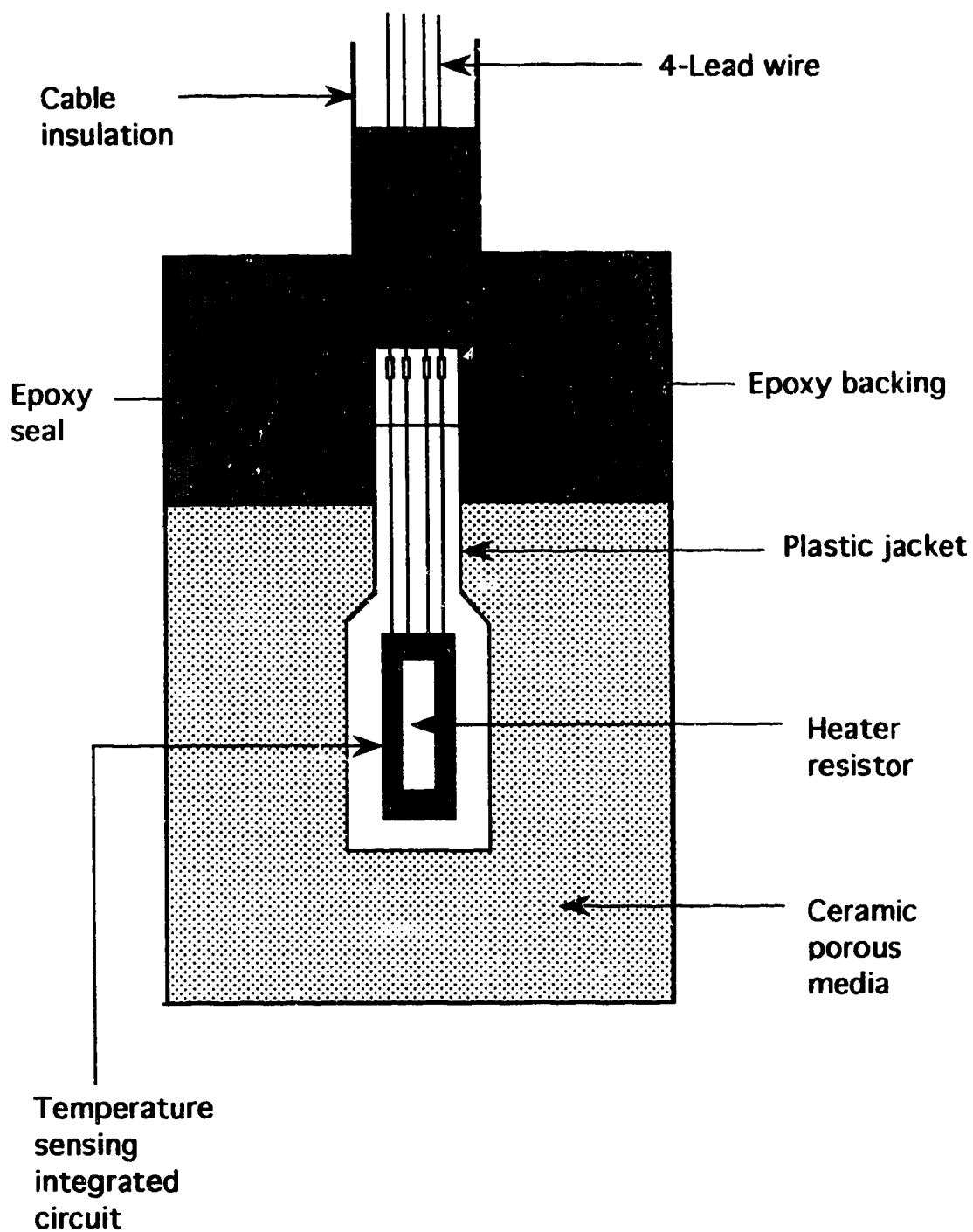


Figure 3.14: A Cross Section of the AGWA-II Thermal Conductivity Sensor
(After Phene et al., 1971 a)

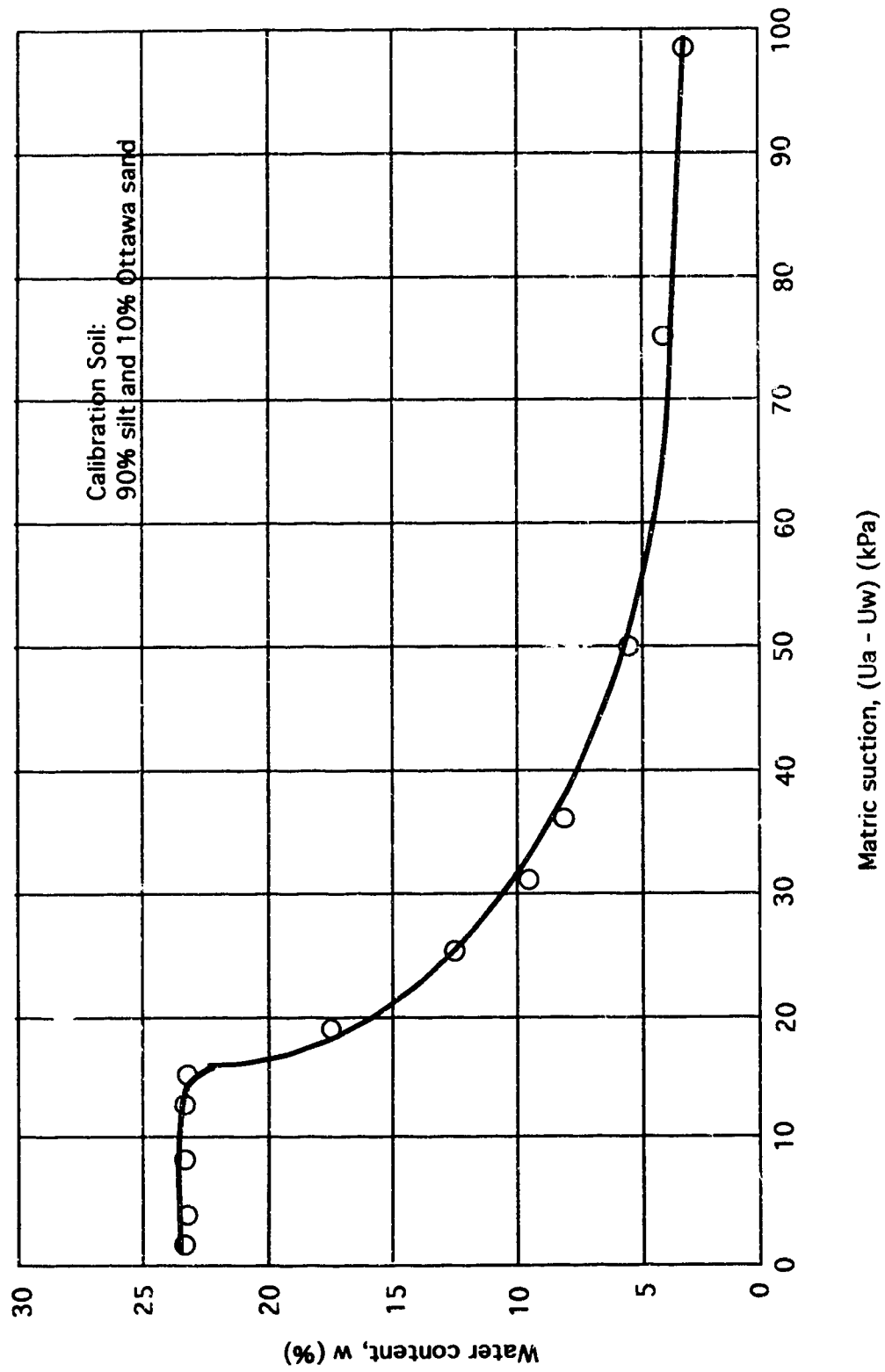


Figure 3.15: Soil-water Characteristic Curve for the Soil used in the Calibration of the AGWA-II Thermal Conductivity Sensor
(After Fredlund and Wong, 1989)

CHAPTER FOUR

INSTRUMENTED PAVEMENT SECTION

4.1 Introduction

To be able to detect seasonal variation trends in the strength of subgrade and other component layers of the pavement system, the influences of temperature and moisture on the resilient characteristics of these materials must be separated and quantified. To this end, the current research study was initiated to evaluate seasonal changes in the structural adequacy of asphalt concrete pavements within Alberta as measured by surface deflection and/or resilient modulus.

Within the context of this investigation, a two-phase research plan is perceived as a means to achieve the research objectives. The first phase is a field testing program and the second phase is a verification laboratory testing program.

The field testing program involved instrumenting a pavement section, that is representative of a large proportion of the primary highway system within Alberta, with temperature and moisture suction sensors. Falling Weight Deflectometer (FWD) tests were conducted at regular time intervals at various locations within the instrumented section. The output from these tests coupled by simultaneous temperature and moisture suction measurements was used to describe the subgrade resilient characteristics under varying load and environmental conditions normally encountered in Alberta. Details of the instrumentation phase of the field program are presented and discussed in the following sections of this chapter.

4.2 Selection Criteria

During the site selection phase, 21 pavement sites were identified from the Alberta Transportation Pavement Management System (PMS) as being potential for the purposes

of this investigation. The selection criteria that have been put forward for choosing an appropriate site for instrumentation included the following:

- * ***pavement structure and age:*** a granular base (GB) asphalt pavement type with an average age of 5 - 10 years in service was recommended;
- * ***type of subgrade material:*** only CI, CL, or CL-CI soil types were considered;
- * ***pavement geometry:*** a 4-lane divided highway was preferred;
- * ***other factors:*** accessibility to the City of Edmonton was an asset.

After careful examination of all potential sites, and field visits to four, a one kilometre pavement section within highway control section 16:12 north of lake Wabamun, was identified as being suitable for instrumentation. A schematic sketch of the site location is shown in Figure 4.1. Structural, geometric, traffic and other related information pertaining to the chosen site will be detailed below.

4.3 Structure and Geometry of Test Site

Control section 16:12 on Primary Highway 16 is a four-lane divided facility located west of Edmonton between Highway 22 east of Entwistle and the junction with Highway 43, a distance of 51.05 km (Khogali, 1991). Figure 4.2 shows a portion of the highway profile extending from km 18.5 to km 19.5 on the west bound roadway. The mostly westerly 440m of this section lies in a cut whereas the rest of the section is a fill area. The cross section consists of a 7.32m wide asphalt concrete pavement (ACP) with 3.50m outside and 2.40m inside ACP shoulders, shown in Figure 4.3. This section of the highway was constructed in 1983 and is composed of 130mm of asphalt concrete surface, 51mm of asphalt stabilized base, 456mm of granular base course and supported by a CL-CI subgrade soil fill varying from 2 to 3m in height along the section.

A site approximately 171m from the beginning of the selected section was chosen as an appropriate location for instrumentation. This particular site showed no visible distress at the time of installation and satisfied all selection criteria.

4.4 Traffic

In this section, the specific traffic information pertaining to the instrumented site will be summarized.

Traffic Data Systems, previously known as Traffic Information Services, of Alberta Transportation and Utilities publishes annual statistics reports summarizing equivalent single axle loads (ESAL's) and other traffic input characteristics within the Primary and Secondary highways in the Province. Using the information contained in these reports (Kilburn, 1992), historical traffic statistics for control section 16:12 from 1983 to 1991 are summarized and displayed in Tables 4.1 and 4.2. The conversion of the mixed traffic into ESAL's is done using the Alberta Transportation procedure. Details of this procedure can be found elsewhere (Khogali, 1988).

From Table 4.2, the average ESAL/day/direction for the period 1983 to 1991 is 399. This translates to about 1.1 million cumulative ESAL's for the nine-year period. Such traffic is considered to be of medium intensity for this type of highway. As a result, the choice of this section for instrumentation provides a reasonable representation of primary highway traffic within Alberta.

4.5 Environmental Conditions

For the purposes of this study, two main environmental factors are considered essential to monitor; namely, these are temperature and soil moisture.

The selected pavement site is located in central Alberta. This is an area where sub-zero air temperature conditions prevail for a period of approximately five months throughout a typical year (Plewes and Millions, 1985). This consideration coupled with the fact that pavement structures in this region experience frequent seasonal variability in moisture, puts control section 16:12 as one of the most suitable candidates for instrumentation to investigate thaw-weakening behaviour of subgrade soils and the influence that this may have on subgrade resilient modulus.

To the author's knowledge, no temperature and/or moisture data have been collected routinely by Alberta Transportation staff for any of the primary highways. In view of this, specific climatic information, per se, does not constitute a condition to be included among other criteria in the site selection process. Rather, in choosing 16:12 as a candidate for instrumentation, environmental considerations have only been assessed in general terms.

4.6 Instrumentation

The pavement site was instrumented with 12 AGWA-II thermal conductivity suction sensors. These sensors are designed to measure both the temperature and soil matric suction within fine-grained soils. The installation of the instrumentation consisted of two stages. In the first stage, the suction sensors were calibrated at the University of Saskatchewan, Saskatoon, for suctions of up to 400 kPa. This step was necessary to later enable the conversion of the sensor output to suction values. In the second stage, the sensors were installed within the selected site in three sets of four sensors each. One set was placed within the outside shoulder of the pavement while the other two sets were placed within the outside design lane. Within each set, sensors were placed at depths ranging from 0.78m to 1.78m below the top of the pavement surface.

The AGWA-II thermal conductivity suction sensor used in this study is a commercially available sensor. This sensor consists of a porous ceramic block that contains a temperature sensing element and a miniature heater, shown in Figure 4.4. The operation of the sensor is based on the principle of heat dissipation in a porous medium (Phene et al., 1971a and 1971b). When the sensor is inserted into a soil, water will move between the sensor and the soil until moisture stress equilibrium is attained. The equilibrium water content of the sensor is an indication of the suction in the sensor and in the soil. Thus, the sensor indirectly measures the heat-dissipation capacity of the water content in the sensor tip. This is usually achieved by supplying a controlled amount of heat at the centre of the ceramic block, through the heating element, and then measuring the temperature rise at the same point after a fixed period of time. The change in temperature is a function of the water content which can be converted to matric suction through calibration.

In the remaining parts of this chapter, sensor calibration, field installation procedure and method of data collection will be summarized.

4.6.1 Calibration of The AGWA - II Sensors

In this section, details of the calibration procedure used to convert sensor output into soil suction values in terms of kilopascals will be described.

4.6.1.1 Description of Apparatus and Calibration Procedure

The AGWA-II sensors were calibrated at the University of Saskatchewan. The experimental setup used for calibration is shown in Figure 4.5. This setup consists of a 1500 kPa pressure plate extractor, a 25.4cm diameter ceramic plate with a sheet-rubber backing, an insulated enclosure and a data acquisition system. The pressure plate was modified by adding a circular extension ring to the pressure chamber. Twelve circular holes were drilled along the side wall of the extension ring; these holes were required for

the sensor cable to be brought outside the pressure chamber to be hooked up to the data acquisition system. Brass rings, along with split metal pieces and split rubber gaskets were arranged in such a manner that air leakage around the lead wires of the sensors could be eliminated. The air leakage was prevented by the rubber gaskets which were compressed to expand against the side of the hole and against the perimeter of the lead wire as the brass rings were tightened. The ceramic plate of the pressure extractor which has an air entry value of 500 kPa was also modified by installing an additional outlet. This modification was intended for the purpose of removing any entrapped or diffused air that may accumulate beneath the ceramic plate. The insulated enclosure was used to contain the entire pressure plate extractor in order to maintain the ambient temperature within the box at about 0.5 degree Celcius of mean room temperature. The data acquisition system used in calibration consists of a CR10 data logger, an AM32 multiplexor, an external D.C power source, a lap top PC computer and a computer software, the PC208. The software was used for programming the data logger. This system was used to record the response of the sensors in terms of ambient temperature and temperature differences (ΔT^s).

A calibration soil mix composed of 10 percent Ottawa fine sand and 90 percent silt was used to provide contact between the thermal conductivity sensor tip and the ceramic plate (Fredlund and Wong, 1989). Good contact is essential to provide continuity between the water phase in the porous block and in the high air entry ceramic disk.

The ceramic plate was soaked in water for several days to ensure saturation. The AGWA-II sensors were also soaked in water to bring them to saturation. The calibration soil mix, prepared in a slurried form, was placed on the ceramic plate and contained in a lucite ring. The initially saturated sensors were directed through the extension ring holes and then the tips were pushed into the slurry mix. The spaces around the sensors lead

wires were sealed by tightening the brass rings. The pressure plate was then closed, air pressure was applied and the whole assembly was checked for leakage.

After no leakage was detected, calibration was carried out in matric suction increments of 50 kPa, starting from 0 kPa and going to a maximum of 400 kPa. This gave a nine point calibration curve for each sensor. At each pressure increment level, the response of each sensor was monitored until equilibrium was achieved. The sensor response for 0 and 50 kPa was monitored every half an hour. This time interval was increased to one hour for the subsequent pressure increments. Generally, equilibrium was achieved within a 2-day time period for each suction level.

4.6.1.2 Calibration Data

Figure 4.7 shows typical time response curves for three of the AGWA-II sensors for changes in applied pressure during calibration. The values of the ΔT 's at equilibrium for each applied pressure increment and the corresponding suction are used to plot the calibration curve for each sensor. These calibration curves were found to be nonlinear. Using the PC 208 software, second degree polynomial curves were found to suitably describe the behaviour of the calibration data. An example calibration curve for sensor one is depicted in Figure 4.8.

The calibration curves of the remaining sensors, i.e. sensors 2 to 12, are contained in Appendix A.

4.6.2 Installation

The relative locations and depths of the twelve sensors that were installed for this project are as shown in Figures 4.9 and 4.10. Previous experience (Fredlund, 1990) had been that the most critical zone in which suction readings should be obtained is located within the upper 1.20 m of the subgrade soil layer. This is within the average depth of

frost of 2.0m that is frequently encountered within the Province of Alberta (Shields et al., 1965; and Plewes and Millions, 1985). With this in mind, it was decided to have the sensors installed at depths of 0.15, 0.30, 0.60, 0.85 and 1.15 metres from the top of the subgrade layer. Because of the practical difficulty experienced in maintaining exact depths for all sensors, a 5 to 15 % variation is considered acceptable. This is shown in Figure 4.10.

A major concern about using the AGWA-II sensors is the installation procedure. It was noted before that a good soil-to-sensor contact is essential to obtain reliable suction measurements. This consideration coupled with the fact that the AGWA-II sensors are quite fragile, necessitates extreme care to be exercised when these sensors are being installed to avoid breaking them. One acceptable procedure for installing such sensors in the field involves excavating a trench or boring a large-diameter borehole to the required depth following which the sensors are to be installed into the side of the excavation by hand. But since a public highway is involved, this procedure was deemed to be too disruptive. As a result, an alternative method for installation was selected. The selected procedure employed in the current study was typical of the one that was used in a project near Regina, Saskatchewan, in 1989. The steps involved in this procedure are as follows (Klimochko, 1990):

- (1) A hole 125mm in diameter was bored through the asphalt concrete pavement and into the subgrade approximately 300mm above the required depth that the sensor was to be placed at. This was done using a drill rig.
- (2) A 75mm diameter Shelby tube was pushed to obtain soil sample extending from the bottom of the borehole down to the required depth at which the sensor was to be placed. This was also expected to produce a flat surface for installing the sensor.

- (3) A hole at the bottom of the Shelby spoon sample cavity was then punched for fitting the sensor into. A sledge hammer and a rod whose end was equipped with an adapter similar in diameter and length to that of the sensor was used. Care was taken not to make the punched hole any deeper than necessary. The length corresponding to the required depth of the tip of sensor, was marked on the installation rod. By driving the rod to the marked length, a punched hole with an exact depth was obtained. This was done to ensure that the bottom of the sensor when inserted would be in full contact with the soil.
- (4) The sensor was inserted using a special wire rod. This rod was approximately 9mm in diameter with one end bent out 90 degrees, approximately 40mm and then bent again so as to form the letter "c". The sensor was held against the wire rod by pulling back on the electrical cable while it was being guided into the punched hole located in the bottom of the Shelby sample cavity. After the sensor was inserted into the punched hole, the technician pushed gently on the insertion rod to ensure that good sensor-to-soil contact was made.
- (5) After the sensor was installed in the punched hole, dry powdered kaolin was backfilled into the hole to approximately 75mm above the sensor. The fact that the kaolin backfill was dry is important in that it was done to ensure that the backfill be void-free to provide for a good sensor-to soil contact. It is to be noted, however, that one disadvantage of using dry kaolin is that it is not at the same moisture equilibrium as the surrounding clay soil in the vicinity of the sensor. This might result in some moisture transfer which in turn could affect the sensor readings in the process. However, it was believed that the advantage of the void-free backfill far out weighs the disadvantage of the soil being at different moisture content. Moreover, with time the dry kaolin will come to equilibrium with the surrounding clay.

- (6) The remainder of the hole up to the top of the subgrade was backfilled with a crumbly clay material similar to that in which the hole was situated. The moisture content of this backfill material was appreciably less than that existing in the in situ material. Again, the dryer soil was used to get around the backfilling problem.
- (7) After all the sensors were installed at the desired depths and locations, a series of trenches for laying the cable from each sensor to the location of the data acquisition box were cut into the pavement to a depth of approximately 50mm. The data acquisition system was located in a water-tight box, situated at approximately 2.0m from the edge of the outside shoulder on the north side slope.
- (8) After the cables from the sensors were laid in the trenches, the trenches were backfilled with a granular material and were topped off with some cold-mix patching material.
- (9) The ends of the electrical cables coming out of the trenches were then connected to the appropriate terminals of the AM32 multiplexor residing inside the data acquisition box. The PC208 software was used to download the program that commenced data monitoring and collection.

A set of photographs displaying the steps involved in the above outlined installation procedure is shown in plates 4.1 to 4.8

4.7 Temperature and Soil Suction Data Collection

The same data acquisition system used during the calibration phase was used for the field monitoring phase. Two external batteries for powering the system were used to replace the D.C power supply. The whole assembly was placed in a water tight container to prevent moisture from getting inside the box and damaging both the data logger and the multiplexor. The PC208 software was used to program the CR10 unit to record temperature and moisture suction measurements every two hours. This was synchronized

to reflect real time (instantaneous) measurements.

The installation of the twelve thermal conductivity gauges was completed on November 7, 1990. Monitoring and retrieval of temperature and soil suction data commenced on the same day. A four-week period was found adequate for site visits to retrieve the data. This was determined in view of the fact that the external batteries powering the system need to be recharged once every month to maintain the data being collected.

On April 6, 1991 site visit to retrieve the data, it was discovered that the data acquisition system had suffered a major break down. After investigation, it was found that drainage water from the pavement shoulder edge had leaked into the data acquisition box and caused a short circuit within the multiplexor component of the data acquisition assembly. Further investigations showed that only the multiplexor was rendered unoperational with all other components being in good condition. From these investigations it was evident that the data acquisition box had not been sealed properly, as expected.

After the leakage problem was detected, efforts were made to replace the defective data acquisition system with a new one and make sure that the new system would be more secured against future hazardous operational conditions. A new multiplexor unit was ordered from the manufacturer and different alternatives were considered to ensure safe operation of the new data acquisition system. Finally it was decided that instead of burying the new system into the ground, it should be placed inside a water-tight container which will in turn be clamped to a steel post and left hanging in the air an adequate distance in order that drainage water would not get to it. The setup of the new monitoring system was completed on July 17, 1991 and temperature and soil suction data collection

resumed. This continued until September 15, 1992 without any more problems being detected.

4.8 Summary

This chapter gives an overview of the details of the instrumentation part of the field testing program. This includes the selection criteria used, the specifics of the test site selected, traffic and environmental considerations, calibration and installation of the thermal conductivity sensors and temperature and soil suction data monitoring and retrieval.

Sensor calibration constitutes a major portion of the work completed towards fulfilling the objectives of the field testing program. A detailed description of the calibration procedure followed together with example outputs were given.

The fact that the AGWA-II sensors are very fragile necessitated a particular routine to be followed when installing these sensors. This technique has proved successful. The details of the installation procedure were also given.

Temperature and soil suction data collection started in early November of 1990. The monitoring was interrupted in the first week of April 1991 due to improper sealing of the data acquisition box which resulted in drainage water leaking into the box and causing a short circuit within the multiplexor component of the data acquisition assembly. This rendered the system unoperational. The malfunction was soon discovered and remedial measures were undertaken.

Successful data monitoring covered the first winter of 1990-91 from November to April, and after remedial measures over one calendar year. The latter included a summer period, a second winter followed by a spring and a second summer period.

References

1. Fredlund, D.G. and D.K.H. Wong (1989), "*Calibration of Thermal Conductivity Sensors for Measuring Soil Suction*," ASTM Geotechnical Journal, GTJODJ, Vol. 12, Number 3, pp. 188-194.
2. Fredlund, D.G. (1990), *Private Communications*, Professor of Civil Engineering, University of Saskatchewan.
3. Khogali, W.I. (1988), "*A Parametric Evaluation of a Mechanistic-Empirical Design Procedure for Asphalt Concrete Pavements*," M.Sc. Thesis, University of Alberta, Spring 1988.
4. Khogali, W.I., K.O. Anderson, J.K. Gan and D.G. Fredlund (1991), "*Installation and Monitoring of Thermal Conductivity Suction Sensors in a Fine-Grained Subgrade Soil Subjected to Seasonal Frost*," Proceedings of the Second Symposium on Road and Airport Pavement Response Monitoring Systems, West Lebanon, New Hampshire, U.S.A., September 12-16, pp. 153-167.
5. Kilburn, P. (1992), *Private Communications*, Managing Engineer, Traffic Data Systems, Alberta Transportation and Utilities.
6. Klimochko, D. (1990), Saskatchewan Department of Highways and Transportation, *Private Communications*.
7. Phene, C.J., C.J. Hoffman and S.L. Rawlins (1971a), "*Measuring Soil Matrix Potential in situ by Sensing Heat Dissipation within a Porous Body: I. Theory and Sensor Construction*," Soil Science Society of America Proceedings, 35: 27-33.
8. Phene, C.J., C.J. Hoffman and S.L. Rawlins (1971b), "*Measuring Soil Matrix Potential in situ by Sensing Heat Dissipation within a Porous Body: II. Experimental Results*," Soil Science Society of America Proceedings, 35: 225-229.
9. Plewes, S.L. and K.A. Millions (1985), "*Possible Failure Mode for Problem Full-Depth Pavements*," Proceedings, Canadian Technical Asphalt Association, 30: 232-259.
10. Shields, B.P. and J.M. Dacyszyn (1965), "*Seasonal Variations in Flexible Pavement Strength*," Proceedings, Canadian Good Road Association, 42: 394-409.

Table 4.1: Traffic Volume History for Hwy 16 (1983-1991)

Hwy ID and location	Year	AADT	ASDT
16:12 W OF 765 E OF FALLIS	1983	5130	6250
16:12 W OF 765 E OF FALLIS	1984	5100	6220
16:12 W OF 765 E OF FALLIS	1985	4830	5910
16:12 W OF 765 E OF FALLIS	1986	5620	7030
16:12 W OF 765 E OF FALLIS	1987	5280	6310
16:12 W OF 765 E OF FALLIS	1988	-	-
16:12 W OF 765 E OF FALLIS	1989	6310	7550
16:12 W OF 765 E OF FALLIS	1990	6460	7720
16:12 W OF 765 E OF FALLIS	1991	6530	7840

Table 4.2: Traffic Volume Breakdown and ESAL Statistics for Hwy 16 (1983-1991)

Year	AADT	Percent Trucks		ESAL/Day/Direction		
		SUT %	TTC %	SUT	TTC	Total
1983	5130	4.2	8.3	60	292	352
1984	5100	4.2	8.4	60	294	354
1985	4830	3.6	7.9	49	261	310
1986	5620	4.4	8.6	69	331	400
1987	5280	3.6	7.9	53	286	339
1988	-	-	-	-	-	-
1989	6310	5.3	10.2	94	440	534
1990	6460	4.1	8.4	75	373	448
1991	6530	4.2	8.4	76	377	453

HWY - HIGHWAY

ESAL - EQUIVALENT SINGLE AXLE LOAD

AADT - AVERAGE ANNUAL DAILY TRAFFIC

ASDT - AVERAGE SUMMER DAILY TRAFFIC

SUT - SINGLE UNIT TRUCKS (1 SUT = .56 ESAL)

TTC - TRACTOR-TRAILOR COMBINATIONS (1 TTC = 1.37 ESAL)

TOTAL = (SUT + TTC)

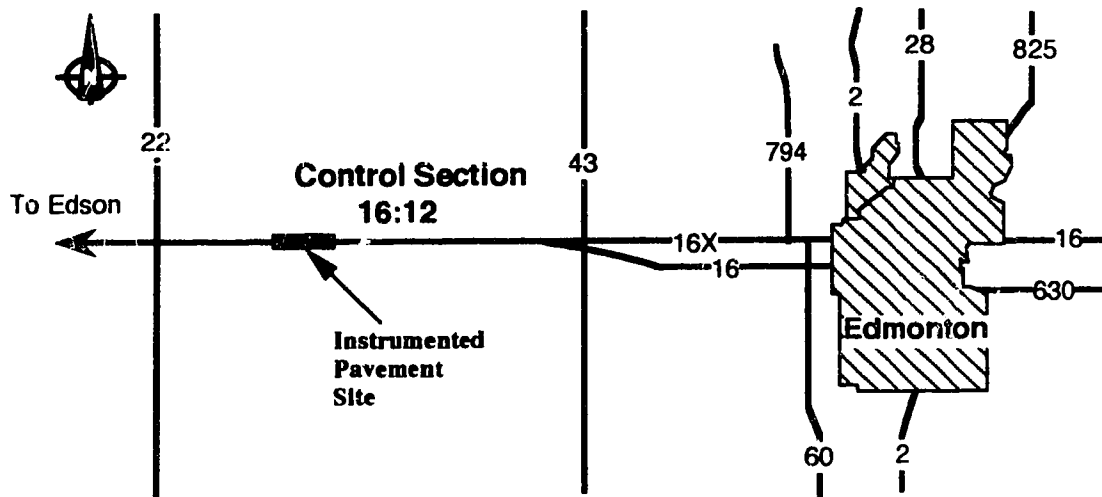


Figure 4.1: A Schematic Sketch of Site Location

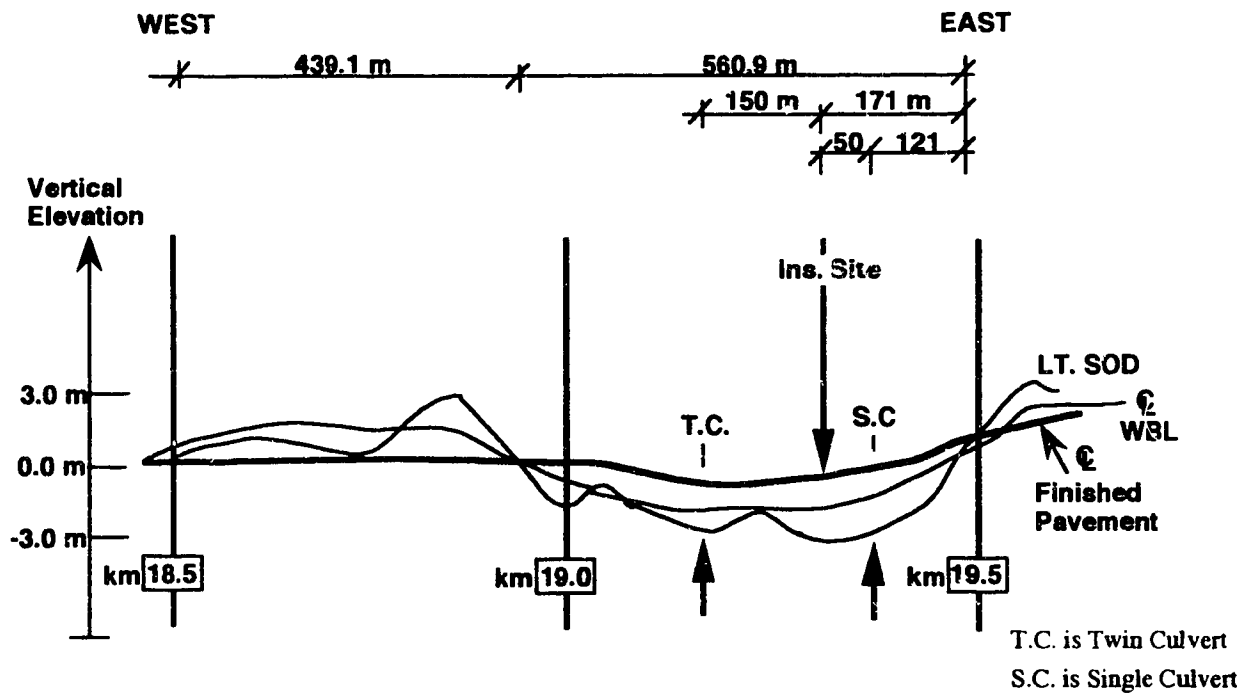


Figure 4.2: Selected Pavement Section Profile

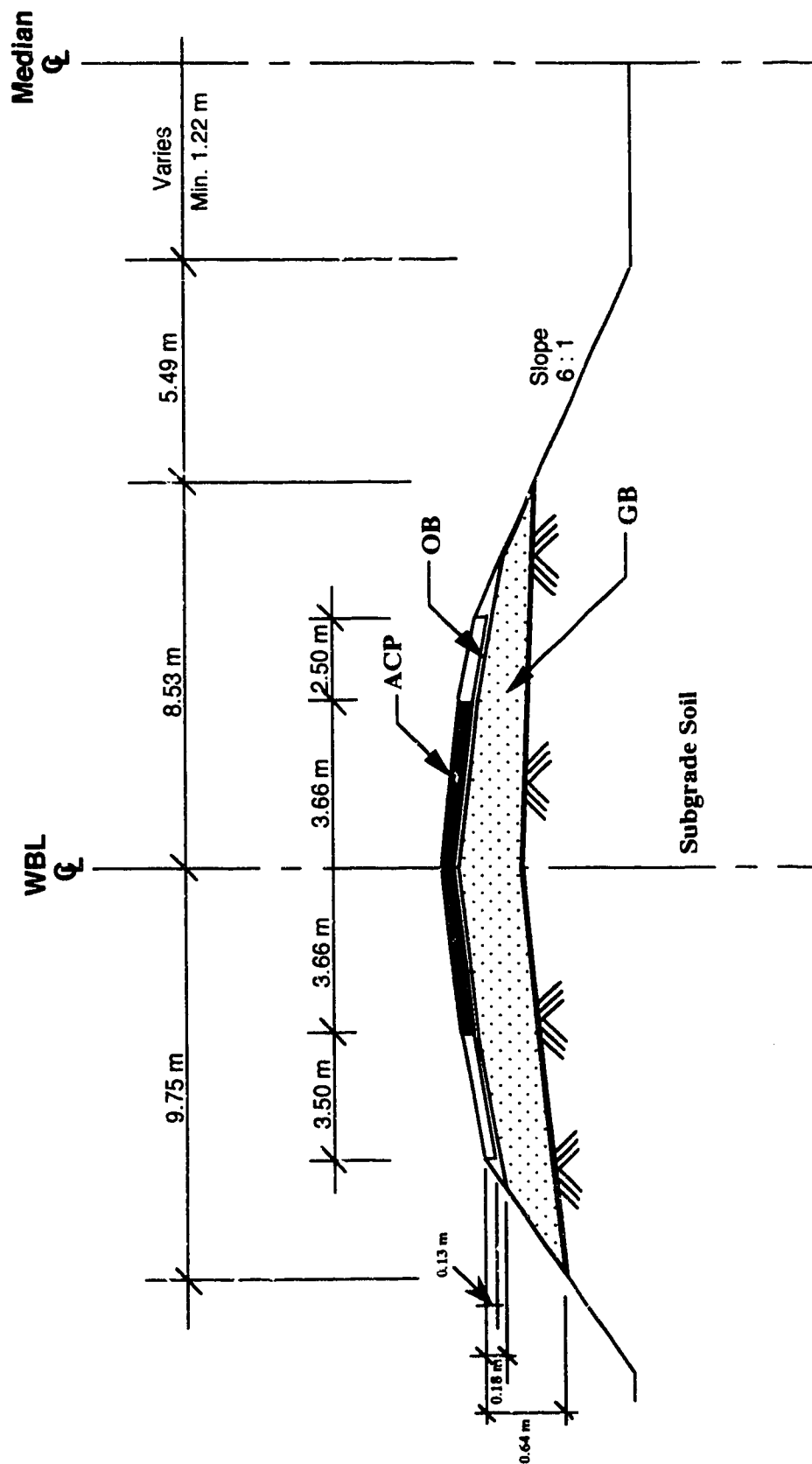


Figure 4.3: Selected Pavement Cross-Section

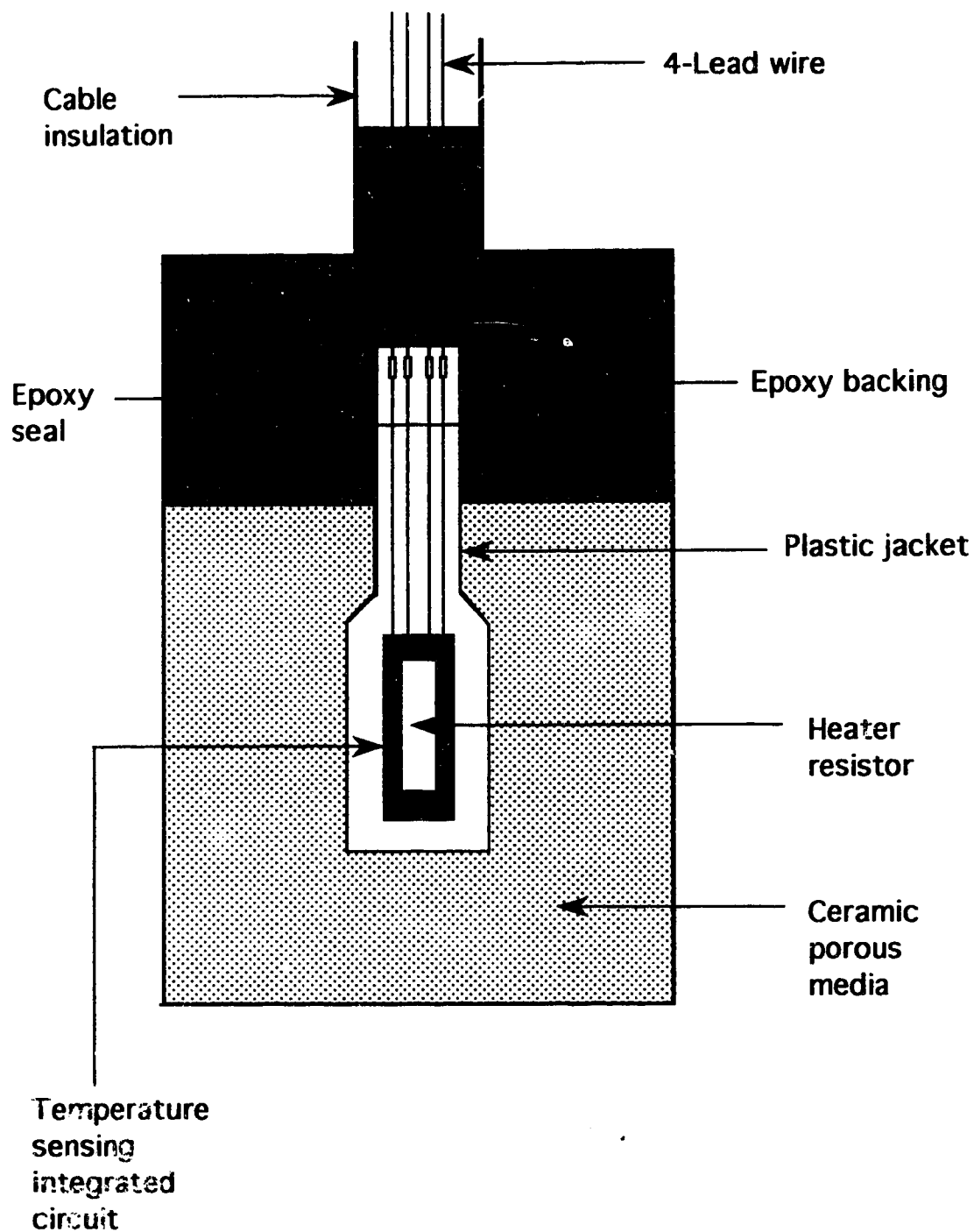


Figure 4.4: A Cross Section of the AGWA-II Thermal Conductivity Sensor
(After Phene et al., 1971 a)

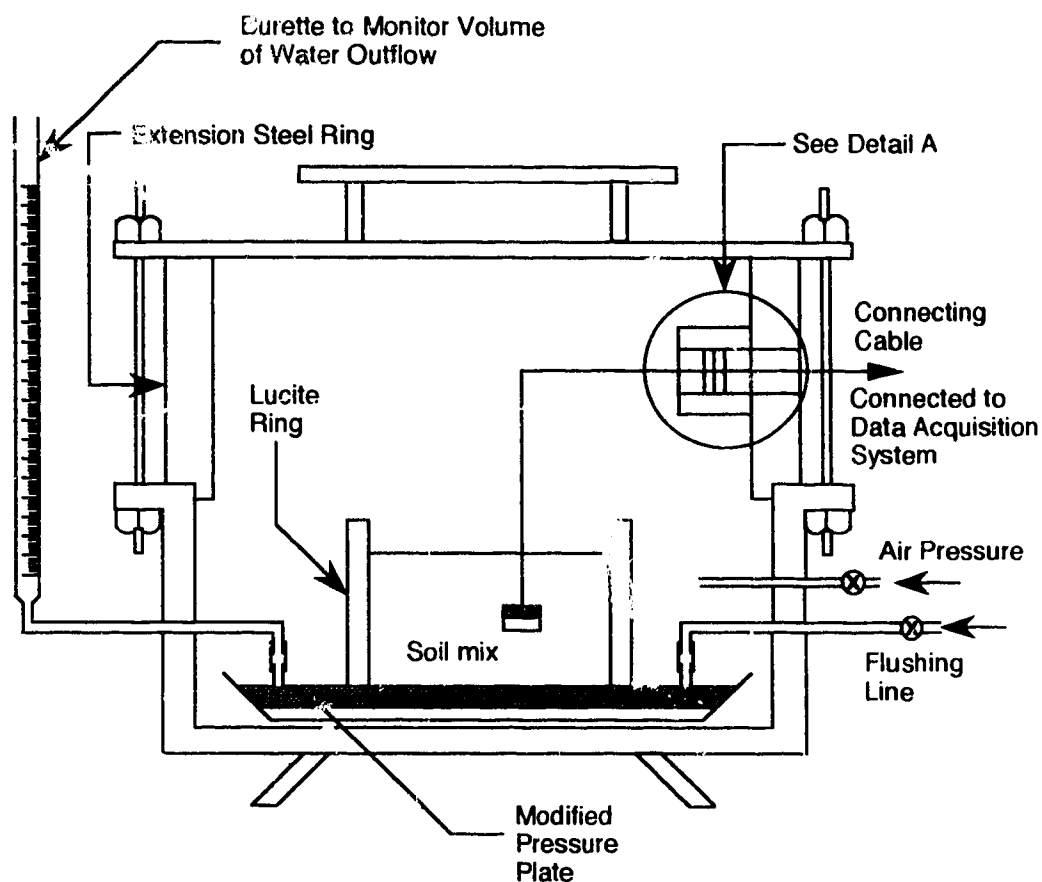


Figure 4.5: Calibration Apparatus

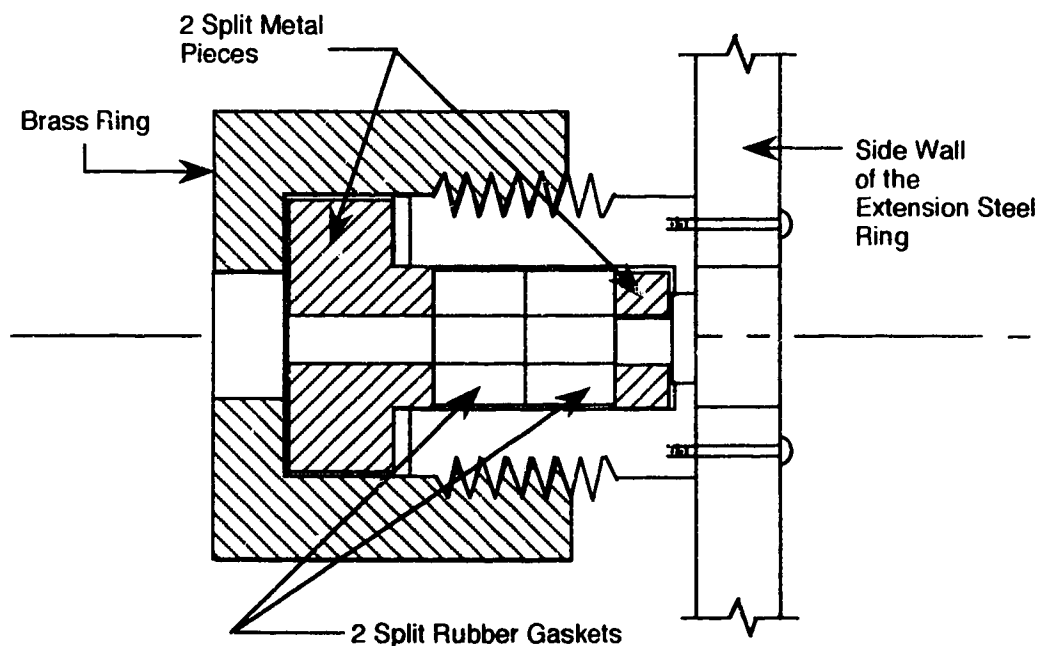


Figure 4.6: Calibration Apparatus - Detail A

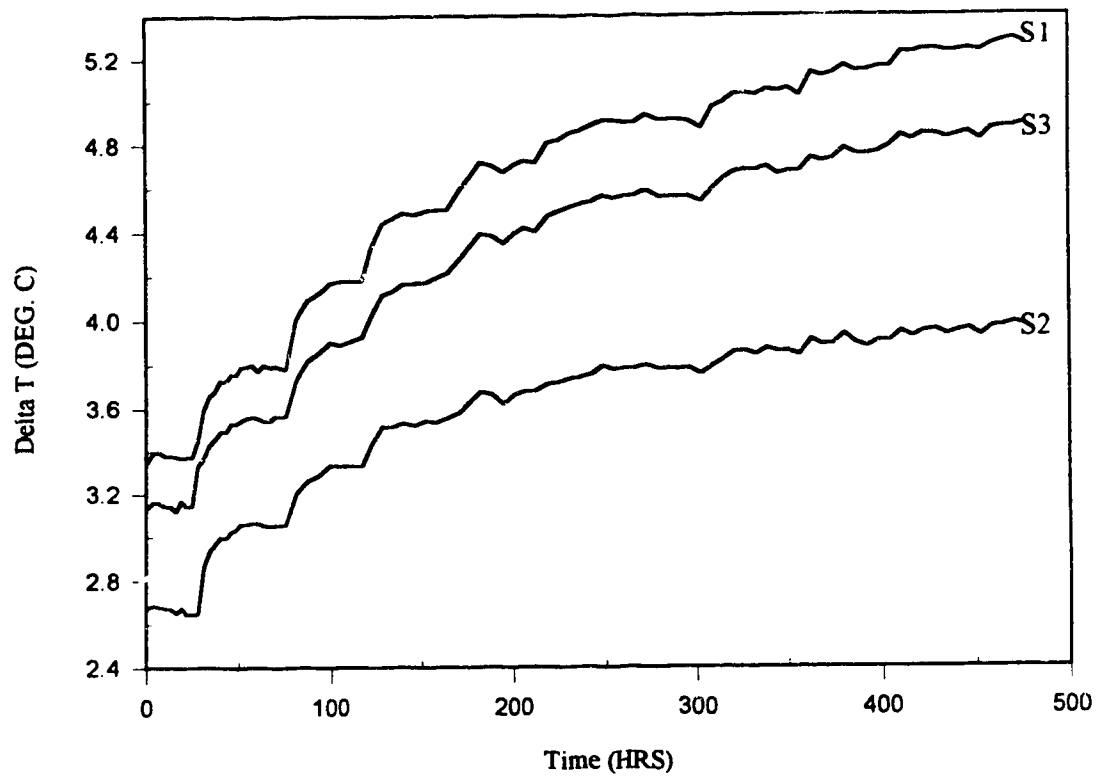


Figure 4.7: Time Response Curves for Sensors 1, 2, 3

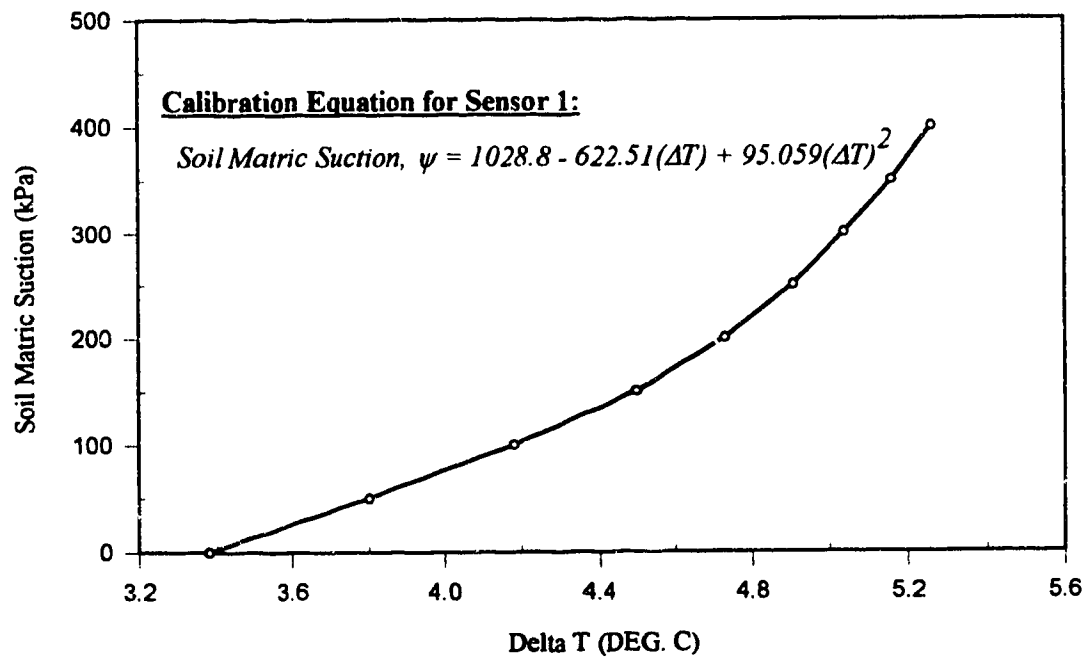


Figure 4.8: Calibration Curve for Sensor 1

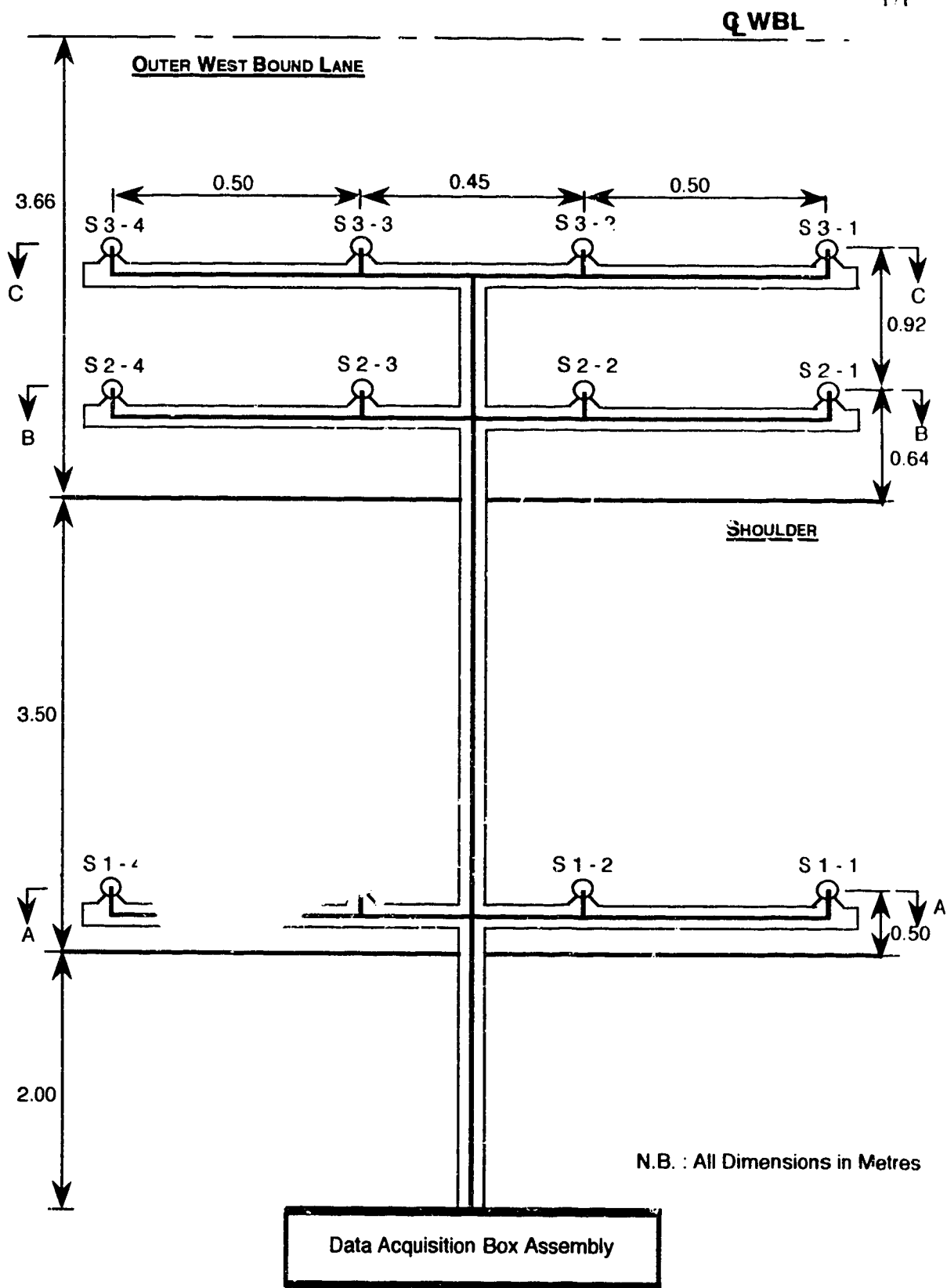
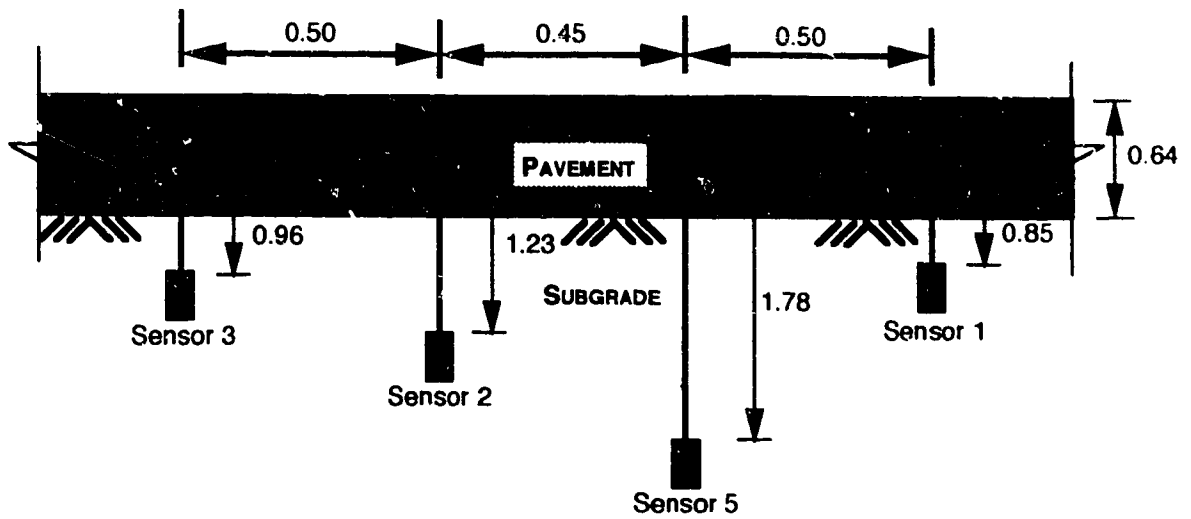
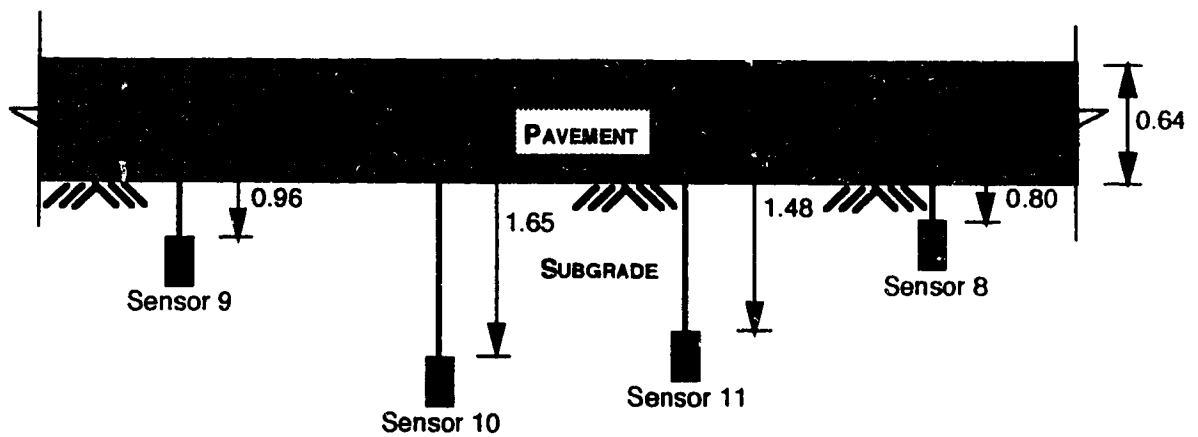


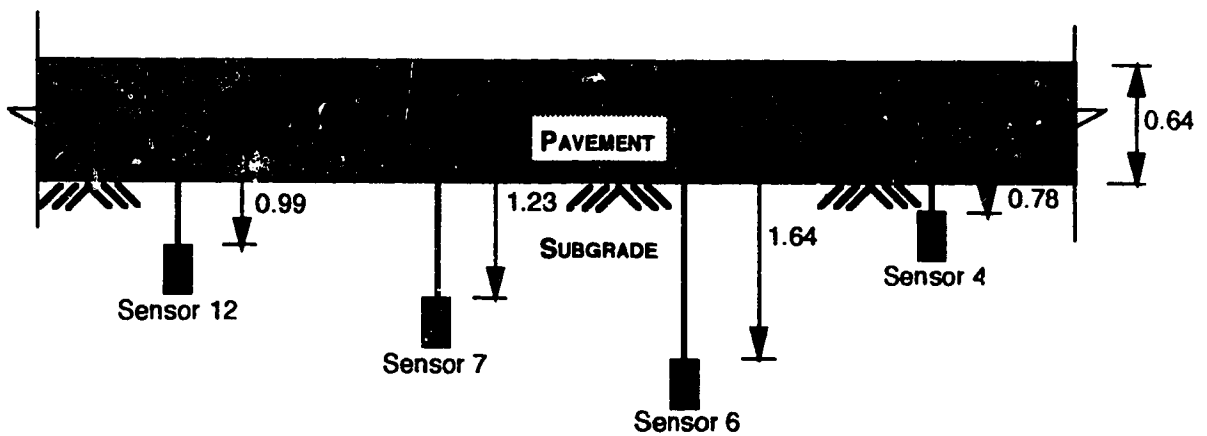
Figure 4.9: Instrumentation Layout



X - sectional View A - A



X - sectional View B - B



X - sectional View C - C

Note: All dimensions
in metres

Figure 4.10: Sensors Depth Locations

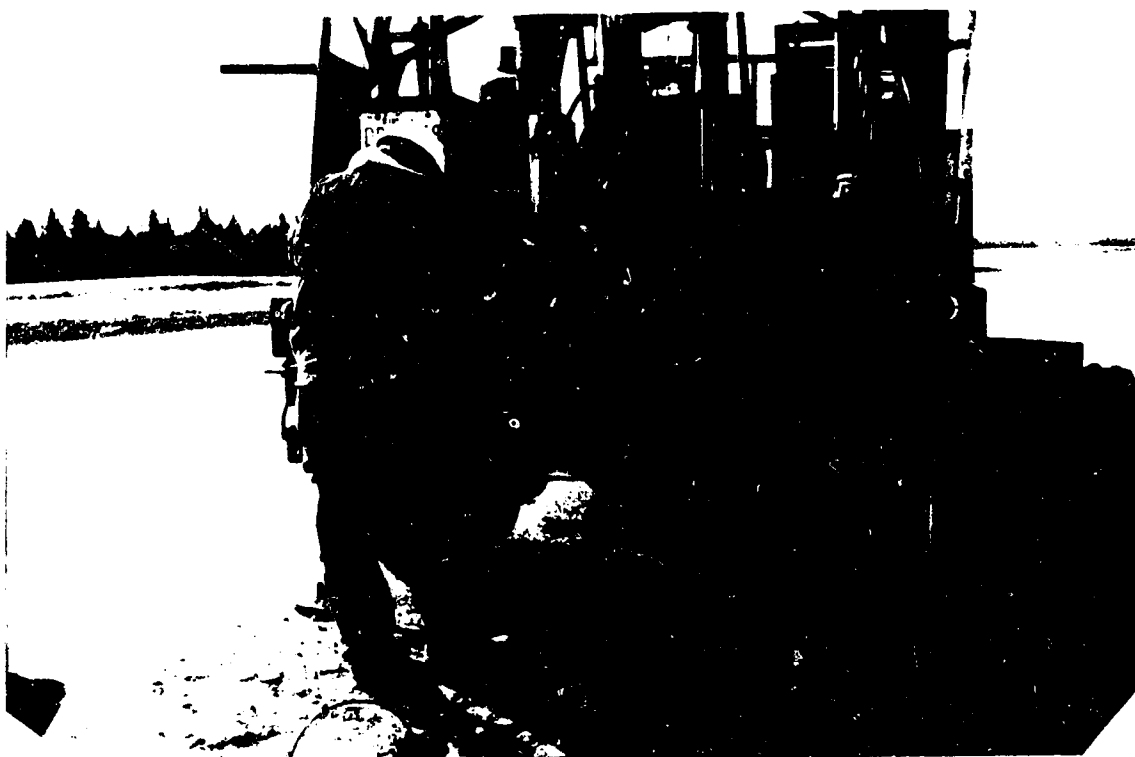


Plate 4.1: Preparation of a Pilot Hole for Instrumentation



Plate 4.2: Obtaining an Undisturbed Shelby Sample

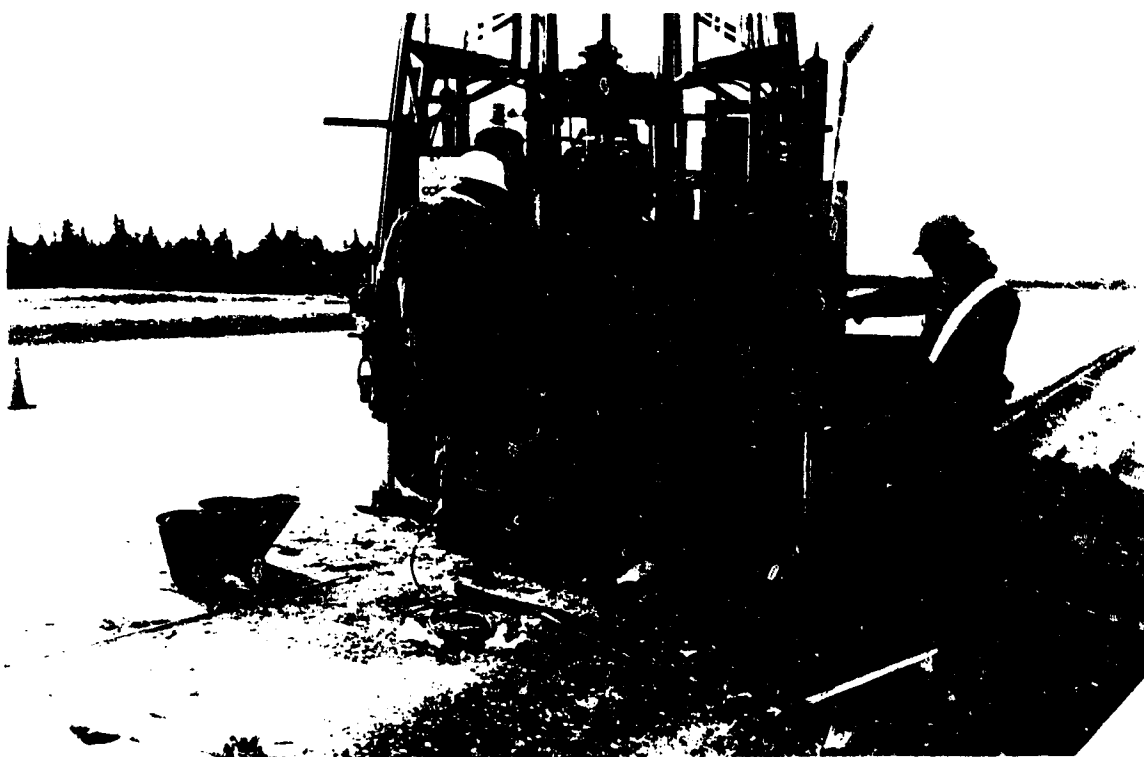


Plate 4.3: Preparation of a Punched Hole at the Bottom of the Shelby Cavity to Host the AGWA-II Sensor

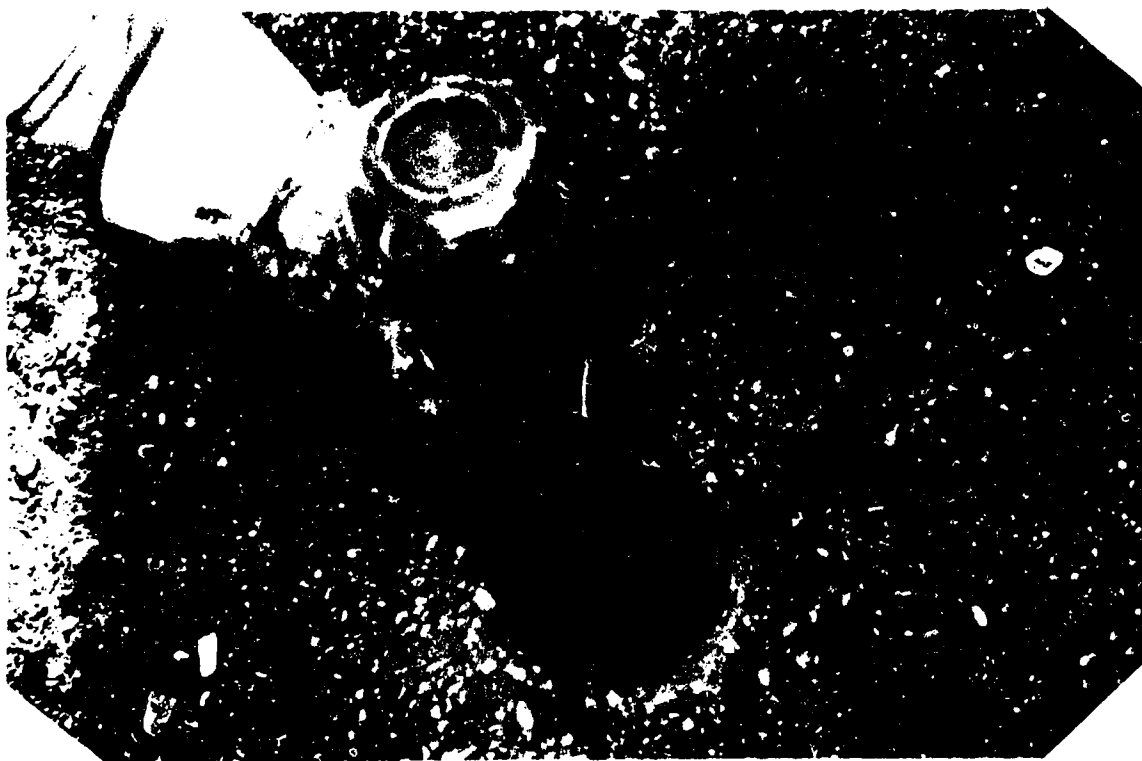


Plate 4.4: Finished Pilot Hole



Plate 4.5: A Picture Showing the AGWA-II Sensor with the Special Rod used to Situate the Sensor Inside the Prepared Hole



Plate 4.6: Preparation of Transverse and Longitudinal Trenches for Laying Sensors' Cables



Plate 4.7: A Picture Showing the Connection of the Sensors' Cables to the Data Acquisition Box

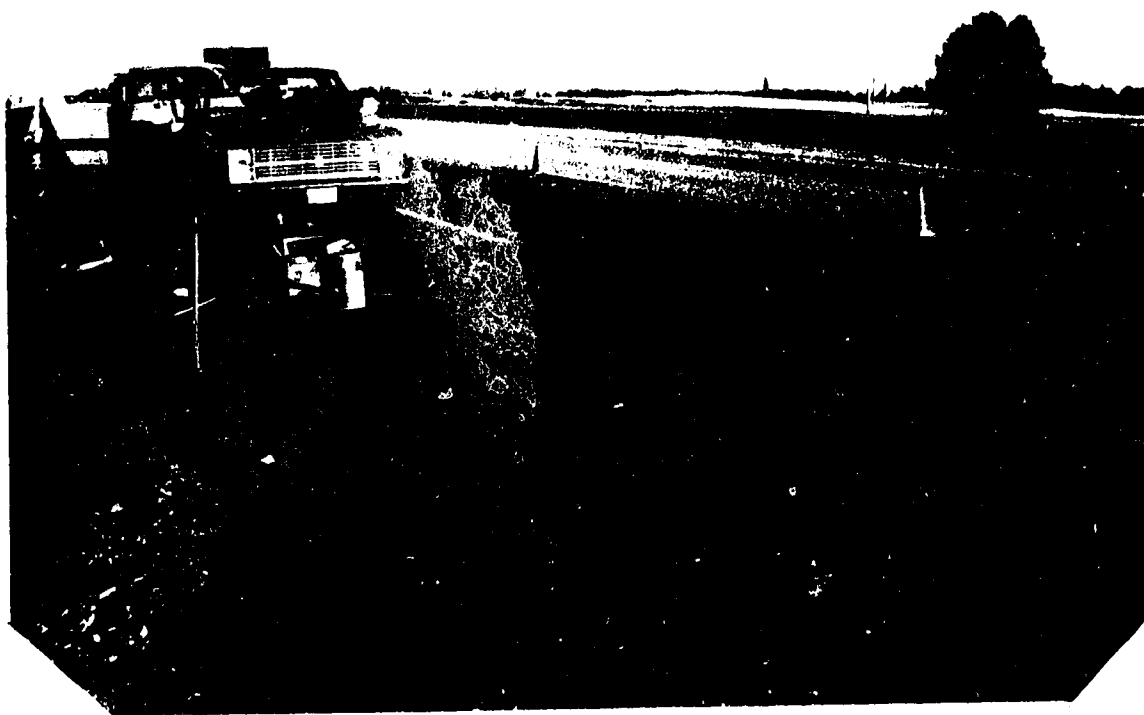


Plate 4.8: Finished Instrumented Site

CHAPTER FIVE

LABORATORY CHARACTERIZATION OF FINE-GRAINED SUBGRADE SOILS

5.1 General

This chapter overviews the general framework of the laboratory testing phase of the current research. The chapter is divided into three major sections. In the first section, a description of the resilient modulus test system developed for the laboratory investigation is given. The second section deals with the identification of the soil samples tested and the method of sample preparation for repeated load testing. In the third section, specifics regarding the test procedure used and an outline of the testing program carried out are described briefly.

5.2 Resilient Modulus Test Equipment

The main objective of the laboratory testing program was to determine, experimentally, the resilient modulus of the fine-grained cohesive subgrade material retrieved from the instrumented highway section and to relate this parameter to stress-state conditions prevailing in the field. To fulfill this objective, a repeated loading triaxial apparatus was needed. An equipment designed and constructed after the model of Seed and Fead (1959) was developed with the help of the technical staff of both the Civil Engineering Department at the University of Alberta and the Environmental Department of the Alberta Research Council. This new equipment is similar to the apparatus used earlier by Dasmopatra (1972) and Hadipour (1987) for determining the resilient characteristics of subgrade soils and asphalt concrete mixes, respectively.

A steel framework of the form shown in Plate E.2 was built for seating three triaxial cells along with their loading devices and other equipment needed for their operation. Each triaxial chamber was equipped with an individual load cell for the purpose of measuring the applied repetitive deviator stress.

Load was applied to the soil specimen in the triaxial cell through a bellofram operated on compressed air. Three solenoid valves, mounted on a loading panel, were used to regulate the magnitude of air pressure applied to each triaxial cell. When the valve is open, air pressure is transmitted to the soil specimen through the bellofram. When the valve is closed, air is forced to pass through an exhaust pipe in the valve and the load is removed. The movement of the solenoid-operated three-way valve was controlled by an electronic timing unit.

The specimen inside the triaxial cell was also subjected to an all around confining pressure. This pressure was applied to the specimen through a pressure supply valve located in the base of the triaxial cell. No water medium was used for transmitting the confining pressure to the soil specimen, rather the triaxial cell was filled with compressed air which acts as the medium for applying the confining pressure. The confining pressure was recorded by a pressure transducer. The transducer was mounted on the loading panel and was connected to the triaxial cell through a third inlet in the base of the triaxial chamber.

Two thermocouples encased in a plastic tube were used to monitor the temperature of the soil specimen. The measurements were performed at locations 2.54 cm from the top and 2.54 cm from the bottom of the sample, respectively.

The specimen was loaded axially by applying the repetitive deviator stress under a prescribed constant confining pressure. Axial deformation was measured by an externally mounted linear variable differential transducer (LVDT). The LVDT was clamped to the loading arm of the triaxial cell applying the load and the moving end was screwed to the cell cap. The magnitude of the axial load was measured by a load cell which sat with a firm contact on the piston of the triaxial cell.

The monitoring of the number of load applications to the test specimen and the measurement of all the required stress, strain and temperature data were performed automatically by a data acquisition system controlled by a 286 personal computer.

During any particular test, a graphical form of the collected data, i.e. repetitive deviator stress, confining pressure, axial strain and temperature, was continuously displayed on the computer monitor to ensure that the system is working properly. This feature enabled the immediate recognition of any system malfunction and/or improper seating of the tested soil specimen.

The triaxial cell used in testing was a standard size chamber suitable for testing cylindrical samples 102 mm (4 in.) in diameter by 204 mm (8 in.) high, as described by Bishop and Henkel (1962), except that the recess under the base was adjusted so that the cell could sit on the seat in the frame. A threaded hole on the cap of the triaxial cell was made for the LVDT to be screwed to the cap to provide a reference point for deformation measurements.

Plates E.1 to E.4 show the resilient modulus testing system with further details being given in Appendix E.

5.3 Soil Sample Classification and Grouping

The test soils used in this phase of the study come from the instrumented pavement site. Representative cores from different depths within the subgrade layer were obtained using 102 mm diameter Shelby tubes. The material was left in the 300 mm long Shelby tubes and kept tightly wrapped to prevent moisture loss until just before extraction for resilient modulus testing.

Shovel samples of the natural subgrade were also obtained from the back slope of the shoulder area within the instrumented roadway section. Specimens from this material were prepared in the laboratory for resilient modulus testing purposes.

At the beginning, it was intended to test the soil samples obtained from the field cores in their undisturbed condition. However, unsuccessful sample extraction from the Shelby tubes necessitated the use of remolded samples for the resilient modulus testing program. Although resilient moduli values obtained from remolded soil specimens are expected to be different from those under undisturbed field conditions, it is the prime objective of this study to determine the resilient moduli-stress relationships over the whole spectrum of stress state conditions anticipated to prevail in the field at any point in time during the service life of the highway pavement under consideration. Therefore, the use of remolded soil samples instead of undisturbed samples appears to be justified.

The retrieved subgrade soil material was divided into five groups. Each group represents a specific depth location within the subgrade layer with the last group i.e. soil group 6 being representative of the material obtained from the back slope of the shoulder area. Routine soil tests were performed on these soil groups. This included Atterberg limits, material classification, grain-size distribution, in situ subgrade moisture and field density determinations and standard Proctor tests. Clay X-ray diffraction analyses were also performed on the different soil groups (AT & U, 1995). Tables 5.1 (a) and (b)

summarize the basic soil properties obtained from the aforementioned tests for all soil groups. It should be mentioned that the main reasons behind conducting the above described tests are:

- 1) To obtain the in situ subgrade soil material characteristics.
- 2) To assist in soil sample preparation for resilient modulus testing purposes.

5.4 Resilient Modulus Testing

In this section, the details of the repeated load tests performed will be reviewed. This includes description of the method of soil sample preparation, the test procedure adopted and a summary of the steps followed in conducting the resilient modulus test.

5.4.1 Preparation of Soil Samples

As mentioned previously, reconstituted test specimens were made in the laboratory from a representative portion of the bulk samples.

The soil sample preparation procedure adopted can be summarized as follows:

- (1) Subgrade soil material retrieved from the field was placed in large pans and oven-dried at 110 °C for twenty four hours.
- (2) Dried soil was then crushed and passed through a 5000 μm opening mesh (No. 4 sieve).
- (3) Material passing through the 5000 μm sieve was mixed with distilled water to obtain the desired moisture content. Usually an extra one half percent water was added to allow for evaporation during mixing. Soil was mixed thoroughly by hand for five minutes. Mechanical mixing using the mixer available in the laboratory was not possible because of the large amount of soil required for the preparation of the test samples. After mixing was completed, wet soil was placed in a plastic bag and sealed tightly. The bag was then stored in the moisture room for twenty four

hours to allow for moisture migration within the soil. This was done to ensure uniform water distribution within the soil mass.

- (4) After the twenty four period, the wet soil was removed from the moisture room and hand compacted using the standard ASTM D698-78 Test. The test involves using a 2.49 kg (5.5 lb) drop-hammer hand compactor with a 306 mm (12 in.) free fall distance. The mold used for compaction was a 102 mm (4 in.) diameter by 204 mm (8 in.) long split type mold with a 51 mm (2 in.) collar at the top. Trial compactions were performed to determine which procedure could be used to attain the standard ASTM D698-78 densities. It was found that soil compacted in five layers with twenty-five blows per layer is sufficient to produce the required density. To control the uniformity of samples, material required for preparation of one sample was divided into five equal parts. Each part was then placed in the compaction mold and spread evenly by hand after which twenty-five blows of the drop-hammer were applied around the mold. After the last blow to the fifth layer, the collar was removed and the excess material was trimmed.
- (5) Compacted specimens were then wrapped in many layers of plastic wrap and stored in the moisture room until time for resilient modulus testing. Following the above procedure, several samples for each soil group were prepared at different prescribed moisture contents. The range of moisture content used was intended to bracket the water range of critical moisture conditions. This resulted in molding moisture contents in the range of ± 2 percent of optimum water content as determined from a standard Proctor compaction curve for each soil group.

5.4.2 Test Protocol

An important consideration in carrying out any resilient modulus testing study is the selection of an appropriate test procedure. From the literature, several options are available. Examples include the Asphalt Institute test method developed in 1973 for full depth airfield pavements and the established AASHTO T274-82 (1982) procedure. After

careful examination of the features and merits and demerits of the various test methods available, it was decided to choose the recently adopted standard AASHTO T 294-92 test procedure (1992) for the purposes of this investigation.

The AASHTO T 294-92 procedure is a modified version of the AASHTO T 274-82 test method. This procedure was originally developed by a group of researchers in Austin, Texas in 1989 to fulfill the SHRP program needs for evaluating the resilient characteristics of cohesive soils and unbound granular materials. The test was developed with the intention of producing more uniform test results and thus providing a common platform for comparison of test results obtained by different investigators and/or transportation department laboratories. Furthermore, redundancy in load sequence application inherent in the former AASHTO T 274-82 procedure has been removed. This greatly improved the testing procedure and made the time needed for test execution considerably shortened.

The T 294-92 procedure consists of two parts. One part deals with testing unbound granular materials while the second part describes the steps to be followed in testing cohesive fine-grained subgrade soils. Only the part that illustrates testing cohesive subgrade soils will be described here.

The test procedure identifies cohesive subgrade materials as soil Type 2. The testing method consists of applying a repeated axial deviator stress of fixed magnitude, load duration and cycle duration to a cylindrical test specimen. During testing, the specimen is subjected to a dynamic deviator stress and a static all-around stress provided by means of a triaxial pressure chamber. The resilient (recoverable) axial deformation response of the specimen is measured and used in conjunction with the deviator stress to calculate the resilient modulus.

The load sequence during the test depends on soil designation. For material Type 2 (i.e. fine-grained subgrade soils), the load sequence shown in Table 5.2 is followed. Five levels of deviator stress and three levels of confining pressure are used to cover the practical range of stresses expected to prevail under in situ conditions. Unconfined tests (i.e. with zero confining pressure) are not used since such stress state never occurs under in situ conditions. Also, deviator stresses less than 14 kPa (2 psi) are not used because practical experience has shown that major dispersion in the test results occurs at small stress levels (Pezo et al., 1991). The high dispersion is suspected to be the product of the small resilient deformation which can not be measured accurately and sometimes is not bigger than the noise of the recorded signal.

The number of load applications to the test sample at any particular combination of deviator and confining stress levels is limited to 100 repetitions. This is done based on extensive research findings that report that changes experienced in resilient modulus values after 100 load applications are insignificant. A failure criterion is also included in the test procedure to eliminate samples with large permanent deformations. A soil specimen is considered failed if it experiences permanent vertical strain greater than 10 percent.

The external loading source required by the test protocol is a closed-loop electro-hydraulic system. However, the author's experience with the open-loop air system used in the current study serves to illustrate that such a system is equally capable of providing the prescribed load duration and cycle duration specified by the AASHTO T 294-92 procedure. The main advantage of using an open-loop air system is its relatively cheap overall cost compared to the more expensive closed-loop hydraulic system. A haversine stress pulse with load duration of 0.1 sec and a cycle duration of 1 sec as recommended by

the test procedure has been used in the current investigation. The shape and characteristics of this load pulse, shown in Figure 5.1, is a true representation of the shape of a truck load on the pavement as reported by Thompson and Robnett (1976). It is also similar to the load pulse generated by non-destructive testing devices such as the Falling Weight Deflectometer.

The triaxial cell fluid used for the provision of the all-around static pressure is air. This confining pressure was monitored by a pressure transducer with an accuracy of 0.7 kPa (0.1 psi) as specified by the AASHTO T 294-92 procedure. Criteria for selecting load cell and LVDT's to be used in the test are also specified by the testing protocol and depend on sample diameter. Recommended working ranges are shown in Table 5.3. These guidelines, however, were not followed exactly during the current study. Rather, load cells with 450 kg (1000 lb) capacity and LVDT's with ± 6.4 mm (± 0.25 in) range were used.

5.4.3 Conducting The Resilient Modulus Test

The following steps illustrate the routine used in testing the reconstituted soil samples:

- (1) The compacted soil specimen was removed from the moisture room and the diameter, D , the length, H_1 , and weight, W_{w1} of the cylindrical sample were measured and recorded.
- (2) The specimen was then grouted at each end to an aluminum circular plate using a hydrostone paste (Plaster of Paris). This was done because other researchers experience with resilient modulus testing (Pezo et al., 1991) showed that good contact between tested specimen and end platens is an important factor in evaluating M_r . Grouting has also proved useful in adjusting any unevenness in the ends of the tested sample.

- (3) After the specimen was grouted to the end platens, the new length of the specimen (with the platens) was measured and recorded as H_2 . The weight of the wet specimen, with the platens, W_{w2} , was also recorded.
- (4) Sample was then placed inside the triaxial chamber and two rubber membranes were placed around the specimen to prevent moisture loss or air migration during testing.
- (5) Testing was started by first subjecting the sample to a conditioning stage. For cohesive materials, the T 294-92 procedure recommends the application of 200 repetitions of a 28 kPa (4 psi) deviator stress under a 42 kPa (6 psi) confining pressure. This conditioning stage was intended to eliminate the effects of the interval between compaction and loading and also of initial loading versus reloading. The conditioning also aids in minimizing the effects of initially imperfect contact between the end platens and the test specimen (in other words, help in correctly seating the loading ram on the top of the tested specimen).
- (6) After conditioning was completed, the testing sequence displayed in Table 5.2 was followed. This consisted of applying 100 repetitions of each one of the specified deviator stresses of 14, 28, 42, 56, and 70 kPa (2, 4, 6, 8, and 10 psi) in ascending order at each level of the specified confining pressures of 42, 28, and 14 kPa (6, 4, and 2 psi) in descending order. This resulted in 15 sets of test data that could be used to compute 15 different moduli values at the different stress states.
- (7) At the completion of the loading sequences, the confining pressure was reduced to zero and the triaxial cell was disassembled.
- (8) The length, H_3 , and diameter, d , of the specimen after the test were measured and recorded.
- (9) The tested specimen was weighed and then placed in the oven and left to dry at 110 °C for 24 hours.

- (10) The moisture content of the soil sample was then computed from the wet and dry weights of the tested specimen.

An example worksheet used in recording the resilient modulus test results is shown in Figure 5.2.

5.5 Scope and Limitations of The Laboratory Testing Program

The laboratory testing phase was initiated to examine, in depth, how the resilient modulus of cohesive subgrade soils is affected by the following parameters:

- i) Soil matric suction
- ii) Deviator stress
- iii) Confining pressure
- iv) Soil density
- v) Temperature

Only one type of subgrade soil has been investigated in this study. The soil chosen represents a typical subgrade material that is frequently encountered in the Province of Alberta. It is a medium to low plasticity silty clay material that classifies as a CL-CI type soil according to the Unified Soil Classification System. This soil also classifies as a soil Type 2 according to the AASHTO T 294-92 Resilient Modulus Test Procedure.

Inability to continuously monitor soil matric suction under repeated loading test conditions necessitated the estimation of this parameter from water content-matric suction relations known as moisture retention curves. Because of the anticipated significant effect of matric suction on the resilient modulus, great care was exercised in estimating this parameter from the moisture retention curves. Continuous measurement of the other parameters during the repeated loading test did not present any problem.

The results obtained from repeated load tests are accurate within the error range of the devices used. This includes loading cells, pressure transducer, LVDT's, and temperature-measuring thermocouples. Further details on this are contained in chapter 6.

5.5 Summary

This chapter gives an overview of the specifics of the laboratory testing program pertaining to the current investigation. The chapter consists of three main parts. In the first part, a description of the resilient modulus testing system was given. This included both the resilient modulus testing apparatus and the data acquisition system used for data monitoring and collection.

In the second part, the details pertaining to the resilient modulus testing were presented. This included the preparation of the test specimens, the description of the test procedure used, and the steps involved in conducting the actual test.

In the third part, the scope and limitations of the test program were highlighted. This included the parameters being studied, the type of subgrade soil being investigated, and the limitations of the resilient modulus system being used in carrying out the investigation.

The results obtained from the laboratory testing program and the interpretation of these results will be presented and discussed in chapter six.

References

1. AASHTO (1982), "*Standard Method of Test for Resilient Modulus of Subgrade Soils - AASHTO Designation: T 274-82*," AASHTO Methods of Sampling and Testing, pp. 1157-1177. (N.B.: This test procedure is discontinued as of 1992)
2. AASHTO (1992), "*Resilient Modulus of Unbound Granular Base/Subbase Materials and Subgrade Soils - SHRP Protocol P46: AASHTO Standard Test Designation T 294-92*," American Association of State Highway and Transportation Officials.
3. Alberta Transportation and Utilities (1995), "*Bulk and Glycolated Clay XRD Analysis*," An Internal Report Prepared by Chemical & Geological Laboratories Inc. for AT&U Roadway Engineering Branch.
4. Dasmohapatra, D.K. (1973), "*An Investigation into the Application of Elastic Theory to Predict Deflections in Full-Depth Asphalt Pavements*," M.Sc. Thesis, University of Alberta, Edmonton, Canada.
5. Hadipour, K. (1987), "*Materials Characterization of Recycled Asphalt Concrete Pavements*," Ph.D. Thesis, University of Alberta, Edmonton, Canada.
6. The Asphalt Institute (1973), "*Full Depth Asphalt Pavements for Air Carrier Airports*," Manual Series No. 11 (MS-11).
7. Bishop, A.W. and D.J. Henkel (1962), "*The Measurement of Soil Properties in the Triaxial Cell*," Second Edition, Arnold Publishers.
8. Pezo, R.F., D. Kim, K.H. Stokoe and W.R. Hudson (1991), "*A Reliable Resilient Modulus Testing System*," Transportation Research Board Record 1307, Washington, D.C., pp. 90-98.
9. Seed, H.B. and J.W.N. Fead (1959), "*Apparatus for Repeated Load Test in Soils*," Special Technical Publication No. 254, American Society for Testing and Materials.
10. Thompson, M.R. and Q.R. Robnett (1976), "*Final Report: Resilient Properties of Subgrade Soils*," Transportation Engineering Series No. 14, University of Illinois at Urbana-Champaign.

Table 5.1(a): Properties of Tested Subgrade Soils

Soil Property	Soil # 1	Soil # 2	Soil # 3	Soil # 5	Soil # 6
Location (from top of Subgrade)	0.16 m	0.33 m	0.59 m	1.07 m	Side Slope
% Passing Sieve 5000 (μm)	96	95	100	97	95
% Passing Sieve 400 (μm)	93	92	97	94	93
% Passing Sieve 160 (μm)	64.5	-	-	-	-
% Passing Sieve 80 (μm)	43.9	51.2	64.6	59.1*	59*
% Passing Sieve 60 (μm)	41	49	63	62	60
Soil Classification (Unified System)	SC	CI - CL	CI	CI	CI
Soil Description	clayey sand	sandy clay	sandy clay	sandy clay	sandy clay
Liquid Limit, % (LL)	30.0	32.0	37.8	38.1	36.3
Plasticity Index, % (PI)	12.7	12.3	21.3	20.5	17.5
Proctor Max. Density (kg/m^3)	1851	1825	1800	1768	1770
Optimum Moisture Content (%)	14.8	15.7	16.3	16.9	17.4
% Silt Content	29	35	38	43	44
% Clay Content	12	14	25	19	16
Specific Gravity (G_s)	2.792	2.756	2.769	2.760	2.787

* indicates an error in measurements

Table 5.1(b): Bulk Fraction X-Ray Diffraction Data

Soil #	Qtz	Plag	KFd	Cal	Dol	Sid	Pyr	Kaol	Ill	Smec	Total Clay
G 1	59.1	11.1	3.6	1.4	2.2	-	-	3.2	6.5	12.9	22.6
G 2	55.8	23.8	tr	-	0.9	-	-	2.1	6.4	11.0	19.5
G 3	45.7	14.0	tr	2.9	1.6	-	2.5	6.2	12.3	14.8	33.3
G 5	56.8	11.9	5.3	1.4	1.4	-	-	3.2	11.6	8.4	23.2
G 6	57.2	4.1	tr	tr	tr	-	-	5.5	15.0	18.2	38.2

Qtz - Quartz; Plag - Plagioclase feldspar; KFd - Potassium feldspar; Cal - Calcite; Dol - Dolomite; Sid - Sidrite; Pyr - Pyrite; Kaol - Kaolinite; Ill - Illite; Smec - Smectite; **Total Clay = Kaol + Ill + Smec**

Table 5.2 Load Sequence for Testing Soil Type 2

Sequence Number	Conf. Pres. σ_3 (kPa)	Dev. Stress σ_d (kPa)	# of Load Applications
1	42	14	100
2	42	28	100
3	42	42	100
4	42	56	100
5	42	70	100
6	28	14	100
7	28	28	100
8	28	42	100
9	28	56	100
10	28	70	100
11	14	14	100
12	14	28	100
13	14	42	100
14	14	56	100
15	14	70	100

Table 5.3: Recommended Load Cell and LVDT Ranges for Different Test Specimen Configurations

Sample Diameter (cm)	Load Cell Capacity (kg)	LVDT Range (cm)
7.11	45.45	± 0.127
10.16	272.73	± 0.254
15.24	636.36	± 0.635

Notes: 1 kPa = 0.143 psi
 1 cm = 0.394 in.
 1 kg = 0.455 lb

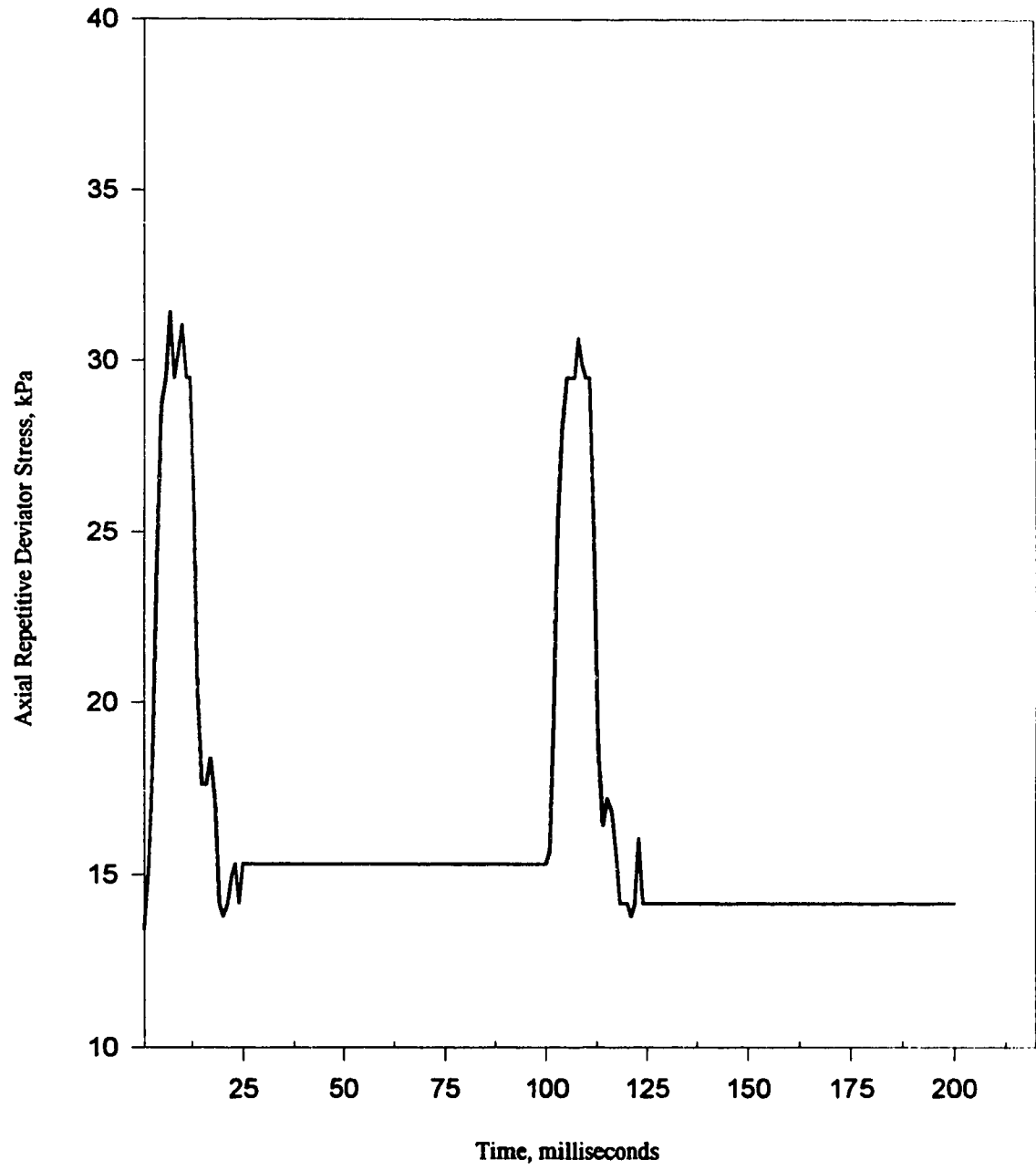


Figure 5.1: Typical Load Trace Produced by Resilient Modulus Testing Equipment

Figure 5.2: Example Worksheet for Recording Resilient Modulus Test Results

RESILIENT MODULUS TESTING DATA COLLECTION SHEET

Sample Identification: (a) Group # _____
 (b) Location _____
 (c) Test Date _____

Sample Characteristics:

	<u>As Received from AT & U Labs</u>	<u>At Time of Testing</u>
1.	Avg. Dia. , D, (in.) = _____	d* = _____; _____; _____ D _____
2.	Avg. Height, H, (in.) = _____	h* = _____; _____; _____ H1 _____
		h* = _____; _____; _____ H2 _____
		d** = _____; _____; _____ D _____
		h** = _____; _____; _____ H3 _____
		h** = _____; _____; _____ H4 _____
3.	Wet Weight, W _w , (g) = _____	Wet Weight, W _{w1} *, (g) = _____
		Wet Weight, W _{w2} *, (g) = _____
		Wet Weight, W _{w3} **, (g) = _____
4.		Dry Weight, W _{d1} , (g) = _____
		Dry Weight, W _{d2} , (g) = _____
5.	Moisture Content, m.c. = _____ %	m.c.1 = _____
		m.c.2 = _____
6.		Wet Volume, V _w , (ml) = _____
7.		Bulk Density (kg/m ³) = _____
8.		Dry Density (kg/m ³) = _____

Testing Specifications:

Test Bay _____ Total # of Reps = _____

Seating Pressure _____ (psi)

Instrumentation Balance(s) @ Beginning of Test

1. LVDT = _____ x 10⁻³ (in.)
2. Load Cell = _____ (lb)
3. Pressure Transducer = _____ x 10⁻² (psi)

Figure 5.2: Continued

Instrumentation Balance(s) @ End of Test

1. **LVDT** = _____ $\times 10^{-3}$ (in.)
2. **Load Cell** = _____ (lb)
3. **Pressure Transducer** = _____ $\times 10^{-2}$ (psi)

Testing Sequence:

Conditioning 200 Reps of a 4 psi Deviator stress @ a confining pressure of 6 psi

Testing 100 Reps of

- | | | |
|-----|------------|-------------|
| 1. | p3 = 6 psi | pd = 2 psi |
| 2. | p3 = 6 psi | pd = 4 psi |
| 3. | p3 = 6 psi | pd = 6 psi |
| 4. | p3 = 6 psi | pd = 8 psi |
| 5. | p3 = 6 psi | pd = 10 psi |
| | | |
| 6. | p3 = 4 psi | pd = 2 psi |
| 7. | p3 = 4 psi | pd = 4 psi |
| 8. | p3 = 4 psi | pd = 6 psi |
| 9. | p3 = 4 psi | pd = 8 psi |
| 10. | p3 = 4 psi | pd = 10 psi |
| | | |
| 11. | p3 = 2 psi | pd = 2 psi |
| 12. | p3 = 2 psi | pd = 4 psi |
| 13. | p3 = 2 psi | pd = 6 psi |
| 14. | p3 = 2 psi | pd = 8 psi |
| 15. | p3 = 2 psi | pd = 10 psi |

Data File Naming

G?-??CON.dat & G?-??CON.tmp (for conditioning)

G?-??.dat & G?-??tmp (for load sequence)

where:

first ?	Group #
second ?	Sample #
third ?	Load sequence #

Figure 5.2: Continued

Notes:

* indicates status @ beginning of test

** indicates status @ end of test

H1 = height of soil sample with no grouting (at beginning of test - wet soil)

H2 = height of soil sample with grouting (at beginning of test - wet soil)

H3 = height of soil sample with grouting (at end of test - wet soil)

H4 = height of soil sample with no grouting (at end of test after 24 hrs - dry soil)

Ww1 = wet weight of sample with no grouting (at beginning of test)

Ww2 = wet weight of sample with grouting (at beginning of test)

Ww3 = wet weight of sample with grouting (at end of test)

Wd1 = dry weight of sample with grouting (after 24 hrs after test)

Wd2 = dry weight of sample with no grouting (after 24 hrs after test)

m.c.1 = moisture content (using non grouted sample condition)

m.c.2 = moisture content (using grouted sample condition)

Plate 1 (with dry grouting) = ----- inches ; P1 (used)= ----- in. & ----- g

Plate 2 (with dry grouting) = ----- inches ; P2 (used)= ----- in. & ----- g

Further Notes (if any!):

1.

2.

3.

4.

5.

6.

7.

8.

9.

CHAPTER SIX

PRESENTATION AND DISCUSSION OF LABORATORY TEST RESULTS

6.1 Introduction

The primary objective of the laboratory testing program was to examine, in depth, the resilient deformation characteristics of cohesive subgrade soils in Alberta, with particular regard to changing seasonal trends as induced by environmental factors such as temperature and moisture variations. To achieve this goal, an extensive repeated loading laboratory testing scheme was formulated to investigate how the subgrade resilient modulus is affected by the following parameters:

- i) Soil matric suction, ψ
- ii) Deviator stress, σ_d
- iii) Confining pressure, σ_3
- iv) Soil density, γ_d
- v) Temperature.

To reduce the research scope to a manageable size, only one type of subgrade soil was investigated in this study. The selected soil represents a typical subgrade material that is frequently encountered in primary highways in Alberta. It is a low to medium plasticity, silty clay material that classifies as a CI-CL type soil according to the Unified Soil Classification System.

Another limitation that was put on the research is the fact that the current state of technology does not permit continuous monitoring of soil matric suction under repeated-loading test conditions. This necessitated the estimation of this parameter from water content-matric suction relations known as moisture retention curves. Because of the

anticipated significant effect of matric suction on the resilient modulus, great care was exercised in obtaining this parameter from the moisture retention curves. Continuous measurement of other parameters of interest during the repeated loading test did not present any problem.

The resilient modulus results obtained from repeated load tests are accurate within the error ranges of the measurement devices used. This includes loading cells, pressure transducer, LVDT's and temperature-measuring thermocouples. For further details consult Appendix E.

6.2 Planning the Laboratory Testing Program

As has been mentioned previously, the test soil specimens used in this phase of the study came from the instrumented pavement site. Representative cores from various depths within the subgrade layer were obtained using 102mm diameter Shelby tubes. The retrieved soil samples were taken from depths at 0.16m, 0.33m, 0.59m and 1.07m from the top of the subgrade layer. These soils were designated as soil group 1, soil group 2, soil group 3 and soil group 5, respectively. Shovel samples of the natural subgrade, i.e. unprepared subgrade, were also obtained from the side slope of the area of the instrumented roadway section. This material was designated as soil group 6.

Several classical soil tests were performed on all soil groups for the purposes of identification and classification of these soils. The results of these tests are displayed in Table 5.1 in chapter 5 and in Figures 6.1 to 6.6 in the current chapter.

Beside the Proctor maximum dry density and optimum moisture content values obtained for each soil group, the actual field densities and in situ moisture contents of the retrieved soil samples were also determined. These values were plotted for soil groups 1, 2, 3, and 5 and they were denoted by the triangular symbols shown in Figures 6.2 to 6.5.

From Figures 6.3 through 6.5, it is clear that the points representing the field conditions of moisture and dry density for soil groups 2, 3 and 5 all fall within, or very near, the specified range of 95% to 99% maximum dry density set by AT&U for compacted subgrade fill sections. However, the same observation does not hold true for soil group 1. For this soil group a field density value corresponding to approximately 92% Proctor maximum dry density was obtained. This low density which may have been brought about by an error in sampling is not reliable and therefore can not be trusted to represent the in situ conditions of the upper portion of the subgrade soil layer. Also in the case of soil group 6, no measurement point representing field conditions was drawn since this soil was a loose material that was obtained from the side slope area of the instrumented section.

Further tests to determine the “water content-matric suction” relations, commonly referred to as soil moisture retention curves, for the different soil groups were also performed.

The laboratory experimental program involved three stages:

- (1) preparing soil samples for resilient modulus testing,
- (2) conducting the repetitive load tests, and
- (3) establishing the relationship(s) between soil matric suction and soil water content.

The procedures used for sample preparation and for conducting the resilient modulus test have already been described in chapter 5. This description also included the selection of ranges of values of the different factors to be investigated. However, such practice was not applied equally to all the parameters studied. No ranges were set forth for either the soil density or the temperature. Rather, values of soil density obtained through the compaction of test specimens and actual temperature conditions monitored

during resilient modulus testing were recorded and later used in the analysis of these two parameters.

6.3 Establishing the Relationship(s) between Soil Matric Suction and Soil Water Content

The relations between the soil matric suction and the soil water content have been determined for all the soil groups included in the current research. This was done to enable the inference of matric suction values from measurements of soil water content.

The relationship between soil water content and soil water suction is identified in the literature by various names such as water retention function, moisture characteristic, and capillary pressure-saturation curve (Klute, 1986). The soil water content is usually expressed on weight basis while soil suction is expressed in units of energy per unit volume (a unit that is dimensionally equivalent to force per unit area or pressure).

The determination of the water retention function, or curve, usually involves establishing a series of equilibria between water in the soil sample and a body of water at known potential (Klute, 1986).

Another property of the water retention curve is that it is hysteretic. This means that the water retention curve obtained by wetting the soil is different from that obtained by drying the soil. The drainage curve usually yields higher suction values than the wetting curve for the same water content. In the current investigation, water retention curves for the various soil groups were obtained using the adsorption procedure, i.e. one that produces drainage water retention curves. Although this is different from the procedure used for preparing the soil test specimens for resilient modulus testing (absorption process), the justification was that hysteresis effects can be considered negligible for all practical purposes. This consideration was further imposed by the fact that the test had to

be carried out at the Soil Science Department due to the unavailability of the equipment needed to perform the test in the laboratories of the Civil Engineering Department.

It is worthy to note that the retention curves for the various soil groups were obtained using disturbed soil samples. The use of disturbed soil specimens was justified based on the suggested evidence in the literature that a unique relationship does exist between matric suction and soil water content irrespective of the soil dry density (Croney and Coleman, 1960; Olson and Langfelder, 1965; and Fredlund and Krahn, 1972).

The water retention curves obtained for the various soils studied in this research are shown in Figures B.1 to B.5 in Appendix B.

6.4 Resilient Modulus Test Results and Analysis Methodologies

Repeated loading tests on the five soil groups were performed to obtain their resilient characteristics. This involved testing twenty eight reconstituted samples from the various groups. In the following sections of this chapter, test results will be displayed and discussed on a group by group basis.

Two analysis strategies were followed in interpreting the test results. The first strategy involved plotting the resilient modulus against the various stress and environmental parameters and commenting on the trends observed in these graphs.

In the second strategy, models for predicting the resilient modulus for the particular soil group using stress and/or environmental parameters were developed. These models were postulated using multiple linear regression techniques. The validity of the model(s) in predicting the resilient modulus response was carefully checked using different diagnostic statistical analyses.

6.4.1 Graphical Analysis Method

6.4.1.1 Test Results of Soil Group #1

Soil group 1 represents the subgrade soil material retrieved from depth 0.16m below the top of the subgrade layer. This material was classified as an SC-type soil according to the Unified Soil Classification System. The characteristics of this soil are displayed in Table 5.1 and in Figure 6.2.

Samples prepared in the laboratory from this soil were tested after two to three days from the time of their preparation. Four specimens were prepared at moisture contents of 14.3%, 15.4%, 15.9% and 18% respectively. This corresponds to a water content range from - 0.5% dry of optimum to + 3.2% wet of optimum. Repeated load tests, using the AASHTO T 294-92 Procedure, were conducted on the four soil samples and the results obtained are shown in Figures 6.7 to 6.9

Resilient modulus values for soil group 1 ranged from 8 to 127.5 MPa for the range of water content investigated. This corresponds to a subgrade strength range of approximately 1 to 12 CBR (Shell, 1978). One way of interpreting the test results, is to examine graphically the effect of each stress state variable on the resilient modulus.

(i) $M_r - \sigma_d$ relationship:

Figures 6.7 (a) through 6.7 (c) show the variation of resilient modulus with deviator stress for soil group 1. The general trend that was observed in all of these figures is that resilient modulus decreases with increasing deviator stress. This trend is more pronounced at high levels of confining pressure and/or soil matric suction. It was also seen that near the optimum moisture content, i.e. 14.8%, the rate of decrease in the resilient modulus was very pronounced with a slight increase in the deviator stress especially in the low range of deviator stresses (up to 42 kPa). This is indicated by the

shape of the two curves representing matric suctions of 170 kPa (or 15.4% water content) and 218 kPa (14.3% water content). This observation is in agreement to that reported by Dasmohapatra in 1973.

It was observed that for samples compacted wet of optimum moisture content, the rate of decrease in resilient modulus with increase in the deviator stress was moderate or very little.

From Figures 6.7 (a) to 6.7 (c), it is also noticeable that the influence of soil matric suction on the resilient modulus is more pronounced than that of the deviator stress. This point will be discussed in detail in the next section.

(ii) $M_r - \psi$ relationship:

The resilient modulus, M_r , versus matric suction, ψ , relationship at three different levels of confining pressure is shown in Figures 6.8 (a) to 6.8 (c). From these figures, it was observed that the resilient modulus increases as matric suction increases. Moreover, it is clearly evident that matric suction has a very pronounced effect on the resilient modulus. For example, for the range of the water content investigated, i.e. -0.5% to $+3.2\%$ above optimum, and confining pressure of 14 kPa, the resilient modulus increases by seven orders of magnitude (from about 10 MPa to more than 80 MPa).

The effect of the deviator stress, σ_d , in influencing the $M_r - \psi$ relation is minimal especially at low levels of confining pressure. On the other hand, the influence of σ_3 on the $M_r - \psi$ relation is more predominant. This can be illustrated by the observation that for a change of 28 kPa, or 4 psi, in σ_3 , the corresponding increase in M_r , for the same value of matric suction, equals 47 MPa (this can be seen by comparing the M_r values of Figures 6.8 (a) and 6.8 (c) at a deviator stress, σ_d , of 14 kPa).

It is also seen that the effect of matric suction on the resilient modulus is more pronounced at high levels of matric suction. For example, from Figure 6.8 (a), a change in matric suction from 92 kPa to 170 kPa produces a change of about 10 MPa in the resilient modulus, whereas for a change in matric suction from 170 kPa to 218 kPa, the corresponding change in M_r is about 60 MPa. This trend is also observable in Figures 6.8 (b) and 6.8 (c).

(iii) $M_r - \sigma_3$ relationship:

Figures 6.9 (a) to 6.9 (e) show the relationship between the resilient modulus and the confining pressure, σ_3 . The general trend in all these figures indicates that M_r increases as σ_3 increases. The increase in M_r is more pronounced at high levels of matric suction. This phenomenon can be interpreted based on the fact that at high levels of matric suction (i.e. low levels of water content) the voids within the soil structure are largely filled with air, which is a highly compressible fluid and therefore an increase in the confining pressure produces a significant increase in the soil stiffness, as measured by its resilient modulus. On the other hand, for soil specimens compacted at water contents above optimum (i.e. low matric suction), the increase in M_r due to an increase in σ_3 will not be significant because of the fact that the soil voids are now largely filled with water which is an incompressible fluid.

It is also noticed that, for samples compacted dry of optimum (i.e. at high suction levels), the influence of the confining pressure on the resilient modulus increases with increased deviator stress up to a certain value then decreases with further increase in deviator stress. This can be illustrated by the following example. Let us consider the case of the soil sample having matric suction of 218 kPa. Under a deviator stress of 14 kPa, an increase in σ_3 from 14 kPa to 42 kPa produces a corresponding increase in M_r of about 45 MPa. At a higher deviator stress of 42 kPa, and under the same σ_3 and ψ conditions,

the increase in M_r becomes 50 MPa. As we increase the deviator stress further to 70 kPa, the increase in M_r drops from 50 to about 22.5 MPa.

The influence of σ_d on the $M_r - \sigma_3$ relation for samples compacted wet of optimum can be viewed by examining the trend of the two curves representing soil suction values of 152 kPa and 92 kPa, respectively. By looking at these two curves, Figures 6.9 (a) to 6.9 (e), it can be seen that as the deviator stress is increased, from 14 kPa to 70 kPa, the effect of σ_3 on M_r gradually diminishes.

6.4.1.2 Test Results of Soil Group #2

Soil group 2 represents the subgrade soil horizon at depth 0.33m below the top of the subgrade layer. This material was classified as a CI-CL type soil according to the Unified Soil Classification System. It is a low to medium plasticity clay material with the characteristics shown in Table 5.1 and Figure 6.3.

Five soil samples were prepared at moisture contents of 15.1%, 16.1%, 16.9%, 17.7%, and 18.7%. This covers a water content range of – 0.6% dry of optimum to +3.0% wet of optimum. The corresponding suction range obtained from the water retention curve for this soil is from 132 kPa to 258 kPa. Repeated load tests were conducted on the prepared specimens and the results are displayed in Figures 6.10 to 6.12

Resilient modulus values for this soil group ranged from 8.2 to 100 MPa for the range of water content studied. This corresponds to a subgrade strength range of about 1 to 10 CBR based on the relationship developed by Shell Company in 1978.

(i) $M_r - \sigma_d$ Relationship:

The resilient modulus-deviator stress relationship for soil group 2 is displayed in Figures 6.10 (a) through 6.10 (c). The general trend observed before for soil group 1 is

repeated again here. Furthermore, the influence of σ_d on M_r appears to be more significant in the case of this soil group than in the case of the previous soil group.

For samples compacted wet of optimum (i.e. samples with matric suction values of 184 kPa, 160 kPa, and 132 kPa), the rate of decrease in resilient modulus due to increase in deviator stress is more pronounced than that for samples compacted dry of optimum (i.e. samples with suction values of 212 kPa and 258 kPa). This is contrary to the behaviour of soil group 1. This phenomenon indicates that this type of subgrade soil is more sensitive to changes in deviator stress at low levels of matric suction than at high levels of matric suction.

It is also observed that increasing the confining pressure slightly seems to affect significantly the $M_r - \sigma_d$ relationship especially at low levels of matric suction. This is quite evident from the shape of the curves representing matric suction levels of 184 kPa, 160 kPa, and 132 kPa.

From Figures 6.10 (a) to 6.10 (c), it is also evident that matric suction has a greater influence on the resilient modulus-deviator stress relationship than that of the confining pressure. For example, a change in matric suction of 126 kPa (corresponding to a total change of 2.6% in water content), produces a change in resilient modulus of between 55 to 75 MPa depending on the level of confining pressure at which the specimen had been tested. On the other hand, increasing the confining pressure from 14 kPa to 42 kPa produces a maximum change in the resilient modulus of about 35 MPa (as depicted by the curve representing the soil specimen having a matric suction value of 184 kPa, in Figure 6.10 (c)).

(ii) $M_r - \psi$ Relationship:

The influence of soil matric suction on the resilient modulus for this soil group is depicted in Figures 6.11 (a) through 6.11 (c). As matric suction increases so does the resilient modulus. This continues up to a value of suction of 212 kPa, or 2% above optimum water content, after which a drop in resilient modulus occurs. This is observed to occur at all levels of confining pressures. Also, the greatest amount of change in M_r values is observed to occur between matric suction values of 184 kPa and 212 kPa, i.e. +1.2% to +2.0% above optimum water content. This observation indicates that this type of soil is more susceptible to changes in stiffness, as afflicted by matric suction, in the water content range of 1 to 2% above optimum.

The effect of the deviator stress in influencing the $M_r - \psi$ relationship is more pronounced for this soil than the previous soil group. This is characterized by the relatively great dispersion observed for the various curves representing the different deviator stress conditions, shown in Figures 6.11 (a) to 6.11 (c). This effect is further augmented by increasing the confining pressure from 14 kPa to 42 kPa.

Among the three stress state variables, i.e. matric suction, deviator stress, and confining pressure, suction is the most influential in affecting the resilient modulus. For the range of water content investigated, i.e. 0.6% dry of optimum to 3% wet of optimum, the change in M_r induced by matric suction is about 2.3 to 3.5 times greater than that induced by σ_d , and 3.5 to 14 times greater than that induced by σ_3 for all soil samples tested.

(iii) $M_r - \sigma_3$ Relationship:

Figures 6.12 (a) to 6.12 (e) show the relationship between the resilient modulus and the confining pressure at five levels of deviator stress. The resilient modulus is found to increase as the confining pressure increases. The change in M_r is observed to be

greater in the middle range of matric suction values, i.e. 160 kPa to 212 kPa, than at either the low suction or high suction range values. This again confirms the earlier finding that this soil group is more susceptible to changes in stiffness, as produced by a change in the stress state conditions, within the water content range of 1 to 2% above optimum than at any other water content level.

Changing the deviator stress conditions appears to influence the $M_r - \sigma_3$ relationship in two ways. First, as the level of the deviator stress is increased, the $M_r - \sigma_3$ curves shift to a lower order of magnitude. This continues up to a deviator stress level of 42 kPa. Second, by increasing the deviator stress beyond 42 kPa, this causes the confining pressure to have lesser influence on the resilient modulus.

The trend shown in Figures 6.12 (a) to 6.12 (e) again substantiates the conclusion arrived at earlier that the influence of matric suction in affecting the resilient modulus far outweighs the effects of both the deviator stress and the confining pressure.

6.4.1.3 Test Results of Soil Group #3

Soil group 3 represents the subgrade soil material extracted from depth 0.59m below the surface of the subgrade layer. This material is a medium plasticity clay soil that classifies as a CI soil type with the characteristics displayed in Table 5.1 and Figure 6.4.

Only three soil specimens were prepared from this soil group at moisture contents of 17%, 17.1%, and 18.2%, respectively. The preparation of extra soil specimens at optimum and below optimum water content was not successful due to difficulties encountered in compacting these specimens (the cylindrical samples prepared were too dry to hold together). Consequently, the range of water content investigated for this soil was only from +0.7% to +1.9% above optimum water content. The corresponding matric suction values obtained from the water retention curve ranges from a minimum of 346 kPa

to a maximum of 377 kPa. This is a very narrow range which will be seen later to limit the interpretation of the resilient modulus test results for this particular soil group.

Figures 6.13 to 6.15 contain the test results obtained from repeated load testing for this soil group. From these figures, resilient modulus values ranged from 54 to 104 MPa. This corresponds to a strength range of 5 to 10 CBR.

(i) $M_r - \sigma_d$ Relationship:

The relationship between the resilient modulus and the deviator stress for soil group 3 is displayed in Figures 6.13 (a) to 6.13 (c). These plots show that as the deviator stress is increased, the resilient modulus decreases. However, there seems to be some scatter in the data at low levels of deviator stress. This is particularly evident at both low and high levels of confining pressure, see Figures 6.13 (a) and 6.13 (c). Also, the rate of decrease in the resilient modulus seems greater at low levels of matric suction than at high levels. This suggests that this soil is more sensitive to changes in deviator stress at wet of optimum moisture contents than near optimum water content. This is in agreement with the same observation noted before for soil group 2. No conclusions can, however, be drawn for the dry of optimum range since no soil specimen was fabricated and tested under such conditions.

It is further observed that as the level of the confining pressure is increased, the trend in the $M_r - \sigma_d$ relationship becomes more pronounced. In other words, the rate of decrease of M_r as a function of σ_d increases with increased σ_3 .

(ii) $M_r - \psi$ Relationship:

Figures 6.14 (a) through 6.14 (c) illustrate the relationship between soil matric suction and the resilient modulus pertaining to group 3. The resilient modulus is a direct function of matric suction. As suction increases so does the resilient modulus. The

magnitude of increase in the resilient modulus varies from a minimum of 10 MPa to a maximum of 32 MPa, for the range of water content studied, depending on the levels of both the deviator stress and the confining pressure. It was also observed that the M_r - ψ curves representing σ_d of 14 kPa and σ_d of 28 kPa behave in a different manner to the other curves especially at low and high levels of confining pressure. This may be attributed to measurement and/or computational errors in the M_r values obtained at the aforementioned low deviator stress levels.

Further, the influence of the deviator stress in affecting the M_r - ψ relation seems to be of an equal magnitude to that of the confining pressure.

(iii) M_r - σ_3 Relationship:

The effect of changing the confining pressure in relation to the resilient modulus is shown in Figures 6.15 (a) through 6.15 (e). The general trend indicates that as the confining pressure value is increased, the resilient modulus increases as well. However, the increase seems to be greater at low levels of deviator stress than at high levels.

Moreover, changing the confining pressure by a small amount appears to be more significant in affecting the resilient modulus than the matric suction parameter. This is true for all levels of deviator stress.

6.4.1.4 Test Results of Soil Group #5

Soil group 5 is representative of the subgrade soil material taken from depth 1.07m from the top of the subgrade layer. This material is a medium plasticity clay soil that classifies as a CI soil type, similar to soil group 3. The characteristics of soil group 5 are depicted in Table 5.1 and Figures 6.5.

Three soil samples were fabricated from this soil group for the purposes of repeated load testing. The samples were prepared at prescribed moisture contents of 17.1%, 18.2%, and 19.1%, respectively. This covers a water content range of +0.2% to +2.2% above optimum. The corresponding matric suction values obtained from the water retention curve varies between 232 kPa and 310 kPa.

The results from the repeated loading testing for this soil group are displayed in Figures 6.16 to 6.18. The resilient modulus values ranged from about 31 MPa to about 105 MPa, i.e. from 3 to 10 CBR.

(i) $M_r - \sigma_d$ Relationship:

The resilient modulus was found to be significantly dependent on the deviator stress. As the deviator stress is increased, the modulus decreases. This is shown in Figures 6.16 (a) to 6.16 (c).

For samples compacted 2% wet of optimum water content, e.g. for the curve representing matric suction of 232 kPa, the resilient modulus decreased to about 50% of its initial value over the whole range of deviator stress investigated, i.e. 14 kPa to 70 kPa. This phenomenon was observed to occur irrespective of the level of the applied confining pressure.

The effect of the deviator stress on the resilient modulus seems to decrease appreciably as the level of matric suction is increased. This is apparent from the $M_r - \sigma_d$ curves representing matric suction levels of 270 and 310 kPa, respectively. This observation shows that soil group 5 is more susceptible to changes in stiffness at wet of optimum moisture content conditions than at near optimum water content conditions. This is again in agreement with what has been observed before for both soil groups 2 and 3.

(ii) $M_r - \psi$ Relationship:

Figures 6.17 (a) through 6.17 (c) show the relationship between matric suction and the resilient modulus for soil group 5. The observed trend in these figures is that as matric suction increases, the resilient modulus also increases. For the range of the water content studied (+0.2 to +2.2% wet of optimum), the resilient modulus increased by a factor of 170% from its initial value. This is almost twice the effect the deviator stress had on the resilient modulus.

(iii) $M_r - \sigma_3$ Relationship:

The relation between the confining pressure and the resilient modulus for this soil group is depicted in Figures 6.18 (a) through 6.18 (e). Increasing the confining pressure results in a corresponding increase in the resilient modulus. This increase is more pronounced at low levels of matric suction than at high levels. The rate of increase was also found to depend on the level of the deviator stress applied. As the deviator stress is increased the rate decreases until it reaches a minimum at σ_d of 70 kPa.

6.4.1.5 Test Results of Soil Group #6

Soil group 6 represents the natural subgrade soil material that was retrieved from the side slope of the area of the instrumented pavement section. This material also classifies as a CI soil, with the characteristics shown in Table 5.1 and Figure 6.6.

Five samples were prepared from this soil group at prescribed moisture contents of 18%, 18.5%, 19%, 19.8%, and 20.7%, respectively. This corresponds to a range of water content of +0.6% to +3.3% above optimum water content.

The results of the repeated load tests for this soil are displayed in Figures 6.19 to 6.21. The resilient modulus values ranged from about 8.4 MPa to about 83 MPa. This corresponds to a soil strength range of slightly less than 1 to 8 CBR.

(i) $M_r - \sigma_d$ Relationship:

The resilient modulus-deviator stress relation at various levels of soil matric suction and applied confining pressure is depicted in Figures 6.19 (a) to 6.19 (c). Regardless of the fact that this soil group was not retrieved from the prepared subgrade layer material but rather from the side slope of the shoulder area of the instrumented section, the same trend observed before for the $M_r - \sigma_d$ relationship for the other soil groups was again evident. As the applied deviator stress increases, the resilient modulus decreases. The rate of decrease is of a moderate magnitude resembling that for soil group 1 (material taken from the top of the prepared subgrade layer). This rate becomes more pronounced as the level of confining pressure is increased.

From figures 6.19 (a) to 6.19 (c), it is clear that the effect of matric suction on resilient modulus is far greater than that of the deviator stress. For example, changing the matric suction from 139 kPa (i.e. 3.3% wet of optimum water content) to 260 kPa (i.e. 0.6% wet of optimum) at a deviator stress value of 14 kPa and confining pressure of 14 kPa, increases the resilient modulus from about 10 MPa to about 60 MPa, see Figure 6.19 (a). This is far greater than the effect of changing the deviator stress from 14 kPa to 70 kPa (which brings about a maximum decrease in M_r of 17 MPa as shown in Figure 6.19 (a) for the $M_r - \sigma_d$ curve representing soil suction of 225 kPa).

The rate of decrease in the resilient modulus resulting from increasing the deviator stress appears to be of the same order of magnitude for all levels of matric suction at any particular level of confining pressure.

(ii) $M_r - \psi$ Relationship:

Figures 6.20 (a) through 6.20 (c) show the resilient modulus-matric suction relation for soil group 6. Again the same trend observed before for the other soil groups repeats itself here. Generally as the matric suction level is increased, the resilient modulus

also increases. The increase in modulus value ranges from 50 MPa to 70 MPa (about 5 to 7 fold of the initial value of M_r) depending on the levels of both the applied deviator stress and confining pressure. It was also observed that for a change in matric suction from 216 kPa to 225 kPa, there is a corresponding decrease in the resilient modulus. This is in contrast to the general trend. This phenomenon may be due to a measurement error that occurred during the estimation of the matric suction value especially in view of the fact that the two suction levels represent samples that are compacted at 18.8% and 19% water contents, respectively.

The influence of the deviator stress on the $M_r - \psi$ relationship is moderate at low and intermediate levels of confining pressure and increases significantly at high levels of confining pressure.

(iii) $M_r - \sigma_3$ Relationship:

The effect of the confining pressure on the resilient modulus is illustrated in Figures 6.21 (a) through 6.21 (e). As the confining pressure level is increased from 14 kPa to 42 kPa, the resilient modulus was observed to increase as well. However, the effect of σ_3 on M_r is not as appreciable as that induced by either the deviator stress or the matric suction. It was also observed, as with the case for the other soil groups, that the effect of σ_3 on M_r diminishes gradually as the level of the deviator stress is increased.

Soil samples compacted at high suction levels, e.g. 216, 225, and 260 kPa, exhibit greater change in the resilient modulus value, as induced by changes in σ_3 , than those experienced at low suction levels. This is evident at all levels of the deviator stress (see Figures 6.21 (a) through 6.21 (e)).

6.4.1.6 General Remarks on the Graphical Analysis Procedure

From the previous discussion of the test results pertaining to all soil groups, the following general conclusions can be drawn:

- (1) Among the three stress state variables studied, matric suction appears to be the most significant in affecting the resilient modulus parameter. The selection of the matric suction, rather than the water content %, as an independent parameter influencing the resilient modulus is deemed more appropriate based on the following:
 - (i) Soil suction is a fundamental soil property that reflects mechanical behaviour of unsaturated soils (Fredlund et al., 1975; Edil and Krizek, 1976).
 - (ii) A small error in the estimation of the moisture content in the wet of optimum region may lead to a very large error in the mechanical properties whereas it takes considerably large values of suction to cause the same error. In other words, the use of matric suction in predicting the mechanical response of unsaturated soils is more accurate than moisture content. This gives matric suction a definite analytical advantage over the moisture content parameter.
 - (iii) Technology is available today for routinely measuring soil matric suction in situ both non destructively and with great accuracy. This permits the utilization of laboratory results to predict in situ soil behaviour.
- (2) Although four of the five studied soil groups classify as CI soil type, the range of matric suction for each soil group differs substantially from the others. This further illustrates that the use of soil type as a parameter for analyzing the resilient behaviour of soils is inappropriate and may lead to ambiguous results.
- (3) The effects of the deviator stress and the confining pressure on the resilient modulus confirms the findings of earlier research works (Seed et al., 1957 and 1962; Dasmohapatra, 1973). However, these effects are far less important than that of soil matric suction.
- (4) The susceptibility of CI and/or CI-CL soils (such as soil groups 2, 3, 5, and 6 studied in the current research) to changes in stiffness seem to be greater within the water

content range of 1% to 2% wet of optimum than at any other level of moisture content.

- (5) The mechanical behaviour of soil group 6, i.e. the material that was retrieved from the side slope of the shoulder area of the instrumented pavement section, resembles very closely that of soil group 1, soil material taken from the top of the subgrade layer. This means that the results of these two soils can be grouped together to help in better understanding the mechanical behaviour of the top portion of the subgrade layer within the instrumented section.

Another alternative for presenting the resilient modulus test results in a graphical format is through the use of the moisture-density relationship, or Proctor curve, for the particular soil in question. This can be accomplished by using the Proctor plot as a background for displaying the laboratory-obtained modulus test results. Examples illustrating this for the various soil groups tested during the current investigation are shown in Figures 6.22 to 6.26. In these figures, the black dots refer to the laboratory tested soil specimens pertaining to each soil group. The location of every soil sample tested is indicative of both the sample dry density and its moisture content. The number written beside each dot represents the resilient modulus value, in MPa, obtained at a deviator stress of 14 kPa and a confining pressure of 14 kPa. The selection of these stress levels, although arbitrary, is believed to reflect actual in situ conditions.

The presentation of the test results in the fashion described above, i.e. using the moisture-density relationship, enables the visualization of the material structural strength in view of other soil characteristics such as optimum moisture content, maximum dry density and soil type. Furthermore, such presentation can be incorporated in pavement construction records for the purpose of future pavement maintenance and/or rehabilitation.

The graphical analysis procedure(s) described previously is a simple and effective way of presenting the laboratory test results. Nevertheless, the following constitutes some of the concerns and limitations pertaining to this analysis strategy:

- (1) The procedure is too elaborate. This means that many graphical representations of the various stress state variables versus the resilient modulus are needed to identify the effects of each of those parameters on the resilient characteristics of the soil under consideration.
- (2) Individual graphical displays of the M_r versus each of the stress state parameters make "interaction" or "overlapping" effects of these parameters on M_r difficult to discern. This problem, however, can be minimized to a certain degree by constructing three dimensional graphs. In such graphs, the simultaneous influence of any two of the stress parameters, at a fixed level of the third stress parameter, on the resilient modulus can be identified and interpreted. Examples of 3-D graphs plotted for M_r versus σ_d and ψ , and for M_r versus σ_d and σ_3 for soil groups 1, 2, and 6 are shown in Figures 6.27 to 6.29 and Figures 6.30 to 6.32, respectively. The use of the 3-D graphs is also limited in the sense that it can accommodate a maximum of three independent parameters. For discerning the effects of more than three variables on M_r , other analytical tools should be used.
- (3) Disaggregation of data, in the manner required for graphical results interpretation, may lead to confusion of how M_r is affected by each and/or all of the stress state variables (i.e. the graphical analysis procedure can not provide a global picture of the resilient modulus as a function of the stress state variables).
- (4) The degree of association, or influence, between a particular stress state variable and M_r may be misleading in a graphical environment. For example, σ_d (for all soil groups) appears to be significant in affecting M_r . However, this conclusion is not

totally correct. This point will be further clarified in the next section that deals with the development of the M_r predictive models for the various soil groups.

In summary, the graphical analysis procedure provides a good diagnostic tool for qualitative evaluation of the effects of the different stress state parameters on the resilient modulus. However, the method falls short in providing quantitative measures of the effects of these parameters on the resilient modulus. This calls for an alternative analysis strategy. One such a choice will be the use of statistical multiple linear regression techniques to postulate predictive resilient moduli models in terms of the pertinent stress state variables.

6.4.2 Postulated Predictive Resilient Modulus Models

As discussed previously, a second analysis strategy was envisioned to interpret the results of the laboratory testing program. This consisted of applying multiple linear regression techniques to develop models that describe the resilient behaviour of the various soil groups.

For each soil group, several models were examined in order to obtain the most sound model that best predicts the resilient modulus parameter. Several transformations of the data including the logarithm and the natural logarithm of dependent and/or independent variables were tried. Models in which the natural logarithmic transformation was used proved to be the most satisfactory. Consequently, the resilient modulus, for all soil groups, was modeled using the following form:

$$\ln M_r = B_0 + B_1 \ln \psi + B_2 \ln \gamma_d + B_3 \ln T + B_4 \ln(f(\sigma)) \quad (6.1)$$

where,

M_r = resilient modulus, kPa

ψ = matric suction ($u_a - u_w$), kPa

γ_d	=	soil dry density, kg/m ³
T	=	average soil temperature, °C
$f(\sigma)$	=	a stress function, kPa (the ratio of the second stress invariant to the octahedral shear stress, i.e. J_2/T_{oct} , was found to be adequate for describing the behaviour of all soil groups)

Table 6.1 shows the results of the regression analysis performed on the test data of the various soil groups. The number n in this table refers to the number of sets of test data used in the analysis. R^2 represents the coefficient of determination obtained for each model. $S.E.$ refers to the standard deviation of the dependent variable (i.e. $\ln M_r$) about the regression line. As it can be seen in Table 6.1, R^2 for all soil groups are, for the most part, reasonably good.

Detailed discussion of each of the models obtained will now follow

6.4.2.1 Soil Group 1

After several trials, the model arrived at to describe the resilient modulus of the first soil group was of the following form:

$$\ln M_r = 3.28 + 0.205 \ln(J_2/T_{oct.}) + 1.046 \ln(\psi_m) \quad (6.2)$$

where,

M_r	=	resilient modulus, kPa
J_2/T_{oct}	=	stress function described above, kPa (in the case of the triaxial test this equals $\frac{9\sigma_3^2 + 6\sigma_3\sigma_d}{\sqrt{2}\sigma_d}$)
ψ_m	=	soil matric suction, ($u_a - u_w$), kPa

This model has a coefficient of determination, R^2 , of 0.70 which indicates a relatively strong degree of association (or correlation) between the resilient modulus and the two independent parameters (i.e. $r=0.84$). The standard deviation of $\ln M_r$ about the regression line, S.E. = 0.201, implies that there is no much scatter in the data used to obtain the model. Furthermore, the relation also suggests that there are no reasons to doubt that a linear relationship does exist between the natural log of the resilient modulus and that of the matric suction and the stress function. This conclusion is evident from the F-value for the equation (F-value = 276.3 provides a significant F of probability = 0.0000).

Other diagnostics were also performed on equation 6.2 to validate all the underlying assumptions pertaining to multiple linear regression (SPSS for Windows-release 6.0, 1993).

It is worth noting that all stress state variables were examined for their effects on the resilient modulus. However, only matric suction and the stress function J/T_{oct} appear to be statistically significant in influencing the resilient modulus parameter for this soil group. Moreover and upon examining the regression coefficients in equation 6.2, it is evident that the effect of matric suction on M_r is more pronounced than that of traffic induced stresses (1.046 compared to 0.205). This finding emphasizes the importance that environmental factors have on affecting the structural capacity of fine-grained subgrade soils. This conclusion is not readily visual when using the graphical analysis procedure.

6.4.2.2 Soil Group 2

For this soil group, the model developed was of the following form:

$$\ln M_r = -4.87 + 0.246 \ln(J/T_{oct}) + 2.704 \ln(\psi_m) \quad (6.3)$$

where,

M_r = resilient modulus, kPa

ψ_m = soil matric suction, kPa

J_2/T_{oct} = ratio of the second stress invariant to the octahedral shear stress, kPa

The R^2 value for the model is 0.73 and the S.E. ($\ln M_r$) is 0.258. This indicates a strong linear relationship between the natural logarithm of the resilient modulus on one side and the natural logarithms of the independent variables, i.e., J_2/T_{oct} and ψ_m , on the other side. Like soil group 1, the resilient modulus for soil group 2 appears to be a function of both matric suction and traffic induced stresses. Also, the influence of the matric suction on M_r seems to be even greater in the case of this soil group than for soil group 1. This can be visually examined by looking at the magnitude of the regression coefficients of both independent variables (0.246 for J_2/T_{oct} as compared to 2.704 for ψ_m).

The diagnostic checks performed before for equation 6.2 were again repeated for equation 6.3 to ensure its validity.

6.4.2.3 Soil Group 3

Several regression equations were examined for soil group 3. The final model arrived at which was thought of as representing the resilient modulus of this soil was of the following form:

$$\ln M_r = 10.17 + 0.188 \ln(J_2/T_{oct}) \quad (6.4)$$

where,

J_2/T_{oct} = ratio of the second stress invariant to the octahedral shear stress

Equation 6.4 has an R^2 - value of 0.67 and an F-value of 86.616 (probability = 0.0000). This indicates a linear relationship of reasonable strength between the natural logarithm of the resilient modulus on one hand and the natural logarithm of the stress

function J_2/T_{oct} on the other hand. The S.E. of $\ln M_r$ equals 0.094 which reflects a very small scatter in the data used to obtain equation 6.4. Although this looks good from a prediction point of view, this conclusion is a little bit misleading. The reason behind this is the fact that the range of the matric suction parameter, i.e. ψ_m , investigated for this soil is small compared to previous soil groups. This factor is believed to have contributed to the observed finding as well as to eliminating ψ_m from being included as a significant parameter in the postulated model.

6.4.2.4 Soil Group 5

The resilient modulus model developed for this soil group takes the following form:

$$\ln M_r = 9.55 + 0.302 \ln(J_2/T_{oct}) \quad (6.5)$$

Equation 6.5 has an R^2 -value of 0.61 and an F-value of 53.524 (probability = 0.0000) which indicates a strong linear relationship between the natural logarithm of the modulus and the natural logarithms of the stress function J_2/T_{oct} . An estimated S.E. for $\ln M_r$ of 0.229 is comparable with S.E.'s obtained for soil groups 1 and 2. However, soil group 5 appears to behave in a similar way to that of soil group 3. This is evident from the shape of equation 6.5 as compared to that of equation 6.4. This is again attributed to the small range of ψ_m investigated for soil group 5.

The fact that a much smaller range of matric suction was examined in the case of both soil groups 3 and 5 is due to some difficulties encountered during the testing of these soils. The main difficulty is the fact that a small amount of soil material, for both soil groups, was retrieved from the instrumented site. This made the remolding of the required soil specimens at some moisture contents, notably on the dry of optimum side of the moisture-density relation for the particular soil group in question, unattainable.

6.4.2.5 Soil Group 6

The predictive model developed that describes the resilient characteristics of soil group 6 is given by the following expression:

$$\ln M_r = -6.40 + 0.312 \ln(J_2/T_{oct}) + 2.819 \ln(\psi_m) \quad (6.6)$$

where all the parameters shown in the equation are as defined previously.

This model has a high R^2 -value of 0.90 and a significant F-value (probability = 0.0000) of 326.892. This indicates that the natural logarithm of the resilient modulus is highly correlated with the natural logarithms of both the stress state parameter J_2/T_{oct} and the soil matric suction. The S.E. of $\ln M_r$ obtained for this soil group is 0.155 indicating a good model fit.

The influence of matric suction on M_r is clearly more profound than that of the traffic induced stress variable J_2/T_{oct} . This can be seen by comparing the magnitude of the regression coefficient for matric suction, 2.819, with that of the stress state function, 0.312. This finding confirms the trend observed before for the other soil groups that environmental effects on M_r appear to be more significant than those associated with traffic induced stresses.

6.5 Summary and Conclusions

This chapter presents and interprets the research findings from the laboratory testing program. The purpose of the laboratory phase of the current research was to study the resilient deformation characteristics of a typical fine-grained subgrade soil in Alberta, with particular emphasis on the phenomenon of seasonal variations as afflicted upon by environmental factors such as temperature and soil moisture.

An extensive repeated loading testing scheme was formulated to investigate how the subgrade resilient modulus is affected by various stress state variables. These variables included both traffic induced stresses and environmental factors. The traffic induced stresses consisted of the vertical deviator stress and the confining pressure. Average soil temperature and soil matric suction comprised the two environmental factors investigated in this study.

Only one type of subgrade material was examined in this research. The selected soil represents a typical subgrade material that is frequently encountered in many primary highways in Alberta. This material is a medium plasticity silty clay soil that classifies as a CI type soil according to the Unified Soil Classification System.

The subgrade soil material used in this study was retrieved from an instrumented pavement site that is located within control section 16:12 along primary Highway 16 west of Edmonton. The material retrieved from the test site was grouped into five groups on the basis of the depths from which they have been extracted. This was done to see whether the location of the specific soil group within the subgrade would have any influence on its structural characteristics i.e. whether the subgrade soil stiffness varies with depth or not.

Several classical soil tests were performed on the various soil groups to obtain the necessary information required for the preparation of the soil samples for resilient modulus testing. Also, soil moisture retention curves were obtained for all soil groups. This was done to enable the estimation of the soil matric suction parameter since present technology does not permit the measurement of this variable during repeated load testing.

Several soil specimens were prepared from the various soil groups at different prescribed moisture content conditions. These specimens were tested using the repeated loading test system developed at the University of Alberta. Two analysis strategies were utilized in interpreting the results obtained from the laboratory testing program. The first strategy involved using different graphical displays of the resilient modulus parameter versus the various individual stress state variables to identify general trends and highlight the relative importance of each of the independent parameters on the resilient modulus value. An alternative for displaying the resilient modulus test results for pavement construction purposes was also proposed. This took the form of plotting the test results on a moisture-density diagram. In the second strategy, the individual effect and/or interaction effects of each stress state variable was quantified. This is accomplished by developing prediction models for the resilient modulus parameter in terms of the significant stress state variables.

The general conclusions that can be drawn from the research results of the laboratory testing program are as follows:

- (1) The graphical analysis approach by itself is not sufficient to provide full-scope interpretation of the test data. In other words, it only gives a qualitative estimation of the influences of the various stress state parameters on the resilient modulus. This shortcoming can be rectified by developing predictive moduli models through the use of multiple linear regression analysis techniques. It should be mentioned, however, that proper diagnostic checks must be performed on the postulated models to ensure their validity and accuracy. In the current research exercise, verification of the developed models was carried out with great caution.
- (2) Conclusive evidences from both the graphical and the statistical analysis procedures, strongly indicate that environmental factors (as represented by soil matric suction)

are more significant in affecting the resilient modulus than their counterparts of traffic induced stresses (as represented by the stress ratio J_2/T_{oct}). In other words, seasonal variations in soil matric suction have more devastating consequences on the resilient modulus than those pertaining to traffic induced stresses.

- (3) The layering effect within the subgrade material seems to have very little impact on the resilient modulus. This is evident from the ranges of the resilient modulus of the various soil groups (between 8 and 100 MPa or 1 to 10 CBR).
- (4) Although the range of soil stiffness for all soil groups is almost the same, however, each group has its own distinct resilient modulus expression. This serves to illustrate the point that even if various soils have the same range of structural strength, this consideration by itself alone is not sufficient to draw conclusions about the resilient behaviour of these soils under different climatic conditions. Such predictions can only be made if there exists a mathematical expression that uniquely relates the resilient modulus, or any other mechanistic response, to other stress state variables. Within the general framework of the current research objectives, the task of developing such expressions for the particular subgrade soil studied is believed to have been successfully achieved.
- (5) The resilient modulus was found to be strongly influenced by traffic induced stresses such as the deviator stress and the confining pressure. In all cases (soil groups 1 through 6), such influence was found to be best represented by a stress function that incorporates the effects of both the deviator stress and the confining pressure simultaneously. The candidate stress function used in the current study is a ratio of the second stress invariant, J_2 , to the octahedral shear stress, T_{oct} . Findings from the current investigation confirm and substantiate similar research results reported by Cole et al. (1986) from an earlier research work on granular soils.

- (6) Examination of the developed resilient modulus models reveals that changes in the soil dry density, γ_d , has very little effect, if any, on the M_r value. This phenomenon can be explained in view of the fact that the influence of such parameter, i.e. γ_d , on M_r has already been taken care of through the consideration of the effects of both the confining pressure and the soil matric suction. This is understandable since these two parameters are found to be highly correlated with the soil dry density.
- (7) From Figures 6.22 to 6.26, it is clear that both matric suction, ψ , and soil dry density, γ_d , have significant effects on M_r . This is particularly evident in the range from 95% to 99% of maximum dry density as shown in the aforementioned figures. Although this conclusion appears to be in contrast to conclusion (6) above, at least for the part concerning the dry density, it is not really so. This can be explained in view of the fact that both ψ and γ_d have significant effects on M_r , however, the influence of ψ on M_r far outweighs the influence of γ_d . Furthermore, upon analysing the resilient modulus test results in a quantitative fashion, such as the one employed to develop the predictive models, only parameters that are highly correlated with M_r got identified as being significant. Other parameters, although could be significant, do not appear in the regression equation, especially if they are highly correlated with other independent variables. This turned out to be the case for γ_d that was found to be highly correlated with both the matric suction itself and the confining pressure contained in the stress function that appeared in the postulated equations, i.e. (J_2/T_{oct}) .

The research approach followed in the current laboratory investigation produced good and consistent results in terms of characterizing seasonal variations in subgrade stiffness that is based on mechanistic measures. The applicability of this approach to

studying other soil types can further be improved by adopting the following recommendations:

- (i)** A well statistically-designed experiment should be devised to fulfill the specific testing needs pertaining to the particular soil to be studied. This means that no special standardized test procedure, such as the AASHTO T 294-92 used here, is required. Rather, the researcher should develop his/her own test Protocol to satisfy his/her particular research objectives. This typically involves the selection of the appropriate ranges of the various parameters to be investigated.

The above recommendation is further substantiated by the following finding. During the analysis to develop the above discussed resilient moduli relations, it was found that the resilient modulus obtained at any particular stress state test conditions is highly correlated with moduli values obtained in previous test runs for the same test specimen. This was true for all soil groups tested. The implication of this finding is that every prepared soil sample must be tested under only one set of stress conditions or otherwise, test results from repeated loading triaxial testing should be interpreted using time series analysis techniques.

- (ii)** In determining the soil water retention characteristics pertaining to the specific soil under investigation, an identical procedure to the one used in preparing soil samples for repeated load testing should be followed for obtaining the soil retention curves. This means that sorption curves rather than desorption curves should be obtained and used. This provides for more accurate estimates of the soil matric suction parameter.
- (iii)** In addition to the calibration of the individual components comprising the repeated load testing system, a separate calibration of the system as a whole is strongly recommended. Such calibration is usually performed using some type of a

“standard specimen” with known resilient characteristics (Pezo et al., 1991). This calibration was not performed during the current research study due to difficulties encountered in obtaining the necessary calibration specimen(s) to perform this task.

References

1. AASHTO (1992), "*Resilient Modulus of Unbound Granular Base/Subbase Materials and Subgrade Soils - SHRP Protocol P46: AASHTO Standard Test Designation T-294-92*," American Association of State Highway and Transportation Officials.
2. Cole, D., D. Bentley, G. Durell and T. Johnson (1986), "*Resilient Modulus of Freeze-Thaw Affected Granular Soils for Pavement Design and Evaluation: Part 1. Laboratory Tests on Soils from Winchendon, Massachusetts, Test Sections*," CRREL Report 86-4, 71 p.
3. Croney, D. and J.D. Coleman (1960), "*Pore Pressures and Suction in Soils*," Pore Pressures and Suction in Soils Conference, Butterworths, London, England.
4. Dasmohapatra, D.K. (1973), "*An Investigation into the Application of Elastic Theory to Predict Deflections in Full-Depth Asphalt Pavements*," M.Sc. Thesis, University of Alberta, Edmonton, Alberta, Canada.
5. Edil, T.B. and R.J. Krizek (1976), "*Influence of Fabric and Soil-Water Potential on the Mechanical Behaviour of a Kaolinitic Clay*," *Geoderma*, Vol. 15, pp. 831-840.
6. Fredlund, D.G. and J. Krahn (1972), "*On Total, Matric and Osmotic Suction*," *Soil Science*, Vol. 114, No. 5, November, pp. 339-348.
7. Fredlund, D.G., A.T. Bergan and E.K. Sauer (1975), "*Deformation Characterization of Subgrade Soils for Highways and Runways in Northern Environments*," *Canadian Geotechnical Journal*, Vol. 12, No. 2, pp. 213-223.
8. Klute, A (1986), "*Methods of Soil Analysis - Part 1: Physical and Mineralogical Methods, 26: Water Retention: Laboratory Methods*," *Agronomy*, No. 9 (Part 1), Soil Science Society of America, pp. 635-660.
9. Olson, R.E. and L.J. Langfelder (1965), "*Pore Pressures in Unsaturated Soils*," *Journal of Soil Mechanics and Foundation Division, ASCE*, Vol. 91, SM4.
10. Pezo, R.F., D. Kim, K.H. Stokoe and W.R. Hudson (1991), "*A Reliable Resilient Modulus Testing System*," *Transportation Research Board Record* 1307, Washington, D.C., pp. 90-98.
11. Seed, H.B. and R.L. McNeill (1957), "*Soil Deformation Under Repeated Stress Applications*," *Proceedings, Conference on Soils for Engineering Purposes*, Universidad de Mexico.
12. Seed, H.B., C.K. Chan and C.E. Lee (1962), "*Resilience Characteristics of Subgrade Soils and Their Relation to Fatigue Failures in Asphalt Pavements*," *Proceedings*, Vol. 1, First International Conference on the Structural Design of Asphalt Pavements, University of Michigan, Ann Arbor, Michigan, pp. 611-636.

13. Shell (1978), "*Shell Pavement Design Manual - Asphalt Pavements and Overlays for Road Traffic*," Shell International Petroleum, London.
14. Norusis, M.J./SPSS Inc (1993), "SPSS for Windows Base System User's Guide - Release 6.0," SPSS Inc., Chicago, Illinois, pp. 316-322.

Table 6.1: Results of Regression Analysis performed on Various Soil Groups

Soil Group	Regression Equation	n	R ²	S.E.
#1	$\text{Ln } M_r = 3.28 + 0.205 \text{ Ln}(J_2/T_{oct}) + 1.046 \text{ Ln}(\psi_m)$	45	0.70	0.201
#2	$\text{Ln } M_r = -4.87 + 0.246 \text{ Ln}(J_2/T_{oct}) + 2.704 \text{ Ln}(\psi_m)$	75	0.73	0.258
#3	$\text{Ln } M_r = 10.17 + 0.188 \text{ Ln}(J_2/T_{oct})$	45	0.67	0.094
#5	$\text{Ln } M_r = 9.55 + 0.302 \text{ Ln}(J_2/T_{oct})$	37	0.61	0.229
#6	$\text{Ln } M_r = -6.40 + 0.312 \text{ Ln}(J_2/T_{oct}) + 2.819 \text{ Ln}(\psi_m)$	75	0.90	0.155

Notes:

S.E. refers to the standard deviation of “Ln M_r ” about the regression line.

R² is the coefficient of determination of the model(s).

n indicates the sample size used to generate the regression equation(s).

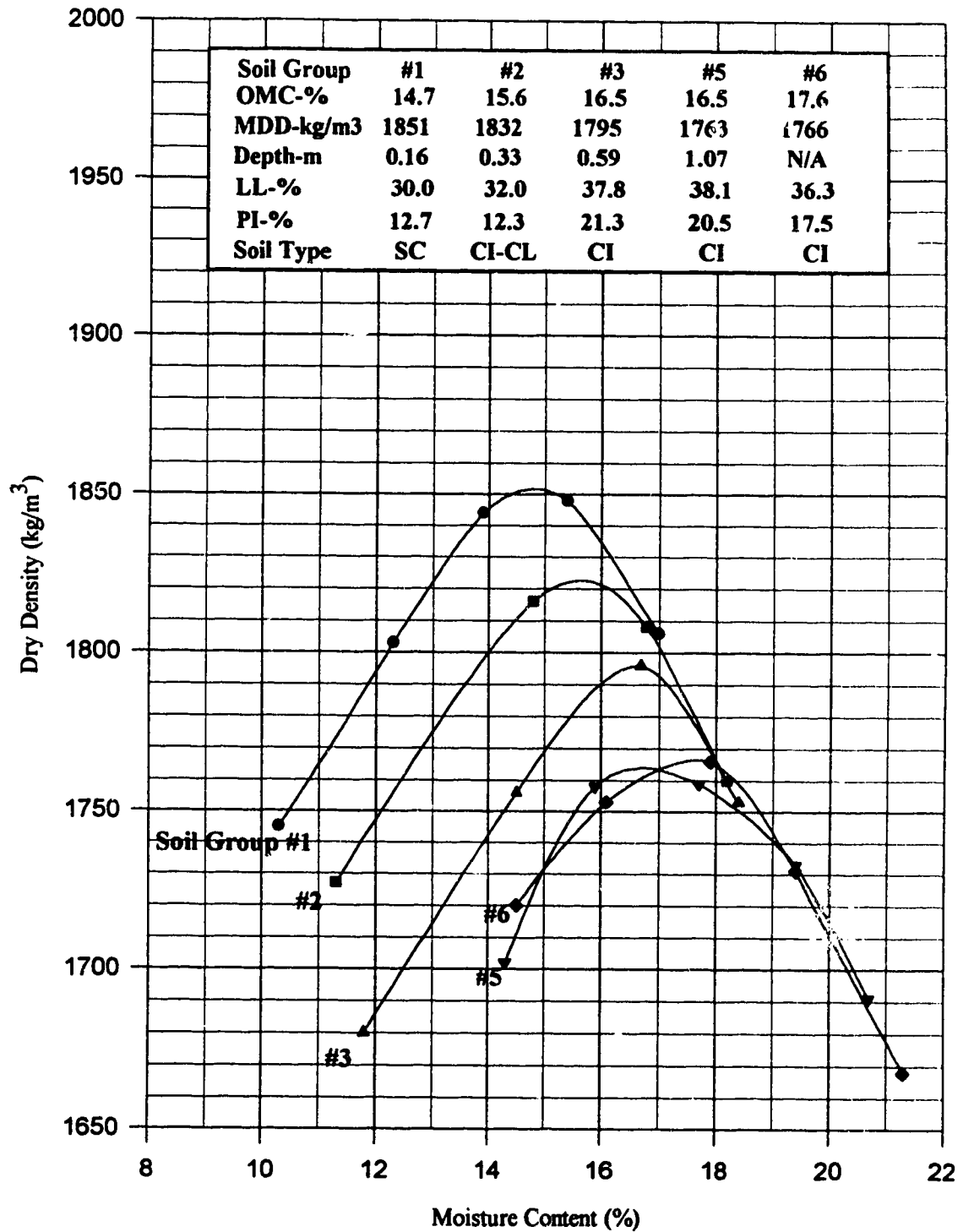


Figure 6.1: Moisture -Density Report for Soils Sampled from CS 16:12

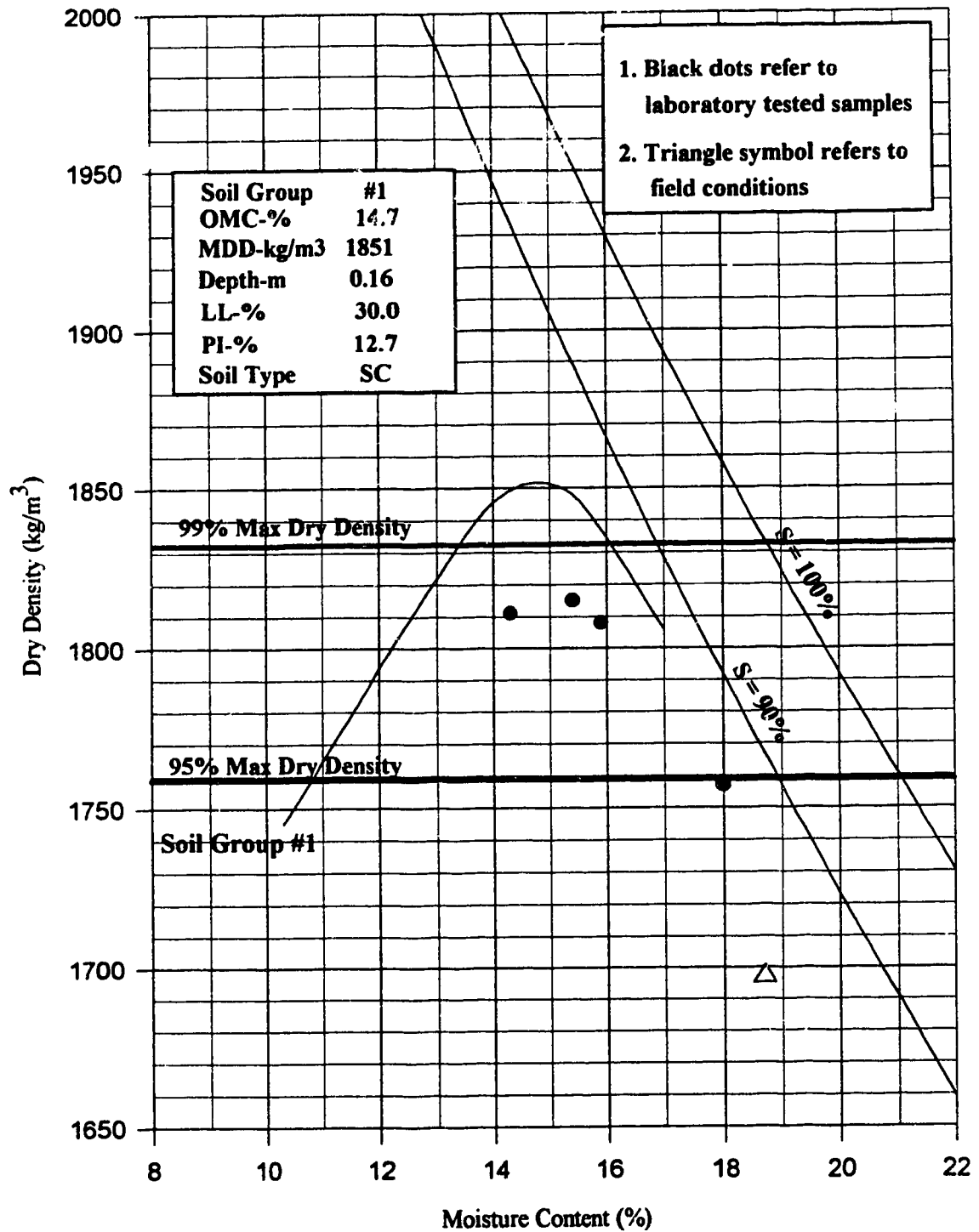


Figure 6.2: Moisture - Density Relation for Soil Group # 1

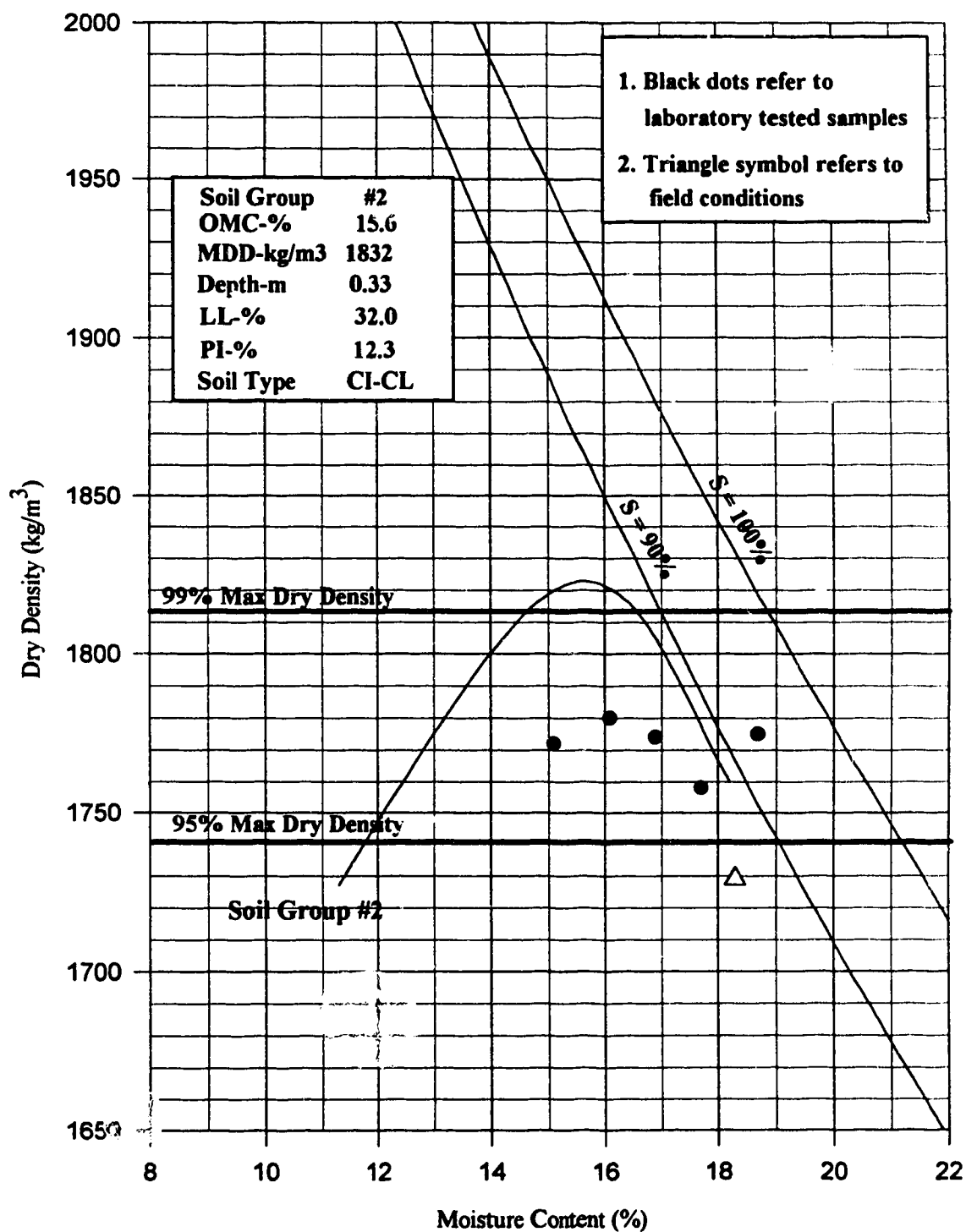


Figure 6.3: Moisture - Density Relation for Soil Group #2

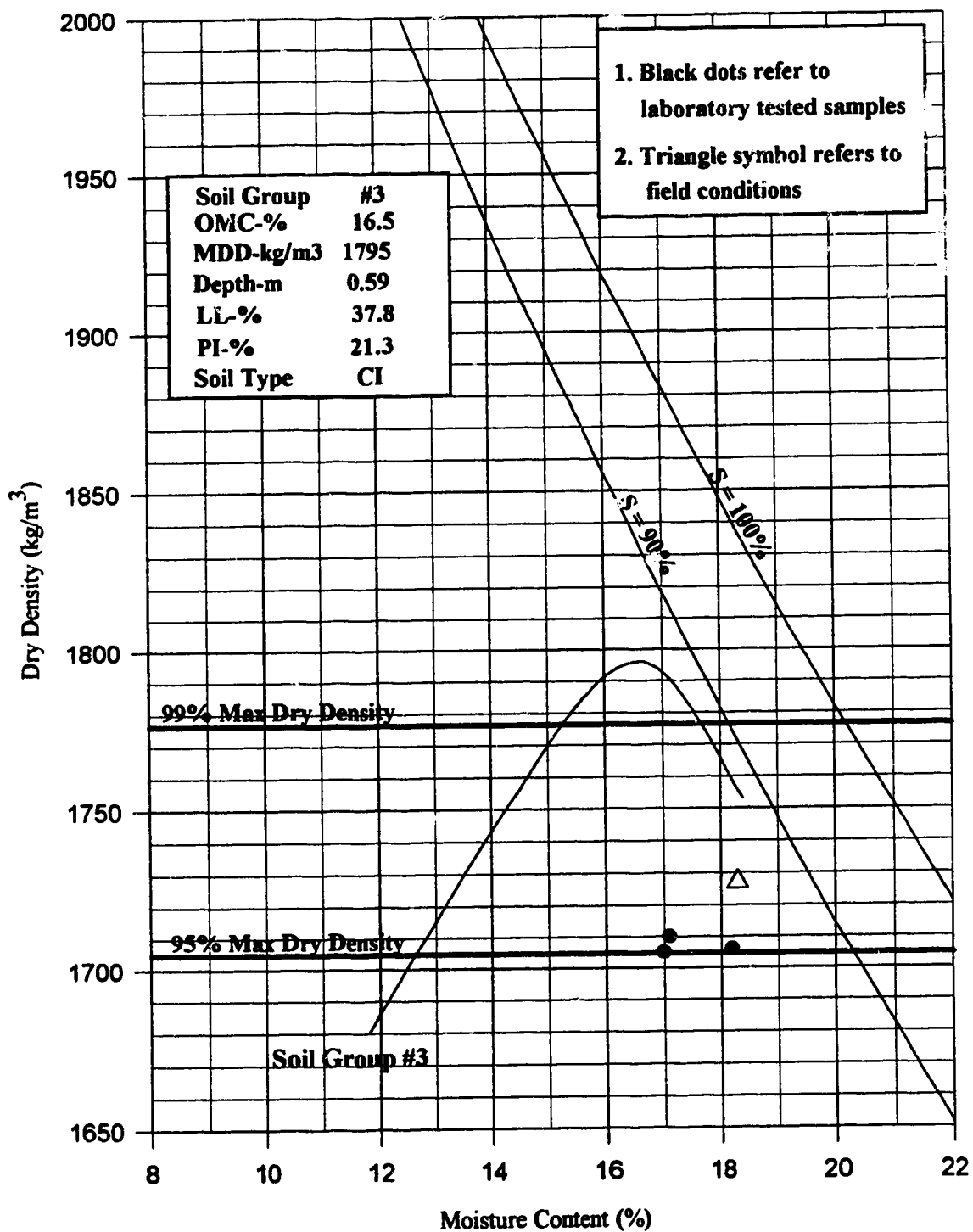


Figure 6.4: Moisture - Density Relation for Soil Group # 3

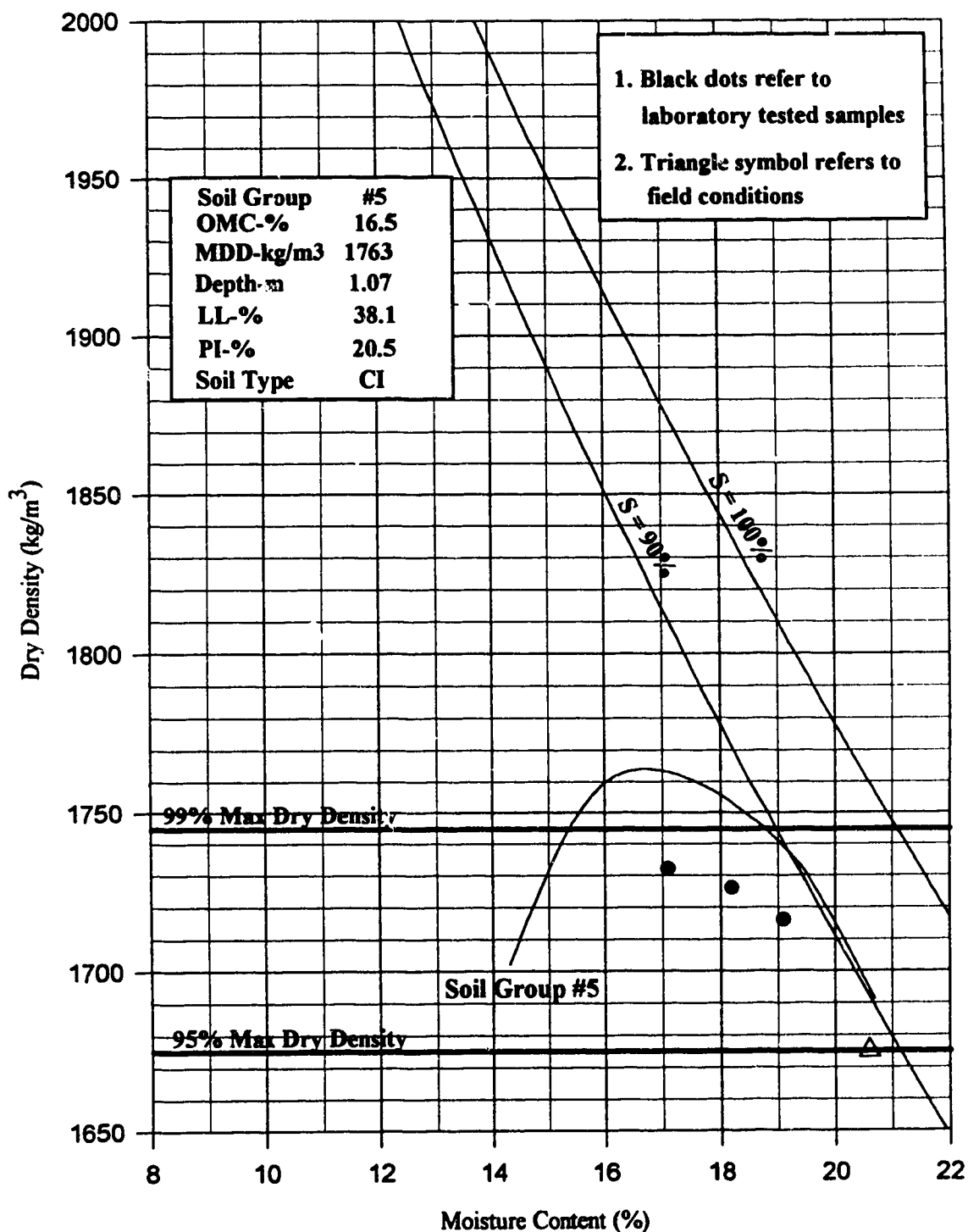


Figure 6.5: Moisture - Density Relation for Soil Group # 5

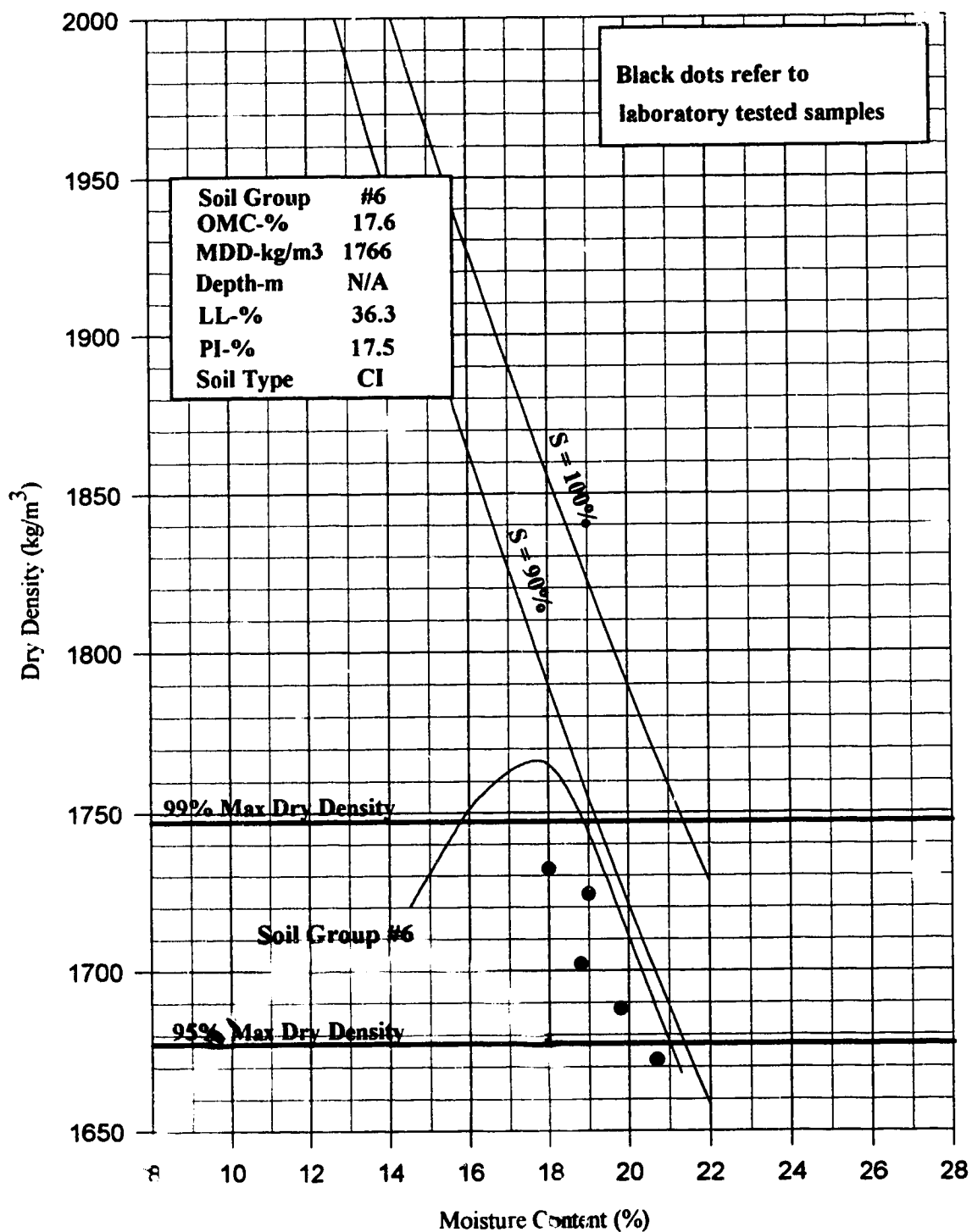


Figure 6.6: Moisture - Density Relation for Soil Group # 6

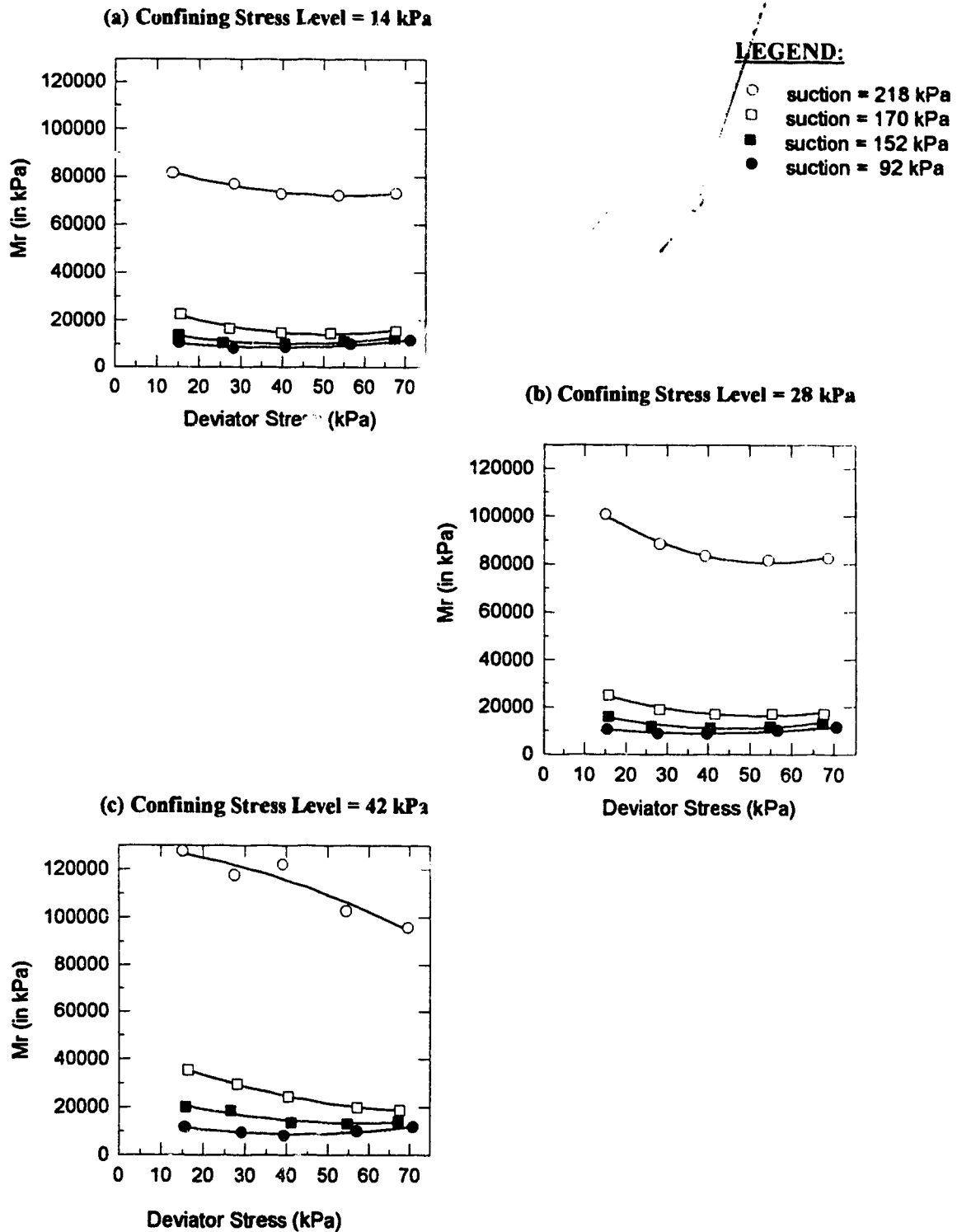


Figure 6.7: Resilient Modulus *versus* Deviator Stress for Soil Group 1

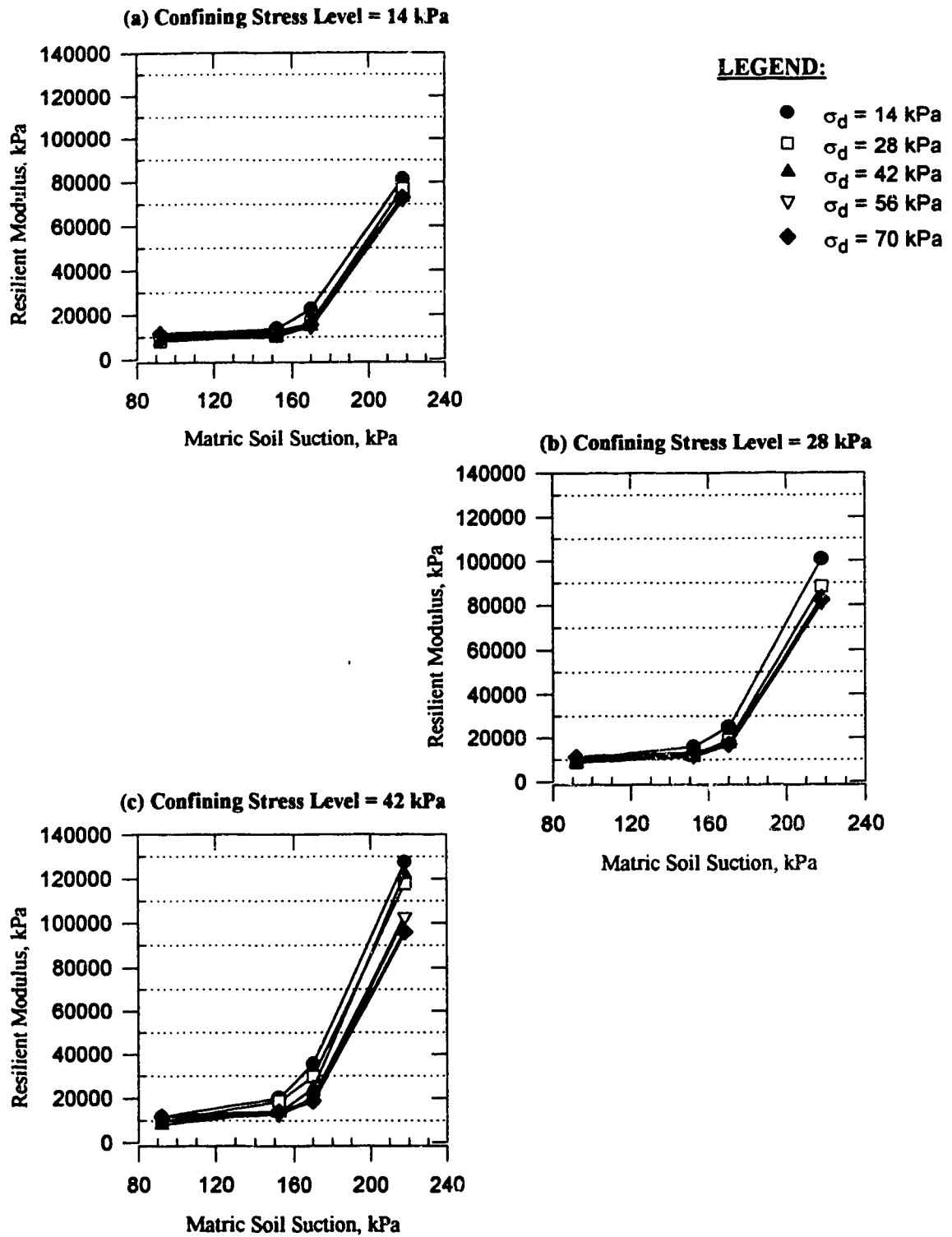


Figure 6.8: Resilient Modulus *versus* Soil Matric Suction for Soil Group 1

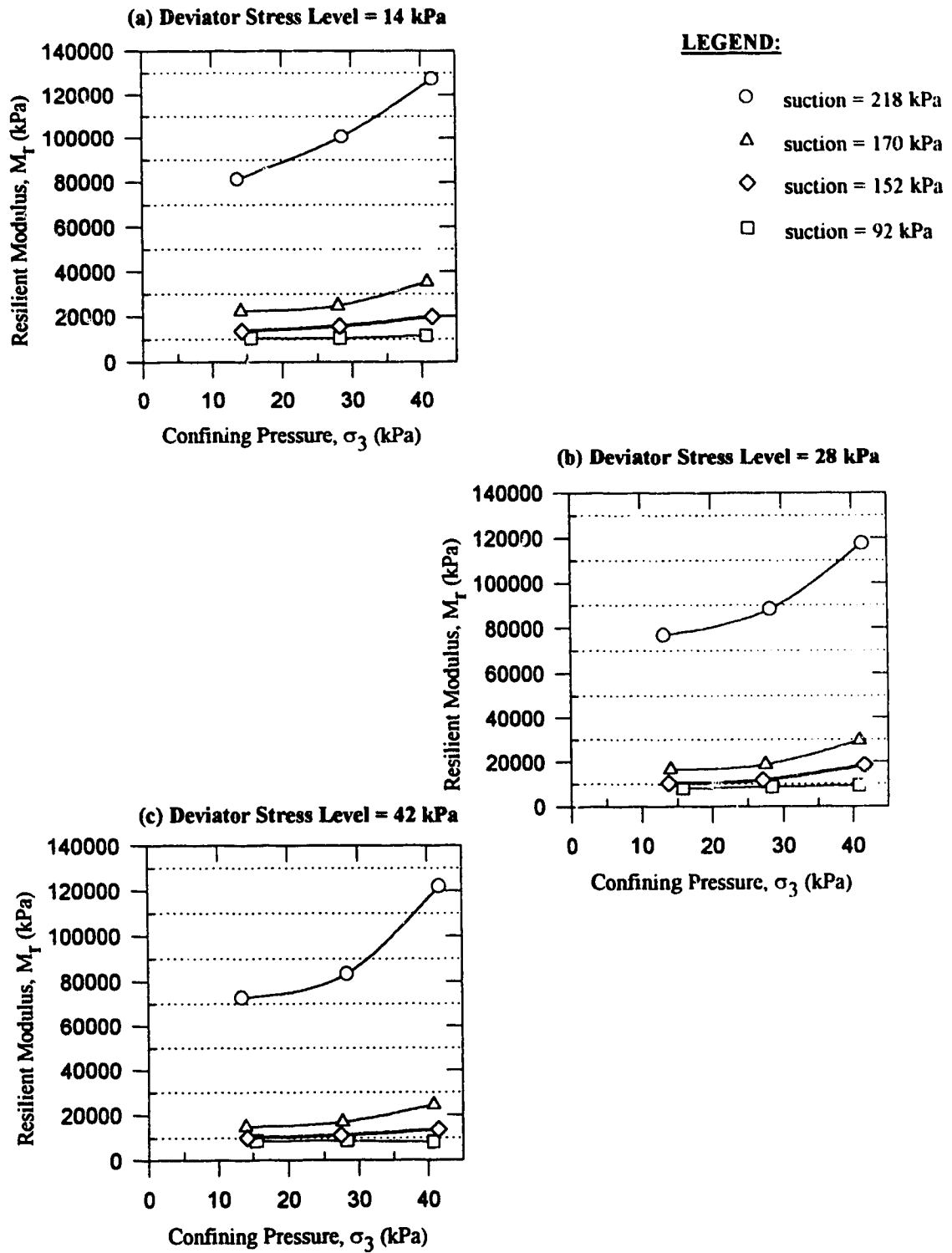
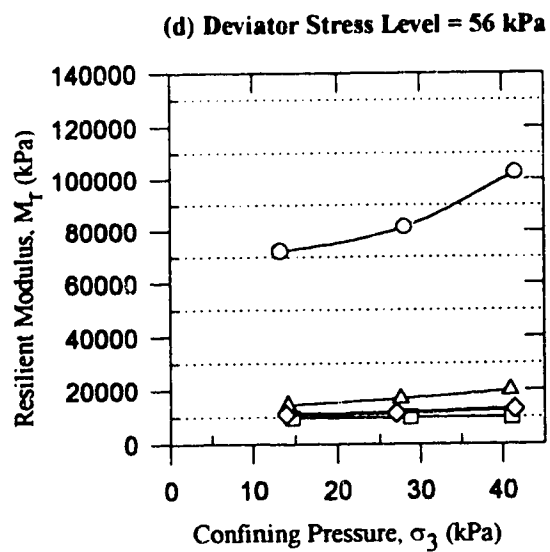


Figure 6.9: Resilient Modulus *versus* Confining Pressure Soil Group 1



LEGEND:

- suction = 218 kPa
- △ suction = 170 kPa
- ◇ suction = 152 kPa
- suction = 92 kPa

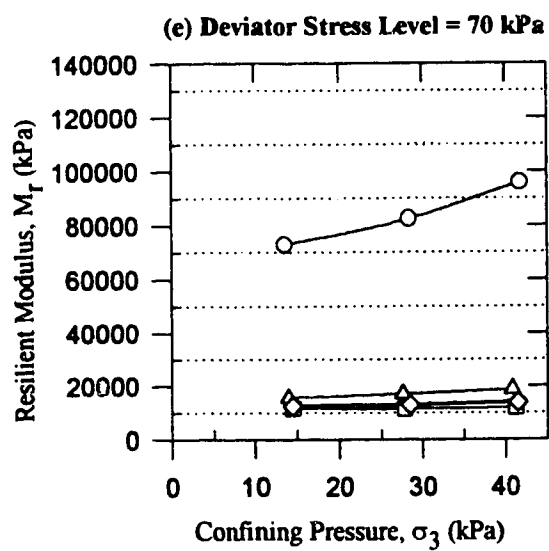


Figure 6.9: Continued

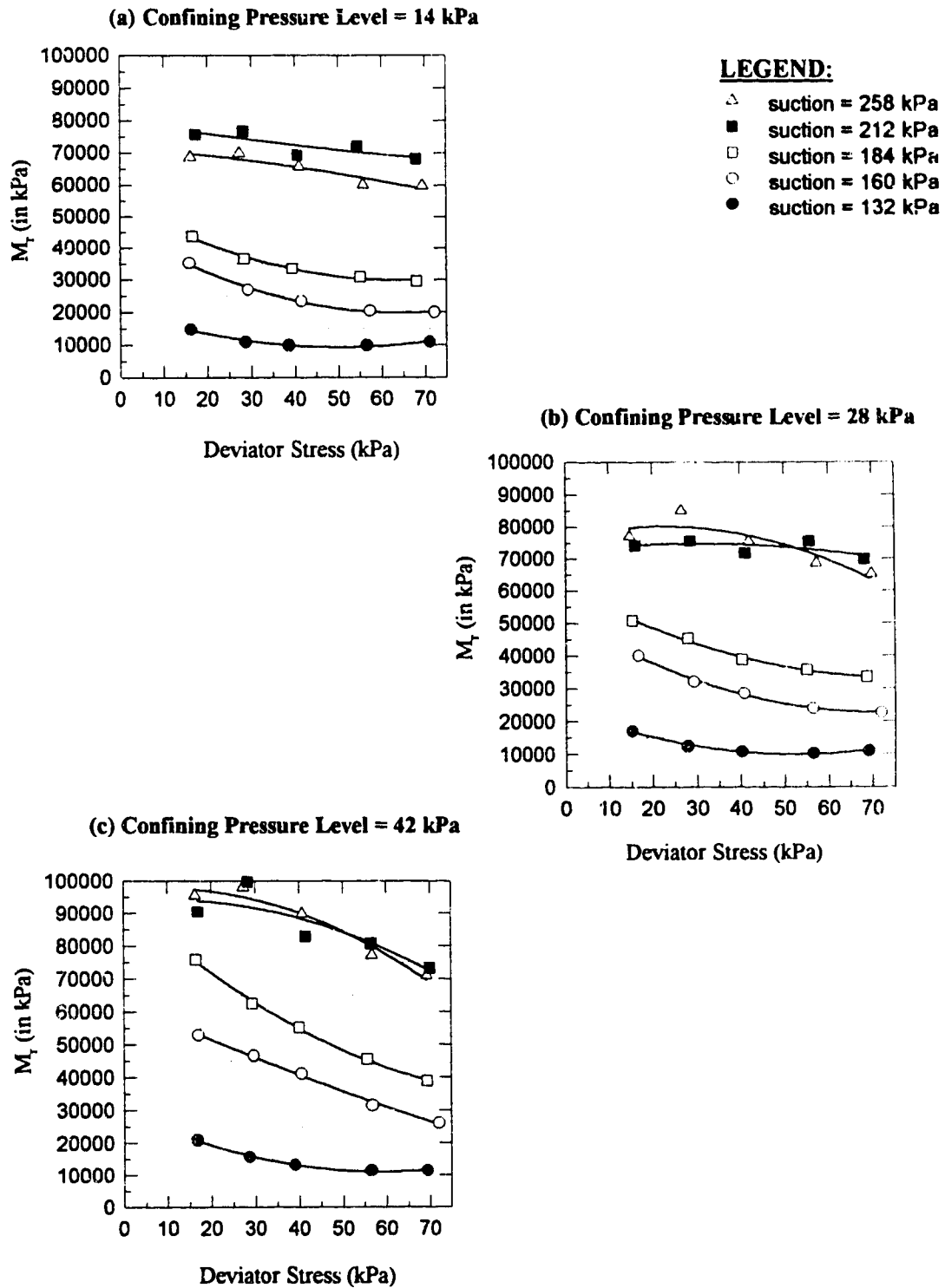


Figure 6.10: Resilient Modulus *versus* Deviator Stress for Soil Group 2

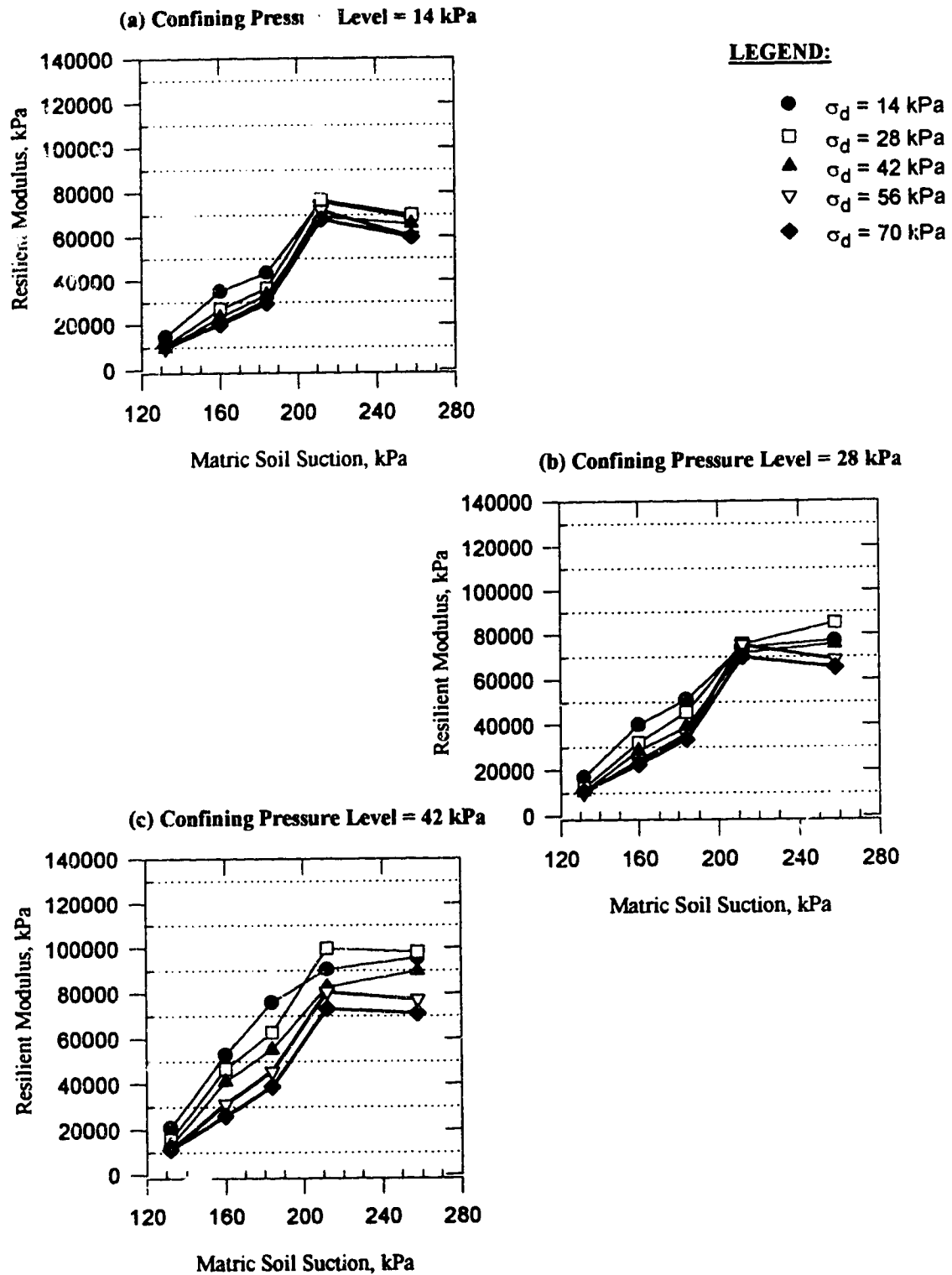


Figure 6.11: Resilient Modulus *versus* Matric Suction for Soil Group 2

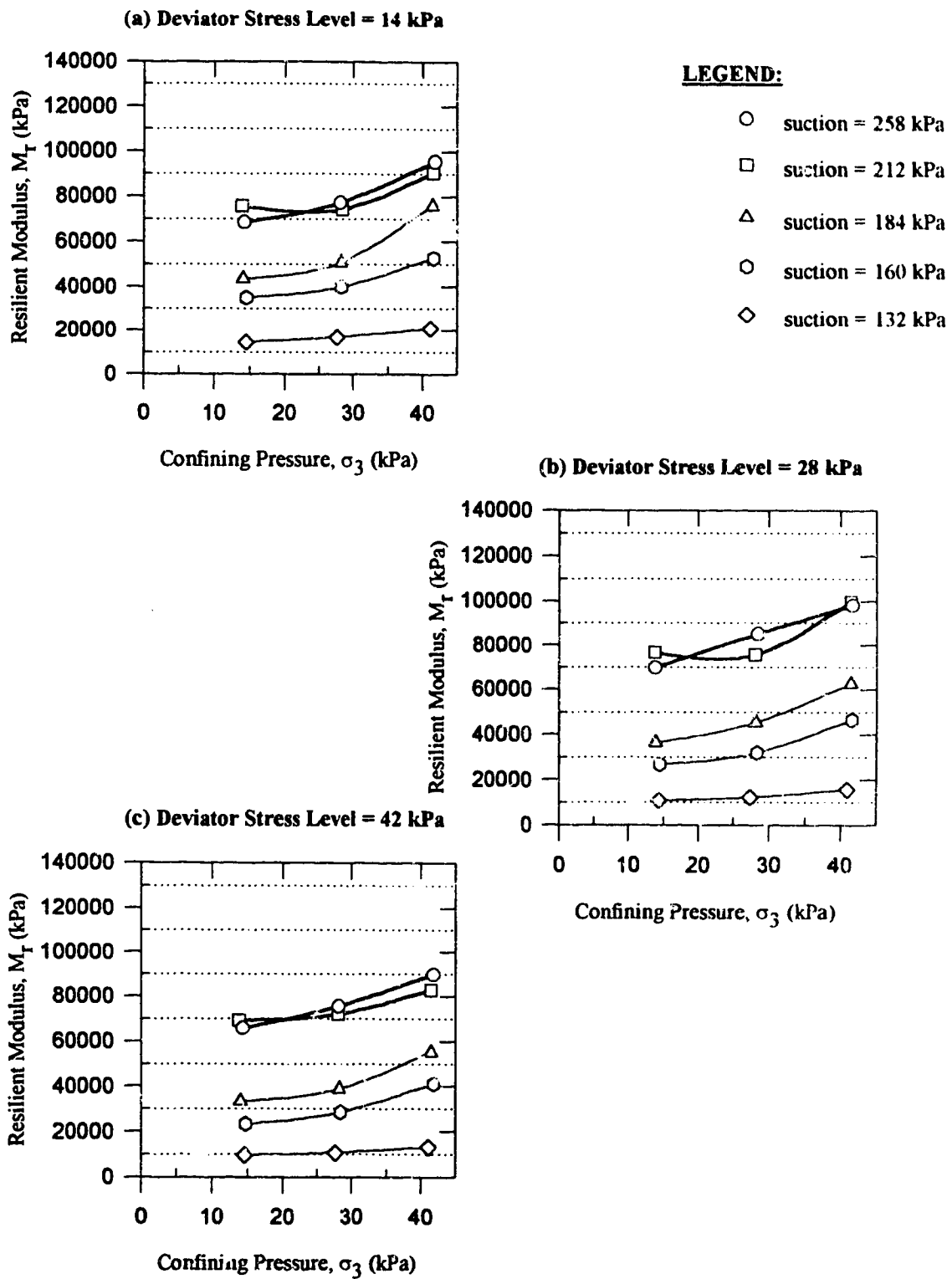
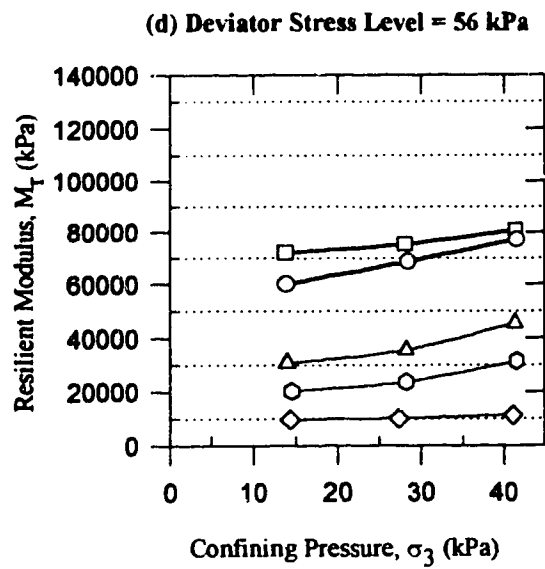


Figure 6.12: Resilient Modulus *versus* Confining Pressure for Soil Group 2



LEGEND:

- suction = 258 kPa
- suction = 212 kPa
- △ suction = 184 kPa
- ◇ suction = 160 kPa
- ◇ suction = 132 kPa

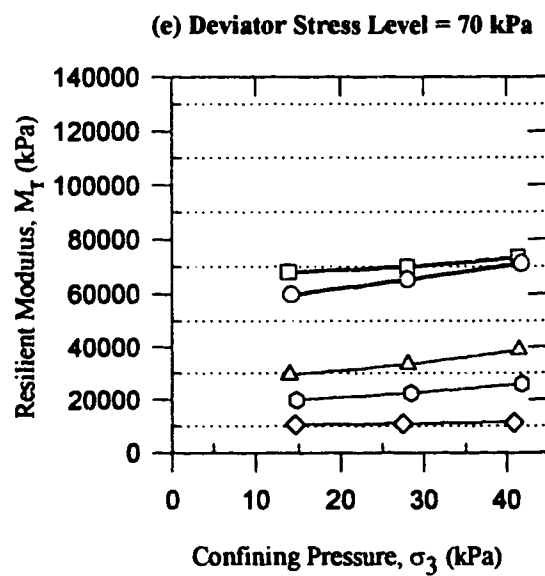


Figure 6.12: Continued

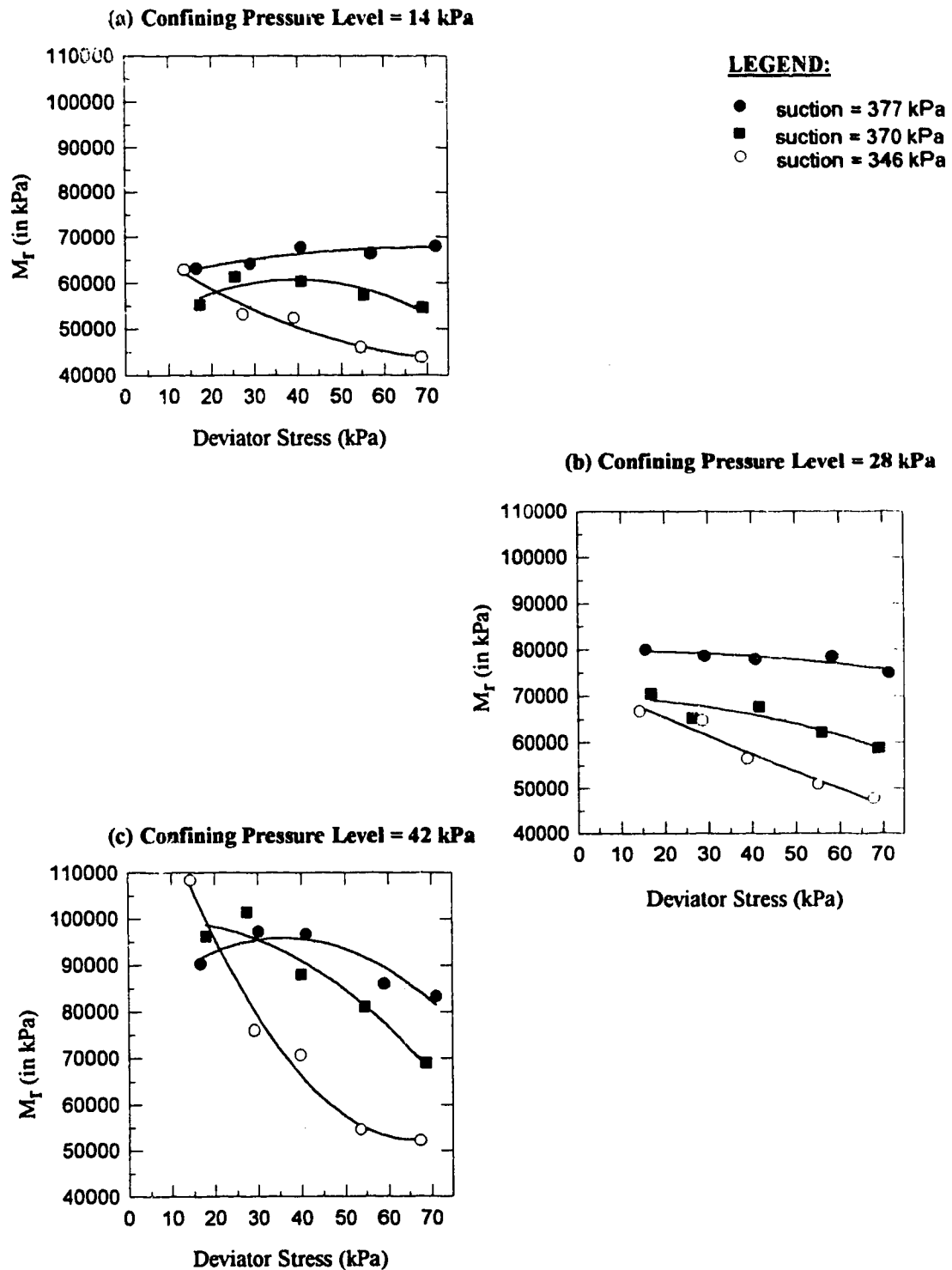


Figure 6.13: Resilient Modulus *versus* Deviator Stress for Soil Group 3

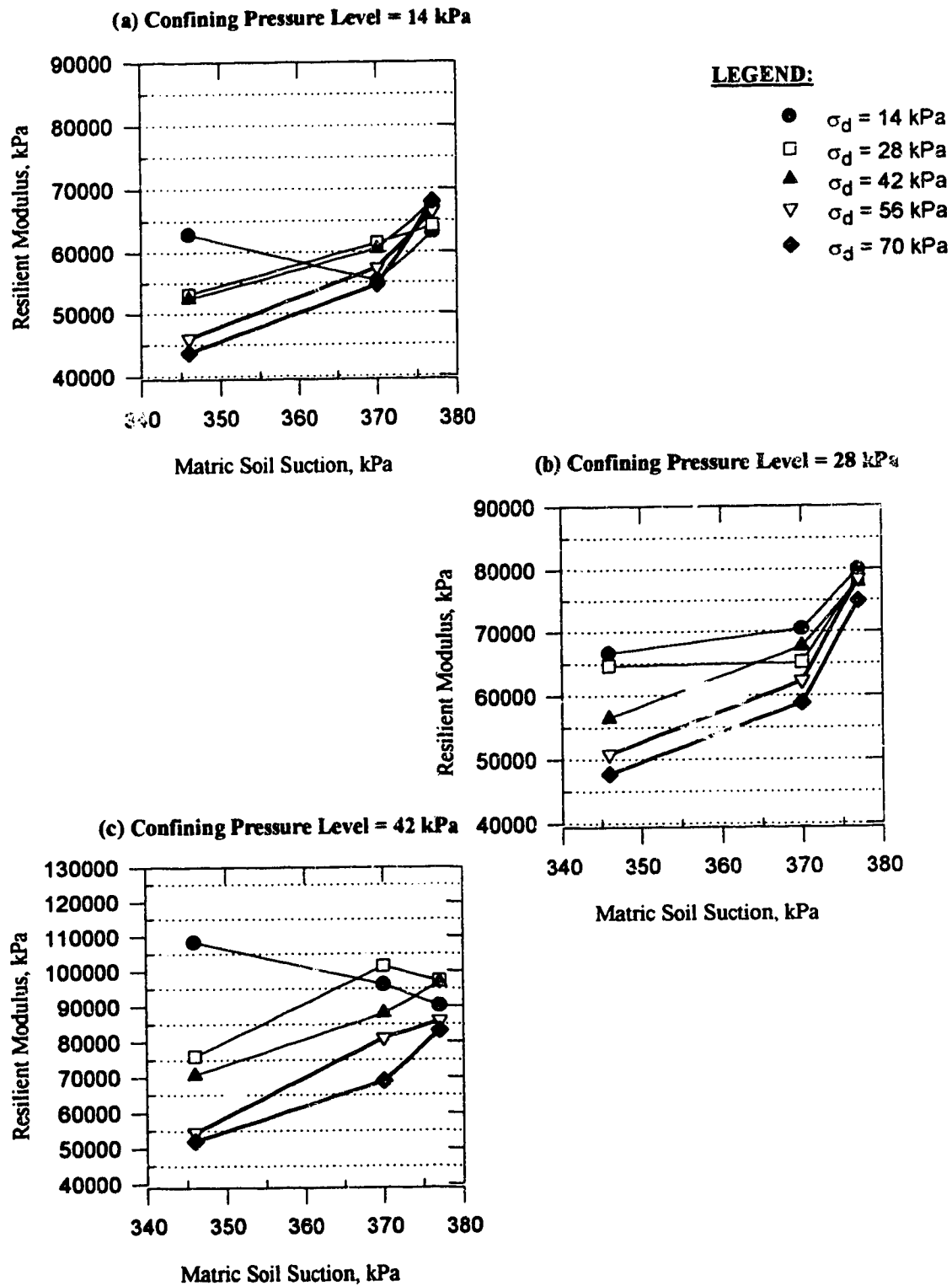


Figure 6.14: Resilient Modulus *versus* Matric Suction for Soil Group 3

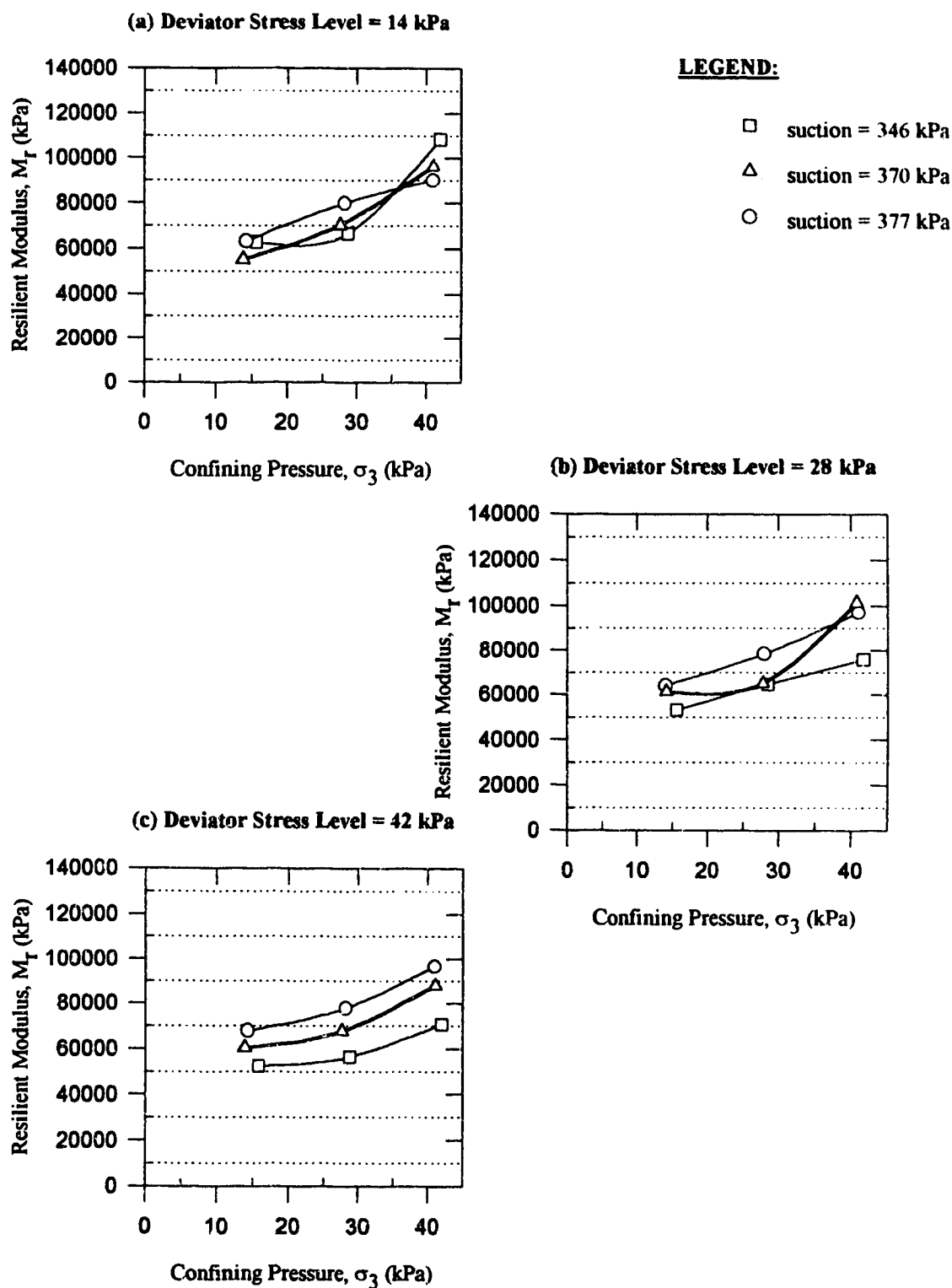
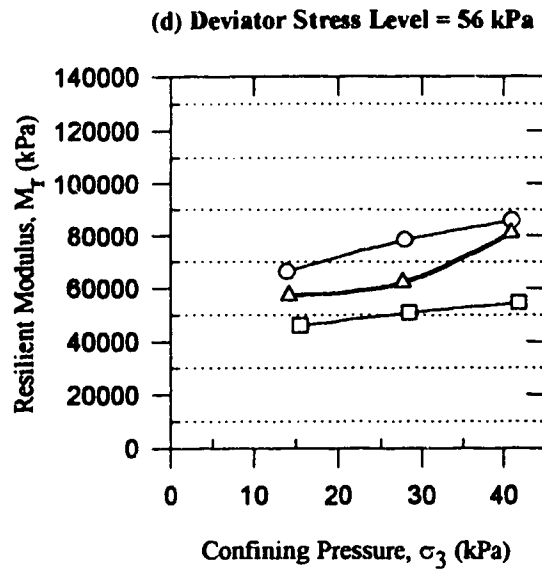


Figure 6.15: Resilient Modulus versus Confining Pressure for Soil Group 3



LEGEND:

- suction = 346 kPa
- △ suction = 370 kPa
- suction = 377 kPa

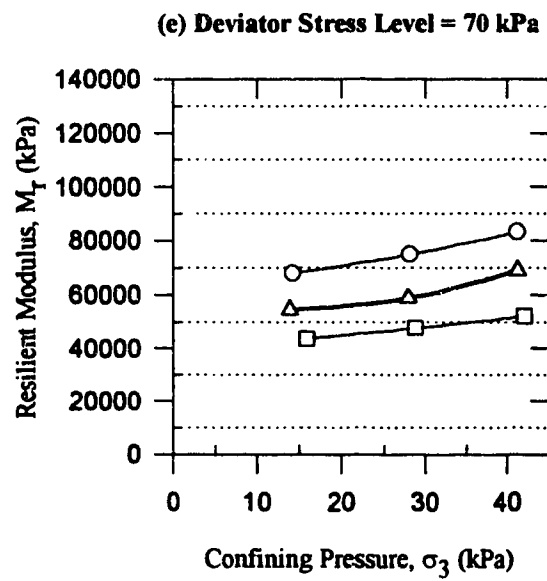


Figure 6.15: Continued

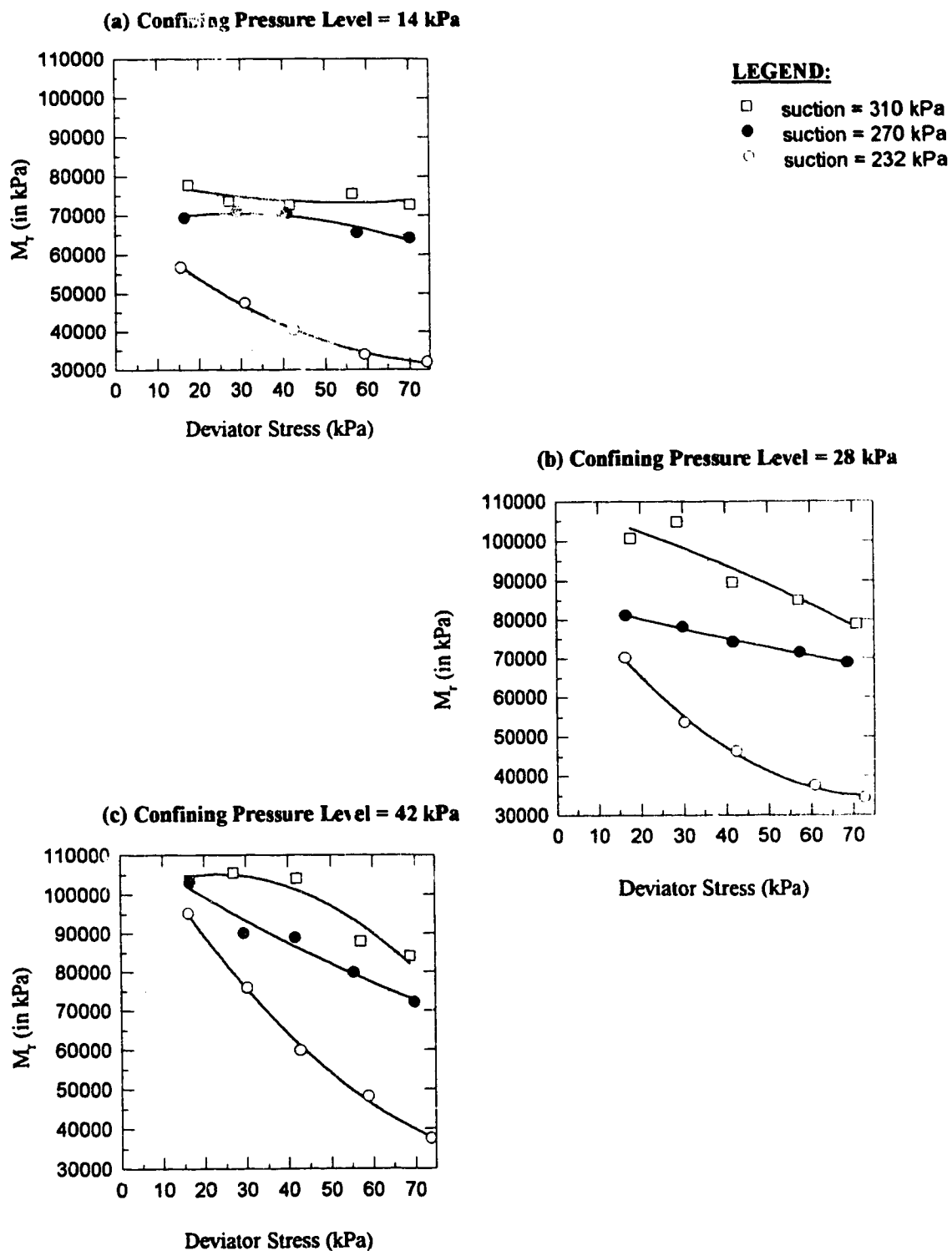


Figure 6.16: Resilient Modulus *versus* Deviator Stress for Soil Group 5

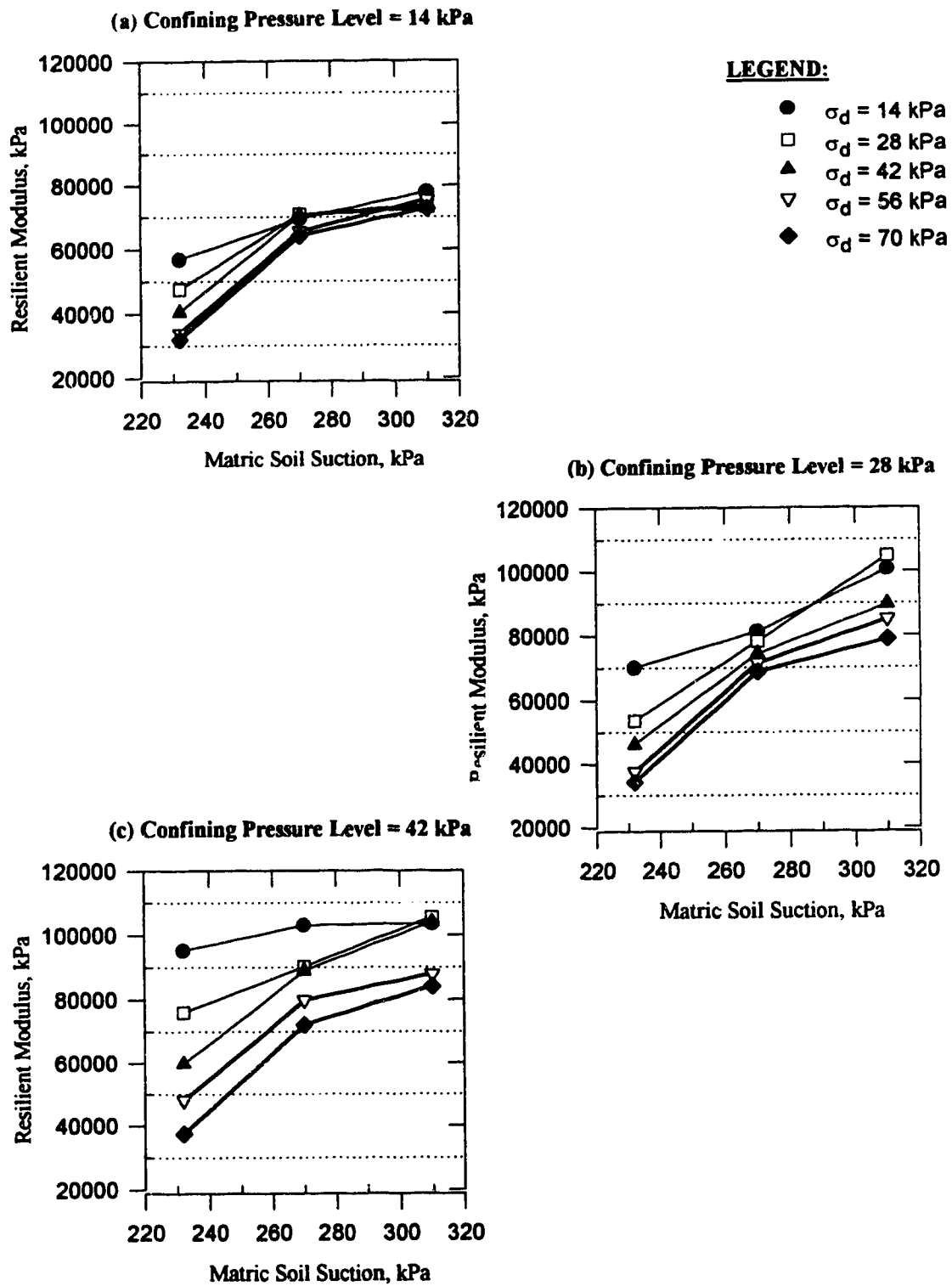


Figure 6.17: Resilient Modulus versus Matric Suction for Soil Group 5

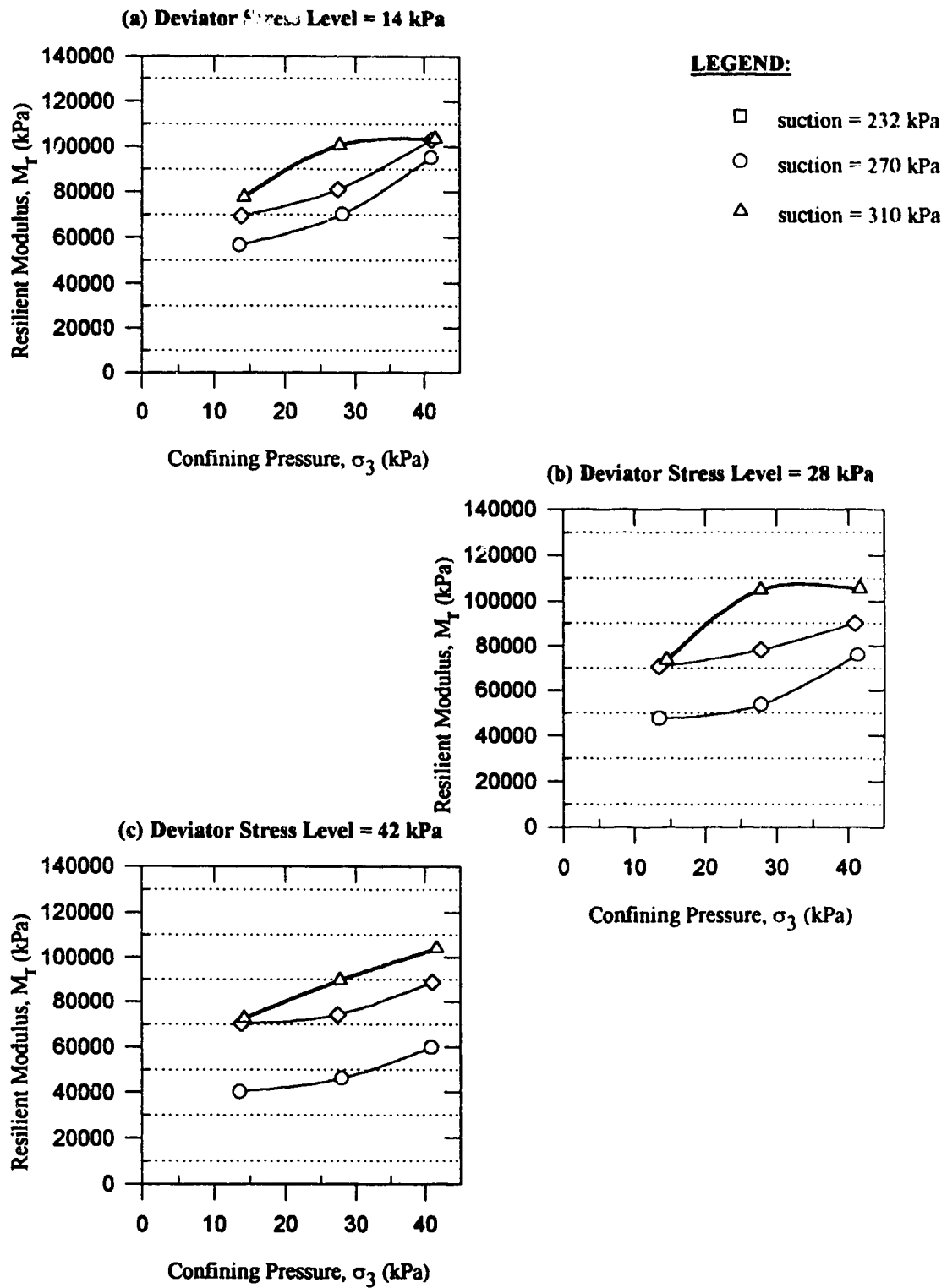
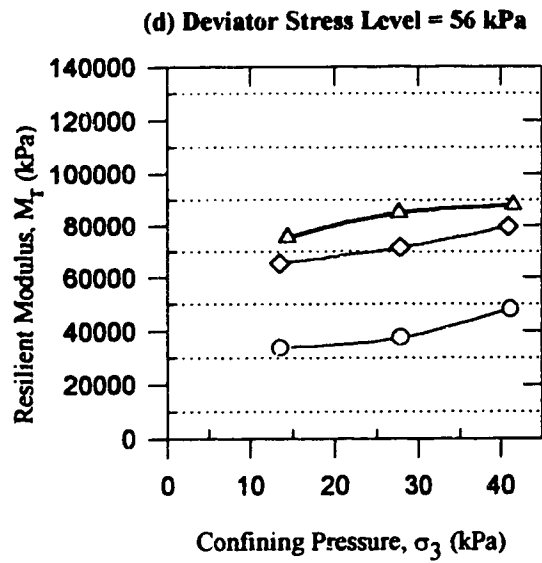


Figure 6.18: Resilient Modulus *versus* Confining Pressure for Soil Group 5



LEGEND:

- suction = 232 kPa
- suction = 270 kPa
- △ suction = 310 kPa

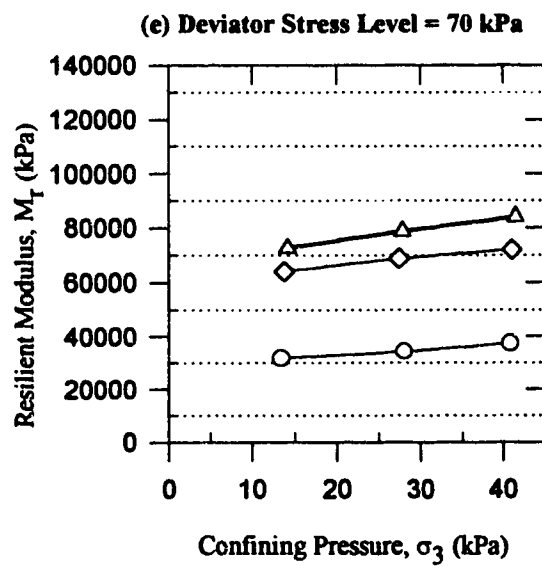


Figure 6.18: Continued

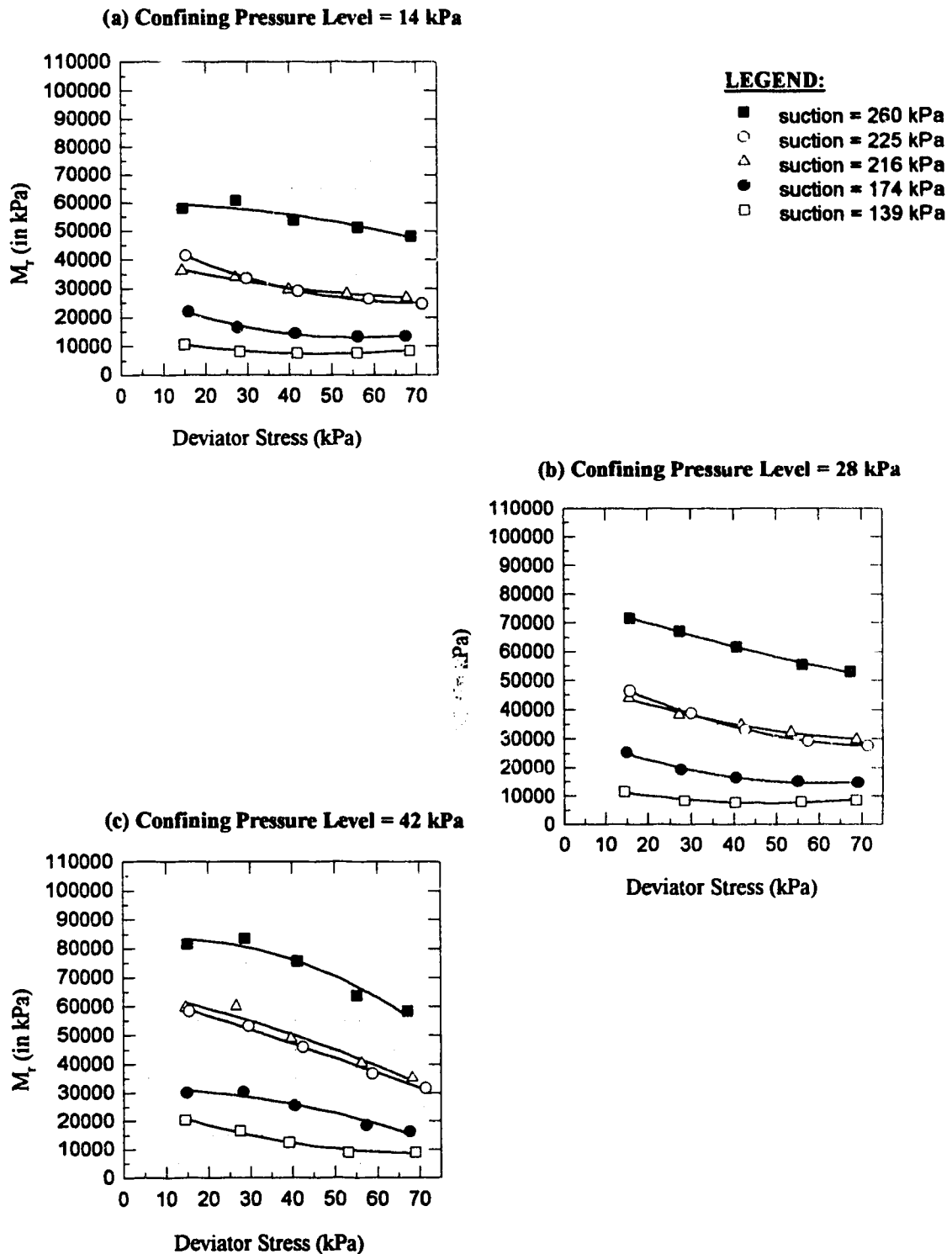


Figure 6.19: Resilient Modulus *versus* Deviator Stress for Soil Group 6

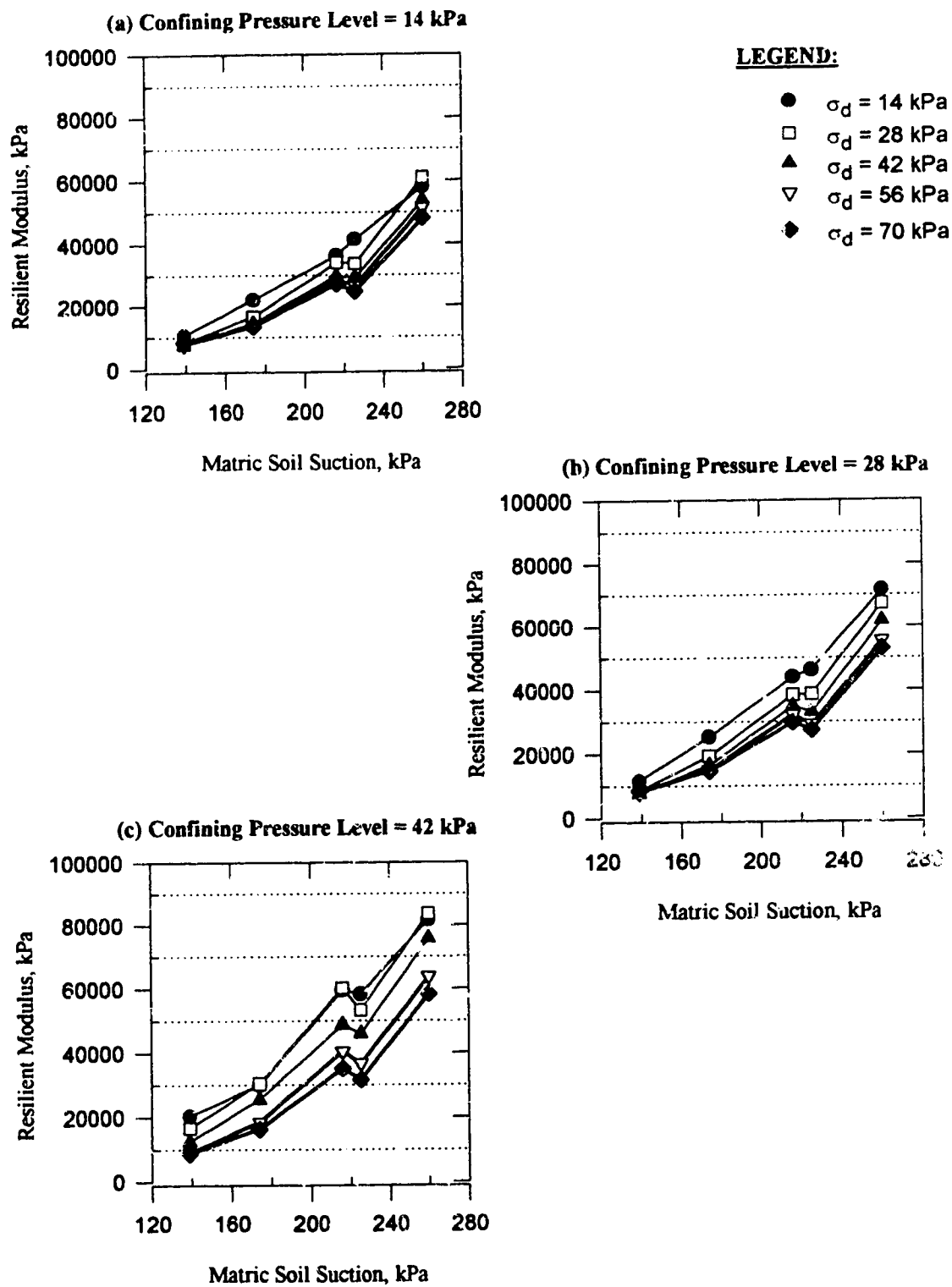


Figure 6.20: Resilient Modulus *versus* Matric Suction for Soil Group 6

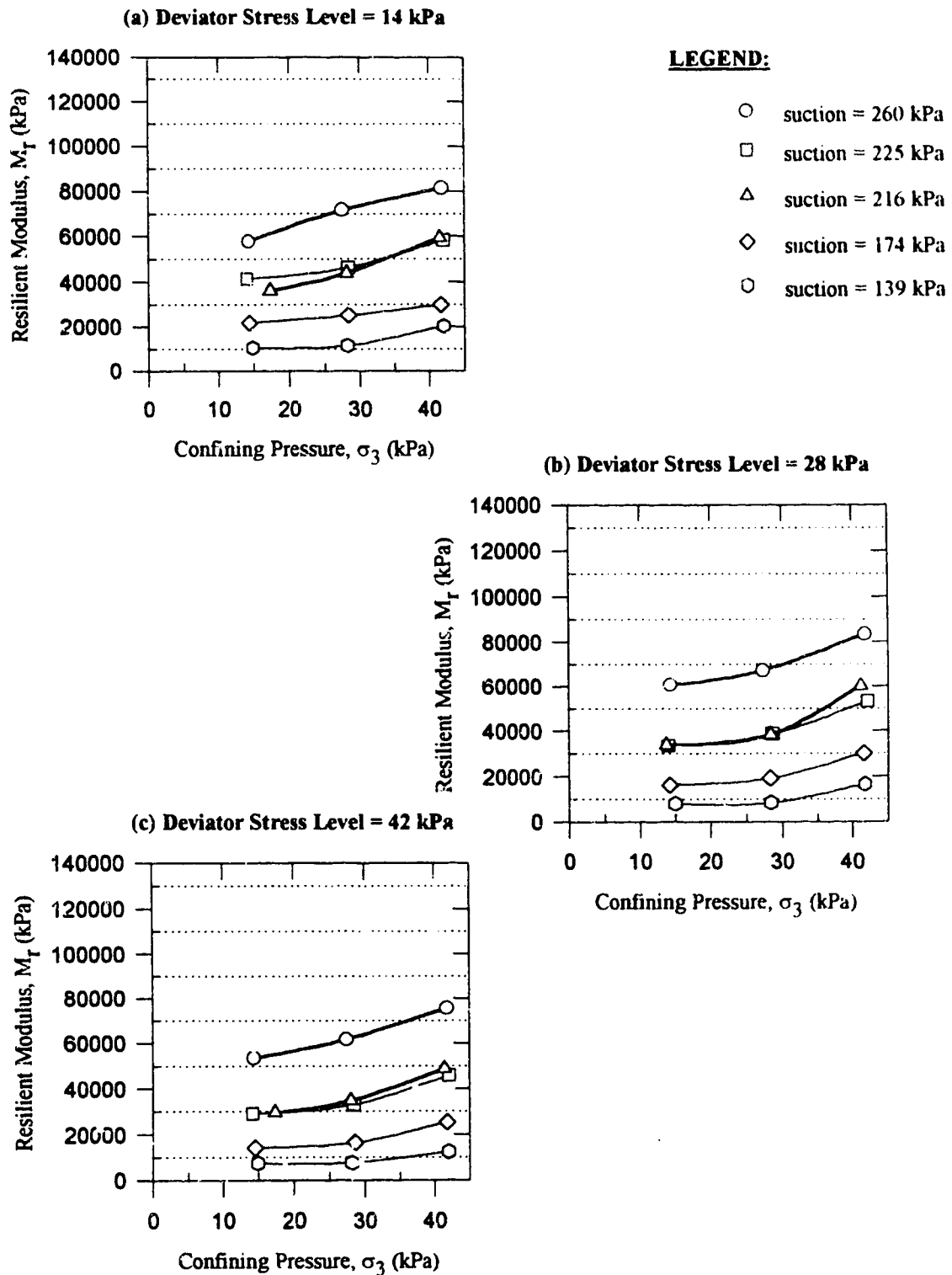
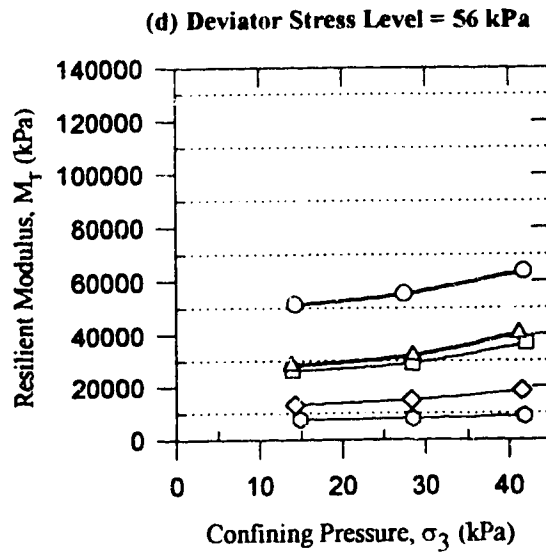


Figure 6.21: Resilient Modulus *versus* Confining Pressure for Soil Group 6



LEGEND:

- suction = 260 kPa
- suction = 225 kPa
- △ suction = 216 kPa
- ◇ suction = 174 kPa
- suction = 139 kPa

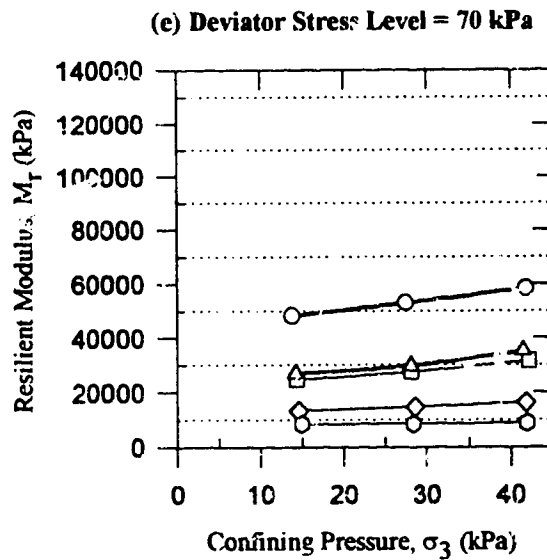


Figure 6.21: Continued

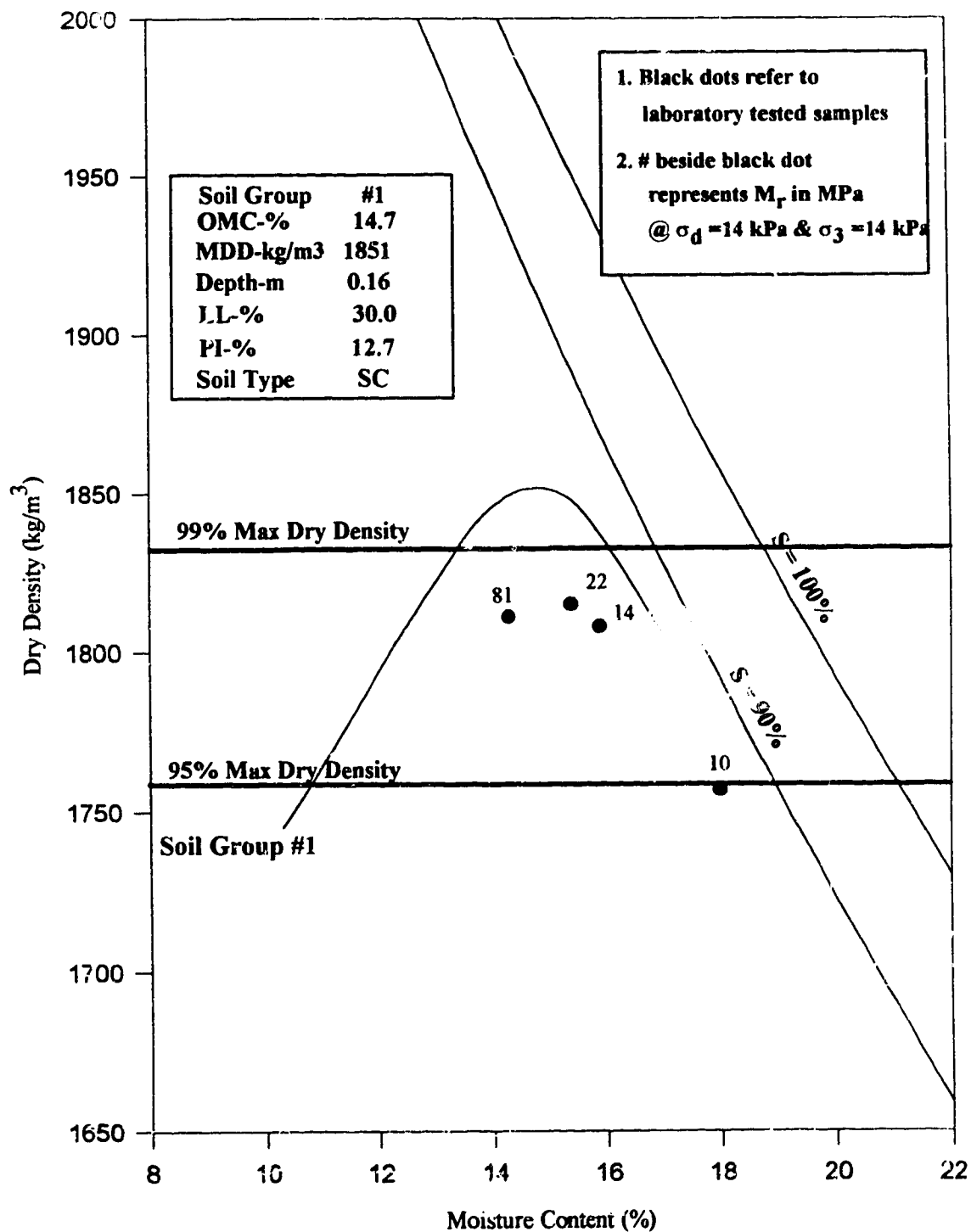


Figure 6.22: Selected Resilient Moduli for Soil Group # 1

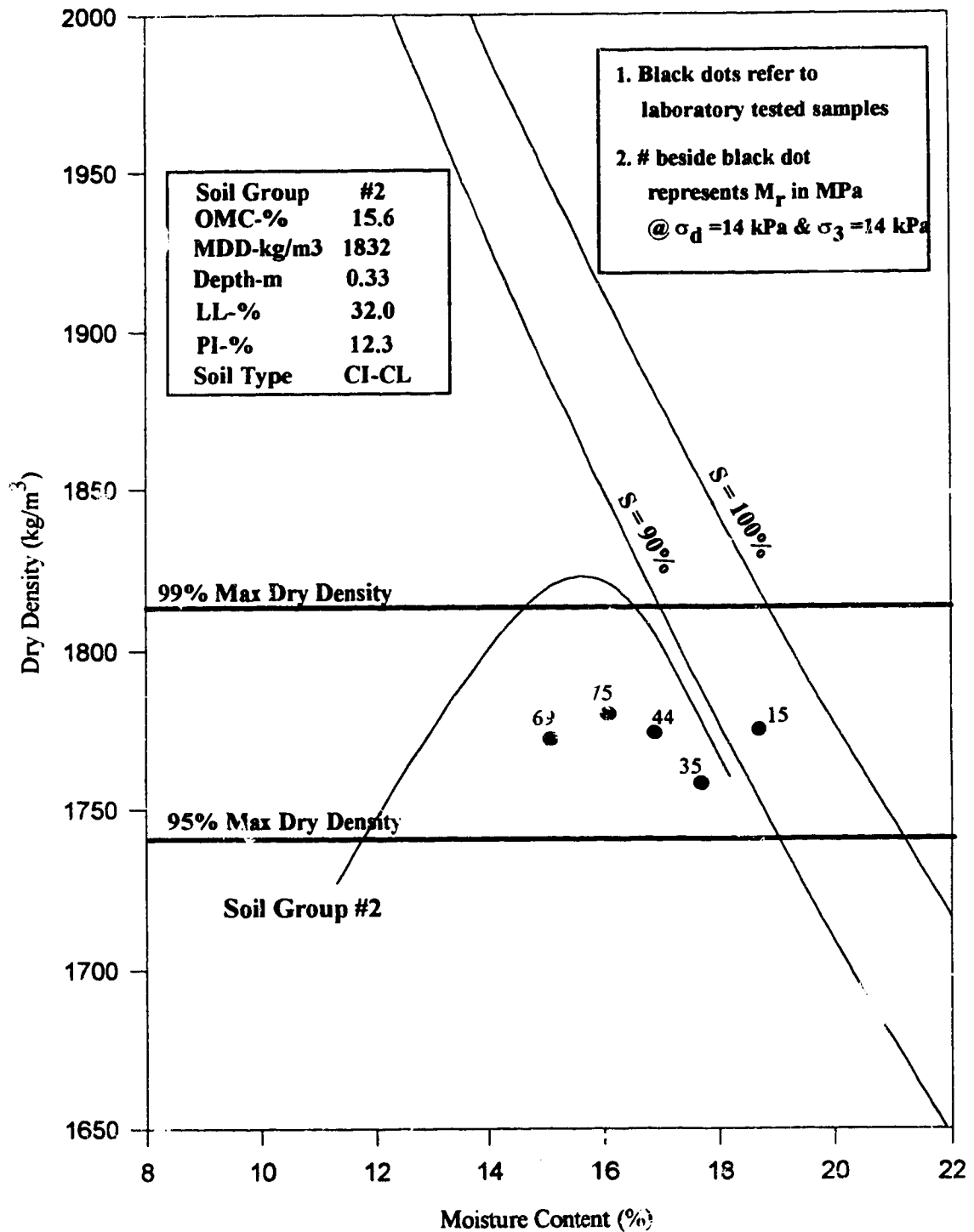


Figure 6.23: Selected Resilient Moduli for Soil Group #2

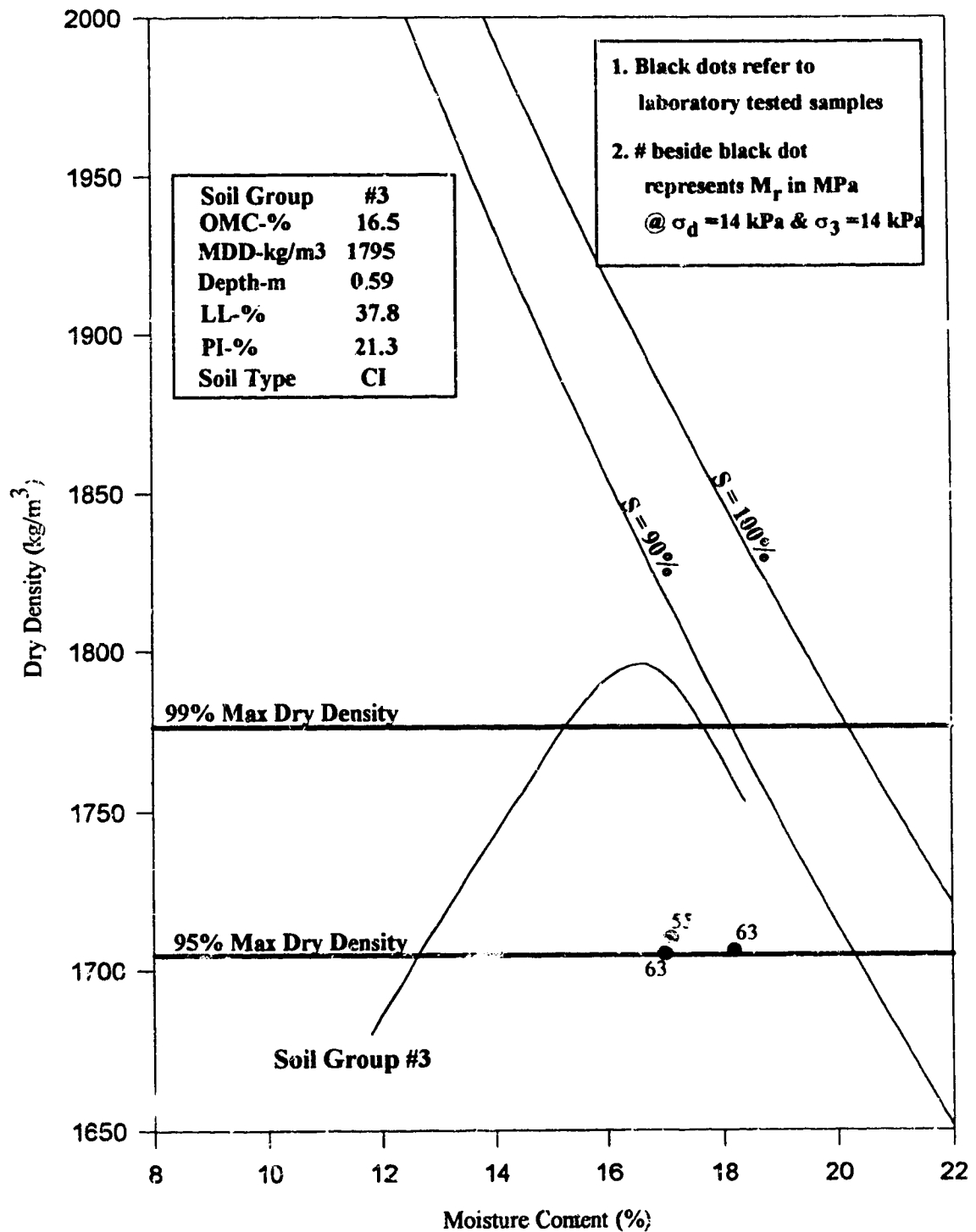


Figure 6.24: Selected Resilient Moduli for Soil Group # 3

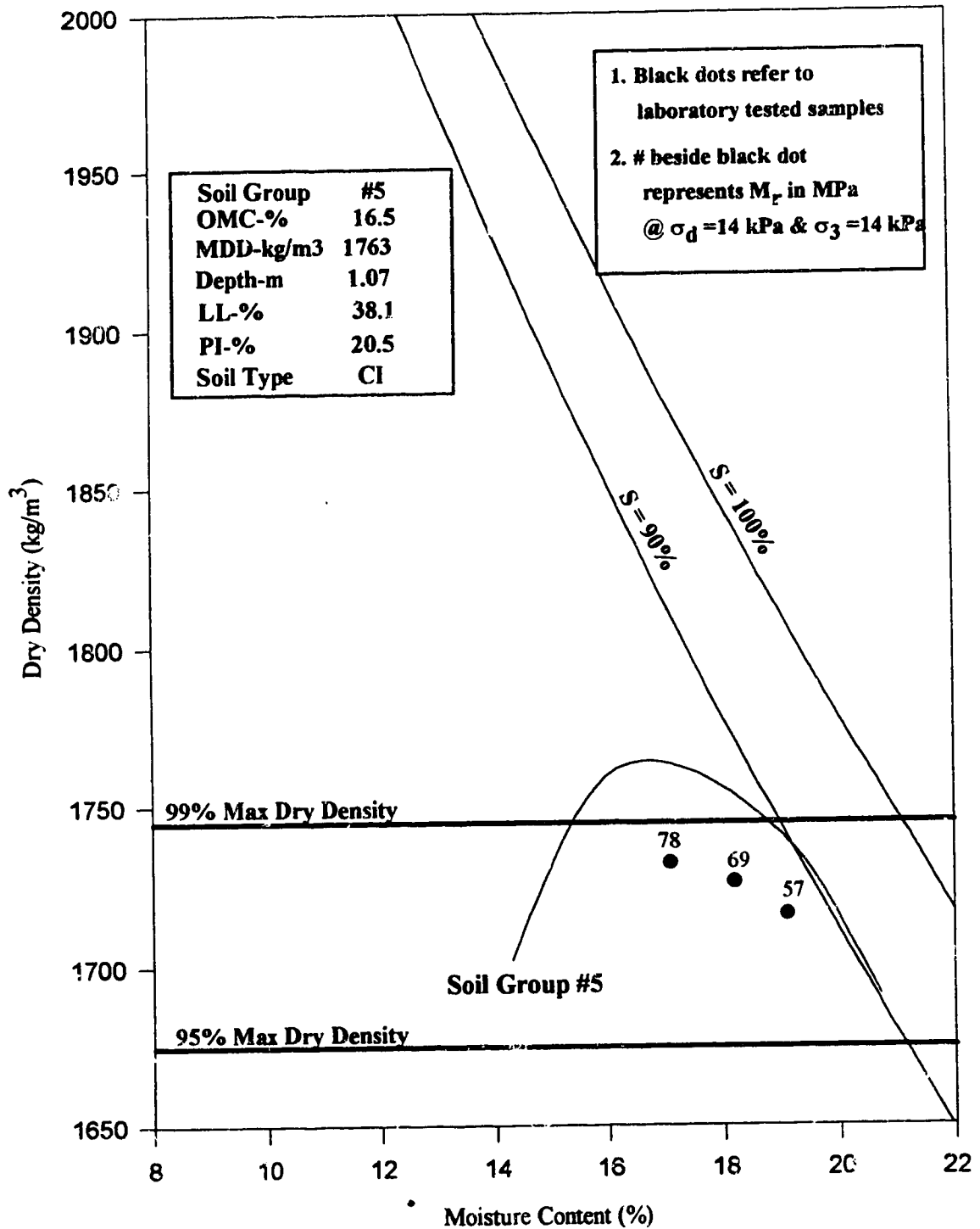


Figure 6.25: Selected Resilient Moduli for Soil Group # 5

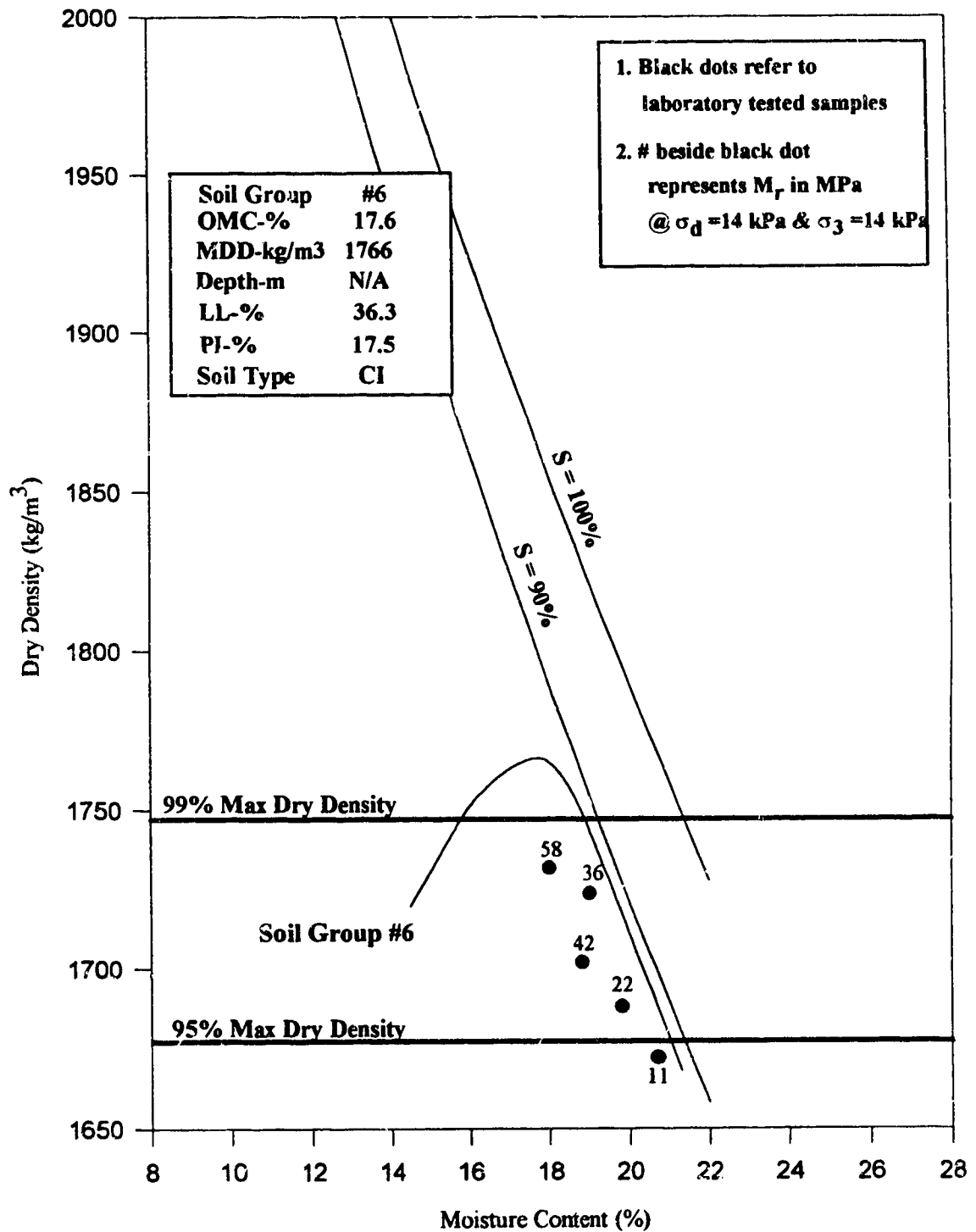


Figure 6.26: Selected Resilient Moduli for Soil Group # 6

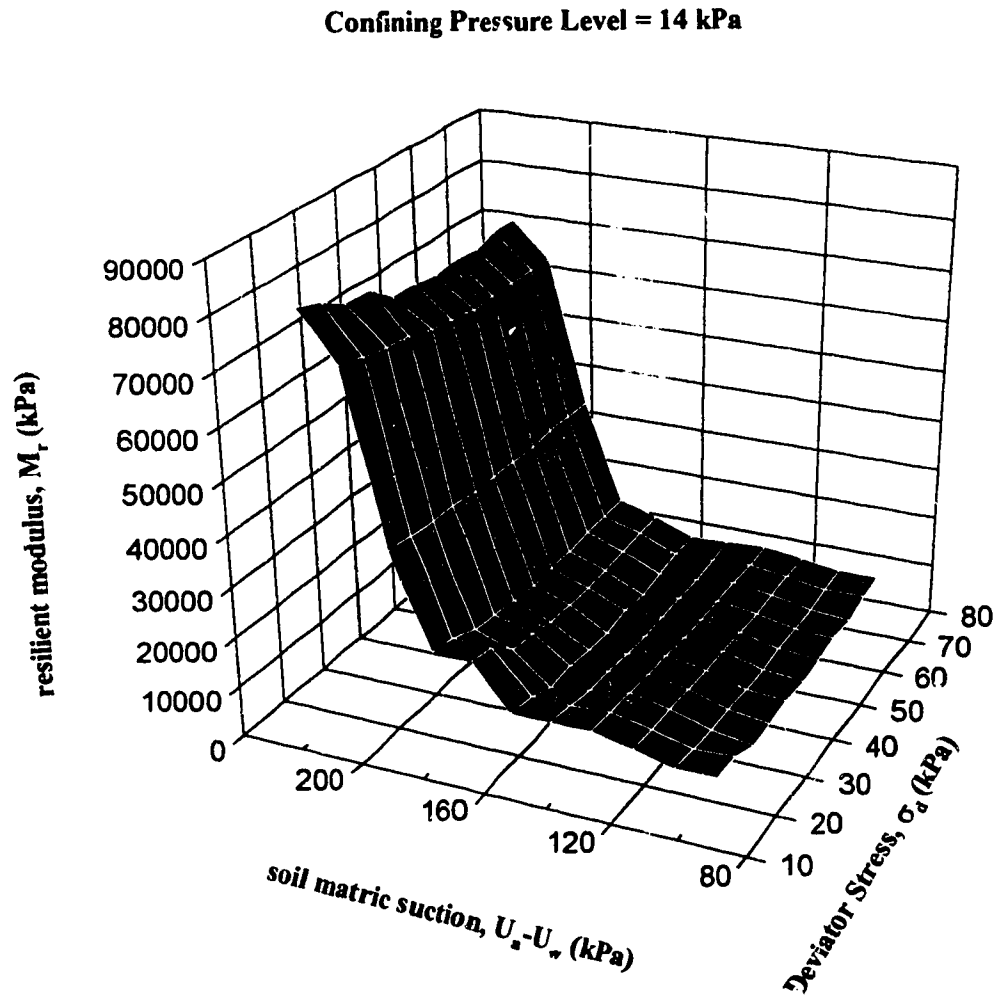


Figure 6.27: Variation of Resilient Modulus with σ_d and ψ for Soil Group 1

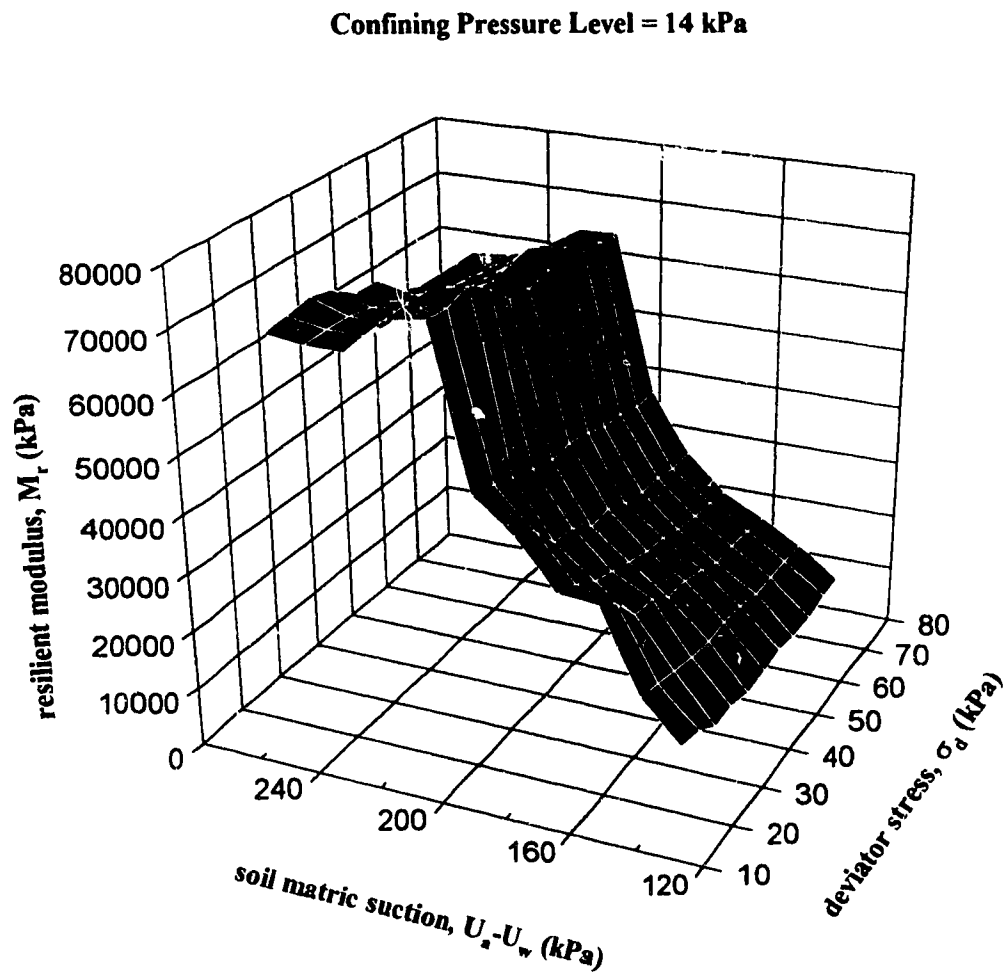


Figure 6.28: Variation of Resilient Modulus with σ_d and ψ for Soil Group 2

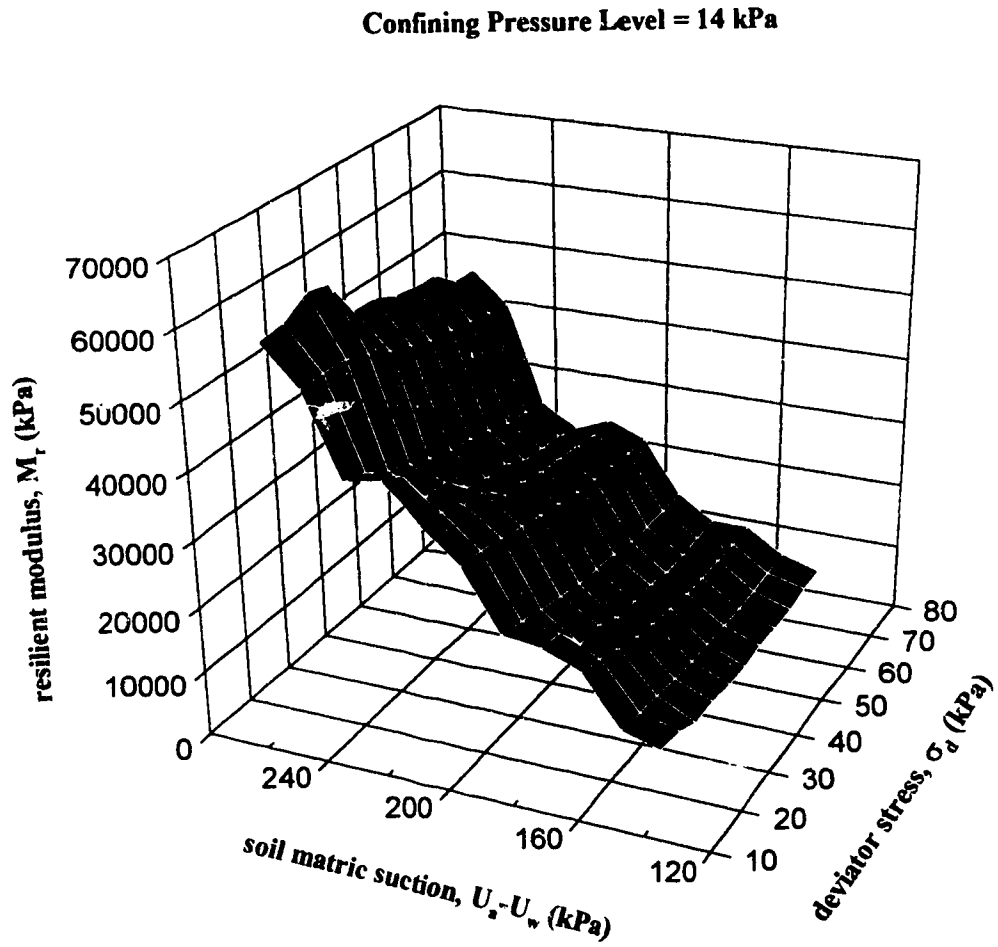


Figure 6.29: Variation of Resilient Modulus with σ_d and ψ for Soil Group 6

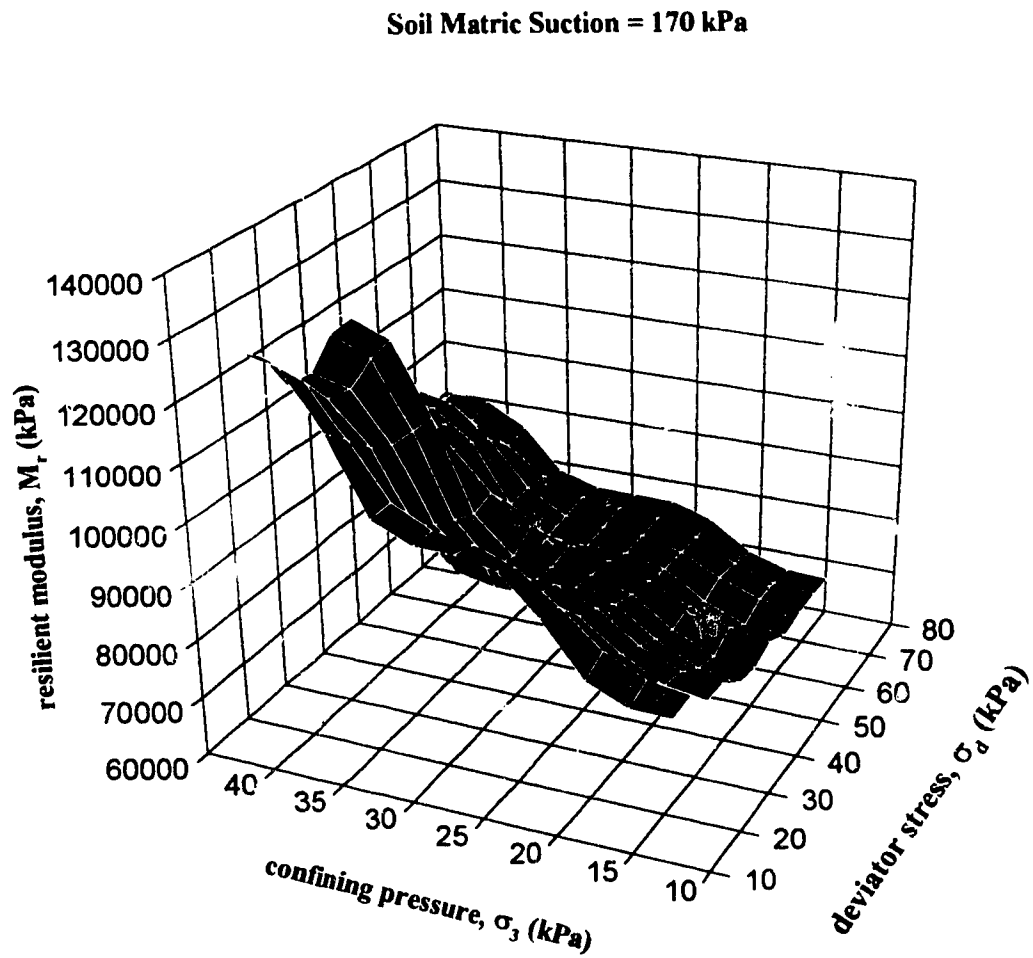


Figure 6.30: Variation of Resilient Modulus with σ_d and σ_3 for Soil Group 1

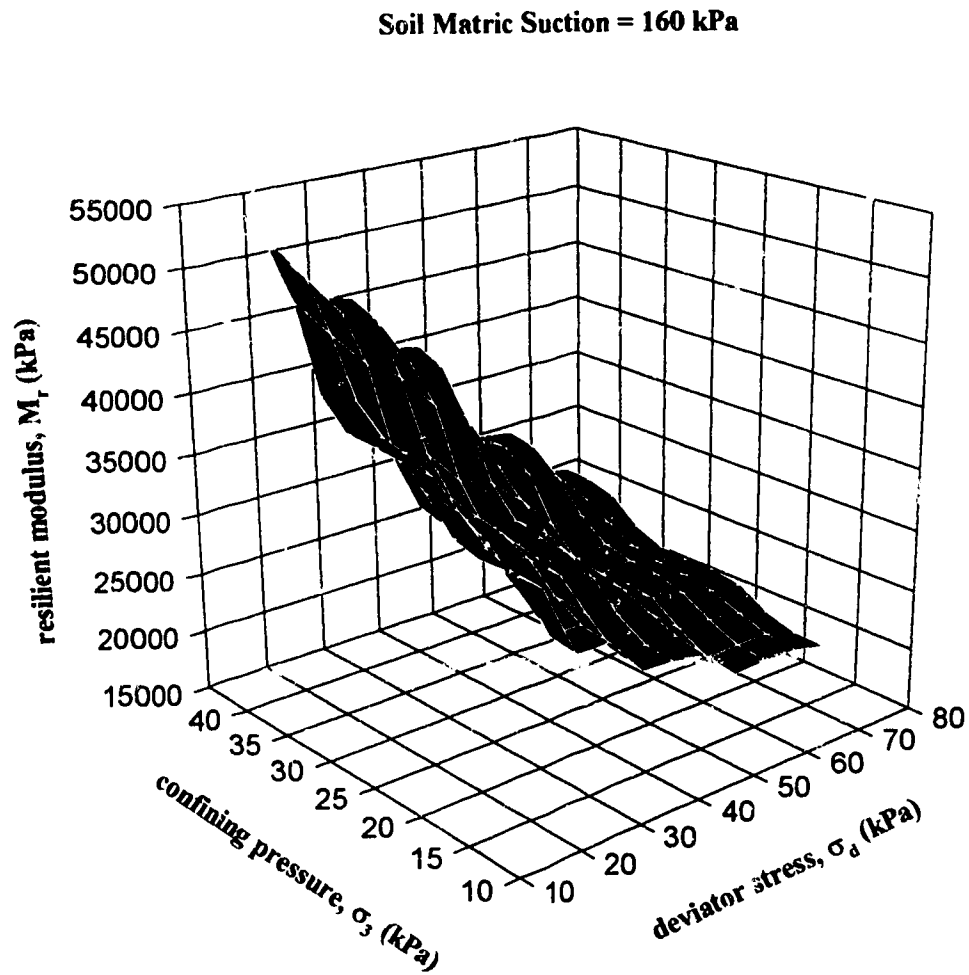


Figure 6.31: Variation of Resilient Modulus with σ_d and σ_3 for Soil Group 2

Soil Matrix Suction = 216 kPa

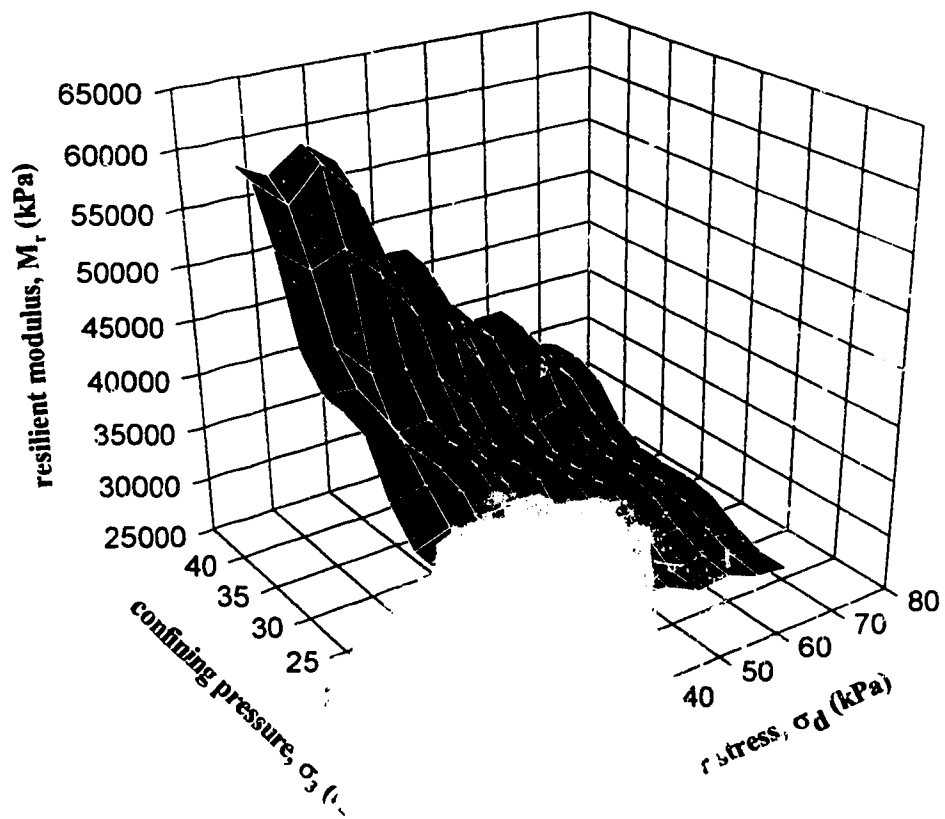


Figure 6.32: Variation of Resilient Modulus with σ_d and σ_3 for Soil Group 6

CHAPTER SEVEN

PRESENTATION AND DISCUSSION OF FIELD TESTING PROGRAM RESULTS

7.1 Introduction

This chapter summarizes the research findings from the field testing phase of the current investigation. The details of the field testing program were given in Chapter Four of this thesis. In summary, a one kilometre section on Highway 16, approximately 80 km west of Edmonton, was instrumented with 12 thermal conductivity sensors for the purpose of monitoring temperature and soil matric suction at different depth locations within the subgrade layer. Falling Weight Deflectometer (FWD) tests were also conducted at regular time intervals at various locations within the instrumented section. Data collected from these tests and from temperature and soil suction measurements is presented and discussed in the following sections of this chapter.

7.2 Objectives of The Field Testing Program

The main objectives of the field testing program can be summarized as follows:

- (1) Develop a procedure for monitoring temperature and matric suction distribution trends within a typical subgrade soil material in Alberta.
- (2) Assess the effects of seasonal variations in temperature and matric suction on flexible pavement structural capacity to withstand traffic loadings particularly during the thaw-weakening period in the spring time.
- (3) Investigate the possibility of implementing mechanistic measures, such as the resilient modulus determined from back-calculation analysis, for pavement design and rehabilitation.

The degree of success achieved in fulfilling these goals is addressed in detail in the following parts of this chapter.

7.3 Temperature and Matric Suction Data

Monitoring and collection of temperature and matric suction data spanned a period of approximately two years from November 7, 1990 to September 15, 1992. The measurements were performed at each sensor location every two hours using an automated data acquisition system. This system suffered a temporary breakdown during the period from April 6, 1991 to July 16, 1991, as a result of drainage water ingress inside the data acquisition box. The problem, which has been explained in detail in chapter four, was discovered and remedied and data collection resumed again on July 17, 1991. The consequences of this incident was a loss of about three and a half months of temperature and suction data. Although this loss occurred during a critical monitoring period, i.e. spring of 1991, it was felt that the data collected during the spring of 1992 would make up for the loss and would shed some light on the distribution trends of temperature and soil suction within the subgrade layer during the normal thaw-weakening time. This assumption, of course, implies that there are no significant differences in the distribution trends of temperature and matric suction during any particular time interval, such as the spring period, from one year to the next year.

Based on the information given previously in chapter three pertaining to the behaviour of unsaturated soils under both freezing and non freezing conditions, temperature and moisture suction data obtained during the current study will be interpreted and discussed.

7.4 Presentation and Discussion of Temperature and Soil Suction Results

Although both temperature and soil matric suction measurements were collected automatically every two hours for the whole duration of the two-year monitoring period, seasonal trends for these parameters were plotted for data recorded only every forty eight and every twenty four hours, respectively. This was done to avoid the excessive

fluctuations that were observed to occur when all the data collected every two hours was plotted. Examples illustrating this for temperature and suction data are shown in Figures C.1 and C.2 in Appendix C, respectively.

Initial analysis of temperature and soil matric suction data takes the form of plotting these measurements versus time to identify seasonal distribution trends. Figures C.3 to C.14 in Appendix C present the temperature and suction results of the twelve sensors that were installed in Control Section 16:12. Each figure consists of two plots. The first plot on the top of the page displays the variations in temperature at the specific sensor location together with variations measured in daily air temperature. The bottom plot of each figure shows the variations in soil matric suction throughout the seasons.

The time of monitoring and collection of the temperature and soil suction data can be divided into two distinct intervals. The first interval extends from November 7, 1990 to April 6, 1991 while the second interval spans the period from July 17, 1991 to September 15, 1992. During the period from April 6, 1991 to July 16, 1991, no data was collected due to the malfunction in the data acquisition system. This incident was noted to at the beginning of this chapter and is explained in detail in chapter four.

Attempts to relate the outputs of the different sensors together based on spatial and depthwise distances were also made. These are shown in Figures 7.1 to 7.6.

7.4.1 Temperature Variations

It should be mentioned that the temperature measurements plotted every forty eight hours were chosen to represent a particularly selected time of the day. This means that the plotted data does not represent any minimum, maximum or average daily temperature values. This was done since the emphasis in the current research is on

identifying only the general temperature trends and not on obtaining actual temperature measurement indices. It should also be mentioned that the measurements of the daily air temperature were performed using a thermocouple unit that is placed inside the data acquisition equipment box. The precision of this method for recording air temperature is quite reasonable based on the fact that the data acquisition box was clamped to a steel post and left hanging in the air. Furthermore, the fact that the data acquisition box was made of a fibre glass material implies that temperature measurements performed inside the box will not be significantly different from actual air temperatures outside the box since this material does not constitute any thermal barrier between the temperature conditions inside and outside the data acquisition box.

Based on the discussion, given in Appendix C, pertaining to temperature seasonal variations as monitored by the AGWA-II sensors and from Figures 7.1 to 7.6, the following main findings can be drawn:

- (1) In general, the AGWA-II sensors used in this study seem to provide good and consistent temperature measurements throughout the seasons. One observation that seems to substantiate and confirm this finding is that sensors at shallow depths responded faster to changes in air temperature than other sensors at deeper locations. This observation is consistent for all sensor groups and agrees reasonably well with the theoretical aspects of temperature distribution in situ.
- (2) It is clear that there is a great deal of fluctuations in the recorded daily air temperature. However, temperature measurements performed at each sensor location within the subgrade soil layer do not exhibit the same kind of fluctuations. This indicates that daily temperature changes within the subgrade are moderate and can therefore be accommodated for by recording temperature measurements once

every two or more days i.e. there is no need for continuous monitoring every two hours.

7.4.2 Soil Matric Suction Variations

In order to examine the effect of the sensor location on its measured response, two sets of figures were drawn. Within the first set, measured outputs of sensors located at the same transverse distance from the pavement shoulder edge were grouped together. This is shown in Figures 7.1 to 7.3. The second set includes measured responses of sensors that are located at approximately the same depth and same longitudinal distance but at different transverse distances from the pavement shoulder edge. This is depicted in Figures 7.4 through 7.6 inclusive.

From Figures 7.1 to 7.3, the following conclusions can be drawn:

- (1) It is evident that during the first monitoring period there are more variations in suction readings obtained from sensors located closer to the pavement edge than from those located further away from the pavement edge. This is illustrated by the variations shown in the shoulder and outer wheel path (OWP) areas as compared to those in the inner wheel path (IWP) area. The reason behind this may be the fact that water usually drains to the side ditch close to the pavement shoulder. This will, in turn, provide for an ample supply of water that can move freely and quickly to regions within the pavement structure that are close to the pavement edge. The consequence of this will be that the soil at such locations will experience more fluctuations in moisture content which will be accompanied by mutual fluctuations in matric suction. Therefore, sensors installed at these locations will record more variations in suction than those recorded by further away sensors.

(2) It is also observed that after the first winter i.e. 1990-1991, the suction measurements obtained from sensors close to the pavement edge do not differ much from those obtained from sensors located further away from the pavement edge. Several reasons are thought of as contributing to this behaviour:

(i) freezing and thawing of fine-grained soils may induce some volume changes. These volume changes, which are dependent on soil suction, may become excessive and lead to either soil expansion or contraction. If the latter mechanism prevails, then the soil will shrink away from the sensor causing a gap between the sensor and the surrounding soil. Once the sensor has separated from the soil, the soil suction reading registered will reflect only the amount of water remaining within the sensor porous tip. On the other hand, if the gap between the sensor and the soil becomes filled with water, this will increase the rate of heat transfer due to the induced heat pulse and will consequently lead to errors in sensor readings.

(ii) A big transverse crack was observed to develop within the instrumented section immediately after the first winter period elapsed. This crack might have provided a passage for rain water to flow to sensors' locations and consequently cause a reduction in the recorded soil suction.

(iii) The backfilling of sensors' holes and/or longitudinal trenches for laying out sensors' lead wires may have not been done properly. This might have eventually caused preferential flows of water along the wires leading to the sensors and caused the observed reduction in the measured suction values.

(3) Sensors, within the same group, that are located at approximately the same depths and at different longitudinal distances recorded equal suction values for almost the whole monitoring period. Examples of such sensors are sensors 1 and 2 in Figure 7.1 and sensors 8 and 9 in Figure 7.2. This indicates that the effect of the

longitudinal distance on the sensor response is less important than the effect of either the transverse distance or the depthwise location.

- (4) Variation in soil suction during the winter time is difficult to interpret. However, it is evident that the AGWA-II sensors function equally well during both the frozen and the non-frozen periods. One benefit that could be gained by examining the behaviour of the thermal conductivity sensors during the frozen period, is to make sure that these sensors are still working properly to provide reliable and consistent measurements of the soil matric suction after the first freezing and thawing period elapses.
- (5) There is no significant change in soil matric suction observed during both the thaw weakening and summer periods. This is characterized by changes in matric suction for the surface sensors in the order of 10 to 50 kPa and for deeper sensors in the order of 10 to 25 kPa. Linking this to seasonal variations in subgrade soil stiffness during such critical periods will be discussed in details in the following sections that deals with FWD deflection testing.

Combined examination of the trends shown in both Figures 7.1 to 7.3 and Figures 7.4 to 7.6 reveals that the role that the transverse distance, from pavement edge, plays in influencing measured suction values far outweighs the role of either the longitudinal or the depthwise distances.

7.5 FWD Deflection Testing

As a part of the field investigation, a non-destructive field testing program was carried out. This consisted of conducting FWD deflection tests at 50m intervals on both the outer and inner west bound lanes in the vicinity of the instrumented site. The lateral positioning of the FWD tests were in the outer wheel path of the outer lane and the centre

line of the inner lane, respectively. Figure 7.7 shows a plan view of the FWD test locations. The philosophy behind the particular testing scheme displayed in Figure 7.7 is that uniformly spaced test points over the full length of the selected pavement section are expected to provide more information on the longitudinal variability in the pavement than more closely spaced test points over shorter subsections.

The purpose of the FWD testing is to use the measured dynamic deflection in conjunction with temperature and soil matric suction data to study the phenomenon of seasonal variations in subgrade stiffness.

In carrying out deflection tests, a Dynatest model 8000 FWD system was used. This equipment is owned and operated by the Alberta Transportation and Utilities Department of Highways. The Dynatest 8000 FWD system consists of three main units:

- (i) A Dynatest 8002E FWD Trailer.
- (ii) A Dynatest 9000 System Processor.
- (iii) An IBM PC compatible computer with an attached printer.

The 8002E FWD trailer houses a loading plate, a strain-gauge-type load transducer (load cell), seven velocity transducers (geophones) for deflection measurements, and a dropping-weight system for the provision of the impulse load. The method of applying the dynamic load and measuring the resulting deflections was outlined previously in chapter two. The load pulse generated by the drop approximates a haversine wave of load duration of 25-30 milliseconds. By varying the drop heights and drop weights, a force range of 7 to 120 kN can be obtained. Deflection is measured by using up to nine velocity transducers. Only seven transducers were used in the current study with one at the centre of the loading plate and the remainder mounted on a bar that is lowered automatically with the loading plate.

The Dynatest 9000 System Processor is a compact, microprocessor based electronic unit that is interfaced with both the FWD trailer and the IBM PC computer. The main functions of this Processor are the following

- (i) Control of the FWD trailer hydraulics.
- (ii) Condition, scan, digitize and transmit measured load and deflection signals to the IBM PC computer for data display and storage.
- (iii) Perform continuous monitoring of the whole system to reveal any functional or operational errors.

The 9000 System Processor is powered by a 12 VDC battery.

The Computer/Printer assembly is used for input of control and site/test identification data as well as for displaying, editing, storing and printing of FWD test data.

Specifications pertaining to each main unit of the Dynatest 8000 FWD System as well as further details on equipment maintenance and calibration can be found in the system manuals (Dynatest 8000 FWD Test System, Owners Manual, Part 1 and 2, 1991).

7.5.1 Test Protocol and Planned FWD Tests

To accomplish the objectives of the field testing phase, an extensive deflection testing program was planned and executed. Testing spanned a period of two years from October 15, 1990 to October 27, 1992. Forty test points were located and marked with white paint within the one kilometre pavement section shown in Figure 7.7. The FWD tests carried out were performed in accordance with the following scheme:

- (i) Once a week every week for the period of March 1st to May 31st.
- (ii) Once every two weeks for the period of June 1st to June 31st.

(iii) Once every three weeks thereafter. This was continued until no further deflection readings could be obtained.

The aforementioned test sequence was followed as close as possible, however, sometimes it was difficult to adhere to that. Two reasons that contributed to this difficulty were:

- (1) Unpredicted weather conditions and/or unexpected sensor malfunction that hindered the operation of the FWD equipment.
- (2) Unusual time conflicts between scheduled deflection tests pertaining to the instrumented section and those carried out routinely by Alberta Transportation and Utilities Roadway Engineering Department for inventory purposes.

As a result, actual testing dates differed slightly from the above given schedule. Table 7.1 shows these dates for all deflection tests performed.

In carrying out the testing program, the following test protocol was followed (FWD Field Operation Manual Version 2.1, 1992):

- (1) The Dynatest 8000 FWD equipment is moved to the specific test point and the loading plate and transducers are hydraulically lowered until the assembly touched the pavement surface.
- (2) An eleven-drop sequence is used at each test location. This consisted of three drops to seat the FWD loading plate followed by eight drops that are performed from heights h1, h2, h3, h4, h1, h2, h3 and h4, respectively. These drop heights correspond to approximate applied loads of 26.7 kN, 40.0 kN, 53.3 kN and 71.1 kN, respectively with a target tolerance error of $\pm 10\%$. The mass used to achieve the target loads was a 200 kg mass.
- (3) Load and deflection data is then measured and displayed on the computer screen. The sensor locations are measured from the centre of the applied dynamic load and are set at: 0, 300, 600, 900, 1200, 1500 and 1800 millimetres, respectively.

- (4) Temperature readings at approximately 50 mm below the asphalt concrete surface are also recorded every two hours.
- (5) The loading plate and sensors are then hydraulically lifted, and the equipment is ready to move to the next test location.
- (6) All the test data pertaining to the forty test locations within the instrumented section for any particular test date is stored in a single computer file. A special data collection software, the Dynatest FWD Field Program, is used for inputting the necessary information concerning the tested highway and for recording the test results. Two versions of this software were used in the current investigation, namely: edition 20 and edition 25. Example outputs showing these two formats are displayed in Figure D.1 and D.2 in Appendix D. Additional information pertaining to the description of the data collection software can be found elsewhere (AT & U FWD Field Operation Manual Version 2.1, 1992).

It should be mentioned that, two test runs, or repetitions, were performed on each test date. A full run, i.e. forty test locations, usually takes about two hours to complete. These test repetitions were conducted to examine the effect of time of the day on measured deflections.

Apart from the fact that different deflection spacings and load sequences are used by the different department of highways and agencies, for example the SHRP Standard Procedure, to achieve their testing goals, all the other test steps listed above are common among these agencies.

7.5.2 Analysis of Deflection Data

As stated previously, in chapter two, deflection data can be interpreted using one of two approaches (AASHTO 1986 and 1993). Namely, these are:

- (1) Direct deflection analysis.
- (2) Back-calculation of layer moduli.

The first approach involves visual examination of deflection data trends and patterns through the utilization of one or more deflection parameters. This approach is simple and can be used very successfully to discern several deflection-performance relationships for many application purposes. However, this methodology possesses some inherent disadvantages such as:

- (i) The rate of deterioration of pavements depends on critical stresses and strains in the different layers rather than merely surface deflections. This makes deflection criteria and stress or strain criteria incompatible. Ullidtz (1987) presented an example substantiating this fact.
- (ii) Deflection measurements cannot be applied directly as input in any of the currently available mechanistic-empirical pavement design procedures.

The second approach, on the other hand, is more appropriate for use in pavement structural evaluations that are based on mechanistic responses such as critical stresses and/or strains (Ullidtz and Stubstad, 1985; Huang, 1993). Although numerous studies and research efforts have been completed during the past two decades in the area of modulus back-calculation, many problems connected to this methodology still remain to be solved. Some of these problem areas were identified and discussed by many engineers and highway researchers (Uddin et al., 1986; Rwebangira et al., 1987; Briggs and Nazarian, 1989; Stolle and Hein, 1989; Chang et al., 1992; Stolle and Jung, 1992; and Mahoney et al., 1993).

In the present study, deflection measurements collected from the instrumented section were analyzed using both of the aforementioned procedures. Specifics pertaining to each analysis will be detailed in the following sections.

7.5.3 Presentation and Discussion of Deflection Results

This section deals with the presentation and analysis of the FWD deflection data collected from the instrumented site. The primary objective of the analysis is to identify and quantify seasonal variations in the structural stiffness of the subgrade soil layer. During the current analysis, several FORTRAN computer programs and EXCEL macros were developed to automate the handling of the huge deflection data base. Listings of some of these computer codes are contained in Appendix D.

In the pursuit of accomplishing the research objectives, both data analysis techniques, discussed previously, were employed. First, the direct deflection analysis method was used to discern seasonal trends and to see whether further investigation is warranted. This is then followed by the application of a modulus back-calculation procedure to quantify the observed seasonal variations. The details pertaining to each of these analyses and the research findings obtained follow.

7.5.3.1 Deflection Interpretation Analysis

The term “deflection interpretation” as used in this thesis refers to the direct use of representative deflections and/or deflection bowl parameters as a means of describing the structural adequacy of the pavement, without relating this directly to the fundamental properties of the component materials that comprise the pavement structure. Uddin et al. (1985) listed a number of these deflection parameters as used by other researchers to assess pavements.

During the present study, several deflection parameters were investigated to characterize pavement seasonal variations. These parameters were the central deflection (δ_c), the impulse stiffness modulus (*ISM*), fourth sensor deflections (δ_4), seventh sensor deflections (δ_7), and deflection basin areas (*BA* & *ba*). Central deflections are those

measured at the point of application of the dynamic impulse load. The *ISM* is defined by Bush (1987) as the ratio of the applied FWD load to the corresponding central deflection. The ratio of the fourth (or the seventh) sensor deflection measured at any time to the same sensor deflection measured during the fall is used as an indication of the change in subgrade stiffness. This ratio was introduced by Janoo and Berg (1990) and is called the subgrade stiffness index (*SSI*). Although in Janoo and Berg's work only fourth sensor deflections were used to obtain the *SSI*, in the current study subgrade stiffness ratios based on both fourth and seventh sensor deflections were used. In the present discussion, *SSID4* refers to values of the ratio based on fourth sensor deflections whereas *SSID7* refers to values based on seventh sensor deflections.

In the case of the basin area parameter, two basin areas were studied. The first basin area (*BA*) involves the area above the deflection curve that is bounded by the deflection curve and all the seven sensor deflection ordinates. The second basin area (*ba*) refers to the area bounded by the deflection curve and the fourth, fifth, sixth and seventh sensor deflections.

A FORTRAN Computer program called BOWL was developed to compute the aforementioned deflection parameters. This Program uses as input the FWD deflection data collected in the field. The Program accepts both edition 20 and edition 25 FWD data formats. Listing of the BOWL Program can be found in Appendix D.

Using the BOWL Program, deflection data collected during 1990-91 and 1991-92 seasons was analyzed and the results were displayed in Figures 7.8 to 7.18. It should be mentioned that although deflection data was collected under four different loads (i.e. 26.7, 40.0, 53.3 and 71.1 kN), only the data pertaining to load levels 40 kN and 53.3 kN were included in the present analysis. These load levels were of interest because one

corresponds to the standard single axle load of 80 kN (i.e. 40 kN wheel load), and the other (53.3 kN) represents high tire pressure loadings, since the same loading plate of diameter 300mm is used, that may be more detrimental to pavements during thaw-weakening periods.

Deflection Basin Area

As mentioned earlier, two different formulations of the deflection basin area parameter were used to study the seasonal variations in subgrade stiffness. During this analysis exercise it became apparent that the *ba* parameter is more desirable for characterizing subgrade stiffness than the other basin area parameter. This is because, unlike the deflection basin area *BA*, the former parameter is free from any temperature-related influences. Consequently, only the *ba* parameter is used in the subsequent discussion and results interpretation.

The ratio of the basin area computed for any specific test data to the basin area corresponding to the fall conditions of that year was plotted against time. This is shown in Figures 7.8 and 7.9 for the two load levels investigated. As can be seen from these figures, four values of the basin area ratio were obtained at any particular test date. These values reflect the conditions within the fill and cut sections of both the outer and inner lanes of the instrumented pavement section.

From Figures 7.8 and 7.9, several observations can be made:

- (i) During the first monitoring period, a large reduction in stiffness was observed to occur as the subgrade layer started thawing. This is characterized by a change in the basin area ratio from 0.2, representing the frozen condition, to 1.1 at the thaw-weakened condition. The change happened over a relatively short period of time of approximately one month (from March 20, 1991 to April 25, 1991).

- (ii) After the first rapid change in subgrade stiffness, it was observed that a period of almost constant stiffness prevails. This period spanned about three months (from late April or early May to end of July, 1991). After that a gradual recovery in stiffness took place until the subgrade finally converged to the normalized fall value of 1.0.
- (iii) Changes in subgrade stiffness during the second monitoring period (i.e. 1992) resembled the pattern observed in 1991, however, the 1992 changes were more pronounced than those observed during the first monitoring period. This is demonstrated by an increase in the basin area ratio from 1.1 to 1.2 and from 1.2 to 1.3 for the two load levels studied, respectively. The reason behind this further decrease in stiffness can be attributed to the existence of the transverse crack noted earlier.
- (iv) It was also noticed that the level of the applied load, e.g. 40 kN or 53 kN, affects the magnitude of the seasonal variations. Such an effect has a similar order of magnitude to that occurring between years (e.g. between 1991 and 1992 - see finding (iii) above).

Subgrade Strength Index (SSI)

Another measure that was used for characterizing the subgrade seasonal behaviour was the subgrade stiffness index, SSI. The variations in SSI with time are shown in Figures 7.10 to 7.13. Figures 7.10 and 7.11 display these variations for load level 40 kN based on fourth sensor and seventh sensor deflections, respectively, whereas Figures 7.12 and 7.13 show these variations for load level 53 kN. From these figures, it is evident that the same observations noted before for the basin area ratio are also applicable here, namely:

- (i) A large reduction in subgrade stiffness occurs upon thawing. This is indicated by a change in subgrade stiffness index ratio from 0.2 during the period of frozen subgrade to 1.1 under thawed conditions.
- (ii) After the rapid change observed in subgrade stiffness, a second period of more or less constant stiffness prevails. This is characterized by a constant SSI ratio of 1.1 persisting for about three months. After that a gradual recovery in stiffness took place until the subgrade finally converged to its normal value, i.e. an SSI of 1.0.

Moreover, it appears that both the fourth sensor and seventh sensor deflections provide comparable results. This can be seen by comparing Figures 7.10 and 7.11, and Figures 7.12 and 7.13. This finding indicates that any of these sensor deflections can be used interchangeably to obtain the required SSI parameter.

Central Deflections

Central deflections have long been used by many researchers to characterize pavement seasonal variations. Traditionally, this took the form of comparing Benkleman Beam spring rebound values, defined as the sum of the average deflection plus two standard deviations, with average fall rebound values obtained during the 60-day period prior to the inception of freezing (Shields and Dacyszyn, 1965; and Christison and Leung, 1988). In keeping with these efforts that extended over a period of more than 20 years of pavement research in Alberta, it was decided to include this parameter, i.e. central deflection, within the current study. It should be emphasized, however, that central deflections referred to in the present investigation are those induced by the FWD dynamic load and are measured at the centre of the loading plate while those studied by earlier researchers refer to static deflections measured by the Benkleman Beam device under an 80 kN (i.e. 18-kips) single axle load.

When centre deflections are used, it is recommended (Bush, 1987; and Christison and Leung, 1988) that temperature adjustments be made to measured deflections to account for the deflection of the asphalt concrete surface layer at high temperatures (typically summer conditions). In the present analysis, temperature adjustment factors were derived for both the fill and cut areas within the tested pavement section. The procedure suggested by Christison and Leung (1988) for obtaining these factors was successfully employed in the current investigation. Four temperature adjustment equations resulted from this. These relations can be listed as follows:

(i) ***Fill - outer wheel path area, (F-OWP),***

$$\text{Log D1} = \text{Log D2} - 0.00836 (T2 - T1) \quad (7.1)$$

$$\text{with, } n = 16 \quad R^2 = 0.94 \quad \text{S.E (Log D1)} = 0.0213$$

(ii) ***Cut - outer wheel path area, (C-OWP),***

$$\text{Log D1} = \text{Log D2} - 0.00803 (T2 - T1) \quad (7.2)$$

$$\text{with, } n = 16 \quad R^2 = 0.92 \quad \text{S.E (Log D1)} = 0.0192$$

(iii) ***Fill - centre line of inner lane, (F - IC),***

$$\text{Log D1} = \text{Log D2} - 0.0111 (T2 - T1) \quad (7.3)$$

$$\text{with, } n = 16 \quad R^2 = 0.97 \quad \text{S.E (Log D1)} = 0.0217$$

(iv) ***Cut - centre line of inner lane, (C - IC),***

$$\text{Log D1} = \text{Log D2} - 0.0130 (T2 - T1) \quad (7.4)$$

$$\text{with, } n = 16 \quad R^2 = 0.94 \quad \text{S.E (Log D1)} = 0.0264$$

where,

D1 = central deflection measured at reference temperature T1,

D2 = central deflection measured at temperature T2,

T1 = reference temperature taken as 21°C.

n = number of data sets used to generate the regression equations.

R^2 = coefficient of determination of model(s).

S.E (Log D1) = standard deviation of Log D1 about the regression line.

Equations 7.1 to 7.4 are displayed graphically in Figure 7.14. It was felt that by segregating the central deflection data in the fashion described above, any differences in behaviour of this data with respect to temperature influences will be discernible. This strategy proved successful. From Figure 7.14, it is clear that although the analysis was performed on FWD central deflections collected from a short pavement stretch of only one kilometre long, substantially different temperature corrections should be applied to centre deflections based on where those deflections are measured (i.e. whether in a fill or a cut area or whether within the outer or inner lane). Further examination of the four temperature adjustment curves reveals that the difference between the F-OWP and the C-OWP data is small and for all practical purposes it can be neglected. On the other hand, differences between the F-IC and the C-IC data and also between the outer wheel path area of outer lane data and centre line of inner lane data are significant and can not be ignored. It follows that only F-OWP and C-OWP data can be combined together to obtain one global equation for this set of data. This reduces the number of the temperature adjustment equations to three instead of four. The new equations are as follows:

(i) ***Combined F-OWP and C-OWP data,***

$$\text{Log D1} = \text{Log D2} - 0.00806 (T_2 - T_1) \quad (7.5)$$

$$\text{with, } n = 32 \quad R^2 = 0.93 \quad \text{S.E (Log D1)} = 0.0197$$

(ii) ***Fill - centre line of inner lane, (F - IC), (same equation as 7.3 above)***

$$\text{Log D1} = \text{Log D2} - 0.0111 (T_2 - T_1) \quad (7.3)$$

$$\text{with, } n = 16 \quad R^2 = 0.97 \quad \text{S.E (Log D1)} = 0.0217$$

(iii) ***Cut - centre line of inner lane, (C - IC), (same equation as 7.4 above)***

$$\text{Log D1} = \text{Log D2} - 0.0130 (T_2 - T_1) \quad (7.4)$$

$$\text{with, } n = 16 \quad R^2 = 0.94 \quad \text{S.E (Log D1)} = 0.0264$$

Further aggregation of the data to obtain one universal equation to represent all the collected central deflections proved to be inadequate. This conclusion was arrived at upon examining the regression model developed for all central deflection data which showed that the three sets of data, i.e. all OWP, F-IC and C-IC, represent different statistical populations. The previous discussion serves to illustrate the point that the use of centre deflections in characterizing pavement stiffness must be accompanied by careful evaluation of the appropriate temperature adjustment factors.

The results pertaining to the analysis of central deflections are portrayed in Figures 7.15 through 7.17. Upon examining Figures 7.15 and 7.16, the importance of applying temperature corrections to measured deflections becomes evident. Without temperature adjustments, seasonal variations in subgrade stiffness become obscured and no specific pattern is discernible.

Figure 7.17 shows the variations in the corrected central deflection ratio with the season. This ratio is obtained in a manner similar to that of the rebound deflection ratio used previously with Benkleman Beam data (Shields and Dacyszyn, 1965). From Figure 7.17, the following observations are noted:

- (i) A substantial decrease in subgrade stiffness occurred as this layer started thawing. This is demonstrated by a change in the corrected central deflection ratio from 0.3 at the frozen state to more than 1.3 at the thaw-weakened state.
- (ii) After the subgrade reached a minimum stiffness around April 25, 1991, a remarkable recovery took place within a relatively short time, less than two weeks, and the new subgrade stiffness approached very rapidly the normalized fall value of 1.0.

- (iii) Seasonal variations in structural stiffness observed during the 1992 year appear strange and can not be explained.

From the aforementioned discussion, it is clear that all the observations noted before for the basin area ratio and *SSI* apply equally well to the corrected central deflection ratio. However, a distinct peak in the corrected central deflection ratio, marking a unique low stiffness, is quite evident compared to other deflection parameters. This leads to the conclusion that seasonal variations as measured by the central deflection parameter might represent changes in pavement stiffness that are not totally comparable to those measured by other deflection parameters such as the basin area ratio and/or the subgrade stiffness index. While the basin area ratio and the *SSI* parameter describe conditions pertaining to the subgrade layer, corrected central deflection ratio provides stiffness assessment of the overall pavement structure.

Impulse Stiffness Modulus (ISM)

The *ISM* is another alternative of using central deflections for pavement structural evaluation. This alternative was employed in the current analysis and the results are displayed in Figure 7.18. From this figure, it can be concluded that the role of the *ISM* parameter in detecting seasonal variations in subgrade soils may be limited. Again, this can be attributed to the fact that *ISM*, like central deflections, also requires the application of temperature corrections. Moreover, seasonal variations in stiffness as measured by this parameter reflect conditions concerning the overall pavement structure and not the subgrade foundation layer alone.

7.5.3.2 Modulus Back-calculation Analysis

Back-calculation analysis is another attractive alternative for evaluating pavement stiffness. The technique involves computing pavement layer moduli using measured deflection basins. Essentially, this consists of finding a set of layer moduli that would,

theoretically, produce a deflection basin that matches the measured deflection basin to within a specified tolerance. Although the moduli obtained cannot be said to be truly the actual moduli of the pavement materials, they can still be used to adequately model the behaviour of the pavement under actual traffic loads. Such moduli are in essence "effective" and not "real" material properties. Extra details pertaining to how these moduli can actually be obtained using any of the currently available back-calculation procedures, can be found in chapter two of this thesis.

The use of back-calculation techniques is more promising than mere "deflection interpretation" analysis in that they:

- (1) link the measured pavement response, i.e. deflections, to the in situ properties of the component materials in a more rational fashion, and
- (2) provide directly the inputs needed for the application of mechanistic-empirical procedures for pavement design and/or rehabilitation.

From among the many available computer programs that can be used for performing the modulus back-calculation analysis, MODULUS (Uzan et al., 1988) was the program of choice selected for the current study. This program has several features and advantages that favors its use over other programs. Most notable among these are its speed, availability and the consistency of obtained results. A full list of all the other advantages was given by Lytton (1989).

It should be mentioned that in obtaining the back-calculated layer moduli, only the deflections measured at the 40 kN load level were used in the analysis. No attempts were made to analyze the deflection basins measured at other load levels. Moreover, the layer thicknesses used in the back-calculation analysis were obtained from the AT&U construction records. In other words, no attempts were made to obtain the actual layer

thicknesses at the time when the FWD tests were performed. Although this consideration constitutes a major uncertainty in the part dealing with the precision of back-calculated ACP and GB moduli, it is believed to have minimal, or no, effect on the estimated SG moduli.

Using the MODULUS Program, effective moduli were computed for the asphalt concrete (ACP) layer, the granular base (GB) layer and the subgrade (SG) layer. This was done for two sets of deflection data that were collected at different times during the day for each test date. The first data set was usually collected between 10:00 AM and 12:00 PM, while the second data set was collected between 12:00 PM and 2:00 PM. Results from these analyses are displayed graphically in Figures 7.19 through 7.30. Figures 7.19 to 7.24 deal with the first set of data, while Figures 7.25 to 7.30 portray the results of the second set.

Based on the first set of data, i.e. Figures 7.19 to 7.24, the following observations can be made:

- (1) Variations in ACP moduli throughout the seasons do not follow any recognizable pattern. This can be attributed to the fact that the deflections used in the back-calculation analysis were not adjusted for temperature effect. As a result, the ACP moduli displayed in Figures 7.19 and 7.20 do not represent the actual effective moduli for this layer. Since the emphasis in this research is on the seasonal variations pertaining to the subgrade layer, no further attempts were made to correct the initially obtained ACP layer moduli.
- (2) The modulus of the granular base material seems to drop significantly and within a short period of time, approximately two weeks, from about 900 MPa to less than 140 MPa in the OWP area, and from about 1400 MPa to less than 140 MPa in the

IC area. This event occurred in both fill and cut areas of the instrumented section during the first year. The observed phenomenon is linked with the thawing of the GB layer after the first winter season. During the second year, however, it appears that deflection testing commenced after the GB layer had completely thawed. This is characterized by the disappearance of the sudden drop in stiffness observed previously during the first year.

- (3) There seems to be very little change in GB stiffness, as measured by the modulus value, during spring and summer months (beginning of April to early October). The value of the GB modulus for this period ranged from 105 MPa to 170 MPa for the fill area, and from 60 MPa to 115 MPa for the cut area.
- (4) In the case of the subgrade layer, i.e. SG, the following several conclusions can be drawn:
 - (i) Like the granular base material, the subgrade also experiences significant reduction in stiffness as the process of thaw commences. This is characterized by a change in SG modulus from about 800 MPa to less than 150 MPa in fill areas, and from about 800 MPa to less than 100 MPa in cut areas. Furthermore, in the case of the subgrade layer, the change was observed to take place over a longer period of time of approximately one to one and a half months (from March 20, 91 to April 30, 91 as shown in Figures 7.23 and 7.24).
 - (ii) The sharp reduction observed in the subgrade modulus reached a minimum of 140 MPa for the fill section and a minimum of 85 MPa of the cut section around May 7th for both the 1991 and 1992 years. After that, the modulus remained almost constant, for both fill and cut areas, within ± 10 MPa of the minima reached. This continued for a period of approximately three months (early May to early August) after which a gradual recovery in modulus value was observed to occur. The magnitude of this recovery was small in the case of the fill section

(about 20 MPa or 14% increase in M_r) and relatively large in the case of the cut section (about 25 MPa or 29% increase in M_r).

- (iii) From the previous observations, it is clear that the modulus value for the fill area is significantly greater than that for the cut area. The difference is in the order of about 55 MPa or 65% of the modulus of the weaker section (i.e. the cut area). This finding clearly indicates that the subgrade material contained within the fill section is of a superior quality to that contained within the cut section. Such superiority is attributed to the fact that subgrade materials in fill areas are usually placed in greater thicknesses of well compacted layers as compared to their counterparts in cut areas. As a result, the overall stiffness of the subgrade layer in fill sections increases significantly.
- (iv) It is also observed that moduli obtained at the instrumented site location are closer to fill moduli than cut moduli. This is expected since the instrumented site lies within the fill area. However, exact agreement between fill and instrumented site moduli could not be achieved because of two reasons: first, the transverse crack that was observed to develop, after the first winter season, in the vicinity of the instrumented section seems to affect the deflections measured at that location. This in turn affected the back-calculated moduli. Second, the procedure followed in obtaining representative moduli values for the fill area involved a great deal of data aggregation and reduction and as a consequence of that differences between fill and instrumented site moduli may have been magnified. Nevertheless, the close agreement observed between the modulus values obtained for the fill area and their corresponding counterparts at the instrumented site location suggests that either of these moduli can be used interchangeably to represent the other.

- (v) From Figures 7.23 and 7.24, it can be seen that representative moduli values obtained at either the outer wheel path area (OWP) or the centre line of the inner lane area (IC) are comparable and show more or less the same trend.
- (vi) Lastly, seasonal variations observed in the subgrade stiffness, as characterized by back-calculated moduli, appears to be identical for both the 1991 and the 1992 seasons.

Upon comparing the two sets of data analyzed, i.e. Figures 7.19 to 7.24 with Figures 7.25 to 7.30, the same conclusions arrived at for the 10:00 AM data set apply equally well to the 12:00 PM data set. The only difference between the two sets of results, however, is the observed reduction in the ACP layer moduli for the 12:00 PM set. This can be attributed to the fact that measured deflections used in the computation of ACP moduli for the 12:00 PM set, tend to be larger in magnitude, due to warmer temperatures prevailing during mid-day, than those obtained in the early morning period. This effect could have been corrected for by adjusting measured deflection data for temperature effects before carrying on with the back-calculation of the layer moduli. However, since the emphasis in the current research is on evaluating seasonal variations within the subgrade layer only, no further attempts were made to carry on with the aforementioned adjustments. In conclusion, it appears that deflections measured during any time of the day can safely be used for back-calculating granular base and cohesive subgrade soil moduli without any serious loss in accuracy of the obtained values. In other words, this means that temperature does not affect granular base and/or subgrade moduli in any significant way.

7.5.3.3 Correlating Temperature and Suction Data with Back-Calculated Moduli

Another method that was attempted to quantify seasonal variations in subgrade stiffness involved correlating the back-calculated layer moduli with other measured

responses of temperature, suction and computed in situ stresses. This is accomplished using multiple linear regression techniques in a fashion similar to that employed for laboratory resilient modulus data presented in chapter six.

Prior to the development of the aforementioned empirical models, stresses at various locations within the subgrade layer were computed using a computer program called KENLAYER. This Program, which was developed by Huang (1993), models flexible pavements as systems of multi-linear elastic layers. The program uses various structural, geometric and traffic inputs to compute mechanistic responses of stresses, strains and deflections at various locations within the pavement structure. Inputs used to compute the stresses in the current analysis were back-calculated moduli obtained from FWD deflection tests performed at the times shown in Table 7.1. Other inputs were Poissons' ratios assumed equal to 0.35, 0.35, and 0.40 for the ACP, the GB, and the SG layers, respectively. As built layer thicknesses of 130mm, 51mm, and 456mm for the respective ACP, OB, and GB layers were also used. Further details pertaining to the description of the KENLAYER Program and its operation can be found elsewhere (Huang, 1993). The reason for using this Program in the current study stems from the fact that traffic-induced stress data is needed in the following analysis. Ideally, such data should have been obtained through direct in situ measurements utilizing pressure gauges. At the time when soil suctions sensors were installed, the option of including pressure gauge devices was not considered due to financial and time constraints associated with the research study.

Using computed stresses obtained at various suction sensor locations and measured temperature and matric suction data, various models were developed that linked these responses to back-calculated subgrade moduli. It should be mentioned that only the sensors installed within the outer lane were considered in this analysis. Other sensors

installed in the shoulder area were excluded from the analysis since no FWD tests were performed at those locations.

The following are the models arrived at using regression analysis:

$$(1) \quad M_r = 144,867 + 24,780 (J_2/T_{oct.}) + 2,046 T \quad (7.6)$$

$$(n=31, R^2=0.77, S.E.(M_r)=7,703)$$

$$(2) \quad M_r = 224,714 + 18,709 (J_2/T_{oct.}) \quad (7.7)$$

$$(n=22, R^2=0.74, S.E.(M_r)=3,807)$$

$$(3) \quad M_r = 236,243 + 49,732 (J_2/T_{oct.}) + 1,383 T \quad (7.8)$$

$$(n=21, R^2=0.83, S.E.(M_r)=9,131)$$

$$(4) \quad M_r = 255,671 + 107,395 (J_2/T_{oct.}) - 294 \psi_m \quad (7.9)$$

$$(n=21, R^2=0.84, S.E.(M_r)=6,275)$$

$$(5) \quad M_r = 213,429 + 39,188 (J_2/T_{oct.}) \quad (7.10)$$

$$(n=18, R^2=0.82, S.E.(M_r)=32,603)$$

$$(6) \quad M_r = 61,292 + 61,186 (J_2/T_{oct.}) + 29,455 (\sigma_d) \quad (7.11)$$

$$(n=15, R^2=0.99, S.E.(M_r)=4,347)$$

where, M_r = back-calculated subgrade modulus, in MPa
 $J_2/T_{oct.}$ = ratio of second stress invariant to octahedral shear stress
 T = subgrade temperature, in °C
 ψ_m = soil matric suction, in MPa
 σ_d = deviator stress, in MPa

The first four equations are the relations obtained for the individual sensors 4,9, 11 and 6 located at 0.14m, 0.32m, 0.84m and 1.00m below the top of the subgrade, respectively. As it can be seen, the relations developed for deeper sensors, i.e. 11 and 6 or equations 7.8 and 7.9, have higher R^2 value compared to those obtained for sensors at shallow depths. This implies that the “effective” back-calculated moduli represent best the structural conditions at greater depths within the subgrade than those at shallower depths. Upon examining the first four equations further, it is also apparent that both traffic

induced stresses, represented by (J_s/T_{α}) parameter, and environmental induced stresses, T and ψ_m , influence back-calculated moduli with the effect of the former, i.e. traffic induced stresses, being more significant. This is contrary to findings from the laboratory phase and it is believed to have been brought about by the fact that the ranges of ψ_m measured in situ are much smaller than their counterparts in the laboratory testing phase.

Combining the data pertaining to shallow-depth sensors together and those pertaining to deeper sensors together, and performing the regression analysis again produced the relations given above by equations 7.10 and 7.11. Equation 7.10 represents combined data of sensors 4 and 9 (i.e. depth horizon 0.14 - 0.32 m below top of subgrade), whereas equation 7.11 represents the results of deeper sensors (i.e. sensor 11 and 6 at depth horizon 0.84 - 1.00 m below top of subgrade). From both equations 7.10 and 7.11, it is again apparent that back-calculated moduli represent better the structural conditions prevailing at greater depths within the subgrade than those existing at shallow depths (R^2 of 0.99 and S.E. (M_r) of 4,347 compared to R^2 of 0.82 and S.E. (M_r) of 32,603, respectively).

From the previous discussion, it is again confirmed that back-calculated moduli are function of both traffic induced stresses and environmental factors. However, the form of the model obtained during the field investigation phase is arithmetic as compared to the natural log model obtained during the laboratory investigation phase. The main reason behind this is believed to be attributed to the substantially different ranges of traffic induced and environmental stresses investigated within each phase of the current research.

7.6 Summary and Conclusions

This chapter included a presentation and discussion of the research findings obtained from the field testing phase. The purpose of the field testing program was to

investigate the phenomenon of seasonal variations in subgrade stiffness under prevailing in situ conditions. To this end, a pavement section within a primary highway, HWY 16, in Alberta was selected and instrumented with thermal conductivity sensors to measure temperature and soil suction data at various locations within the subgrade layer. This data coupled with FWD deflection measurements performed at regular time intervals throughout the course of the seasons were used to achieve the research goals.

The present chapter is divided into two main sections. The first section deals with the presentation and analysis of the temperature and soil suction data collected from the instrumented section during the two-year monitoring period. The analysis took the form of plotting this data versus time to identify the seasonal distributional trends of these climatic factors at various depth locations within the subgrade soil layer.

Presentation, analysis and interpretation of the FWD deflection data comprise the second section of this chapter. Two methods of analysis were employed. The first method involves direct interpretation of deflection data while the second method utilizes measured deflections to back-calculate basic material properties that can subsequently be used as stiffness indicators. The former technique is simple and provides an acceptable general picture of the overall seasonal variations within the pavement structure. However, it is the latter technique that provides more quantitative evaluation of what is happening in subgrade stiffness from season to season. Furthermore, results obtained using the back-calculation approach are readily applicable to currently available mechanistic-empirical pavement design procedures.

The following are the main research findings obtained from the field investigation phase:

- (1) A system for monitoring temperature and soil matric suction distributions within cohesive fine-grained subgrade soils was developed. The developmental stages of this system consisted of three tasks. First, evaluating the applicability of a commercially available thermal conductivity sensor, i.e. the AGWA-II model, for the purposes of monitoring both temperature and soil matric suction seasonal trends within cohesive fine-grained subgrade soils under actual field conditions. Second, developing an automated data acquisition system for monitoring and collecting the required field data. Third, developing a procedure, or a set of procedures, for analyzing and interpreting the collected temperature and soil matric suction data based on current state-of-the-knowledge concerning the mechanical behaviour of unsaturated cohesive subgrade soils. The developed system was tested, under actual field conditions, and proved satisfactory for the purposes of flexible pavement design and rehabilitation.
- (2) Two problems were encountered during the monitoring of temperature and matric suction measurements. One problem is connected to the placement of the data acquisition equipment box while the other problem has to do with the fragility of the installed sensors. During the time of installation, it was conceived that placing the data acquisition assembly in a water-tight box and then burying that box in the back slope of the instrumented section was the best alternative to avoid vandalism. However, this option proved to be a wrong choice since after the first winter season, drainage water from the thawed subgrade started ingressing inside the data acquisition box, which was not sealed properly, and caused a major breakdown of the monitoring system. The problem was detected and remedied by replacing the defective data acquisition system with a new one. However, while doing this, another alternative was selected for situating the data acquisition box. This consisted of clamping the box to a steel post and left hanging in the air an adequate

distance away from the reach of any drainage water. This choice was successful and no further monitoring problems were detected.

- (3) It was noticed that some of the AGWA-II sensors ceased to function properly immediately after installation while others failed after a period of about one year. Of the twelve sensors installed, five failed. This corresponds to a mortality rate of about 42%. Upon investigating the reason(s) behind this relatively high rate of failure, it became apparent that the AGWA-II sensors are quite fragile in nature and as such they require extremely careful handling during both calibration and installation processes. This feature confines the use of the AGWA-II sensors to research purposes only until a more sturdy construction of these sensors become available to facilitate their use for routine monitoring of soil matric suction under actual field conditions.
- (4) The AGWA-II thermal conductivity sensors used in this study provide consistent monitoring of matric suction under both freezing and non-freezing conditions. However, interpretation of suction results during the frozen period is difficult due to the significant role played by the latent heat of fusion of the soil water in affecting thermal conductivity measurements. Nevertheless, the extensive discussion presented in Chapter Seven and in Appendix C, pertaining to the behaviour of the aforementioned sensors during the frozen period, proved useful in assuring that the sensors continued functioning after the first winter season. This confirms and substantiates research findings obtained by other investigators (Fredlund et al., 1991) concerning the applicability of the AGWA-II sensors for long term monitoring of matric suction under both frozen and non frozen conditions.
- (5) Typical values of matric suction obtained during the thaw-weakening and summer periods ranged from 10 to 80 kPa for sensors installed near the top of the

subgrade, and from 10 to 40 kPa for sensors installed at deeper locations. This indicates that there are no significant seasonal changes in the soil suction parameter for the particular case study pursued in the present research.

- (6) Two different strategies for analyzing and interpreting the FWD deflection data were established. The first methodology involved identifying seasonal changes in subgrade stiffness via graphical analysis of a number of deflection parameters while the second methodology involved back-calculating fundamental material properties, namely the resilient modulus, to be used as potential stiffness indicators.
- (7) Four deflection parameters, namely, the basin area ratio (*ba*), the subgrade stiffness index based on fourth and seventh sensors deflections (*SSID4* & *SSID7*), the impulse stiffness modulus (*ISM*) and the corrected central deflection ratio, were chosen to investigate seasonal variations in subgrade stiffness. All studied parameters, with the exception of the corrected central deflection ratio and the *ISM*, seem adequate for describing seasonal changes in subgrade stiffness. On the other hand, seasonal variations as measured by the central deflection parameter and the *ISM* appear to provide an assessment of changes occurring within the overall pavement structure rather than within the subgrade layer. This leads to the conclusion that central deflection is not a good parameter to use for assessing seasonal changes occurring within the subgrade soil layer. However, it is the other parameters, i.e. *ba*, *SSID4* & *SSID7*, that are useful for accomplishing such an objective.
- (8) Conclusive evidence from deflection data analyses indicate that significant reduction in subgrade stiffness occurs as this layer starts thawing. After this initial reduction, a long period of unchanged subgrade stiffness of about three months prevails. This is then followed by a gradual increase in subgrade stiffness. In

terms of back-calculated moduli, the thawed subgrade modulus within the fill section was found to equal 85% of the fall fill section modulus whereas for the cut section it was about 71% of the fall cut section modulus. This indicates that the moduli in cut section experience larger seasonal fluctuations than their counterpart fill moduli.

- (9) Subgrade back-calculated fill moduli were found to be 65% greater than their counterparts in cut area. This is expected, although not in the deterministic sense, and it is indicative of the superiority of the cohesive material in fill area compared to that used in cut area. Such superiority is attributed mainly to the fact that subgrade materials in fill sections are usually placed in greater thicknesses of well compacted layers as compared to their counterparts in cut sections. The result of this will be an overall increase in the subgrade stiffness within the fill area.
- (10) Careful examination of field subgrade moduli computed from two different deflection data sets that were collected at different times during the day reveals that seasonal variations, as characterized by changes in subgrade stiffness, are insensitive to temperature influences. This means that deflections used in the back-calculation procedure need not be adjusted for temperature effects.
- (11) Attempts to empirically correlate back-calculated moduli with measured responses of temperature, soil suction and computed in situ stresses did not produce satisfactory results. Reasons behind this may be: (a) insufficient amount of data needed for the analysis; (b) narrow ranges of values of some of the parameters used in the analysis, e.g. soil suction; (c) use of a layered elastic model for stress and moduli computations that assumes a constant modulus value for the full extent of each layer rather than varying the modulus from point to point within the layer.

References

1. AASHTO (1986), "*AASHTO Guide for Design of Pavement Structures*," American Association of State Highway and Transportation Officials.
2. AASHTO (1993), "*AASHTO Guide for Design of Pavement Structures*," American Association of State Highway and Transportation Officials.
3. Briggs, R. C. and S. Nazarian (1989), "*Effects of Unknown Rigid Subgrade Layers on Back-calculation of Pavement Moduli and Predictions of Pavement Performance*," Transportation Research Record 1227, Washington, D.C., pp. 183-193.
4. Bush, A. J. III (1987), "*Development of a Pavement Evaluation Method for Low Volume Airfield Pavements*," Ph.D. dissertation, University of Illinois, Urbana-Champaign.
5. Christison, J. T. and P. S. Leung (1988), "*Temperature Adjustment Factors for Benkelman Beam Rebound Deflections and Seasonal Variations in Pavement Strength*," Internal Report No. HTE 88/07.
6. Chang, D., J. M. Roesset and K. H. Stokoe II (1992), "*Nonlinear Effects in Falling Weight Deflectometer Tests*," Transportation Research Record 1355, Washington, D.C., pp. 1-7.
7. Dynatest, (1991), "*Dynatest 8000 FWD Test System Owners Manual: Part 1 and 2*."
8. Fredlund, D. G., J. K. Gan and H. Rahardjo (1991), "*Measuring Negative Pore Water Pressures in a Freezing Environment*," Transportation Research Record 1307, Washington, D.C., pp. 291-299.
9. _____ (1992), "*Falling Weight Deflectometer (FWD) Field Operation Manual: Version 2.1*," Internal Specifications, Pavement Evaluation Unit, Alberta Transportation and Utilities, Alberta, Canada.
10. Huang, Y. H. (1993), "*Pavement Analysis and Design*," Prentice-Hall, Inc.
11. Janoo, V. C and R. L. Berg (1990), "*Thaw Weakening of Pavement Structures in Seasonal Frost Areas*," Transportation Research Record 1286, Washington, D.C., pp. 217-233.
12. Lytton, R. L. (1989), "*Back-calculation of Pavement Layer Properties*," Nondestructive Testing of Pavements and Back-calculation of Moduli, ASTM STP 1026, A. J. Bush III and Y. G. Baladi, Eds., American Society for Testing and Materials, Philadelphia, pp. 7-38.

13. Mahoney, J. P., B. C. Winters, N. C. Jackson and L. M. Pierce (1993), "*Some Observations About Back-calculation and Use of a Stiff Layer Condition*," Transportation Research Record 1384, Washington, D.C., pp. 8-14.
14. Plewes, S. L. and K. A. Millions (1985), "*Possible Failure Mode for Problem Full-Depth Pavements*," Canadian Technical Asphalt Association Proceedings, Montreal, Quebec, Canada, pp. 232-259.
15. Rwebangira, T., R. G. Hicks and M. Truebe (1987), "*Sensitivity Analysis of Selected Back-calculation Procedures*," Transportation Research Record 1117, Washington, D.C., pp. 25-37.
16. Sattler, P. and D. G. Fredlund (1989), "*Use of Thermal Conductivity Sensors to Measure Matrix Suction in the Laboratory*," Canadian Geotechnical Journal, Vol 26, No. 3, pp. 491-498.
17. Shields, B. P. and J. M. Dacyszyn (1965), "*Seasonal Variations in Flexible Pavement Strength*," Proceedings of the 1965 Convention of the Canadian Good Roads Association, pp. 394-409.
18. Stolle, D. F. and D. Hein (1989), "*Parameter Estimates of Pavement Structure Layers and Uniqueness of the Solution*," Nondestructive Testing of Pavements and Back-calculation of Moduli, ASTM STP 1026, A. J. Bush III and Y. G. Baladi, Eds., American Society for Testing and Materials, Philadelphia, pp. 313-322.
19. Stolle, D. F. and F. W. Jung (1992), "*Simplified, Rational Approach to Falling Weight Deflectometer Data Interpretation*," Transportation Research Record 1355, Washington, D.C., pp. 82-89.
20. Uddin, W., A. H. Meyer, W. R. Hudson and K. H. Stokoe II (1985), "*Project-Level Structural Evaluation of Pavements Based on Dynamic Deflections*," Transportation Research Record 1007, Washington, D.C., pp. 37-45.
21. Uddin, W., A. H. Meyer and W. R. Hudson (1986), "*Rigid Bottom Considerations for Nondestructive Evaluation of Pavements*," Transportation Research Record 1070, Washington, D.C., pp. 21-29.
22. Ullidtz, P. and R. N. Stubstad (1985), "*Analytical-Empirical Pavement Evaluation Using the Falling Weight Deflectometer*," Transportation Research Record 1022, Washington, D.C., pp. 36-44.
23. Ullidtz, P. (1987), "*Pavement Analysis*," Elsevier Publication, Amsterdam.
24. Uzan, J., R. L. Lytton and E. P. Germann (1988), "*General Procedure for Back-calculating Layer Moduli*," First International Symposium on Nondestructive

Testing of Pavements and Back-calculation of Moduli, American Society for Testing Materials, Baltimore, MD.

25. Williams, P. J. (1964a), "*Specific Heat and Apparent Specific Heat of Frozen Soils*," Geotechnique, Vol. 14, No. 2, pp. 133-142.
26. Williams, P. J. (1964b), "*Unfrozen Water Content of Frozen Soils and Soil Moisture Suction*," Geotechnique, Vol. 14, No. 3, pp. 231-246.
27. Wong, D. K. H. and A. Ho (1987), "*An Evaluation of a Thermal Conductivity Sensor for the Measurement of Soil Matric Suction*," Test-Track Program and Lime-Modified Clay Research Program, Saskatchewan Highways and Transportation, Internal Report Prepared by the Geotechnical Group of the Department of Civil Engineering, University of Saskatchewan.

Table 7.1: Dates of FWD Deflection Tests Performed on Highway 16**1991 Season****1992 Season**

Calendar Date	File ID	Calendar Date	File ID
March, 20, 1991	H1612m4 fwd	March, 27, 1991	H1612m1 f20
March, 27, 1991	H1612m5 fwd	April, 03, 1991	H1612m2 f20
April, 03, 1991	H1612m6 fwd	April, 15, 1991	H1612m3 f20
April, 10, 1991	H1612m7 fwd	April, 22, 1991	H1612m4 f20
April, 18, 1991	H1612m8 fwd	April, 29, 1991	H1612m5 f20
April, 26, 1991	H1612m9 fwd	May, 13, 1991	H1612m6 f20
May, 02, 1991	H1612m10 fwd	May, 27, 1991	H1612m7 f20
May, 08, 1991	H1612m11 fwd	May, 29, 1991	H1612m8 f20
May, 22, 1991	H1612m12 fwd	June, 12, 1991	H1612m9 f20
May, 31, 1991	H1612m13 fwd	June, 24, 1991	H1612m10 f20
June, 11, 1991	H1612m14 fwd	July, 16, 1991	H1612m11 f20
June, 26, 1991	H1612m15 fwd	August, 05, 1991	H1612m12 f20
July, 10, 1991	H1612m16 fwd	August, 27, 1991	H1612m13 f20
July, 31, 1991	H1612m17 fwd	September, 17, 1991	H1612m14 f20
August, 22, 1991	H1612m18 fwd	October, 15, 1991	H1612m15 f20
September, 12, 1991	H1612m19 fwd	October, 27, 1991	H1612m16 f20
October, 09, 1991	H1612m20 fwd		

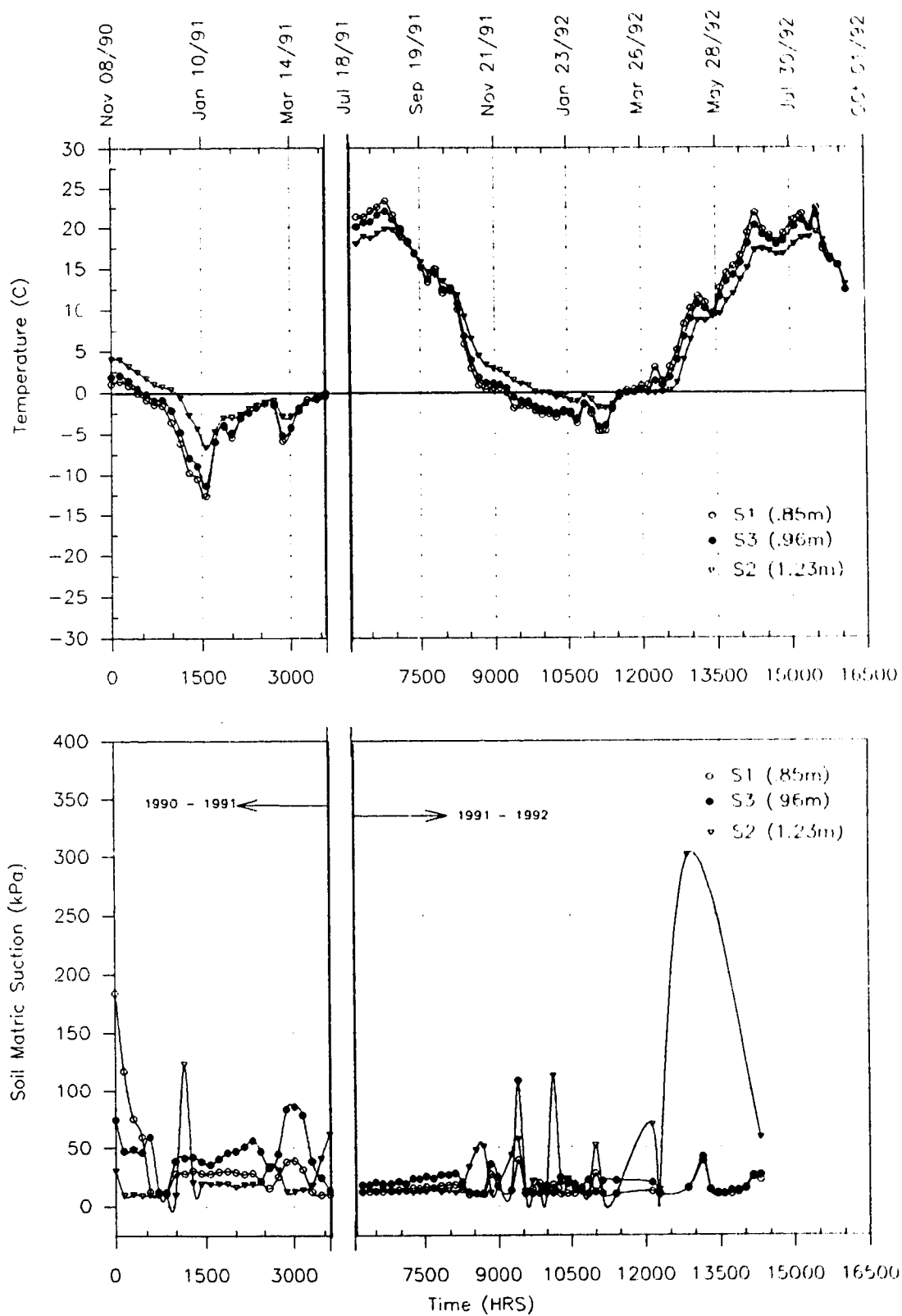


Figure 7.1: Seasonal Variation in Temperature and Soil Matrix Suction for Sensors 1, 2, 3 (SHOULDER Area)

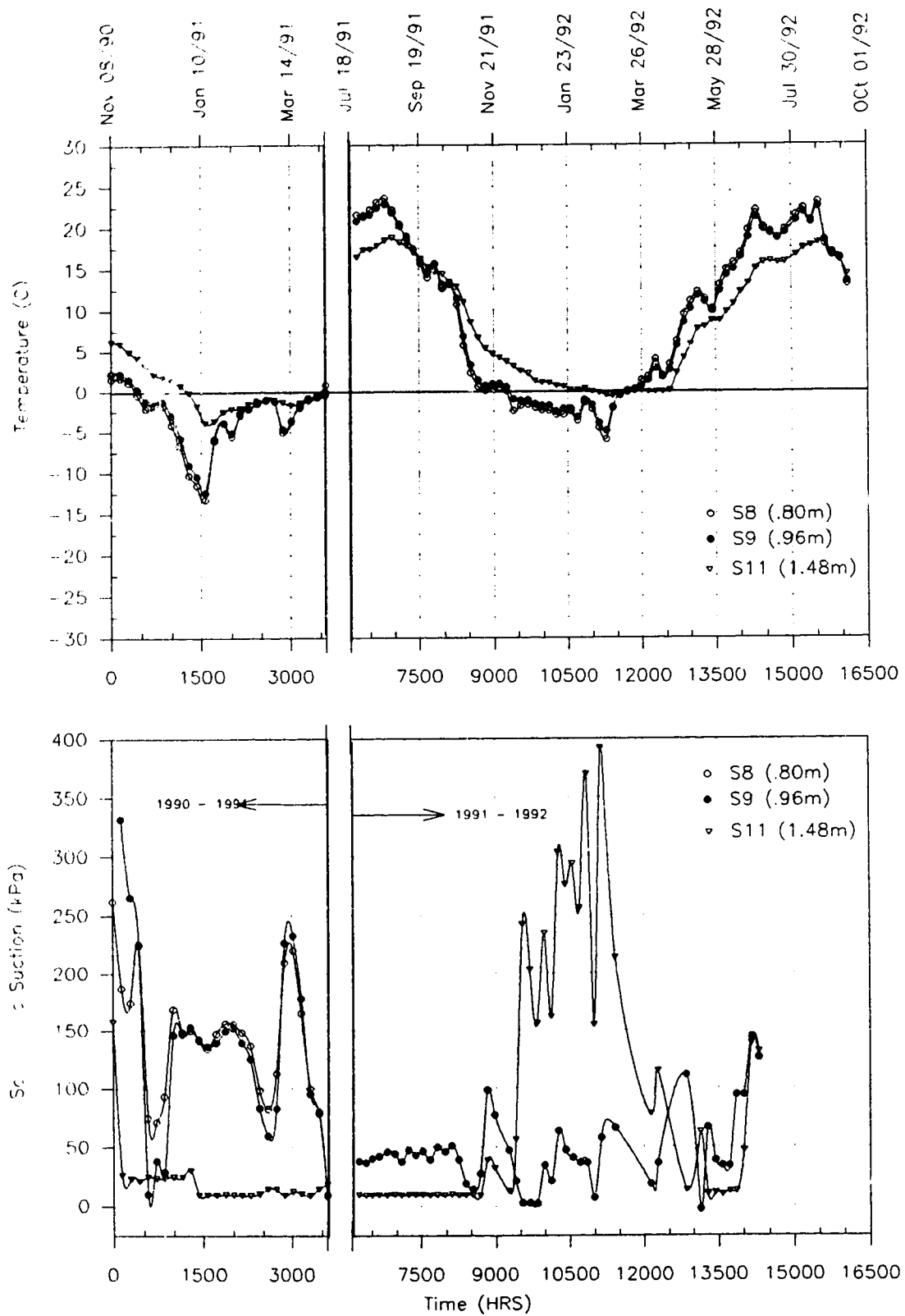


Figure 7.2: Seasonal Variation in Temperature and Soil Matric Suction for Sensors 8, 9, 11 (OWP Area)

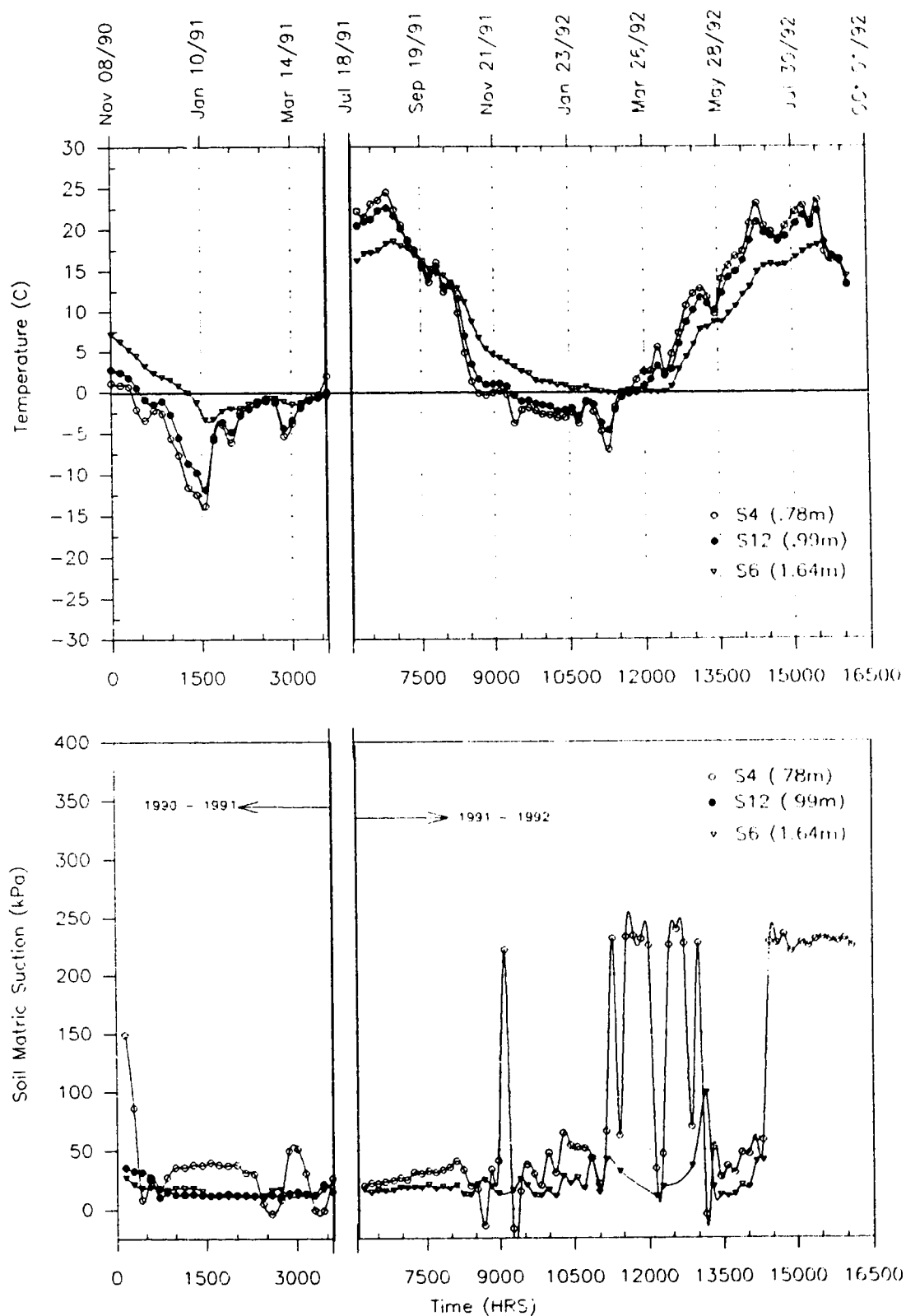


Figure 7.3: Seasonal Variation in Temperature and Soil Matrix Suction for Sensors 4, 6, 12 (IWP Area)

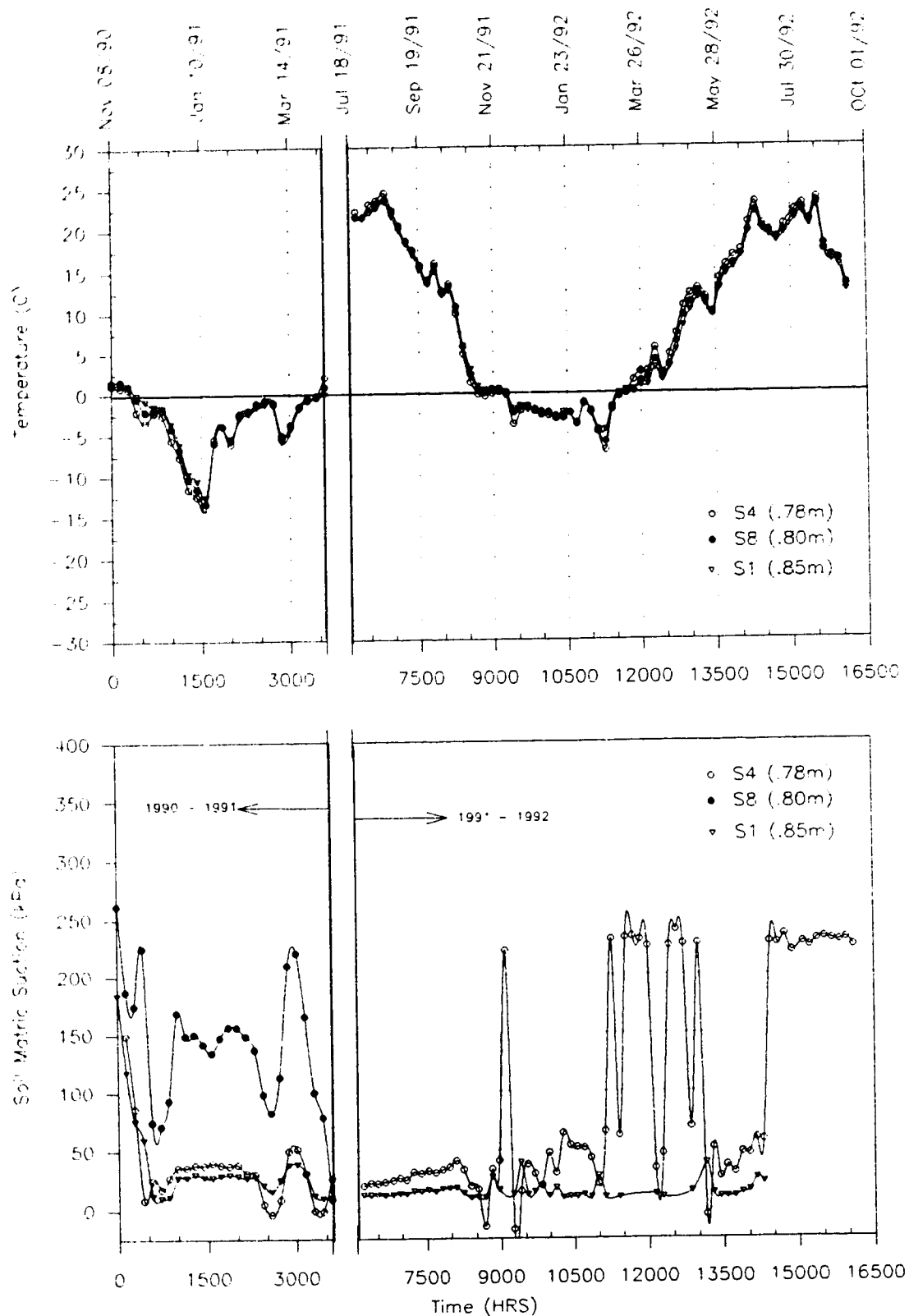


Figure 7.4: Seasonal Variation in Temperature and Soil Matrix Suction for Sensors 1, 4, 8
(Depth Horizon 0.14 – 0.21m below Top of Subgrade)

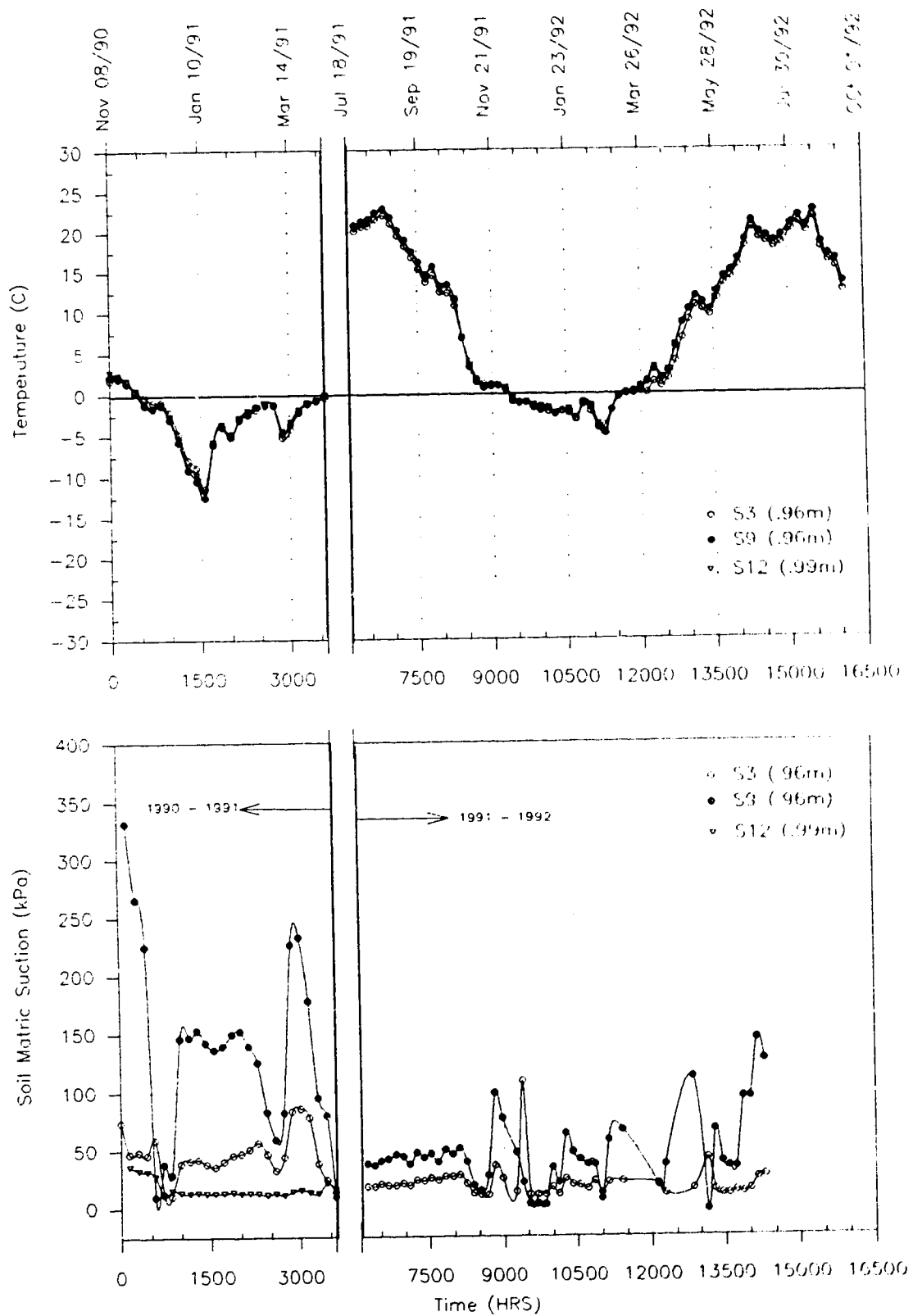


Figure 7.5: Seasonal Variation in Temperature and Soil Matrix Suction for Sensors 3, 9, 12
(Depth Horizon 0.32 - 0.35m below Top of Subgrade)

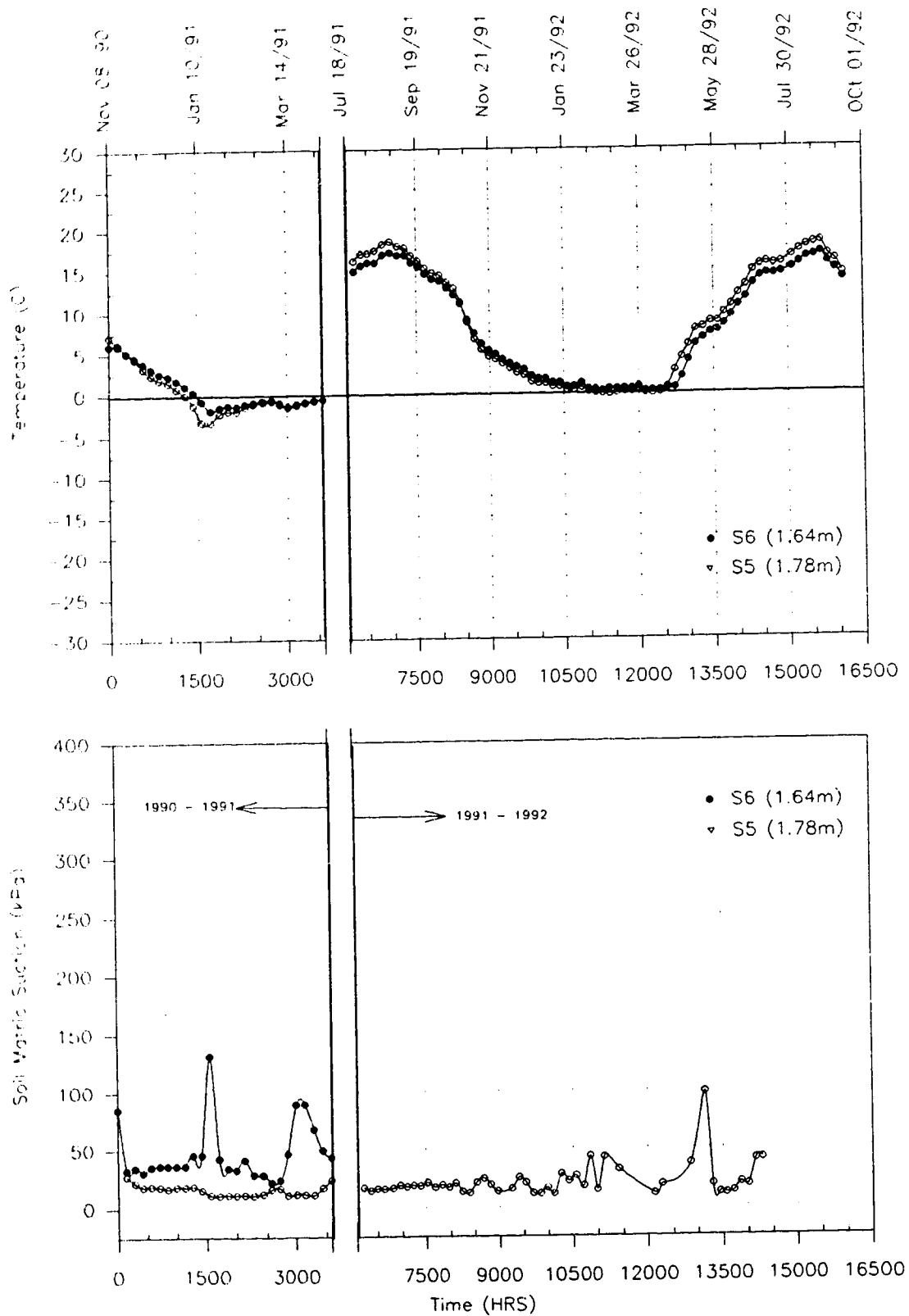
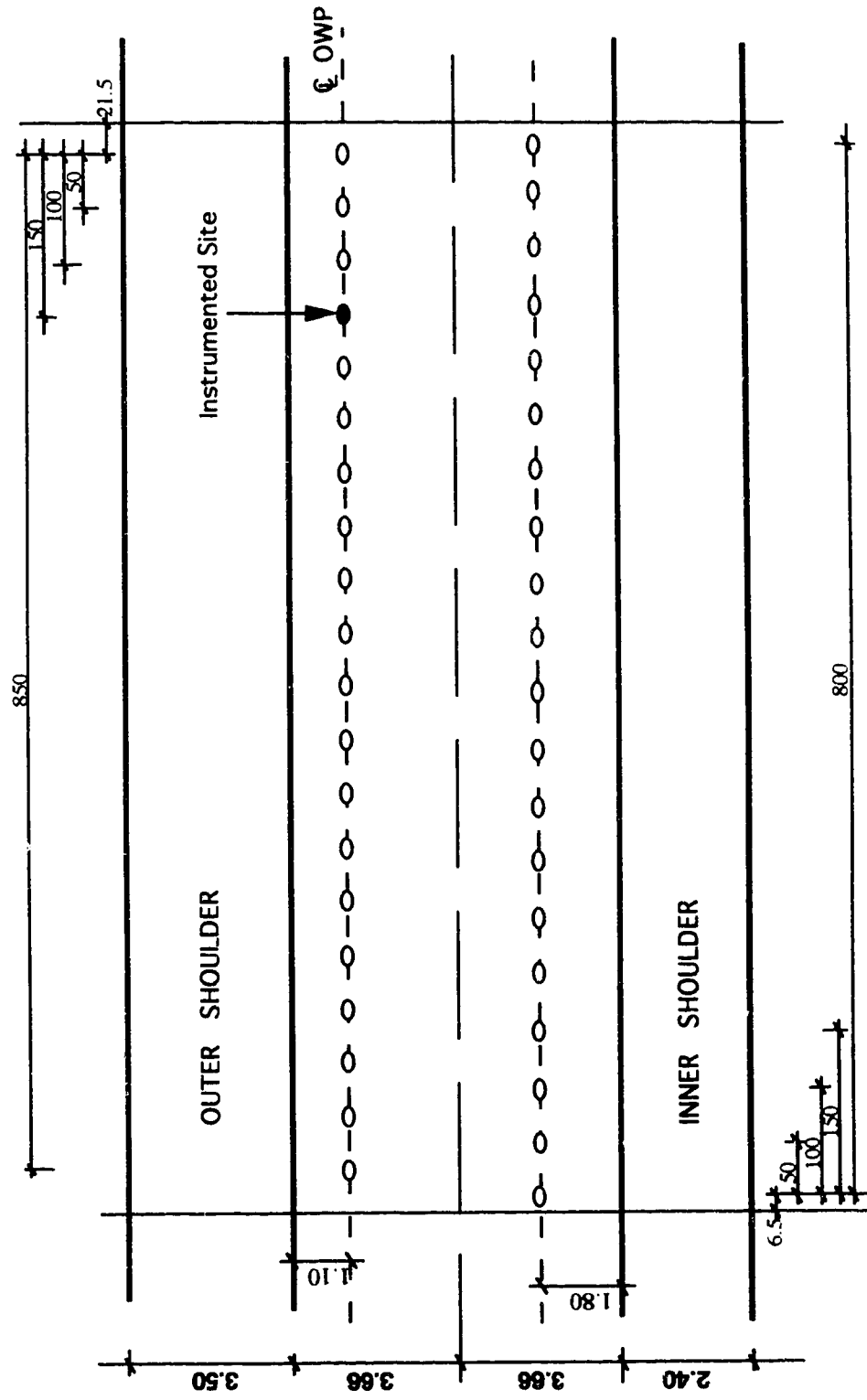


Figure 7.6: Seasonal Variation in Temperature and Soil Matric Suction for Sensors 5, 6
(Depth Horizon 1.00 – 1.14m below Top of Subgrade)



Note: All Dimensions
in metres

Figure 7.7: Plan View of FWD Test Locations

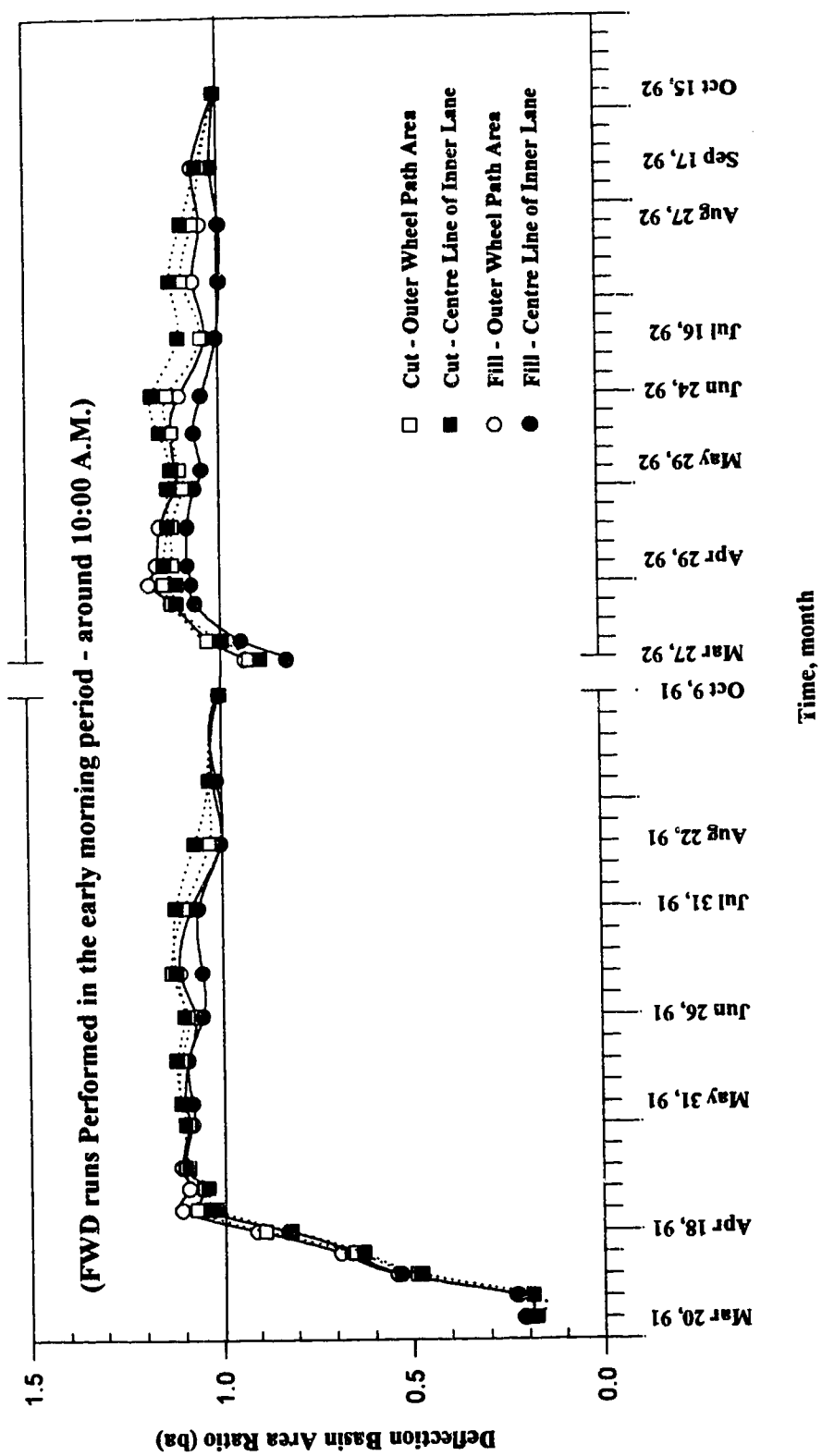


Figure 7.8: Variation of Deflection Basin Area Ratio with Season for Both Cut and Fill Sections (under FWD load of 40 kN)

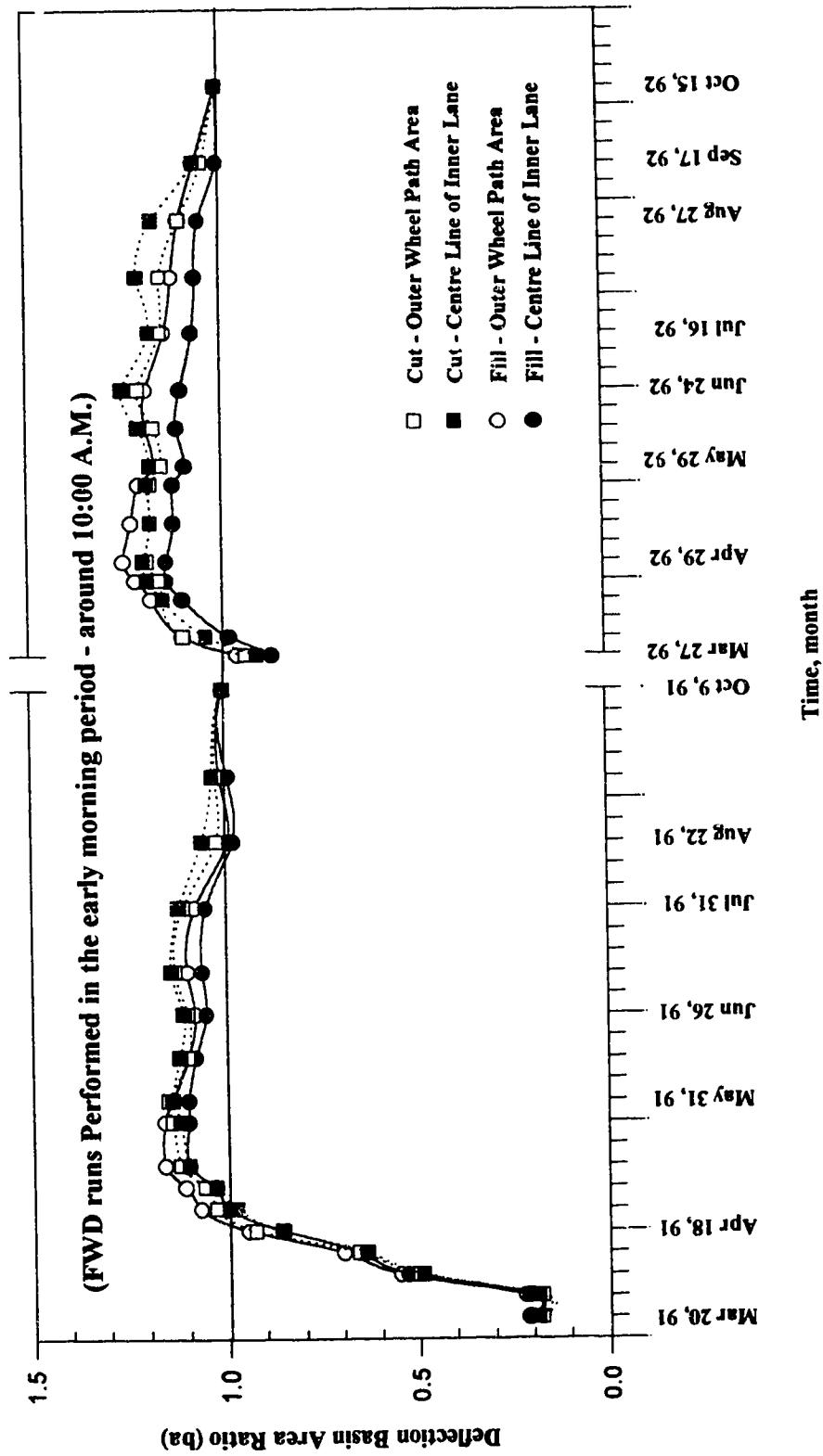


Figure 7.9; Variation of Deflection Basin Area Ratio with Season for Both Cut and Fill Sections (under FWD load of 53 kN)

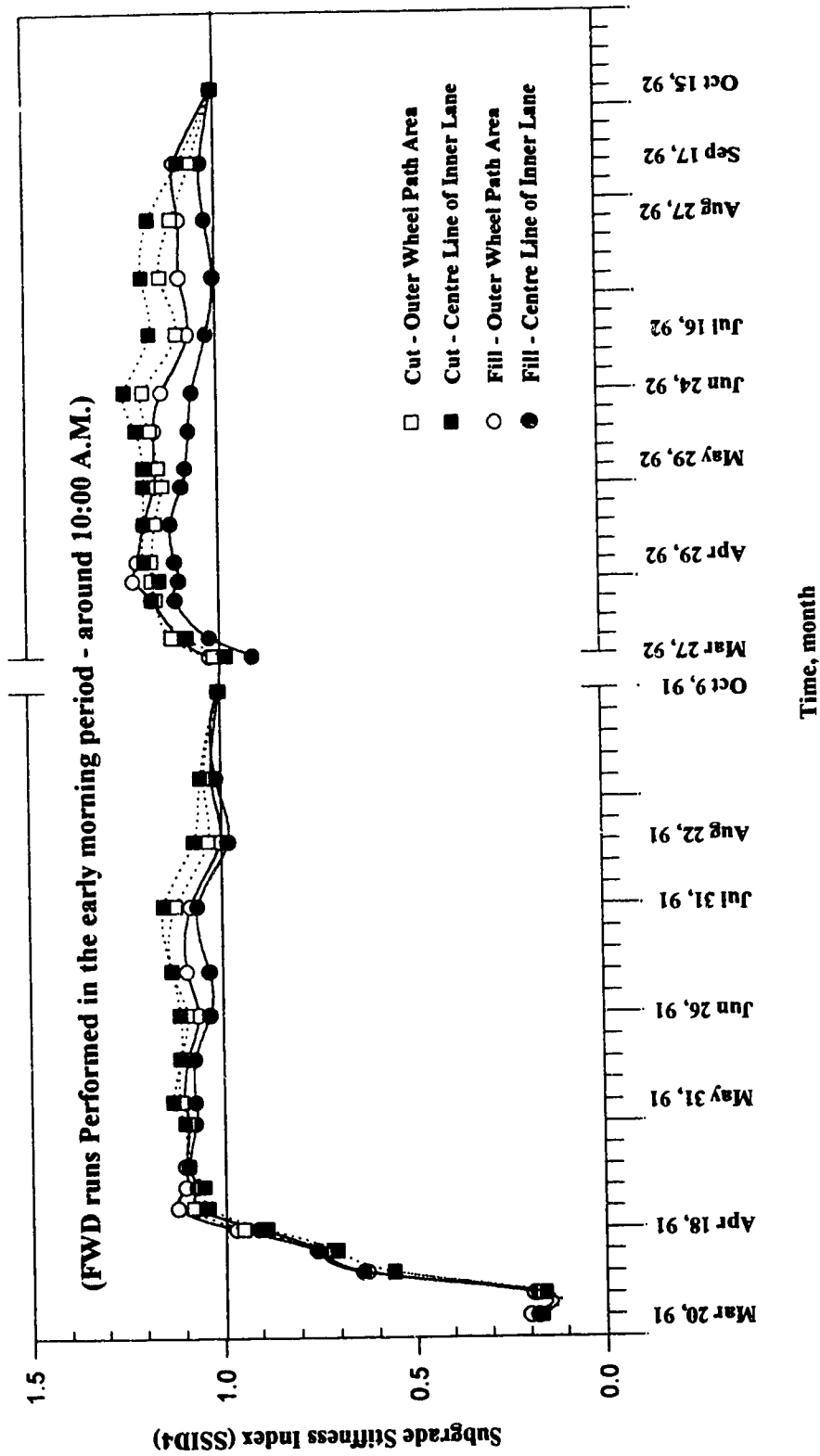


Figure 7.10: Variation of Subgrade Stiffness Index, SSID4, with Season for Both Cut and Fill Sections (under FWD load of 40 kN)

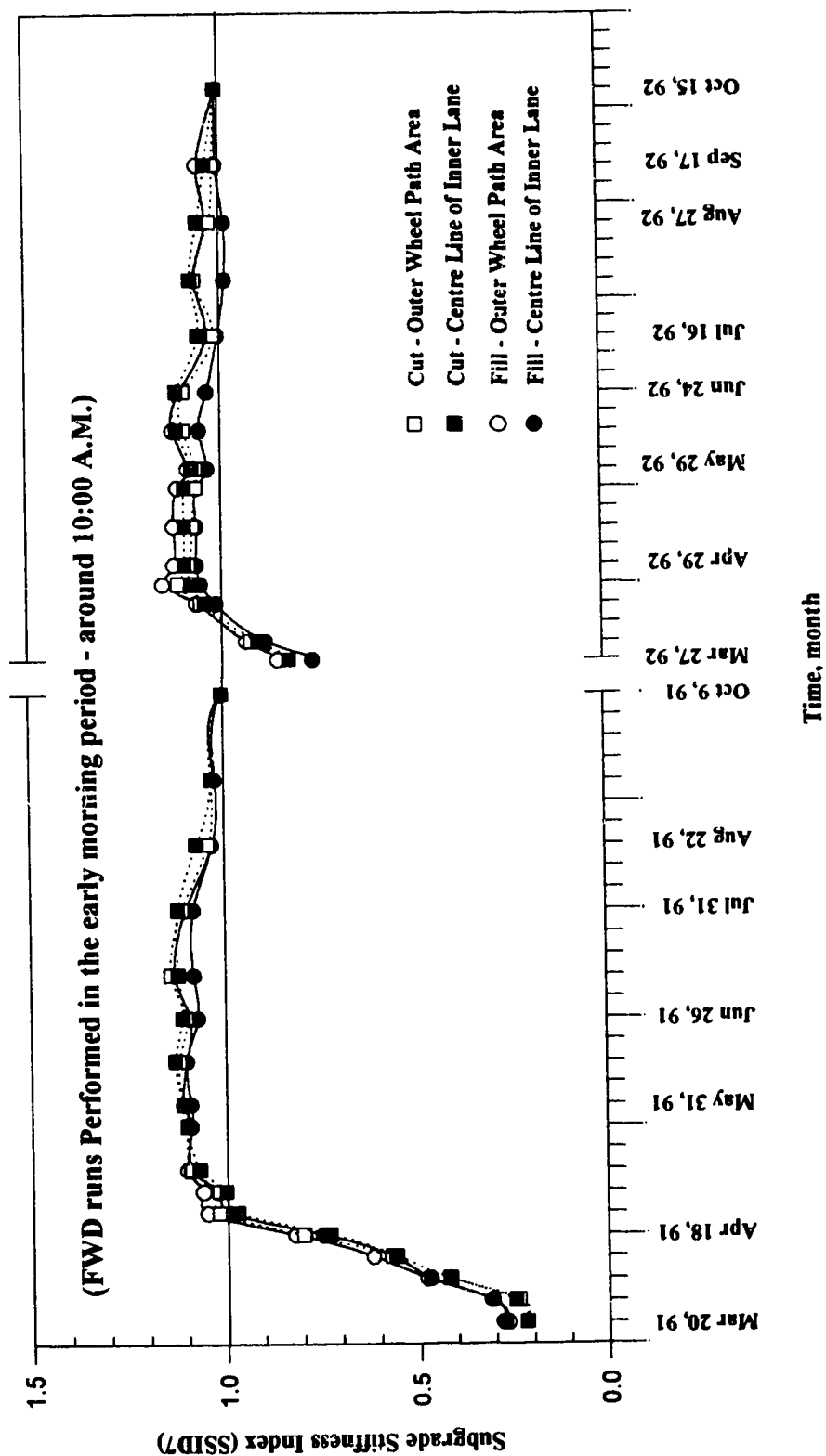


Figure 7.11: Variation of Subgrade Stiffness Index, SSID7, with Season for Both Cut and Fill Sections (under FWD load of 40 kN)

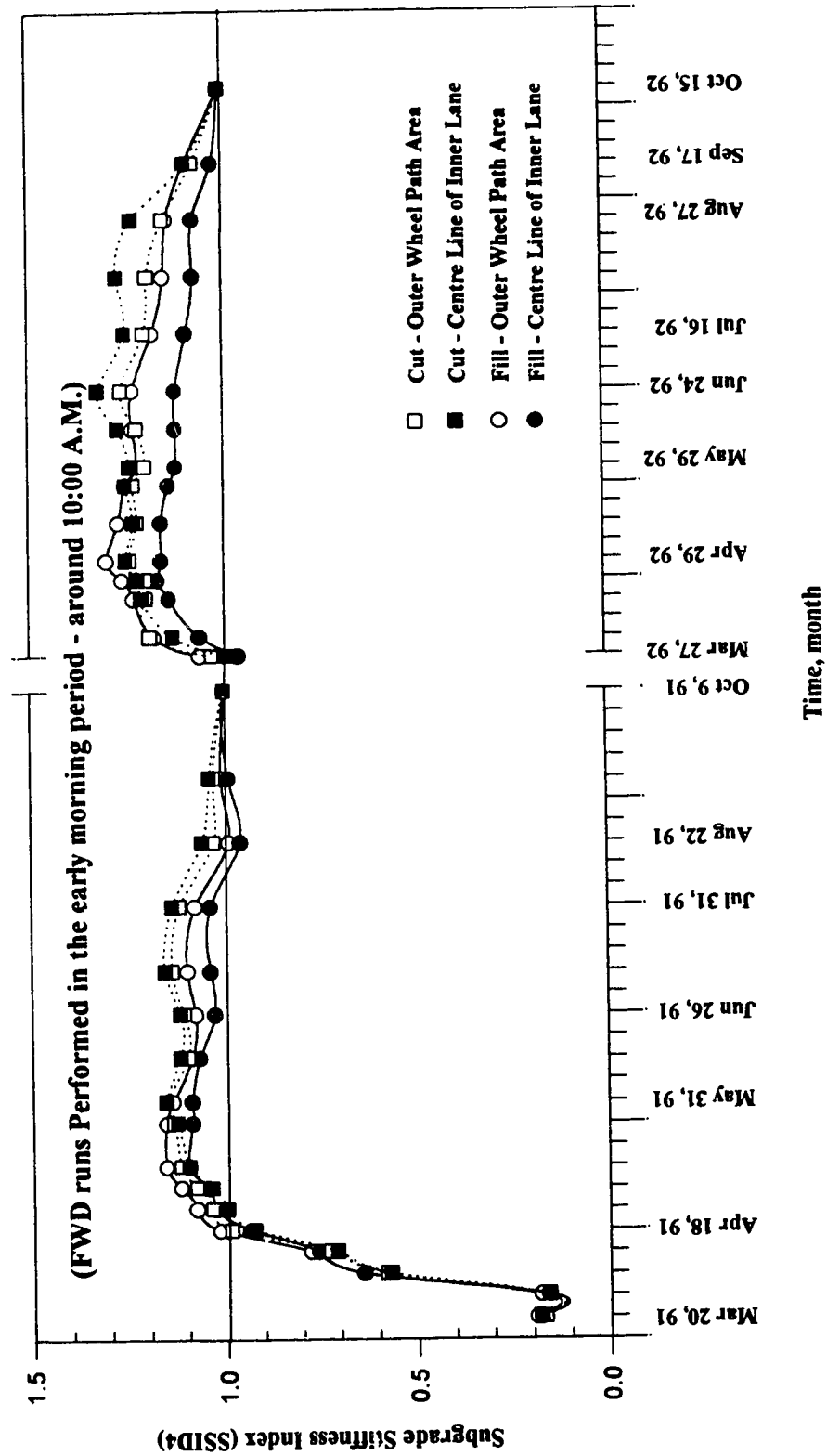


Figure 7.12: Variation of Subgrade Stiffness Index, SSId4, with Season for Both Cut and Fill Sections (under FWD Load of 53 kN)

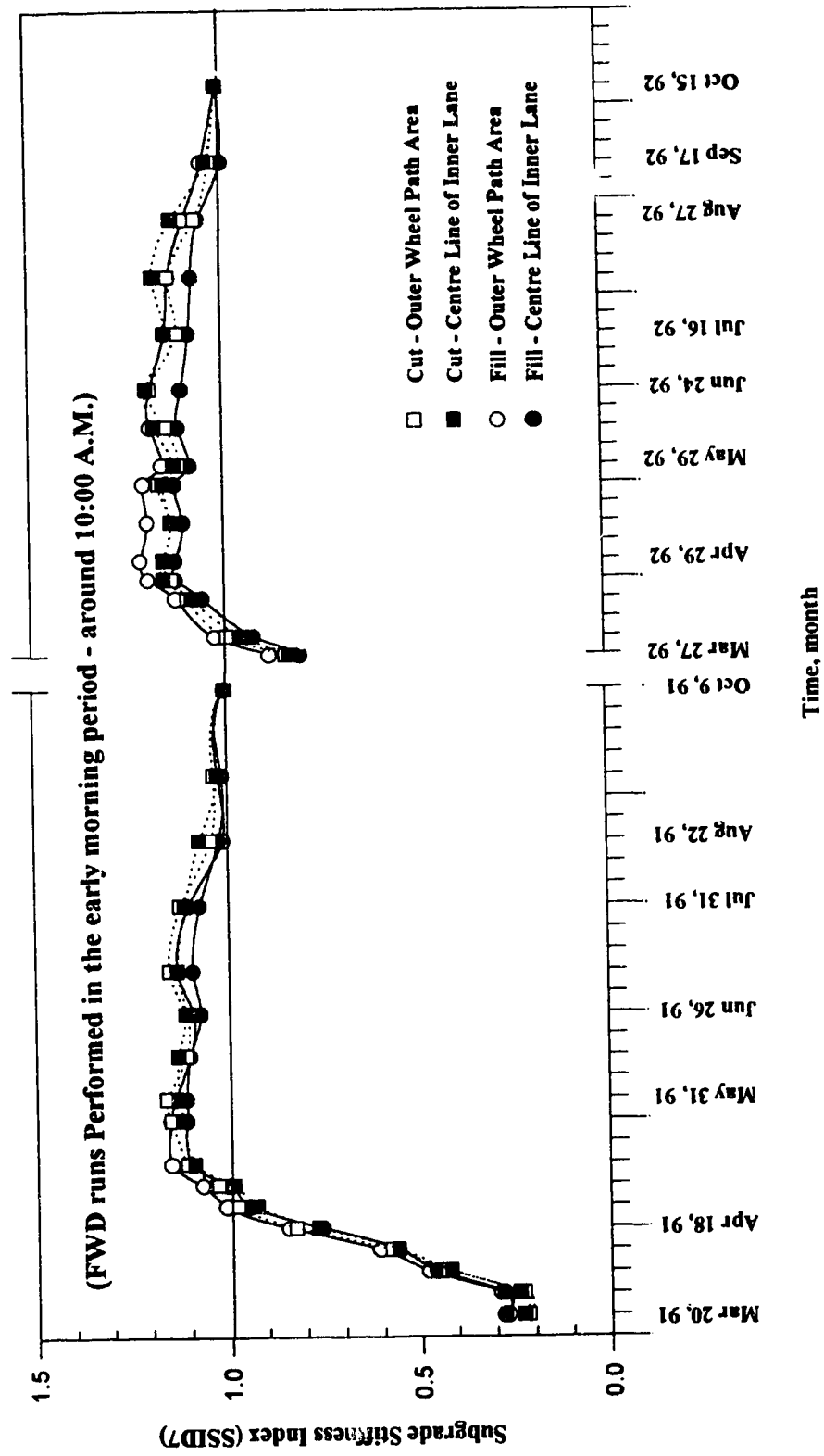


Figure 7.13: Variation of Subgrade Stiffness Index, SSID7, with Season for Both Cut and Fill Sections (under FWD Load of 53 kN)

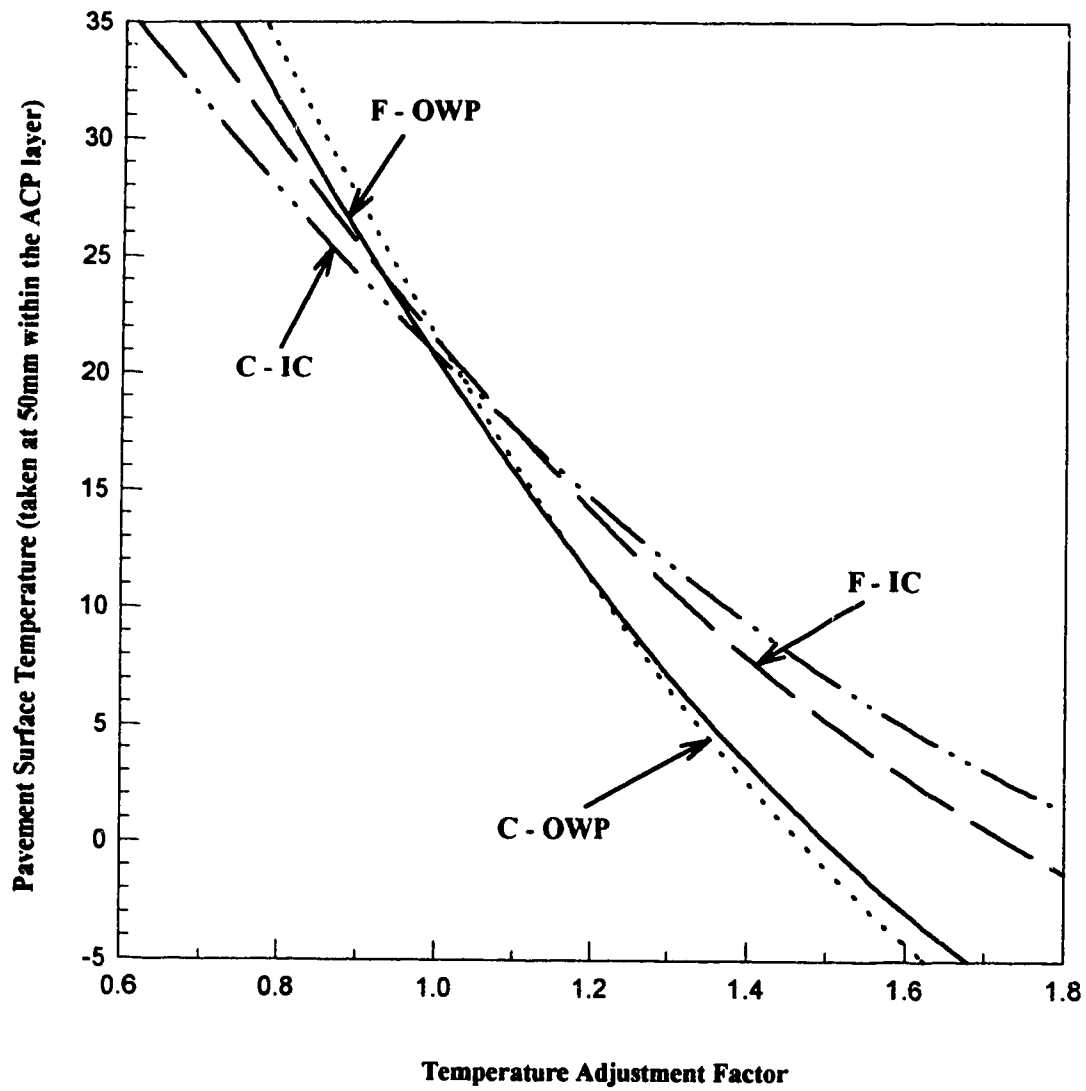


Figure 7.14: Temperature Adjustment Factor Curves for Central Deflection

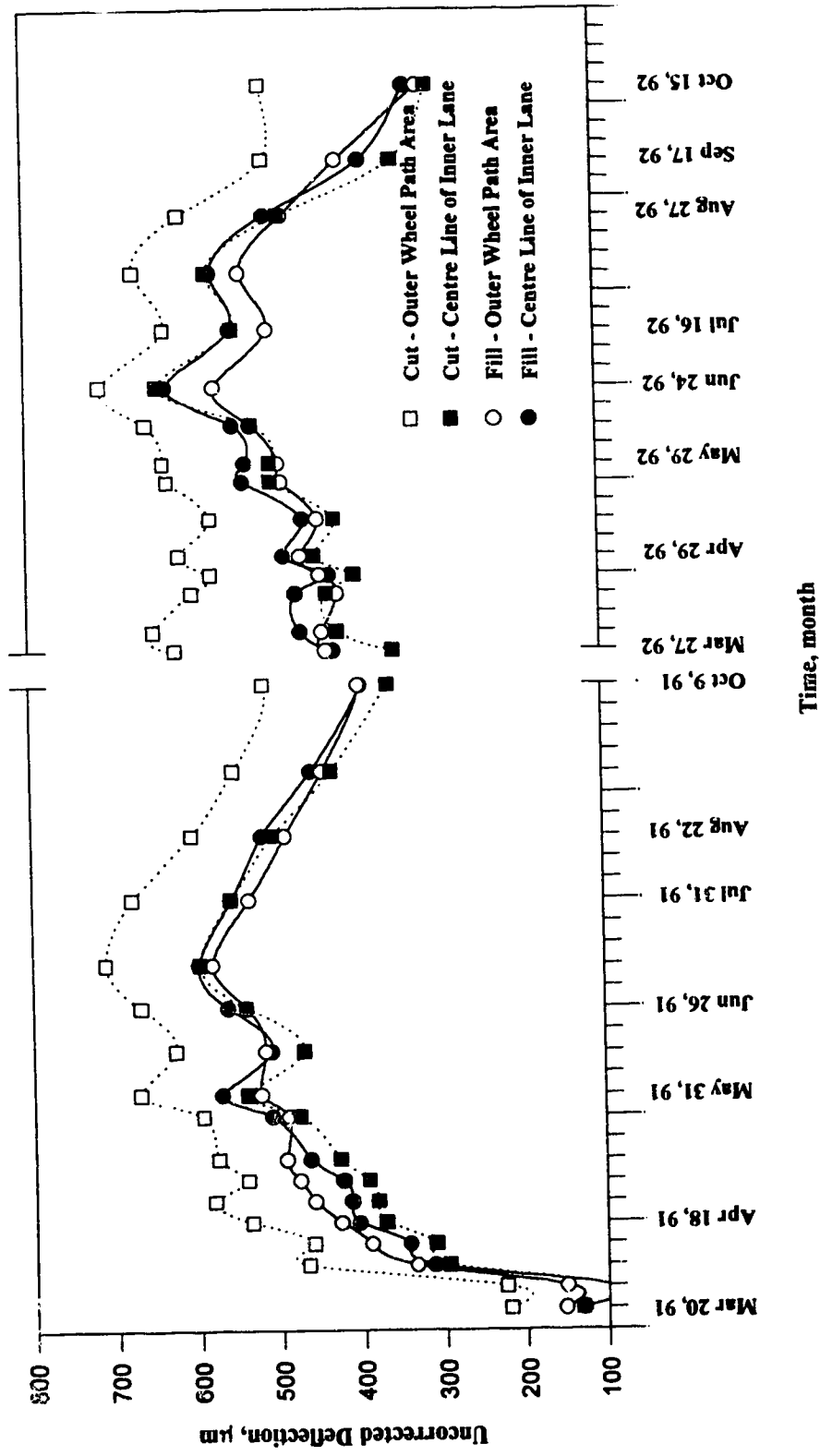


Figure 7.15: Variation of Actual Central Deflection with Season for Both Cut and Fill Sections (under 40 kN load)

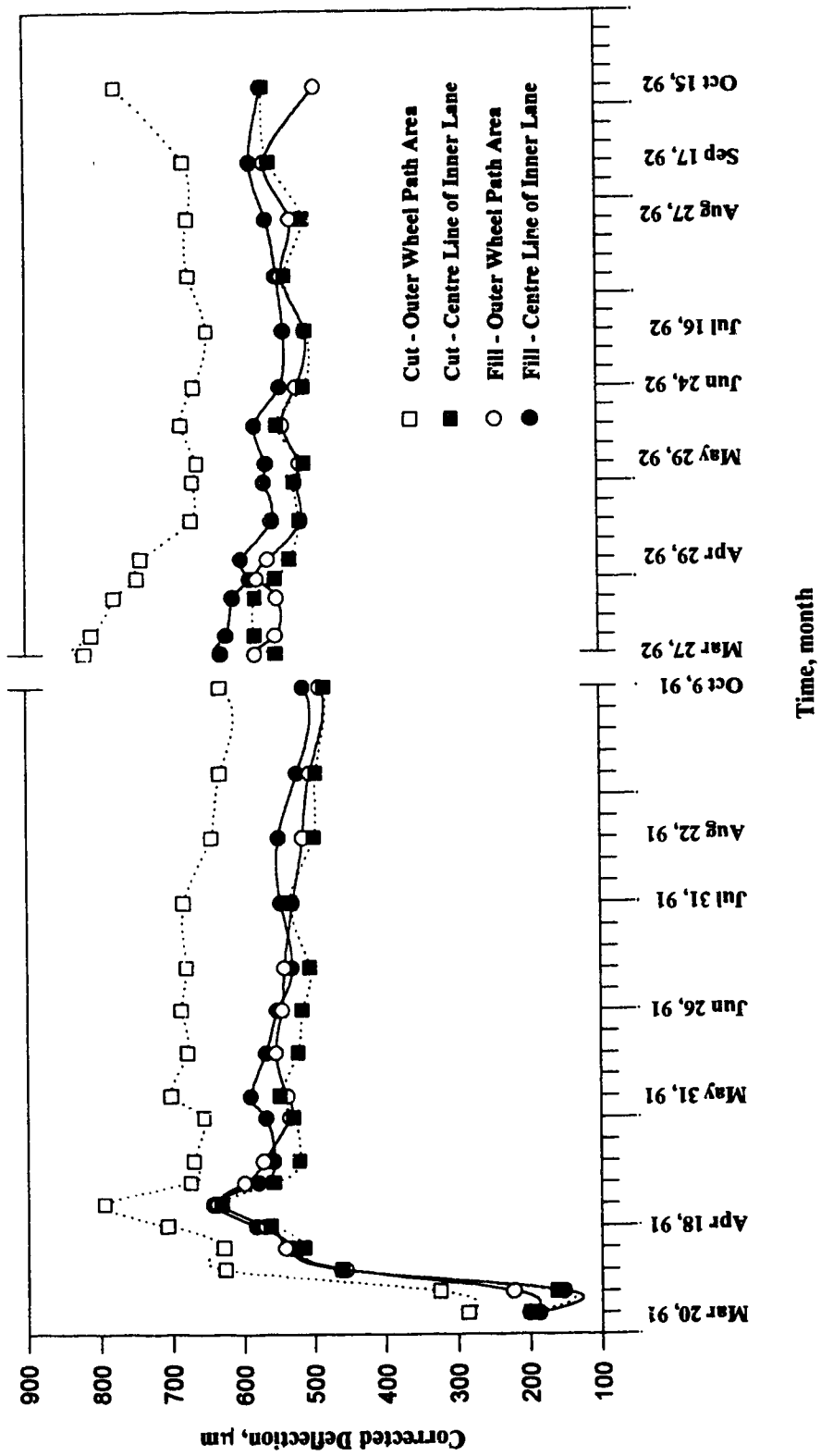


Figure 7.16: Variation of Corrected Central Deflection with Season for Both Cut and Fill Sections (under 40 kN load)

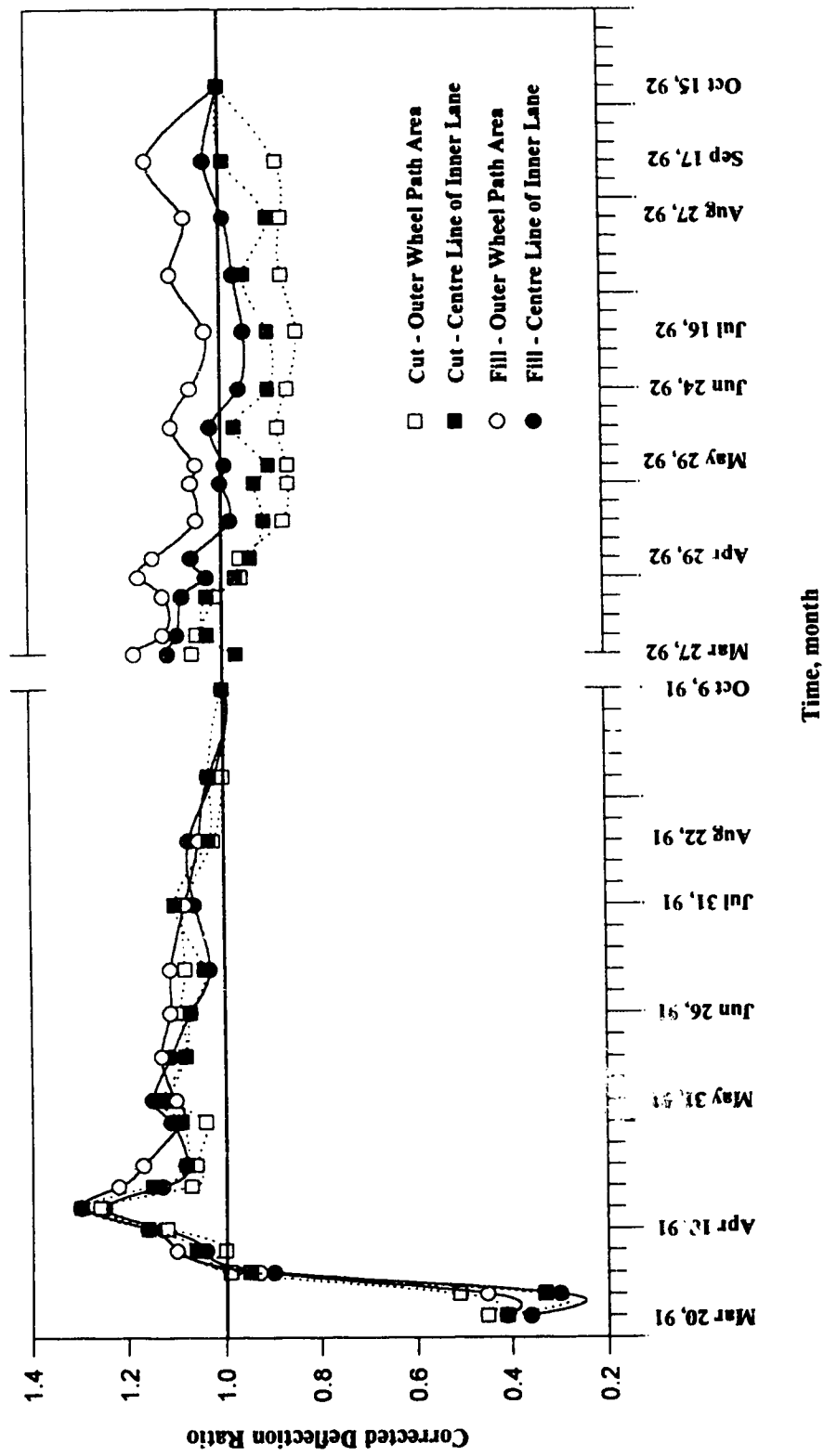


Figure 7.17: Variation of Corrected Central Deflection Ratio with Season for Both Cut and Fill Sections (under 40 kN load)

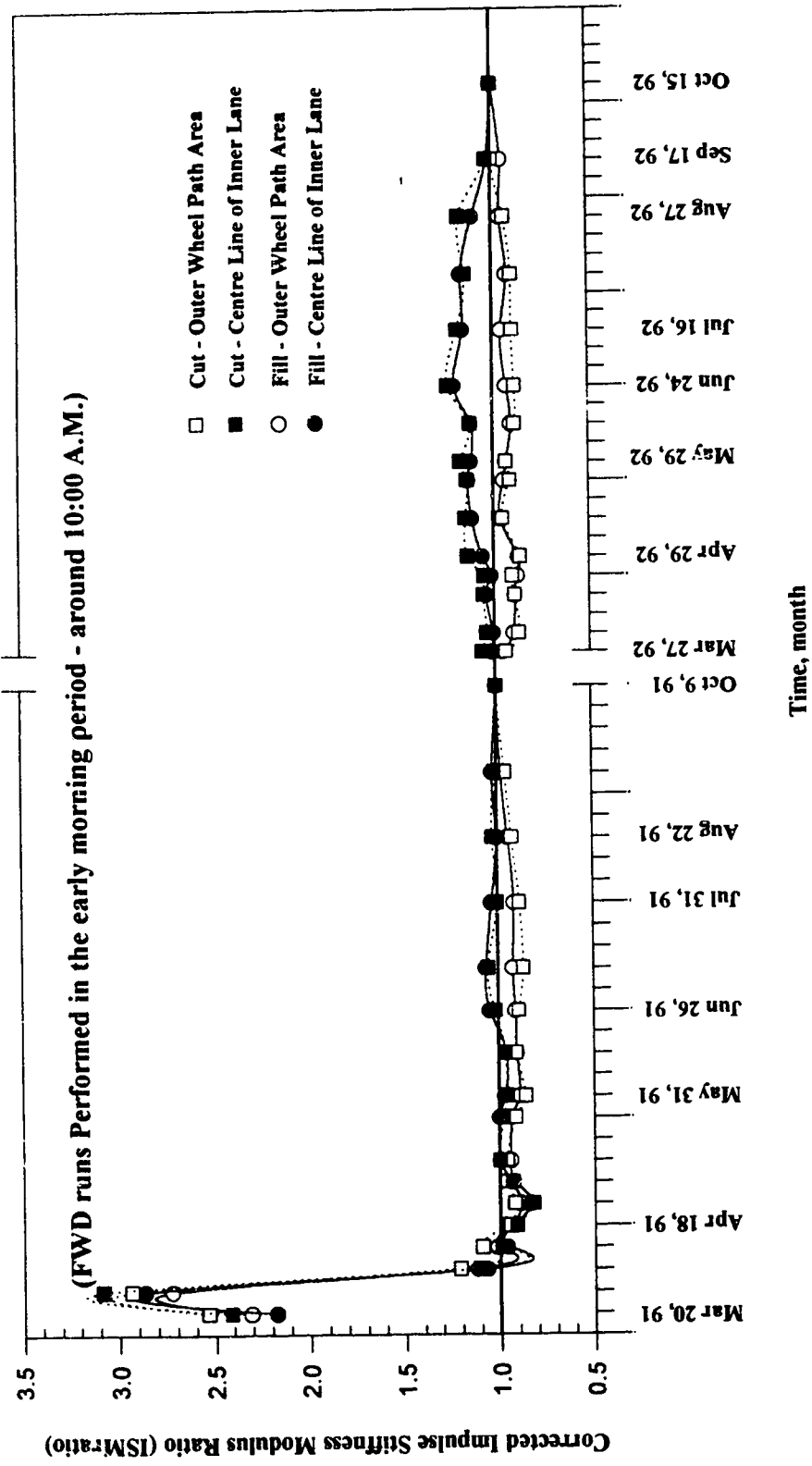


Figure 7.18: Variation of Corrected Impulse Stiffness Modulus Ratio, ISMratio, with Season for Both Cut and Fill Sections (under 40 kN load)

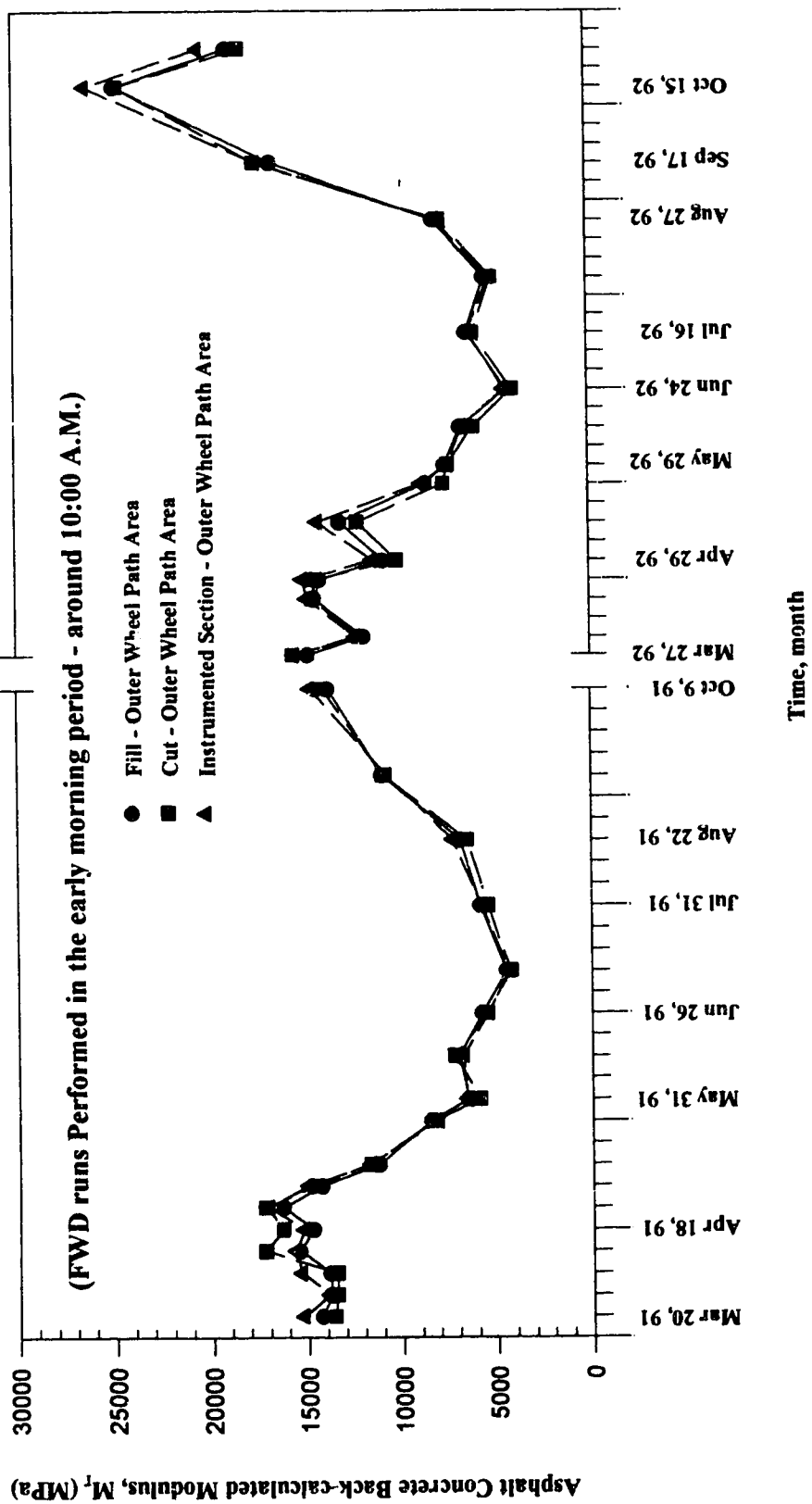


Figure 7.19: Variation of ACP Back-calculated Modulus with Season for the Sections in OWP Area

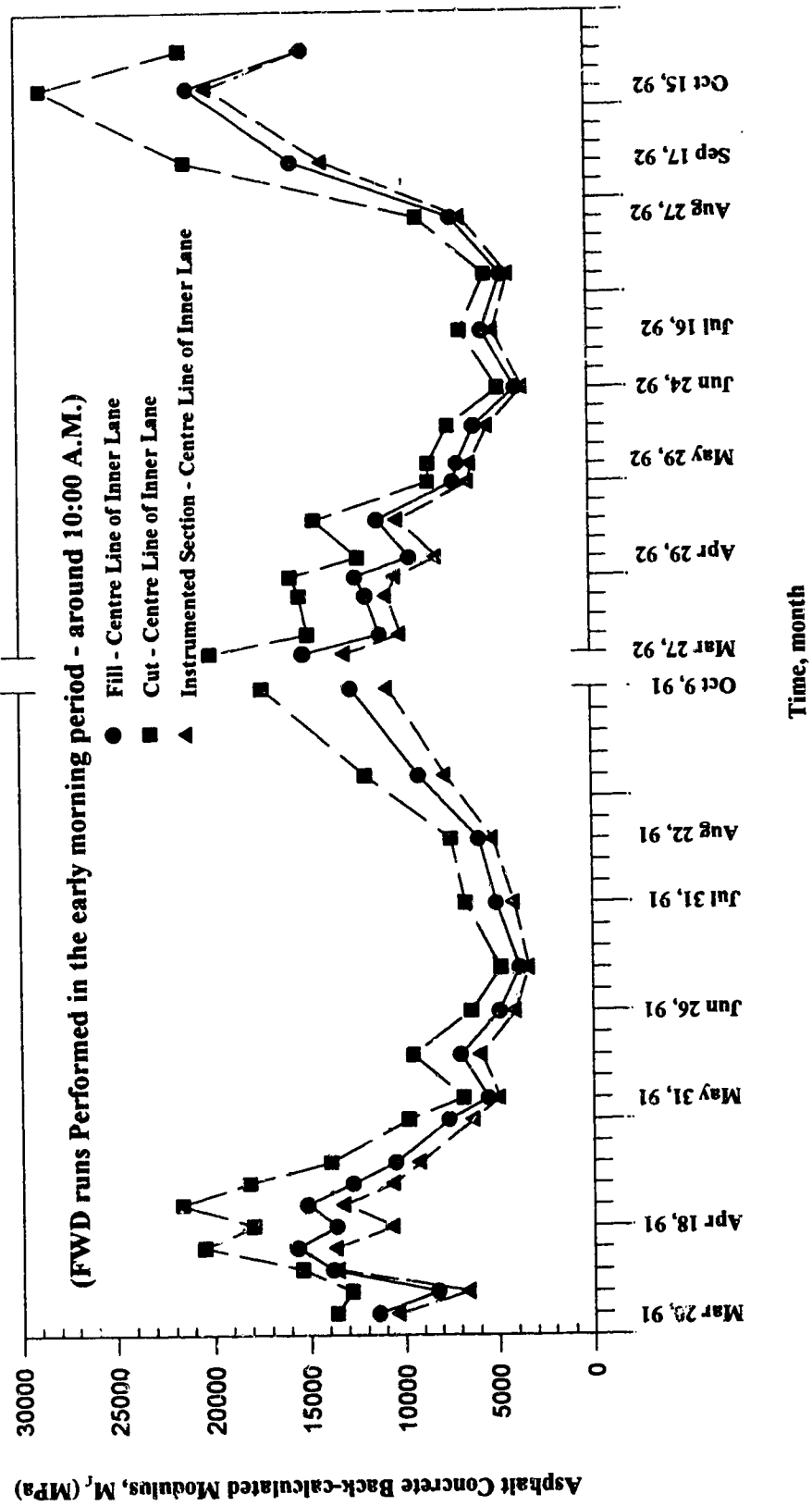


Figure 7.20: Variation of ACP Back-calculated Modulus with Season for the Sections in IC Area

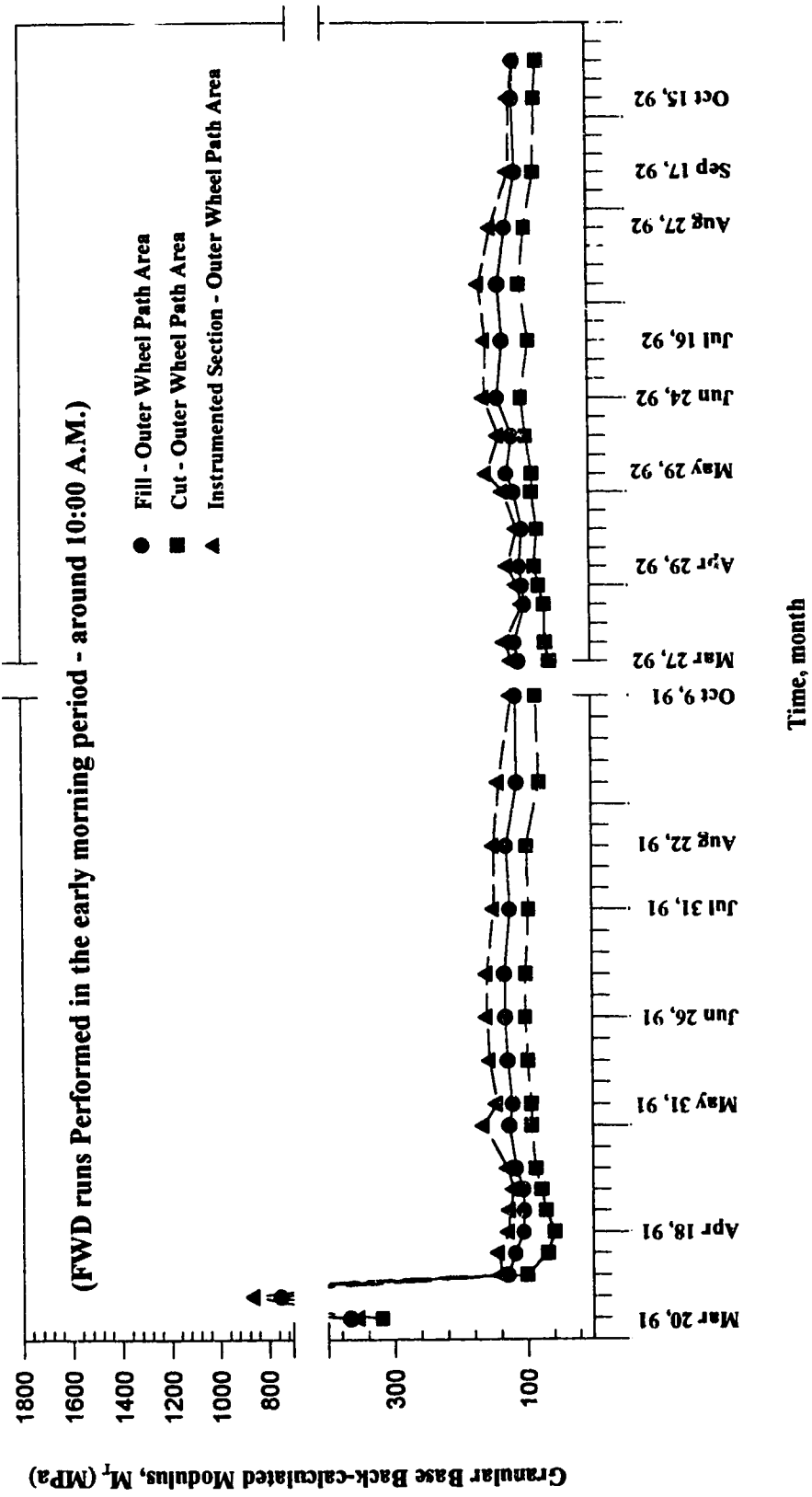


Figure 7.21: Variation of GB Back-calculated Modulus with Season for the Sections in OWP Area

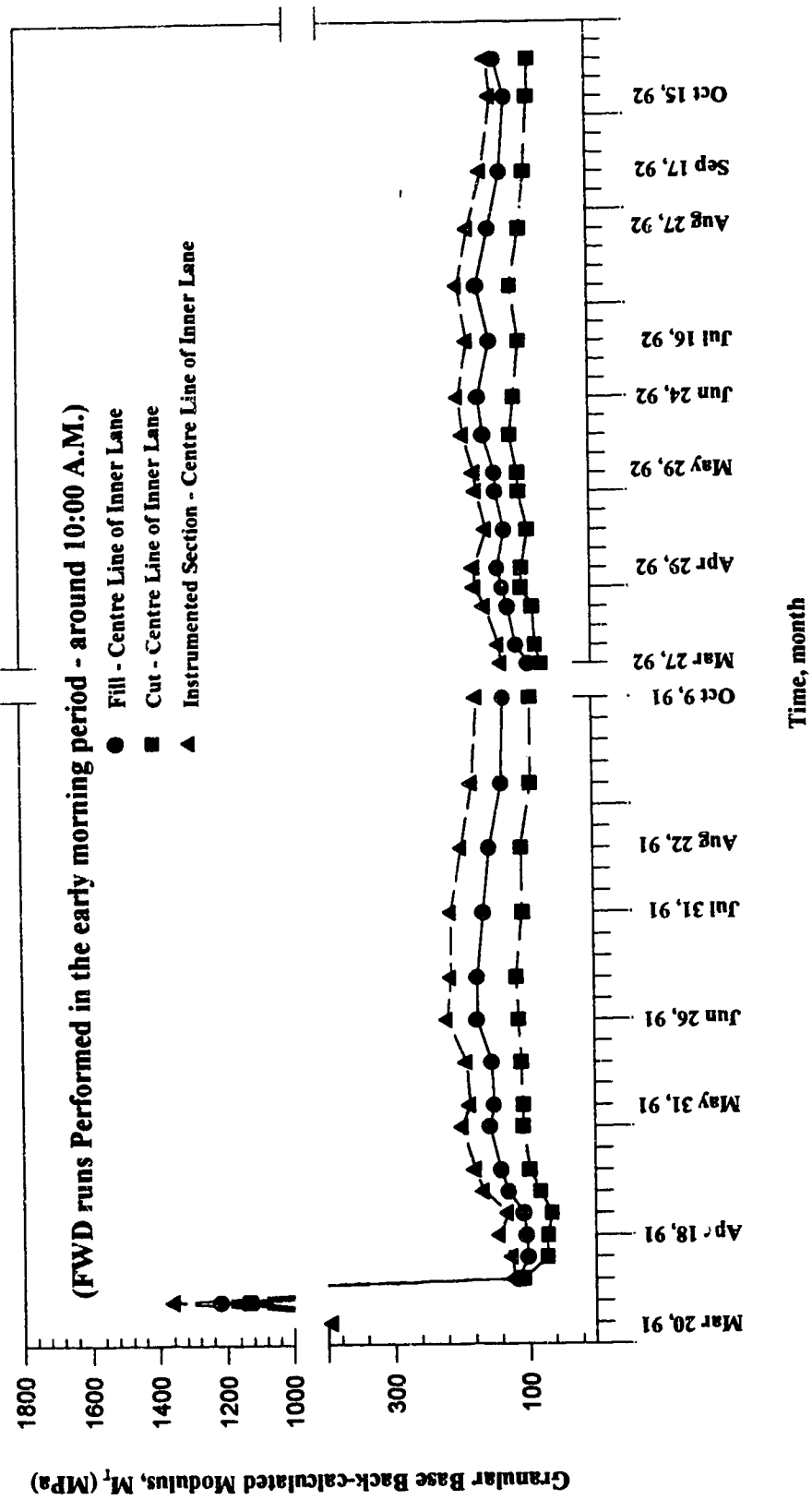


Figure 7.22: Variation of GB Back-calculated Modulus with Season for the Sections in IC Area

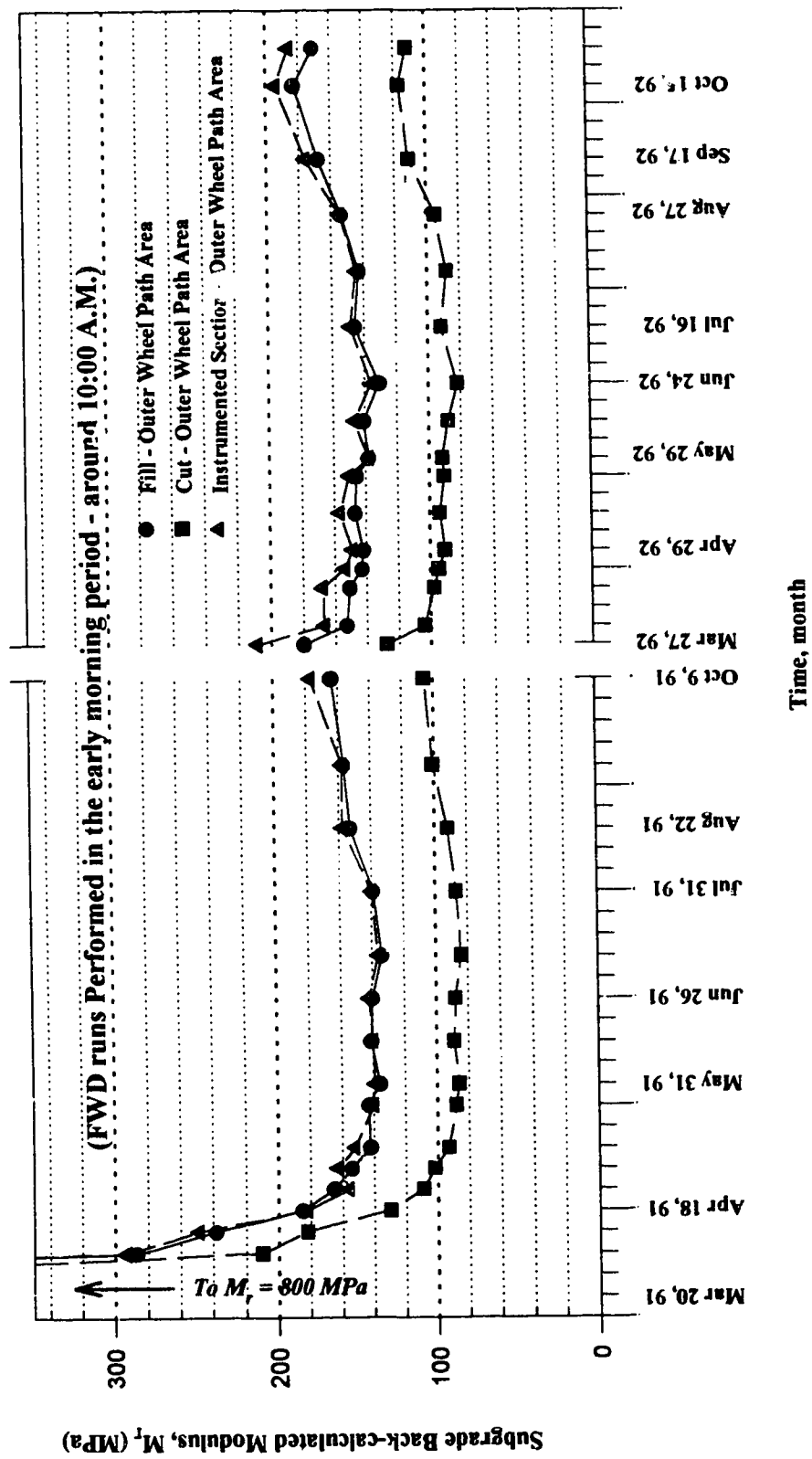


Figure 7.23: Variation of SG Back-calculated Modulus with Season for the Sections in OWP Area

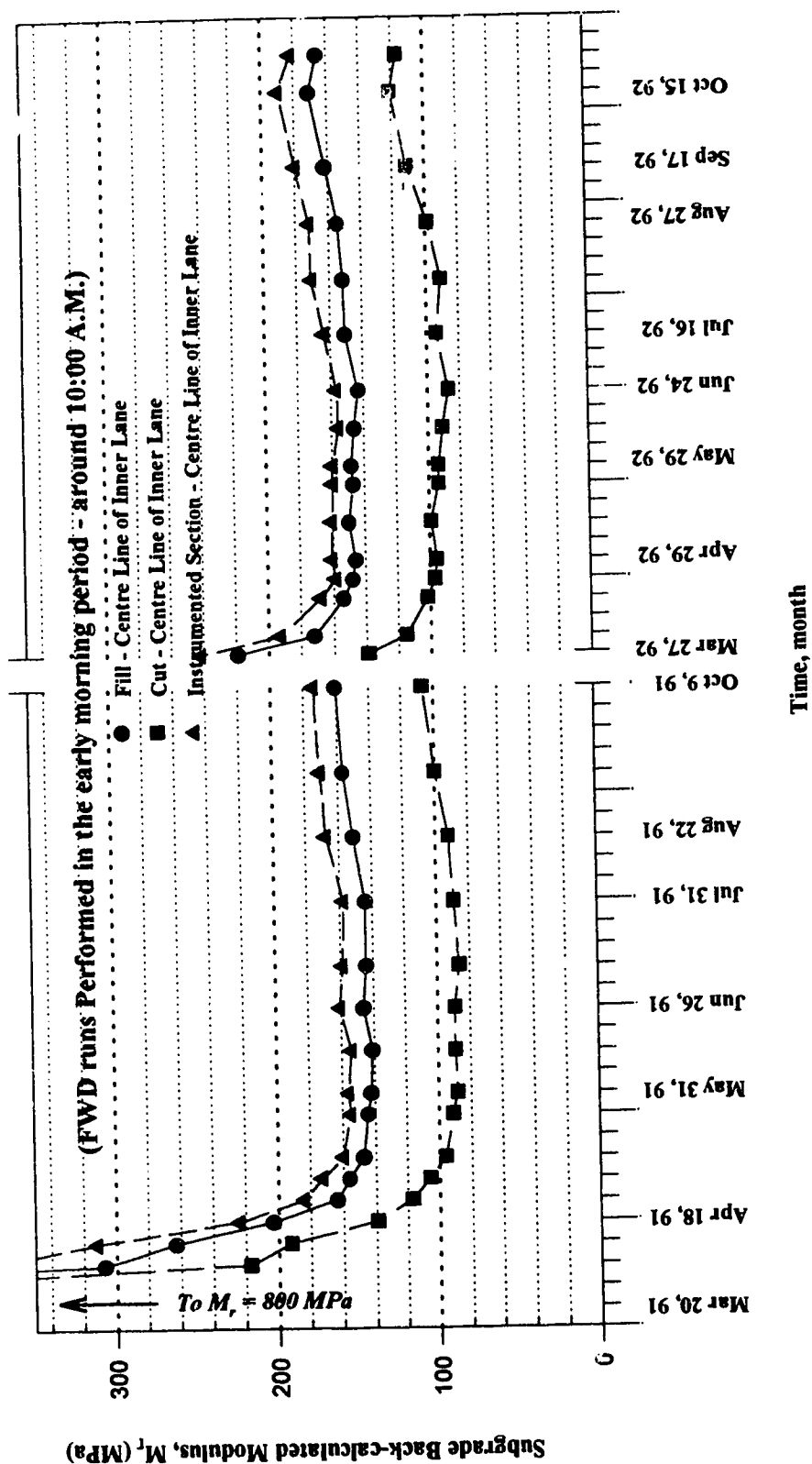


Figure 7.24: Variation of SG Back-calculated Modulus with Season for the Sections in IC Area

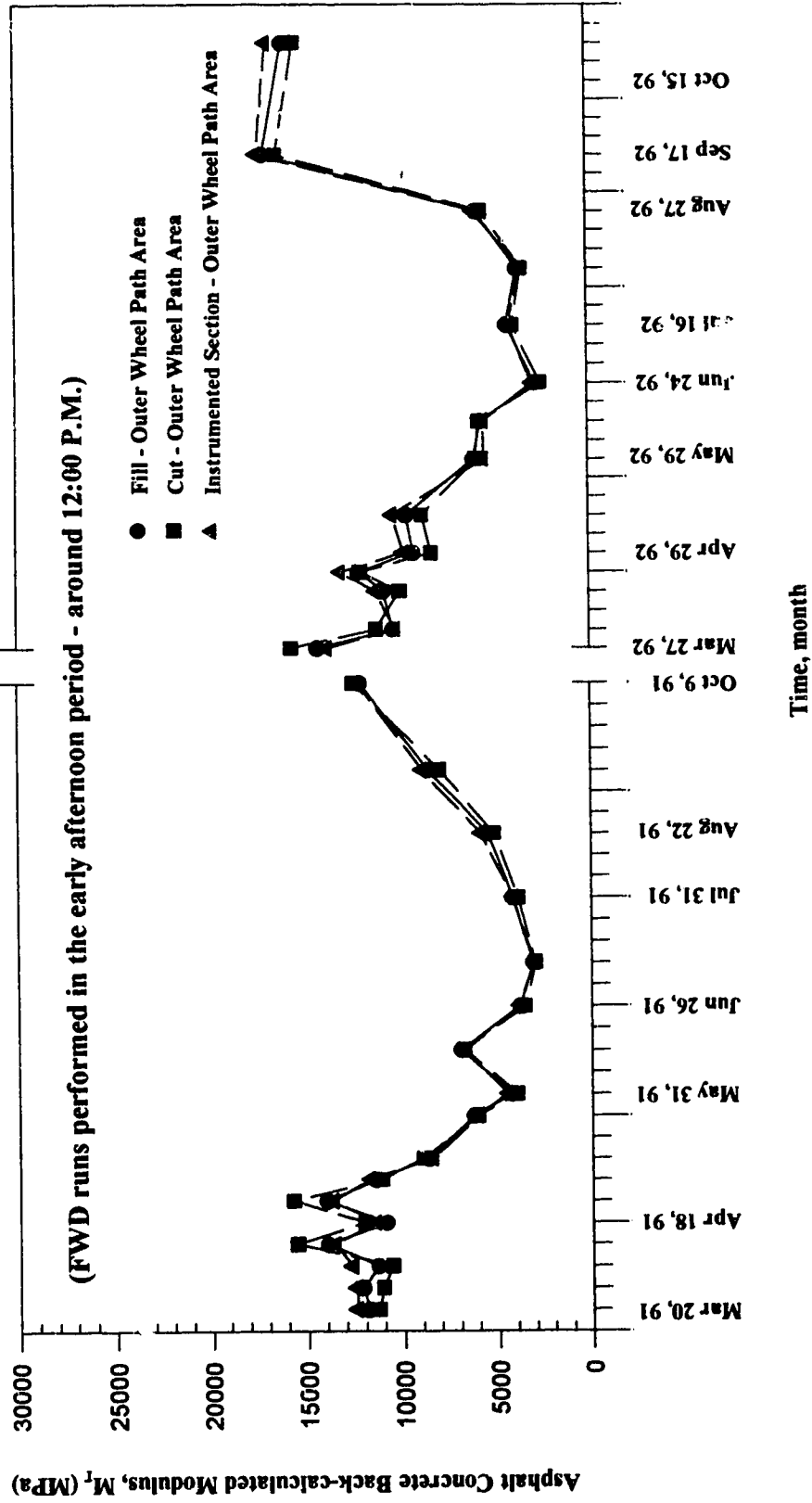


Figure 7.25: Variation of ACP Back-calculated Modulus with Season for the Sections in OWP Area

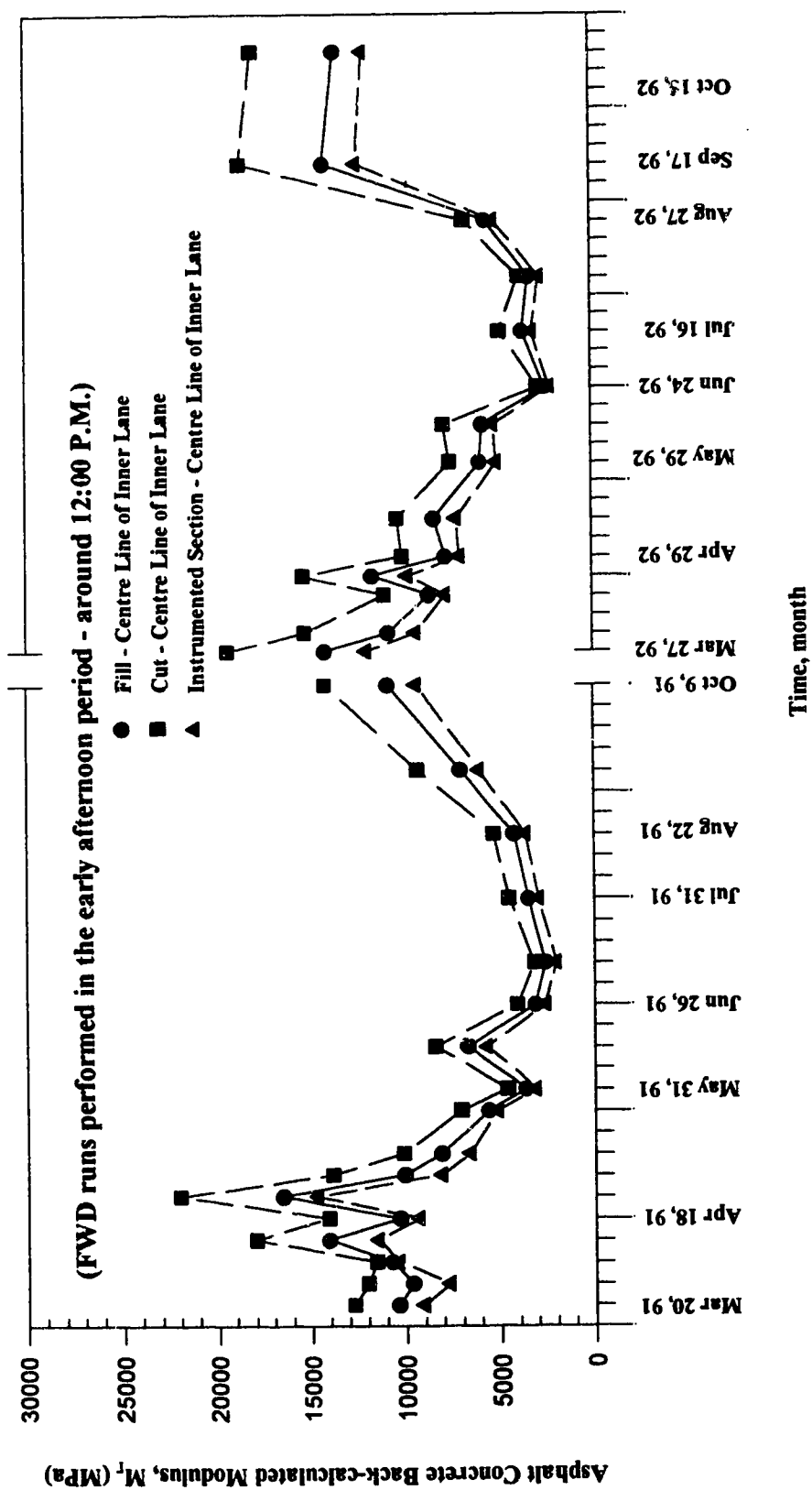


Figure 7.26: Variation of ACP Back-calculated Modulus with Season for the Sections in IC Area

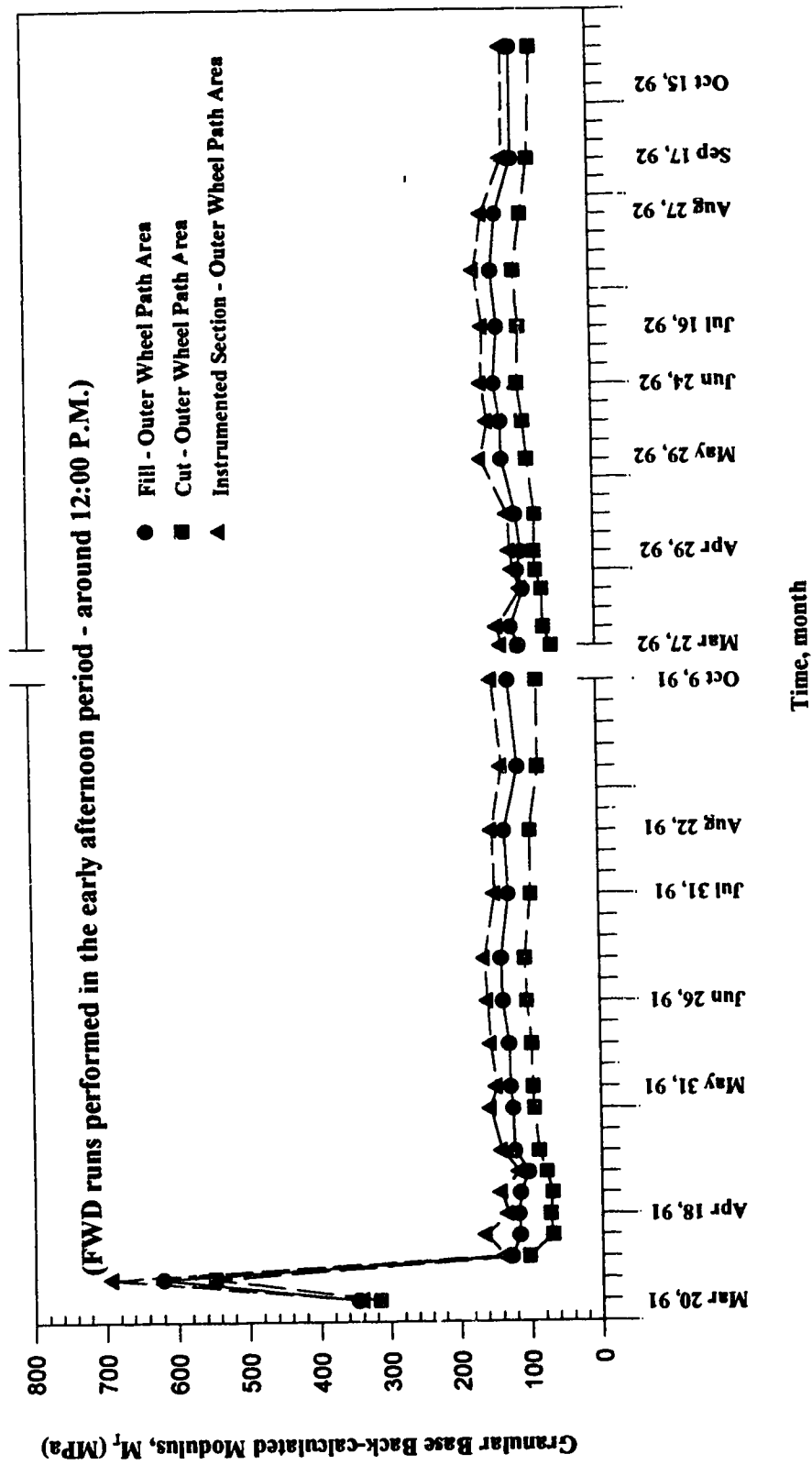


Figure 7.27: Variation of GB Back-calculated Modulus with Season for the Sections in OWP Area

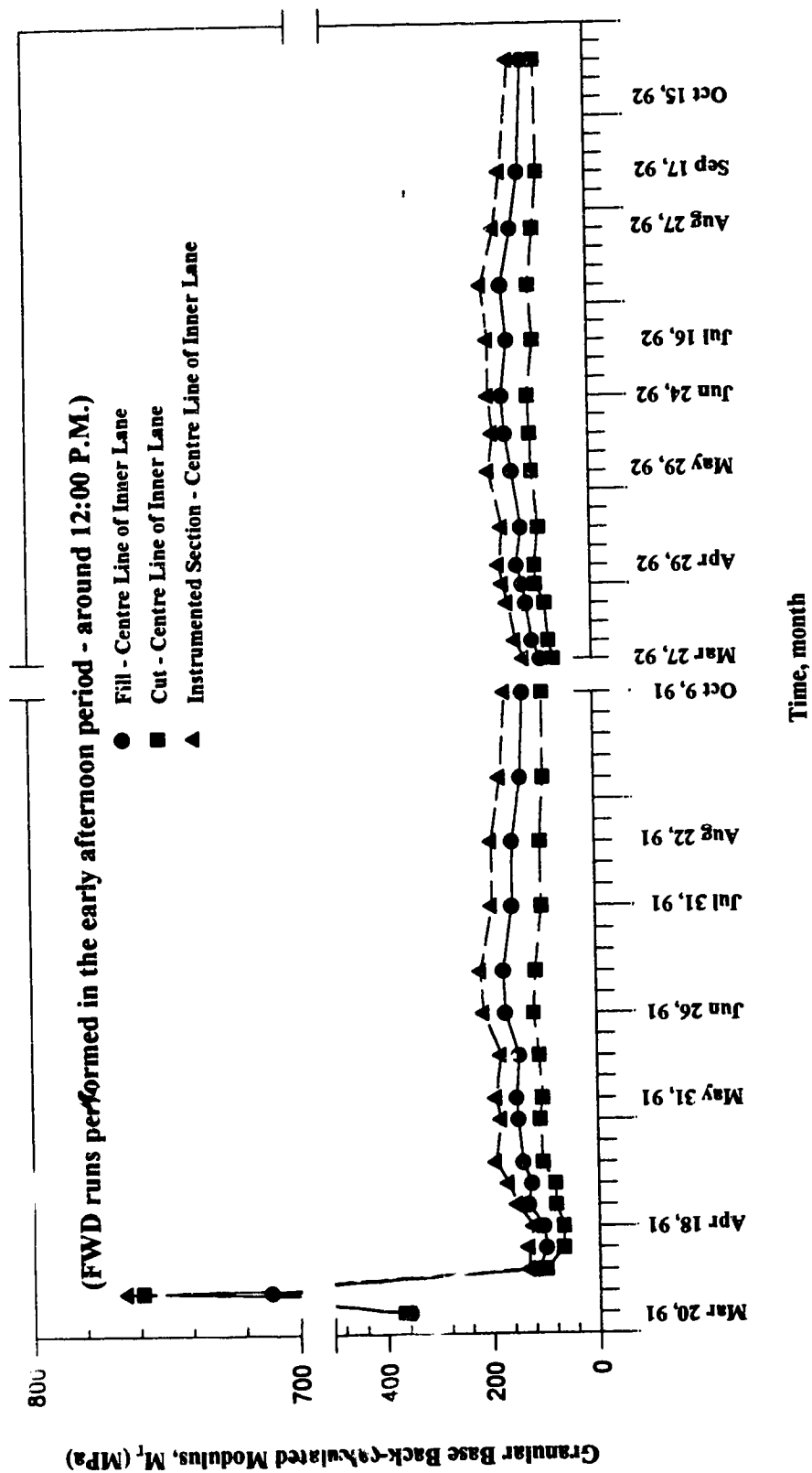


Figure 7.28: Variation of σ_B Back-calculated Modulus with Season for the Sections in IC Area

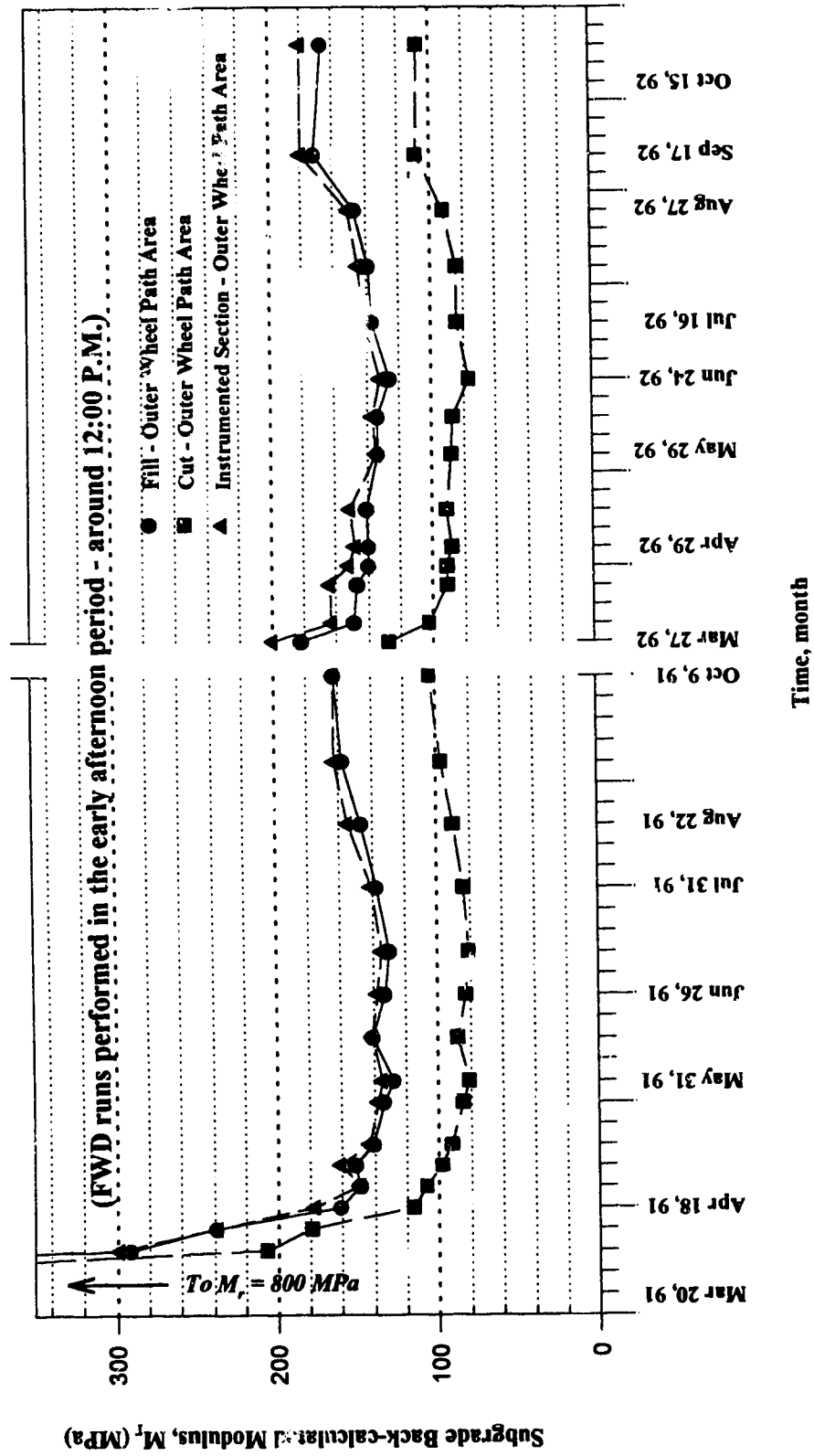


Figure 7.29: Variation of SG Back-calculated Modulus with Season for the Sections in OWP Area

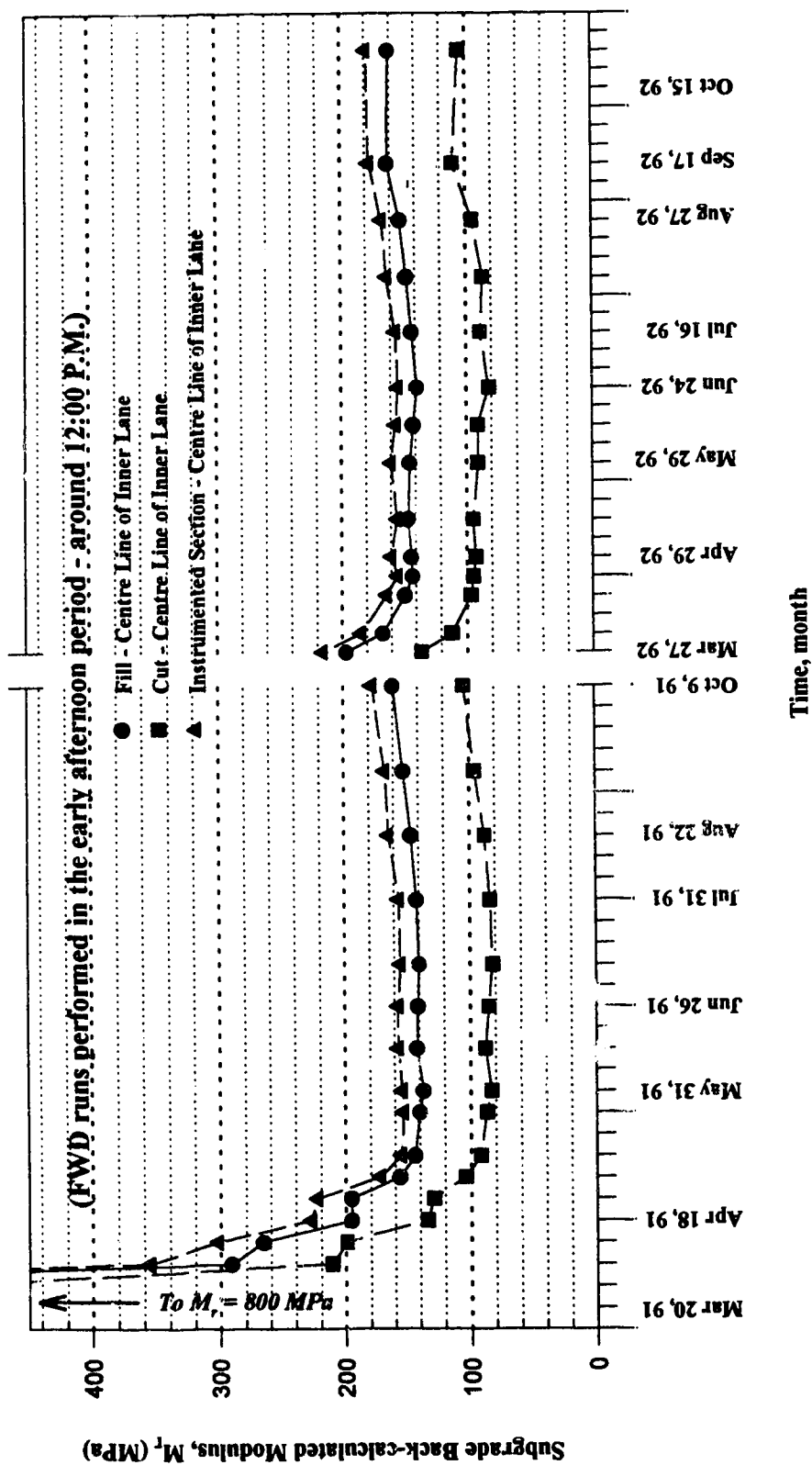


Figure 7.50: Variation of SG Back-calculated Modulus with Season for the Sections in IC Area

CHAPTER EIGHT

SUMMARY, CONCLUSIONS AND RECOMMENDATIONS

8.1 General

This study was aimed at achieving a better understanding of the phenomenon of seasonal variations in the structural strength of subgrade materials for pavements structures situated in cold climates for the purpose of future implementation of mechanistic-empirical pavement design procedures. The main objective of the investigation was to establish a way for measuring seasonal variations. The specifics of this involved identifying and quantifying the influences of both temperature and soil matric suction on the stiffness of cohesive subgrade soils in Alberta.

State-of-the-art reviews pertaining to current methodologies used for evaluating the structural adequacy of in-service pavements and for measuring soil matric suction were completed. This led to conceiving a two-phase investigation for accomplishing the research objectives. The first phase was an extensive field testing program of an in-service pavement while the second phase comprised a laboratory testing program for determining the resilient modulus of a typical subgrade soil.

The field testing program consisted of instrumenting a pavement section that is representative of the primary highway system within the Province of Alberta, with thermal conductivity suction sensors. Details pertinent to the instrumentation phase of the field testing program were given in Chapter Four. Falling Weight Deflectometer deflection tests were conducted at various locations within the instrumented section. This was done at different time intervals throughout the seasons, for two consecutive years, with

particular emphasis on the spring time. Output from these tests were used to back-calculate the resilient moduli of the various component layers of the pavement structure. The back-calculated moduli in conjunction with temperature and soil suction measurements were then linked to describe changes in subgrade resilient characteristics under varying environmental conditions.

Within the scope of the laboratory testing phase, extensive repeated load testing on reconstituted samples of the subgrade material taken from the instrumented site were conducted to obtain representative resilient moduli values under different loading, temperature and moisture conditions. Predictive moduli relationships linking the laboratory resilient modulus of the subgrade material to the stress state variables were postulated.

In order to fulfill the objectives of the laboratory testing phase, a repeated loading resilient modulus testing system was developed. The equipment used in this testing utilizes an open-loop air system for providing the external load. Further details concerning the development of this system and its operation are included in Chapter Five and in Appendix E of this thesis.

8.2 Major Research Findings

The main research findings from the laboratory testing program can be summarized as follows:

- (1) Two analysis strategies have been developed to interpret the laboratory obtained resilient moduli of subgrade soils. The first approach is a graphical procedure that serves as a first step to qualitatively analyze the repeated load data whereas the second approach is an analytical procedure that uses statistical techniques to

quantitatively determine the effects of the various stress state variables on the resilient modulus.

- (2) Conclusive evidences from both the graphical and the statistical analysis procedures, clearly indicate that the resilient modulus of cohesive subgrade soils is a function of both soil matric suction and traffic induced stresses as represented by the stress ratio J/T_{oct} . This finding is in good agreement with earlier research work reported by Cole et al. (1986) on granular soils.
- (3) The layering effect within the subgrade material seems to have very little impact on the resilient modulus. This is evident from the ranges of the resilient modulus of the various soil groups (between 8 and 100 MPa or approximately 1 to 10 CBR).
- (4) Although the range of soil strength for all soil groups is almost the same, however, each group has its own distinct resilient modulus expression. This serves to illustrate the point that even if various soils have the same range of structural strength, this consideration by itself alone is not sufficient to draw conclusions about the resilient behaviour of these soils under different climatic conditions. Such predictions can only be made if there exists a mathematical expression that uniquely relates the resilient modulus of the subgrade soil to other stress state variables. Within the general framework of the current research objectives, the task of developing such expressions for typical CI and CI-CL subgrade soils is believed to have been successfully accomplished.
- (5) The effect of the soil dry density, γ_d , on the resilient modulus is not shown explicitly in any of the postulated predictive moduli models for the various soil groups studied. This is because γ_d is highly correlated with soil matric suction and by identifying ψ as significant in affecting M_r , the influence of γ_d on M_r would have already been taken care of.

The following are the main research findings from the field investigation phase:

- (1)** A system for monitoring temperature and soil matric suction distributions within cohesive fine-grained subgrade soils has been developed. This system uses thermal conductivity sensors, of the AGWA-II model, for measuring temperature and soil suction. The developed system has been tested under actual field conditions and found adequate for the purposes of flexible pavement design and rehabilitation.
- (2)** Few technical problems have been encountered during the development of the “temperature - soil suction” monitoring system. These problems deal mainly with the fragility of the sensors to breakage during calibration and field instrumentation, and with the choice of where to place the system’s data acquisition assembly.
- (3)** A high mortality rate of about 42% confines the use of the AGWA-II sensors to research purposes only until a more sturdy construction of these sensors become available to facilitate their use for routine monitoring of soil matric suction under actual field conditions.
- (4)** Despite their fragility, the AGWA-II thermal conductivity sensors used in the current study provided consistent monitoring of matric suction under both freezing and non-freezing conditions. However, interpretation of suction results during the frozen period is difficult due to the significant role played by the latent heat of fusion of the soil water in affecting thermal conductivity measurements. From a pavement engineering standpoint, soil suction monitoring during the frozen period is not needed since the damage to the pavement structure during this period is very minimal.

- (5) Not much variation in soil matric suction has been recorded during both the spring and the summer periods. Typical values obtained during these two periods ranged from 10 to 80 kPa for sensors installed near the top of the subgrade, and from 10 to 55 kPa for sensors installed at deeper locations. This indicates that there are no significant seasonal changes in the soil suction parameter for the particular case study pursued in the present research.
- (6) Two different strategies for analyzing and interpreting the FWD deflection data have been established. The first methodology involved identifying seasonal changes in subgrade strength via graphical analysis of a number of deflection parameters while the second methodology involved back-calculating fundamental material properties, namely the resilient modulus, to be used as potential strength indicators. Both methodologies give comparable results with the back-calculation procedure being more favored over the deflection interpretation method.
- (7) Three deflection parameters have been found to adequately characterize seasonal variations in subgrade stiffness. These are the basin area ratio (*ba*), the subgrade strength index based on fourth sensor deflections (*SSID4*) and the subgrade strength index based on seventh sensor deflections (*SSID7*). The impulse stiffness modulus (*ISM*) and the corrected central deflection ratio (δ_c ratio) appear to provide an assessment of seasonal changes occurring within the overall pavement structure rather than within the subgrade layer. This leads to the conclusion that central deflections and/or *ISM* are not good parameters to use for assessing seasonal changes occurring within the subgrade soil layer.
- (8) Conclusive evidence from deflection data analyses indicate that significant reduction in subgrade stiffness occurs as this layer starts thawing. After this initial

reduction, a long period of unchanged subgrade stiffness of about three months prevails. This is then followed by a gradual increase in subgrade stiffness.

- (9) In terms of back-calculated moduli, the thawed subgrade modulus within the fill section was found to equal 85% of the fall fill section modulus whereas for the cut section it was about 71% of the fall modulus in the cut section. This indicates that the moduli in the cut section experience larger seasonal fluctuations than their counterparts in the fill section.
- (10) Subgrade back-calculated fill moduli were found to be 65% greater than their counterparts in cut area. This is expected, although not in the deterministic sense, and it is indicative of the superiority of the cohesive material in fill area compared to that used in cut area. Such superiority is attributed mainly to the fact that subgrade materials in fill sections are usually placed in greater thicknesses of well compacted layers as compared to their counterparts in cut sections. The result of this will be an overall increase in the subgrade strength within the fill area.
- (11) Careful examination of field subgrade moduli computed from two different deflection data sets that were collected at different times during the day reveals that seasonal variations, as characterized by changes in subgrade stiffness, are insensitive to temperature influences. This means that deflections used in the back-calculation procedure need not be adjusted for temperature effects.
- (12) Attempts to empirically correlate back-calculated moduli with measured responses of temperature, soil suction and computed in situ stresses did not produce satisfactory results. Reasons behind this may be: (a) insufficient amount of data needed for the analysis; (b) narrow ranges of values of some of the parameters

used in the analysis, e.g. soil suction; (c) use of a layered elastic model for stress and moduli computations that assumes a constant modulus value for the full extent of each layer rather than varying the modulus from point to point within the layer.

8.3 Linking Laboratory and Field Results

Findings from both laboratory and field testing investigations emphasize the significant dependence of the resilient modulus of cohesive subgrade soils on both environmental factors and traffic induced stresses. However, linking field back-calculated moduli to laboratory obtained moduli produced less than satisfactory results. Several reasons might have contributed to this. These can be listed as follows:

- (i)** During the laboratory evaluation of the subgrade soil resilient characteristics, the actual stress pulse applied to the lab sample and the actual time dependent response of the sample are not known accurately. This is because these responses were measured by the load cell and the displacement transducer outside, and not inside, the triaxial chamber that contains the tested soil specimen. This carried out practice assumes that the resilient response of the tested soil sample will be the same whether the measurements are performed on the outside or the inside of the triaxial chamber. As a consequence of this, the calculation of the resilient modulus may have been subjected to a number of random errors (instrument error) and systematic errors (assumption that the material is elastic and that the peak load and strain measured outside the triaxial cell fully characterize the material).
- (ii)** Also, during the laboratory testing phase, five soil groups were identified that represent different soil horizons within the subgrade layer. However, during the field back-calculation analysis, the subgrade layer was treated as being elastic with one modulus value that is constant throughout the full extent of the layer. This

assumption which was imposed by the limitations of the computer programs used in the back-calculation of the field moduli and in the computations of in situ stress is believed to have contributed the most to the disagreement that was observed to occur between field and laboratory determined moduli.

- (iii)** The stress pulse used to obtain the lab modulus has a loading time that is substantially different from that applied by the FWD equipment to the in service pavement. This in turn produces different stress distribution within the lab sample as compared to that existing under the FWD loading.
- (iv)** The range of the soil suction parameter measured in situ also differed greatly from that set during the lab tests. This might have caused the soil matric suction to appear as an insignificant parameter in the postulated predictive field moduli models.

In view of the above discussed reasons, the gap between the field and laboratory results can be narrowed down by adopting the following guide lines:

- (i)** Use the resilient modulus test system developed in the current research study to obtain predictive moduli relationships for the particular cohesive subgrade soil in question.
- (ii)** Incorporate the laboratory predictive moduli relationships obtained from repeated load testing as input to modify currently available computer programs that calculate mechanistic responses within pavement structures.
- (iii)** Use such modified computer program(s) to calculate stresses, strains and deflections and compare the results obtained with measured FWD deflections for possible match. When match between measured and calculated deflections occurs,

retain the moduli values used in the computation as the “effective moduli” representing the various pavement layers of the particular pavement structure analyzed.

8.4 Recommendations and areas of Future Research

- (1)** The impact of environmental factors, as represented by temperature and soil matric suction, on subgrade resilient characteristics is more significant than that of traffic induced stresses. This implies that quantification of such effects for all types of cohesive subgrade soils in Alberta constitutes an urgent task that should be accomplished in order to expedite and enhance the current design and rehabilitation practices used for maintaining asphalt concrete pavements in Alberta.
- (2)** Since the subgrade back-calculated fill section moduli were found to be significantly greater than their counterparts in the cut section, it is recommended that current specifications prepared by Alberta Transportation and Utilities pertaining to grade construction be revised. Specifically, the requirement for excavation to be carried to a depth of 0.6m below the designed subgrade surface, should be increased to maximize the performance of newly constructed pavements. This will provide for more uniformity between cut and fill sections.
- (3)** Further verification of the developed Resilient Modulus Test System (RMTS) should be carried out before this system can be used on routine basis for obtaining predictive resilient moduli models. The use of a “standard test specimen” of known stiffness (Pezo et al., 1991) to calibrate the system as a whole is strongly recommended.

- (4)** The suitability of the AGWA-II sensors for monitoring soil matric suction in situ and a solution to the fragility problem of these sensors should be checked for a variety of flexible pavement types (e.g. thin versus thick asphalt concrete pavement structures).

APPENDIX A

CALIBRATION CHARACTERISTICS OF "AGWA-II" THERMAL CONDUCTIVITY SENSORS

- A-1 Calibration Curves of Installed AGWA-II Sensors**
- A-2 Limits of Accuracy of Installed AGWA-II Sensors**

A-1 Calibration Curves of AGWA-II Thermal Conductivity Sensors

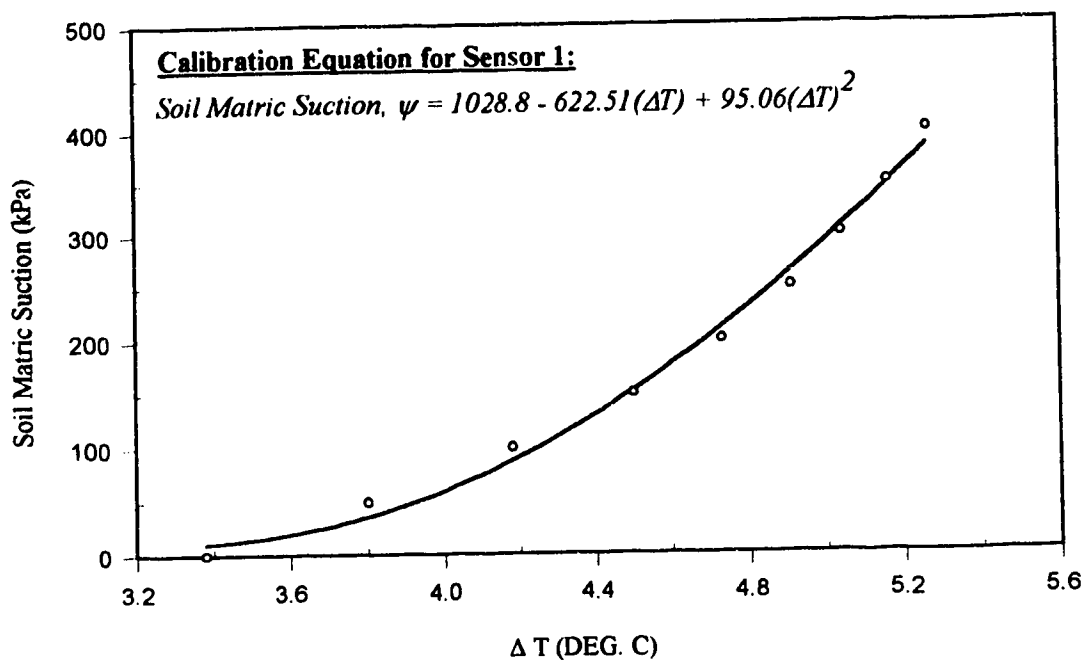


Figure A.1: Calibration Curve for Sensor 1

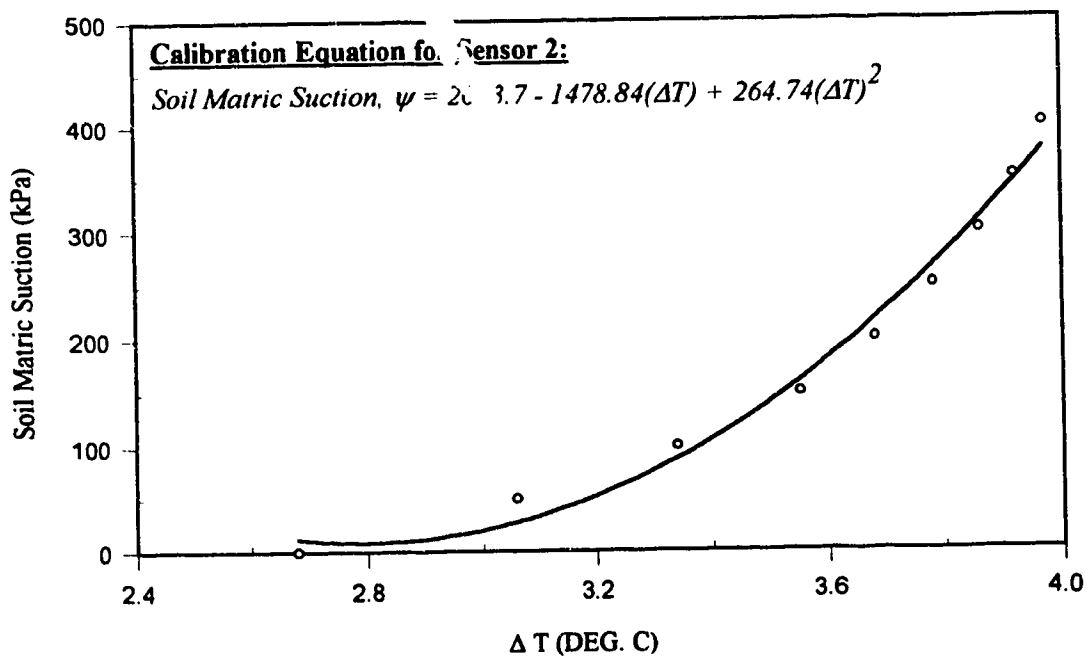


Figure A.2: Calibration Curve for Sensor 2

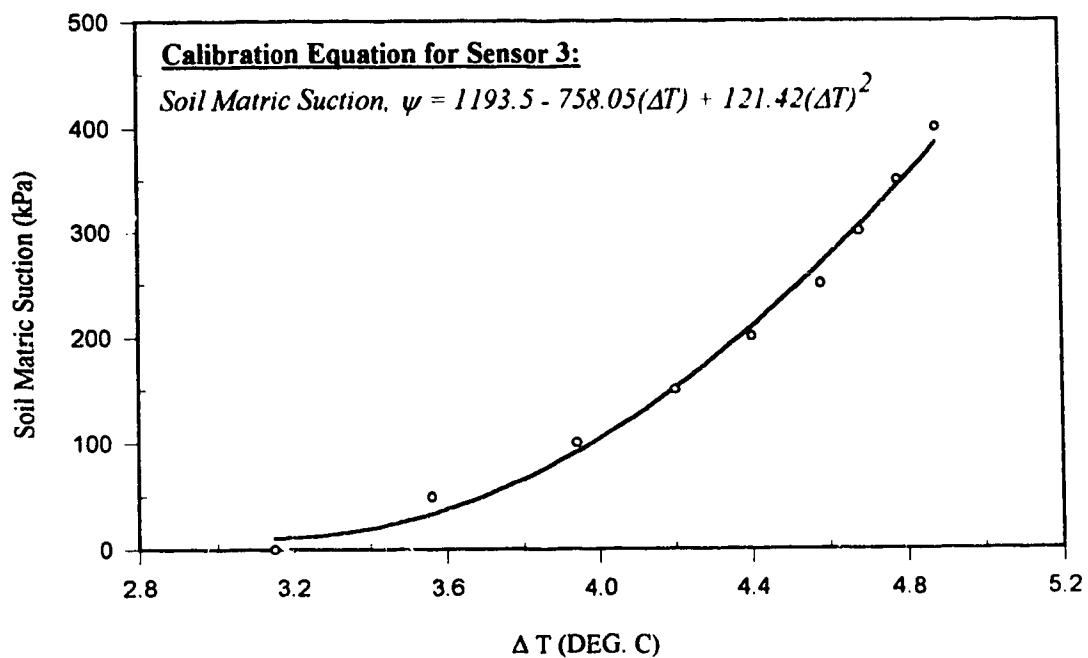


Figure A.3: Calibration Curve for Sensor 3

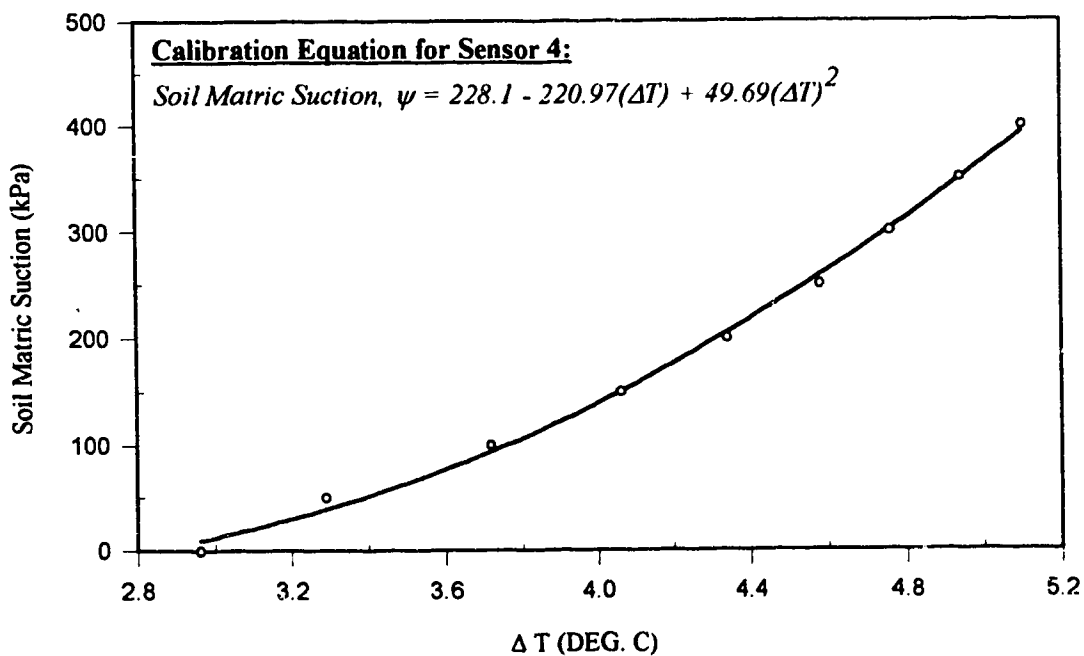


Figure A.4: Calibration Curve for Sensor 4

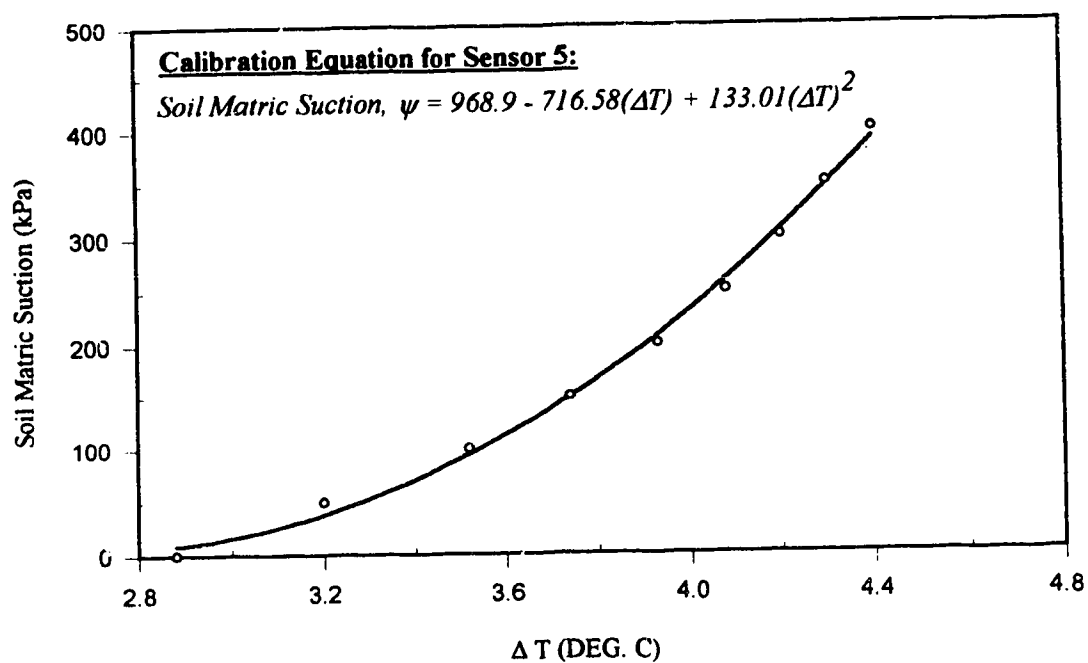


Figure A.5: Calibration Curve for Sensor 5

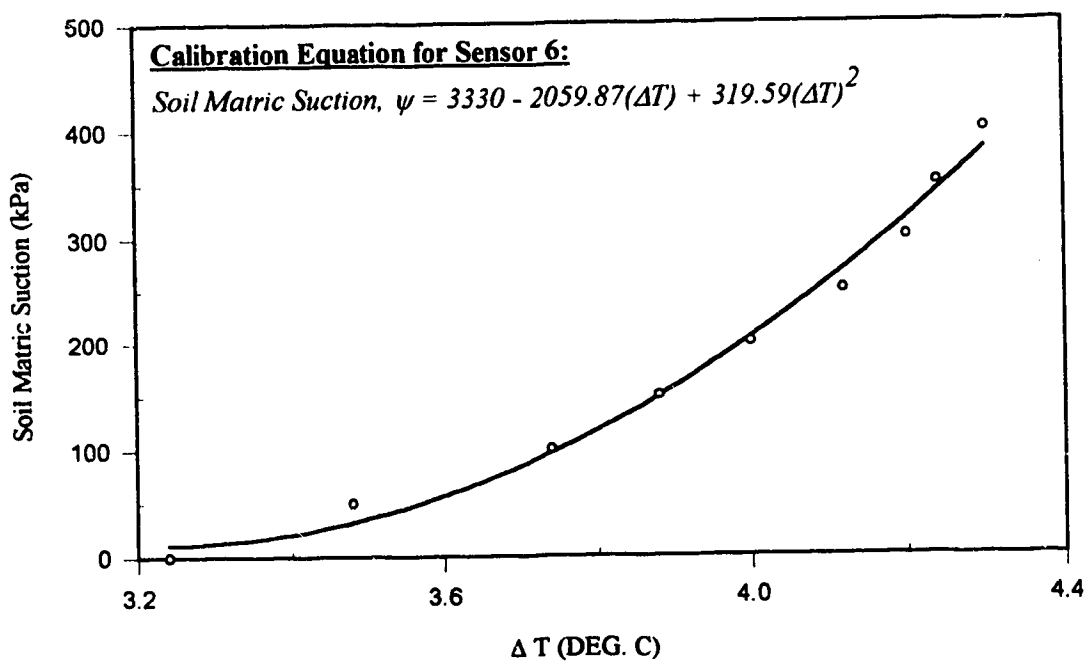


Figure A.6: Calibration Curve for Sensor 6

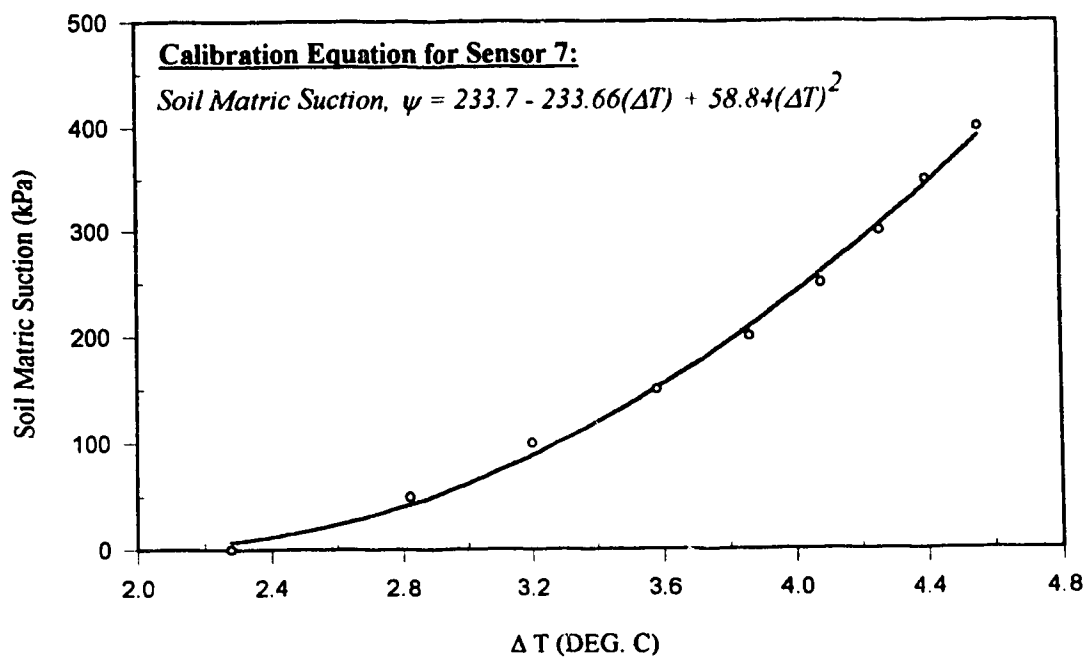


Figure A.7: Calibration Curve for Sensor 7

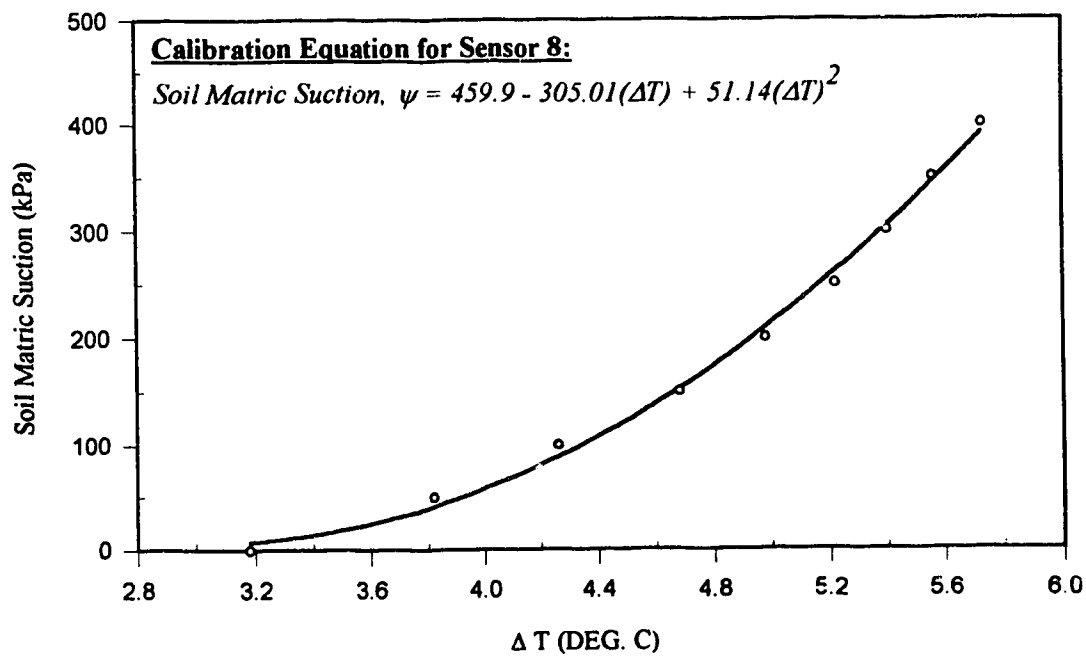


Figure A.8: Calibration Curve for Sensor 8

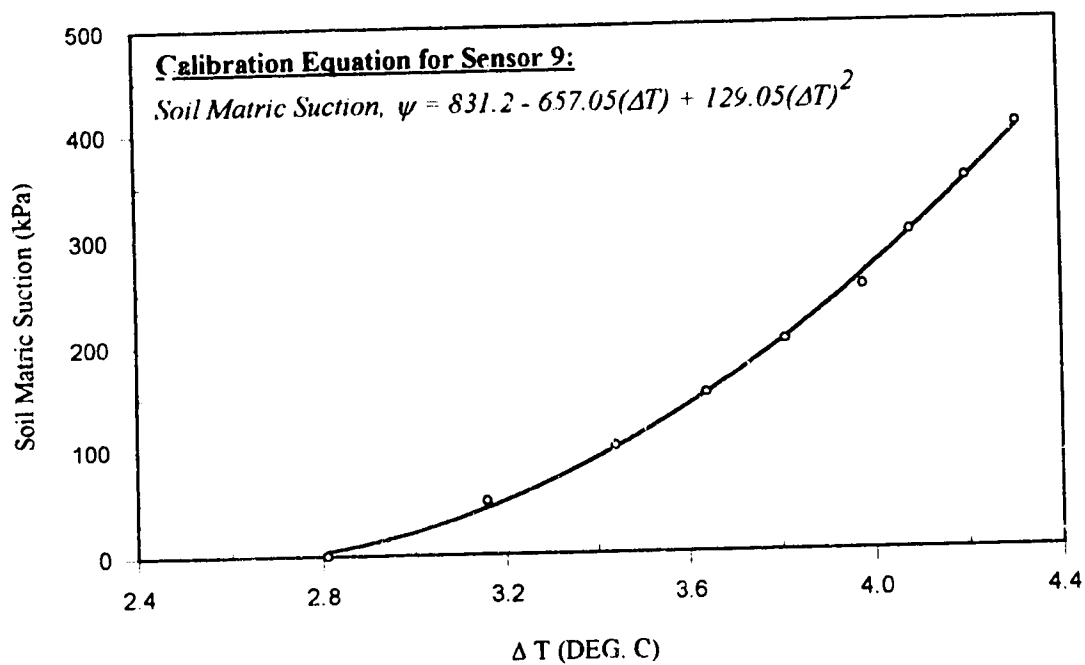


Figure A.9: Calibration Curve for Sensor 9

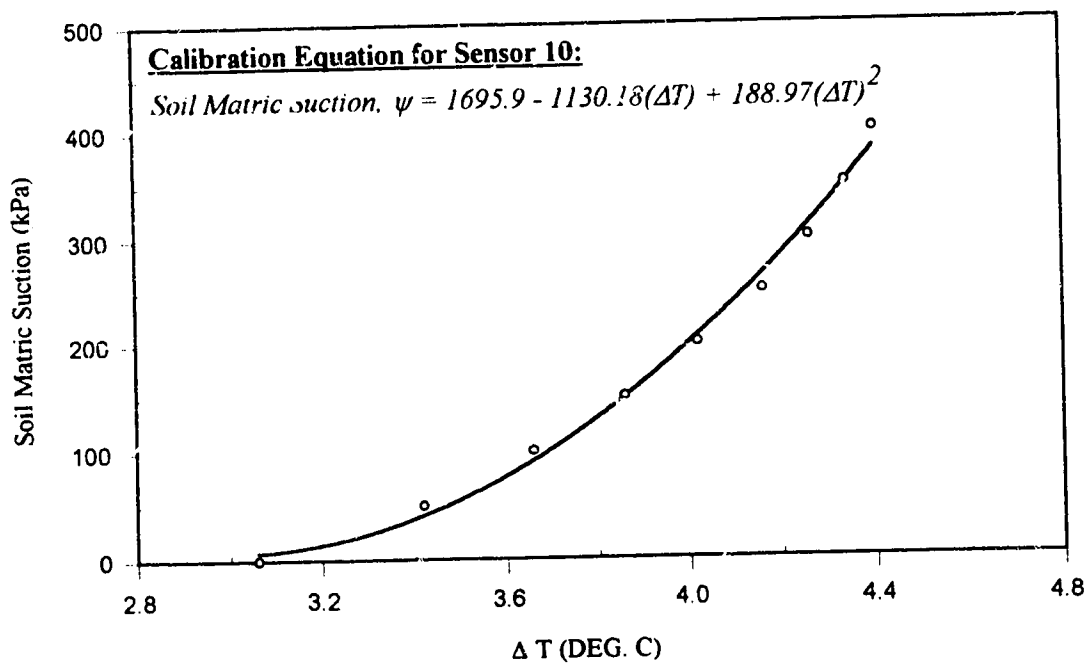


Figure A.10: Calibration Curve for Sensor 10

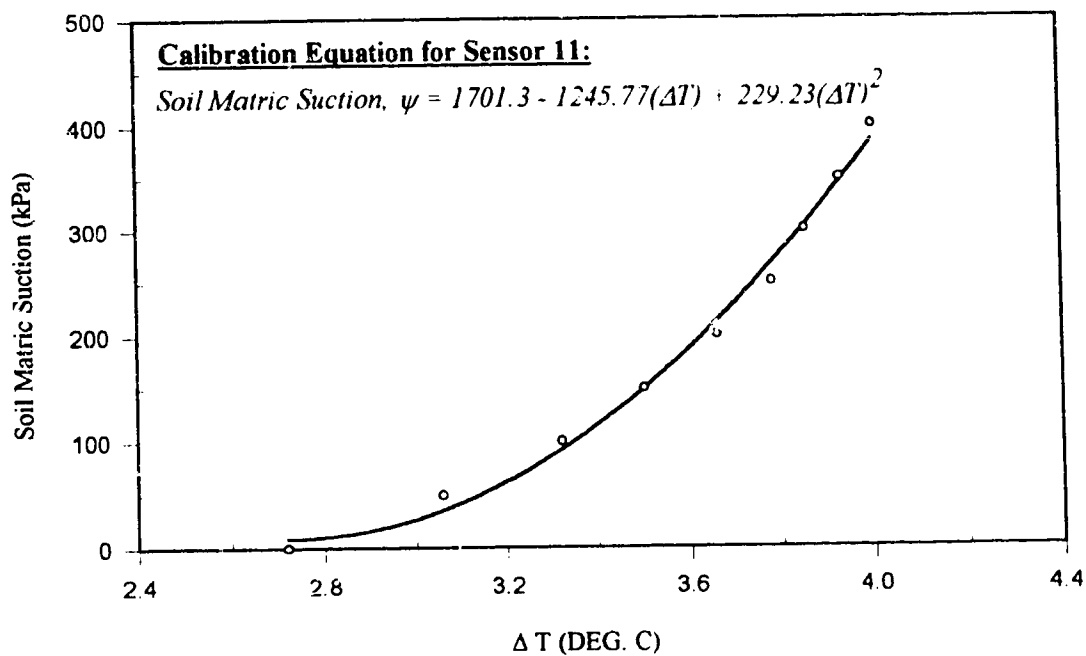


Figure A.11: Calibration Curve for Sensor 11

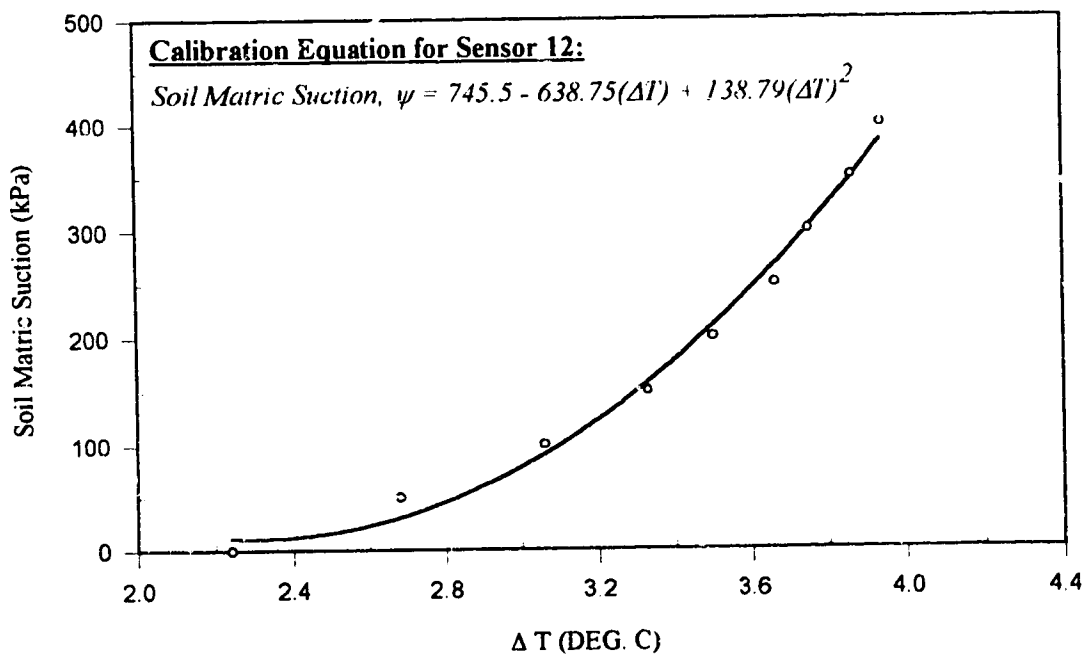


Figure A.12: Calibration Curve for Sensor 12

Table A.1: Limits of Accuracy of Installed AGWA-II Sensors

SENSOR #	Location & Depth	Accuracy in the Range 0 - 175 kPa	Accuracy in the Range 175 - 400 kPa
S 1	Shoulder @ 0.21m	12.5	37.4
S 2	Shoulder @ 0.59m	15.6	70.9
S 3	Shoulder @ 0.32m	13.3	42.9
S 4	IWP @ 0.14m	13.3	27.1
S 5	Shoulder @ 1.14m	16.0	43.4
S 6	IWP @ 1.00m	21.7	64.7
S 7	IWP @ 0.59m	10.6	31.2
S 8	OWP @ 0.16m	9.4	25.8
S 9	OWP @ 0.32m	16.1	40.5
S 10	OWP @ 1.01m	13.8	58.5
S 11	OWP @ 0.84m	16.6	62.8
S 12	IWP @ 0.35m	10.2	47.1

- Notes:** 1. Accuracy (in columns three and four above) is expressed as kPa per 0.1 °C.
2. The calibration curves shown in Figures A.1 to A.12 were approximated by bilinear curves to obtain the accuracy limits displayed in Table A.1 above. All breakage points were observed to occur at a suction value of 175 kPa.
3. The depth referred to in column two of the above table is measured from the top of the subgrade layer (in metres).

APPENDIX B

WATER RETENTION CURVES FOR TESTED SUBGRADE SOIL GROUPS

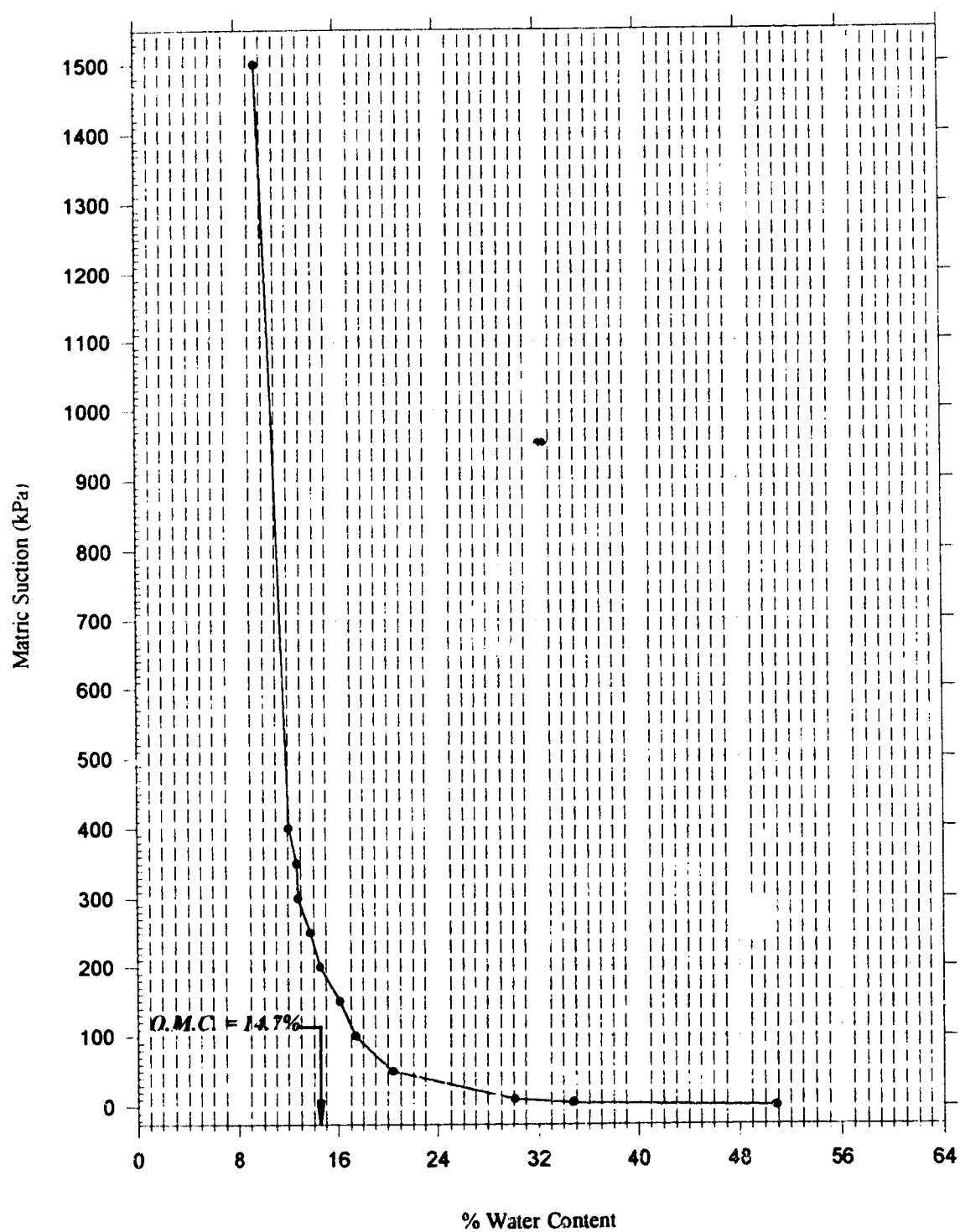


Figure B.1: Moisture Retention Curve for Soil Group 1

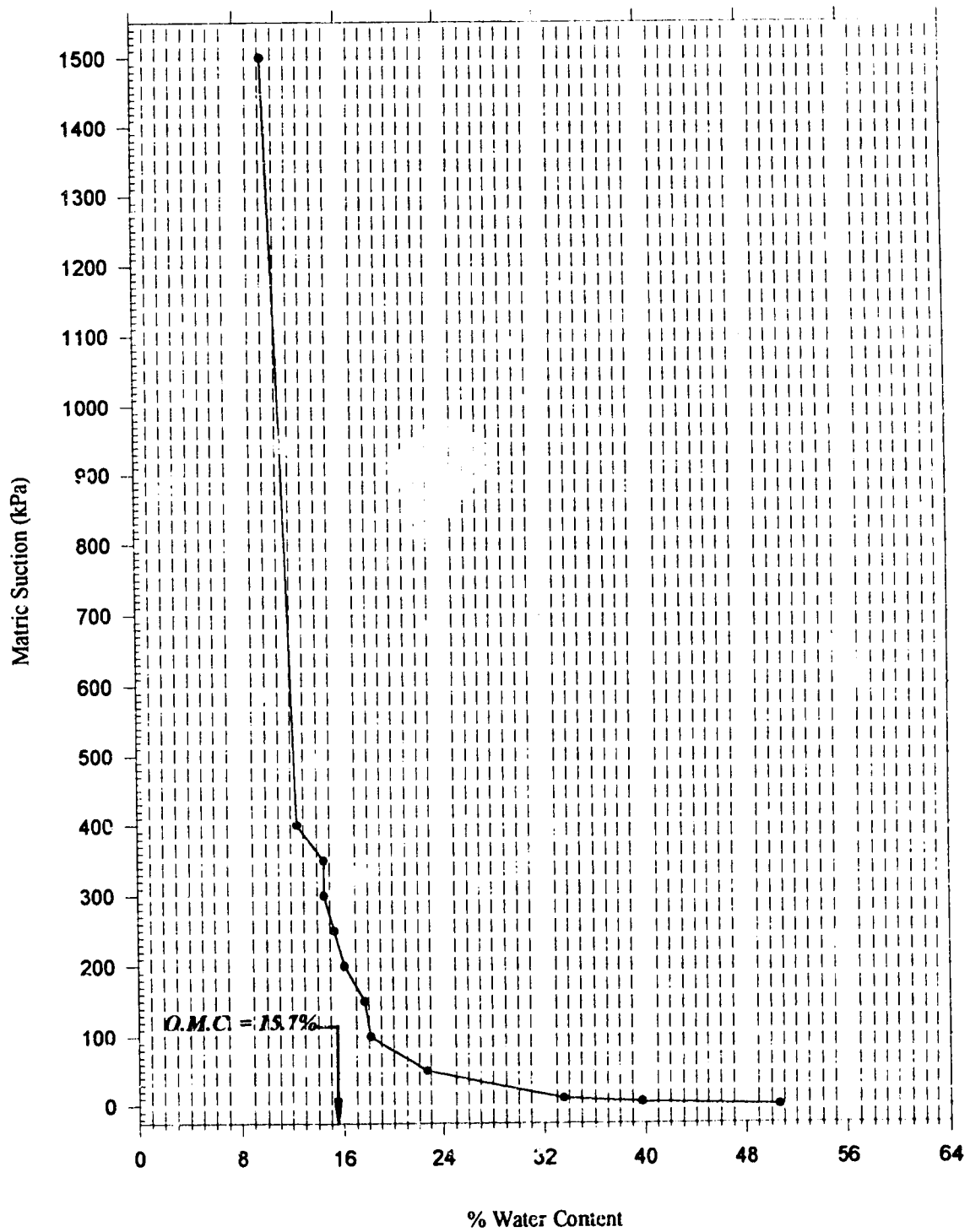


Figure B.2: Moisture Retention Curve for Soil Group 2

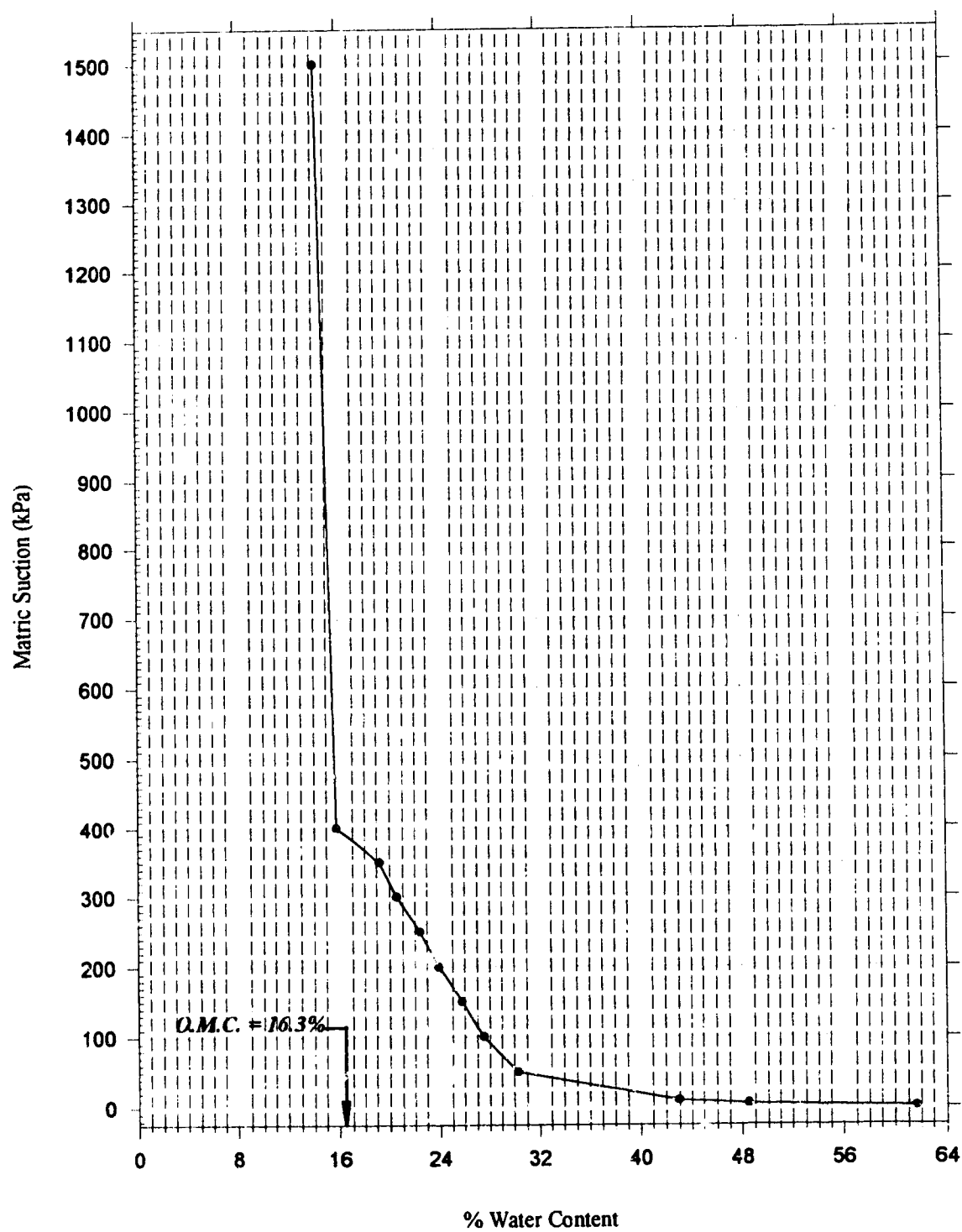


Figure B.3: Moisture Retention Curve for Soil Group 3

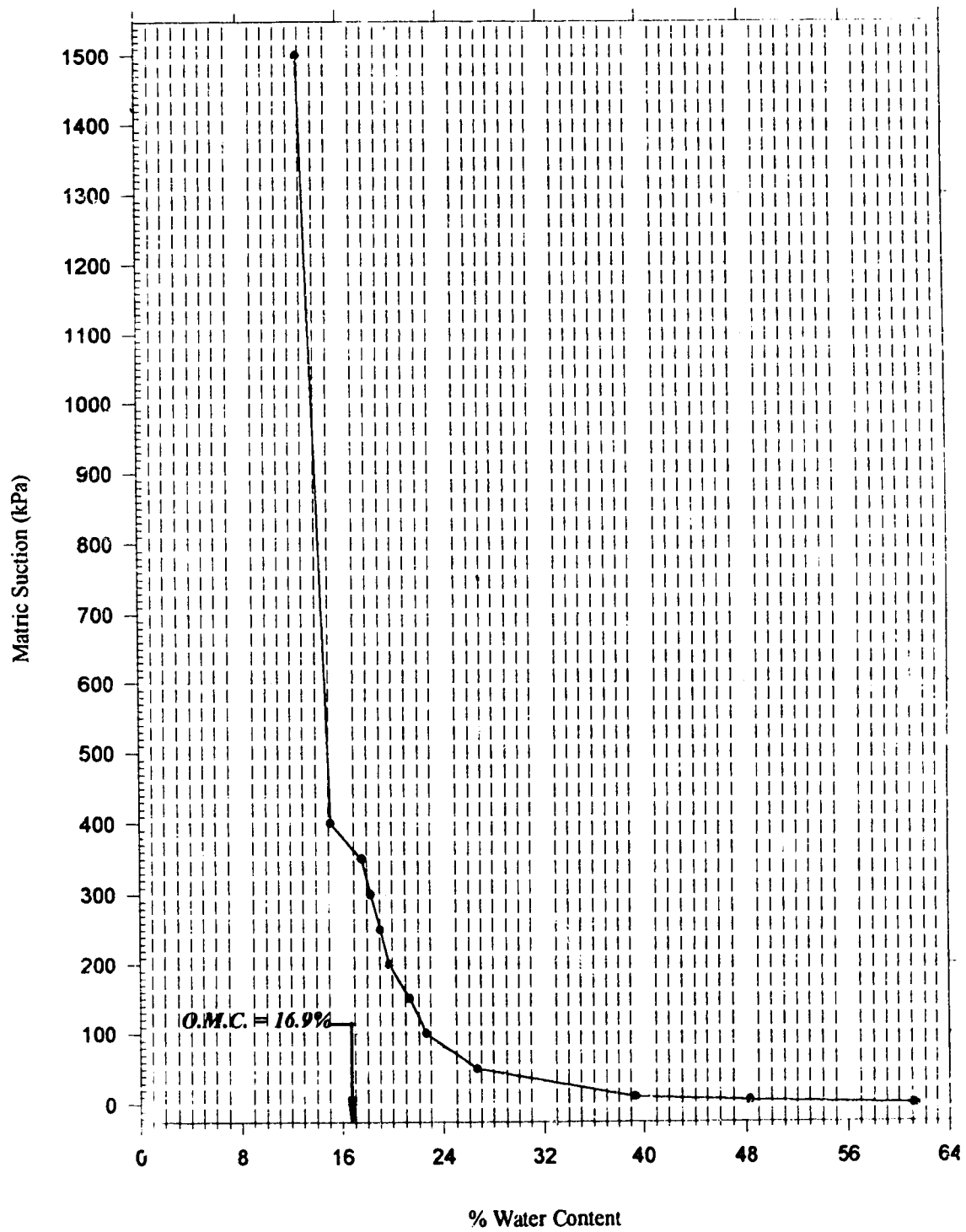


Figure B.4: Moisture Retention Curve for Soil Group 5

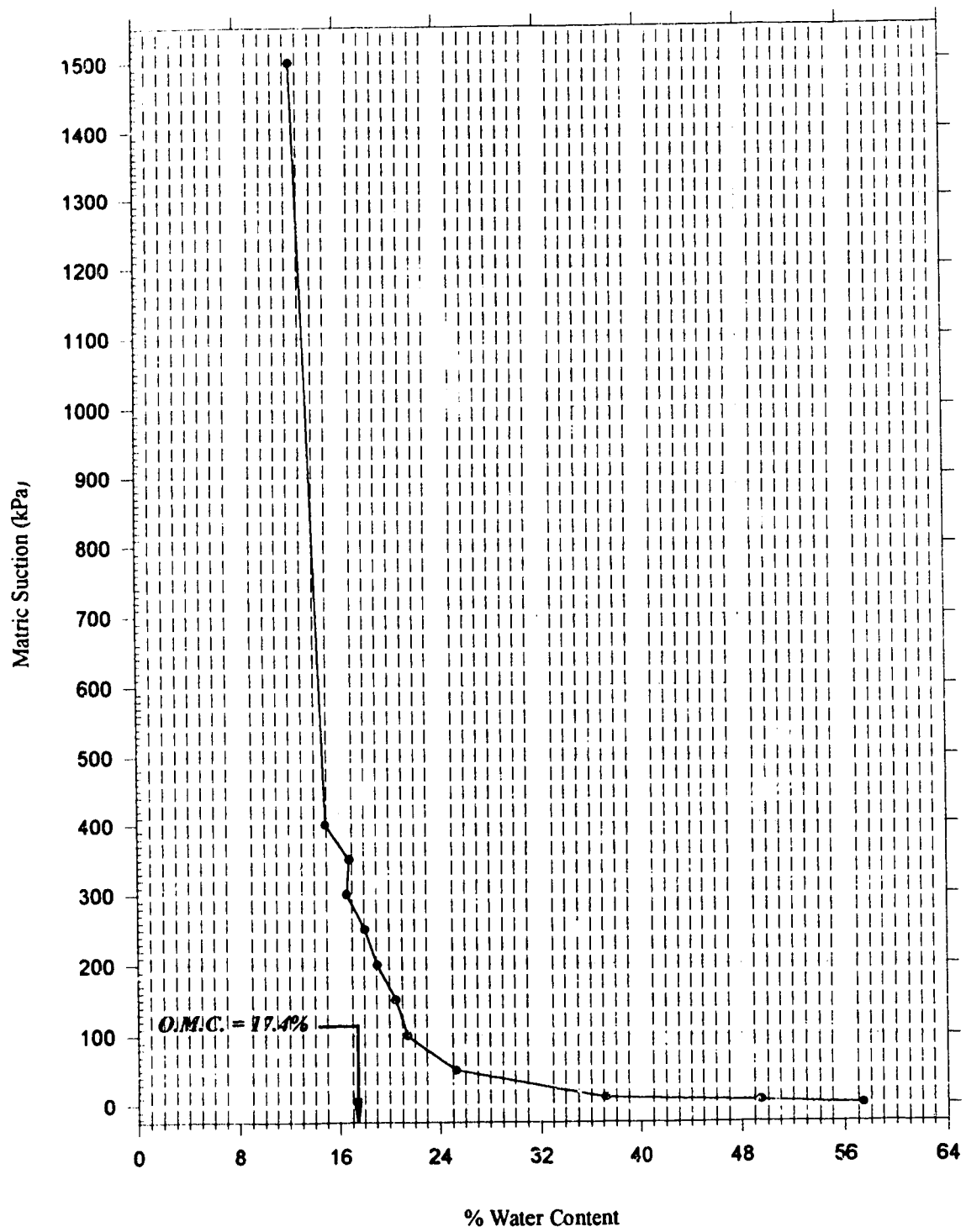


Figure B.5: Moisture Retention Curve for Soil Group 6

APPENDIX C

TEMPERATURE AND SOIL MATRIC SUCTION DATA FROM THE INSTRUMENTED SITE (HIGHWAY CONTROL SECTION 16:12)

- C-1 Data Presentation**
- C-2 Individual Sensor Responses**
- C-3 Limits of Sensors' Calibration**

C.1 Data Presentation

In this section two figures are displayed that show the format chosen to present the temperature and soil matric suction data. Figure C.1 is composed of two plots. The top plot displays the temperature data collected every forty eight-hour while the bottom plot represents the temperature data monitored every two-hour interval. This applies for both air temperature and the temperature measured at the particular sensor location. Figure C.2 is analogous to Figure C.1 except that the former represents matric suction data recorded every twenty four hours and every two hours for the top and bottom plots, respectively.

C.2 Individual Sensor Responses

Figures C.3 to C.14 display the individual sensor response for all installed sensors. Each of these figures consists of two plots: a top plot that shows the seasonal variation in temperature measurements and a bottom plot that displays the seasonal variation in soil matric suction. Commentary and discussions pertaining to these figures are given below.

C.1.1 Temperature Variations

Upon examining the temperature variation curves shown in Figures C.3 through C.14, the following observations can be drawn:

- (1) It is clear that there is a great deal of fluctuations in the recorded daily air temperature. However, temperature measurements performed at each sensor location within the subgrade soil layer do not exhibit the same kind of fluctuations. This indicates that daily temperature changes within the subgrade are moderate and can therefore be accommodated for by recording temperature measurements once every two or more days i.e. there is no need for continuous monitoring every two hours.

- (2) The freezing front during the first winter season (1990-1991) appears to have reached the top of the subgrade layer around November 23, 1990. This is apparent from the location of the 0°C isotherm of sensor 4 which is situated near the top of the subgrade at a depth of 0.78 m from the pavement surface i.e. 0.14m from the top of the subgrade. Further examination of the temperature data reveals that by January 9, 1991, the freezing front has reached a depth of about 1.14m below the top of the subgrade i.e. 1.78m from the pavement surface. This is depicted by the temperature curve for sensor 5 (the deepest sensor), shown in Figure C.7. By examining the air temperature curves, it can also be seen that the minimum air temperature reached was about -5°C. This occurred around January 10, 1991. The minimum air temperature recorded, i.e. -13°C, does not reflect realistically the minimum air temperature experienced during this winter. This is because the collection of the air temperature data was not started at the same time as for the other temperature measurements but rather at a later time. Based on these observations, the average depth of frost within the instrumented pavement section appears to be lying within about 2.00m from the pavement surface. This observation is in good agreement with earlier research findings reported by Shields and Dacyszyn (1965) and by Plewes and Millions (1985).
- (3) Thawing during the first monitoring period, i.e. November 7, 1990 to April 16, 1991, seems to have started around the beginning of April, 1991 (approximately April 2, 1991). From temperature curves, it is clear that sensor 4 started thawing first. This is then followed by sensor 8. Unfortunately, the progress of thaw after that could not be followed due to the malfunction of the data acquisition system experienced between April 6, 1991 and July 16, 1991. Upon resuming data monitoring again from July 17, 1991 onward, all temperature curves show that thawing was already complete at all sensor locations and that high temperature

values indicative of the summer season were prevailing. This can be seen in Figures C.3 through C.14 between July 18, 1991 and September 15, 1992.

- (4) Following the temperature distributional trends for the second year, the freezing front was observed to have reached the top of the subgrade around November 2, 1991. This is also indicated by the 0°C isotherm of the sensor closest to the top of the subgrade layer, i.e. sensor 4. This time, however, it took more than 100 days (actually 109 days) for the frost line to reach the deepest sensor, i.e. sensor 5. This is about one and a half months longer than the time needed to freeze the deepest sensor during the first winter season. Based on this observation and the general trend in temperature variations depicted in Figures C.3 through C.14, it is quite evident that the winter of 1990-1991 was more severe than that of 1991-1992.
- (5) In general, the AGWA-II sensors used in this study seem to provide good and consistent temperature measurements throughout the seasons.

C.1.2 Moisture Variations

The variation in soil matric suction with time was plotted for data points collected every twenty-four hours as mentioned previously. It was observed that when plotting the suction data in this fashion, the general shape of the "matric suction-time" relationship does not change significantly from that when all the data collected every two hours was plotted. This can be seen by comparing the two plots shown in Figure C.2. The only noticeable difference between these two plots, however, is the existence of occasional high matric suction values for the data plotted every two hours. The occurrence of these spikes is unexplainable and can only be attributed either to a temporary malfunction of the particular sensor in question or to a wrongful interpretation of the matric suction value using the specific sensor's calibration curve.

It should be mentioned also that only soil suction values in the range 0 kPa to 400 kPa were plotted. Other values higher than 400 kPa were not considered since they lie outside the calibration range for all installed sensors. Figure C.15 illustrates the magnitude of the error that could be involved when trying to interpret soil suction values beyond the upper and lower limits of calibration. Thus, no attempts have been made to interpret such values in the present discussion.

As it has been mentioned previously in chapter four, the twelve AGWA-II sensors used in the current investigation were installed in their air-dry condition. This was done for two reasons. First, an initially dry sensor provides a more accurate measure of suction because there will be a smaller exchange of water between the soil and the installed sensor. This can be explained in view of the fact that an initially air-dry sensor normally has a water content of about 1% whereas an initially saturated sensor has a water content of about 96% (Sattler and Fredlund, 1989). Natural water contents of soils usually range from 20% to 40% (Fredlund and Pickett, 1982) in the current study the actual range is 18.2% to 26%). Therefore, a larger amount of water that is needed to flow from the soil to the sensor, or vice versa, will occur when the sensor is initially dry. Second, due to the fact that a large amount of water will occur between an initially dry sensor and the surrounding soil, a longer time will be required for equilibrium to occur between the installed sensor and the surrounding soil. This is clearly evident from Figures C.3 through C.14. In general, it was observed that equilibrium between the sensor and the surrounding soil was achieved in about 4 to 8 days (i.e. 100 - 200 hours after installation). This finding is in good agreement with other researchers' work (Wong and Ho, 1987; and Sattler and Fredlund, 1989).

The presentation and discussion of soil matric suction distribution trends during the two-year monitoring period will be divided into two sections:

- (A) Matric suction trends observed during freezing and thawing of the subgrade soil.
- (B) Matric suction trends observed during the non frozen periods.

(A) Matric Suction Variations during Freezing and/or Thawing:

Upon examining Figures C.3 through C.14, it seems that all sensors, with the exception of sensor 7, appear to respond in a similar manner. It was observed that as the subgrade soil starts freezing, approximately 16 days after sensor installation, the matric suction drops sharply and then increases rapidly to approximately the same suction values. This phenomenon, which was also reported by other investigators (Fredlund et al., 1991), can be explained in view of the fact that during freezing, the soil-water starts turning into ice. In fine-grained soils, this transformation normally occurs over an extended range of negative temperatures below 0°C. The result of this process will be a gradual release of the latent heat of fusion of water which will cause the specific heat capacity of the water within the porous sensor to peak sharply and then decrease rapidly as the temperature is lowered further below 0°C as shown in Figure 3.5 in chapter three. At the same time as ice starts forming, the apparent thermal conductivity of the water inside the sensor will increase since the thermal conductivity of ice is four times greater than that of unfrozen water. The combined effect of a decreasing apparent specific heat capacity and an increasing overall thermal conductivity would mean a net increase in the overall thermal diffusivity (this can be seen by referring to equation 3.21 in chapter three). As a result, the temperature rise produced by the heat pulse, used during soil suction measurement, will be small. This small rise in the temperature of the sensor would then be interpreted from the sensor's calibration curve as a decreasing soil suction.

Now, after a major portion of the water within the porous sensor turns into ice, the measured temperature rise due to the heat pulse will depend upon the proportions of both the ice and the remaining unfrozen water, and also upon the quantity of air bubbles that

may be entrapped during the freezing process. It is this amount of entrapped air that is expected to lower the overall thermal conductivity of the porous sensor and thus gives rise to the observed high sensor readings in the frozen state (Fredlund et al., 1991).

Towards the end of the first monitoring period, i.e. from November 7, 1990 to April 6, 1991, the subgrade layer was observed to have started thawing. This would be followed by parallel thawing of the ice within the porous block of the installed sensors. As the ice within these sensors start thawing, a gradual increase in the heat capacity of the sensor occurs (following again the behaviour depicted in Figure 3.5). This increase in the heat capacity of the sensor will cause the temperature rise due to the heat pulse to be small. The consequence of this will again be a sudden drop in suction measurements as the temperature increases towards 0°C.

The above-discussed phenomena that occurred during the first freezing and thawing cycle were observed to happen again during the second monitoring period i.e. from July 17, 1991 to September 15, 1992. However, the picture is somewhat confused during this period. This can be attributed mainly to the existence of those unexplainable spikes that have been alluded to at the beginning of this section.

Although some explanation pertaining to the response of thermal conductivity sensors under freezing and thawing conditions was given, this is actually an oversimplification of what most likely happens in soils during these processes. The greatest difficulty in providing a full explanation of what actually happens during freezing and thawing, lies mainly in the role that the latent heat of fusion of soil-water plays during the phase transformation. As Williams (1964(a) and (b)) stated earlier, even if one could successfully determine the amounts of heat quantities involved in temperature changes in soil in the laboratory, the precise determination of such quantities in situ is difficult, if not

totally impossible, due to the several factors influencing the freezing of the soil moisture pertaining to any soil type. Nevertheless, the aforementioned explanations serve to interpret things reasonably well based on the current state-of-knowledge for obtaining soil suction measurements using thermal conductivity sensors.

Another benefit that could be gained by examining the behaviour of the thermal conductivity sensors during the frozen period, is to make sure that these sensors are still working properly to provide reliable and consistent measurements of the soil matric suction after the first freezing and thawing period elapses.

(B) Matric Suction Trends during the Unfrozen Periods:

By examining Figures C.3 to C.14 after the first winter season, it is evident that there are less variations in soil suction measurements during this monitoring period than those recorded during the first monitoring period. This can be explained in lieu of the fact that freezing and thawing of fine-grained soils may induce some volume changes. These volume changes, which are dependent on soil suction, may become excessive and lead to either soil expansion or contraction. If the latter mechanism prevails, then the soil will shrink away from the sensor causing a gap between the sensor and the surrounding soil. Once the sensor has separated from the soil, the soil suction reading registered will reflect only the amount of water remaining within the sensor porous tip. On the other hand, if the gap between the sensor and the soil becomes filled with water, this will increase the rate of heat transfer due to the induced heat pulse and will consequently lead to errors in sensor readings. Therefore, it appears that either one of these two mechanisms occurred and the result is a consistent decrease in the suction readings after the first freeze/thaw cycle.

Other reasons that might have contributed towards the decrease in suction measurements observed after the first thaw are:

- (i) A big transverse crack was observed to develop within the instrumented section immediately after the first winter period elapsed. This crack might have provided a passage for rain water to flow to sensors' locations and consequently cause a reduction in the recorded soil suction.
- (ii) The backfilling of sensors' holes and/or longitudinal trenches for laying out sensors' lead wires may have not been done properly. This might have eventually caused preferential flows of water along the wires leading to the sensors and caused a reduction in the measured suction values.

In general, the majority of the matric suction values recorded during the first monitoring period ranged from 0 kPa to 85 kPa while those measured during the second monitoring period ranged from 10 kPa to 50 kPa. Within the sensitivity measurement limitations of the various installed sensors (see Table A.1 in Appendix A), these ranges correspond to actual matric suction values of between 0 kPa and 70 kPa for the first period, and 0 kPa and 35 kPa for the second period. This finding indicates that the observed seasonal variations in soil suction throughout the two-year monitoring period is not as large as it has been speculated previously. The implications of this finding on the structural strength of the subgrade soil will be discussed in more details in the section dealing with FWD deflection testing.

Of all the sensors monitored, only three were observed to have recorded higher suction values compared to the remaining sensors. These are sensors # 4, # 8 and # 9. Sensors 8 and 9 measured exceptionally high suction readings during the first monitoring period while sensor 4 exhibited similar behaviour during the second monitoring period. The behaviour of sensors 8 and 9 can be attributed to the fact that the observed high suction readings were obtained when these two sensors were in a frozen state. This can

be seen upon examining the two temperature curves pertaining to these sensors as shown in Figures C.10 and C.11. On the other hand, the observed trend for sensor 4, during the second monitoring period, can be explained in view of the fact that this sensor is the most closest to the pavement surface. Sensor 4 was located within the upper 16 cm of the subgrade soil layer (see Figure 4.10 in chapter four). This location makes the sensor more susceptible to seasonal drying and wetting than other sensors located at greater depths. Another factor that might have also helped in augmenting this effect is the fact that the transverse crack that has developed within the instrumented section was actually observed to have been originated at the location where sensor 4 was installed. This crack then extended to the other edge of the pavement.

Careful examination of Figure C.9 reveals that sensor 7 appears to behave differently from all other sensors. Although the temperature variation curve for this sensor is in line with the other temperature curves of other sensors, however, soil suction readings recorded by sensor 7 seem erratic and do not follow any recognizable pattern. The fact that the ceramic tip of this sensor was broken during calibration and that about half of its original height was lost may be the reason behind this behaviour. This is because the heat pulse generated during suction measurement will not be fully contained within the ceramic tip of the sensor and as a result measurements will depend not only on the thermal conductivity of the porous tip but also on the thermal conductivity of the surrounding soil. In other words, the measured sensor outputs will be converted into soil suction readings using the wrong calibration curve. Although this incident was known prior to sensor installation, it was believed that it may still be worth putting this sensor in and monitor it closely in hopes that the remaining part of the sensor tip will be enough to contain the generated heat pulse. However, judging from the actual sensor response as observed in situ proves the incorrectness of this assumption.

In addition to sensor 7, sensors 5, 8, 10 and 12 also behaved in an unexpected manner during the second monitoring period. Some explanations pertaining to the behaviour of these sensors may be summarized as follows:

- (1) For sensor 5, some difficulty was experienced during the installation of this device. Due to its deep location, approximately 1.78m from the pavement surface, not enough indentation could be made to ensure a snug fit of this sensor with the surrounding soil. Another problem that was observed to happen is that the sensor fractured during installation. These two reasons, coupled with the effect of the first freeze/thaw cycle might have lead to the sensor being separated from the surrounding soil. Consequently, measured suction readings during this period will be dependent on the amount of remaining water content of the porous tip and as such can not be considered reliable.
- (2) In the case of sensor 8, the device was observed to fracture during installation, same as sensor 5, however, no immediate problem was observed to occur as a consequence of this. This conclusion was arrived at by comparing the response of this sensor with the response of another sensor, i.e. sensor 9, at a comparable depth location. From Figures C.10 and C.11, it is clear that both sensors gave consistent results during the first monitoring period. However, after a complete cycle of freezing and thawing, sensor 8 started behaving erratically. This is depicted by the recorded response shown in Figure C.10 as of July 17, 1991 onward.
- (3) Sensor 10 was observed to have suffered a similar incident to that of sensor 7. However, the partial loss of this sensor porous material was smaller compared to that of sensor 7. This actually slowed down the deterioration of the remaining part of the sensor ceramic block and gave a wrong impression that the sensor is registering correct suction values during the first monitoring period. After one

complete freeze/thaw cycle, the sensor response started deteriorating rapidly and soon thereafter the device stopped functioning properly. This is characterized by the erratic sensor response shown in Figure C.12 from July 17, 1991 onward. It should be emphasized that the sensor response during the first monitoring period is also doubtful, especially in view of the fact that this sensor is located deeply in the subgrade, about 1.65m from pavement surface, where high suction measurements are not common (contrary to what the sensor actually measured during this period).

- (4) No problem was detected for sensor 12 during either calibration or installation. Nonetheless, the sensor ceased to function properly after the first winter of 1990-1991. No explanations can be provided as to the reasons behind this behaviour.

C-3 Limits of Sensors' Calibration

Figure C.15 is an example that illustrates the consequences of extrapolating soil suction measurements beyond the limits of calibration pertaining to the specific sensor in question.

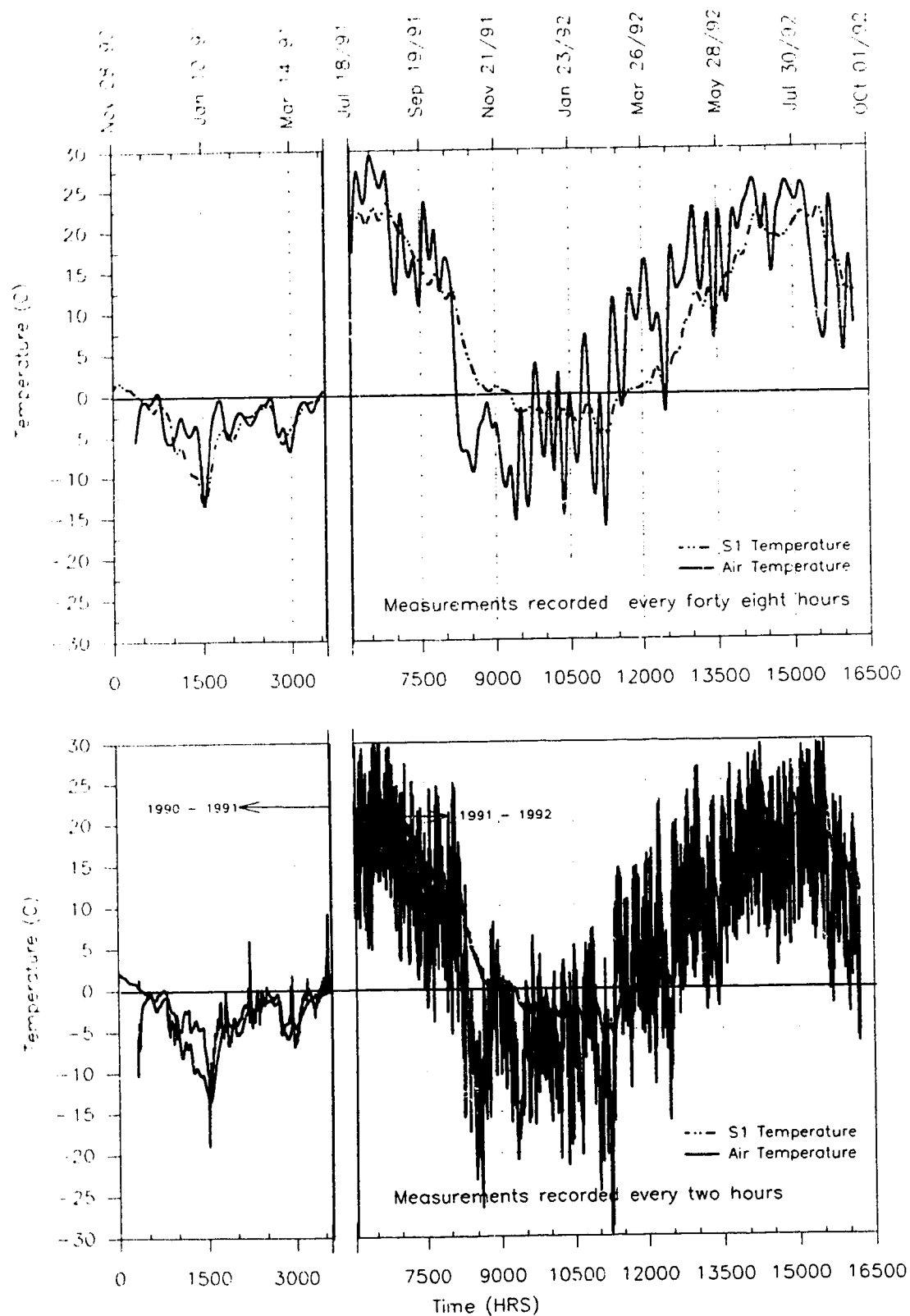


Figure C.1: Seasonal Variation in Temperature for Sensor 1

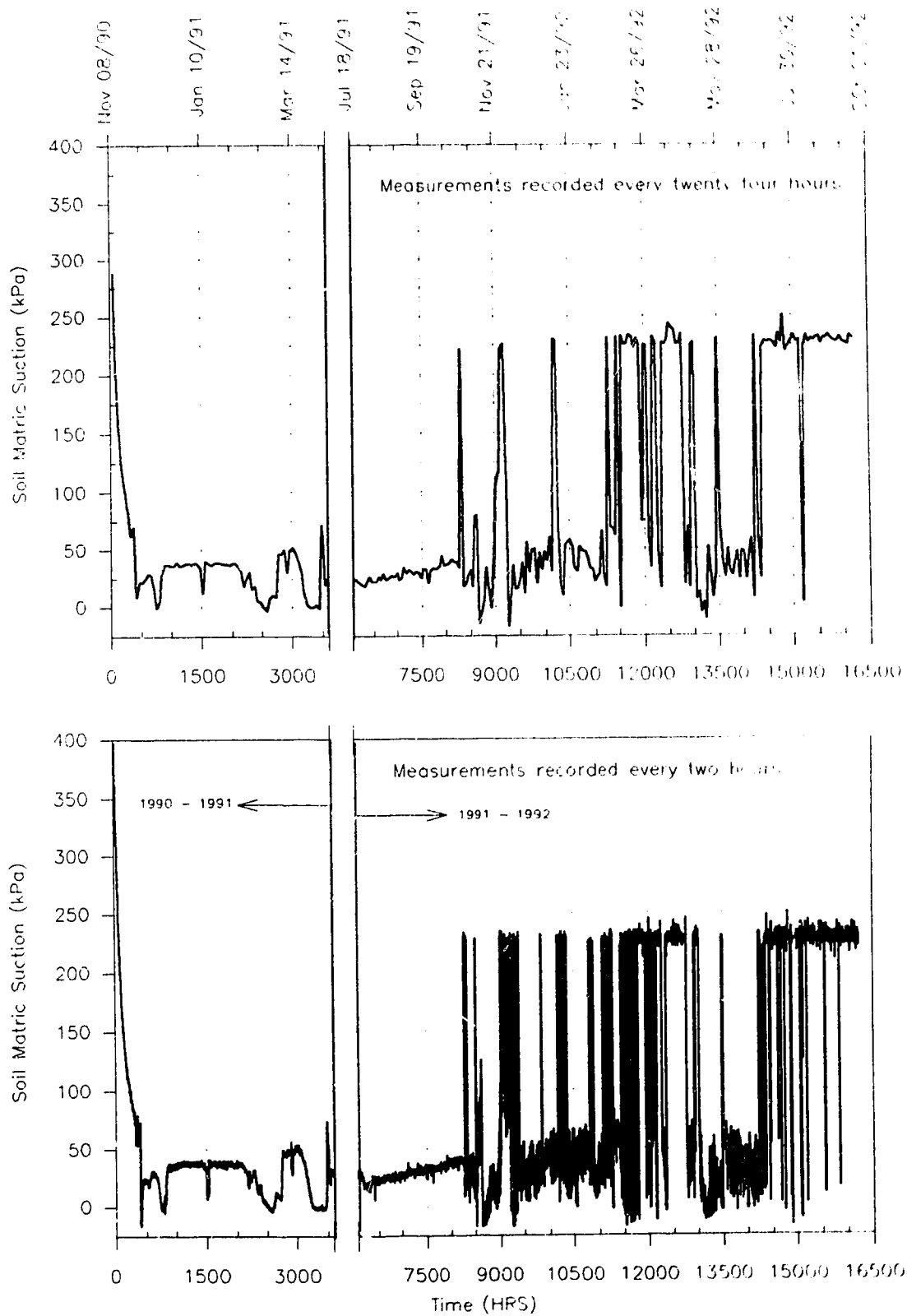


Figure C.2: Seasonal Variation in Soil Matrix Suction for Sensor 4

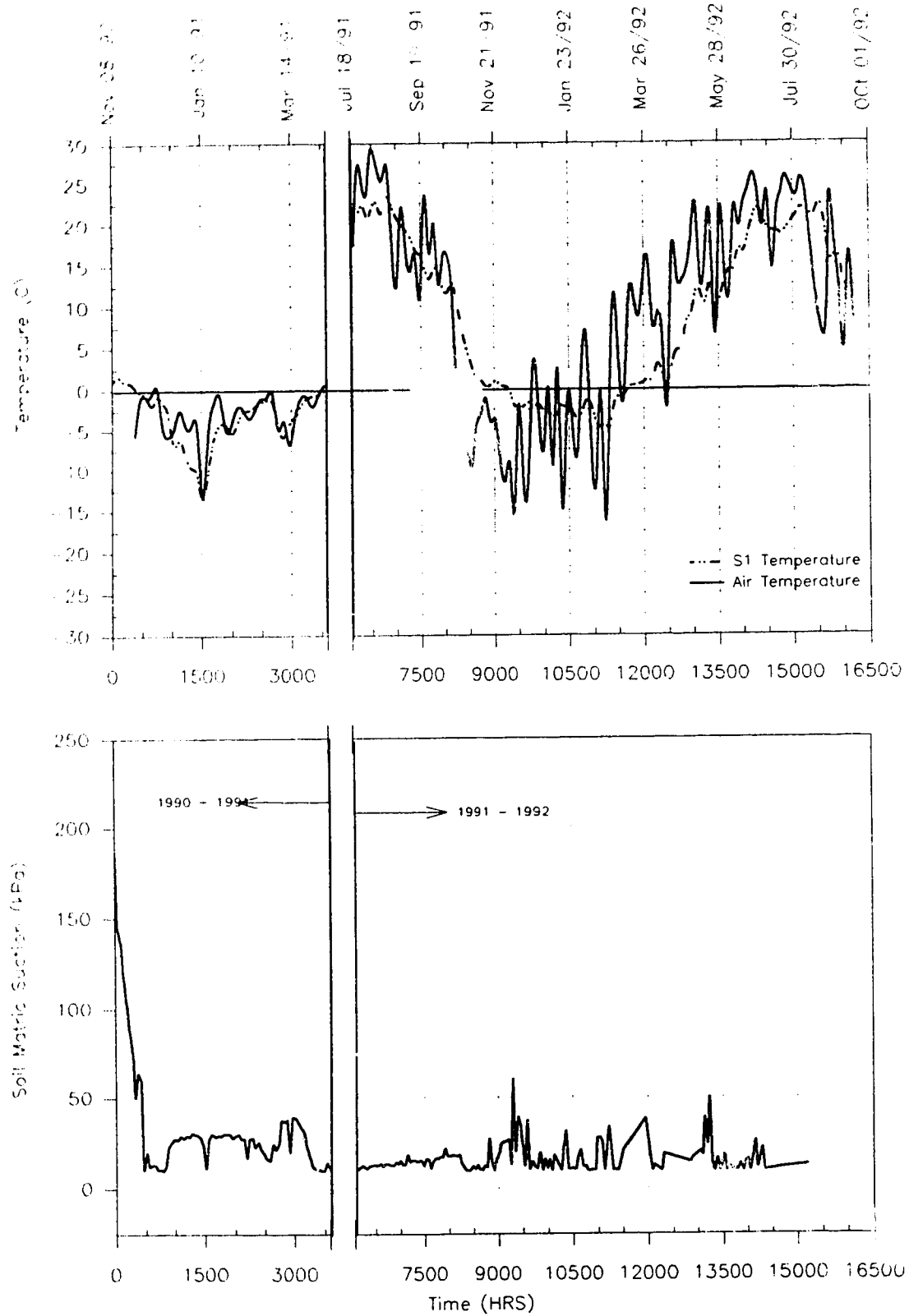


Figure C.3: Seasonal Variation in Temperature and Soil Matrix Suction for Sensor 1 (@ depth of 0.21m)

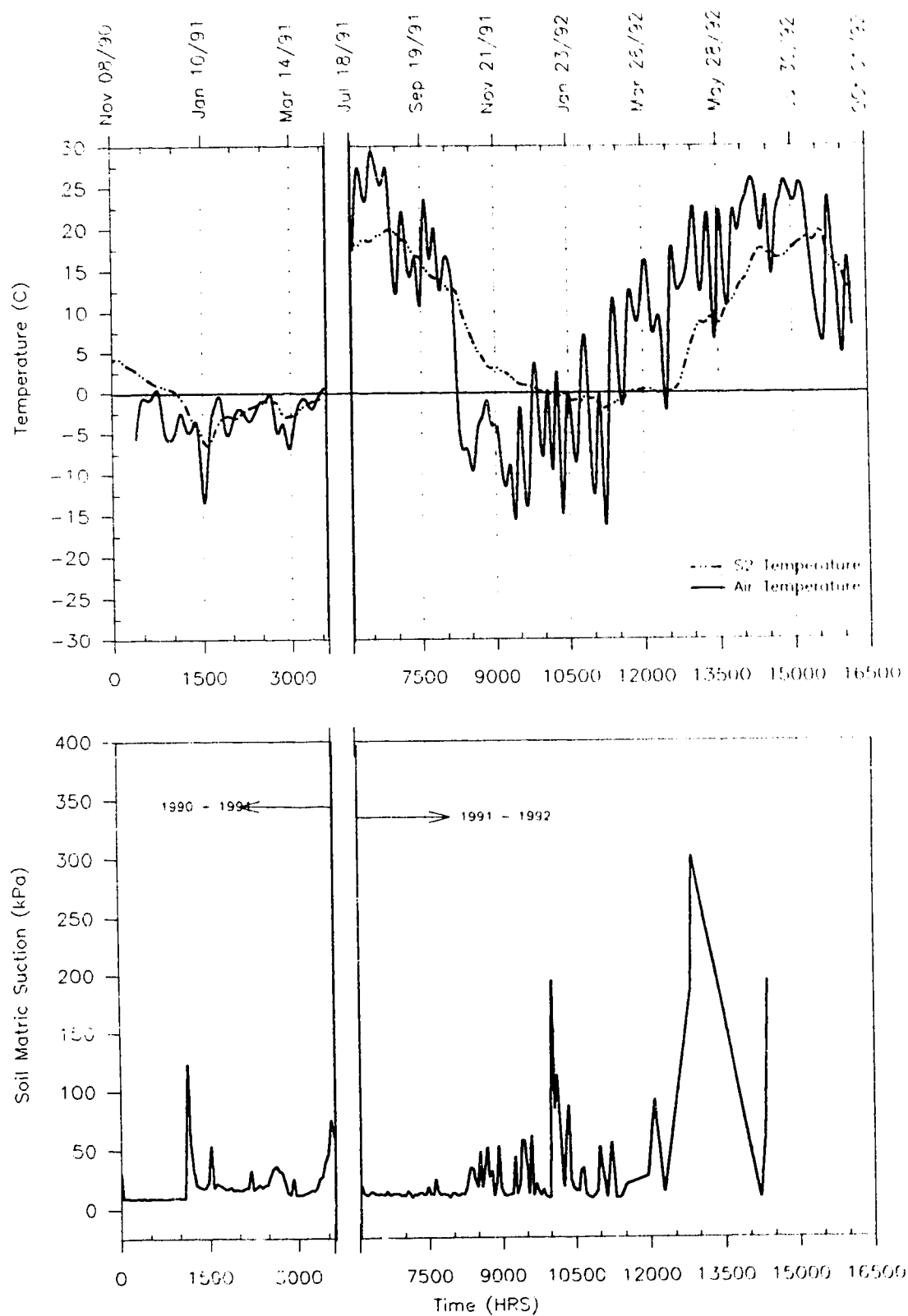


Figure C.4: Seasonal Variation in Temperature and Soil Matrix Suction for Sensor 2 (@ depth of 0.59m)

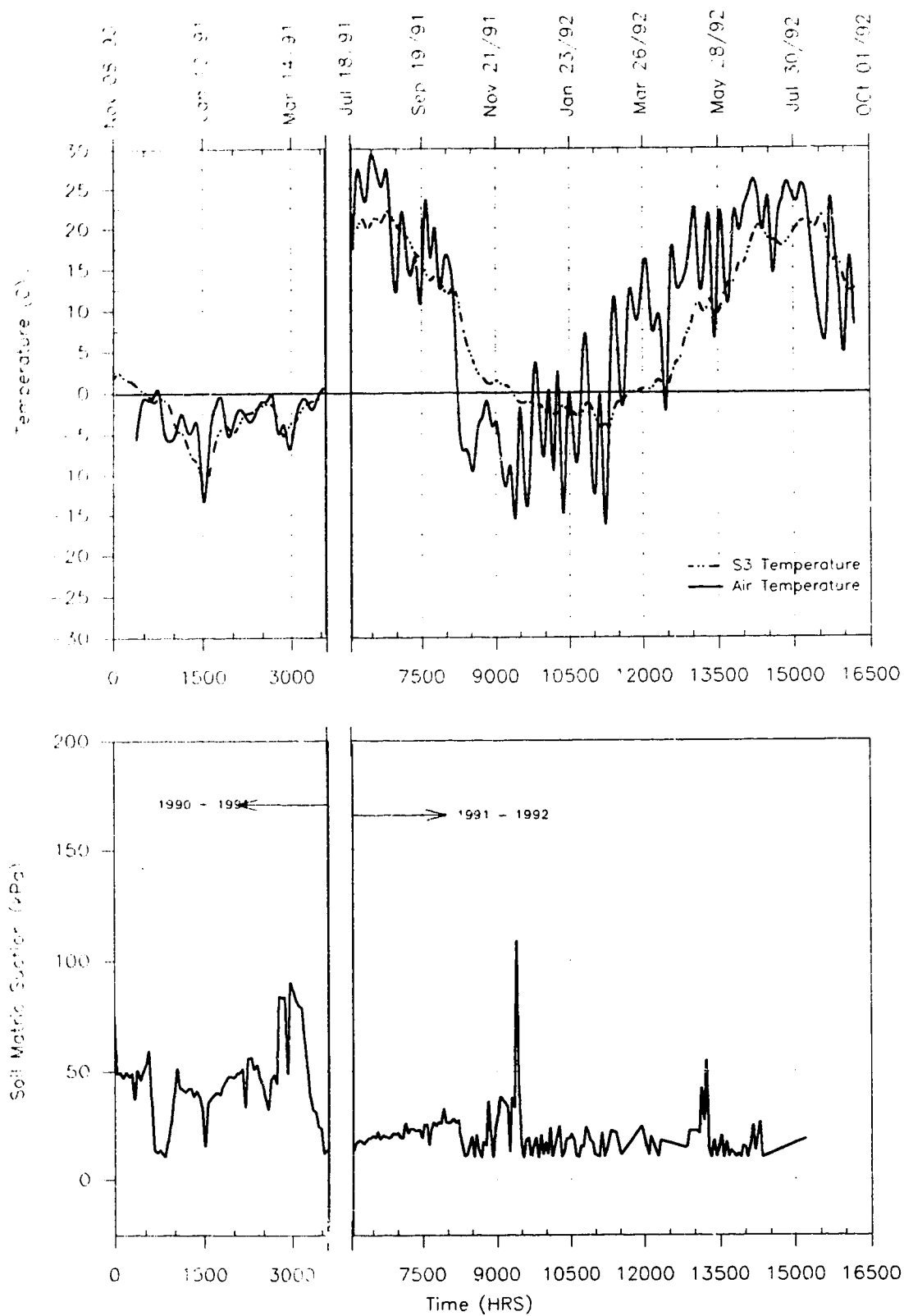


Figure C.5: Seasonal Variation in Temperature and Soil Matrix Suction for Sensor 3 (@ depth of 0.32m)

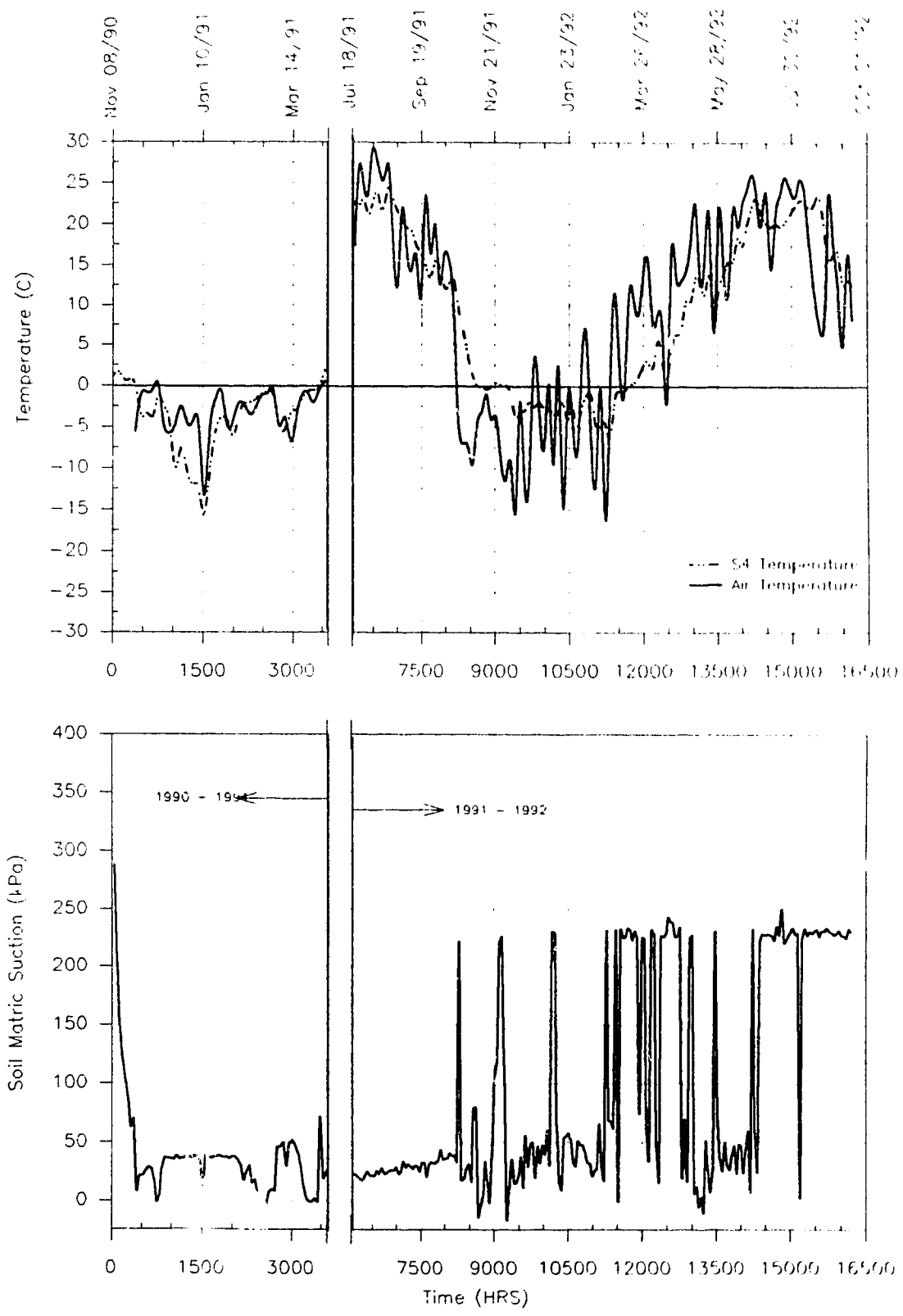


Figure C.6: Seasonal Variation in Temperature and Soil Matrix Suction for Sensor 4 (@ depth of 0.14m)

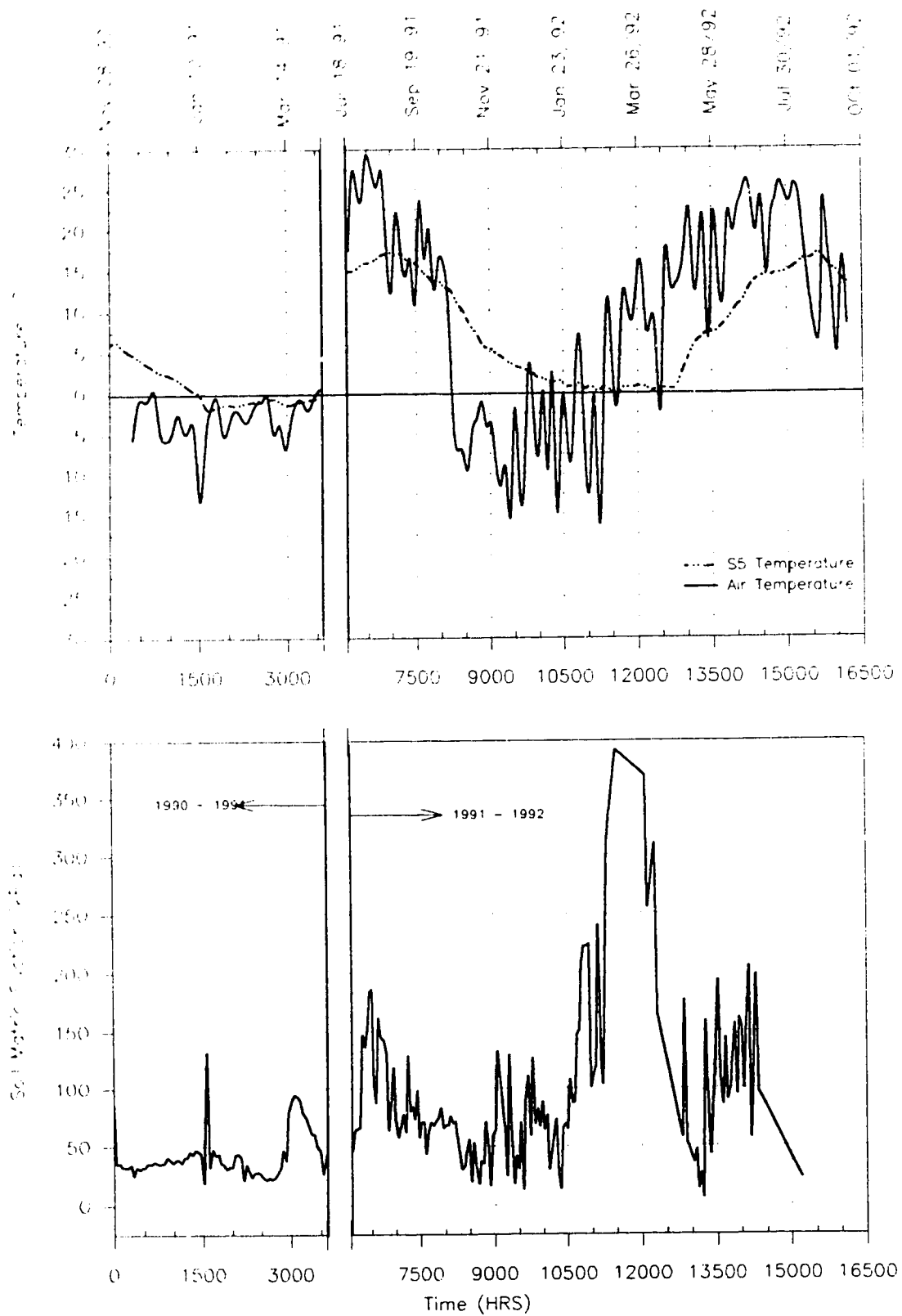


Figure C.7: Seasonal Variation in Temperature and Soil Matrix Suction for Sensor 5 (@ depth of 1.14m)

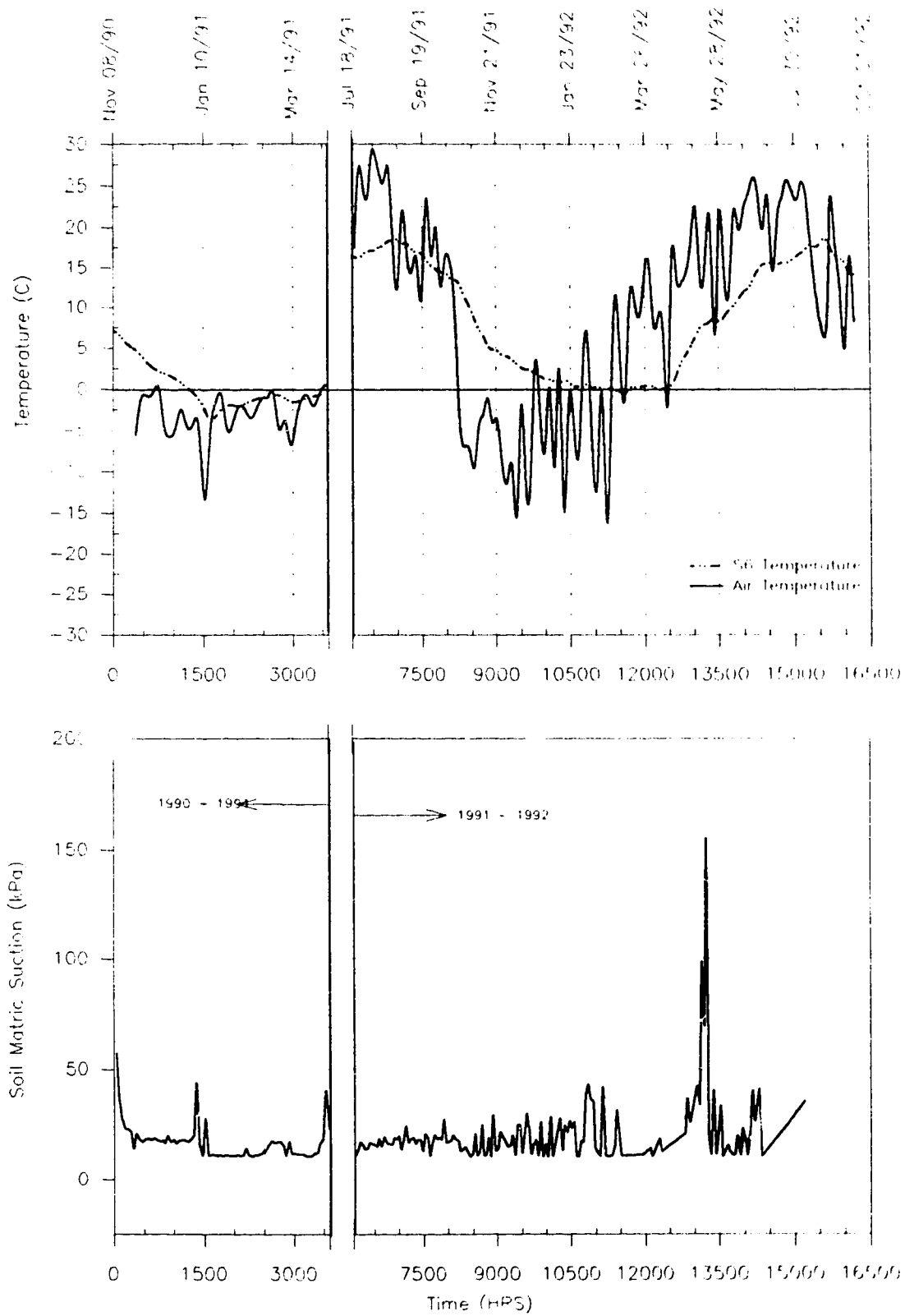


Figure C.8: Seasonal Variation in Temperature and Soil Matrix Suction for Sensor 6 (@ depth of 1.00m)

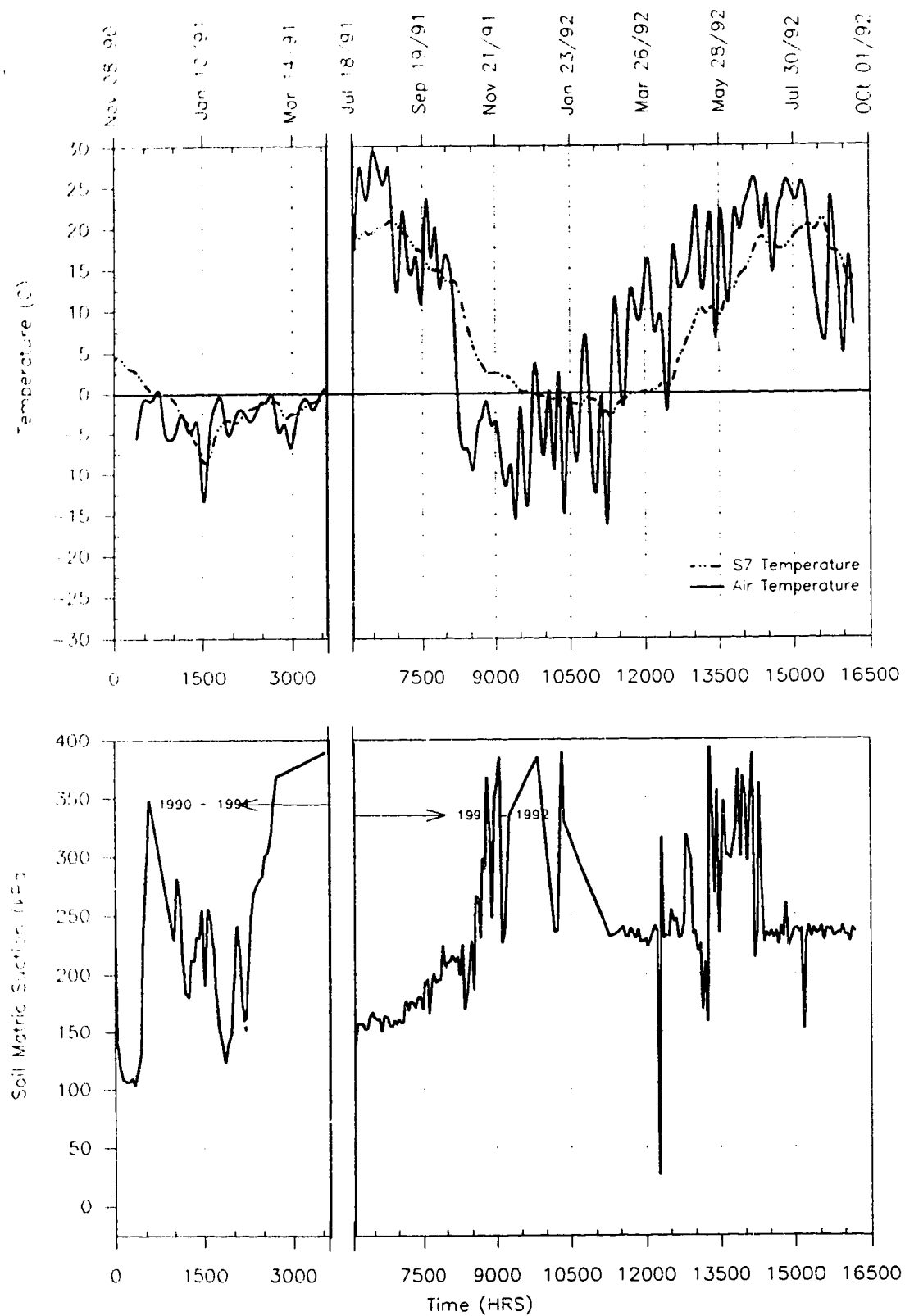


Figure C.9: Seasonal Variation in Temperature and Soil Matric Suction for Sensor 7 (@ depth of 0.59m)

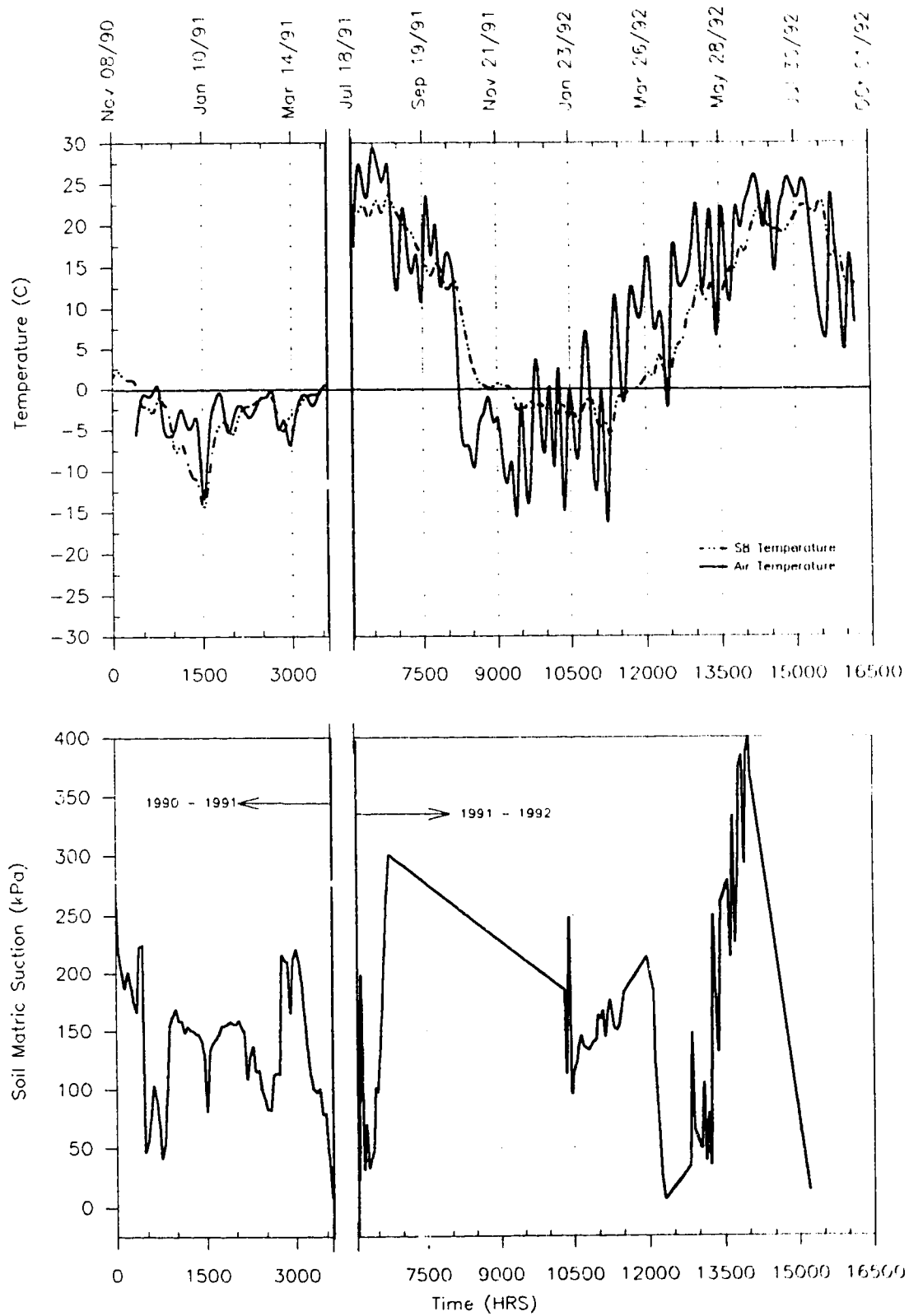


Figure C.10: Seasonal Variation in Temperature and Soil Matrix Suction for Sensors 8 (@ depth of 0.16m)

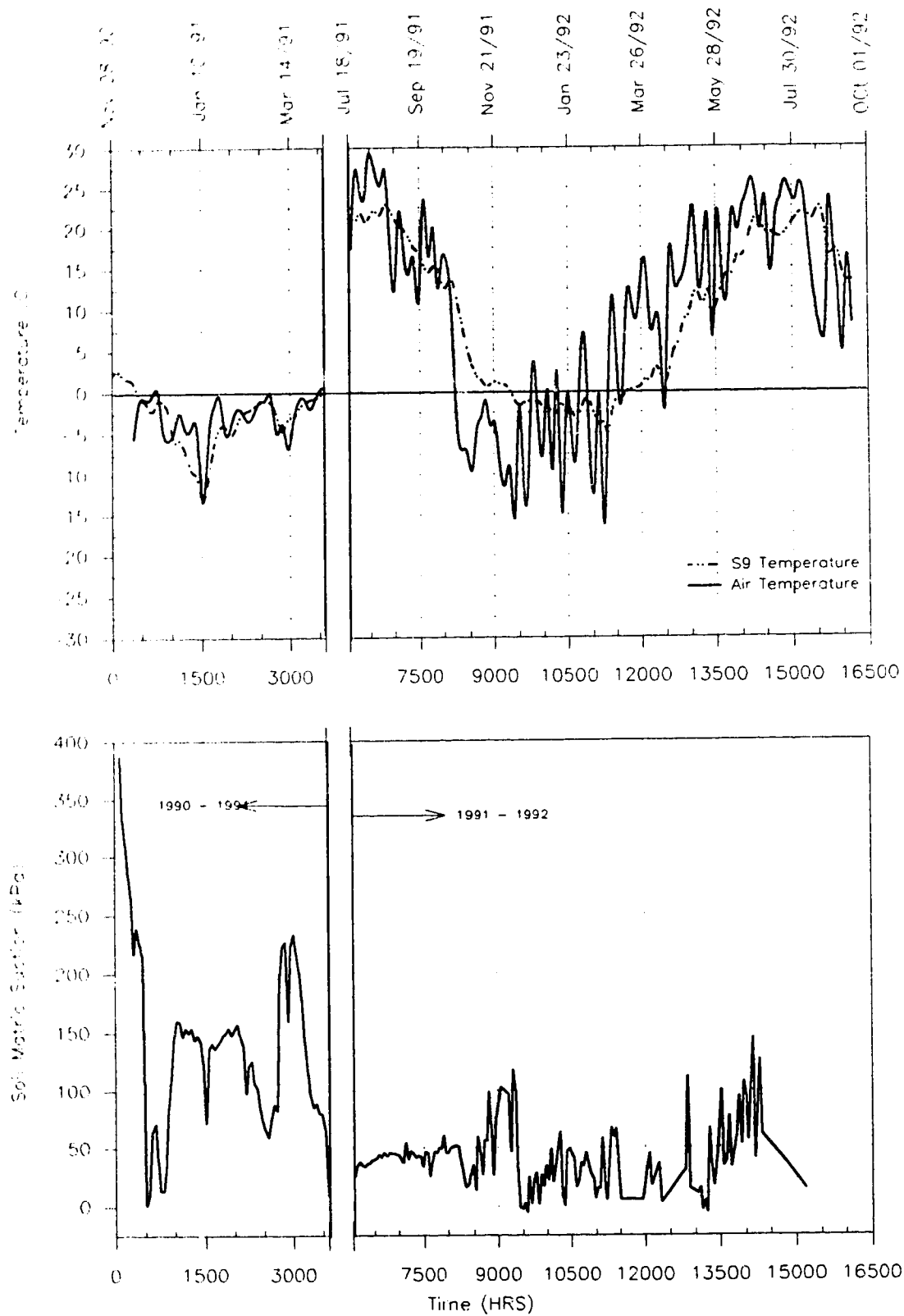


Figure C.11: Seasonal Variation in Temperature and Soil Matric Suction for Sensor 9 (@ depth of 0.32m)

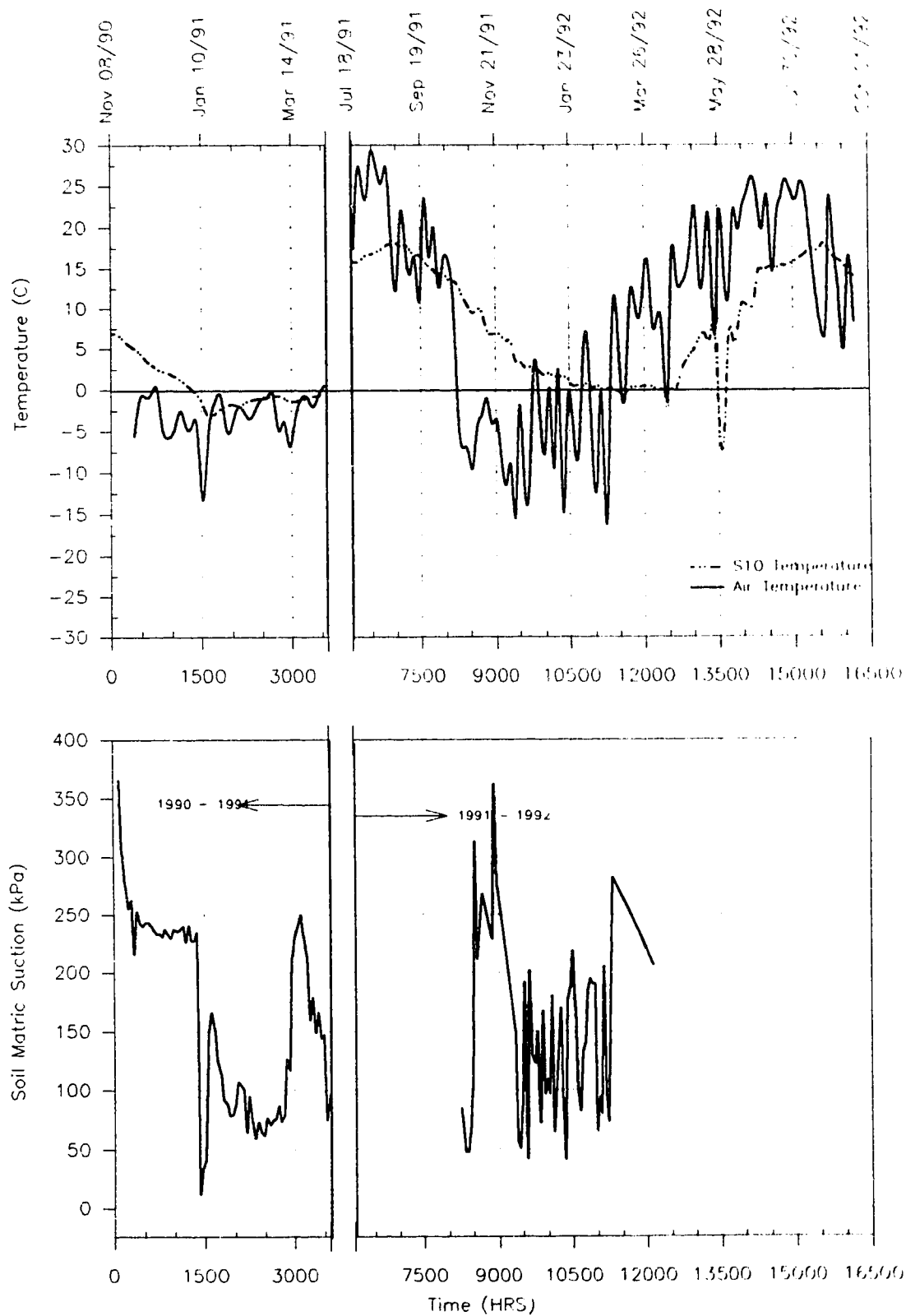


Figure C.12: Seasonal Variation in Temperature and Soil Matrix Suction for Sensor 10 (@ depth of 1.01m)

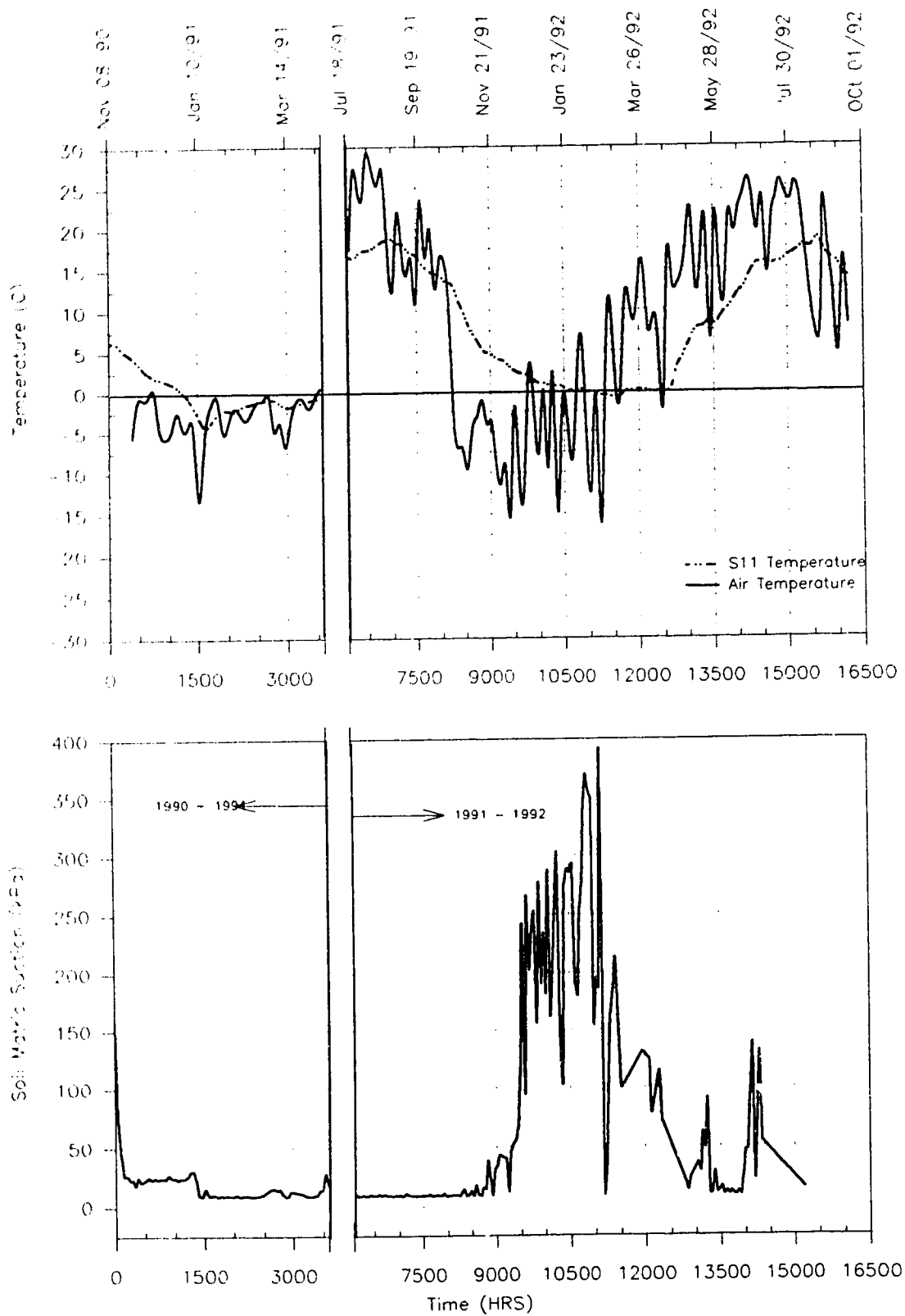


Figure C.13: Seasonal Variation in Temperature and Soil Matric Suction for Sensor 11 (@ depth of 0.84m)

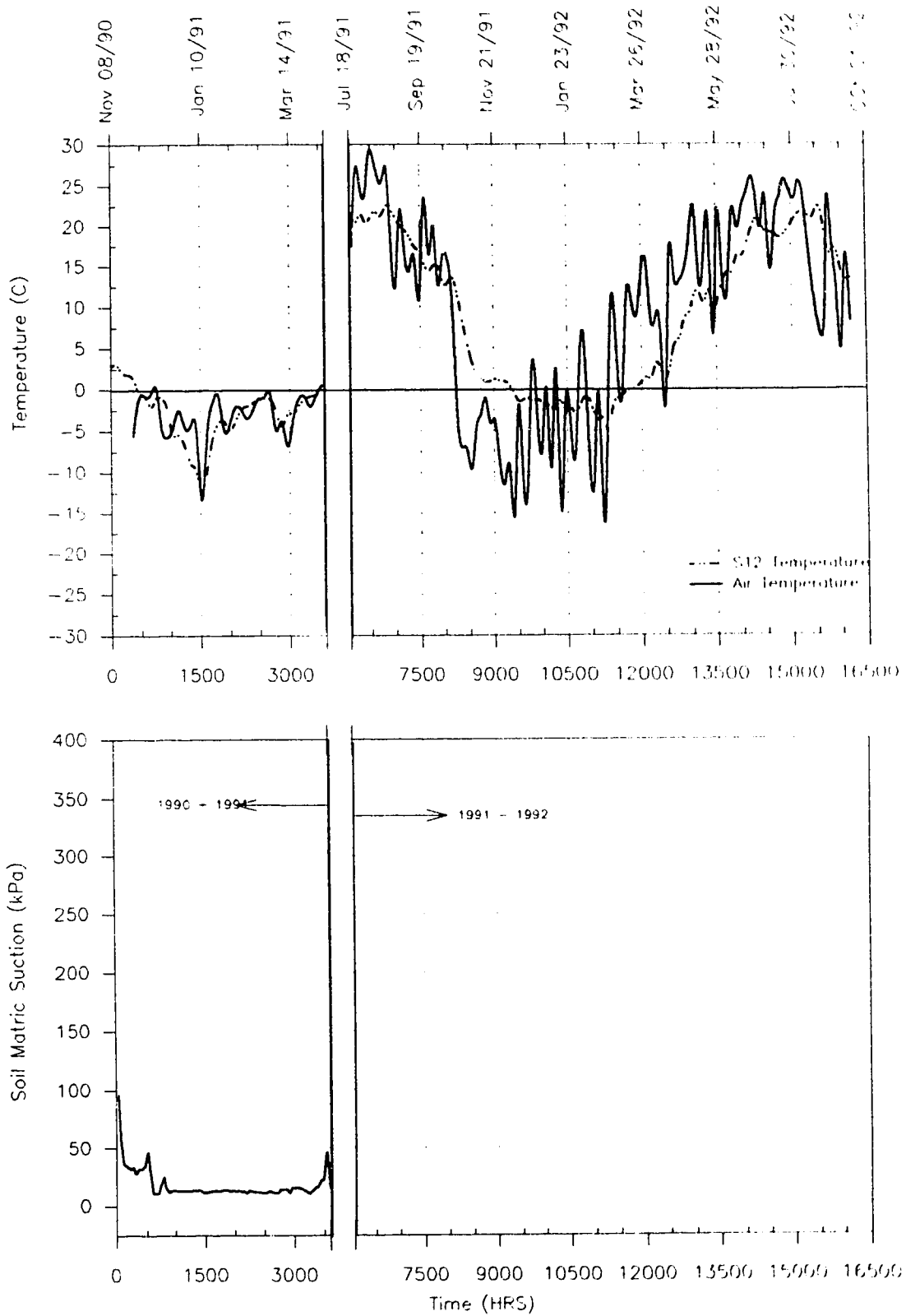


Figure C.14: Seasonal Variation in Temperature and Soil Matrix Suction for Sensor 12 (@ depth of 0.35m)

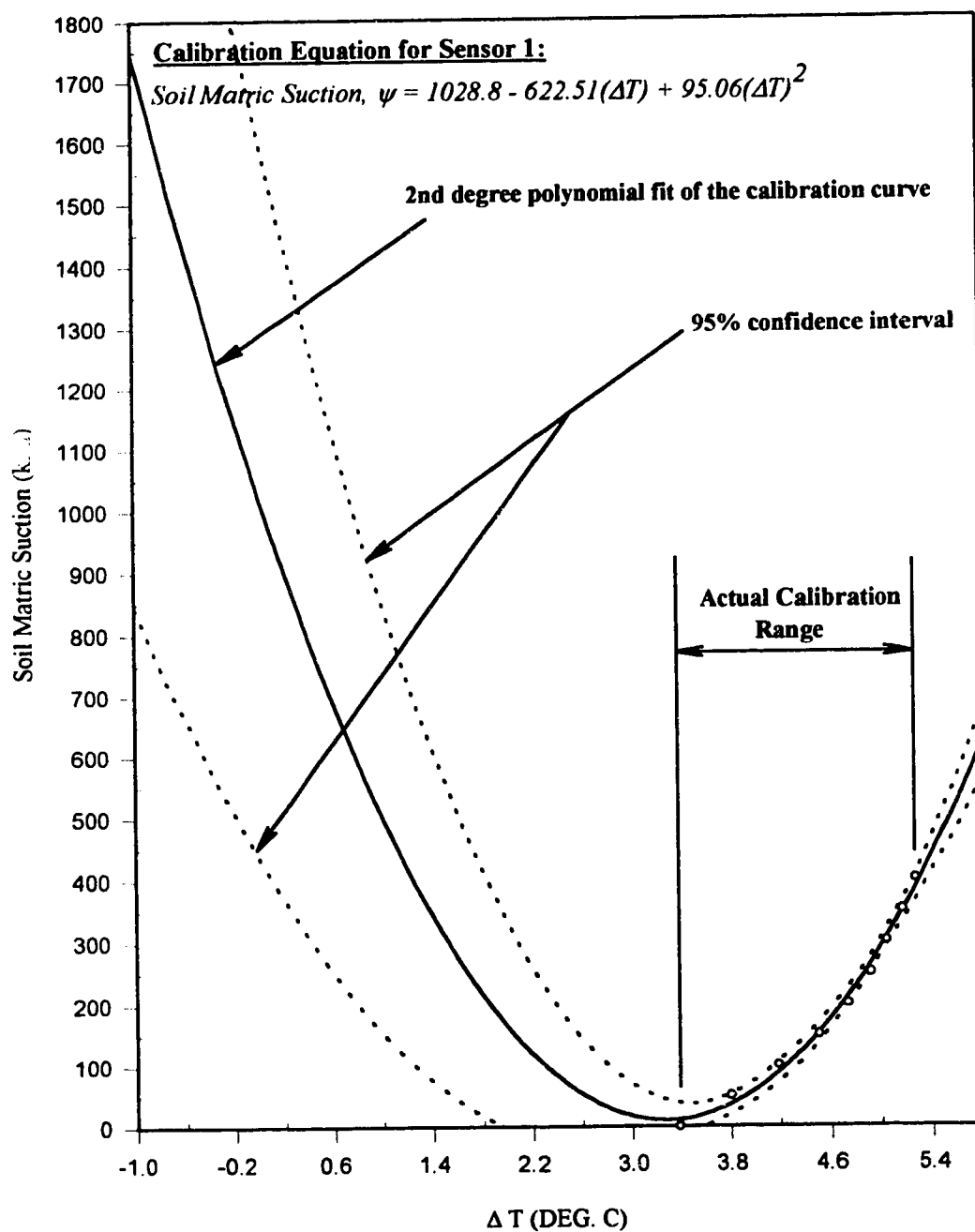


Figure C.15: Extended Calibration Curve for Sensor 1

APPENDIX D

FALLING WEIGHT DEFLECTOMETER DATA AND ANALYSIS TOOLS

D-1 Examples of FWD Field Program Outputs

D-2 Listing of Computer Program BOWI,

D.1 Examples of FWD Field Program Outputs

Figure D.1: Example Output of FWD Field Program - Edition 20

```

R32 397 910508H1612M1136F20
700031008002-06875394.3902111 8
150 0 300 600 900 120015001800
A:\UOA91\ .FWD
007010 H1612M11 Km 18.50 - 19.50
S 0.976WBIC14 00 11 400
S 0.976WBIC14 00 11 400
0' 100'273037300 .976
8 15 3.5 5 2 15 2 8
Ld 116 1 95.1
D1 931 1 1.092
D2 932 1 1.100
D3 933 1 1.066
D4 934 1 1.087
D5 935 1 1.122
D6 936 1 1.096
D7 937 1 1.081
D0 938 1 1.134
D0 939 1 1.082
D* ***** 1 1
Kleparchuk, Vic
00010000.....
13 2 6 2 .....
*Km 18.50 - 19.50

*
.....
0 0Peak...
12345678901.....
CCC123412341111111111111111111111111111
.....
*****
...
.....
.....
uoa1
*Km 18.50 - 19.50

S 0.000WBOO12 00 9 I00957
382 176 130 86 57 40 31 26
583 288 212 143 95 68 51 42
794 409 303 207 139 100 76 63
1075 505 376 260 175 127 97 79
377 174 128 85 56 40 31 25
577 287 211 142 94 68 51 42
787 407 302 207 138 100 76 62
1072 503 375 259 175 127 96 79

```

Figure D.1: Continued

S 0.050WBOO12 00 9 I00959
 384 192 142 93 60 42 30 25
 582 310 230 153 99 69 50 40
 784 437 326 219 145 100 73 58
 1065 541 406 276 184 127 92 73
 381 189 141 92 60 42 30 25
 579 309 230 153 100 69 50 40
 782 436 325 220 146 101 73 58
 1062 539 405 277 185 128 93 74

S 0.101WBOO12 00 9 I01001
 387 208 155 104 68 47 34 26
 581 335 241 168 112 79 56 44
 776 470 352 242 163 115 82 64
 1057 580 439 304 207 148 105 81
 380 208 153 101 67 46 33 25
 577 331 249 168 112 79 56 43
 773 466 352 241 163 116 82 63
 1056 579 440 304 207 148 105 81

S 0.150WBOO12 00 8 I01003
 361 367 354 95 64 42 31 24
 561 565 531 183 110 74 53 41
 773 761 706 240 161 108 76 60
 1044 931 856 308 206 137 97 75
 360 364 353 95 64 44 31 24
 556 560 528 161 109 73 52 41
 770 758 707 239 161 108 76 60
 1043 929 857 308 207 137 97 75

S 0.201WBOO12 00 10 I01005
 377 157 118 77 49 33 23 19
 581 261 193 129 83 56 40 33
 782 364 272 183 119 81 59 47
 1056 454 339 232 152 103 75 60
 374 156 114 75 48 32 23 19
 574 259 191 127 82 56 40 32
 778 362 269 182 118 81 58 47
 1052 451 338 230 151 104 75 60

S 0.250WBOO12 00 9 I01007
 375 161 117 74 45 30 23 18
 572 265 190 123 76 51 37 30
 779 371 268 177 110 74 54 45
 1048 464 337 224 141 95 69 56
 371 159 115 74 45 30 23 19
 572 265 190 123 76 51 37 29
 781 370 268 177 110 74 54 46
 1046 463 337 224 142 96 70 57

Figure D.2: Continued

S 0.050WBOO 19.000 0 180309530120000013

397	226	178	149	114	89	55	37	27	21
586	341	270	230	178	139	87	58	43	33
780	469	375	322	251	199	126	86	64	48
1056	596	477	411	324	258	166	114	86	66
391	223	174	147	112	87	54	37	27	20
582	339	268	229	176	138	87	58	43	34
776	467	373	320	249	197	126	86	64	50
1049	593	476	409	322	257	166	114	85	66

S 0.100WBOO 19.000 0 180309550120000013

385	246	198	167	130	103	65	44	32	24
577	374	303	260	204	163	104	73	53	41
776	509	415	357	285	230	150	104	77	59
1047	643	525	453	365	298	196	138	103	79
382	243	196	167	130	102	67	46	32	25
573	369	300	257	202	161	103	72	52	40
776	506	412	356	284	228	149	104	77	59
1041	639	521	451	363	296	196	138	103	79

S 0.150WBOO 19.000 0 180309590120000013

387	360	306	274	176	142	66	41	28	21
577	520	448	402	266	172	106	66	48	37
774	701	600	539	366	245	153	98	70	54
1041	879	752	675	465	318	200	128	92	72
386	355	306	274	175	109	66	41	28	21
572	519	445	400	265	172	107	67	49	39
776	698	599	539	365	246	153	98	70	54
1043	878	749	672	464	318	200	129	92	72

S 0.200WBOO 19.000 0 180310010120000013

391	198	157	132	101	78	47	30	21	17
579	300	241	206	158	122	76	50	36	29
782	413	334	286	222	174	109	74	54	44
1046	524	424	363	284	225	143	97	73	59
390	195	157	132	101	77	48	31	22	17
576	298	241	204	155	121	76	51	38	32
780	411	331	283	218	171	108	73	55	44
1041	521	421	360	282	223	142	96	72	58

S 0.250WBOO 19.000 0 180310030120000013

388	192	150	124	92	69	40	26	20	17
579	292	229	193	145	110	65	43	34	28
780	398	315	267	202	157	95	62	51	45
1046	504	400	342	261	204	125	83	67	56
382	188	149	124	92	71	42	28	23	19
575	294	230	194	146	112	68	48	38	33
778	397	314	267	202	157	95	63	50	40
1039	501	399	339	260	203	124	83	65	54

D.2 Listing of Computer Program BOWL used in FWD Deflection Analysis

```

CHARACTER*12 IFILE,OFILE,OFILE1,OFILE2,OFILE3,OFILE4,IFILER,OFILEM
CHARACTER*1 CH(20)
CHARACTER*80 DUM
CHARACTER*8 IDENT
CHARACTER*4 DUM1,DUM2
CHARACTER*5 TEMP
CHARACTER*5 DUM3
CHARACTER*3 TAIR
CHARACTER*2 LANE
DIMENSION DEFLEC(9),DEFM(4,7),DEFS(8,9),DEFT(4,9),BA(4),SA(4)
DIMENSION SMI(4),BASAV(100,4),SASAV(100,4),D4SAV(100,4)
DIMENSION D1SAV(100,4),SMISAV(100,4),D7SAV(100,4)
DIMENSION BARAT(4),SSID4(4),SSID7(4),SARAT(4),CDCORR(4),SMIRAT(4)
DIMENSION LAV1(4),LAV2(4),LAV3(4),LAV4(4)
DIMENSION BARAV1(4),BARAV2(4),BARAV3(4),BARAV4(4)
DIMENSION SARAV1(4),SARAV2(4),SARAV3(4),SARAV4(4)
DIMENSION SSI4V1(4),SSI4V2(4),SSI4V3(4),SSI4V4(4)
DIMENSION SSI7V1(4),SSI7V2(4),SSI7V3(4),SSI7V4(4)
DIMENSION SMIAV1(4),SMIAV2(4),SMIAV3(4),SMIAV4(4)
DIMENSION SMIRV1(4),SMIRV2(4),SMIRV3(4),SMIRV4(4)
REAL KPOST
DIMENSION LOADM(4),LOADS(8)
REAL MU2MIL,KM2MI,KG2LBS
WRITE(*,*) 'CONVERSION REQUIRED ?'
READ(*,17) DUM
17 FORMAT(A1)
WRITE(*,*) 'ENTER NUMBER OF DEFLECTION READINGS IN REFERENCE FILE'
READ(*,*) NDEFR
WRITE(*,*) 'ENTER NUMBER OF DEFLECTION READINGS IN INPUT FILES'
READ(*,*) NDEFI
KM2MI=1.
KG2LBS=1.
MU2MIL=1.
IF((DUM.EQ.'y').OR.(DUM.EQ.'Y')) THEN
  KM2MI=1/1.6104
  KG2LBS=1/.062850
  MU2MIL=1/25.4
ENDIF
WRITE(*,*) 'ENTER NUMBER OF INPUT FILES'
READ(*,*) NFILES
WRITE(*,*) 'ENTER REFERENCE FILE NAME'
READ(*,*) IFILER
WRITE(*,*) 'ENTER MASTER DEFLECTION OUTPUT FILE NAME'
READ(*,*) OFILEM
OPEN(6,FILE=OFILEM,STATUS='NEW')
WRITE(6,290)
DO 260 NUM=1,NFILES
  OPEN(7,FILE=IFILER,STATUS='OLD')
  DO 778 J=1,4
    LAV1(J)=0
    LAV2(J)=0

```

```

LAV3(J)=0
LAV4(J)=0
BARAV1(J)=0.0
BARAV2(J)=0.0
BARAV3(J)=0.0
BARAV4(J)=0.0
SARAV1(J)=0.0
SARAV2(J)=0.0
SARAV3(J)=0.0
SARAV4(J)=0.0
SSI4V1(J)=0.0
SSI4V2(J)=0.0
SSI4V3(J)=0.0
SSI4V4(J)=0.0
SSI7V1(J)=0.0
SSI7V2(J)=0.0
SSI7V3(J)=0.0
SSI7V4(J)=0.0
SMIAV1(J)=0.0
SMIAV2(J)=0.0
SMIAV3(J)=0.0
SMIAV4(J)=0.0
SMIRV1(J)=0.0
SMIRV2(J)=0.0
SMIRV3(J)=0.0
SMIRV4(J)=0.0
778 CONTINUE
WRITE(*,*) 'ENTER INPUT FILE NAME'
READ(*,*) IFILE
WRITE(*,*) 'ENTER OUTPUT FILE MAIN NAME'
READ(*,*) OFILE
READ(OFILE,4) (CH(I),I=1,12)
DO 55 I=1,12
55 IF(CH(I).EQ.' ') GO TO 77
77 I=I-1
WRITE(OFILE1,4) (CH(J),J=1,I),'1',' ','O','U','T'
WRITE(OFILE2,4) (CH(J),J=1,I),'2',' ','O','U','T'
WRITE(OFILE3,4) (CH(J),J=1,I),'3',' ','O','U','T'
WRITE(OFILE4,4) (CH(J),J=1,I),'4',' ','O','U','T'
OPEN(1,FILE=IFILE,STATUS='OLD')
OPEN(2,FILE=OFILE1,STATUS='NEW')
OPEN(3,FILE=OFILE2,STATUS='NEW')
OPEN(4,FILE=OFILE3,STATUS='NEW')
OPEN(5,FILE=OFILE4,STATUS='NEW')
4 FORMAT(12(A1))
READ(IFILE,4) (CH(I),I=1,12)
WRITE(*,4) (CH(I),I=1,12)
K=0
DO 7 I=1,12
K=K+1
IF(CH(I).EQ.' ') GO TO 2
7 CONTINUE
2 DO 8 J=K,12
CH(J)=' '
8 CONTINUE
LANE=' W'

```

```

IDENT='007 10 '
DO 150 I=1,37
  READ(7,3) DUM
150 CONTINUE
  DO 160 I=1,200
    READ(7,13,END=170) DUM1,KPOST
    KPOST=KM2MI*KPOST
    DO 180 J=1,8
      READ(7,*,END=170) LOAD,(DEFLEC(K),K=1,NDEFR)
      LOAD=KG2LBS*LOAD
      LOADS(J)=LOAD
      DO 190 I1=1,NDEFR
        DEFLEC(I1)=MU2MIL*DEFLEC(I1)
        DEFS(J,I1)=DEFLEC(I1)
190 CONTINUE
180 CONTINUE
      DO 200 J=1,4
        LOADM(J)=.5*(LOADS(J)+LOADS(J+4))
        DO 210 I1=1,NDEFR
          DEFT(J,I1)=.5*(DEFS(J,I1)+DEFS(J+4,I1))
210 CONTINUE
200 CONTINUE
        DO 220 J=1,4
          IF(NDEFR.EQ.9) THEN
            DEFM(J,1)=DEFT(J,1)
            DEFM(J,2)=DEFT(J,3)
            DO 230 K=5,9
              DEFM(J,K-2)=DEFT(J,K)
230 CONTINUE
            ELSE
              DO 370 K=1,7
                DEFM(J,K)=DEFT(J,K)
370 CONTINUE
            ENDIF
220 CONTINUE
            DO 240 J=1,4
              SMI(J)=LOADM(J)/DEFM(J,1)
              BA(J)=(1800.0-0.0)/18.0*(DEFM(J,1)+4.0*DEFM(J,2)+2.0*DEFM(J,3)+
&4.0*DEFM(J,4)+2.0*DEFM(J,5)+4.0*DEFM(J,6)+DEFM(J,7))
              SA(J)=300*(DEFM(J,4)*0.5+DEFM(J,5)+DEFM(J,6)+DEFM(J,7)*0.5)
240 CONTINUE
              DO 140 J=1,4
                BASAV(I,J)=BA(J)
                SASAV(I,J)=SA(J)
                D1SAV(I,J)=DEFM(J,1)
                D4SAV(I,J)=DEFM(J,4)
                D7SAV(I,J)=DEFM(J,7)
                SMISAV(I,J)=SMI(J)
140 CONTINUE
160 CONTINUE
170 DO 5 I=1,37
  READ(1,3) DUM
5 CONTINUE
  WRITE(2,24)
  WRITE(3,24)
  WRITE(4,24)

```

```

WRITE(5,24)
DO 10 I=1,200
  READ(1,13,END=320) DUM1,KPOST,DUM2,TEMP,DUM3,TAIR
  KPOST=KM2MI*KPOST
  DO 12 J=1,8
    READ(1,*,END=320) LOAD,(DEFLEC(K),K=1,NDEFI)
    LOAD=KG2LBS*LOAD
    LOADS(J)=LOAD
    DO 11 I1=1,NDEFI
      DEFLEC(I1)=MU2MIL*DEFLEC(I1)
      DEFS(J,I1)=DEFLEC(I1)
11  CONTINUE
12  CONTINUE
    DO 120 J=1,4
      LOADM(J)=.5*(LOADS(J)+LOADS(J+4))
      DO 110 I1=1,NDEFI
        DEFT(J,I1)=.5*(DEFS(J,I1)+DEFS(J+4,I1))
110  CONTINUE
120  CONTINUE
    DO 333 J=1,4
      IF(NDEFI.EQ.9) THEN
        DEFM(J,1)=DEFT(J,1)
        DEFM(J,2)=DEFT(J,3)
        DO 334 K=5,9
          DEFM(J,K-2)=DEFT(J,K)
334  CONTINUE
        ELSE
          DO 777 K=1,7
            DEFM(J,K)=DEFT(J,K)
777  CONTINUE
          ENDIF
333  CONTINUE
    DO 130 J=1,4
      SMI(J)=LOADM(J)/DEFM(J,1)
      BA(J)=(1800.0-0.0)/18.0*(DEFM(J,1)+4.0*DEFM(J,2)+2.0*DEFM(J,3)+
&4.0*DEFM(J,4)+2.0*DEFM(J,5)+4.0*DEFM(J,6)+DEFM(J,7))
      SA(J)=300*(DEFM(J,4)*0.5+DEFM(J,5)+DEFM(J,6)+DEFM(J,7)*0.5)
130  CONTINUE
    DO 250 J=1,4
      BARAT(J)=BA(J)/BASAV(I,J)
      SARAT(J)=SA(J)/SASAV(I,J)
      SSID4(J)=DEFM(J,4)/D4SAV(I,J)
      SMIRAT(J)=SMI(J)/SMISAV(I,J)
      SSID7(J)=DEFM(J,7)/D7SAV(I,J)
C    CDCORR(J)= FACTOR* DEFM(J,1)
250  CONTINUE
    DO 270 J=1,4
      IF(I.LE.12) THEN
        LAV1(J)=LAV1(J)+LOADM(J)
        BARAV1(J)=BARAV1(J)+BARAT(J)
        SARAV1(J)=SARAV1(J)+SARAT(J)
        SSI4V1(J)=SSI4V1(J)+SSID4(J)
        SSI7V1(J)=SSI7V1(J)+SSID7(J)
        SMIAV1(J)=SMIAV1(J)+SMI(J)
        SMIRV1(J)=SMIRV1(J)+SMIRAT(J)
      ENDIF

```

```

IF((I.GT.12).AND.(I.LE.20)) THEN
LAV2(J)=LAV2(J)+LOADM(J)
BARAV2(J)=BARAV2(J)+BARAT(J)
SARAV2(J)=SARAV2(J)+SARAT(J)
SSI4V2(J)=SSI4V2(J)+SSID4(J)
SSI7V2(J)=SSI7V2(J)+SSID7(J)
SMIAV2(J)=SMIAV2(J)+SMI(J)
SMIRV2(J)=SMIRV2(J)+SMIRAT(J)
ENDIF
IF((I.GT.20).AND.(I.LE.31)) THEN
LAV3(J)=LAV3(J)+LOADM(J)
BARAV3(J)=BARAV3(J)+BARAT(J)
SARAV3(J)=SARAV3(J)+SARAT(J)
SSI4V3(J)=SSI4V3(J)+SSID4(J)
SSI7V3(J)=SSI7V3(J)+SSID7(J)
SMIAV3(J)=SMIAV3(J)+SMI(J)
SMIRV3(J)=SMIRV3(J)+SMIRAT(J)
ENDIF
IF(I.GT.31) THEN
LAV4(J)=LAV4(J)+LOADM(J)
BARAV4(J)=BARAV4(J)+BARAT(J)
SARAV4(J)=SARAV4(J)+SARAT(J)
SSI4V4(J)=SSI4V4(J)+SSID4(J)
SSI7V4(J)=SSI7V4(J)+SSID7(J)
SMIAV4(J)=SMIAV4(J)+SMI(J)
SMIRV4(J)=SMIRV4(J)+SMIRAT(J)
ENDIF
270 CONTINUE
WRITE(2,23)I,LOADM(1),(CH(L),L=1,8),(DEFM(1,K),K=1,7),TEMP,TAIR,
&BA(1),SA(1),SMI(1),BARAT(1),SARAT(1),SSID4(1),SSID7(1),SMIRAT(1)
WRITE(3,23)I,LOADM(2),(CH(L),L=1,8),(DEFM(2,K),K=1,7),TEMP,TAIR,
&BA(2),SA(2),SMI(2),BARAT(2),SARAT(2),SSID4(2),SSID7(2),SMIRAT(2)
WRITE(4,23)I,LOADM(3),(CH(L),L=1,8),(DEFM(3,K),K=1,7),TEMP,TAIR,
&BA(3),SA(3),SMI(3),BARAT(3),SARAT(3),SSID4(3),SSID7(3),SMIRAT(3)
WRITE(5,23)I,LOADM(4),(CH(L),L=1,8),(DEFM(4,K),K=1,7),TEMP,TAIR,
&BA(4),SA(4),SMI(4),BARAT(4),SARAT(4),SSID4(4),SSID7(4),SMIRAT(4)
10 CONTINUE
320 DO 280 J=1,4
LAV1(J)=LAV1(J)/12.0
LAV2(J)=LAV2(J)/8.0
LAV3(J)=LAV3(J)/11.0
LAV4(J)=LAV4(J)/9.0
BARAV1(J)=BARAV1(J)/12.0
BARAV2(J)=BARAV2(J)/8.0
BARAV3(J)=BARAV3(J)/11.0
BARAV4(J)=BARAV4(J)/9.0
SARAV1(J)=SARAV1(J)/12.0
SARAV2(J)=SARAV2(J)/8.0
SARAV3(J)=SARAV3(J)/11.0
SARAV4(J)=SARAV4(J)/9.0
SSI4V1(J)=SSI4V1(J)/12.0
SSI4V2(J)=SSI4V2(J)/8.0
SSI4V3(J)=SSI4V3(J)/11.0
SSI4V4(J)=SSI4V4(J)/9.0
SSI7V1(J)=SSI7V1(J)/12.0
SSI7V2(J)=SSI7V2(J)/8.0

```

```

      SSI7V3(J)=SSI7V3(J)/11.0
      SSI7V4(J)=SSI7V4(J)/9.0
      SMIAV1(J)=SMIAV1(J)/12.0
      SMIAV2(J)=SMIAV2(J)/8.0
      SMIAV3(J)=SMIAV3(J)/11.0
      SMIAV4(J)=SMIAV4(J)/9.0
      SMIRV1(J)=SMIRV1(J)/12.0
      SMIRV2(J)=SMIRV2(J)/8.0
      SMIRV3(J)=SMIRV3(J)/11.0
      SMIRV4(J)=SMIRV4(J)/9.0
280  CONTINUE
      DO 310 J=1,4
        WRITE(6,300) J,(CH(L),L=1,8),LAV1(J),BARAV1(J),SARAV1(J),SSI4V1(
&J),SSI7V1(J),SMIAV1(J),SMIRV1(J)
        WRITE(6,300) J,(CH(L),L=1,8),LAV2(J),BARAV2(J),SARAV2(J),SSI4V2(
&J),SSI7V2(J),SMIAV2(J),SMIRV2(J)
        WRITE(6,300) J,(CH(L),L=1,8),LAV3(J),BARAV3(J),SARAV3(J),SSI4V3(
&J),SSI7V3(J),SMIAV3(J),SMIRV3(J)
        WRITE(6,300) J,(CH(L),L=1,8),LAV4(J),BARAV4(J),SARAV4(J),SSI4V4(
&J),SSI7V4(J),SMIAV4(J),SMIRV4(J)
310  CONTINUE
      WRITE(6,330)
330  FORMAT(///)
      CLOSE(UNIT=1)
      CLOSE(UNIT=2)
      CLOSE(UNIT=3)
      CLOSE(UNIT=4)
      CLOSE(UNIT=5)
      CLOSE(UNIT=7)
260  CONTINUE
300  FORMAT(I3,' ',8(A1),' ',I6,' ',6((F8.2),' '))
      3  FORMAT(A80)
13  FORMAT(A4,F5.3,A4,A5,A5,A3)
23  FORMAT(I6,' ',I6,' ',8(A1),' ',7((F6.2),' '),A5,' ',A3,' ',
&F8.1,' ',F8.1,' ',F7.1,' ',5((F6.2),' '))
24  FORMAT('LOC,LOADM,FWDRUN,D1,D2,D3,D4,D5,D6,D7,TEMP,TAIR,BA,ba,
&ISM,BAr,SAr,SSID4,SSID7,ISM,CDcorrected')
290  FORMAT('SEQ,FWDRUN,LOAD,BAratio,SAratio,SSID4,SSID7,ISM,ISMratio')
15  STOP
      END

```

APPENDIX E

RESILIENT MODULUS TRIAXIAL TEST SYSTEM

- E-1 Introduction**
- E-2 Repeated Loading Triaxial Test Equipment**
- E-3 Automated Data Recording System**
- E-4 Data Processing and Handling**
- E-5 Listing of Computer Programs Used for Repeated Loading Tests.**

E.1 Introduction

One of the major objectives of the testing program undertaken during this study was to establish the resilient modulus relationship(s) for typical cohesive subgrade soil(s) frequently encountered in the Province of Alberta. To fulfill this purpose, repeated loading triaxial test equipment together with an automated data acquisition system were needed.

This appendix contains the detailed description of the testing apparatus and the data acquisition system together with the computer programs used for recording and analyzing the data.

E.2 Repeated Loading Triaxial Test Equipment

E.2.1 Description of the Test Apparatus

The layout for the resilient modulus test apparatus is shown in Figure E.1. Description of the various components that comprise the system is given below. Corresponding reference letters are included in Figure E.1 to facilitate the identification of the different parts.

- A Bellofram** This is a 102mm diaphragm air cylinder used for applying the repetitive deviator stress to the test specimen inside the triaxial cell.
- B Load cell** This device is a custom-made load cell that is used to measure the axial repetitive stress applied to the specimen. It has an operating range of 0 to 570 kg. A detailed schematic of this device is shown in Figure E.2. The load cell used for resilient modulus testing during this investigation has been calibrated for a range of 0 to 440 kg. The calibration curve obtained is shown in Figure E.3.
- C Linear Variable Differential Transducer (LVDT)** This is an electrical displacement transducer which measures the specimen axial deformation. The LVDT's used

were Trans-Tek displacement transducers DC_DC series 240, model 0242-0000 with a displacement range of $\pm 6.35\text{mm}$ in full scale. A schematic of this unit and a typical calibration curve used for converting voltage output into displacement output are shown in Figures E.4(a) and E.4(b) respectively.

D Triaxial Chamber The triaxial chamber used in this investigation was of a standard size for testing a 102mm diameter by 204 diameter long cylindrical specimen. The central area of the base of the triaxial cell is supported by the testing machine frame. The clear removable cylinder of the cell is made of a 9.5mm thin perspex. The loading ram is a 19mm diameter stainless steel rod with a hemispherical end to seat the loading cell. The top cap of the triaxial cell contains two exit spouts that are equipped with two one-way valves. One valve, when opened, is used to ensure that the medium used for applying the confining pressure is filling the triaxial cell. The other valve is a pressure safety valve that is used to automatically release the cell pressure if it exceeds a certain value (in the current testing program, this pressure is set at 175 kPa). The base of the triaxial cell contains valves for the connection of the confining pressure as well as the pressure transducer lines. The pressure capacity of the triaxial cell is 100 kPa. Extra details pertaining to the description of the triaxial cell can be found in section E.2.2.

Air Pressure Reservoir Tank (Not shown in the figure) This is a cylindrical tank used for the storage of compressed air. It has sufficient capacity to provide the pressure requirements for the three triaxial chambers. In the current investigation, however, only one triaxial cell, the middle bay, was used and compressed air from a pressure line was used directly without the need for storage in the reservoir tank. This practice proved sufficient for providing the pressure requirements needed for the purposes of the current resilient modulus testing program.

E Air Pressure Regulators These units are installed on the regulator and distribution panel to regulate the air pressure to the triaxial cell (both the repetitive axial pressure and the constant all-around confining pressure). The operating range of the regulators is 14 to 1000 kPa.

F Air Pressure Gauges These gauges are installed after the air pressure regulators and indicate the air pressure being supplied by that particular line. Two types of these gauges were mounted on the regulator and distribution panel. The first type has an operating range of 0 to 1100 kPa and is used to indicate the repetitive deviator axial stress. The second type has an operating range of 0 to 200 kPa and is used to indicate the amount of all-around confining pressure supplied to the triaxial cell.

G Counter This is a four digit electric counter connected to the solenoid valve and is used to record the number of load applications to the test specimen.

H Pressure Transducer (Mounted on the back of the regulator and distribution panel with its location being indicated by the 3-way valve) This is a pressure sensor that is used to monitor the confining pressure in the three triaxial cells. This gauge is manufactured by Durham Instruments. The model used is P724-0025 with an operating range of 0 to 350 kPa. In order to measure the confining pressure in each of the three triaxial cells, a four-way valve is used. The sensor is connected to one arm while the other three arms are connected to the triaxial cells. By using a three-way valve switch, the pressure from two triaxial cells is shut off and the pressure from the third cell is read by the transducer.

Solenoid Valve (Mounted on the back of the regulator and distribution panel – not shown in figure) This valve controls the flow of pressurized air from the air pressure line to the bellofram. The unit also provides an exhaust vent for air from

the bellofram. The operation of the three-way solenoid valve is controlled by a solenoid pulser unit which electrically opens and closes the three-way valve. The units used are Ascolectic - catalog 8300 number D64RF with an operating range of 0 to 840 kPa.

- I **Solenoid Pulser** The solenoid pulser is a custom made unit that was developed to control the operation of the three-way solenoid valve. The unit consists of an electronic timing circuit of resistors, capacitors and an LM555 timer microcomputer chip which act to form a pulsating signal. By adjusting the proportion of the various components in the circuit, the frequency and duration of loading can be controlled. Adjusting the dynamic pulse rate and pulse width is made accessible through the use of three exterior knobs. This unit can provide up to a 50-millisecond on-load time.
- J **Signal Conditioner** The signal conditioner unit is used to amplify and condition the signals from the load cells, LVDT's, pressure transducer and thermocouples. An ESP-16 board that acts as a multiplexor is built into the signal conditioner box. This cord collects the amplified signals from the pressure transducer and the thermocouples and sends them to the DAS-8 card installed inside the computer. The DAS-8 card transforms the signals from the analog format into a digital format. The load cells signals are also amplified inside the signal conditioner box and sent together with the LVDT's signals to the DAS-8 card. These signals, however, do not pass through the EXP-16 card.
- K **Computer and Data Logger** The computer collects the data from the LVDT, the load cell, the two thermocouples and the pressure transducer. The computer used is a Pro-Spec 286 IBM clone with 1 MB of RAM, 40 MB hard drive and two disc drives. The operating system used was DOS version 4.1. The data logging card, DAS-8, is installed inside the computer. This card collects and converts the output

voltages from the different measuring devices into binary bits for storage in the computer. A computer software was developed using “QuickBASIC” to initialize the computer and collect the data. Extra details on the data acquisition system is given in section E.3.

E.2.2 Description of the Triaxial Chamber

Figure E.5 shows the principal features of the triaxial cell used in the current testing program. For item identification refer to the corresponding numbers as shown in the figure and described below.

- 1 **Loading Room** This is a 19mm diameter round stainless steel rod. It is used to transfer the repetitive axial load from the bellofram to the test specimen inside the cell.
- 2 **Air Release Valve** This valve releases the air pressure from the triaxial cell. It is also used to indicate when the cell is full with water when this is used as a medium for applying the confining pressure.
- 3 **Rubber O-Rings** These rings are used to seal the specimen with the rubber membrane and to seal the perspex cylinder to the top and bottom plates of the triaxial cell.
- 4 **Loading Cap** This is a 102mm diameter by 16mm thick aluminum disc with a depression on its top surface to seat the hemispherical end of the loading ram. This plate evenly distributes the applied load over the entire surface area of the test specimen.
- 5 **Soil Specimen** The triaxial chamber used in this study can accommodate a 204mm high x 102mm diameter cylindrical specimen. The specimen is enclosed within a rubber membrane and sealed with O-rings at both ends.

- 6 Rubber Membrane Two rubber membranes were used to enclose the test specimen. The objectives of the membranes were to prevent moisture loss from the soil sample during testing and to bring the thermocouple assembly in contact with the specimen to facilitate temperature measurements.
- 7 Perspex Cylinder This cylinder is 289mm high with a 197mm outer diameter and a 178mm inner diameter.
- 8 Pressure Transducer Connection Valve This valve enables the connection of a line to the pressure transducer for the purpose of measuring the confining pressure.
- 9 Triaxial Chamber Base Plate This constitutes the base of the triaxial cell. It contains three inlets. Two of these inlets are equipped with valves that are used for supplying and measuring the confining pressure inside the cell. The third inlet is used as an exit for the load wires of the thermocouples.
- 10 Confining Pressure Connection Valve This valve supplies the confining pressure to the triaxial chamber.
- 11 Thermocouple Assembly The thermocouple assembly consists of a thin plastic tube that contains two thermocouples. The thermocouples used are type T (i.e. Copper-constantan) thermocouples with a diameter of 0.508mm and a load wire length of 1830mm. Temperature measurements were performed at locations 25mm from each end of the test specimen.
- 12 Mounting Screws Three equally spaced 12.7mm diameter threaded rods and three studs used to seal the triaxial cell.
- 13 Top Cap of the Triaxial Chamber The top cap contains the pressure safety valve, the air release valve, the entrance for the load ram as well as a threaded hole for the seating of the LVDT core.

14 Pressure Safety Valve This valve is set to release the cell pressure automatically when it exceeds a certain value. The threshold pressure used is 175 kPa. This safety feature is included in the design of the load cell to cater for the fact that compressed air rather than water is used as the confining pressure medium. In the absence of such safety precaution, the cell might explode without warning if something went wrong during testing.

E.3 Automated Data Recording System

A data acquisition system was developed to collect data from the triaxial test. The raw data was first recorded and stored in the computer using a data acquisition software. The recorded data was then processed using other computer programs to compute the required resilient characteristics of the tested soil. All the computer software used for data recording and processing were developed during the course of this study. Following is a description of the hardware and software that comprise the data logging system.

E.3.1 Data Acquisition Hardware

The data acquisition hardware consists of an IBM compatible microcomputer, an EXP-16 board, a DAS-8 board and a solenoid pulser. Figure E.6 shows a schematic diagram of the overall data acquisition system and how it is connected to the resilient modulus test equipment (RME). The letters A, B, C and D refer to the RME unit, the signal conditioner box, the 286 microcomputer and the solenoid pulser, respectively.

(i) Computer Hardware:

The computer used was a 286 PRO-SPEC IBM clone with 1 MB RAM and a 40 MB hard drive. A 287 math coprocessor chip was installed inside the computer to speed up the data collection and computation processes. The computer also comes with one 5.25-in drive and a 3.5-in drive. This enables storing the test data in either the hard drive or in back up floppy disks.

(ii) MetraByte EXP-16 Board:

The MetraByte Universal Expansion Interface, Model No. EXP-16 is an expansion multiplexer/amplifier system that can be used with any data acquisition system. The EXP-16 board can accommodate up to 16 channels of analog information. This board also amplifies, filters and conditions the input signals from the test. The EXP-16 board then multiplexes all the collected signals into one channel (#7 in this system) which is fed to the DAS-8 Board. The EXP-16 also provides a system for temperature measurements using standard type thermocouples. This board is installed inside the signal conditioner box and is connected to the DAS-8 board through a ribbon cable. For further information pertaining to the EXP-16 board, refer to the EXP-16 Manual published by MetraByte Corporation.

(iii) DAS-8 Board:

The DAS-8 board is an 8 channel 12 bit high speed analog/digital converter and timer/counter board for the IBM and IBM compatible P.C.'s. This board was used to collect part of the test data in analog form and convert all data collected by this board and the EXP-16 board from the analog format into a digital format for use by the computer. The DAS-8 board has a full scale input for each channel of ± 5 volts with a resolution of 0.00244 volts (2.44 millivolts). The A/D conversion time is typically 25 microseconds with 35 microseconds maximum.

The DAS-8 board comes with a pre-programmed software package that allows the user to configure the board to his/her own needs. The board also has a programmable counter timer that provides periodic interrupts for the A/D converter. For further information regarding the DAS-8 board and how it can be programmed for test data collection, refer to the DAS-8 Manual published by the manufacturer, MetraByte Corporation.

(iv) Solenoid Pulser

The function and operation of the solenoid pulser have previously been described in section E.2.1. The solenoid pulser box contains two separate components. A pulser that is used for generating the dynamic repetitive load and a channel selection multiplexor that is used to activate the designated loading bay.

E.3.2 Data Acquisition Software

The second step in the development of the data acquisition system was the writing of a computer software to accomplish this objective, QuickBASIC program was written. This program made use of the software provided with the DAS-8 board and a graphical library program called Lab Windows.

The software supplied with the DAS-8 board provides the I/O driver routine that controls the functions of the DAS-8 card. This routine is called "Das8-BIN" and can be accessed from QuickBASIC using call statements. On the other hand, Lab Windows software provides extensive graphical libraries that can be used by the QuickBASIC program to display the collected data on the screen in a graphical form. This feature was deemed essential to detect any anomalies in the system during repeated load testing.

The program uses the timer built in the DAS-8 board to collect the test data. This timer is triggered by the solenoid pulser unit. Upon activation of the solenoid pulser unit, it simultaneously sends two signals, one to the solenoid valve and the other to the DAS-8 board inside the computer. The solenoid valve signal controls the operation of the air rams that load the specimen while the other signal invokes the DAS-8 board to start recording the measured data from the load cells, the LVDT's, the pressure transducer and the thermocouples. This continues for 100 milliseconds which constitutes the on-load time period. This is then followed by a 900 milliseconds off-load period during which the A/D converter within the DAS-8 board converts the collected analog information into

digital information. Further computations done by the software are also performed during the off-load period to convert the digital information from binary computer code into engineering units. The collected test data, in engineering units, are then stored temporarily in the computer RAM. This process is repeated every second until the test ends. Upon completion of the repeated load test, the collected data is permanently stored in user specified files.

The QuickBASIC program written for the repeated loading test is illustrated in section E.5.1. It contains all the information and comments pertaining to the test which makes it self-explanatory.

E.4 Data Processing and Handling

Several computer programs were used to process the collected test data. These programs were written in FORTRAN and were used to compute the resilient modulus and permanent deformation values. The permanent deformation was computed as follows:

$$E_p = 100 \frac{[H_1 - H_2 DIF(I)]}{H_1}$$

where,

E_p = percent permanent deformation

H_1 = initial sample thickness

$H_2 DIF(I)$ = final sample thickness (as defined in
PDEF-IC-FOR & PDEF-IIc-For
programs in section E.5.2)

The resilient modulus was computed as follows:

$$M_R = \frac{DSTRS(I)}{RSTRN(I)}$$

where,

M_R = resilient modulus in psi (later converted into kPa.

DSTRS(I) = Deviator stress in psi (as defined in the MCALC-IC.FOR & MCLC-IIC.FOR programs in section E.5.2)

RSTRN(I) = recoverable axial strain (as defined in the MCALC-IC.FOR & MCLC-IIC.FOR programs in section E.5.2)

The listing of these computer programs together with example output files are displayed in section E.5.2.

E.5 Listing of Computer Programs Used for Repeated Loading Tests

E.5.1 Triaxial Test Data Logging Program (MODULUZZ.BAS)

'Program MODULUZZ.BAS Used for Resilient Modulus Testing.

"" This program is used to control the repeated triaxial load
'test and to monitor and record the required test
'parameters."

```
*****
'*-----*
'*  Program for DAS-8 used in array mode 5 and Lab Windows  *
'*-----*
*****

  DIM d%(6)
  COMMON SHARED d%()
  DECLARE SUB DAS8 (mode%, BYVAL dummy%, FLAG%)
*****
```

'[1] Dimensioning the arrays required to store the collected data

GETMEM (45000&)

DIM a%(250)
DIM b%(16)

DIM CH0#(500) 'CJC readings
DIM CH1#(10025) 'LVDT CELL A, B or C
DIM CH4#(10025) 'LOAD CELL A, B or C

DIM CH7#(10025) 'PRESSURE TRANS
DIM CH7#(10010) 'PRESSURE
 'TRANS

DIM PP#(30) 'LOAD CELL A (RESET EVERY SEC.)

DIM TT(138)
DIM btemp%(16)

```

DIM CHEX0#(401)    'SAME AS CH7
DIM CHEX1#(401)    'TEMP CELL A
DIM CHEX2#(401)    'TEMP CELL B
DIM CHEX3#(401)    'TEMP CELL C
DIM CHEX4#(401)    'NOT USED
DIM CHEX5#(401)    'TEMP DUMMY THICK
DIM CHEX6#(401)    'TEMP DUMMY THICK
DIM CHEX7#(401)    'TEMP DUMMY THICK
DIM CHEX8#(401)    'TEMP DUMMY THICK
DIM CHEX9#(401)    'TEMP DUMMY THICK
DIM CHEX10#(401)   'TEMP DUMMY THICK
DIM CHEX11#(401)   'TEMP DUMMY THICK
DIM CHEX12#(401)   'TEMP DUMMY THIN
DIM CHEX13#(401)   'TEMP DUMMY THIN
DIM CHEX14#(401)   'TEMP DUMMY THIN
DIM CHEX15#(401)   'NOT USED

```

'a%() will be filled with the acquired data. In Rev's earlier than 4.32
'this array would have to be placed in the COMMON area. As a result 'only
small amounts of data could be aquired. In Rev's 4.32, Mode 5 has 'been
changed. Here if d%(0) is a -1 then d%(2) will have the offset and 'd%(3)
will have the segment of the array one wishes to place the data in. 'This
allows a user to aquire upto 32k of readings.

'NOTE that is d%(0) is not -1 then Mode 5 will operate as before

[II] System selection (This step involves selecting Bay 1, 2 or 3 for M_R testing).

```

SCREEN 0, 0, 0
KEY OFF
WIDTH 80

```

```

DO
CLS
LOCATE 1, 10
INPUT "Enter System Number (1,2,3) "; sysnum%
LOOP UNTIL sysnum% >= 1 OR sysnum% <= 3

```

```

load% = sysnum% + 3
load$ = STR$(load%)

```

```

dis$ = STR$(sysnum%)

ON ERROR GOTO ERROREND
ON KEY(1) GOSUB KEYONE
KEY(1) ON

GOSUB 50000      'LOAD TEMPERATURE LINEARIZATION TABLE

'Make initial screen announcement

  CLS

'-----
'[ III ] Create the graphical display on the screen ( This step involves using the
''LABWINDOWS software to create graphical strip charts and numeric ports on the
''screen for displaying the measured data) .
'-----

  CALL GrfLReset(0, 0, 1, 1)
  CALL SetPlotMode(0)

  portsize% = 150      'Number of points in strip charts
  SCOUNT% = 0

port1% = CreatePort(0, 64, 30, 30)
CALL SetAxLbIVis(0, 0)

port2% = CreateStripChart (32, 64, 64, 30, -100.0, 400.0, 0.0, 1.0, portsize% * 25, 1, 1)
CALL SetAxLbIVis(0, 0)
port3% = CreateStripChart (50, 32, 50, 30, -5000.0, 5000.0, 0.0, 1.0, portsize% * 25, 1,
1)
CALL SetAxLbIVis(0, 0)
port4% = CreateStripChart (0, 32, 45, 30, 0.0, 75.0, 0.0, 1.0, portsize% * 25, 1, 1)
CALL SetAxLbIVis(0, 0)
port5% = CreateStripChart (50, 0, 50, 30, -300.0, 500.0, 0.0, 1.0, portsize%, 1, 1)
CALL SetAxLbIVis(0, 0)
port6% = CreateStripChart (64, 32, 30, 30, -2047.0, 2047.0, 0.0, 1.0, portsize%, 1, 1)
CALL SetAxLbIVis(0, 0)
port7% = CreateStripChart (0, 0, 30, 30, -100.0, 100.0, 0.0, 1.0, portsize%, 2, 1)
CALL SetAxLbIVis(0, 0)
port8% = CreateStripChart (32, 0, 30, 30, -2047.0, 2047.0, 0.0, 1.0, portsize%, 1, 1)
CALL SetAxLbIVis(0, 0)
port9% = CreateStripChart (64, 0, 30, 30, -2047.0, 2047.0, 0.0, 1.0, portsize%, 1, 1)
CALL SetAxLbIVis(0, 0)

portA% = CreateNumericPort(0, 94, 1, 8, 2, "", "")

```

```

portC% = CreateNumericPort(0, 25, 1, 8, 2, "", "")
portD% = CreateNumericPort(30, 25, 1, 8, 2, "", "")
portE% = CreateNumericPort(65, 94, 1, 8, 2, "", "")
portF% = CreateNumericPort(30, 5, 1, 8, 2, "", "")

portB% = CreateStripChart(64, 64, 30, 30, -2047, 2047, 0, 1, portsize%, 1, 1)
CALL SetAxLblVis(0, 0)

CALL SetActivePort(port1%)
CALL SetTitle("Load P (CH " + load$ + ")")
CALL SetGrdFrame(1)
CALL SetAxGridVis(1, 0)
CALL SetAxGridVis(0, 0)

CALL SetActivePort(port2%)
CALL SetTitle("Load lbs (CH " + load$ + ")")
CALL SetGrdFrame(1)
CALL SetAxGridVis(1, 1)
CALL SetAxGridVis(0, 1)

CALL SetActivePort(port3%)
CALL SetTitle("Presure PSI X 100 (CH 7)")
CALL SetGrdFrame(1)
CALL SetAxGridVis(1, 1)
CALL SetAxGridVis(0, 1)

CALL SetActivePort(port4%)
CALL SetTitle("Dis in. X 1000 (CH " + dis$ + ")")
CALL SetGrdFrame(1)
CALL SetAxGridVis(1, 1)
CALL SetAxGridVis(0, 1)

CALL SetActivePort(port5%)
CALL SetTitle("TEMP (Deg C X 10) SYS # " + dis$)
CALL SetGrdFrame(1)
CALL SetAxGridVis(1, 1)
CALL SetAxGridVis(0, 1)

CALL SetActivePort(port6%)
CALL SetTitle("Channel EX1")
CALL SetGrdFrame(1)
CALL SetAxGridVis(1, 0)
CALL SetAxGridVis(0, 0)

```

```
CALL SetActivePort(port7%)
CALL SetGrdFrame(1)
CALL SetAxGridVis(1, 0)
CALL SetAxGridVis(0, 0)
```

```
CALL SetActivePort(port8%)
CALL SetGrdFrame(1)
CALL SetAxGridVis(1, 0)
CALL SetAxGridVis(0, 0)
```

```
CALL SetActivePort(port9%)
CALL SetGrdFrame(1)
CALL SetAxGridVis(1, 0)
CALL SetAxGridVis(0, 0)
```

GOSUB TITLEPAGE ' This command bring in the title page screen

'-----
'**[IV] This part sets up the DAS-8 card (This involves initializing the card, setting the
'built-in timer rate for channel scanning and select the channels to be scanned).**
'-----

360 '

400 '--- Step 1: Initialize DAS-8 with mode 0 -----

484 CLS

 b% = &H300

486

490 d%(0) = b% 'I/O address of DAS-8 (change to suit)

500 MD% = 0 'initialize mode

510 FLAG% = 0 'declare error variable

520 CALL DAS8(MD%, VARPTR(d%(0)), FLAG%)

530 IF FLAG% <> 0 THEN PRINT "Error in initialization": STOP

540 '

600 '--- Step 2: Set timer rate -----

610 MD% = 10 'Mode 10 for setting counter configuration

620 d%(0) = 2 'Operate on counter #2

630 d%(1) = 3 'Configuration #2 = rate generator

640 CALL DAS8(MD%, VARPTR(d%(0)), FLAG%)

650 IF FLAG% <> 0 THEN PRINT "Error in setting counter 2 configuration": STOP

660 '

670 'Prompt user for desired sample rate

680 CLS

690 F = 100

700 ' Output frequency = 2386.4/N KHz

710 N = 6000

720 IF N < 2 OR N > 65535! THEN

```

PRINT "Warning! A sample rate of "; F; " samples/sec is outside the range
of Counter 2"

```

```

GOTO 690

```

```

END IF

```

```

730 MD% = 11      'Mode 11 to load counter

```

```

740 d%(0) = 2      'Operate on counter #2

```

```

750 d%(1) = 7356    '(11.77 MHz / 2) / 7,356 = 800 reading / sec.

```

```

                'OR 80 readings / 100 msec. = 10 readings /channel

```

```

760 CALL DAS8(MD%, VARPTR(d%(0)), FLAG%)

```

```

770 IF FLAG% <> 0 THEN PRINT "Error in loading counter 2": STOP

```

```

780 'Pin 6 (Counter 2 Out) should now be producing the selected frequency.

```

```

790 '

```

```

800 'Now fetch duration of scan

```

```

810

```

```

    DS = .2

```

```

820 'Translate duration in a number of conversions for mode 5

```

```

830 'Number of conversions = duration x sample rate

```

```

840 'NC = DS * F

```

```

850 '

```

```

900 '--- Step 3: Select the channel to scan -----

```

```

910 'Note this program only looks at one channel, but by setting LL% and UL%

```

```

920 'to the desired scan limits, the channels will be stored in array A%

```

```

930 'in the order scanned, for example if LL% = 1 and UL% = 3 then:-

```

```

940 '          A%(0) = channel 1 data

```

```

950 '          A%(1) = channel 2 data

```

```

960 '          A%(2) = channel 3 data

```

```

970 '          A%(3) = channel 1 data etc.

```

```

980 'The rest of the program can be modified to handle multiple channel

```

```

990 'graphs and data files.

```

```

1000 MD% = 1      'Set scan limits, mode 1

```

```

    LL% = 0

```

```

1010 d%(0) = LL%

```

```

1020 UL% = 7

```

```

    d%(1) = UL%      'sample on one channel only

```

```

1030 CALL DAS8(MD%, VARPTR(d%(0)), FLAG%)

```

```

1040 IF FLAG% <> 0 THEN PRINT "Error in setting channel scan limits": STOP

```

```

1050 '

```

```

GOTO 4000

```

Mode5:

```

1250 MD% = 5      'Mode 5, do conversions direct to array
1260 d%(0) = -1    'Set to -1 to indicate that d%(2) will have offset
                  'and d%(3) will have segment of array
1261 d%(2) = VARPTR(a%(0))
1262 d%(3) = VARSEG(a%(0))
      NC = 200
1270 d%(1) = NC      'Number of conversions NC = .2 * 100
1280
1290 CALL DAS8(MD%, VARPTR(d%(0)), FLAG%)
1300 IF FLAG% <> 0 THEN
      BEEP
      GOTO 1250
      'PRINT "Error in setting mode 5": STOP
END IF

```

'----- MOVE DATA TO CHANNEL ARRAYS -----

'-----
'**[V] Data conversion within the DAS-8 card (This step involves converting the data
'collected by the DAS-8 card from a binary format into engineering units of load,
'displacement and degree Celcius).**
'-----

COUNT% = 0

1305

FOR COUNT% = 0 TO 24

CH0#(lop%) = a%(0 + (COUNT% * 8))

IF sysnum% = 1 THEN

CH4#(COUNT% + SCOUNT%) = (.71345029 * (a%(3 + sysnum% + (COUNT%
* 8))))

CH1#(COUNT% + SCOUNT%) = (.12754 * (a%(sysnum% + (COUNT% * 8))))

END IF

IF sysnum% = 2 THEN

CH4#(COUNT% + SCOUNT%) = (.68732394 * (a%(3 + sysnum% + (COUNT%
* 8))))

CH1#(COUNT% + SCOUNT%) = (.12726 * (a%(sysnum% + (COUNT% * 8))))

END IF

```

IF sysnum% = 3 THEN
  CH4#(COUNT% + SCOUNT%) = (.67403314 * (a%(3 + sysnum% + (COUNT%
* 8))))
  CH1#(COUNT% + SCOUNT%) = (.12896 * (a%(sysnum% + (COUNT% * 8))))
END IF

```

```

CH7#(COUNT% + SCOUNT%) = (2.44 * (a%(7 + (COUNT% * 8))))

```

```

PP#(COUNT%) = a%(3 + sysnum% + (COUNT% * 8))    'channel 4 load cell

```

```

NEXT COUNT%

```

```

1306

```

```

      SCOUNT% = SCOUNT% + 25    'INCREMENT SCAN COUNT 25 FOR 25
READINGS EVER SEC.

```

```

1310 RETURN

```

```

'-----
[ VI ] Reading and plotting collected data (This step involves reading channels 0 to 7
'on DAS-8 and channels 0 to 15 on EXP-16 cards and displaying the collected data
'graphically on the screen. This include axial repetitive load, axial displacement,
'confining cell pressure and temperature measurements in actual engineering units).
'-----

```

```

4000

```

```

CALL SetPlotMode(0)
CALL GrfPrint(0, 0, "Press F1 to stop test! ")

```

```

DO
  PLT = TIMER

```

```

      GOSUB Mode5      'Reads DAS-8 channels 0 to 7
      GOSUB MODE22    'Reads EXP-16 channels 0 to 15

```

```

4003

```

```
'st=TIMER + 1
```

```
GOSUB PLOT1
```

```
GOSUB PLOT2
```

```
GOSUB PLOT3
```

```
GOSUB PLOT4
```

```
GOSUB PLOT5
```

```
IF grferr <> 0 THEN GOTO GRPHERR
```

```
'EPLT = TIMER - PLT
```

```
GOSUB PLOTA
```

```
GOSUB PLOTB
```

```
GOSUB PLOTD
```

```
GOSUB PLOTE
```

```
GOSUB PLOTF
```

```
lop% = lop% + 1
```

```
IF lop% >= 299 THEN GOTO KEYONE
```

```
LOOP
```

```
END
```

```
'---- Display 'a on screen and return to menu -----
```

```
4010 CLS
```

```
4020 LOCATE 25, 1: PRINT "Press any key to STOP/START display, <ESC> key to  
return to data storage menu "; : LOCATE 1, 1
```

```
4030 PRINT "Time    Channel data (volts)"
```

```
4040 FOR I = 0 TO NC
```

```
4050 PRINT I / F, a%(I) * 5 / 2048
```

```
4060 a$ = INKEY$
```

```
4070 IF a$ = CHR$(27) THEN I = NC + 3
```

```
4080 IF a$ <> "" THEN GOTO 4140
```

```
4090 NEXT I
```

```
4100 IF I = NC + 3 GOTO 1400
```

```
4110 COLOR 0, 7: PRINT " Press any key to return to data storage menu "; : COLOR 7,  
0
```

```
4120 IF INKEY$ = "" GOTO 4120
```

```
4130 GOTO 1400
```

```
4140 FOR K = 1 TO 50: NEXT K 'delay
```

```
4150 IF INKEY$ = "" GOTO 4150
```

```
4160 GOTO 4090
```

4170 END

KEYONE:

```
CALL SetDisplayMode(0)      ' This return the display back to QuickBASIC
text screen
```

'[VII] This part saves the test data to two ASCII files (The first file, called 'xxxxxxx.dat, contains the load-deformation data while the second, named 'xxxxxxx.tmp, contains the temperature data).

FILEDATA:

```
CLS
LOCATE 3, 1
INPUT "Enter Data File Name "; DAFN$
IF LEN(DAFN$) > 7 THEN GOTO FILEDATA

LOCATE 5, 1
INPUT "Enter Drive (A, B, C) "; DRNUM$
LOCATE 7, 1
INPUT "Enter Sub Directory "; SUB$
IF LEN(SUB$) > 0 THEN SUB$ = SUB$ + "\"

LOCATE 9, 1
OPFL$ = DRNUM$ + "\" + SUB$ + DAFN$
PRINT "Data will be saved to files "; OPFL$; " .DAT and .TMP "

LOCATE 11, 1
INPUT "Is this file name and drive correct (Y/N) ? "; YN$
YN$ = UCASE$(YN$)
IF YN$ = "N" THEN GOTO FILEDATA

TB$ = CHR$(9)

CLS

PRINT "SAVING DATA FILE"

OPEN OPFL$ + ".DAT" FOR OUTPUT AS #1
PRINT #1, "SYSTEM NUMBER"; TB$; sysnum%
PRINT #1, "Displacement"; TB$; "Applied Load"; TB$; "Cell Pressure"

FOR SCAN% = 0 TO lop% * 25
    LOCATE 5, 1
    PRINT "PERCENTAGE DONE ";
```

```

        PRINT USING "###"; (SCAN% / (lop% * 25) * 100)
        PRINT #1, CH1#(SCAN%); TB$;
        PRINT #1, CH4#(SCAN%); TB$; CH7#(SCAN%)
    NEXT SCAN%
CLOSE 1
CLS
PRINT "SAVING TEMPERATURE FILE "

OPEN OPFL$ + ".TMP" FOR OUTPUT AS #1
    PRINT #1, "SYSTEM NUMBER"; TB$; sysnum%

    PRINT #1, "Temp A"; TB$; "Temp B"; TB$; "Temp C"; TB$; "Temp Dumb
1"; TB$; "Temp Dumb 2"; TB$; "Temp Dumb 3";
    PRINT #1, TB$; "Temp Dumb 4"; TB$; "Temp Dumb 5"; TB$; "Temp Dumb
6"; TB$; "Temp Dumb 7";
    PRINT #1, TB$; "Temp Dumb 8"; TB$; "Temp Dumb 9"
    FOR SCAN% = 0 TO lop%
        LOCATE 5, 1
        PRINT "PERCENTAGE DONE ";
        PRINT USING "###"; (SCAN% / (lop% * 10) * 1000)

        PRINT #1, CH0#(SCAN%); TB$; CHEX1#(SCAN%); TB$;
CHEX2#(SCAN%); TB$; CHEX3#(SCAN%); TB$;
        PRINT #1, CHEX4#(SCAN%); TB$; CHEX5#(SCAN%); TB$;
CHEX6#(SCAN%); TB$; CHEX7#(SCAN%); TB$;
        PRINT #1, CHEX8#(SCAN%); TB$; CHEX9#(SCAN%); TB$;
CHEX10#(SCAN%); TB$;
        PRINT #1, CHEX11#(SCAN%); TB$; CHEX12#(SCAN%); TB$;
CHEX13#(SCAN%); TB$;
        PRINT #1, CHEX14#(SCAN%); TB$; CHEX15#(SCAN%); TB$;
    NEXT SCAN%
CLOSE 2
END
RETURN

```

PLOT1:

```

CALL SetActivePort(port1%)
CALL SetPlotMode(0)
CALL SetLblColor(15)

```

```

'CALL SetYDataType (1)
CALL SetAxAuto(1, 0)

```

```

CALL SetAxRange(1, -100, 400, 10)

CALL RemovePlots(port1%)
CALL GrfYCurv2D(PP#(), 25)
RETURN

PLOT2:
  CALL SetActivePort(port2%)
  CALL GrfStrip(port2%, CH4#(), (lop% * 25), 25, 0)
RETURN

PLOT3:
  CALL SetActivePort(port3%)
  CALL GrfStrip(port3%, CH7#(), (lop% * 25), 25, 0)
RETURN

PLOT4:
  CALL SetActivePort(port4%)
  CALL GrfStrip(port4%, CH1#(), (lop% * 25), 25, 0)
RETURN

PLOT5:
  CALL SetActivePort(port5%)
  SELECT CASE sysnum%
    CASE 1
      CALL GrfStrip(port5%, CHEX1#(), lop%, 1, 0)

    CASE 2
      CALL GrfStrip(port5%, CHEX2#(), lop%, 1, 0)

    CASE 3
      CALL GrfStrip(port5%, CHEX3#(), lop%, 1, 0)
  END SELECT

RETURN

PLOT6:
  CALL SetActivePort(port6%)
  CALL GrfStrip(port6%, CH5#(), lop%, 1, 0)
RETURN

PLOT7:
  CALL SetActivePort(port7%)

```

```

      'CALL GrfStrip (port7%, CHPL7#(), 0, 2, 0)
RETURN

```

```

PLOT8:
      CALL SetActivePort(port8%)
      CALL GrfStrip(port8%, CH7#(), lop%, 1, 0)
RETURN

```

```

PLOT9:
      CALL SetActivePort(port9%)
      CALL GrfStrip(port9%, CH7#(), lop%, 1, 0)
RETURN

```

```

PLOTA:
      CALL SetActivePort(portA%)
      CALL GrfNumeric(portA%, lop%)
      CALL GrfLReset(0, 0, 0, 0)
RETURN

```

```

PLOTB:
      CALL SetActivePort(portC%)
      CALL GrfNumeric(portC%, CH1#(lop% * 25))
      CALL GrfLReset(0, 0, 0, 0)
RETURN

```

```

PLOTD:
      CALL SetActivePort(portD%)
      CALL GrfNumeric(portD%, CH7#(lop% * 25))
      CALL GrfLReset(0, 0, 0, 0)
RETURN

```

```

PLOTF:
      CALL SetActivePort(portF%)
      IF sysnum% = 1 THEN
        CALL GrfNumeric(portF%, CHEX1#(lop%))
      END IF

      IF sysnum% = 2 THEN
        CALL GrfNumeric(portF%, CHEX2#(lop%))
      END IF

      IF sysnum% = 3 THEN
        CALL GrfNumeric(portF%, CHEX3#(lop%))
      END IF

```

```

      CALL GrfLReset(0, 0, 0, 0)
RETURN

```

```

PLOTE:

```

```

      CALL SetActivePort(portE%)
      CALL GrfNumeric(portE%, CH4#(lop% * 25))
      CALL GrfLReset(0, 0, 0, 0)
RETURN

```

```

MODE22:

```

```

      MD% = 1
      d%(0) = 7
      d%(1) = 7
      CALL DAS8(MD%, VARPTR(d%(0)), FLAG%)
      NC = 16
      LO% = 0
      UO% = 15
      AV% = 10

      MD% = 22
      d%(0) = 3 + 0 'INTERRUPT LEVEL 3
      d%(1) = -1
      d%(6) = VARPTR(b%(0))
      d%(7) = VARSEG(b%(0))
      d%(2) = NC 'NUMBER OF CONVERSIONS
      d%(3) = LO% 'EXP-16 CHANNEL LOW
      d%(4) = UO% 'EXP-16 CHANNEL HIGH
      d%(5) = AV% 'NUMBER OF AVERAGES PER CHANNEL

```

```

      CALL DAS8(MD%, VARPTR(d%(0)), FLAG%)
      IF FLAG% < 0 THEN
        PRINT "ERROR IN MODE 22"
        STOP
      END IF

```

```

      SSTIME = TIMER + 2

```

```

DO

```

```

      MD% = 20
      CALL DAS8(MD%, VARPTR(d%(0)), FLAG%)

```

```

        IF FLAG% <> 0 THEN
            BEEP
            STOP

        END IF'

PRINT d%(1), FLAG%, NC

LOOP UNTIL d%(1) >= NC

FOR CONTEMP% = 1 TO 15
    CONTEMPDATA% = b%(CONTEMP%)
    GOSUB TEMPC
    btemp%(CONTEMP%) = INT(TC * 10)
NEXT CONTEMP%

CHEX0#(lop%) = b%(0)           'pressure measurement
CHEX1#(lop%) = btemp%(1)       'The rest are Temperature T type
CHEX2#(lop%) = btemp%(2)       'thermocouple measurements
CHEX3#(lop%) = btemp%(3)
CHEX4#(lop%) = btemp%(4)
CHEX5#(lop%) = btemp%(5)
CHEX6#(lop%) = btemp%(6)
CHEX7#(lop%) = btemp%(7)
CHEX8#(lop%) = btemp%(8)
CHEX9#(lop%) = btemp%(9)
CHEX10#(lop%) = btemp%(10)
CHEX11#(lop%) = btemp%(11)
CHEX12#(lop%) = btemp%(12)
CHEX13#(lop%) = btemp%(13)
CHEX14#(lop%) = btemp%(14)
CHEX15#(lop%) = btemp%(15)

MD% = 1
d%(0) = 0
d%(1) = 7
CALL DAS8(MD%, VARPTR(d%(0)), FLAG%)

RETURN

```

5110

'[VIII] This part is a subroutine used for displaying a title page on the screen at the beginning of the test. The title page contains the name of the software developed together with further instructions as what to do next.'

TITLEPAGE:

```

CLS
LOCATE 1, 12
PRINT "University of Alberta, Department of Civil Engineering"
LOCATE 2, 28
PRINT "Transportation Division"
LOCATE 4, 25
PRINT "RESILIENT MODULUS TESTING SOFTWARE"
LOCATE 6, 30
PRINT "Written by Dale Lathe"
LOCATE 20, 26
PRINT "PRESS ANY KEY TO START TEST!"

```

```

DO
LOOP UNTIL INKEY$ <> ""

```

RETURN

ERROREND:

```

CALL SetDisplayMode(0)
CLS
PRINT "ERROR # "; ERR; " ON LINE "; ERL
PRINT "Press any key to continue "
DO
LOOP UNTIL INKEY$ <> ""

```

```

GOSUB FILEDATA
STOP

```

GRPHERR:

```

CALL SetDisplayMode(0)
CLS
PRINT "ERROR # "; grferr
PRINT "Press any key to continue "
DO
LOOP UNTIL INKEY$ <> ""
END

```

'[IX] *This part involves converting temperture data from binary format into degree Celcius.*

TEMPC:

CJC = CH0#(lop%) / 10

V = CONTEMPDATA% / 51920

'VT = (1000 * V) + .992 + ((CJC - 25) * .040667)'VT in mV

GOSUB 51000

RETURN

50000 '----- Table lookup data for T type thermocouple -----

50010 'Run this subroutine only in the initialization section of your program

50020 'Number of points, voltage step interval (mV), starting voltage (mV)

NT = 138

SIT = .2

SVT = -6.4

50050 'Temperature at -6.4mv, -6.2mV, -6.0mV etc.

50060 DATA -324.6,-253.7,-229.4,-213.5,-199.8,-187.8,-176.8,-166.6,-157.0,-147.9

50070 DATA -139.2,-131.0,-123.0,-115.4,-108.0,-100.8,-93.8,-87.0,-80.4,-74.0

50080 DATA -67.7,-61.5,-55.4,-49.4,-43.6,-37.9,-32.2,-26.7,-21.2,-15.8

50090 DATA -10.5,-5.2,-0.0, 5.1, 10.2, 15.3, 20.3, 25.2, 30.1, 34.9

50100 DATA 39.7, 44.5, 49.2, 53.8, 58.4, 63.0, 67.6, 72.0, 76.5, 80.9

50110 DATA 85.3, 89.7, 94.0, 98.3, 102.6, 106.8, 111.1, 115.3, 119.4, 123.6

50120 DATA 127.7, 131.8, 135.9, 139.9, 143.9, 148.0, 151.9, 155.9, 159.9, 163.8

50130 DATA 167.7, 171.6, 175.5, 179.3, 183.2, 187.0, 190.8, 194.6, 198.4, 202.1

50140 DATA 205.9, 209.6, 213.3, 217.0, 220.7, 224.4, 228.1, 231.7, 235.4, 239.0

50150 DATA 242.6, 246.2, 249.8, 253.4, 256.9, 260.5, 264.0, 267.6, 271.1, 274.6

50160 DATA 278.1, 281.6, 285.1, 288.6, 292.1, 295.5, 299.0, 302.4, 305.8, 309.3

50170 DATA 312.7, 316.1, 319.5, 322.9, 326.3, 329.6, 333.0, 336.4, 339.7, 343.1

50180 DATA 346.4, 349.7, 353.0, 356.4, 359.7, 363.0, 366.3, 369.6, 372.8, 376.1

50190 DATA 379.4, 382.6, 385.9, 389.2, 392.4, 395.6, 398.9, 402.1

50200

50210 FOR I = 0 TO NT - 1

READ TT(I)

NEXT I

50220 RETURN

50230 '

51000 '----- Interpolation routine to find T thermocouple temperature -----

51010 'Entry variables:-

51020 ' CJC = cold junction compensator temperature in deg. C.

51030 ' V = thermocouple voltage in volts

51040 'Exit variables:-

51050 ' TC = temperature in degrees Centigrade

51060 ' TF = temperature in degrees Fahrenheit

51070 'Execution time on std. IBM P.C. = 46 milliseconds

51080 'Perform CJC compensation for T type

51090 $VT = (1000 * V) + .992 + (CJC - 25) * .040667$ 'VT in mV

51100 '

51110 'Find look up element

51120 $ET = INT((VT + 6.4) / .2)$ 'SIT = .2 SVT = -6.4

51130 IF ET < 0 THEN

TC = TT(0)

GOTO 51170 'Out of bounds, round to lower limit

END IF

51140 IF ET > NT - 2 THEN

TC = TT(137)

GOTO 51170 'Out of bounds, round to upper limit

END IF

51150 'Do interpolation

51160 $TC = TT(ET) + (TT(ET + 1) - TT(ET)) * (VT - ET * SIT - SVT) / SIT$ Centigrade

51170 $TF = (TC * 1.8) + 32$ 'Fahrenheit

51180 RETURN

Table E.1: Typical Resilient Modulus Raw Data File**SYSTEM NUMBER 2**

Displacement	Applied Load	Cell Pressure
37.66896	24.05634	631.96001
37.54170	27.49296	636.84001
37.79622	32.99155	634.40001
38.30526	43.30141	619.76001
39.70512	51.54930	631.96001
39.83238	52.92394	639.28001
40.46868	56.36056	627.08001
40.46868	52.92394	636.84001
40.34142	54.29859	631.96001
40.34142	55.67324	636.84001
40.72320	52.92394	627.08001
40.59594	52.92394	636.84001
40.34142	46.73803	624.64001
39.32334	36.42817	634.40001
38.68704	31.61690	629.52001
38.94156	31.61690	636.84001
38.43252	32.99155	631.96001
38.55978	30.92958	634.40001
38.05074	25.43099	627.08001
37.79622	24.74366	636.84001
37.79622	25.43099	634.40001
37.79622	26.80563	634.40001
37.79622	27.49296	627.08001
37.79622	25.43099	639.28001
37.66896	27.49296	631.96001
37.54170	28.18028	622.20001
37.79622	35.05352	636.84001
38.81430	45.36338	624.64001
39.83238	50.17465	631.96001
40.21416	52.92394	631.96001
40.34142	52.92394	634.40001
40.72320	52.92394	631.96001
40.59594	54.98592	631.96001
40.59594	53.61127	629.52001
40.59594	52.92394	629.52001
40.85046	52.92394	627.08001
40.97772	44.67606	634.40001
39.45060	33.67887	636.84001
37.79622	29.55493	624.64001
38.30526	30.92958	636.84001
38.30526	30.24225	634.40001
38.17800	28.18028	619.76001
37.79622	25.43099	634.40001
37.92348	25.43099	622.20001

37.92348	25.43099	639.28001
37.54170	24.74366	634.40001
37.79622	25.43099	619.76001
37.79622	28.86761	636.84001
37.66896	25.43099	617.32001
37.66896	25.43099	636.84001
37.92348	25.43099	634.40001
37.54170	27.49296	627.08001
37.66896	32.30423	631.96001
38.30526	40.55211	627.08001
39.32334	49.48732	636.84001
39.83238	52.92394	631.96001
40.34142	55.67324	629.52001
40.72320	52.92394	636.84001
40.34142	55.67324	631.96001
40.34142	36.36056	624.64001
40.97772	53.61127	631.96001
40.97772	52.92394	636.84001
40.59594	47.42535	617.32001
39.57786	35.05352	631.96001
38.81430	29.55493	634.40001
38.81430	32.99155	624.64001
38.30526	31.61690	636.84001
38.30526	29.55493	631.96001
38.05074	27.49296	619.76001
37.79622	27.49296	631.96001
37.66896	24.74366	629.52001
37.92348	24.05634	619.76001
37.79622	24.74366	636.84001
37.92348	25.43099	631.96001
37.54170	25.43099	622.20001
37.28718	25.43099	627.08001
37.79622	26.80563	634.40001
37.79622	30.92958	631.96001
38.30526	39.17746	634.40001
39.06882	49.48732	636.84001
40.08690	52.92394	636.84001
40.46868	55.67324	634.40001
40.46868	55.67324	636.84001
40.34142	54.29859	636.84001
40.85046	53.61127	627.08001
40.72320	54.98592	631.96001
40.72320	54.98592	631.96001
40.85046	51.54930	622.20001
40.34142	43.98873	639.28001
39.06882	32.99155	631.96001
38.43252	30.92958	627.08001
38.55978	34.36620	624.64001
38.30526	28.18028	636.84001
38.17800	25.43099	636.84001
37.79622	26.11831	634.40001
37.79622	25.43099	624.64001

37.79622	24.74366	634.40001
37.79622	24.74366	636.84001
37.79622	24.05634	631.96001
37.79622	25.43099	617.32001

KEY:

- [1] System Number refers to the load bay used in test (2 is the middle bay in Figure E.1)
- [2] Displacement refers to the LVDT readings. (inch /1000)
- [3] Applied Load refers to the repetitive axial load readings. (lb)
- [4] Cell Pressure refers to the confining pressure readings. (psi x 100)

Note:

*** This is a typical stress-strain data file that is produced by MODULUZZ.BAS Program**

- (1) The data shown in the table above are those pertaining to only four load cycles.
- (2) Every load cycle contains three sets of test data , i.e. displacement, axial load and confining pressure, of twenty five readings each.

E.5.2 Triaxial Test Data Processing Programs

(I) Permanent Deformation Programs

Two programs, PDEF-IC and PDEF-IIC, are used for permanent deformation computation. The two programs are identical with only one exception. PDEF-IC is used to analyze the first load sequence data where the initial sample height is to be input manually whereas PDEF-IIC program is used to analyze the test data for the remaining load sequences utilizing soil sample height(s) computed from previous runs of either PDEF-IC or PDEF-IIC.

(a) Program PDEF-IC for used for Computation of Permanent Deformation

```
"  IMPLICIT REAL*8 (A-H,O-Z)"
"  CHARACTER *12 FILE5,FILE7,FILE8,FILE6,FILE4"
"  CHARACTER *80 TITLE1,TITLE2"
"  CHARACTER *4 NUMBERS
"  CHARACTER *1 CH(4)
"  DIMENSION HF(200), HFA(200),HFINAL(4),DIF(4),HQART(4)"
"  DIMENSION H2DIF(4),DLDDIF(4),HFFDIF(4)"
"  WRITE(*,201)"
201 FORMAT (' ENTER GROUP NUMBER AND LOAD SEQUENCE NUMBER ')
"  READ (*,*) NUMBERS"
"  READ (NUMBERS,11) (CH(I),I=1,4)"
11 FORMAT(12(A1))
"  IF(CH(4).EQ.' ') THEN
"    IF(CH(3).EQ.' ') THEN
"      WRITE(FILE5,11) 'G',CH(1),'-',CH(2),' ','D','A','T'"
"      WRITE(FILE7,11) 'D',CH(1),'-',CH(2),' ','D','A','T'"
"      WRITE(FILE8,11) 'D','H','F','A',CH(1),'-',CH(2),' ','D','A','T'"
"      WRITE(FILE6,11) 'D','H',CH(1),'-',CH(2),' ','D','A','T'"
"      WRITE(FILE4,11) 'D','D','T','F',CH(1),'-',CH(2),' ','D','A','T'"
"    ELSE
"      WRITE(FILE5,11) 'G',CH(1),'-',CH(2),CH(3),' ','D','A','T'"
"      WRITE(FILE7,11) 'D',CH(1),'-',CH(2),CH(3),' ','D','A','T'"
"      WRITE(FILE8,11) 'D','H','F','A',CH(1),'-',CH(2),CH(3),' ','D','A'
"      &','T'"
"      WRITE(FILE6,11) 'D','H',CH(1),'-',CH(2),CH(3),' ','D','A','T'"
"      WRITE(FILE4,11) 'D','D','T','F',CH(1),'-',CH(2),CH(3),' ','D','A'
"      &','T'"
"    ENDIF
"  ELSE
"    WRITE(FILE5,11) 'G',CH(1),'-',CH(2),CH(3),CH(4),' ','D','A','T'"
"    WRITE(FILE7,11) 'D',CH(1),'-',CH(2),CH(3),CH(4),' ','D','A','T'"
```

```

"    WRITE(FILE8,11) 'D','H','F','A',CH(1),'-',CH(2),CH(3),CH(4),',',
"    &'D','A','T'"
"    WRITE(FILE6,11) 'D','H',CH(1),'-',CH(2),CH(3),CH(4),',', 'D','A',
&'T'
"    WRITE(FILE4,11) 'D','D','T','F',CH(1),'-',CH(2),CH(3),CH(4),',',
"    &'D','A','T'"
    ENDIF
"    OPEN (UNIT=5,FILE=FILE5,STATUS='OLD')
"    OPEN (UNIT=7,FILE=FILE7,STATUS='NEW')
"    OPEN (UNIT=8,FILE=FILE8,STATUS='NEW')
"    OPEN (UNIT=6,FILE=FILE6,STATUS='NEW')
"    OPEN (UNIT=4,FILE=FILE4,STATUS='NEW')
"    READ (5,220)TITLE1
"    READ (5,220)TITLE2
220 FORMAT(A80)
"    WRITE(*,203)"
203 FORMAT (' ENTER NUMBER OF DATA SETS')
"    READ (*,*) NSETS
"    WRITE(*,204)"
204 FORMAT (' ENTER NUMBER OF POINTS  ')
"    READ (*,*) NVARs"
"    WRITE(*,230) "
230 FORMAT(' ENTER H1 ')
"    READ (*,*) H1"
"    WRITE(*,290) "
290 FORMAT(' ENTER PBALANCE ')
"    READ (*,*) PBAL"
"    WRITE(7,221)"
" 221 FORMAT(' LV1  , LV25  , LC1  , LC25  , LV25-LV1"
"    & ,LC25-LC1 , LVCUM  , HF(I)  , HFA(I) , LCCUM, "
& P3AVG ')
    ACUM=0.0
    BCUM=0.0
    CCUM=0.0
    CCUMT=0.0
"    DO 100 I=1,NSETS"
"      DO 101 J=1,NVARs"
"        READ(5,*) A,B,C"
"        IF(J.EQ.1) A1 = A
"        IF(J.EQ.1) B1 = B
"        IF(J.EQ.NVARs) A25 = A
"        IF(J.EQ.NVARs) B25 = B
"        CCUM=CCUM+C
"        CCUMT=CCUMT+C
101 CONTINUE

```

```

DIFA = A25-A1
DIFB = B25-B1
ACUM=ACUM+DIFA
BCUM=BCUM+DIFB
P3AVG=CCUM/NVARS
HF(I) = H1-(ACUM/1000.0)
IF(I.EQ.1) HFA(1) = (H1+HF(1))/2.0
IF(I.NE.1) HFA(I) = (HF(I-1)+HF(I))/2.0
"  WRITE(7,223)A1,A25,B1,B25,DIFA,DIFB,ACUM,HF(I),HFA(I),BCUM,P3AVG"
IF(I.EQ.1) AINIT = A1
IF(I.EQ.25) DIF(1) = A25-AINIT
IF(I.EQ.50) DIF(2) = A25-AINIT
IF(I.EQ.75) DIF(3) = A25-AINIT
IF(I.EQ.100) DIF(4) = A25-AINIT
CCUM=0.0
100 CONTINUE
  CCUMTA=((CCUMT/NSETS/NVARS)-PBAL)/100
" 223 FORMAT(11(F11.5,','))"
"  WRITE(7,224)ACUM,BCUM,CCUMTA"
" 224 FORMAT('LVCUM =',F15.9,', LCCUM =', F15.9,', P3GA =', F15.9)"
  H2= H1 - (ACUM/1000.0)
  DL= 100*((H1 - H2)/H1)
  HFF = (H1 + H2)/2.0
"  DO 113 I=1,4"
    H2DIF(I)= H1 - (DIF(I)/1000.0)
    DLDIF(I)= 100*((H1 - H2DIF(I))/H1)
    HFFDIF(I) = (H1 + H2DIF(I))/2.0
113 CONTINUE
"  WRITE(7,231)H2,HFF,DL"
" 231 FORMAT(' H2 =',F15.9,', HFF =', F15.9,', DL =', F15.9)"
"  DO 102 I=1,NSETS"
"    WRITE(8,236)HFA(I)"
102 CONTINUE
236 FORMAT(F15.9)
"  WRITE(8,236)"
"  DO 110 I=1,4"
    HFINAL(I)=H1-DIF(I)/1000.0
"  WRITE(6,238) HFINAL(I)"
110 CONTINUE
238 FORMAT(F15.9)
"  WRITE(7,250)"
250 FORMAT('QUARTER      DIF(I) ')
"  WRITE(4,251)"
251 FORMAT('QUARTER      H2DIF(I)   DLDIF(I)   HFFDIF(I)')
"  DO 115 I=1,4"

```

```
"  WRITE(7,246)I,DIF(I)"
"  WRITE(4,247)I,H2DIF(I),DL DIF(I),HrFDIF(I)"
115 CONTINUE
" 246 FORMAT(I3,5X,F15.9)"
" 247 FORMAT(I3,3(3X,F15.9))"
  STOP
  END
```

(b) Program PDEF-III.for used for Computation of Permanent Deformation

```

"  IMPLICIT REAL*8(A-H,O-Z)"
"  CHARACTER *12 FILE5,FILE7,FILE8,FILE6,FILE4,FILE3      "
"  CHARACTER *80 TITLE1,TITLE2"
  CHARACTER *4 NUMBERS
  CHARACTER *1 CH(4)
"  DIMENSION HF(200), HFA(200),HINIT(4),DIF(4),HINITF(4)"
"  DIMENSION HCDIF(4),DLDDIF(4),HFFDIF(4)"
"  WRITE(*,201)"
201 FORMAT (' ENTER GROUP NUMBER AND LOAD SEQUENCE NUMBER ')
"  READ (*,*) NUMBERS"
"  READ (NUMBERS,11) (CH(I),I=1,4)"
11 FORMAT(12(A1))
"  WRITE(*,270)"
270 FORMAT (' ENTER INPUT FILE NAME FOR HINITIAL ')
"  READ (*, '(A)') FILE4"
  IF(CH(4).EQ.' ') THEN
    IF(CH(3).EQ.' ') THEN
      "  WRITE(FILE5,11) 'G',CH(1),'-',CH(2),',',',D','A','T'"
      "  WRITE(FILE7,11) 'D',CH(1),'-',CH(2),',',',D','A','T'"
      "  WRITE(FILE8,11) 'D','H','F','A',CH(1),'-',CH(2),',',',D','A','T'"
      "  WRITE(FILE6,11) 'D','H',CH(1),'-',CH(2),',',',D','A','T'"
      "  WRITE(FILE3,11) 'D','D','T','F',CH(1),'-',CH(2),',',',D','A','T'"
    ELSE
      "  WRITE(FILE5,11) 'G',CH(1),'-',CH(2),CH(3),',',',D','A','T'"
      "  WRITE(FILE7,11) 'D',CH(1),'-',CH(2),CH(3),',',',D','A','T'"
      "  WRITE(FILE8,11) 'D','H','F','A',CH(1),'-',CH(2),CH(3),',',',D','A'
      "  &','T'"
      "  WRITE(FILE6,11) 'D','H',CH(1),'-',CH(2),CH(3),',',',D','A','T'"
      "  WRITE(FILE3,11) 'D','D','T','F',CH(1),'-',CH(2),CH(3),',',',D','A'
      "  &','T'"
    ENDIF
  ELSE
    "  WRITE(FILE5,11) 'G',CH(1),'-',CH(2),CH(3),CH(4),',',',D','A','T'"
    "  WRITE(FILE7,11) 'D',CH(1),'-',CH(2),CH(3),CH(4),',',',D','A','T'"
    "  WRITE(FILE8,11) 'D','H','F','A',CH(1),'-',CH(2),CH(3),CH(4),',',',
    "  &'D','A','T'"
    "  WRITE(FILE6,11) 'D','H',CH(1),'-',CH(2),CH(3),CH(4),',',',D','A',"
    "  &'T'
    "  WRITE(FILE3,11) 'D','D','T','F',CH(1),'-',CH(2),CH(3),CH(4),',',',
    "  &'D','A','T'"
  ENDIF
"  WRITE(*,271)      "
271 FORMAT(' ENTER THE QUARTER OF HINIT TO BE USED (1 TO 4)')

```

```

"  READ (*, *  QUART"
"  OPEN (UNIT=5,FILE=FILE5,STATUS='OLD')"
"  OPEN (UNIT=4,FILE=FILE4,STATUS='OLD')  "
"  OPEN (UNIT=7,FILE=FILE7,STATUS='NEW')"
"  OPEN (UNIT=8,FILE=FILE8,STATUS='NEW')"
"  OPEN (UNIT=6,FILE=FILE6,STATUS='NEW')"
"  OPEN (UNIT=3,FILE=FILE3,STATUS='NEW')      "
"  READ (5,220)TITLE1"
"  READ (5,220)TITLE2"
"  DO 110 I=1,4"
"    READ (4,*) HINIT(I)"
110 CONTINUE
220 FORMAT(A80)
"  WRITE(*,203)"
203 FORMAT (' ENTER NUMBER OF DATA SETS')
"  READ (*,*) NSETS"
"  WRITE(*,204)"
204 FORMAT (' ENTER NUMBER OF POINTS  ')
"  READ (*,*) NVARs"
"  WRITE(*,290)"
290 FORMAT (' ENTER PBALANCE  ')
"  READ (*,*) PBAL"
"  WRITE(7,221)"
" 221 FORMAT('  LV1  ,  LV25  ,  LC1  ,  LC25  ,  LV25-LV1"
"    & , LC25-LC1 , LVCUM  , HF(I)  , HFA(I) ,  LCCUM  "
"    & P3AVG  ')"
"    ACUM=0.0
"    BCUM=0.0
"    CCUM=0.0
"    CCUMT=0.0
"  DO 100 I=1,NSETS"
"    DO 101 J=1,NVARs"
"      READ(5,*) A,B,C"
"      IF(J.EQ.1) A1 = A
"      IF(J.EQ.1) B1 = B
"      IF(J.EQ.NVARs) A25 = A
"      IF(J.EQ.NVARs) B25 = B
"      CCUM=CCUM+C
"      CCUMT=CCUMT+C
101 CONTINUE
"    DIFA = A25-A1
"    DIFB = B25-B1
"    ACUM=ACUM+DIFA
"    BCUM=BCUM+DIFB
"    P3AVG=CCUM/NVARs

```

```

HF(I) = HINIT(IQUART)-(ACUM/1000.0)
IF(I.EQ.1) HFA(1) = (HINIT(IQUART)+HF(1))/2.0
IF(I.NE.1) HFA(I) = (HF(I-1)+HF(I))/2.0
"  WRITE(7,223)A1,A25,B1,B25,DIFA,DIFB,ACUM,HF(I),HFA(I),BCUM,P3AVG"
IF(I.EQ.1) AINIT = A1
IF(I.EQ.25) DIF(1) = A25-ANIT
IF(I.EQ.50) DIF(2) = A25-ANIT
IF(I.EQ.75) DIF(3) = A25-ANIT
IF(I.EQ.100) DIF(4) = A25-ANIT
CCUM=0.0
100 CONTINUE
  CCUMTA=((CCUMT/NSETS/NVARS)-PBAL)/100
" 223 FORMAT(11(F11.5,' '))"
"  WRITE(7,224)ACUM,BCUM,CCUMTA"
" 224 FORMAT('LVCUM = ',F15.9,', LCCUM = ', F15.9,', P3GA = ', F15.9)"
  H2= HINIT(IQUART) - (ACUM/1000.0)
  DL= 100*((HINIT(IQUART) - H2)/HINIT(IQUART))
  HFF = (HINIT(IQUART) + H2)/2.0
"  DO 113 I=1,4"
    H2DIF(I)= HINIT(IQUART) - (DIF(I)/1000.0)
    DLDIF(I)= 100*((HINIT(IQUART) - H2DIF(I))/HINIT(IQUART))
    HFFDIF(I) = (HINIT(IQUART) + H2DIF(I))/2.0
113 CONTINUE
"  WRITE(7,231)H2,HFF,DL"
" 231 FORMAT(' H2 = ',F15.9,', HFF = ', F15.9,', DL = ', F15.9)"
"  DO 102 I=1,NSETS"
"    WRITE(8,236)HFA(I)"
102 CONTINUE
236 FORMAT(F15.9)
"  WRITE(8,236)"
"  WRITE(7,291)"
291 FORMAT(' IQUART  DIF(I) ')
"  WRITE(3,292)"
292 FORMAT(' IQUART  H2DIF(I)  DLDIF(I)  HFFDIF(I) ')
"  DO 112 I=1,4"
    HINITF(I)= HINIT(IQUART)-DIF(I)/1000.0
"    WRITE(6,238) HINITF(I)"
"    WRITE(7,246)I,DIF(I)"
"    WRITE(3,251)I,H2DIF(I),DLDIF(I),HFFDIF(I)"
112 CONTINUE
" 251 FORMAT(I3,3(3X,F15.9))"
" 246 FORMAT(I3,5X,F15.9)"
238 FORMAT(F15.9)
  STOP
  END

```

(c) Example Output Files of PDEF-IC and PDEF-IIC Programs

Table E.2: Typical Output File Produced by Program PDEF-IC (File D1-11.dat)

LV1	LV25	LC1	LC25	LV25-LV1	LC25-LC1	LVCUM	HF(I)	HFA(I)	LCCUM	P3AVG
37.66896	37.66896	24.05634	27.49296	0.00000	3.43662	0.00000	6.91600	6.91600	3.43662	632.54561
37.54170	37.66896	28.18028	25.43099	0.12726	-2.74930	0.12726	6.91587	6.91594	0.68732	630.39841
37.92348	37.54170	25.43099	25.43099	-0.38178	0.00000	-0.25452	6.91625	6.91606	0.68732	630.00801
37.28718	37.79622	25.43099	25.43099	0.50904	0.00000	0.25452	6.91575	6.91600	0.68732	631.96001
37.54170	37.92348	27.49296	27.49296	0.38178	0.00000	0.63630	6.91536	6.91555	0.68732	629.71521
37.79622	37.79622	27.49296	27.49296	0.00000	0.00000	0.63630	6.91536	6.91536	0.68732	631.86241
37.66896	37.79622	25.43099	25.43099	0.12726	0.00000	0.76356	6.91524	6.91530	0.68732	630.78881
37.66896	37.66896	24.05634	26.80563	0.00000	2.74930	0.76356	6.91524	6.91524	3.43662	633.13121
37.66896	37.66896	27.49296	26.11831	0.00000	-1.37465	0.76356	6.91524	6.91524	2.06197	631.96001
37.79622	37.92348	26.11831	25.43099	0.12726	-0.68732	0.89082	6.91511	6.91517	1.37465	631.17921
37.92348	37.79622	25.43099	26.11831	-0.12726	0.68732	0.76356	6.91524	6.91517	2.06197	630.98401
37.79622	37.54170	27.49296	25.43099	-0.25452	-2.06197	0.50904	6.91549	6.91536	0.00000	632.83841
37.66896	37.79622	24.74366	26.11831	0.12726	1.37465	0.63630	6.91536	6.91543	1.37465	630.10561
37.79622	37.79622	26.11831	26.80563	0.00000	0.68732	0.63630	6.91536	6.91536	2.06197	630.49601
37.79622	37.79622	27.49296	27.49296	0.00000	0.00000	0.63630	6.91536	6.91536	2.06197	631.56961
37.66896	37.79622	25.43099	25.43099	0.12726	0.00000	0.76356	6.91524	6.91530	2.06197	631.76481
37.92348	37.79622	25.43099	26.80563	-0.12726	1.37465	0.63630	6.91536	6.91530	3.43662	629.71521
37.54170	37.79622	28.18028	26.80563	0.25452	-1.37465	0.89082	6.91511	6.91524	2.06197	630.39841
37.54170	37.79622	27.49296	25.43099	0.25452	-2.06197	1.14534	6.91483	6.91498	0.00000	628.25121
37.79622	37.92348	25.43099	25.43099	0.12726	0.00000	1.27260	6.91473	6.91479	0.00000	630.49601
37.66896	37.92348	24.74366	26.80563	0.25452	2.06197	1.52712	6.91447	6.91460	2.06197	629.42241
37.54170	37.92348	27.49296	26.11831	0.38178	-1.37465	1.90890	6.91403	6.91428	0.68732	630.88641
37.79622	37.66896	27.49296	25.43099	-0.12726	-2.06197	1.78164	6.91422	6.91415	-1.37465	630.49601
37.66896	37.79622	25.43099	26.11831	0.12726	0.68732	1.90890	6.91409	6.91415	-0.68732	630.30081
37.66896	37.79622	26.11831	26.11831	0.12726	0.00000	2.03616	6.91396	6.91403	-0.68732	629.42241
37.79622	37.79622	25.43099	27.49296	0.00000	2.06197	2.03616	6.91396	6.91396	1.37465	631.47201
37.66896	37.79622	25.43099	27.49296	0.12726	2.06197	2.16342	6.91384	6.91390	3.43662	631.08161
37.92348	37.92348	25.43099	25.43099	0.00000	0.00000	2.16342	6.91384	6.91384	3.43662	630.00801

37.66896	37.79622	24.05634	28.86761	0.12726	4.81127	2.29068	6.91371	6.91377	8.24789	630.49601
37.66896	37.66896	25.43099	25.43099	0.00000	0.00000	2.29068	6.91371	6.91371	8.24789	633.71681
37.79622	37.79622	24.05634	25.43099	0.00000	1.37465	2.29068	6.91371	6.91371	9.62254	630.20321
37.66896	37.66896	28.86761	26.80563	0.00000	-2.06197	2.29068	6.91371	6.91371	7.56055	630.88641
37.54170	37.79622	26.80563	27.49296	0.25452	0.68732	2.54520	6.91345	6.91358	8.24789	631.86241
37.79622	37.79622	28.18028	28.18028	0.00000	0.00000	2.54520	6.91345	6.91345	8.24789	629.22721
37.79622	37.79622	28.18028	28.18028	0.00000	0.00000	2.54520	6.91345	6.91345	8.24789	631.27681
37.79622	37.79622	28.18028	28.18028	0.00000	0.00000	2.54520	6.91345	6.91345	8.24789	632.15521
37.66896	37.79622	28.18028	28.18028	0.00000	0.00000	2.54520	6.91345	6.91345	8.24789	631.27681
37.41444	37.79622	26.11831	26.80563	0.12726	0.68732	2.67246	6.91333	6.91339	8.93521	629.03201
37.79622	37.79622	27.49296	28.86761	0.38178	1.37465	3.05424	6.91295	6.91314	10.30986	630.59361
37.79622	37.79622	28.18028	25.43099	0.00000	-2.74930	3.05424	6.91295	6.91295	7.56056	631.47201
37.79622	37.79622	26.11831	27.49296	0.00000	1.37465	3.05424	6.91295	6.91295	8.93521	630.98401
37.66896	37.79622	25.43099	27.49296	0.12726	2.06197	3.18150	6.91282	6.91288	10.99718	630.88641
37.54170	37.79622	26.80563	24.74366	0.25452	-2.06197	3.43602	6.91256	6.91269	8.93521	631.37441
37.79622	37.66896	26.80563	25.43099	-0.12726	-1.37465	3.30876	6.91269	6.91263	7.56056	630.88641
37.28718	37.79622	26.11831	25.43099	0.50904	-0.68732	3.81780	6.91218	6.91244	6.87324	631.08161
37.54170	37.79622	27.49296	25.43099	0.25452	-2.06197	4.07232	6.91193	6.91205	4.81127	629.42241
37.54170	37.66896	26.11831	28.18028	0.12726	2.06197	4.19958	6.91180	6.91186	6.87324	631.96001
37.54170	37.79622	27.49296	28.86761	0.25452	1.37465	4.45410	6.91155	6.91167	8.24789	631.27681
37.92348	37.66896	25.43099	25.43099	-0.25452	0.00000	4.19958	6.91180	6.91167	8.24789	631.17921
37.66896	37.66896	25.43099	27.49296	0.00000	2.06197	4.19958	6.91180	6.91180	10.30986	630.59361
37.66896	37.92348	28.18028	26.11831	0.25452	-2.06197	4.45410	6.91155	6.91167	8.24789	630.00801
37.66896	37.79622	25.43099	26.11831	0.12726	0.68732	4.58136	6.91142	6.91148	8.93521	629.22721
37.79622	37.79622	27.49296	27.49296	0.00000	0.00000	4.58136	6.91142	6.91142	8.93521	629.91041
37.92348	37.79622	25.43099	27.49296	-0.12726	2.06197	4.45410	6.91155	6.91148	10.99718	629.22721
37.28718	37.79622	27.49296	27.49296	0.50904	0.00000	4.96314	6.91104	6.91129	10.99718	629.22721
37.54170	37.92348	25.43099	26.80563	0.38178	1.37465	5.34492	6.91066	6.91085	12.37183	629.32481
37.66896	37.79622	24.74366	25.43099	0.12726	0.68732	5.47218	6.91053	6.91059	13.05915	630.69121
37.66896	37.79622	25.43099	27.49296	0.12726	2.06197	5.59944	6.91040	6.91046	15.12113	631.17921
37.66896	37.92348	26.80563	24.74366	0.25452	-2.06197	5.85396	6.91015	6.91027	13.05915	631.76481
37.54170	37.79622	24.05634	26.11831	0.25452	2.06197	6.10848	6.90989	6.91002	15.12113	629.03201
37.66896	37.79622	27.49296	25.43099	0.12726	-2.06197	6.23574	6.90976	6.90983	13.05915	631.17921
37.79622	37.66896	28.18028	27.49296	-0.12726	-0.68732	6.10848	6.90989	6.90983	12.37183	631.47201
37.92348	37.92348	25.43099	25.43099	0.00000	0.00000	6.10848	6.90989	6.90989	12.37183	630.30081

37.66896	37.79622	27.49296	24.74366	0.12726	-2.74930	6.23574	6.90976	6.90983	9.62254	630.98401
37.66896	37.79622	25.43099	27.49296	0.12726	2.06197	6.36300	6.90964	6.90970	11.68451	631.56961
37.79622	37.79622	25.43099	25.43099	0.00000	0.00000	6.36300	6.90964	6.90964	11.68451	630.39841
37.54170	37.66896	25.43099	26.11831	0.12726	0.68732	6.49026	6.90951	6.90957	12.37183	629.91041
37.92348	37.79622	25.43099	25.43099	-0.12726	0.00000	6.36300	6.90964	6.90957	12.37183	629.32481
37.54170	37.66896	27.49296	26.11831	0.12726	-1.37465	6.49026	6.90951	6.90957	10.99718	631.76481
37.66896	37.66896	27.49296	25.43099	0.00000	-2.06197	6.49026	6.90951	6.90951	8.93521	630.20321
37.79622	37.79622	27.49296	25.43099	0.00000	-2.06197	6.49026	6.90951	6.90951	6.87324	631.76481
37.66896	37.66896	25.43099	28.86761	0.00000	3.43662	6.49026	6.90951	6.90951	10.30986	631.66721
37.66896	37.79622	27.49296	25.43099	0.12726	-2.06197	6.61752	6.90938	6.90945	8.24789	630.39841
37.28718	37.92348	25.43099	26.80563	0.63630	1.37465	7.25382	6.90875	6.90906	9.62254	630.59361
37.41444	37.79622	27.49296	27.49296	0.38178	0.00000	7.63560	6.90836	6.90856	9.62254	629.52001
37.28718	37.79622	25.43099	25.43099	0.50904	0.00000	8.14464	6.90786	6.90811	9.62254	631.08161
37.54170	37.79622	25.43099	24.05634	0.25452	-1.37465	8.39916	6.90760	6.90773	8.24789	629.52001
37.92348	37.66896	25.43099	26.11831	-0.25452	0.68732	8.14464	6.90786	6.90773	8.93521	630.69121
37.66896	37.66896	25.43099	27.49296	0.00000	2.06197	8.14464	6.90786	6.90786	10.99718	630.69121
37.79622	37.79622	25.43099	27.49296	0.00000	2.06197	8.14464	6.90786	6.90786	13.05915	630.10561
37.79622	37.79622	27.49296	26.11831	0.00000	-1.37465	8.14464	6.90786	6.90786	11.68451	630.98401
37.66896	37.54170	27.49296	27.49296	-0.12726	0.00000	8.01738	6.90798	6.90792	11.68451	629.81281
37.41444	37.79622	25.43099	25.43099	0.38178	0.00000	8.39916	6.90760	6.90779	11.68451	630.78881
37.28718	37.79622	25.43099	25.43099	0.50904	0.00000	8.90820	6.90709	6.90735	11.68451	630.88641
37.66896	37.92348	26.80563	25.43099	0.25452	-1.37465	9.16272	6.90684	6.90696	10.30986	629.22721
37.79622	37.66896	27.49296	28.18028	-0.12726	0.8732	9.03546	6.90696	6.90690	10.99718	630.30081
37.79622	37.79622	25.43099	26.11831	0.00000	0.68732	9.03546	6.90696	6.90696	11.68451	629.42241
37.28718	37.92348	25.43099	25.43099	0.63630	0.00000	9.67176	6.90633	6.90665	11.68451	629.71521
37.79622	37.66896	27.49296	27.49296	-0.12726	0.00000	9.54450	6.90646	6.90639	11.68451	628.93441
37.79622	37.28718	28.18028	28.18028	-0.50904	0.00000	9.03546	6.90696	6.90671	11.68451	629.91041
37.54170	37.92348	26.11831	25.43099	0.38178	-0.68732	9.41724	6.90658	6.90677	10.99718	629.81281
37.54170	37.79622	25.43099	26.11831	0.25452	0.68732	9.67176	6.90633	6.90646	11.68451	630.20321
37.54170	37.92348	27.49296	26.80563	0.38178	-0.68732	10.18080	6.90582	6.90601	8.24789	629.42241
37.66896	37.79622	28.18028	25.43099	0.12726	-2.74930	10.30806	6.90569	6.90576	5.49859	630.10561
37.79622	37.66896	26.11831	25.43099	-0.12726	-0.68732	10.18080	6.90582	6.90576	4.81127	629.91041
37.92348	37.54170	25.43099	25.43099	-0.38178	0.00000	9.79902	6.90620	6.90601	4.81127	630.49601
37.66896	37.92348	26.80563	25.43099	0.25452	-1.37465	10.05354	6.90595	6.90607	3.43662	629.91041

LVCUM = 10.053539962 LCCUM = 3.436619700 P3GA = 5.905731188
H2 = 6.905946460 HFF = 6.910973230 DL = .145366396

QUARTER	DIF (I)
1	0.12726
2	0.00000
3	0.12726
4	0.25452

KEY:

- [1] LV1 is the LVDT reading at the beginning of the loading cycle (inch /1000).
- [2] LV25 is the LVDT reading at the end of the loading cycle (inch/1000).
- [3] LC1 is the load cell reading at the beginning of the loading cycle (lb).
- [4] LC25 is the load cell reading at the end of the loading cycle (lb).
- [5] (LV25-LV1) is the permanent deformation accumulated after each loading cycle (inch/1000).
- [6] (LC25-LC1) is the difference in load cell readings between the beginning and end of each loading cycle (lb).
- [7] LVCUM is the cumulative permanent deformation. This is equal the sum of LV25-LV1 (inch/1000).
- [8] HF (I) is the final sample length after each loading cycle (inch).
- [9] HFA (I) is the average sample length after each loading cycle (is = 0.5{HF (1-1) + HF (I)} in inches).
- [10] LCCUM is the cumulative difference in load cell readings between the beginning and end of every loading cycle (lb).
- [11] P3AVG is the uncorrected average confining cell pressure (psi x 100).
- [12] The explanation of the parameters printed after the tabulated data are as follows:
- [a] LVCUM is the final cumulative permanent deformation after 100 repetitions (i.e. the last value printed in the LVCUM column).
- [b] LCCUM is the last value printed in the LCCUM column.
- [c] P3GA is the corrected average confining cell pressure used in the analysis of the data (psi).
- [d] H2 is the final value printed in the HF (I) column.
- [e] HFF is the final sample length at the end of the test derived from $HFF = (\text{Initial sample length} + H2)/2$.
- [f] DL is the percent permanent deformation derived from $DL = 100\{(H1 - H2)/H1\}$, where H1 is the initial sample length.
- [g] QUARTER refers to the quarter number used in the Mr analysis, where the 100 load repetitions were divided into four segments of 25 reps. each.
- [h] DIF (I) refers to the permanent deformation accumulated at the end of each quarter. This is obtained by subtracting the initial LVDT reading at the beginning of the test from the final LVDT reading at the end of the loading cycle of the designated quarter.

Table E.3: Typical Output File Produced by Program PDEF-IC (File DDIF1-11.dat)

QUARTER	H2DIF(I)	DLDF(I)	HFFDF(I)
1	6.91587	0.00184	6.91594
2	6.91600	0.00000	6.91600
3	6.91587	0.00184	6.91594
4	6.91575	0.00368	6.91587

KEY:

- [1] QUARTER refers to the quarter number used in the Mr analysis, where the 100 load repetitions were divided into four segments of 25 reps. each.
- [2] H2DIF(I) refers to the final sample length at the end of quarter (I), where I = 25, 50, 75, or 100 reps. H2DIF(I) is computed from $H2DIF(I) = H - DIF(I)$, where H1 and DIF(I) are as defined before. (inch)
- [3] DLDF(I) refers to the percent permanent deformation accumulated at the end of quarter(I). $DLDF(I) = 100 \{(H1 - H2DIF(I))/H1\}$
- [4] HFFDF(I) refers to the average length of the sample at the end of quarter(I). It is obtained as $HFFDF(I) = \{H1 + H2DIF(I)\}/2$. (inch)

(II) Resilient Modulus Programs

Two programs, MCALC-IC and mCLC-IIC, are used for resilient modulus computations. The two programs are identical with only one exception. MCALC-IC is used to analyze the first load sequence data where the initial sample height is to be input manually whereas MCLC-IIC program is used to analyze the test data for the remaining load sequences utilizing soil sample height(s) computed from previous runs of either MCALC-IC or MCLC-IIC.

(a) Program MCALC-IC for used for Computation of Resilient Modulus

```
"  IMPLICIT REAL*8(A-H,O-Z)"
"  CHARACTER *12 FILE5,FILE6,FILE7,FILE8"
"  CHARACTER *80 TITLE1,TITLE2"
"  CHARACTER *4 NUMBERS
"  CHARACTER *1 CH(4)
"  DIMENSION HFA(200),AF(200),DSTRS(200),RSTRN(200)"
"  DIMENSION RM(200),DST(200),RST(200),RMM(200),P3(200)"
"  WRITE(*,201)"
201 FORMAT (' ENTER GROUP NUMBER AND LOAD SEQUENCE NUMBER ')
"  READ (*,*) NUMBERS"
"  READ (NUMBERS,11) (CH(I),I=1,4)"
11 FORMAT(12(A1))
"  IF(CH(4).EQ.' ') THEN
"  IF(CH(3).EQ.' ') THEN
"    WRITE(FILE5,11) 'G',CH(1),'-',CH(2),',','D','A','T'"
"    WRITE(FILE6,11) 'D','D','T','F',CH(1),'-',CH(2),',','D','A','T'"
"    WRITE(FILE7,11) 'M','R',CH(1),'-',CH(2),',','D','A','T'"
"    WRITE(FILE8,11) 'M','R','Q',CH(1),'-',CH(2),',','D','A','T'"
"  ELSE
"    WRITE(FILE5,11) 'G',CH(1),'-',CH(2),CH(3),',','D','A','T'"
"    WRITE(FILE6,11) 'D','D','T','F',CH(1),'-',CH(2),CH(3),',','D','A'
"    &','T'"
"    WRITE(FILE7,11) 'M','R',CH(1),'-',CH(2),CH(3),',','D','A','T'"
"    WRITE(FILE8,11) 'M','R','Q',CH(1),'-',CH(2),CH(3),',','D','A','T'"
"  ENDIF
"  ELSE
"    WRITE(FILE5,11) 'G',CH(1),'-',CH(2),CH(3),CH(4),',','D','A','T'"
"    WRITE(FILE6,11) 'D','D','T','F',CH(1),'-',CH(2),CH(3),CH(4),',','
"    &'D','A','T'"
"    WRITE(FILE7,11) 'M','R',CH(1),'-',CH(2),CH(3),CH(4),',','D','A','
"    &'T'
"    WRITE(FILE8,11) 'M','R','Q',CH(1),'-',CH(2),CH(3),CH(4),',','D','
"    &'A','T'"
```

```

ENDIF
" OPEN (UNIT=5,FILE=FILE5,STATUS='OLD')
" OPEN (UNIT=6,FILE=FILE6,STATUS='OLD')
" OPEN (UNIT=7,FILE=FILE7,STATUS='NEW')
" OPEN (UNIT=8,FILE=FILE8,STATUS='NEW') "
" READ (5,220)TITLE1"
" READ (5,220)TITLE2"
220 FORMAT(A80)
" READ (6,220)TITLE2"
" WRITE(*,203)"
203 FORMAT (' ENTER # OF DATA SETS AND # OF POINTS')
" READ (*,*) NSETS,NVARS"
" WRITE(*,204)"
204 FORMAT (' ENTER SAMPLE DIAMETER')
" READ (*,*) DIA"
" WRITE(*,240)"
240 FORMAT (' ENTER INITIAL SAMPLE HEIGHT ')
" READ(*,*) H1"
" WRITE(*,276)"
276 FORMAT(' ENTER QUARTER TO BE USED FOR ANALYSIS')
" READ(*,*) IQUART"
" WRITE(7,222)"
" 222 FORMAT(' AMIN  , BMIN  , AMAX  , BMAX  , A25  "
" &, B25, DIFAR, DIFBR , DIFAP , DIFBP, "
" &AF(I) , RSTRN , DSTRS , RM , P3 ')"
" DO 102 I=1,IQUART"
" READ (6,*) I1,R1,R2,HFF ,IF"
102 CONTINUE
" DO 300 I=1,200"
"   RSTRN(I)=0.0
"   DSTRS(I)=0.0
"   RM(I)=0.0
"   RST(I)=0.0
"   DST(I)=0.0
"   RMM(I)=0.0
300 CONTINUE
"   CCUM=0.0
"   PGRAND=0.0
"   DO 100 I=1,NSETS"
"     AMAX=-1000000
"     BMAX=-1000000
"     AMIN=1000000
"     BMIN=1000000
"     CCUM=0.0
"     DO 101 J=1,NVARS"

```

```

"      READ(5,*) A,B,C"
      IF(J.EQ.1) A1=A
      IF(J.EQ.1) B1=B
      IF(J.EQ.NVARS) A25=A
      IF(J.EQ.NVARS) B25=B
      IF(A.LT.AMIN) AMIN = A
      IF(A.GT.AMAX) AMAX = A
      IF(B.LT.BMIN) BMIN = B
      IF(B.GT.BMAX) BMAX = B
      CCUM=CCUM+C
101  CONTINUE
      DIFAR = AMAX-A25
      DIFBR = BMAX-B25
      DIFAP = A25 - A1
      DIFBP = B25 - B1
      P3(I) = CCUM/NVARS
      PGRAND=PGRAND+P3(I)
      RSTRN(I) = DIFAR/HFFDIF/1000.0
      AF(I) = H1 * DIA * DIA *3.14159265359/HFFDIF/4.0
      DSTRS(I) = DIFBR/AF(I)
      RM(I) = DSTRS(I)/RSTRN(I)
"      WRITE(7,200) AMIN,BMIN,AMAX,BMAX,A25,B25,DIFAR,DIFBR,"
"      &DIFAP,DIFBP,AF(I),RSTRN(I),DSTRS(I),RM(I),P3(I)"
100  CONTINUE
      P3AVGF=PGRAND/NSETS/100.0
" 200  FORMAT(13(F11.5,','),F11.0,',',F11.5)"
      RST(1)=(RSTRN(25)+RSTRN(24)+RSTRN(23)+RSTRN(22)+RSTRN(21))/5.0
      RST(2)=(RSTRN(50)+RSTRN(49)+RSTRN(48)+RSTRN(47)+RSTRN(46))/5.0
      RST(3)=(RSTRN(75)+RSTRN(74)+RSTRN(73)+RSTRN(72)+RSTRN(71))/5.0
      RST(4)=(RSTRN(100)+RSTRN(99)+RSTRN(98)+RSTRN(97)+RSTRN(96))/5.0
      DST(1)=(DSTRS(25)+DSTRS(24)+DSTRS(23)+DSTRS(22)+DSTRS(21))/5.0
      DST(2)=(DSTRS(50)+DSTRS(49)+DSTRS(48)+DSTRS(47)+DSTRS(46))/5.0
      DST(3)=(DSTRS(75)+DSTRS(74)+DSTRS(73)+DSTRS(72)+DSTRS(71))/5.0
      DST(4)=(DSTRS(100)+DSTRS(99)+DSTRS(98)+DSTRS(97)+DSTRS(96))/5.0
      RM(1)=(RM(25)+RM(24)+RM(23)+RM(22)+RM(21))/5.0
      RM(2)=(RM(50)+RM(49)+RM(48)+RM(47)+RM(46))/5.0
      RM(3)=(RM(75)+RM(74)+RM(73)+RM(72)+RM(71))/5.0
      RM(4)=(RM(100)+RM(99)+RM(98)+RM(97)+RM(96))/5.0
      K=NSETS/25
"      DO 105 I=1,K"
          RMM(I)=DST(I)/RST(I)
105  CONTINUE
"      WRITE(8,255)"
" 255  FORMAT('  DST(I),  RST(I),  RM(I) ,  RMM(I) ,  P3AVGF ')"
"      DO 106 I=1,K"

```

```
"      WRITE(8,250) DST(I),RST(I),RM(I),RMM(I),P3AVGF"  
106 CONTINUE  
" 250 FORMAT(2(F11.5,','),2(F11.0,','),F7.1)"  
"      WRITE(7,277)HFFDIF"  
" 277 FORMAT('HFFDIF = ',F15.9)"  
      STOP  
      END
```

(b) Program MCLC-IIC.for used for Computation of Resilient Modulus

```

"  IMPLICIT REAL *8(A-H,O-Z)"
"  CHARACTER *12 FILE5,FILE6,FILE7,FILE8,FILE4"
"  CHARACTER *80 TITLE1,TITLE2"
  CHARACTER *4 NUMBERS
  CHARACTER *1 CH(4)
"  DIMENSION AF(200),DSTRS(200),RSTRN(200),P3(200)"
"  DIMENSION RM(200),DST(200),RST(200),RMM(200)"
"  WRITE(*,201)"
201 FORMAT (' ENTER GROUP NUMBER AND LOAD SEQUENCE NUMBER ')
"  READ (*,*) NUMBERS"
"  READ (NUMBERS,11) (CH(I),I=1,4)"
11 FORMAT(12(A1))
  IF(CH(4).EQ.' ') THEN
    IF(CH(3).EQ.' ') THEN
      "  WRITE(FILE5,11) 'G',CH(1),'-',CH(2),' ','D','A','T'"
      "  WRITE(FILE6,11) 'D','D','T','F',CH(1),'-',CH(2),' ','D','A','T'"
      "  WRITE(FILE7,11) 'M','R',CH(1),'-',CH(2),' ','D','A','T'"
      "  WRITE(FILE8,11) 'M','R','Q',CH(1),'-',CH(2),' ','D','A','T'"
      ELSE
      "  WRITE(FILE5,11) 'G',CH(1),'-',CH(2),CH(3),' ','D','A','T'"
      "  WRITE(FILE6,11) 'D','D','T','F',CH(1),'-',CH(2),CH(3),' ','D','A'"
      "  &','T'"
      "  WRITE(FILE7,11) 'M','R',CH(1),'-',CH(2),CH(3),' ','D','A','T'"
      "  WRITE(FILE8,11) 'M','R','Q',CH(1),'-',CH(2),CH(3),' ','D','A','T'"
      ENDIF
    ELSE
      "  WRITE(FILE5,11) 'G',CH(1),'-',CH(2),CH(3),CH(4),' ','D','A','T'"
      "  WRITE(FILE6,11) 'D','D','T','F',CH(1),'-',CH(2),CH(3),CH(4),' ','"
      "  &'D','A','T'"
      "  WRITE(FILE7,11) 'M','R',CH(1),'-',CH(2),CH(3),CH(4),' ','D','A','"
      "  &'T'"
      "  WRITE(FILE8,11) 'M','R','Q',CH(1),'-',CH(2),CH(3),CH(4),' ','D','"
      "  &'A','T'"
      ENDIF
    "  WRITE(*,261)"
261 FORMAT (' ENTER INPUT FILE NAME FOR INITIAL HEIGHT ')
"  READ (*, '(A)') FILE4"
"  OPEN (UNIT=5,FILE=FILE5,STATUS='OLD')"
"  OPEN (UNIT=6,FILE=FILE6,STATUS='OLD')"
"  OPEN (UNIT=4,FILE=FILE4,STATUS='OLD') "
"  OPEN (UNIT=7,FILE=FILE7,STATUS='NEW')"
"  OPEN (UNIT=8,FILE=FILE8,STATUS='NEW') "
"  WRITE(*,265)"
265 FORMAT(' ENTER QUARTER NUMBER FOR HINITIAL TO BE USED ')

```

```

"  READ (*,*) IQUART"
"  READ (5,220)TITLE1"
"  READ (5,220)TITLE2"
"  READ (6,220)TITLE2"
"  DO 115 I=1,IQUART"
"    READ (4,*) HQART "
"    READ (6,*) I1,R1,R2,HFFDIF"
115 CONTINUE
220 FORMAT(A80)
"  WRITE(*,203)"
203 FORMAT (' ENTER # OF DATA SETS AND # OF POINTS')
"  READ (*,*) NSETS,NVARS"
"  WRITE(*,204)"
204 FORMAT (' ENTER SAMPLE DIAMETER')
"  READ (*,*) DIA"
"  WRITE(7,222)"
" 222 FORMAT(' AMIN, BMIN, AMAX, BMAX, A25, B25, DI"
"    &FAR, DIFBR, DIFAP, DIFBP, AF(I) , RSTRN , DSTRS"
"    & , RM , P3 ')"
"  DO 300 I=1,200"
"    RSTRN(I)=0.0
"    DSTRS(I)=0.0
"    RM(I)=0.0
"    RST(I)=0.0
"    DST(I)=0.0
"    RMM(I)=0.0
300 CONTINUE
"  CCUM=0.0
"  PGRAND=0.0
"  DO 100 I=1,NSETS"
"    AMAX=-1000000
"    BMAX=-1000000
"    AMIN=1000000
"    BMIN=1000000
"    CCUM=0.0
"    DO 101 J=1,NVARS"
"      READ(5,*) A,B,C"
"      IF(J.EQ.1) A1=A
"      IF(J.EQ.1) B1=B
"      IF(J.EQ.NVARS) A25=A
"      IF(J.EQ.NVARS) B25=B
"      IF(A.LT.AMIN) AMIN = A
"      IF(A.GT.AMAX) AMAX = A
"      IF(B.LT.BMIN) BMIN = B
"      IF(B.GT.BMAX) BMAX = B

```

```

      CCUM=CCUM+C
101  CONTINUE
      DIFAR = AMAX-A25
      DIFBR = BMAX-B25
      DIFAP = A25-A1
      DIFBP = B25-B1
      P3(I) = CCUM/NVARS
      PGRAND= PGRAND+P3(I)
      RSTRN(I) = DIFAR/HFFDIF/1000.0
      AF(I) = HQART * DIA * DIA * 3.14159265359/HFFDIF/4.0
      DSTRS(I) = DIFBR/AF(I)
      RM(I) = DSTRS(I)/RSTRN(I)
"    WRITE(7,200)
AMIN,BMIN,AMAX,BMAX,A25,B25,DIFAR,DIFBR,DIFAP,DIFBP,"
"    & AF(I),RSTRN(I),DSTRS(I),RM(I),P3(I)"
100  CONTINUE
      P3AVGF=PGRAND/NSETS/100.0
" 200 FORMAT(13(F11.5,','),F11.0,',',F11.5))"
      RST(1)=(RSTRN(25)+RSTRN(24)+RSTRN(23)+RSTRN(22)+RSTRN(21))/5.0
      RST(2)=(RSTRN(50)+RSTRN(49)+RSTRN(48)+RSTRN(47)+RSTRN(46))/5.0
      RST(3)=(RSTRN(75)+RSTRN(74)+RSTRN(73)+RSTRN(72)+RSTRN(71))/5.0
      RST(4)=(RSTRN(100)+RSTRN(99)+RSTRN(98)+RSTRN(97)+RSTRN(96))/5.0
      DST(1)=(DSTRS(25)+DSTRS(24)+DSTRS(23)+DSTRS(22)+DSTRS(21))/5.0
      DST(2)=(DSTRS(50)+DSTRS(49)+DSTRS(48)+DSTRS(47)+DSTRS(46))/5.0
      DST(3)=(DSTRS(75)+DSTRS(74)+DSTRS(73)+DSTRS(72)+DSTRS(71))/5.0
      DST(4)=(DSTRS(100)+DSTRS(99)+DSTRS(98)+DSTRS(97)+DSTRS(96))/5.0
      RM(1)=(RM(25)+RM(24)+RM(23)+RM(22)+RM(21))/5.0
      RM(2)=(RM(50)+RM(49)+RM(48)+RM(47)+RM(46))/5.0
      RM(3)=(RM(75)+RM(74)+RM(73)+RM(72)+RM(71))/5.0
      RM(4)=(RM(100)+RM(99)+RM(98)+RM(97)+RM(96))/5.0
      K=NSETS/25
"    DO 105 I=1,K"
      RMM(I)=DST(I)/RST(I)
105  CONTINUE
"    WRITE(8,255)"
" 255 FORMAT(' DST(I), RST(I), RM(I) , RMM(I) , P3AVGF '"
&)
"    DO 106 I=1,K"
"      WRITE(8,250) DST(I),RST(I),RM(I),RMM(I),P3AVGF"
106  CONTINUE
" 250 FORMAT(2(F11.5,','),2(F11.0,','),F7.1)"
"    WRITE(7,277)HFFDIF"
" 277 FORMAT('HFFDIF=',F15.9)"
      STOP
      END

```

Table E.4: Typical Output File Produced by MCALC-IC and/or MCLC-IIC Program (File MR1-11.dat)

AMIN	BMIN	AMAX	BMAX	A25	B25	DIFAR	DIFBR	DIFAP	DIFBP	AF(I)	RSTRN	DSTRS	RM	P3
37.54170	24.05634	40.72320	56.36056	37.66896	27.49296	1.05424	28.86761	0.00000	3.43662	12.69258	0.00044	2.27437	5150	632.5
37.54170	24.74366	40.97772	54.98592	37.66896	25.43099	3.30876	29.55493	0.12726	-2.74930	12.69258	0.00048	2.32852	4867	630.4
37.54170	24.05634	40.97772	56.36056	37.54170	25.43099	3.43602	30.92958	-0.38178	0.00000	12.69258	0.00050	2.43682	4905	630.0
37.28718	24.05634	40.85046	55.67324	37.79622	25.43099	3.05424	30.24225	0.50904	0.00000	12.69258	0.00044	2.38267	5395	632.0
37.54170	27.49296	40.85046	57.04789	37.92348	27.49296	2.92698	29.55493	0.38178	0.00000	12.69258	0.00042	2.32852	5502	629.7
37.54170	24.05634	40.97772	55.67324	37.79622	27.49296	3.18150	28.18028	0.00000	0.00000	12.69258	0.00046	2.22022	4826	631.9
37.66896	24.05634	40.85046	56.36056	37.79622	25.43099	3.05424	30.92958	0.12726	0.00000	12.69258	0.00044	2.43682	5518	630.8
37.66896	22.68169	40.85046	53.61127	37.66896	26.80563	3.18150	26.80563	0.00000	2.74930	12.69258	0.00046	2.11191	4591	633.1
37.66896	24.74366	40.97772	55.67324	37.66896	26.11831	3.30876	29.55493	0.00000	-1.37465	12.69258	0.00048	2.32852	4867	632.0
37.79622	24.05634	40.85046	56.36056	37.92348	25.43099	2.92698	30.92958	0.12726	-0.68732	12.69258	0.00042	2.43682	5758	631.2
37.66896	25.43099	40.97772	55.67324	37.79622	26.11831	3.18150	29.55493	-0.12726	0.68732	12.69258	0.00046	2.32652	5062	631.0
37.54170	24.05634	40.85046	56.36056	37.54170	25.43099	3.30876	30.92958	-0.25452	-2.06197	12.69258	0.00048	2.43682	5093	632.8
37.54170	24.74366	40.97772	55.67324	37.79622	26.11831	3.18150	29.55493	0.12726	1.37465	12.69258	0.00046	2.32852	5062	630.1
37.66896	25.43099	40.97772	57.04789	37.79622	27.49296	3.18150	28.86761	0.00000	0.68732	12.69258	0.00046	2.27437	4944	630.5
37.28718	25.43099	40.85046	56.36056	37.79622	25.43099	3.05424	30.92958	0.12726	0.00000	12.69258	0.00046	2.32852	5062	631.6
37.66896	25.43099	40.97772	55.67324	37.79622	26.80563	3.18150	28.86761	0.12726	0.00000	12.69258	0.00044	2.43682	5518	631.8
37.54170	25.43099	40.85046	55.67324	37.79622	26.80563	3.05424	28.86761	-0.12726	1.37465	12.69258	0.00046	2.27437	4944	629.7
37.28718	25.43099	40.85046	56.36056	37.92348	25.43099	3.05424	30.92958	0.25452	-1.37465	12.69258	0.00044	2.27437	5150	630.4
37.66896	25.43099	40.85046	55.67324	37.92348	26.80563	2.92698	30.24225	0.25452	-2.06197	12.69258	0.00044	2.43682	5518	628.3
37.54170	24.05634	40.85046	54.98592	37.92348	26.80563	2.92698	29.55493	0.12726	0.00000	12.69258	0.00042	2.38267	5630	630.5
37.66896	25.43099	40.97772	56.36056	37.66896	26.11831	2.92698	28.86761	0.38178	2.06197	12.69258	0.00042	2.32852	5502	629.4
37.54170	25.43099	40.85046	55.67324	37.79622	25.43099	3.30876	30.92958	0.12726	-1.37465	12.69258	0.00042	2.27437	5374	630.9
37.66896	25.43099	40.97772	56.36056	37.66896	25.43099	3.05424	29.55493	-0.12726	-2.06197	12.69258	0.00048	2.43682	5093	630.5
37.28718	25.43099	40.85046	55.67324	37.92348	26.11831	3.05424	30.24225	0.12726	0.68732	12.69258	0.00044	2.32852	5273	630.3
37.66896	24.05634	40.97772	56.36056	37.79622	27.49296	3.18150	28.86761	0.12726	0.00000	12.69258	0.00046	2.38267	5179	629.4
37.66896	25.43099	40.85046	56.36056	37.92348	27.49296	3.05424	28.18028	0.00000	2.06197	12.69258	0.00044	2.27437	5150	631.5
37.54170	25.43099	40.97772	55.67324	37.79622	27.49296	3.18150	30.92958	0.12726	2.06197	12.69258	0.00046	2.22022	4826	631.1
37.54170	25.43099	40.85046	56.36056	37.92348	25.43099	2.92698	30.92958	0.00000	0.00000	12.69258	0.00042	2.43682	5758	630.0
37.28718	24.05634	40.97772	56.36056	37.79622	28.86761	3.18150	27.49296	0.12726	4.81127	12.69258	0.00046	2.16606	4709	630.5
37.28718	25.43099	40.85046	54.98592	37.66896	25.43099	3.18150	29.55493	0.00000	0.00000	12.69258	0.00046	2.32852	5062	633.7
37.79622	24.05634	40.85046	55.67324	37.79622	25.43099	3.05424	30.24225	0.00000	1.37465	12.69258	0.00044	2.38267	5395	630.2
37.41444	24.05634	40.97772	56.36056	37.66896	26.80563	3.30876	29.55493	0.00000	-2.06197	12.69258	0.00048	2.32852	4867	630.9
37.54170	24.05634	40.97772	55.67324	37.79622	27.49296	3.18150	28.18028	0.25452	0.68732	12.69258	0.00046	2.22022	4826	631.9

37.79622	27.49296	40.85046	57.04789	37.79622	28.18028	3.05424	28.86761	0.00000	0.00000	12.69258	0.00044	2.27437	51.50	639.2
37.66896	27.49296	40.85046	57.04789	37.79622	28.18028	3.05424	28.86761	0.00000	0.00000	12.69258	0.00044	2.27437	51.50	631.3
37.66896	27.49296	40.85046	57.04789	37.79622	28.18028	3.05424	28.86761	0.00000	0.00000	12.69258	0.00044	2.27437	51.50	632.2
37.66896	28.18028	40.85046	56.36056	37.79622	28.18028	3.05424	28.18028	0.00000	0.00000	12.69258	0.00044	2.22022	5027	631.3
37.66896	25.43099	40.97772	55.67324	37.79622	26.80563	3.18150	28.86761	0.12726	0.68732	12.69258	0.00046	2.27437	4944	629.0
37.41444	25.43099	40.85046	56.36056	37.79622	28.86761	3.05424	27.49296	0.38178	1.37465	12.69258	0.00044	2.16606	4905	630.6
37.66896	25.43099	41.23224	56.36056	37.79622	25.43099	3.43602	30.92958	0.00000	-2.74930	12.69258	0.00050	2.43682	4905	631.5
37.66896	24.74366	40.85046	56.36056	37.79622	27.49296	3.05424	28.86761	0.00000	1.37465	12.69258	0.00044	2.27437	5150	631.0
37.66896	25.43099	40.97772	56.36056	37.79622	27.49296	3.18150	28.86761	0.12726	2.06197	12.69258	0.00046	2.27437	4944	630.9
37.15992	24.74366	40.85046	56.36056	37.79622	24.74366	3.05424	31.61690	0.25452	-2.06197	12.69258	0.00044	2.49097	5640	631.4
37.54170	25.43099	40.85046	55.67324	37.66896	25.43099	3.18150	30.24225	-0.12726	-1.37465	12.69258	0.00046	2.49097	5179	630.9
37.28718	24.05634	40.97772	56.36056	37.79622	25.43099	3.18150	30.24225	0.50904	-0.68732	12.69258	0.00046	2.38267	5297	631.1
37.54170	25.43099	40.85046	54.98592	37.79622	25.43099	3.18150	30.92958	0.50904	-0.68732	12.69258	0.00046	2.43682	5273	629.4
37.54170	25.43099	40.97772	55.67324	37.66896	28.18028	3.30876	27.49296	0.12726	2.06197	12.69258	0.00044	2.32852	5273	632.0
37.54170	25.43099	40.85046	56.36056	37.79622	28.86761	3.05424	27.49296	0.25452	1.37465	12.69258	0.00044	2.16606	4905	631.3
37.66896	25.43099	40.85046	57.04789	37.66896	25.43099	3.18150	31.61690	-0.25452	0.00000	12.69258	0.00046	2.49097	5415	631.2
37.66896	25.43099	40.97772	55.67324	37.66896	27.49296	3.30876	28.18028	0.00000	2.06197	12.69258	0.00048	2.22022	4641	630.6
37.66896	24.74366	40.97772	55.67324	37.92348	26.11831	3.05424	29.55493	0.25452	-2.06197	12.69258	0.00044	2.32852	5273	630.0
37.66896	25.43099	40.85046	56.36056	37.79622	26.11831	3.05424	30.24225	0.12726	0.68732	12.69258	0.00044	2.38267	5395	629.2
37.79622	25.43099	40.85046	56.36056	37.79622	27.49296	3.05424	28.86761	0.00000	0.00000	12.69258	0.00044	2.27437	5150	629.9
37.66896	24.74366	40.97772	57.73521	37.79622	27.49296	3.18150	30.24225	-0.12726	2.06197	12.69258	0.00046	2.38267	5179	629.2
37.15992	25.43099	40.97772	56.36056	37.79622	27.49296	3.18150	30.24225	0.50904	0.00000	12.69258	0.00046	2.27437	4944	629.2
37.54170	25.43099	40.85046	56.36056	37.92348	26.80563	2.92698	30.24225	0.38178	1.37465	12.69258	0.00042	2.32852	5502	629.3
37.54170	24.74366	40.85046	55.67324	37.79622	25.43099	3.05424	30.24225	0.12726	0.68732	12.69258	0.00044	2.38267	5395	630.7
37.28718	22.69169	40.97772	56.36056	37.79622	27.49296	3.18150	28.18028	0.12726	2.06197	12.69258	0.00046	2.27437	4944	631.2
37.54170	24.74366	40.85046	56.36056	37.92348	24.74366	2.92698	31.61690	0.25452	-2.06197	12.69258	0.00042	2.49097	5886	631.8
37.54170	24.05634	40.85046	57.04789	37.79622	26.11831	3.05424	30.24225	0.25452	2.06197	12.69258	0.00044	2.43682	5518	629.0
37.66896	24.05634	40.85046	56.36056	37.79622	25.43099	3.05424	30.24225	0.12726	-2.06197	12.69258	0.00044	2.43682	5518	631.2
37.66896	25.43099	40.85046	59.10986	37.66896	27.49296	3.18150	31.61690	0.00000	-0.68732	12.69258	0.00046	2.49097	5415	631.5
37.79622	25.43099	40.97772	55.67324	37.92348	25.43099	3.05424	30.24225	0.00000	0.00000	12.69258	0.00044	2.38267	5395	630.3
37.66896	24.74366	40.97772	56.36056	37.79622	24.74366	3.18150	31.61690	0.12726	-2.74930	12.69258	0.00046	2.49097	5415	631.0
37.66896	25.43099	40.97772	55.67324	37.79622	27.49296	3.18150	28.18028	0.12726	2.06197	12.69258	0.00046	2.22022	4826	631.6
37.66896	25.43099	40.97772	55.67324	37.79622	25.43099	3.18150	30.24225	0.00000	0.00000	12.69258	0.00046	2.38267	5179	630.4
37.79622	24.05634	40.97772	55.67324	37.79622	25.43099	3.18150	30.24225	0.12726	0.68732	12.69258	0.00048	2.38267	4980	629.9
37.54170	25.43099	40.97772	56.36056	37.66896	26.11831	3.30876	30.24225	0.00000	0.00000	12.69258	0.00046	2.38267	5179	629.3
37.66896	25.43099	40.97772	55.67324	37.79622	25.43099	3.18150	30.24225	-0.12726	-1.37465	12.69258	0.00050	2.32852	4687	631.8
37.54170	24.74366	41.10498	55.67324	37.66896	26.11831	3.43602	29.55493	0.12726	-2.06197	12.69258	0.00048	2.38267	4980	630.2
37.66896	25.43099	40.97772	55.67324	37.66896	25.43099	3.30876	30.24225	0.00000	-2.06197	12.69258	0.00048	2.38267	5518	631.8
37.66896	25.43099	40.85046	56.36056	37.79622	25.43099	3.05424	30.92958	0.00000	-2.06197	12.69258	0.00044	2.43682		

37.66896	25.43099	40.85046	57.04789	37.66896	28.86761	3.18150	28.18028	0.00000	3.43662	12.69258	0.00046	2.22022	4826	631.7
37.66896	25.43099	40.85046	56.36056	37.79622	25.43099	3.05424	30.92958	0.12726	-2.06197	12.69258	0.00044	2.43682	5518	630.4
37.28718	25.43099	40.97772	56.36056	37.92348	26.80563	3.05424	29.55493	0.63630	1.37465	12.69258	0.00044	2.32852	5273	630.6
37.41444	24.05634	40.85046	57.04789	37.79622	27.49296	3.05424	29.55493	0.38178	0.00000	12.69258	0.00044	2.32852	5273	629.5
37.28718	24.74366	40.97772	56.36056	37.79622	25.43099	3.18150	30.92958	0.50904	0.00000	12.69258	0.00046	2.43682	5297	631.1
37.54170	24.05634	40.97772	55.67324	37.79622	24.05634	3.18150	31.61690	0.25452	-1.37465	12.69258	0.00046	2.49097	5415	629.5
37.66896	23.36901	40.97772	55.67324	37.66896	26.11831	3.30876	29.55493	-0.25452	0.68732	12.69258	0.00048	2.32852	4867	630.7
37.28718	25.43099	40.85046	54.98592	37.66896	27.49296	3.18150	27.49296	0.00000	2.06197	12.69258	0.00046	2.16606	4709	630.7
37.66896	25.43099	40.85046	55.67324	37.79622	27.49296	3.05424	28.18028	0.00000	2.06197	12.69258	0.00044	2.22022	5027	630.1
37.54170	25.43099	40.85046	55.67324	37.79622	26.11831	3.05424	29.55493	0.00000	-1.37465	12.69258	0.00044	2.32852	5273	631.0
37.28718	24.05634	40.97772	56.36056	37.54170	27.49296	3.43602	28.86761	-0.12726	0.00000	12.69258	0.00050	2.27437	4578	629.8
37.41444	24.74366	40.85046	56.36056	37.79622	25.43099	3.05424	30.92958	0.38178	0.00000	12.69258	0.00044	2.43682	5518	630.8
37.28718	25.43099	41.10498	55.67324	37.79622	25.43099	3.30876	30.24225	0.50904	0.00000	12.69258	0.00048	2.38267	4980	630.9
37.54170	25.43099	40.85046	55.67324	37.92348	25.43099	2.92098	30.24225	0.25452	-1.37465	12.69258	0.00042	2.38267	5630	629.2
37.66896	25.43099	40.97772	56.36056	37.66896	28.18028	3.30876	28.18028	-0.12726	0.68732	12.69258	0.00048	2.22022	4641	630.3
37.28718	25.43099	40.85046	57.04789	37.92348	26.11831	3.05424	30.24225	0.00000	0.68732	12.69258	0.00044	2.38267	5395	629.4
37.66896	25.43099	40.85046	56.36056	37.66896	27.49296	3.18150	31.61690	0.63630	0.00000	12.69258	0.00042	2.49097	5886	629.7
37.28718	25.43099	40.85046	55.67324	37.28718	28.18028	3.6328	27.49296	-0.12726	0.00000	12.69258	0.00046	2.27437	4944	628.9
37.28718	24.74366	40.97772	55.67324	37.92348	25.43099	3.05424	30.24225	-0.50904	0.00000	12.69258	0.00052	2.16606	4204	629.9
37.28718	24.74366	40.85046	55.67324	37.79622	26.11831	3.05424	29.55493	0.38178	0.68732	12.69258	0.00044	2.38267	5395	629.8
37.66896	25.43099	40.85046	56.36056	37.79622	25.43099	3.05424	30.92958	0.25452	0.68732	12.69258	0.00044	2.32852	5273	630.2
37.54170	25.43099	40.85046	55.67324	37.92348	25.43099	3.05424	30.92958	0.00000	0.00000	12.69258	0.00044	2.43682	5518	630.8
37.66896	25.43099	40.97772	55.67324	37.66896	28.86761	3.30876	26.80563	0.12726	-3.43662	12.69258	0.00042	2.38267	5630	630.1
37.54170	22.68169	40.97772	56.36056	37.92348	26.80563	3.05424	29.55493	0.00000	0.68732	12.69258	0.00048	2.11191	4414	628.7
37.66896	24.74366	40.85046	55.67324	37.79622	25.43099	3.35424	30.24225	0.12726	-0.68732	12.69258	0.00044	2.32852	5273	629.4
37.66896	24.74366	40.97772	55.67324	37.66896	25.43099	3.30876	30.24225	-0.12726	-2.74930	12.69258	0.00048	2.38267	5395	630.1
37.54170	24.05634	41.10498	55.67324	37.54170	25.43099	3.56328	30.24225	-0.38178	-0.68732	12.69258	0.00048	2.38267	4980	629.9
37.28718	25.43099	40.97772	55.67324	37.92348	25.43099	3.05424	30.24225	0.25452	-1.37465	12.69258	0.00044	2.38267	4624	630.5
													5395	629.9

HFFDIF = 6.91587

KEY:

- [1] AMAX is the maximum LVDT reading during any one load cycle (inch /1000).
- [2] AMIN is the minimum LVDT reading during any one load cycle (inch /1000).
- [3] A25 is the last LVDT reading during any one load cycle (inch /1000).
- [4] BMAX is the maximum load cell reading during any one load cycle (lb).

- [5] BMIN is the minimum load cell reading during any one load cycle (lb).
- [6] B25 is the last load cell reading during any one load cycle (lb).
- [7] DIFAR is the resilient deformation measured during any one load cycle (inch/1000).
- [8] DIFAP is the permanent deformation measured during any one load cycle (inch/1000).
- [9] DIFBR is the amplitude of the applied deviator load and is equal to BMAX - B25 (lb).
- [10] DIFBF is the amount of residual deviator load remaining upon unloading (i.e. = E25 - B25) (lb).
- [11] AF(I) is the surface area of the sample over which the deviator repetitive load is applied (in²). AF(I) changes from one load cycle to the other because the length of the sample changes as permanent deformation accumulates { $AF(I) = H1 \cdot DIA \cdot DIA \cdot 3.14159 / HFFDIF/4$ }.
- [12] DSTRS(I) is the repetitive deviator stress { $= DIFBR / AF(I)$ } (psi).
- [13] RSTRN(I) is the axial resilient recoverable strain { $= DIFAR / HFFDIF/1000$ }
- [14] RM(I) is the computed resilient modulus for every load cycle { $= DSTRS(I) / RSTRN(I)$ } (psi).
- [15] P3 is the uncorrected confining cell pressure measure⁻¹ for each load cycle (psi x 100).
- [16] HFFDIF is the final sample length (inch). This is the length used for strain and resilient modulus computations.

(III) Temperature Computation Program (ARRTEMPF.FOR)

This is a program that is used to calculate the temperature of the soil sample at two locations i.e. at one inch from each end of the specimen. An example output file is also displayed as output file G1-11.TP.

```
"  IMPLICIT REAL*8(A-H,O-Z)"
"  CHARACTER *12 FILE4,FILE5,FILE7"
"  CHARACTER *80 TITLE1,TITLE2"
"  DIMENSION A(1600),CJC(200),TTEMP(200),BTEMP(200)"
"  WRITE(*,201)"
201 FORMAT (' ENTER INPUT FILE NAME ')
"  READ (*,'(A)') FILE4"
"  WRITE(*,202)"
202 FORMAT(' ENTER OUTPUT FILE NAME')
"  READ (*, '(A)') FILE7 "
"  WRITE(*,*) 'ENTER NAME OF ARRANGED FILE'"
"  READ(*,'(A)') FILE5"
"  OPEN (UNIT=4,FILE=FILE4,STATUS='OLD')"
"  OPEN (UNIT=5,FILE=FILE5,STATUS='NEW')"
"  OPEN (UNIT=7,FILE=FILE7,STATUS='NEW')"
"  READ (4,203)TITLE1"
"  READ (4,203)TITLE2"
"  WRITE(5,203)TITLE1"
"  WRITE(5,203)TITLE2"
203 FORMAT(A80)
"  WRITE(*,204)"
204 FORMAT (' ENTER NUMBER OF DATA SETS')
"  READ (*,*) NSETS"
  NUM=16*NSETS
"  READ(4,*) (A(K),K=1,NUM)"
"  DO 110 I=1,NSETS"
"  WRITE(5,208)(A((I-1)*16+J),J=1,16)"
110 CONTINUE
208 FORMAT(16(F8.0))
  CLOSE(UNIT=5)
"  OPEN(UNIT=5,FILE=FILE5,STATUS='OLD')"
"  READ (5,203)TITLE1"
"  READ (5,203)TITLE2"
"  WRITE(*,205)"
205 FORMAT(' ENTER THE NUMBER OF 3 COLUMNS TO BE USED ( 1 TO 16 )')
"  READ (*,*) I1,I2,I3"
"  WRITE(7,206)"
206 FORMAT(' CJC  ,TOPTEMP  ,BOTTEMP  ')"
```

```

" DO 100 I=1,NSETS"
  " READ(5,*) (A(K),K=1,16)"
  " WRITE(7,207)A(I1),A(I2),A(I3)  "
    CJC(I)=A(I1)
    TTEMP(I)=A(I2)
    BTEMP(I)=A(I3)
" 207  FORMAT(3(F6.1,4X','))"
100 CONTINUE
  ACUM=C.0
  BCUM=0.0
  CCUM=0.0
" DO 101 I=1,NSETS"
  ACUM=ACUM+CJC(I)
  BCUM=BCUM+TTEMP(I)
  CCUM=CCUM+BTEMP(I)
101 CONTINUE
  ABAR=ACUM/NSETS/10.0
  BBAR=BCUM/NSETS/10.0
  CBAR=CCUM/NSETS/10.0
  CSS=0.0
  TSS=0.0
  BSS=0.0
" DO 102 I=1,NSETS"
  CSS=CSS+(CJC(I)/10.0-ABAR)*(CJC(I)/10.0-ABAR)
  TSS=TSS+(TTEMP(I)/10.0-BBAR)*(TTEMP(I)/10.0-BBAR)
  BSS=BSS+(BTEMP(I)/10.0-CBAR)*(BTEMP(I)/10.0-CBAR)
102 CONTINUE
  CJCSD=DSQRT(CSS/(NSETS-1))
  TTMPD=DSQRT(TSS/(NSETS-1))
  BTMPD=DSQRT(BSS/(NSETS-1))
" WRITE(7,210)"
" 210 FORMAT(' CJCBAR , TTEMPBAR , BTEMPBAR , CJCSD, TTMPD, BTMPD')
" WRITE(7,209)ABAR,BBAR,CBAR,CJCSD,TTMPD,BTMPD"
" 209 FORMAT(6(F6.1,5X))"
  STOP
  END

```

Table E.5: Typical Computed Temperature Output File (File G1-11.tp)

CJC	TOPTEMP	BOTTEMP
377	132	230
377	132	230
377	132	227
377	132	227
377	132	227
378	133	228
377	132	227
378	133	228
377	135	227
377	135	227
376	131	226
377	132	227
377	132	230
377	132	230
378	136	228
378	136	228
377	132	227
377	132	227
378	136	228
377	135	227
377	132	230
377	132	230
377	132	227
377	132	227
377	132	227
377	132	227
377	129	230
377	129	230
377	132	227
377	132	227
377	132	227
377	132	227
378	133	228
377	132	227
378	133	228
377	132	227
377	132	230
377	132	230
377	132	224
378	133	225
377	132	230
378	133	231
378	133	228
378	133	228
378	133	231
378	133	231

377	132	227
377	132	227
378	133	228
378	133	228
378	136	228
377	135	227
377	132	230
378	133	231
378	133	225
377	132	224
377	135	230
377	135	230
377	132	224
378	132	225
378	133	231
378	133	231
377	132	227
377	132	227
378	133	228
377	132	227
377	132	227
377	132	227
377	132	227
378	133	228
377	132	227
378	133	228
377	132	227
377	132	227
378	133	228
377	135	227
377	135	227
378	133	231
377	132	230
377	135	230
377	135	230
378	130	228
377	129	227
377	132	227
378	133	228
378	133	225
377	132	224
378	133	228
378	133	228
377	132	227
377	132	227
376	133	228
377	132	227
377	132	227
377	132	227
378	133	228
377	132	227

	377	132	227		
	377	132	227		
CJCBAR	TTEMPBAR	BTEMPBAR	CJCSD	TTMPD	BTMPD
37.7	13.3	22.8	0	0.1	0.2

KEY:

- [1] CJC is the temperature reading of the cold junction compensation circuit within the EXP-16 board.
- [2] TOPTTEMP is the temperature reading at the top end of the sample.
- [3] BOTTEMP is the temperature reading at the bottom end of the sample.
- [4] CJCBAR is the average temperature reading of all CJC measurements.
- [5] TTEMPBAR is the average temperature reading of all TOPTTEMP measurements.
- [6] BTEMPBAR is the average temperature reading of all BOTTEMP measurements.
- [7] CJCSD is the standard deviation of the CJC measurements.
- [8] TTMPD is the standard deviation of the TOPTTEMP measurements.
- [9] BTMPD is the standard deviation of the BOTTEMP measurements.
- [9] BOTTEMP measurements are found to be in error and are thus not considered.

All temperature measurements are in degree Celcius x 10

(IV) Compilation Programs

These are programs that are used to group all the test data pertaining to each test specimen together. Two programs are listed here, namely MRCOMPL2.FOR and TEMPCOMP.FOR. The MRCOMPL2.FOR is used to compile stress-strain-modulus data whereas the TEMPCOMP.FOR is used to compile the temperature data. Example output files for each program are also displayed at the end of this section.

(a) Program MRCOMPL2.FOR

```
"  IMPLICIT REAL *8(A-H,O-Z)"
"  CHARACTER *12 FILE5,FILE6"
"  CHARACTER *80 TITLE1
"  DIMENSION DST(80),RST(80),RM(80),RMM(80)"
"  WRITE(*,239)"
239 FORMAT(' ENTER OUTPUT FILE NAME')
"  READ (*, '(A)') FILE6"
"  OPEN (UNIT=6,FILE=FILE6,STATUS='NEW')
"  WRITE(*,290)"
290 FORMAT(' ENTER NUMBER OF DATA FILES')
"  READ(*,*) NFILES"
"  DO 190 IFILE=1,NFILES"
"    WRITE(*,201)"
201  FORMAT (' ENTER INPUT FILE NAME ')
"  READ (*, '(A)') FILE5"
"  OPEN (UNIT=5,FILE=FILE5,STATUS='OLD')"
"  READ (5,220)TITLE1"
"  DO 191 I=1,4"
"    ICOUNT=4*(IFILE-1)+I
"    READ(5,*)DST(ICOUNT),RST(ICOUNT),RM(ICOUNT),RMM(ICOUNT)"
191 CONTINUE
"  CLOSE(UNIT=5)
190 CONTINUE
220 FORMAT(A80)
"  WRITE(6,221)"
"  221 FORMAT('QUART ,DST(I) , RST(I) , RM(I) , RMM(I)')
"  DO 192 I=1,4"
"    DO 193 J=1,NFILES"
"      ICOUNT=4*(J-1)+I
"      IF(J.EQ.1) THEN
"        WRITE(6,300)I,DST(ICOUNT),RST(ICOUNT),RM(ICOUNT),RMM(ICOUNT)"
"      ELSE
"        WRITE(6,301)DST(ICOUNT),RST(ICOUNT),RM(ICOUNT),RMM(ICOUNT)"
"      ENDIF
```

```
193 CONTINUE
"  WRITE(6,302)"
302 FORMAT(' / ')
192 CONTINUE
" 300 FORMAT(I2,',',4(F15.9,','))"
" 301 FORMAT(2X,',',4(F15.9,','))"
  STOP
  END
```

(b) Program TEMPCOMP.FOR

```

"  IMPLICIT REAL*8(A-H,O-Z)"
"  CHARACTER *12 FILE4,FILE5"
"  CHARACTER *80 TITLE1,TITLE2"
  DIMENSION A(16)
"  WRITE(*,*) 'ENTER NUMBER OF INPUT FILES'"
"  READ(*,*) NFILES"
"  WRITE(*,202)"
  202 FORMAT(' ENTER OUTPUT FILE NAME')
"  READ (*, '(A)') FILE5"
"  OPEN (UNIT=5,FILE=FILE5,STATUS='NEW') "
"  WRITE(5,260)"
"  260 FORMAT(' CJCBAR , TTEMPBAR , BTEMPBAR , CJCSD, TTMPSPD,
BTMPSPD') "
"  DO 240 J=1,NFILES"
"    WRITE(*,201)"
  201 FORMAT(' ENTER INPUT FILE NAME ')
"    READ (*, '(A)') FILE4"
"    OPEN (UNIT=4,FILE=FILE4,STATUS='OLD')"
"    DO 220 I=1,102"
"      READ (4,203)TITLE1"
  220 CONTINUE
  203 FORMAT(A80)
"    READ(4,*) B,C
"    WRITE(5,250)
"    CLOSE(UNIT=4)
  240 CONTINUE
"  250 FOR
"    STOP
"    END

```

Table E.6: Typical Output File Produced by MRCOMPL2 (File G1-1.dat)

QUARTER	DST(I)	RST(I)	RM(I)	RMM(I)	P3
1	2.35	0.00045	5284	5278	6.0
	4.09	0.00091	4487	4485	6.0
	5.94	0.00166	3585	3583	6.0
	8.30	0.00289	2874	2874	6.0
	9.86	0.00356	2770	2769	6.0
	2.26	0.00067	3389	3389	4.0
	4.13	0.00151	2741	2739	4.0
	5.96	0.00245	2428	2428	4.0
	7.80	0.00330	2364	2364	4.0
	9.76	0.00396	2464	2464	4.0
	2.12	0.00075	2828	2825	2.0
	3.94	0.00166	2382	2382	2.0
	5.75	0.00267	2153	2153	2.0
	7.55	0.00354	2130	2130	2.0
	9.86	0.00437	2254	2254	2.0
2	2.27	0.00046	4952	4944	6.0
	4.10	0.00095	4342	4339	6.0
	5.85	0.00168	3493	3492	6.0
	8.18	0.00287	2848	2847	6.0
	9.85	0.00362	2719	2718	6.0
	2.32	0.00062	3746	3740	4.0
	4.15	0.00149	2788	2787	4.0
	6.03	0.00245	2463	2462	4.0
	7.96	0.00328	2430	2430	4.0
	9.76	0.00398	2450	2450	4.0
	2.29	0.00068	3340	3339	2.0
	4.01	0.00167	2394	2394	2.0
	5.69	0.00270	2105	2105	2.0
	7.56	0.00360	2098	2098	2.0
	9.77	0.00438	2231	2230	2.0
3	2.35	0.00045	5281	5278	6.0
	4.09	0.00092	4466	4467	6.0
	5.85	0.00168	3494	3492	6.0
	8.27	0.00291	2845	2845	6.0
	9.86	0.00361	2736	2735	6.0
	2.34	0.00063	3715	3708	4.0
	4.16	0.00148	2802	2802	4.0
	6.02	0.00246	2447	2447	4.0
	7.89	0.00328	2410	2410	4.0
	9.78	0.00398	2456	2456	4.0
	2.32	0.00071	3267	3263	2.0
	4.02	0.00165	2434	2433	2.0
	5.77	0.00269	2146	2146	2.0
	7.53	0.00357	2108	2109	2.0

	9.83	0.00436	2254	2254	2.0
4	2.37	0.00046	5134	5115	6.0
	4.06	0.00095	4293	4293	6.0
	5.87	0.00166	3539	3538	6.0
	8.28	0.00289	2867	2867	6.0
	9.79	0.00361	2712	2712	6.0
	2.30	0.00064	3610	3597	4.0
	4.09	0.00150	2731	2731	4.0
	6.03	0.00245	2459	2459	4.0
	8.01	0.00328	2444	2444	4.0
	9.78	0.00397	2463	2462	4.0
	2.24	0.00069	3260	3258	2.0
	3.93	0.00164	2402	2402	2.0
	5.74	0.00268	2141	2140	2.0
	7.48	0.00355	2107	2107	2.0
	9.80	0.00436	2249	2249	2.0

KEY:

- [1] QUARTER is as defined before.
- [2] DST(I) refers to the average deviator stress calculated from the last five stress values at the end of each quarter e.g. for quarter 1,

$$DST(I) = \{DSTRS(21) + DSTRS(22) + DSTRS(23) + DSTRS(24) + DSTRS(25)\}/5$$
- [3] RST(I) refers to the average recoverable strain calculated from the last five strain values at the end of each quarter e.g. for quarter 1,

$$RST(I) = \{RSTRN(21) + RSTRN(22) + RSTRN(23) + RSTRN(24) + RSTRN(25)\}/5$$
- [4] RM(I) refers to the resilient modulus calculated from the last five moduli values at the end of each quarter e.g. for quarter 1,

$$RM(I) = \{RM(21) + RM(22) + RM(23) + RM(24) + RM(25)\}/5$$
- [5] RMM(I) refers to the resilient modulus calculated from the average stress to strain values of the last five load cycles within each quarter e.g. for quarter 1,

$$RMM(I) = \{DST(21)/RST(21)\} + \{DST(22)/RST(22)\} + \{DST(23)/RST(23)\} + \{DST(24)/RST(24)\} + \{DST(25)/RST(25)\}/5$$
- [6] P3 is the cell confining pressure

Note:

- i) Each quarter in the above table contains 15 values of the calculated parameters. These 15 values correspond to the 15 loading sequences specified by the test protocol followed in conducting the laboratory tests.
- ii) Two averaging methods were used to obtain the resilient modulus value for each load sequence {i.e. RM(I) and RMM(I)} this was done to see whether this will have any effect on the value obtained. From the table, it is evident that this is not the case.
- iii) Dimensions applicable to parameters in above table are:
 psi for DST, RM, RMM and P3 & in/in for RST.

Table E.7: Typical Output File Produced by Program TEMPCOMP (File G1-1.tpc)

Load Sequence	CJCBAR	TTEMPBAR	BTEMPBAR	CJCSD	TTMPD	BTMPD
1	37.7	13.3	22.8	0.0	0.1	0.2
2	37.8	13.3	22.8	0.1	0.2	0.2
3	38.1	13.5	23.0	0.1	0.2	0.2
4	38.1	13.5	23.1	0.0	0.2	0.2
5	38.2	13.5	23.1	0.1	0.2	0.2
6	38.4	13.7	23.2	0.0	0.2	0.2
7	38.5	13.8	23.3	0.0	0.2	0.2
8	38.5	13.8	23.4	0.1	0.2	0.2
9	38.6	13.8	23.4	0.1	0.2	0.2
10	38.8	14.0	23.5	0.1	0.2	0.1
11	38.9	14.1	23.6	0.1	0.2	0.2
12	38.9	14.1	23.6	0.0	0.2	0.2
13	38.9	14.1	23.6	0.1	0.1	0.1
14	39.0	14.2	23.7	0.1	0.2	0.2
15	39.2	14.4	23.8	0.0	0.2	0.2

KEY:

[1] All the parameters are as defined in output file G1-11.tp

[2] Load sequence refers to the loading condition(s) used during the test.

All temperature measurements are in degree Celcius x 10

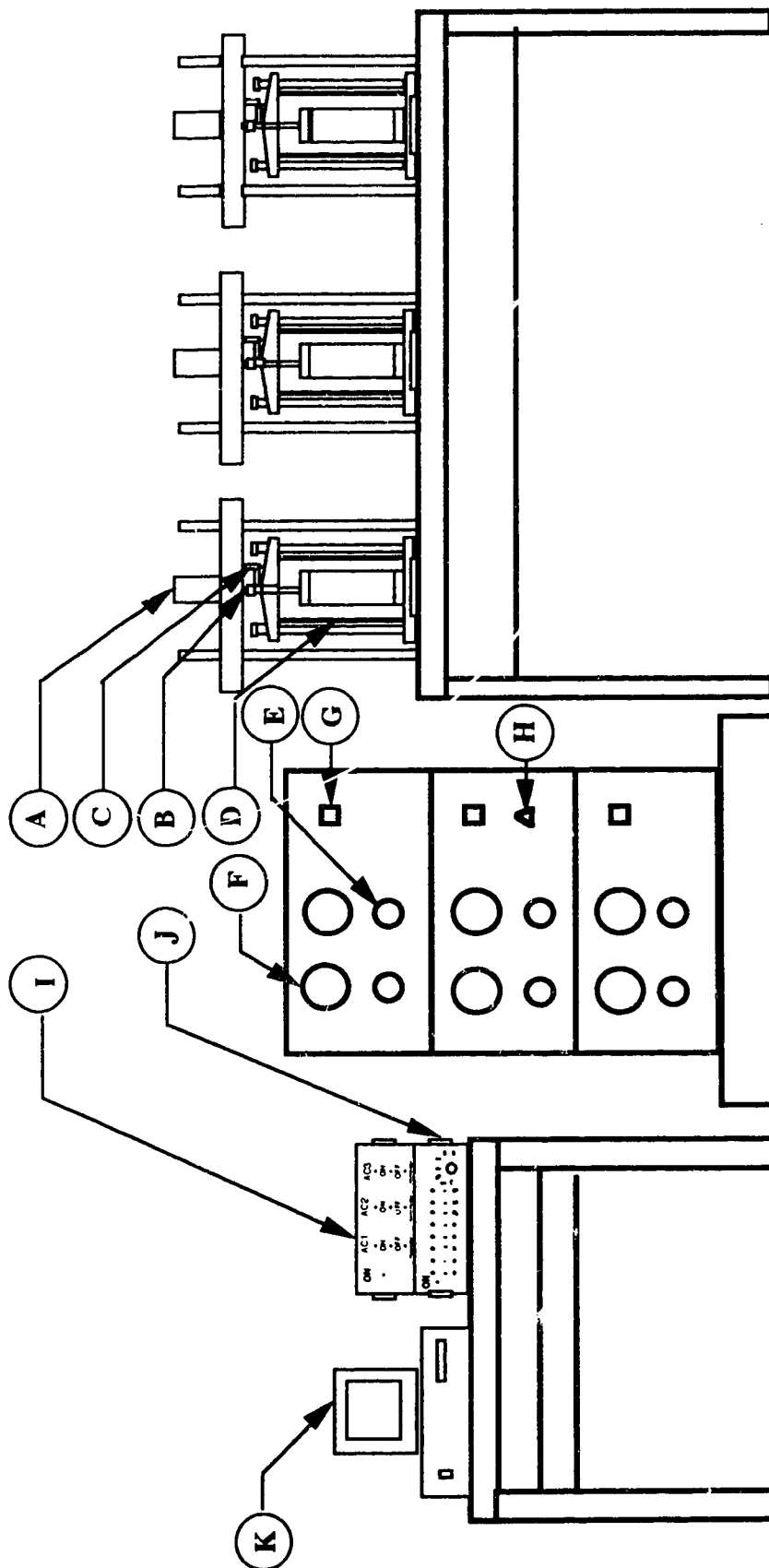


Figure E.1 : Repeated Loading Triaxial Test System

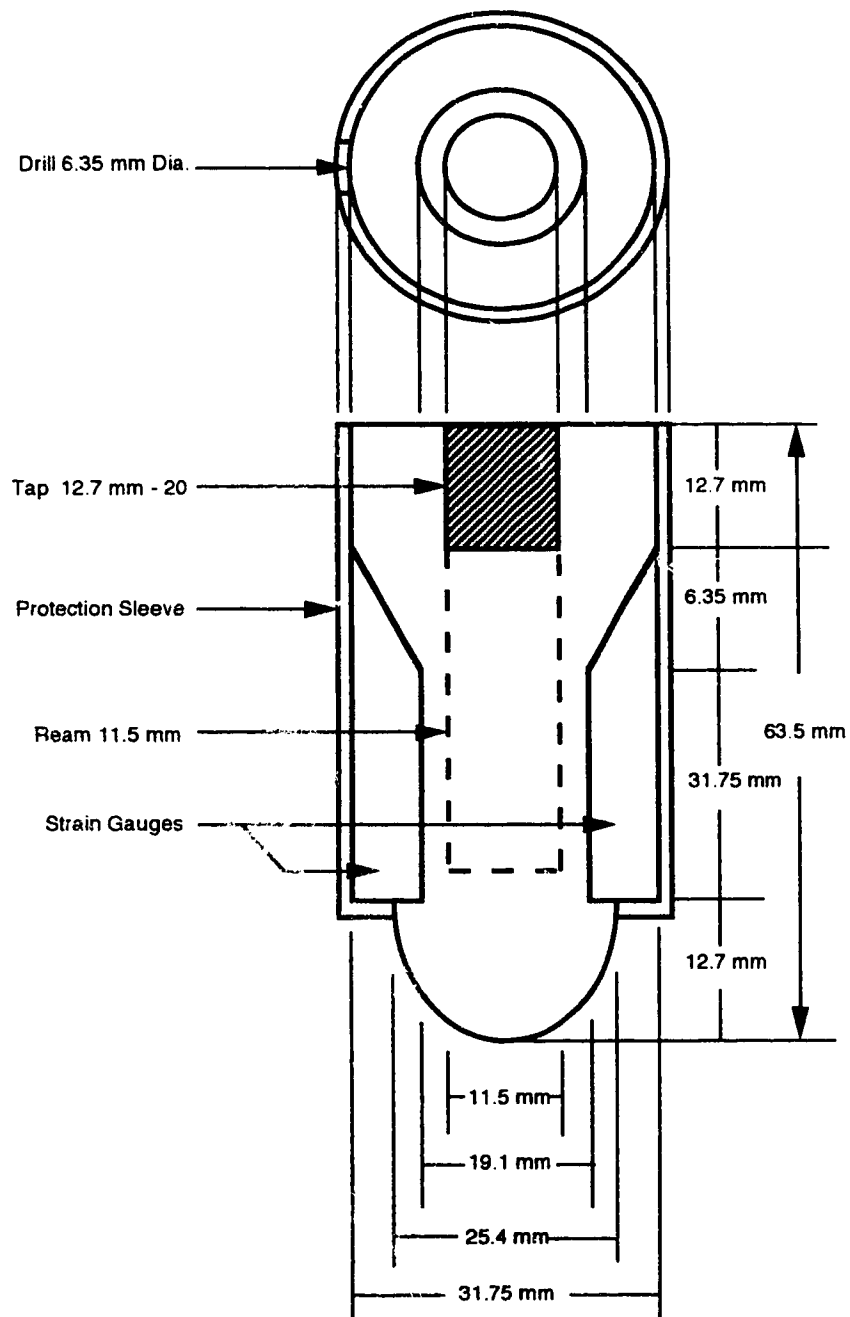


Figure E.2: Cross Sectional and Plan View of the Axial Load Cell Compression Transducer

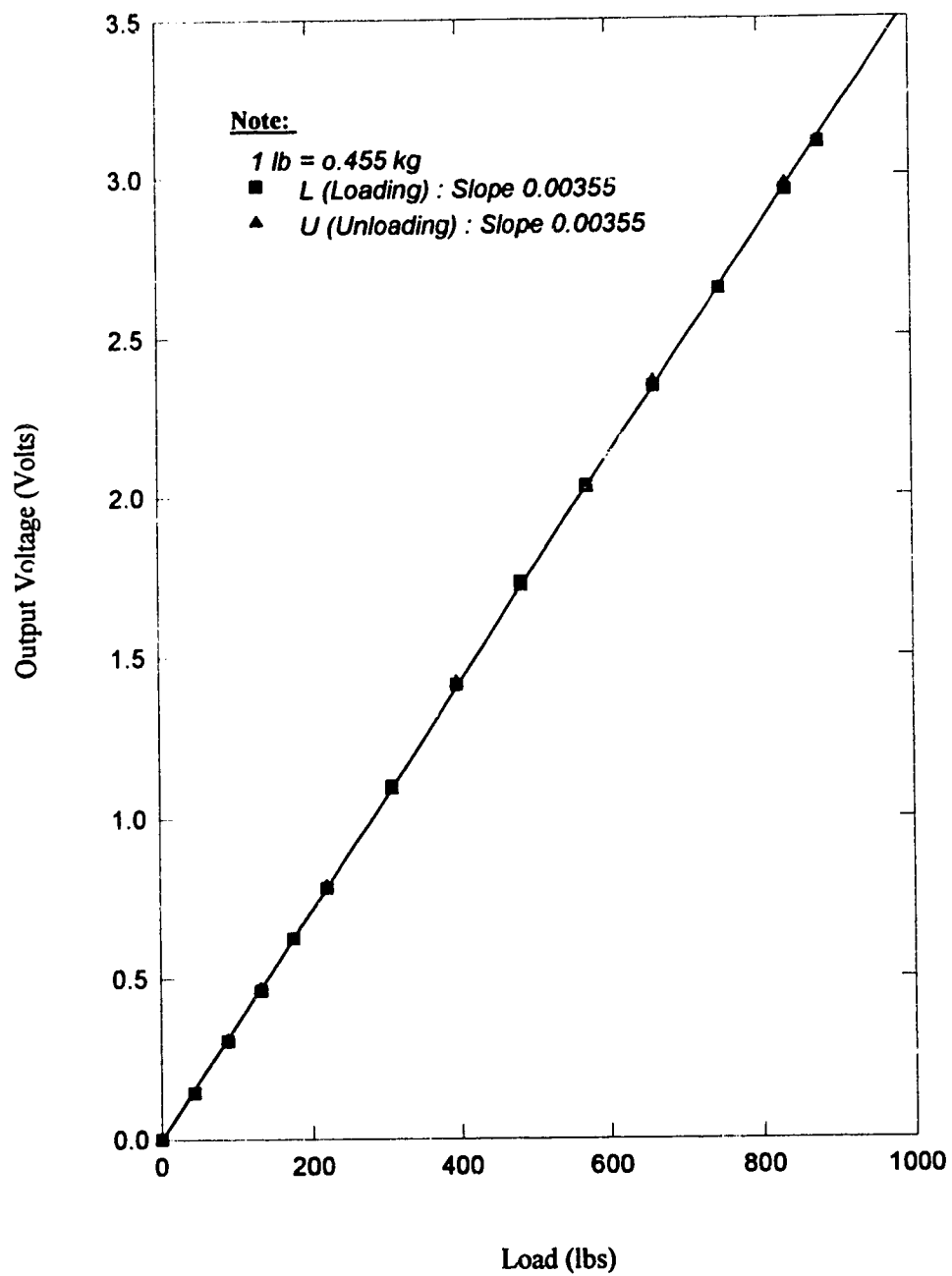


Figure E.3: Calibration Curve for Load Cell "B"

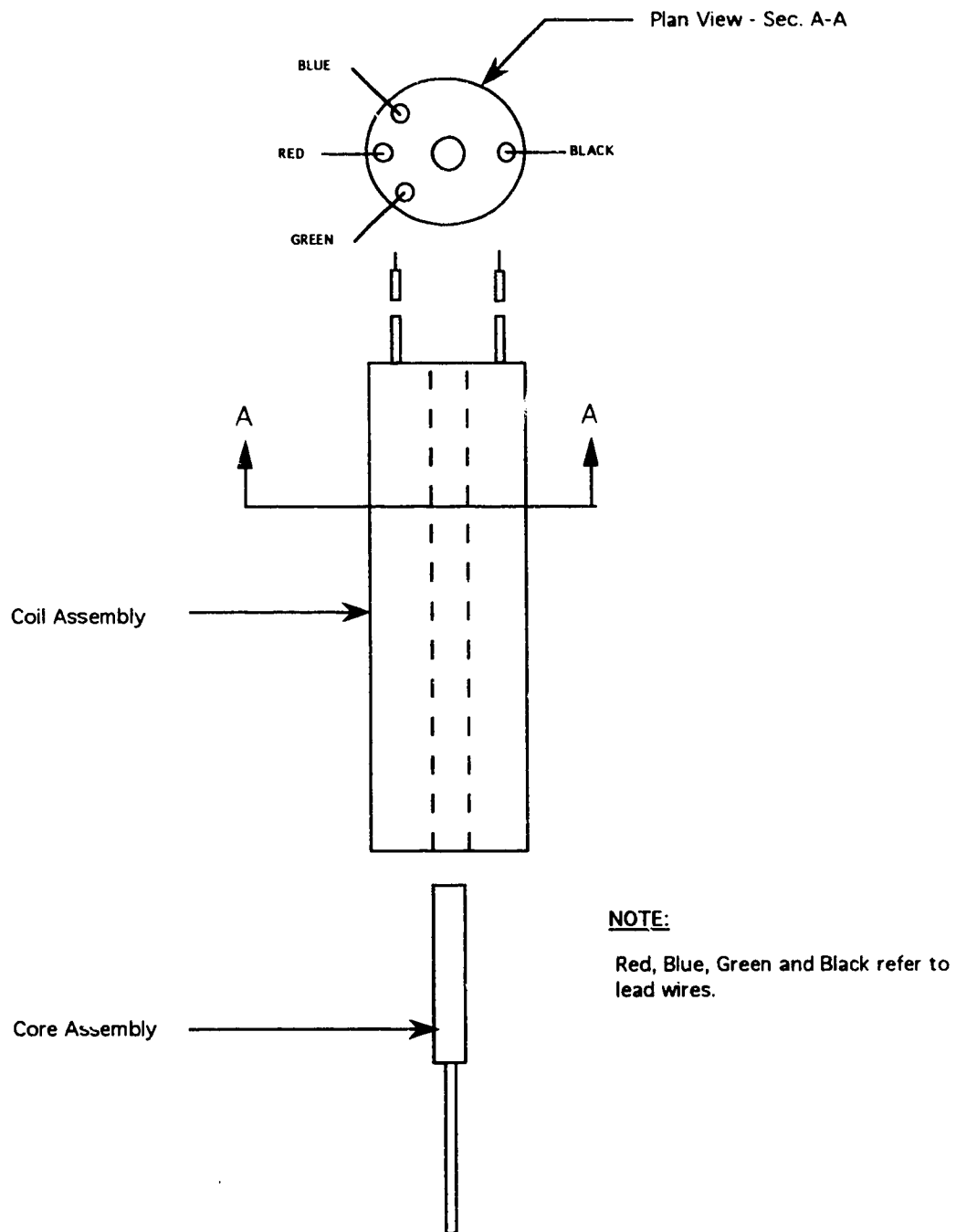


Figure E.4(a): Schematic Diagram of A Typical LVDT - Model DC-DC series 240

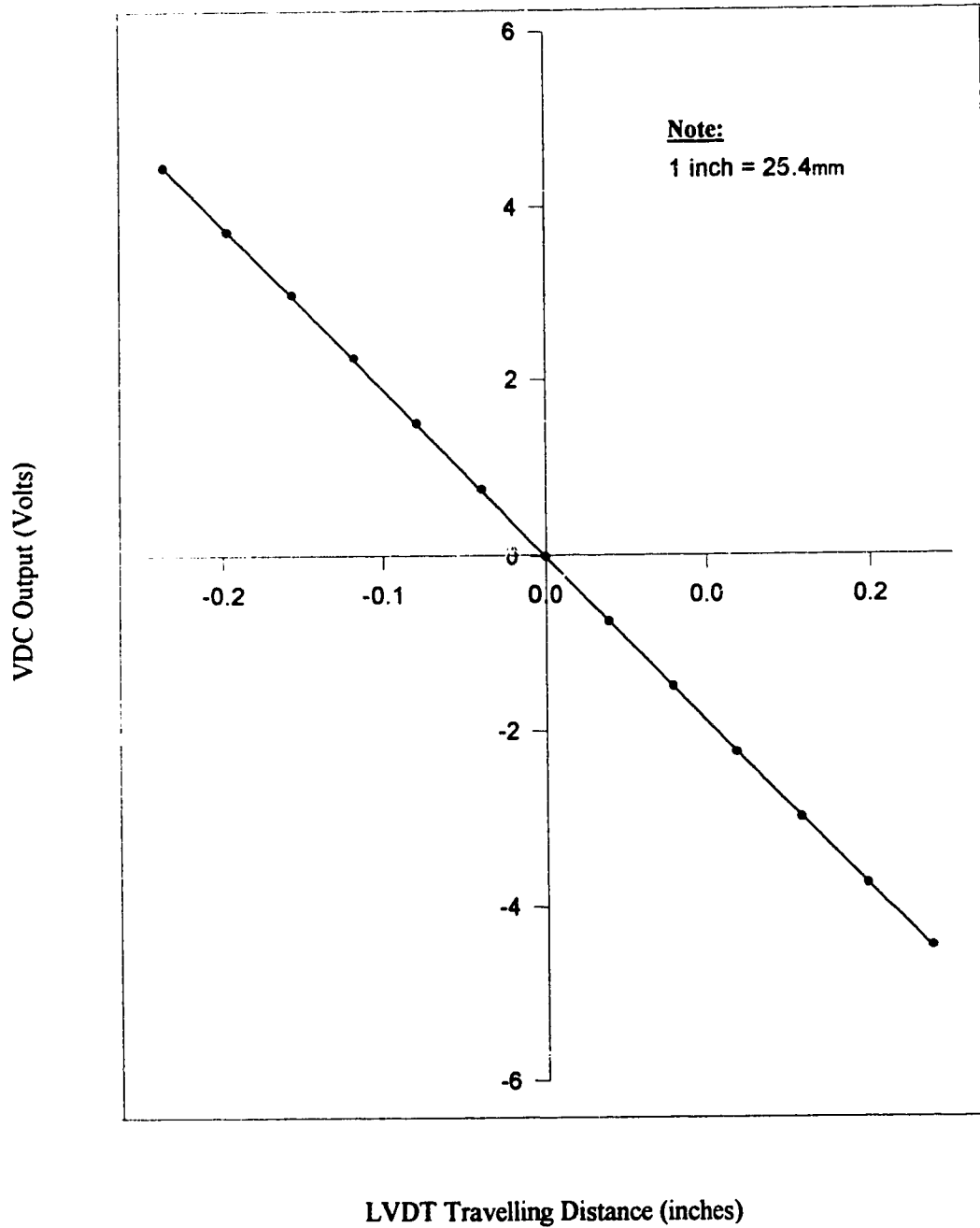


Figure E.4(b): Calibration Curve for LVDT # 2

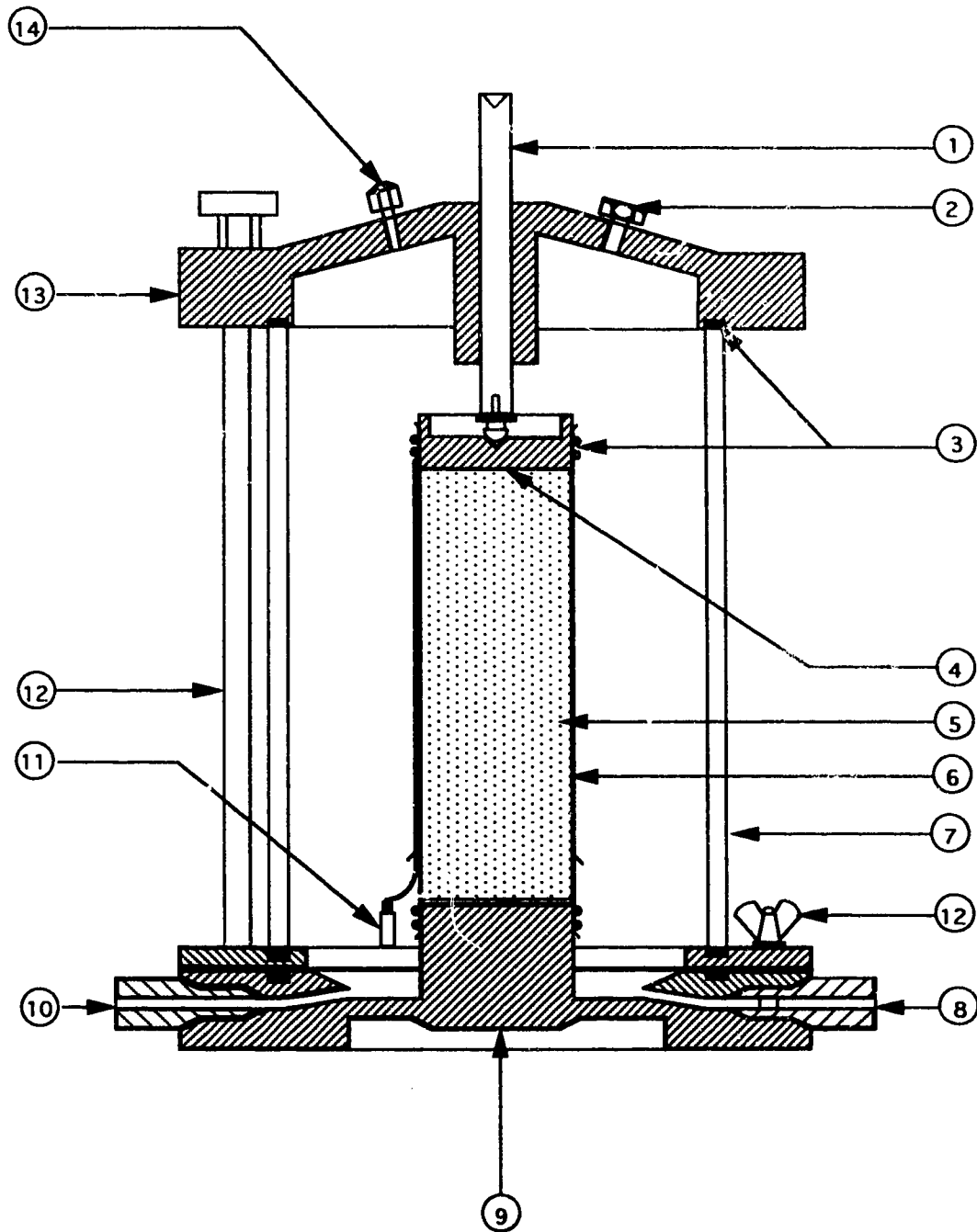


Figure E.5: Repeated Load Triaxial Chamber

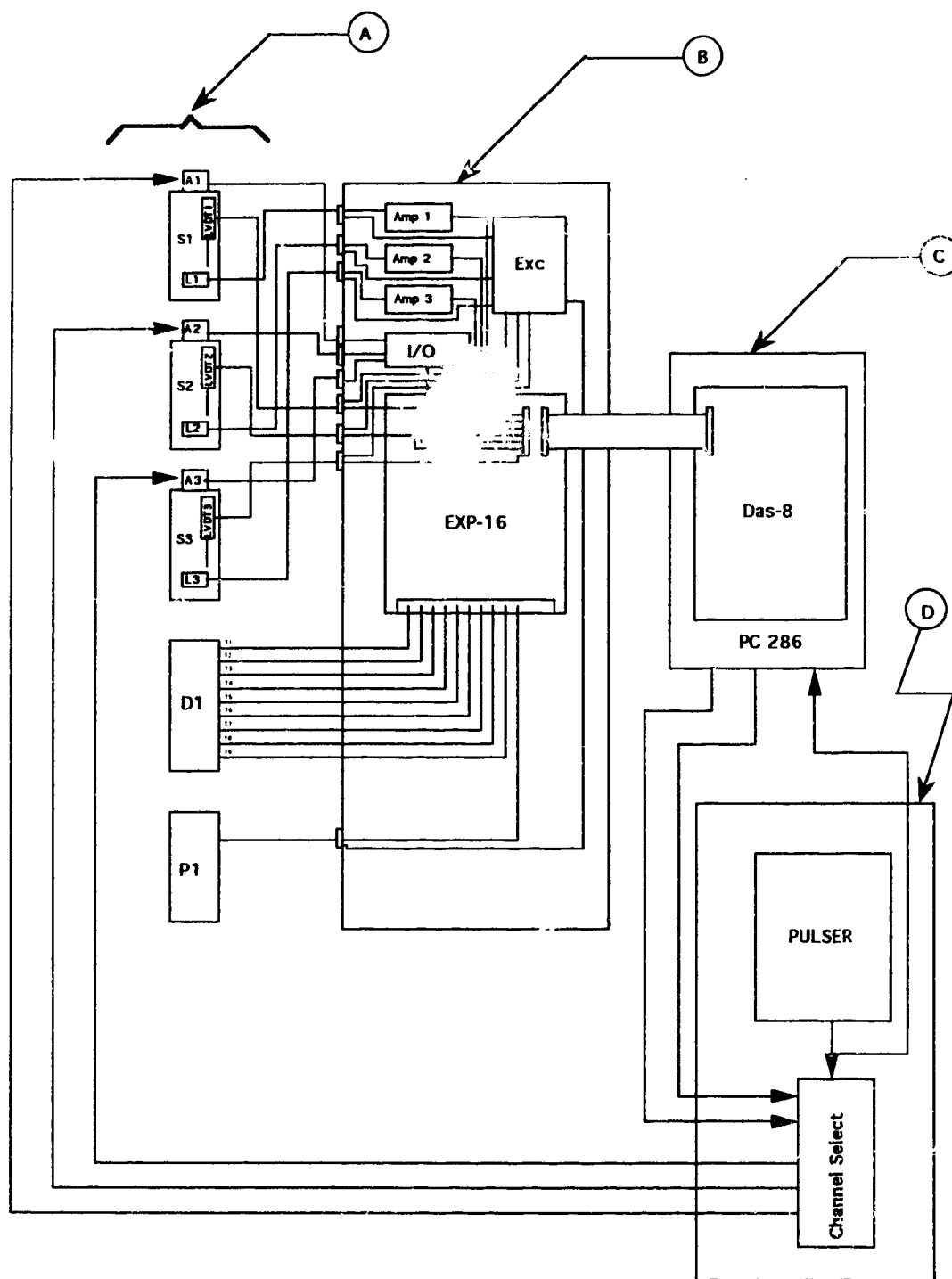


Figure E.6: Schematic Diagram of the Data Acquisition System

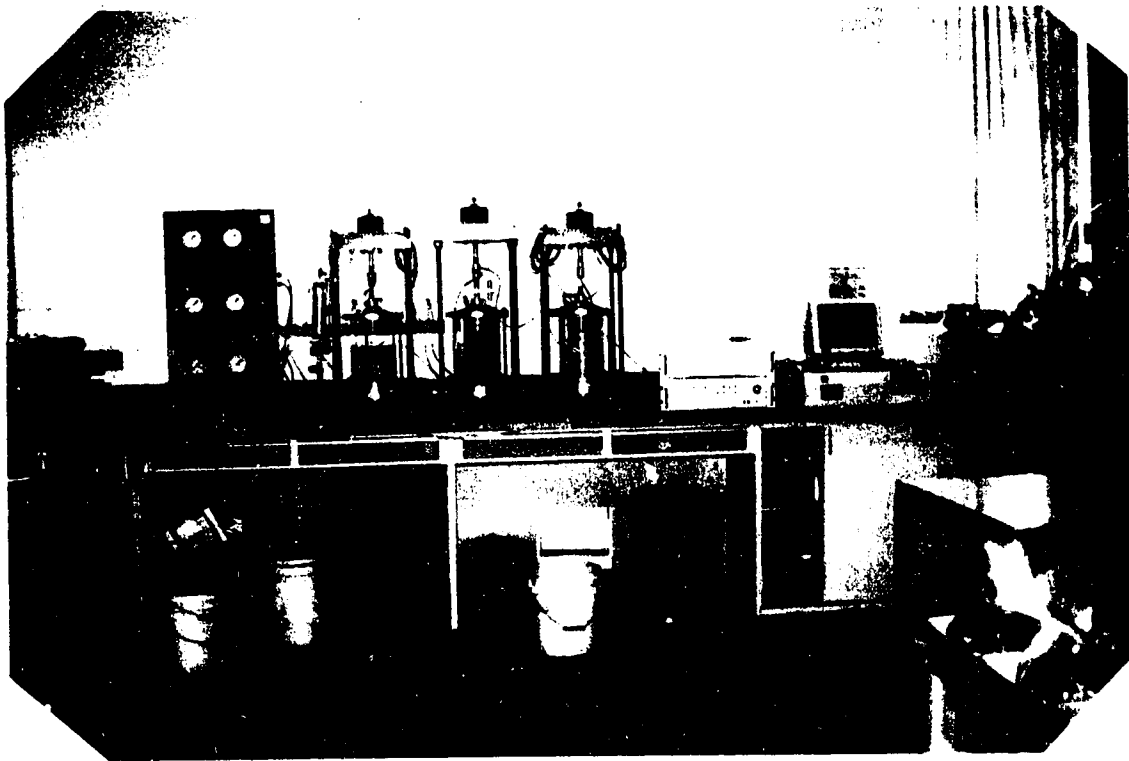


Plate E.1: Resilient Modulus Testing System (RMTS)

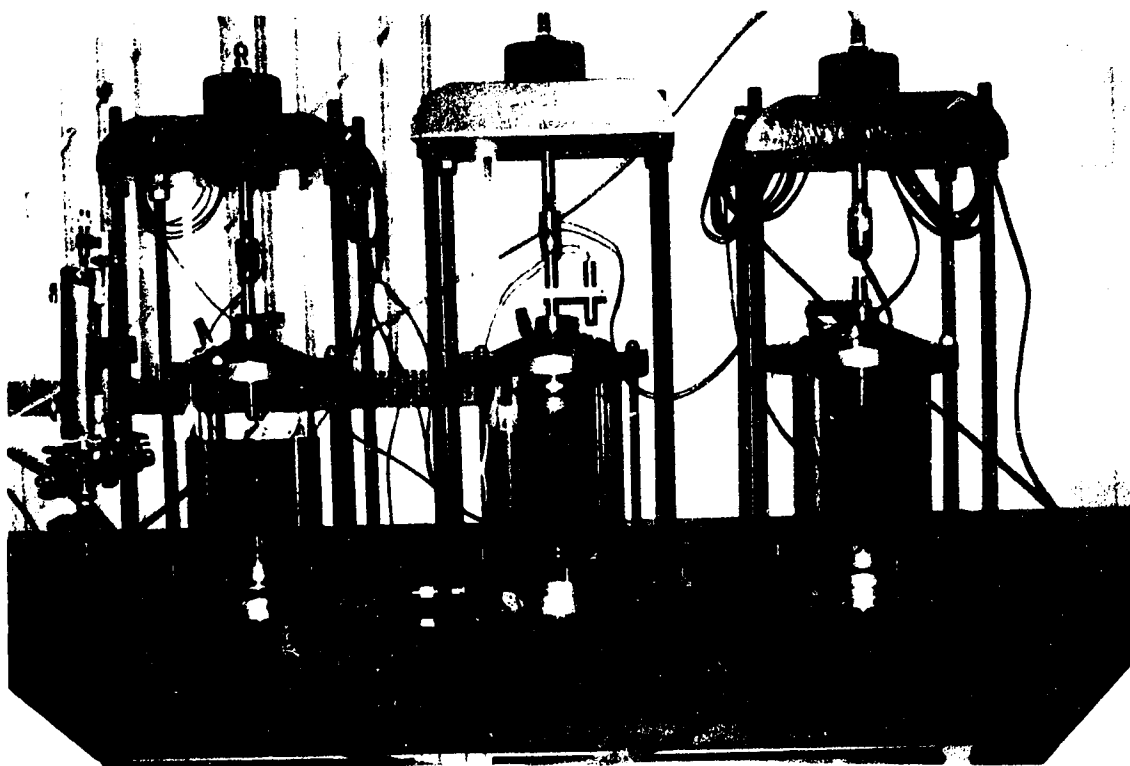


Plate E.2: Loading Frame - Triaxial Chambers Assembly

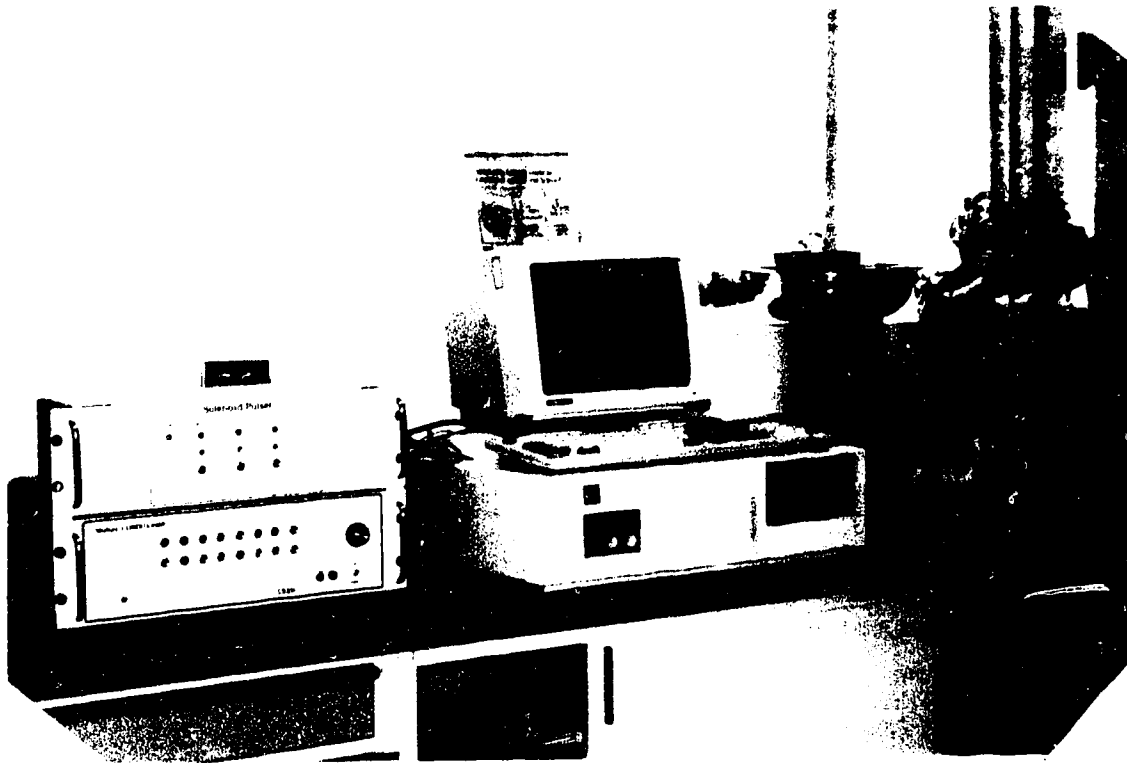


Plate E.3: Data Acquisition Arrangement Used for Operating the RMTS

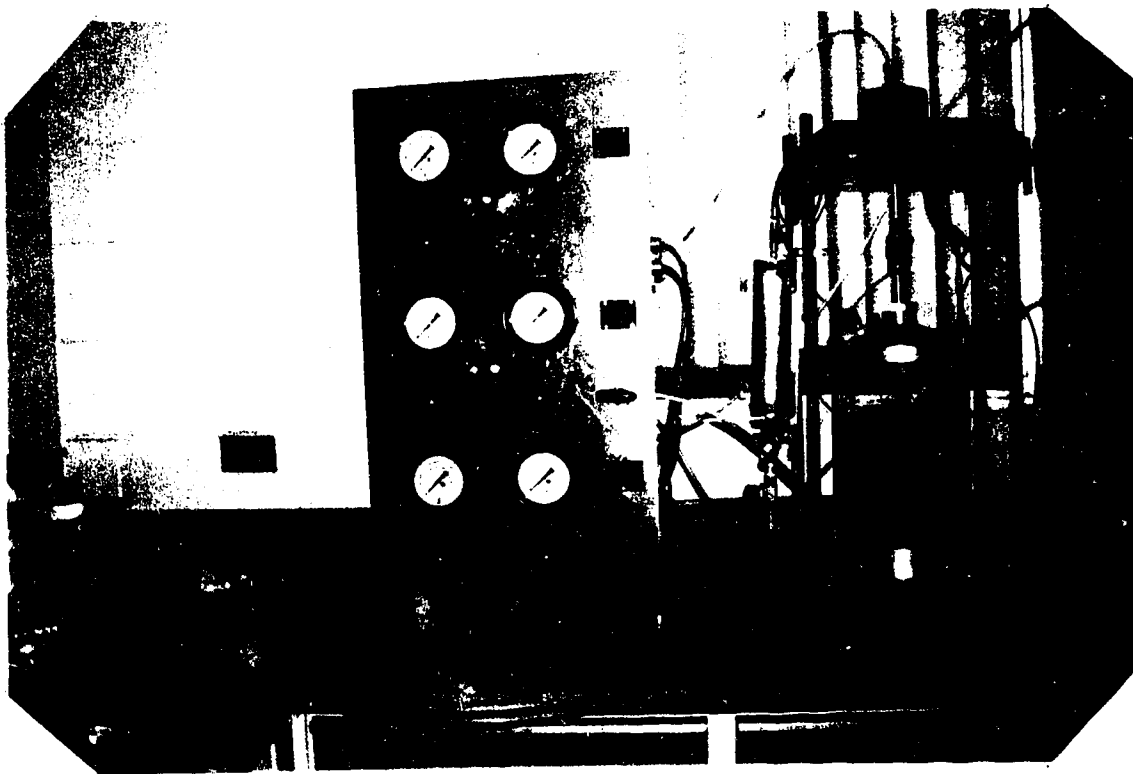


Plate E.4: Loading Panel Used for Setting applied Deviator Stress and Confining Pressure